RUTHENIUM-CATALYZED METATHESIS WITH DIRECTLY FUNCTIONALIZED OLEFINS

by

Marisa L. Macnaughtan

A dissertation submitted in partial fulfillment
of the requirements for the degree of
Doctor of Philosophy
(Chemistry)
in The University of Michigan
2009

Doctoral Committee:

Assistant Professor Marc J. A. Johnson, Co-chair
Associate Professor Adam J. Matzger, Co-chair
Emeritus Professor Arthur J. Ashe III
Professor Mark M. Banaszak Holl
Professor Johannes W. Schwank

© Marisa L. Macnaughtan
2009

Dedication

To my Family:

Mom, Dad, Heather,

Megan, Samuel, Suzanna and Aaron

All my love

Table of Contents

Dedication……...ii

List of Charts…….....x

List of Figures…….....xi

List of Schemes…….…..…xiii

List of Tables…….....……xvi

List of Appendices…….....xviii

List of Abbreviations…….....…xix

Abstract……..…….....xxiii

Chapter 1 Introduction

1.1. Introduction ……...……...1

1.2. An Early History of Olefin Metathesis……...……..2

1.2.1. Initial Mechanistic Debates……...…….3

1.2.2. Discovery of Well-Defined Catalytic Systems……...……...5

1.2.3. Transition Metal Catalyst Choice……..……....5

1.3. Ruthenium Olefin Metathesis Catalysts……..……6

1.3.1. A Brief History……...……...……6

1.3.2. Mechanism……...……..8

1.3.3. Substrate Tolerance……...……9

1.3.4. Tolerance of Halogenated Olefins……9

1.3.5. Schrock verses Fischer Carbene Complexes……...11

1.3.6. Experimental Work involving Fischer Carbene Complexes……..13

1.3.7. DFT Evidence for Fischer Carbene Stability……..15

1.4. Enyne Metathesis……...17

1.5. Alkyne Metathesis…….....19

1.5.1. Current Catalysts……19

1.5.2. Mechanism……..20

1.5.3. Ruthenium Alkylidyne Complexes…….20

1.6. Conclusions……...…….24

1.7. References……..25

Chapter 2 Synthesis, Isolation and Properties of Ruthenium Monohalomethylidene Complexes

2.1. Introduction.....……...……..31

2.2. Ruthenium Monofluoromethylidene Complexes...……32

2.2.1. Synthesis and Isolation……32

2.2.2. Reactivity…….39

2.2.2.1. Metathesis Activity……...39

2.2.2.2. Stoichiometric Metathesis with Ethyl Vinyl Ether……...43

2.2.2.3. Decomposition……..44

2.3. Ruthenium Monochloromethylidene Complexes……...46

2.3.1. Decomposition……46

2.3.2. Synthesis and Observation……...51

2.4. Attempts with Vinyl Bromide…….55

2.5. Conclusions……..56

2.6. Experimental……...57

2.6.1. General Procedures……..57

2.6.2. Materials……..58

2.6.3. Synthetic Procedures…….……...59

2.7. References……...89

Chapter 3 Scope and Limitations of Ruthenium-Based Catalysts for Cross-Metathesis of Vinyl Halides

3.1. Introduction…….92

3.1.1. Reasons for the Failure of Vinyl Halides in CM…….92

3.1.2. The Decomposition Pathway of Monohalomethylidene Complexes……..94

3.1.3. Catalyst Selection……96

3.2. CM Results…….98

3.2.1. CM with Vinyl Fluoride……..98

3.2.2. Synthesis of the Monohalomethylidene Dimer, **3.10**…….100

3.2.3. CM with **3.10-F**…….....……103

3.3. CM with Chlorinated Olefins……104

3.3.1. Results with 1,2-Dichloroethene……104

3.3.2. Vinyl Chloride versus 1,2-Dichloroethene……108

3.3.3. Ruthenium Decomposition during CM……..110

3.3.4. Alkene Isomerization……111

3.4. CM with Vinyl Bromide……...113

3.5. Ring-Opening Cross-Metathesis…….……..114

3.5.1. Vinyl Fluoride……114

3.5.2. Chlorinated Olefins in RO-CM…….....115

3.5.3. Brominated Olefins in RO-CM……..116

3.6. Conclusions……..….117

3.7. Experimental…….117

3.7.1. General Procedures…….……...…117

3.7.2. Materials……118

3.7.3. Synthetic Procedures……..119

3.8. References…….133

Chapter 4 Enyne Metathesis with Vinyl Halides

4.1. Introduction……...136

4.2. Enyne Metathesis (EyM) with Vinyl Halides……...138

4.2.1. EyM with Vinyl Fluoride…….……..138

4.2.2. EyM with Vinyl Chloride…….…….139

4.2.3. EyM with Vinyl Bromide…….…….140

4.3. Regiochemistry……..…140

4.4. Reaction Conditions……...140

4.5. Catalyst Selection……..142

4.5.1. Vinyl Fluoride……....142

4.5.2. Vinyl Chloride and Vinyl Bromide……146

4.6. Stability of the Butadiene Products……...149

4.7. Mechanism……150

4.8. Conclusions……..…152

4.9. Experimental……..……...153

4.9.1. General Procedures……..……..153

4.9.2. Materials……..……..154

4.9.3. Synthetic Procedures……..……....155

4.10. References……...174

Chapter 5 Fischer to Fischer Carbene Olefin Metathesis: Tricking the Ruthenium Catalyst

5.1. Introduction……...175

5.2. Stoichiometric Fischer Carbene Metathesis……..179

5.2.1. 2nd Generation Grubbs Catalyst……179

5.2.2. 3rd Generation Grubbs Catalyst……..180

5.3. Chelated Ruthenium Acetoxycarbene Complex……...182

5.4. CM with Electron-rich Olefins……183

5.4.1. Styryl Acetate……183

5.4.1.1. Synthesis……183

5.4.1.2. Substrate Scope and Yield……...183

5.4.2. Hexenyl Acetate……186

5.4.2.1. Synthesis……186

5.4.2.2. Substrate Scope and Yield……..186

5.4.3. Equilibrium……187

5.4.4. Optimization……..190

5.4.5. Mechanism……190

5.5. Conclusions……...193

5.6. Experimental……194

5.6.1. General Procedures……194

5.6.2. Materials……195

5.6.3. Synthetic Procedures……..195

5.7. References……209

Chapter 6 Synthesis and Reactivity of Ruthenium Benzylidyne Complexes

6.1. Introduction……...212

6.2. Synthesis of Ruthenium Benzylidyne Complexes……214

6.3. Ligand Substitutions……221

6.3.1. Neutral Ligands……..221

6.3.2. Aryloxide and Alkoxide Ligands.……..223

6.4. Ligand Migration…….…….227

6.4.1. Reversible……..227

6.4.1.1. Tetrachlorocatecholate……...227

6.4.1.2. Fluoride……...233

6.4.2. Migration followed by C-H Activation……..235

6.5. Conclusions……...239

6.6. Experimental…….240

6.6.1. General Procedures……240

6.6.2. Materials……241

6.6.3. Synthetic Procedures……..241

6.7. References…….…260

Chapter 7 Conclusions and Future Directions

7.1. Conclusions…….…..264

7.1.1. Ruthenium Monohalomethylidene Complexes…….265

7.1.2. Cross-Metathesis (CM) with Vinyl Halides……..267

7.1.3. Enyne Metathesis (EyM) with Vinyl Halides……268

7.1.4. Fischer to Fischer Cross-Metathesis (FCM)…….…….269

7.1.5. Facile Synthesis of Ruthenium Benzylidyne Complexes……..269

7.2. Future Directions……..270

7.2.1. Metathesis with Vinyl Halides……..….270

7.2.2. Metathesis with Electron-Rich Olefins……..271

7.2.3. Ruthenium Benzylidyne Chemistry……...273

7.3. References…….275

List of Charts

Chart 1.1. Important Ruthenium OM Catalysts……..7

Chart 1.2. Important Fischer Carbene Complexes and Decomposition Products……..….12

Chart 1.3. Previously Synthesized Ru-Benzylidyne Complexes in the Johnson Group…23

Chart 2.1. Important Carbene and Carbide Complexes…….31

Chart 3.1. Important Ruthenium Complexes…….93

Chart 3.2. Possible CM Products (*E/Z*)……..99

Chart 4.1. Important Ruthenium Compounds……..137

Chart 4.2. EyM Products……..139

Chart 5.1. Important Ruthenium Compounds……..176

Chart 5.2. Cross-Products of FCM……..186

Chart 6.1. Previously Synthesized Ru-Benzylidyne Complexes in the Johnson Group……...213

Chart 6.2. Numbered Complexes throughout Chapter 6…….216

Chart 7.1. Some Important Ruthenium Complexes……265

List of Figures

Figure 1.1. Alkyne Metathesis Catalysts……...19

Figure 1.2. Previously Known Acidic Ruthenium Alkylidyne Compounds……..…22

Figure 1.3. Previously Known Ruthenium Alkylidyne Compounds……..…22

Figure 2.1. 50% thermal ellipsoid plot of [Ru(CHF)(H_2IMes)(PCy_3)Cl_2] (**2.13-F**)…..…34

Figure 2.2. 50% thermal ellipsoid plot of [Ru(CHF)(H_2IMes)$(py)_2Cl_2$] (**2.14-F**)…….37

Figure 2.3. 50% thermal ellipsoid plot of [Ru(CHPCy_3)(H_2IMes)Cl_3] (**2.8-Cl**)..…….49

Figure 2.4. 1st order decay of **2.13-Cl**(^{13}C) (14.4 ppm) to **2.8-Cl**(^{13}C) (19.7 ppm)…..….52

Figure 3.1. 50% thermal ellipsoid plot of [Ru(CHF)(H_2IMes)(η-Cl)Cl]$_2$ (**3.10-F**)…….101

Figure 4.1. Steric Effects of Alkyne Binding at the Ru-center: Regiocontrol for the Formation of 1-X-*3*-substituted-1,3-butadienes.…….……152

Figure 5.1. Definitions of Schrock and Fischer Carbene Complexes……..176

Figure 6.1. 50% thermal ellipsoid plot of [Ru(C-*p*-C_6H_4Me)(H_2IMes)Cl_3] (**6.8-Cl**)…..217

Figure 6.2. 50% thermal ellipsoid plot of [Ru(C-*p*-C_6H_4Me)(H_2IMes)I_3] (**6.8-I**)……...218

Figure 6.3. Conformation of **6.10**; Locked on an NMR Timescale…….……226

Figure 6.4. 50% thermal ellipsoid plot of [Ru(≡C-*p*-C_6H_4Me)(H_2IMes)($O_2C_6Cl_4$)I] (**6.19-I**)…….229

Figure 6.5. 50% thermal ellipsoid plot of [Ru(=C(OC_6Cl_4O)(*p*-C_6H_4Me))(H_2IMes) $(C_5D_5N)_2Cl$] (**6.20-Cl/C_5D_5N**)……230

Figure 6.6. 50% thermal ellipsoid plot of [Ru(=C($OC(CF_3)_2CH_2$) (*p*-C_6H_4Me) (H_2IMes)($OC(CF_3)_2CH_3$)] (**6.21**)…….237

Figure 6.7. 50% thermal ellipsoid plot of [Ru(=C($OC(CF_3)_2CH_2$) (*p*-C_6H_4Me) (H_2IMes)($OC(CF_3)_2CH_3$)] (**6.21**).Alternative view…….238

Figure 6.8. NMR spectrum for **6.19-Cl**……...…252

Figure 6.9. ^{1}H NMR spectrum of **6.20-Cl/C_5D_5N**……...254

Figure 7.1. Placement of Electron-Withdrawing Groups on the NHC Ligand…….…...271

List of Schemes

Scheme 1.1. Caulderon and Chauvin Mechanisms……4

Scheme 1.2. Chauvin's CM Experiment.....4

Scheme 1.3. General Mechanism for Olefin Metathesis……8

Scheme 1.4. RCM of α-halo-α,ω-dienes.....……10

Scheme 1.5. NMR MT Experiments…….……13

Scheme 1.6. Treatment of **1.4** with Electron-Rich Olefins…….……...14

Scheme 1.7. Metathesis Activity of Fischer Carbene Complexes with Electron-Rich Olefins…….……...15

Scheme 1.8. Gibbs Free Energy Profile of CM with 1,2-Difluoroethene…….……16

Scheme 1.9. Gibbs Free Energy Profile of CM with 1,2-Dichloroethene……16

Scheme 1.10. General Scheme for EyM……17

Scheme 1.11. Mechanism for EyM……18

Scheme 1.12. The Mechanism for Alkyne Cross-Metathesis……20

Scheme 2.1. Initial Syntheses of **2.13-F** and **2.14-F**……..33

Scheme 2.2. Synthesis of Monofluoromethylidene Complexes…..38

Scheme 2.3. Stoichiometric Metathesis with Ethyl Vinyl Ether…….……..43

Scheme 2.4. Decomposition of **2.13-F**……...……...45

Scheme 2.5. Formation of Terminal Carbide and Phosphoniomethylidene Complexes...47

Scheme 2.6. Proposed Decomposition of the Monohalomethylidene Complexes……47

Scheme 2.7. Formation of the Phosphoniomethylidene Complex from **2.13-F**……48

Scheme 2.8. Stoichiometric Metathesis with Vinyl Bromide……...55

Scheme 2.9. Reactivity of **2.15** in Benzene……...68

Scheme 3.1. Proposed Decomposition of the Monohalomethylidene Complexes…..…..95

Scheme 3.2. Ligand Effect on Carbide Formation……96

Scheme 3.3. Initiation of Precatalysts **3.4-3.6**……...…97

Scheme 3.4. Competition between CM and Decomposition of the Monohalomethylidene Intermediates……..107

Scheme 3.5. Cross-Metathesis verses CM Homodimerization……108

Scheme 3.6. Byproducts from Alkene Isomerization Processes……..111

Scheme 3.7. CM of Allylbenzene under Standard Metathesis Conditions……..112

Scheme 3.8. CM of Allyloxybenzene under Standard Metathesis Conditions……....112

Scheme 4.1. Byproducts of EyM with Vinyl Fluoride……...….146

Scheme 4.2. Byproducts of EyM with Vinyl Chloride……...….147

Scheme 4.3. Byproducts of EyM with Vinyl Bromide……...….148

Scheme 4.4. Proposed Mechanism for EyM with Vinyl Halides: "Alkylidene First"…151

Scheme 4.5. EyM Catalyzed with Compound **4.2**……...152

Scheme 5.1. CM with Electron-Rich Olefins……...……...178

Scheme 5.2. Qualitative Energetic Comparisons of Schrock and Fischer Carbene Complexes……...178

Scheme 5.3. Stoichiometric Fischer Carbene Metathesis (**5.6**)……...179

Scheme 5.4. Stoichiometric Fischer Carbene Metathesis (**5.7**)……...179

Scheme 5.5. General Fischer CM Reaction……181

Scheme 5.6. Reaction of **5.9-F** with Vinyl Acetate……182

Scheme 5.7. Synthesis of Alkenyl Acetate……..183

Scheme 5.8. Mechanism for Fischer Carbene Cross-Metathesis……192

Scheme 5.9. Cycloaddition and Cycloreversion Processes……192

Scheme 5.10. Other Pathways: Fischer to Schrock Conversion…….……193

Scheme 5.11. Degenerate Metathesis; *E/Z* Isomerization……..…..193

Scheme 6.1. Synthetic Pathway to [Ru(C-*p*-C_6H_4Me)(PCy_3)Cl_3] (**6.3-Cl**)…..……..214

Scheme 6.2. Synthesis of [Ru(C-*p*-C_6H_4Me)(H_2IMes)Cl_3] (**6.8-Cl**)……...215

Scheme 6.3. Conversion to [Ru(C-*p*-C_6H_4Me)(H_2IMes)I_3] (**6.8-I**)…….215

Scheme 6.4. Addition of PCy_3 to Chlorinated Benzylidyne Complexes.....222

Scheme 6.5. Addition of PCy_3 to Iodo-Benzylidyne Complexes……....223

Scheme 6.6. Substitutions of Aryloxide Ligands…….225

Scheme 6.7. Synthesis of **6.19-X**…….……228

Scheme 6.8. Synthesis of **6.20-Cl/THF** in THF…….228

Scheme 6.9. Synthesis of **6.20-X/C_5D_5N**……..……..228

Scheme 6.10. Attempted Synthesis of **6.17**…….……233

Scheme 6.11. Observation of the Equilibrium of **6.15** and **6.16**……..235

Scheme 6.12. Synthesis of **6.21**…….…….……236

Scheme 7.1. Products of Monochloromethylidene Deactivation……266

Scheme 7.2. Cross-Metathesis (CM) with Halogenated Olefins…….....267

Scheme 7.3. Ring-Opening CM with Halogenated Olefins……268

Scheme 7.4. Enyne Metathesis with Vinyl Halides……268

Scheme 7.5. FCM with a Variety of Directly Functionalized Olefins……269

Scheme 7.6. Synthesis of a Ruthenium Benzylidyne Compound ……...270

Scheme 7.7. Speculative Removal of H_2IMes…….274

List of Tables

Table 2.1. Crystallographic Data for Complexes **2.13-F**, **2.14-F** and **2.8-Cl**……35

Table 2.2. Selected Bond Lengths and Angles for Complexes **2.13-F**, **2.14-F** and **2.8-Cl**……..……36

Table 2.3. NMR Data for Monofluoromethylidene Compounds……..39

Table 2.4. Catalyzed RCM of Diethyldiallylmalonate……..41

Table 2.5. Catalyzed Self-CM of 1-Hexene……...41

Table 2.6. Selected ^{1}H, ^{13}C, and ^{31}P NMR Data for Comparison with **2.13-Cl(^{13}C)**..…53

Table 2.7. Stoichiometric Metathesis of **2.2-Cl** and Vinyl Chloride…….76

Table 2.8. Stoichiometric Metathesis of **2.2-Cl** and 1,2-Dichloroethylene..…….76

Table 2.9. Stoichiometric Metathesis of **2.2-Cl** and 1-Chloro-1-propene…….77

Table 2.10. Stoichiometric Metathesis of **2.2-Cl** and 1-Chloro-1-propene in the Presence of Diisopropylethylamine……..…….82

Table 3.1. Olefin Cross-Metathesis with Vinyl Fluoride……...99

Table 3.2. Crystallographic Data for Complex **3.10-F**……....102

Table 3.3. Selected Bond Lengths and Angles for Complex **3.10-F**……...103

Table 3.4. Cross-Metathesis Results with 1,2-Dichloroethene……105

Table 3.5. Cross-Metathesis with Vinyl Chloride……...109

Table 3.6. Cross-Metathesis with Brominated Olefins……...…….114

Table 3.7. RO-CM with Vinyl Fluoride……..…115

Table 3.8. RO-CM with Chlorinated and Brominated Olefins…….…..116

Table 3.9. Olefin Cross-Metathesis with Vinyl Fluoride……121

Table 3.10. Olefin Cross-Metathesis Results with 1,2-Dichloroethene..…….122-123

Table 3.11. Olefin Cross-Metathesis with Vinyl Chloride……123

Table 3.12. Olefin Cross-Metathesis with Vinyl Bromide……..……..124

Table 3.13. Olefin RO-CM with Vinyl Fluoride……124

Table 3.14. Olefin RO-CM with Chlorinated and Brominated Olefins……..125

Table 4.1. Reaction Details for NMR Scale Reactions with Vinyl Fluoride……...…144

Table 4.2. Larger Scale EyM Reactions with Vinyl Fluoride…….145

Table 4.3. Reaction Details for NMR Scale Reactions with Vinyl Chloride……..147

Table 4.4. Reaction Details for NMR Scale Reactions with Vinyl Bromide……..…148

Table 4.5. Larger Scale EyM Reactions with Vinyl Chloride and Vinyl Bromide…….149

Table 5.1. Preliminary Substrate Scope Study for Styryl Acetate…..…….185

Table 5.2. Preliminary Substrate Scope Study for 1-Hexenyl Acetate...…….187

Table 5.3. Altering the Concentration of Ethyl Vinyl Ether……189

Table 5.4. Altering the Concentration of Phenyl Vinyl Sulfide……..189

Table 5.5. Altering Catalyst Loading……...190

Table 5.6. FCM with Styryl Acetate in Benzene-d_6……203

Table 5.7. Varying the Concentration of Ethyl Vinyl Ether……205

Table 5.8. FCM with 1-Hexenyl Acetate in Benzene-d_6…….206

Table 5.9. FCM with 1-Hexenyl Acetate in Acetone-d_6……..207

Table 5.10. FCM with Styryl Acetate in Acetone-d_6...……208

Table 6.1. Crystallographic Data for Complexes **6.8-Cl**, **6.8-I**, and **6.19-I**…….219

Table 6.2. Selected Bond Lengths and Angles for Complexes **6.8-Cl**, **6.8-I**, and **6.19-I**……....220

Table 6.3. Crystallographic Data for Complexes **6.20-Cl/C_5D_5N** and **6.22**……231

Table 6.4. Selected Bond Lengths and Angles for Complexes **6.20-Cl/C_5D_5N** and **6.22**……...…232

Table 6.5. NMR Data to Identify **6.16** and **6.15**……..234

List of Appendices

Appendix 1: Crystal Data for [Ru(CHF)(H_2IMes)(PCy_3)Cl_2] (**2.13-F**)……..277

Appendix 2: Crystal Data for [Ru(CHF)(H_2IMes)$(py)_2Cl_2$] (**2.14-F**)…….289

Appendix 3: Crystal Data for [Ru($CHPCy_3$)(H_2IMes)Cl_3] (**2.8-Cl**)……300

Appendix 4: Crystal Data for [Ru(CHF)(H_2IMes)(η-Cl)Cl]$_2$ (**3.10-F**)…….....311

Appendix 5: Crystal Data for [Ru(C-*p*-C_6H_4Me)(H_2IMes)Cl_3] (**6.8-Cl**)…….323

Appendix 6: Crystal Data for [Ru(C-*p*-C_6H_4Me)(H_2IMes)I_3] (**6.8-I**)…….333

Appendix 7: Crystal Data for [Ru(≡C-*p*-C_6H_4Me)(H_2IMes)($O_2C_6Cl_4$)I] (**6.19-I**)……...343

Appendix 8: Crystal Data for [Ru(=C(OC_6Cl_4O-)(*p*-C_6H_4Me))(H_2IMes)$(C_5D_5N)_2Cl$] (**6.20-Cl/C_5D_5N**)…….354

Appendix 9: Crystal Data for [Ru(=C($OC(CF_3)_2CH_2$-)(*p*-C_6H_4Me))(H_2IMes) ($OC(CF_3)_2CH_3$)] (**6.21**)……366

List of Abbreviations

Ac	acyl
AI	alkene isomerization
AM	alkyne metathesis
Anal	elemental analysis
b	broad
3Br-py	3-bromopyridine
^{13}C	carbon-13
ca.	approximately
Calcd	calculated
CM	cross-metathesis
COD	1,5-cyclooctadiene
Cy	cyclohexyl
d	day(s), doublet
D	deuterium
-d_n	deuterated solvent, n = number of deuteriums
DFT	density functional theory
EI	electrospray ionization
Et	ethyl
equiv	equivalents
Eq.	equation
EWG	electron-withdrawing group

EyM	enyne metathesis
^{19}F	fluorine-19
FCM	Fischer carbene cross-metathesis
g	grams
GCMS	gas chromatography-mass spectroscopy
GCOSY	Gradient Correlation Spectroscopy
GOF	goodness of fit
^{1}H	proton
$\{^{1}H\}$	proton decoupled
h	hour(s)
H_2IMes	4,5-dihydro-1,3-bis(mesityl)imidazol-2-ylidene
HSQC	Heteronuclear Single Quantum Coherence
Hz	hertz
i-Pr	isopropyl
$^{n}J_{xy}$	n-bond coupling constant between atoms x and y
K	Kelvin
k	rate constant
L	general neutral donor ligand
m	multiplet, milli-
M	moles/liter, Mega
Me	methyl
Mes	mesityl, 2,4,6-$(CH_3)_3C_6H_2$
mg	milligrams
min	minute(s)
mL	milliliter

mmol	millimole
mol	mole
mol%	mole percent
$NC_{12}H_8$	*N*-carbazole
NHC	general *N*-heterocyclic carbene
NMR	nuclear magnetic resonance
NMR MT	nuclear magnetic resonance magnetization transfer
NOESY	Nuclear Overhauser Enhancement Spectroscopy
OAc	OC(O)Me, acetate
OBz	OC(O)Ph, benzoate
OM	olefin metathesis
ORTEP	Oak Ridge Thermal Ellipsoid Plot
OPv	OC(O)-*t*-Bu, pivalate
OTf	OSO_2CF_3
^{31}P	phosphorus-31
$\{^{31}P\}$	phosphorus decoupled
Ph	phenyl
ppm	parts per million
psig	pressure per square inch gauge
py	pyridine
q	quartet
R	generic alkyl/aryl group unless otherwise defined
RCM	ring-closing metathesis
ROM	ring-opening metathesis
ROMP	ring-opening metathesis polymerization

s	second(s), singlet
t	triplet
TAS-F	tris(dimethylamino)sulfonium difluorotrimethylsilicate
t-Bu	*tert*-butyl
THF	tetrahydrofuran
TMS	trimethylsilyl
TON	number of turnovers per catalyst
X	generic monoanionic ligand, halogen or other heteroatomic group
XRD	X-ray diffraction
°C	degrees Celsius
Å	Angstrom (10^{-10} m)
ΔH	enthalpy of activation
ΔG	Gibbs free energy
δ	chemical shift in ppm downfield from zero
η^n	number of binding sites from a ligand to a metal
μ	bridging ligand
π	pi bond
σ	sigma bond
μL	microliter

Abstract

Olefin metathesis (OM) has become a widely used tool in organic and material syntheses. As catalyst development has advanced, functional group tolerance has increased. Unfortunately, vinyl halides were incompatible with OM catalysts and attempts at cross-metathesis (CM) with vinyl halides failed. Given the usefulness of alkenyl halides in metal-catalyzed cross-coupling reactions, improvement of CM systems employing vinyl halides would be beneficial. Research goals included determining why vinyl halides were not tolerated by ruthenium-based OM catalysts and developing systems in which vinyl halides participate in CM. Ruthenium monohalomethylidene complexes, $[Ru(=CHX)(H_2IMes)LCl_2]$ (X = F, Cl; L = PCy_3, 2 py), which are intermediates in CM with vinyl halides, were found to undergo decomposition through loss of HX, deactivating the catalyst. Decomposition of the monochloromethylidene complexes can be hindered by removing one of the neutral ligands (L) from the system, making CM with chlorinated olefins successful. The monofluoromethylidene complexes synthesized were less susceptible to decomposition. However, the monofluoromethylidene intermediates act as a thermodynamic well, shutting down CM. However, if metathesis product formation is energetically favored, then the thermodynamic stability of the monofluoromethylidene intermediate relative to Ru-alkylidene intermediates can be overcome by this added driving force. Therefore, vinyl fluoride is an effective substrate for ring-opening cross-metathesis with cyclooctene and enyne metathesis with a number of alkynes. We also pioneered a new subfield of OM

referred to as Fischer carbene cross-metathesis (FCM), in which the thermodynamic stability of Fischer carbene complexes was circumvented by removing the need to form a ruthenium alkylidene complex during the catalytic cycle. FCM involves CM of electron-rich olefins such as ethyl vinyl ether with functionalized 1,2-disubstituted alkenes such as styryl acetate to form β-ethoxystyrene. FCM has allowed for productive CM with a number of electron-rich olefins including vinyl fluoride which have previously been detrimental to Ru-based catalysts. Finally, the decomposition process of the monohalomethylidene complexes led to the discovery of a facile synthesis of new Ru-benzylidyne species. The synthesis and reactivity of a number of previously unknown Ru-benzylidyne complexes was studied and has important implications for the development of Ru-based alkyne metathesis catalysts, which have yet to be realized.

Chapter 1

Introduction

1.1. Introduction

Olefin metathesis (OM) has become an increasingly useful synthetic technique for a number of chemical transformations from organic syntheses to polymer formation.[1-4] A number of metal carbene complexes can act as active OM catalysts; however, ruthenium alkylidene complexes have become the favorite of many due to the ability of Ru-based catalysts to retain high activity while maintaining greater stability towards oxygenated and protic functional groups.[1,2] Despite the advances made in OM over the last 50 years, the ability to use vinyl halides in olefin metathesis reactions has not been achieved. Use of vinyl halides in cross-metathesis (CM) would generate facile synthetic techniques of alkenyl halides which are key building blocks in transition-metal catalyzed syntheses, particularly palladium-catalyzed cross-coupling reactions.[5,6,7] The reasons vinyl halides fail to participate in OM reactions has not yet been addressed. Thus, the primary goal of this research project was to determine the reasons vinyl halides fail in olefin metathesis reactions and then alter the system to utilize vinyl halides as effective OM substrates.[8-10] Our studies lead us not only to the reasons vinyl halides shut down OM reactions and ways to use vinyl halides as OM substrates but also to a general method to incorporate a

variety of electron-rich olefins in CM reactions as well as a facile synthesis for Ru alkylidyne species.

1.2 An Early History of Olefin Metathesis

In 1955, Ziegler reported the discovery of metal-catalyzed olefin polymerization. Study of the well-known Ziegler/Natta systems, in which early transition metal catalysts convert olefins to saturated polymers, revealed a secondary reaction in which an unsaturated polymer formed.[11] Meanwhile, at Dupont in 1960, formation of unsaturated ring-opened polynorbornene was observed using a titanium-based catalyst (Eq. 1.1).[12] At the time, ring opening polymerizations of this type were quite unusual.

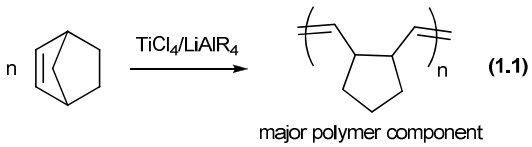

(1.1)

These results led researchers to focus on development of metal-catalyzed systems for the synthesis of unsaturated polymers. The Natta group found that these ring opening polymerizations worked with less strained cyclopentene as well as with highly strained norbornene. The Natta group developed heterogeneous cocatalysts $MoCl_5/Et_3Al$ which gave highly *cis*-alkene polymers and WCl_6/Et_3Al which gave highly *trans*-alkene polymers; demonstrating diastereotopic control (Eq. 1.2).

(1.2)

In 1963, Eleuterio reported the formation of an ethylene-propylene copolymer from propylene and a heterogeneous molybdenum-based catalyst. Off-gases from this reaction contained butenes. Eleuterio proposed carbon-carbon double bond scrambling of the propylene to form ethylene and butene.[1]

The rubber-like properties of the unsaturated polymers formed by the olefin polymerization reactions were of great interest to industry. These metal catalyst systems also yielded 'living' polymer systems making them even more attractive. The Caulderon group at Goodyear began working on new catalytic systems to form unsaturated polymers in the late 60's and proposed a pair-wise exchange mechanism as the propagation step for this chemistry. Calderon coined the term "olefin metathesis" for these reactions and provided strong evidence that the scrambling of carbon-carbon bonds occurred between the olefinic moiety while ruling out transalkylation mechanisms.[13,14]

1.2.1. Initial Mechanistic Debates

By the late 1960's and early 1970's, it was understood that the olefin polymerization reactions occurred by the exchange of partners between two carbon-carbon double bonds as opposed to the association/insertion mechanism of classic Zeigler/Natta systems. Caulderon proposed a pair-wise exchange mechanism, where two olefins are brought together through interaction with the metal catalyst and a 2+2 cycloaddition/cycloreversion occurs around the metal (Scheme 1.1; top);[15,16] Chauvin's

work ruled out the pair-wise exchange and instead proposed that metal carbene complexes were the active species and formation of a metallacyclobutane occurred (Scheme 1.1; bottom).[17] Chauvin demonstrated that the cross-metathesis (CM) of cyclopentene and an acyclic unsymmetric olefin yielded a statistical mixture of three products (Scheme 1.2). The pair-wise mechanism proposed by Caulderon will not give a statistical mixture of the kinetic products observed but will instead favor one of three.[17-19] Further studies ruled out the pair-wise mechanism and supported a metal-carbene complex as the active catalyst.[20,21] However, the only metal carbene complexes known at that time were low oxidation state Fischer carbene complexes. Although these metal carbene complexes were useful for demonstrating a model for the active catalyst, they displayed only sluggish metathesis ability if any.[22]

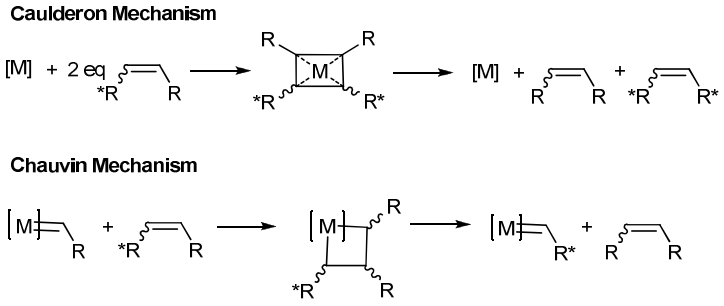

Scheme 1.1. Caulderon and Chauvin Mechanisms

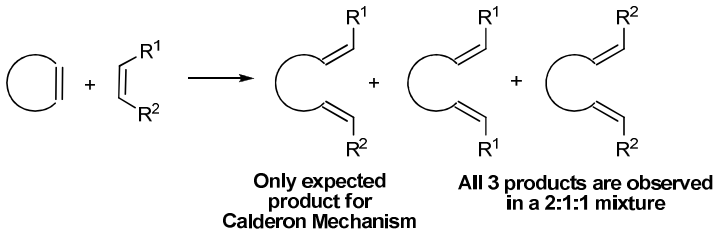

Scheme 1.2. Chauvin's CM Experiment

1.2.2. Discovery of Well-Defined Catalytic Systems

In the late 1970s, Tebbe reported degenerate metathesis between terminal olefins and a well-defined titanium/aluminum complex now known as the Tebbe complex. Isolation of Ti-based metallacycles of the Tebbe complex further verified Chauvin's mechanism for OM.[4,23] Once the mechanism was better understood, focus turned to isolating well-defined OM catalysts. Schrock and Osborn developed and characterized tungsten-based catalysts that were as active as the ill-defined systems. In addition to developing tungsten alkylidene complexes that were active for olefin metathesis, W-based metallacyclobutanes were also observed further verifying the mechanism proposed by Chauvin.[24,25] Throughout the 1980s and 1990s, OM research exploded and a number of metal carbene complexes were developed utilizing a range of transition metals (Ti, Ta, W, Mo, Re, Rh, Ru, Os, Ir) showing varying activities and tolerances for OM.

.

1.2.3. Transition Metal Catalyst Choice

Although the initial isolation of tungsten-based carbene catalysts for OM was a major advance, tungsten, as a very oxophilic metal, was extremely sensitive to a number of functional groups and reaction conditions. The sensitivity of tungsten made tungsten alkylidene complexes impractical as a synthetic tool for OM. Molybdenum-based catalysts exhibited a larger functional group tolerance allowing OM to become a viable tool for organic syntheses.[26] Unfortunately, manipulation of Mo-based catalysts still required stringent air-free and water/alcohol-free conditions. It was not until Grubbs

introduced ruthenium alkylidene catalysts for OM that this process truly became a versatile tool for organic synthesis and polymer synthesis.[27]

1.3. Ruthenium Olefin Metathesis Catalysts

1.3.1. A Brief History

The first well-defined ruthenium catalyst was synthesized in 1990 employing 3,3-diphenylcyclopropene as the alkylidene source. Compound **1.1** (Chart 1.1) catalyzed ring-opening polymerization (ROMP) with highly-strained cycloalkenes but otherwise showed limited activity. Substitution of the triphenylphosphine ligands for tricyclohexylphosphine ligands (**1.2**; Chart 1.1) significantly increased the activity of the catalyst. Catalyst **1.2** was found to catalyze CM of acyclic olefins and affect ring-closing metathesis (RCM) of acyclic dienes. Employing phenyldiazomethane as the alkylidene source in ruthenium-based alkylidene syntheses, complexes **1.3** and **1.4** were synthesized and isolated. Compound **1.4** displayed high catalytic activity comparable to Mo-based catalysts as well as a wide functional group tolerance. This catalyst, known as 1st generation Grubbs catalyst, became widely utilized as an OM catalyst and is still commonly used today. Substitution of one of the tricyclohexylphosphine ligands on **1.4** with an *N*-heterocyclic carbene ligand produced compound **1.5**, known as 2nd generation Grubbs catalyst, which proved to be more active and less prone to decomposition than catalyst **1.4**. Treatment of **1.4** or **1.5** with pyridine or 3-bromopyridine gives rise to new bispyridine Ru carbene complexes (**1.6-1.8**). Although these weakly donating neutral ligands greatly enhance the initiation rate of the metathesis catalysts, compounds **1.6-1.8** were

prone to bimolecular decomposition. Replacement of the second neutral ligand on **1.4** and **1.5** with a chelating ether group results in compounds **1.9** and **1.10** and allows for the catalyst to reside in the 14-electron active form ($Ru(CHR)LCl_2$; L = PCy_3 or H_2IMes) once initiation takes place. On the other hand, initiation of **1.9** and **1.10** was 30 times slower than other catalysts.[1] Chapter 3 covers how this slow initiation actually proves beneficial to CM with vinyl halides. Piers and co-workers developed a phosphoniomethylidene complex **1.11**, which showed decent catalytic activity. Similar to **1.10**, once initiation had taken place, the catalytic species existed as the active 14-electron species. With no second neutral ligand in the system, the inactive 16-electron form of the catalyst does not occur. Since the 14-electron active species is relatively short-lived, the presence of neutral ligands in the reaction mixture increases the longevity of the ruthenium alkylidene intermediates through reassociation to form more stable 16-electron ruthenium species.

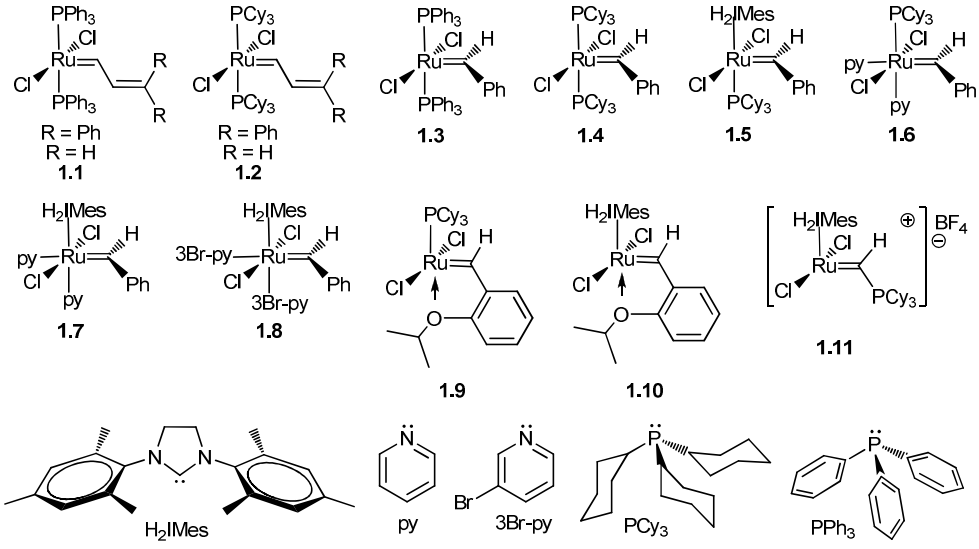

Chart 1.1. Important Ruthenium OM Catalysts

An extensive number and variety of Ru-based OM catalysts have been designed through ligand variation.[1] Chart 1.1 focuses on the Ru complexes that will be pertinent to this thesis.

1.3.2. Mechanism

Extensive mechanistic studies by Grubb's and co-workers on **1.4** and **1.5** revealed that the active catalyst was the 14-electron species. The mechanistic pathway proceeds through initial dissociation of a neutral ligand, followed by association of the olefin to the open coordination site, then a 2+2 cycloaddition between an olefin and the ruthenium alkylidene complex occurs. Cycloreversion followed by dissociation of the olefin then generates a new olefin and a new Ru-alkylidene intermediate (Scheme 1.3).[28-30] Further experimental studies by Piers and co-workers involving the direct observation of a ruthenacyclobutane revealed that the metallocycle unit formed *trans* to the coordinated neutral ligand (Scheme 1.3; L') and retained C_s symmetry.[31]

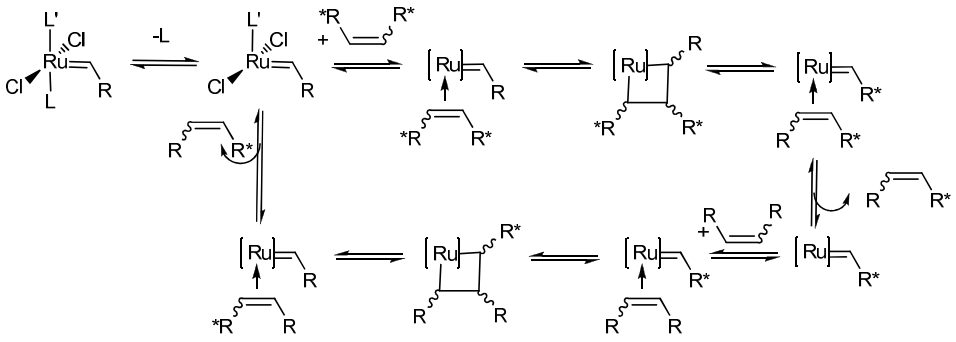

Scheme 1.3. General Mechanism for Olefin Metathesis

1.3.3. Substrate Tolerance

Substrate tolerance increased significantly upon moving from Mo-based catalysts to Ru-based catalysts. Substrate tolerance increased again when comparing **1.4** to **1.5**.[1, 2] Over the years, a number of olefins have been tested for OM activity and have been classified based on their reactivity.[32] As discussed earlier, one class of olefins was often left out in the literature. This group is composed of a subclass of α-heteroatom-substituted olefins in which the heteroatom directly bound to the olefin contains lone-pair electron density. These olefins (*e.g.* vinyl halides, ethyl vinyl ether, phenyl vinyl sulfide) not only failed to participate in metathesis reactions but deactivated the catalyst. Specifically, catalysts such as **1.4** and **1.5** fail to mediate CM of vinyl halides.

1.3.4. Tolerance of Halogenated Olefins

Failure of vinyl halides in Ru-catalyzed CM reactions did not necessarily indicate the inability of the vinyl halide to react with the ruthenium catalyst. Based on the mechanism for OM (Scheme 1.3), a number of pathways could account for the failure of vinyl halides in CM. One possibility is that vinyl halides will not interact with the Ru-catalyst at all. However, a number of examples of catalytic ring-closing metathesis (RCM) reactions involving α-chloro-α,ω-dienes[33, 34] and α-fluoro- α,ω-dienes have been reported with Ru catalysts.[35-37] These RCM results indicate that directly halogenated olefins can participate in metathesis reactions or at least that β-haloruthenacyclobutanes are competent intermediates (Scheme 1.4; top).[29] These results do not address other possible reasons that vinyl halides fail in CM reactions such as the inability to form α-

haloruthenacyclobutanes or the halocarbene intermediates. Neither does it address the potential stability of these intermediates (Scheme 1.4; bottom). Lastly, if the α-haloruthenacyclobutanes or the halocarbene intermediates form, it is also possible that these intermediates undergo a decomposition process that is competitive with CM.

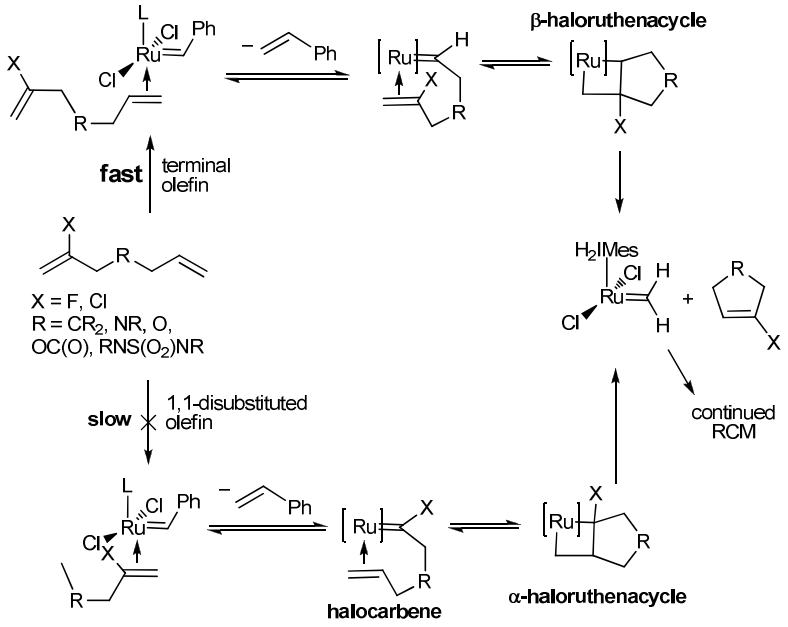

Scheme 1.4. RCM of α-halo-α,ω-dienes.

Certainly, monohalomethylidene complexes are exceptionally rare: there is a single report of four closely related complexes of the form Os(=CHF)(P-*t*-$Bu_2Me)_2$(CO)(X)(Y) (X, Y = F, O_3SCF_3; 2 isomers for X ≠ Y), which were characterized spectroscopically in fluid solution but not isolated.[38] Therefore, we turn to other α-heteroatom-substituted carbene complexes to make predictions as to the chemistry of the

monohalomethylidene complexes which would serve as intermediates in CM reactions of vinyl halides.

1.3.5. Schrock versus Fischer Carbene Complexes

For the purposes of this thesis, we will define Fischer carbene complexes as Ru-carbene complexes with α-heteroatom-substitution on which there is lone-pair electron density (Compounds in Chart 1.2). Schrock carbene complexes will be defined as those Ru-carbene complexes in which no lone-pair electron density is present on the α-moiety of the carbene complex (Compounds in Chart 1.1).

Acyloxycarbene complexes such as **1.12** and **1.13** (Chart 1.2) form isolable complexes but are unstable in solution, forming the corresponding terminal carbide complexes **1.14** and **1.15** (Chart 1.2) cleanly via expulsion of acetic acid.[39] This observation suggests a possible decomposition pathway for complexes of the form $Ru(=CHX)(L)(PCy_3)Cl_2$ (L = PCy_3, H_2IMes; X = halogen) with respect to formation of terminal carbides. This could account for the failure of vinyl halides to undergo productive CM reactions through catalyst deactivation. Carbide formation is not the only mode of Fischer carbene decomposition in the Grubbs system. For example, $Ru(=CHX)(PCy_3)_2Cl_2$ (X = OEt, SPh, and N[carbazole]; **1.19**, **1.21** and **1.22** in Chart 1.2) decompose slowly in solution as well, though the decomposition products are not known except in the case of $Ru(CHOEt)(PCy_3)_2Cl_2$, which forms $Ru(H)(CO)(PCy_3)_2Cl$ (**1.18**) via a first-order reaction with a half-life of 3 h in benzene at 80 °C.[5] Although

decomposition is common for Fischer carbene complexes, it is generally slow and should not compete with CM.

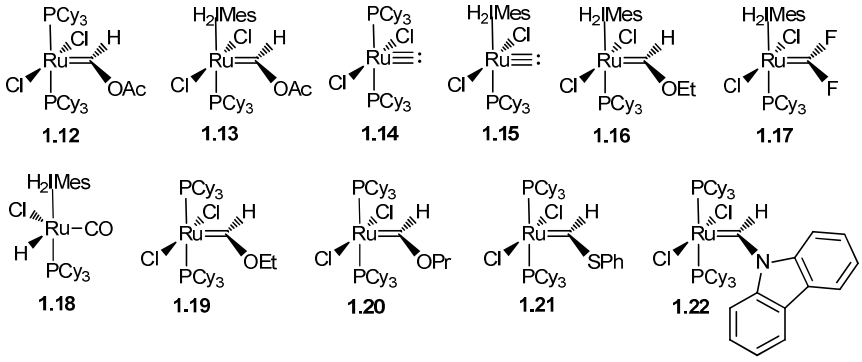

Chart 1.2. Important Fischer Carbene Complexes and Decomposition Products

Alternatively, stabilization of the monohalocarbene complex $Ru(=CHX)(L)(PCy_3)Cl_2$ with respect to PCy_3 dissociation would also interrupt catalysis. This possibility is suggested by the enhanced stability of the difluoromethylidene complex, **1.17,** and ethoxycarbene complex, **1.16**[5] (Chart 1.2) with respect to loss of PCy_3. NMR Magnetization Transfer experiments by Grubbs and co-workers indicate phosphine exchange between complex **1.5** (Chart 1.1) and 1.5 equiv. of free PCy_3 in toluene-d_8 at 80 °C has a rate constant of 0.13 ± 0.01 s^{-1} (Scheme 1.5).[29] However, phosphine transfer between complex **1.17** is not observed even at 100 °C with mixing times up to 50 seconds indicating that dissociation of PCy_3 ($k< 0.01\ s^{-1}$) is extremely slow.[40] This would hinder metathesis with **1.17**. Ethyl vinyl ether is frequently used to terminate ring-opening metathesis polymerization (ROMP) reactions because complex

1.16 is a sluggish CM catalyst.[1] Likewise, complex **1.17** displays almost no metathesis activity.[40]

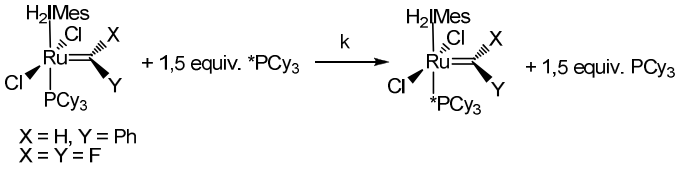

Scheme 1.5. NMR MT Experiments

In addition to slow phosphine dissociation, the carbene moiety itself (=CHX) may contribute to the thermodynamic stability of Fischer carbene complexes with respect to other Ru-alkylidene species. Grubbs and co-workers underscore the thermodynamic stability of Fischer carbene complexes.[5]

1.3.6. Experimental Work involving Fischer Carbene Complexes

In 2002, Grubbs and co-workers reported the interconversion of Fischer carbene complexes. This was the first stoichiometric evidence that Fischer carbene complexes could be active intermediates in some types of metathesis processes. The stoichiometric reaction of 1st generation Grubbs catalyst (**1.4**; Chart 1.1) with ethyl vinyl ether or phenyl vinyl sulfide gave complete conversion to the Fischer carbene complex (**1.19** and **1.21**; Chart 1.2) and styrene (Scheme 1.6; top). Addition of styrene to **1.19** and **1.21** gave no conversion back to **1.4** (Chart 1.1) even at high temperatures and extended times indicating that the equilibrium of this reaction lies far to the right and that **1.19** and **1.21**

are thermodynamically stable with respect to **1.4**. When 1 equivalent of *N*-vinylcarbazole was added to **1.4**, 1 to 16 ratio of **1.4** and **1.22** (Chart 1.2) was observed respectively. The reverse reaction equilibrated to give the same mixture at 60 °C (Scheme 1.6; bottom). Furthermore, treatment of **1.19** with one equivalent of propyl vinyl ether at 80 °C gave a 1 to 1 mixture of **1.19** and **1.20** indicating a thermoneutral reaction (Scheme 1.7; A). In this case, if phosphine liberation were problematic, conversion between the two carbene complexes would not be observed. Therefore, another factor must be contributing to the stability of the ethoxycarbene complex. Treatment of **1.19** with one equivalent of phenyl vinyl sulfide gave a 1 to 1.2 mixture of starting materials and **1.21** (Scheme 1.7; B). However, addition of *N*-vinylcarbazole to either **1.19** or **1.21** had no reaction. The reverse reactions gave complete conversion indicating that compounds **1.19** and **1.21** are thermodynamically stable with respect to **1.22** and **1.4** (Scheme 1.7; C).[5]

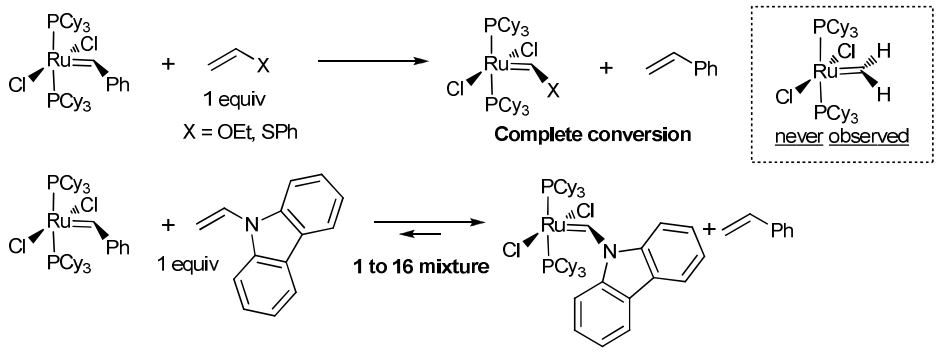

Scheme 1.6. Treatment of **1.4** with Electron-Rich Olefins[5]

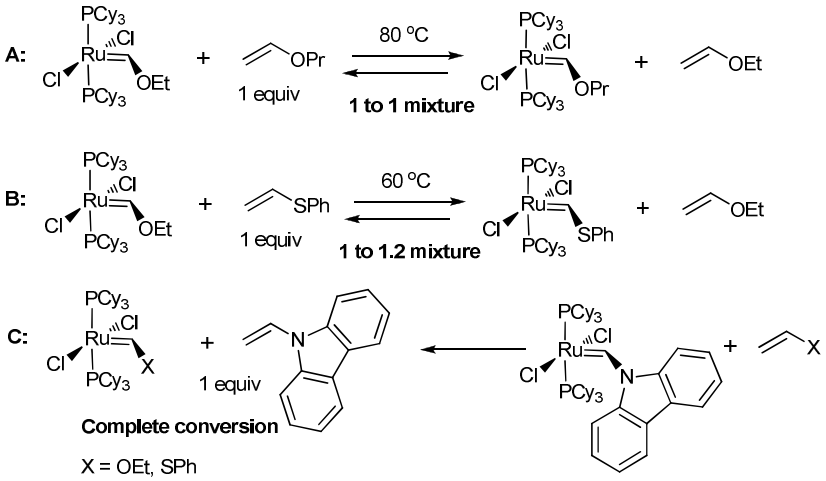

Scheme 1.7. Metathesis Activity of Fischer Carbene Complexes with Electron-rich Olefins[5]

1.3.7. DFT Evidence for Fischer Carbene Stability

In 2007, Fomine reported DFT calculations of the Gibbs free-energy profile of cross-metathesis with 1,2-difluoroethene and 1,2-dichloroethene. The profile for metathesis with 1,2-difluoroethene indicated that the 14-electron ruthenium monofluoromethylidene intermediate is more thermodynamically stable than the 14-electron ruthenium alkylidene complex ($\Delta G = -16.8$ kcal/mol; Scheme 1.8; H_2IPh = 4,5-dihydro-1,3-diphenylimidazol-2-ylidene).[41] Upon moving to 1,2-dichloroethene, the energy difference between the monochloromethylidene complex and the 14-electron alkylidene complexes decreases significantly ($\Delta G = -2.1$ kcal/mol; Scheme 1.9).[41]

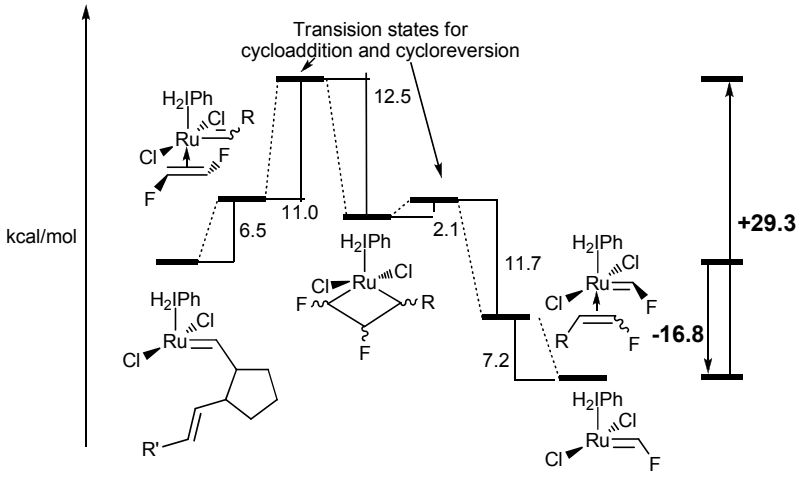

Scheme 1.8. Gibbs Free Energy Profile of CM with 1,2-Difluoroethene.[41]

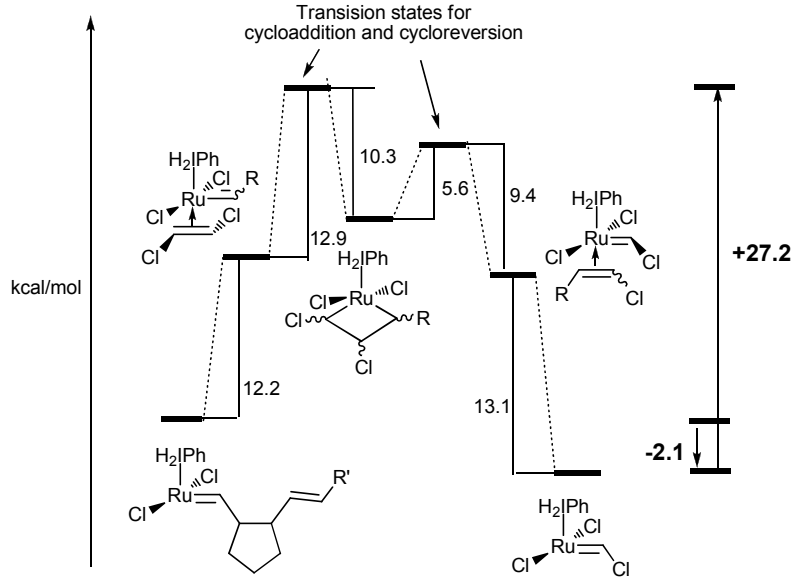

Scheme 1.9. Gibbs Free Energy Profile of CM with 1,2-Dichloroethene.[41]

A second important feature in Scheme 1.8 and 1.9 is the energy barriers around the ruthenacyclobutane intermediate. For 1,2-difluoroethylene, the energy barriers of the two transition states on either side of the ruthenacyclobutane show a 10.4 kcal/mol

difference. The ruthenacycle would be prone to cyclorevert to form the olefin-coordinated monofluoromethyidene complex (Scheme 1.8; right from center) preferentially over the difloro-olefin-coordinated alkylidene complex (Scheme 1.8; left from center). Although Scheme 1.9 has a similar trend, the energy difference between the two transition states is not as dramatic; only 4.7 kcal/mol.

All these data indicate that the carbene ligand itself strongly contributes to the thermodynamic stability of the Ru carbene complex. Once a Fischer carbene complex is formed, it is unlikely to undergo metathesis and reform a Schrock carbene complex without a secondary thermodynamic driving force in the system.

1.4. Enyne Metathesis

Diver demonstrated that although alkyl enol ethers such as ethyl vinyl ether do not undergo intermolecular CM because of the thermodynamic stability of Fischer carbene complexes such as **1.16** (Chart 1.2), alkyl enol ethers will undergo enyne metathesis (EyM) to afford functionalized 1-alkoxy-1,3-butadienes in high yields (Scheme 1.10).[42]

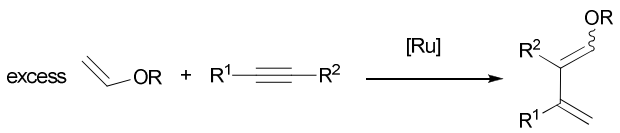

Scheme 1.10. General Scheme for EyM

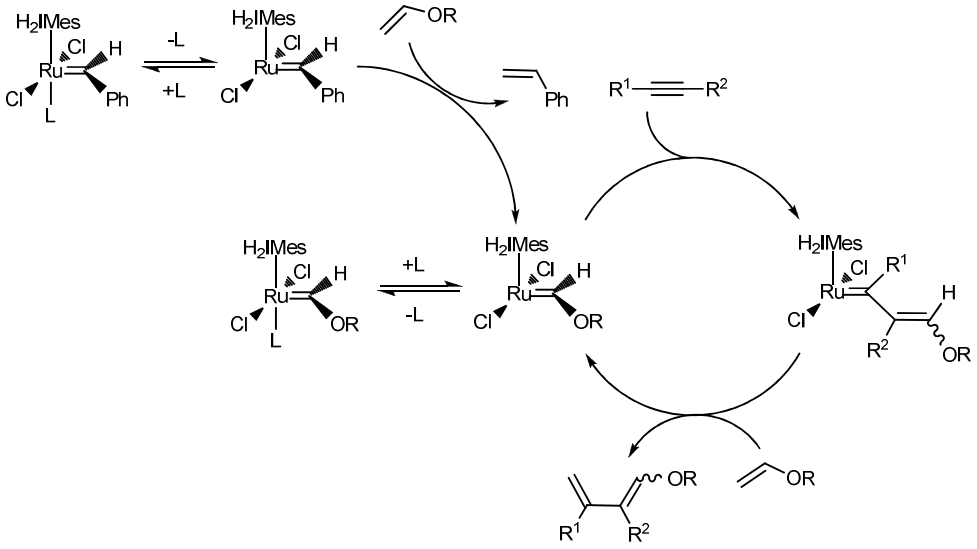

Scheme 1.11. Mechanism for EyM

Diver attributed the ability to overcome the thermodynamic stability of Ru(CHOEt)(H_2IMes)Cl_2 to two factors. First, the enthalpic stability of the newly formed conjugated diene establishes a thermodynamic driving force for EyM. Second, the 14-electron vinylcarbene intermediates, Ru(=CRCR'=CHR")(H_2IMes)Cl_2, are more thermodynamically stable than simple alkylidene complexes; this results in a decreased kinetic barrier for return to a Schrock carbene intermediate from the Fischer carbene intermediate in EyM compared to CM reactions (Scheme 1.11).[42-44] Although vinyl halides do not undergo CM, we speculate that they might undergo EyM in the same way as ethyl vinyl ether. Specifically, fluorinated butadienes would be of interest because although 1-fluoro-1,3-butadiene is well known,[45, 46] substituted derivatives of 1-fluoro-1,3-butadienes are extremely rare. In fact, there is only one other account of the synthesis of 1-fluoro-(2,)3-substituted-1,3-butadienes.[47] In addition to the rarity of these

compounds, fluorinated organic compounds have distinct reactivity and stability profiles that make them frequent targets as pharmaceuticals, agrochemicals, and monomers for a number of materials. Research towards strategies for installation of fluorine units into organic molecules under relatively mild reaction conditions has received a great deal of attention, as some current fluorination techniques are incompatible with certain functional groups.[48-54] Complications arising from this could be circumvented by installation of the fluorine unit through EyM.

1.5. Alkyne Metathesis

1.5.1. Current Catalysts

Alkyne metathesis (AM) has been restricted mostly to tungsten and molybedenum alkylidyne catalysts, although some rhenium alkylidyne complexes will participate in alkyne metathesis (Fig.1.1). [55-58]

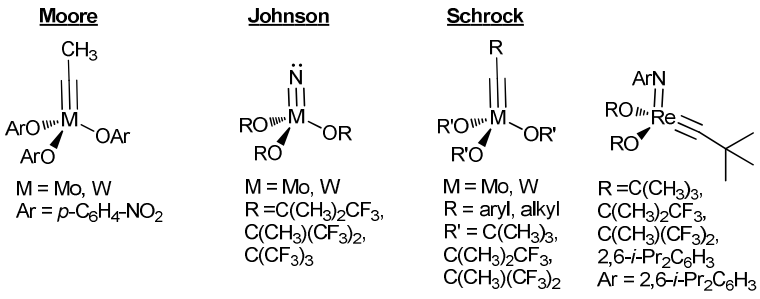

Figure 1.1. Alkyne Metathesis Catalysts

1.5.2. Mechanism

The mechanism for AM is similar to that of OM. An alkyne binds to an open coordination site parallel to the metal alkylidyne moiety (Scheme 1.12).[59-61] Cyclometalation occurs to form a metalocyclobutadiene intermediate. Cycloreversion steps followed by alkyne dissociation produce a new alkyne and metal alkylidyne complex.

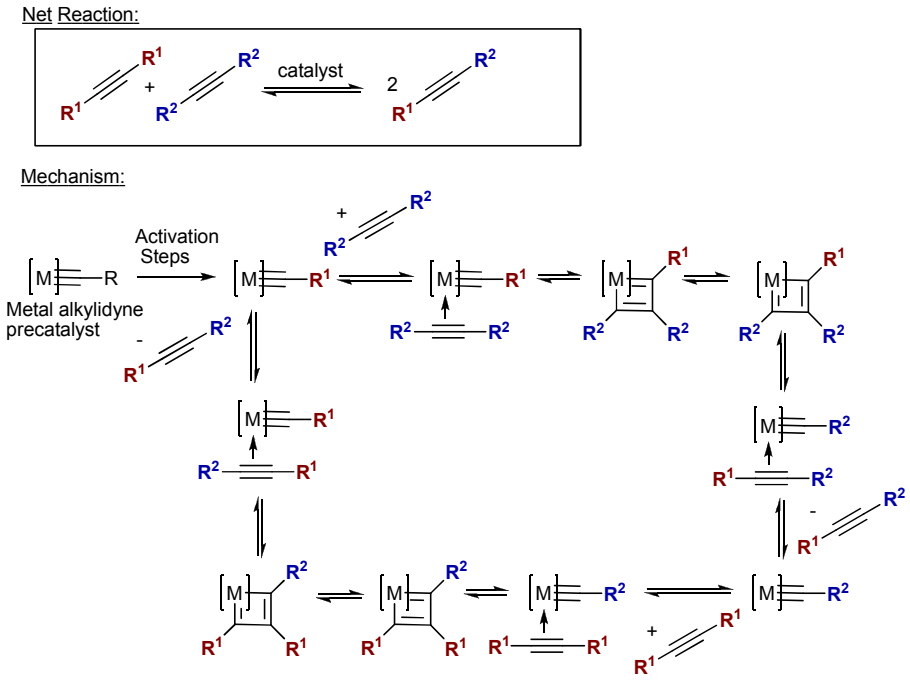

Scheme 1.12. The Mechanism for Alkyne Cross-Metathesis

1.5.3. Ruthenium Alkylidyne Complexes

AM with a ruthenium alkylidyne catalyst is desirable because ruthenium is less oxophilic than tungsten and molybdenum. This would expand functional group tolerance

and solvent choices for AM as well as allow for easier handling techniques because the requirements for a water-free/air-free atmosphere would be less rigorous. Although a number of Ru alkylidyne compounds have been reported, there have been no reports of AM with ruthenium catalysts. Ru carbyne complexes synthesized through protonation of a Ru-allenylidene or –vinylidene complex with a strong acid are shown in Fig. 1.2.[62-73] Addition of a weak base to these compounds causes reversion back to the former vinylidene- or allenylidene species. Therefore, these Ru-alkylidyne complexes are impractical for AM. In general, cationic Ru-alkylidyne species would lack tolerance for most alkyl groups because a cationic Ru alkylidyne compound is prone to deprotonation of the β-proton to form an inactive Ru-vinylidene complex ($[Ru]=C=CR_2$). Roper was able to isolate Ru alkylidyne species bearing strong σ-donating CO ligands.[74-82] Caulton and Fogg synthesized four-coordinate Ru-benzylidyne complexes through treatment of first-generation Grubbs catalyst with 2 equiv. of an aryloxide salt (Fig. 1.3).[83-85] However, AM with these compounds was not reported.

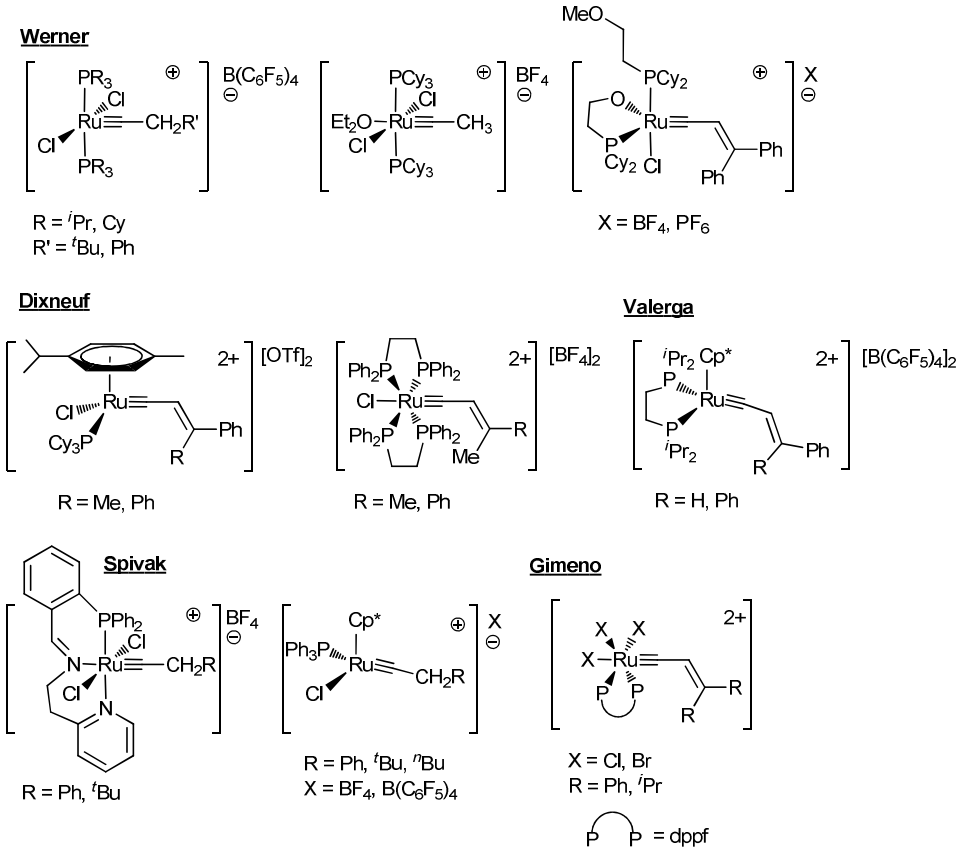

Figure 1.2. Previously Known Acidic Ruthenium Alkylidyne Compounds

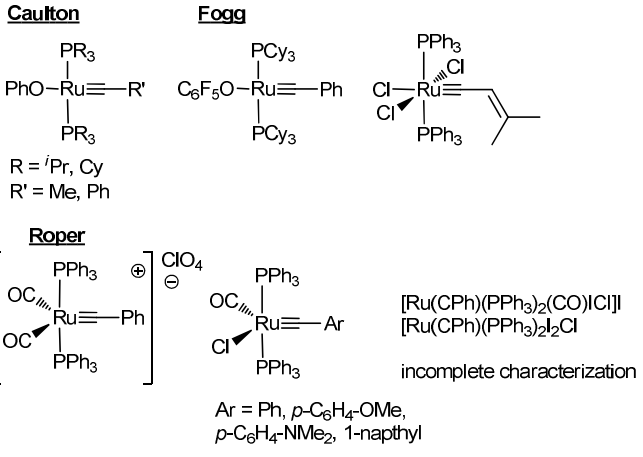

Figure 1.3. Previously Known Ruthenium Alkylidyne Compounds

Steve Caskey in the Johnson group synthesized a number of four-, five-, and six-coordinate Ru-benzylidyne complexes from the common intermediate, **1.23** (Chart 1.3), and also demonstrated a second method to access **1.24-Cl** through treatment of first-generation Grubbs catalyst with an alkyl germylene (Chart 1.3).[86,87] Desired alkyne metathesis activity of these first-generation Ru benzylidyne species was limited. Only cyclooctyne polymerization could be effected with **1.26-I** when activated with thallium(I) trifluoromethanesulfonate. Beyond this, no alkyne metathesis activity was observed although other types of reactivity with alkynes was noted such as alkyne ligation with the square-planar complexes, **1.24**, and alkyne homodimerization with **1.25-F/F**.[86]

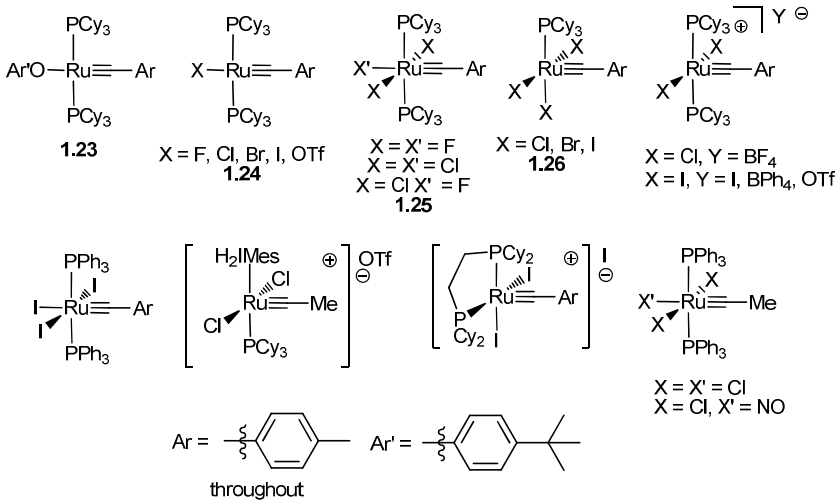

Chart 1.3. Previously Synthesized Ru-Benzylidyne Complexes in the Johnson Group

1.6. Conclusions

Research into olefin metathesis (OM) with vinyl halides has been lacking due to the initial difficulties these substrates caused in OM systems. This thesis will cover the reasons vinyl halides as well as other electron-rich olefins fail to undergo certain metathesis reactions. In addition, the development of successful metathesis systems with vinyl halides and other directly substituted olefins will be discussed including cross-metathesis (CM), ring-opening cross-metathesis (RO-CM), enyne metathesis (EyM) and a new subfield of OM called Fischer carbene cross-metathesis (FCM). Finally, we will focus on methods to exploit the decomposition mechanism of the monohalomethylidene complexes to synthesize Ru-benzylidyne complexes in high yields. The synthesis and reactivity of these Ru-benzylidyne complexes and the direct implications to Ru-catalyzed alkyne metathesis will be addressed.

1.7. References

1. Grubbs, R. H., *Handbook of Metathesis*. Wiley-VCH: Weinheim, 2003; Vol. 1-3.
2. Trnka, T. M.; Grubbs, R. H., The development of L2X2Ru = CHR olefin metathesis catalysts: An organometallic success story. *Accounts Chem. Res.* 2001, *34* (1), 18-29.
3. Connon, S. J.; Blechert, S., Recent developments in olefin cross-metathesis. *Angew. Chem.-Int. Edit.* 2003, *42* (17), 1900-1923.
4. Grubbs, R. H., Olefin metathesis. *Tetrahedron* 2004, *60* (34), 7117-7140.
5. Louie, J.; Grubbs, R. H., Metathesis of Electron-Rich Olefins: Structure and Reactivity of Electron-Rich Carbene Complexes. *Organometallics* 2002, *21*, 2153.
6. Tsuji, J., Reactions of Organic Halides and Pseudohalides. In *Transition Metal Reagents and Catalysts: Innovations in Organic Synthesis*, Wiley: New York, 2000; pp 27-108.
7. Morrill, C.; Grubbs, R. H., Synthesis of functionalized vinyl boronates via ruthenium-catalyzed olefin cross-metathesis and subsequent conversion to vinyl halides. *J. Org. Chem.* 2003, *68* (15), 6031-6034.
8. Macnaughtan, M. L.; Gary, J. B.; Gerlach, D. L.; Johnson, M. J. A.; Kampf, J. W., Cross-Metathesis of Vinyl Halides. Scope and Limitations of Ruthenium-based Catalysts. *Organometallics* 2009, *ASAP*.
9. Macnaughtan, M. L.; Johnson, M. J. A.; Kampf, J. W., Synthesis, Structure, and Olefin Metathesis Activity of Two Ruthenium Monofluoromethylidene Complexes. *Organometallics* 2007, *26* (4), 780-782.
10. Macnaughtan, M. L.; Johnson, M. J. A.; Kampf, J. W., Olefin Metathesis Reactions with Vinyl Halides: Formation, Observation, Interception, and Fate of the Ruthenium-Monohalomethylidene Moiety. *J. Am. Chem. Soc.* 2007, *129* (25), 7708-7709.
11. Ziegler, K.; Holzkamp, E.; Breil, H.; Martin, H., The Mulheim Normal Pressure Polyethylene Process. *Angew. Chem.-Int. Edit.* 1955, *67* (19-2), 541-547.
12. Truett, W. L.; Johnson, D. R.; Robinson, I. M.; Montague, B. A., Polynorbornene Coordiation Polymerization. *J. Am. Chem. Soc.* 1960, *82* (9), 2337-2340.
13. Calderon, N.; Chen, H. Y.; Scott, K. W., Olefin Metathesis- A Noval Reaction for Skeletal Transformations of Unsaturated Hydrocarbons. *Tetrahedron Lett.* 1967, (34), 3327.
14. Calderon, N.; Ofstead, E. A.; Ward, J. P.; Judy, W. A.; Scott, K. W., Olefin Metathesis .I. Acyclic Vinylenic Hydrocarbons. *J. Am. Chem. Soc.* 1968, *90* (15), 4133.
15. Calderon, N., Olefin Metathesis Reaction. *Accounts Chem. Res.* 1972, *5* (4), 127.
16. Calderon, N.; Ofstead, E. A.; Judy, W. A., Mechanistic Aspects of Olefin Metathesis. *Angew. Chem.-Int. Edit. Engl.* 1976, *15* (7), 401-409.
17. Herisson, J. L.; Chauvin, Y., Transformation Catalysts of Olefins by Tungsten Complexes .2. Telomerization of Cyclic Olefins in the Presence of Acyclic Olefins. *Makromolekulare Chemie* 1971, *141* (FEB9), 16.

18. Chauvin, Y., Olefin metathesis: The early days (Nobel lecture). *Angew. Chem.-Int. Edit.* 2006, *45* (23), 3740-3747.
19. Chauvin, Y., Olefin metathesis: The early days (Nobel Lecture 2005). *Adv. Synth. Catal.* 2007, *349* (1-2), 27-33.
20. Grubbs, R. H.; Burk, P. L.; Carr, D. D., Consideration of Mechanism of Olefin Metathesis Reaction. *J. Am. Chem. Soc.* 1975, *97* (11), 3265-3267.
21. Katz, T. J.; Rothchild, R., Mechanism of Olefin Metathesis of 2,2'-Divinylbiphenyl. *J. Am. Chem. Soc.* 1976, *98* (9), 2519-2526.
22. Katz, T. J.; Acton, N., Metathesis Induced by (Phenylmethoxycarbene) Pentacarbonyltungsten. *Tetrahedron Lett.* 1976, (47), 4251-4254.
23. Tebbe, F. N.; Parshall, G. W.; Reddy, G. S., Olefin Homologation with Titanium Methylene-compounds. *J. Am. Chem. Soc.* 1978, *100* (11), 3611-3613.
24. Kress, J. R. M.; Russell, M. J. M.; Wesolek, M. G.; Osborn, J. A., Tungsten(VI) and Molybdenum(VI) Oxo-alkyl Species - Their Role in the Metathesis of Olefins. *J. Chem. Soc.-Chem. Commun.* 1980, (10), 431-432.
25. Kress, J.; Osborn, J. A.; Greene, R. M. E.; Ivin, K. J.; Rooney, J. J., 1st Direct Observation of the Simultaneous Presence and of the Interconversion of Chain-propagating Metal-carbene and Metallacyclobutane Complexes in a Catalytic Olefin Metathesis Reaction - the Ring-opening Polymerization of Norbornene. *J. Am. Chem. Soc.* 1987, *109* (3), 899-901.
26. Fu, G. C.; Grubbs, R. H., The Application of Catalytic Ring-closing Olefin Metathesis to the Synthesis of Unsaturated Oxygen Heterocycles. *J. Am. Chem. Soc.* 1992, *114* (13), 5426-5427.
27. Fu, G. C.; Nguyen, S. T.; Grubbs, R. H., Catalytic Ring-closing Metathesis of Functionalized Dienes by a Ruthenium Carbene Complex. *J. Am. Chem. Soc.* 1993, *115* (21), 9856-9857.
28. Sanford, M. S. Synthetic and Mechanistic Investigations of Ruthenium Olefin Metathesis Catalysts. Ph. D., California Institute of Technology, Pasadena, CA, 2001.
29. Sanford, M. S.; Love, J. A.; Grubbs, R. H., Mechanism and activity of ruthenium olefin metathesis catalysts. *J. Am. Chem. Soc.* 2001, *123* (27), 6543-6554.
30. Sanford, M. S.; Ulman, M.; Grubbs, R. H., New insights into the mechanism of ruthenium-catalyzed olefin metathesis reactions. *J. Am. Chem. Soc.* 2001, *123* (4), 749-750.
31. Romero, P. E.; Piers, W. E., Direct Observation of a 14-Electron Ruthenacyclobutane Relevant to Olefin Metathesis. *J. Am. Chem. Soc.* 2005, *127*, 5032-5033.
32. Chatterjee, A. K.; Choi, T. L.; Sanders, D. P.; Grubbs, R. H., A general model for selectivity in olefin cross metathesis. *J. Am. Chem. Soc.* 2003, *125* (37), 11360-11370.
33. Chao, W. C.; Meketa, M. L.; Weinreb, S. M., Ring-closing metathesis of vinyl chlorides for formation of 5-, 6- and 7-membered carbocyclic and heterocyclic systems. *Synthesis-Stuttgart* 2004, (12), 2058-2061.
34. Chao, W. C.; Weinreb, S. M., The first examples of ring-closing olefin metathesis of vinyl chlorides. *Org. Lett.* 2003, *5* (14), 2505-2507.

35. Marhold, M.; Buer, A.; Hiemstra, H.; van Maarseveen, J. H.; Haufe, G., Synthesis of vinyl fluorides by ring-closing metathesis. *Tetrahedron Lett.* 2004, *45* (1), 57-60.
36. De Matteis, V.; van Delft, F. L.; de Gelder, R.; Tiebes, J.; Rutjes, F., Fluorinated (hetero)cycles via ring-closing metathesis of fluoride- and trifluoromethyl-functionalized olefins. *Tetrahedron Lett.* 2004, *45* (5), 959-963.
37. Salim, S. S.; Bellingham, R. K.; Satcharoen, V.; Brown, R. C. D., Synthesis of heterocyclic and carbocyclic fluoro-olefins by ring-closing metathesis. *Org. Lett.* 2003, *5* (19), 3403-3406.
38. Huang, D. J.; Koren, P. R.; Folting, K.; Davidson, E. R.; Caulton, K. G., Facile and reversible cleavage of C-F bonds. Contrasting thermodynamic selectivity for Ru-CF2H vs F--Os=CFH. *J. Am. Chem. Soc.* 2000, *122* (37), 8916-8931.
39. Caskey, S. R.; Stewart, M. H.; Kivela, J. E.; Sootsman, J. R.; Johnson, M. J. A.; Kampf, J. W., Two Generalizable Routes to Terminal Carbido Complexes. *J. Am. Chem. Soc.* 2005, *127*, 16750-16751.
40. Trnka, T. M.; Day, M. W.; Grubbs, R. H., Olefin metathesis with 1,1-difluoroethylene. *Angew. Chem.-Int. Edit.* 2001, *40* (18), 3441-+.
41. Fomine, S.; Ortega, J. V.; Tlenkopatchev, M. A., Metathesis of halogenated olefins - A computational study of ruthenium alkylidene mediated reaction pathways. *Journal Of Molecular Catalysis A-Chemical* 2007, *263* (1-2), 121-127.
42. Giessert, A. J.; Snyder, L.; Markham, J.; Diver, S. T., Intermolecular enol ether-alkyne metathesis. *Org. Lett.* 2003, *5* (10), 1793-1796.
43. Diver, S. T.; Giessert, A. J., Enyne metathesis (Enyne Bond Reorganization). *Chemical Reviews* 2004, *104* (3), 1317-1382.
44. Schwab, P.; Grubbs, R. H.; Ziller, J. W., Synthesis and applications of RuCl2(=CHR')(PR(3))(2): The influence of the alkylidene moiety on metathesis activity. *J. Am. Chem. Soc.* 1996, *118* (1), 100-110.
45. Cederbalk, P., Preparation, Microwave Transitions and Dipole-Moment of Trans-1-Fluoro-1,3-Butadiene. *Acta Chemica Scandinavica Series a-Physical and Inorganic Chemistry* 1980, *34* (6), 409-413.
46. Cederbalk, P., Microwave-Spectrum and Dipole-Moment of Cis-1-Fluoro-1,3-Butadiene. *Acta Chemica Scandinavica Series a-Physical and Inorganic Chemistry* 1984, *38* (1), 15-21.
47. Lan, Y. F.; Hammond, G. B., Functionalization of monofluoroallene and the synthesis of aryl-substituted conjugated fluorodienes. *Org. Lett.* 2002, *4* (14), 2437-2439.
48. Wipf, P.; Henninger, T. C.; Geib, S. J., Methyl- and (trifluoromethyl)alkene peptide isosteres: Synthesis and evaluation of their potential as beta-turn promoters and peptide mimetics. *J. Org. Chem.* 1998, *63* (18), 6088-6089.
49. Isanbor, C.; O'Hagan, D., Fluorine in medicinal chemistry: A review of anti-cancer agents. *Journal of Fluorine Chemistry* 2006, *127* (3), 303-319.
50. Aneja, R.; Vangapandu, S. N.; Joshi, H. C., Synthesis and biological evaluation of a cyclic ether fluorinated noscapine analog. *Bioorganic & Medicinal Chemistry* 2006, *14* (24), 8352-8358.
51. Wang, M.; Gao, M. Z.; Mock, B. H.; Miller, K. D.; Sledge, G. W.; Hutchins, G. D.; Zheng, Q. H., Synthesis of carbon-11 labeled fluorinated 2-arylbenzothiazoles as

novel potential PET cancer imaging agents. *Bioorganic & Medicinal Chemistry* 2006, *14* (24), 8599-8607.
52. Sket, B.; Zupan, M., Fluorination With Xenon Difluoride .16. Fluorination Of Some Benzocyclenes. *J. Org. Chem.* 1978, *43* (5), 835-837.
53. Thayer, A. M. Constructing Life Sciences Compounds: Fluorinated building blocks are increasingly used as the basis of valuable active molecules. http://pubs.acs.org/cen/coverstory/84/8423cover2.html (accessed May 10).
54. Thayer, A. M. Fabulous Fluorine: Having fluorine in life sciences molecules brings desirable benefits, but the trick is getting it in place and making sought-after building blocks. http://pubs.acs.org/cen/coverstory/84/8423cover1.html (accessed May 10).
55. Schrock, R. R., High oxidation state multiple metal-carbon bonds. *Chemical Reviews* 2002, *102* (1), 145-179.
56. Furstner, A.; Davies, P. W., Alkyne metathesis. *Chem. Commun.* 2005, (18), 2307-2320.
57. Zhang, W.; Kraft, S.; Moore, J. S., Highly active trialkoxymolybdenum(VI) alkylidyne catalysts synthesized by a reductive recycle strategy. *J. Am. Chem. Soc.* 2004, *126* (1), 329-335.
58. Gdula, R. L.; Johnson, M. J. A., Highly Active Molybdenum-Alkylidyne Catalysts for Alkyne Metathesis: Synthesis from the Nitrides by Metathesis with Alkynes. *J. Am. Chem. Soc.* 2006, *128*, 9614-9615.
59. Schrock, R. R., High-Oxidation-State Molybdenum and Tungsten Alkylidyne Complexes. *Accounts Chem. Res.* 1986, *19* (11), 342-348.
60. Woo, T.; Folga, E.; Ziegler, T., Density Functional-Study of Acetylene Metathesis Catalyzed by High Oxidation-State Molybdenum and Tungsten Carbyne Complexes. *Organometallics* 1993, *12* (4), 1289-1298.
61. Zhu, J.; Jia, G.; Lin, Z., Theoretical Investigation of Alkyne Metathesis Catalyzed by W/Mo Alkylidyne Complexes. *Organometallics* 2006, *25*, 1812-1819.
62. Gonzalez-Herrero, P.; Weberndorfer, B.; Ilg, K.; Wolf, J.; Werner, H., The sensitive balance between five-coordinate carbene and six-coordinate carbyne ruthenium complexes formed from ruthenium vinylidene precursors. *Organometallics* 2001, *20* (17), 3672-3685.
63. Jung, S.; Brandt, C. D.; Werner, H., A cationic allenylideneruthenium(II) complex with two bulky hemilabile phosphine ligands. *New Journal of Chemistry* 2001, *25* (9), 1101-1103.
64. Gonzalez-Herrero, P.; Weberndorfer, B.; Ilg, K.; Wolf, J.; Werner, H., The first example of an equilibrium between a carbene and an isomeric carbyne transition metal complex. *Angew. Chem.-Int. Edit.* 2000, *39* (18), 3266-+.
65. Stüer, W.; Wolf, J.; Werner, H.; Schwab, P.; Schulz, M., Carbynehydridoruthenium complexes as catalysts for the selective, ring-opening metathesis of cyclopentene with methyl acrylate. *Angew. Chem.-Int. Edit.* 1998, *37* (24), 3421-3423.

66. Castarlenas, R.; Eckert, M.; Dixneuf, P. H., Alkenylcarbene ruthenium arene complexes as initiators of alkene metathesis: An enyne creates a catalyst that promotes its selective transformation. *Angew. Chem.-Int. Edit.* 2005, *44* (17), 2576-2579.
67. Castarlenas, R.; Vovard, C.; Fischmeister, C.; Dixneuf, P. H., Allenylidene-to-indenylidene rearrangement in arene-ruthenium complexes: A key step to highly active catalysts for olefin metathesis reactions. *J. Am. Chem. Soc.* 2006, *128* (12), 4079-4089.
68. Rigaut, S.; Touchard, D.; Dixneuf, P. H., Amphoteric allenylidene ruthenium complexes and the first dinuclear ruthenium species with a bis-alkenyl carbyne bridging ligand. *Organometallics* 2003, *22* (20), 3980-3984.
69. Bustelo, E.; Jiménez-Tenorio, M.; Mereiter, K.; Puerta, M. C.; Valerga, P., Reactivity of the electron-rich allenylidene-ruthenium complexes [Cp*Ru{=C=C=C(R)Ph}(dippe)][BPh4] (R = H, Ph). X-ray crystal structure of a novel dicationic ruthenium carbyne (CP* = C5Me5; dippe=1,2-bis(diisopropylphosphine)ethane). *Organometallics* 2002, *21* (9), 1903-1911.
70. Beach, N. J.; Jenkins, H. A.; Spivak, G. J., Electrophilic attack on [Cp*Cl(PPh3)Ru(CCHR)]: Carbyne formation vs chloride abstraction. *Organometallics* 2003, *22* (25), 5179-5181.
71. Beach, N. J.; Walker, J. M.; Jenkins, H. A.; Spivak, G. J., Ruthenium vinylidene and carbyne complexes containing a multifunctional tridentate ligand with a PNN donor set. *Journal of Organometallic Chemistry* 2006, *691* (19), 4147-4152.
72. Beach, N. J.; Williamson, A. E.; Spivak, G. J., A comparison of Cp*- and Tp-ruthenium carbyne complexes prepared via site selective electrophilic addition to neutral ruthenium vinylidenes. *Journal of Organometallic Chemistry* 2005, *690* (21-22), 4640-4647.
73. Cadierno, V.; Díez, J.; García-Garrido, S. E.; Gimeno, J., Efficient one-pot synthesis of alpha,beta-unsaturated carbyne complexes fac-[RuX3{ CC(H)= CR2}(dppf)] (X = Cl, Br; R = aryl, alkyl; dppf=1,1 '-bis(diphenylphosphino)ferrocene). *Organometallics* 2005, *24* (13), 3111-3117.
74. Roper, W. R., Carbyne Complexes of Ruthenium and Osmium. In *Transition Metal Carbyne Complexes*, Kreibl, F. R., Ed. Kluwer: Boston, 1993; Vol. 392, pp 155-168.
75. Roper, W. R.; Wright, A. H., Reactions of a Dichlorocarbene-Ruthenium Complex, Rucl2(Ccl2)(Co)(Pph3)2. *Journal of Organometallic Chemistry* 1982, *233* (3), C59-C63.
76. Gallop, M. A.; Roper, W. R., Carbene and Carbyne Complexes of Ruthenium, Osmium, and Iridium. *Advances in Organometallic Chemistry* 1986, *25*, 121-198.
77. Baker, L. J.; Clark, G. R.; Rickard, C. E. F.; Roper, W. R.; Woodgate, S. D.; Wright, L. J., Syntheses and reactions of the carbyne complexes, M(CR)Cl(CO)(PPh3)(2) (M = Ru, Os; R = 1-naphthyl, 2-naphthyl). The crystal structures of [Os(C-1-naphthyl)(CO)(2)(PPh3)(2)]ClO4, Os(=CH-2-naphthyl)Cl-2(CO)(PPh3)(2), and Os(2-naphthyl)Cl(CO)(2)(PPh3)(2). *Journal of Organometallic Chemistry* 1998, *551* (1-2), 247-259.
78. Roper, W. R., Platinum Group-Metals in the Formation of Metal-Carbon Multiple Bonds. *Journal of Organometallic Chemistry* 1986, *300* (1-2), 167-190.

79. Wright, A. H. Ph.D. Thesis. Ph.D. Thesis, University of Auckland, Auckland, New Zealand, 1983.
80. Clark, G. R.; Cochrane, C. M.; Marsden, K.; Roper, W. R.; Wright, L. J., Synthesis and Some Reactions of a Terminal Carbyne Complex of Osmium - Crystal-Structures of Os(=Cr)Cl(Co)(Pph3)2 and Os(=C[Agcl]R)Cl(Co)(Pph3)2. *Journal of Organometallic Chemistry* 1986, *315* (2), 211-230.
81. Clark, G. R.; Edmonds, N. R.; Pauptit, R. A.; Roper, W. R.; Waters, J. M.; Wright, A. H., Octahedral Carbyneosmium(Ii) Complexes. *Journal of Organometallic Chemistry* 1983, *244* (4), C57-C60.
82. Clark, G. R.; Marsden, K.; Roper, W. R.; Wright, L. J., An Osmium-Carbene Complex. *J. Am. Chem. Soc.* 1980, *102* (21), 6570-6571.
83. Coalter, J. N.; Bollinger, J. C.; Eisenstein, O.; Caulton, K. G., R-Group reversal of isomer stability for RuH(X)L-2(CCHR) vs. Ru(X)L-2(CCH2R): access to four-coordinate ruthenium carbenes and carbynes. *New Journal of Chemistry* 2000, *24* (12), 925-927.
84. Amoroso, D.; Snelgrove, J. L.; Conrad, J. C.; Drouin, S. D.; Yap, G. P. A.; Fogg, D. E., An attractive route to olefin metathesis catalysts: Facile synthesis of a ruthenium alkylidene complex containing labile phosphane donors. *Adv. Synth. Catal.* 2002, *344* (6-7), 757-763.
85. Conrad, J. C.; Amoroso, D.; Czechura, P.; Yap, G. P. A.; Fogg, D. E., The first highly active, halide-free ruthenium catalyst for olefin metathesis. *Organometallics* 2003, *22* (18), 3634-3636.
86. Caskey, S. R. Exploration of Ruthenium Carbon Multiple Bond Complexes: Carbenes, Carbynes, and Carbides. Ph.D., University of Michigan, Ann Arbor, 2007.
87. Caskey, S. R.; Stewart, M. H.; Ahn, Y. J.; Johnson, M. J. A.; Rowsell, J. L. C.; Kampf, J. W., Synthesis, Structure, and Reactivity of Four-, Five-, and Six-Coordinate Ruthenium Carbyne Complexes. *Organometallics* 2007, *26*, 1912-1923.
88. Trnka, T. M.; Morgan, J. P.; Sanford, M. S.; Wilhelm, T. E.; Scholl, M.; Choi, T. L.; Ding, S.; Day, M. W.; Grubbs, R. H., Synthesis and activity of ruthenium alkylidene complexes coordinated with phosphine and N-heterocyclic carbene ligands. *J. Am. Chem. Soc.* 2003, *125* (9), 2546-2558.

Chapter 2

Synthesis, Isolation and Properties of Ruthenium Monohalomethylidene Complexes

2.1. Introduction

Over the past two decades, great progress has been made in the development of Ru-based olefin metathesis catalysts that tolerate a wide variety of important functional groups yet display excellent olefin metathesis activity.[1,2] These developments have had an enormous impact on organic and polymer synthesis.[1] However, a few key functional groups are still incompatible with Ru-based catalysts in cross-metathesis (CM) reactions.

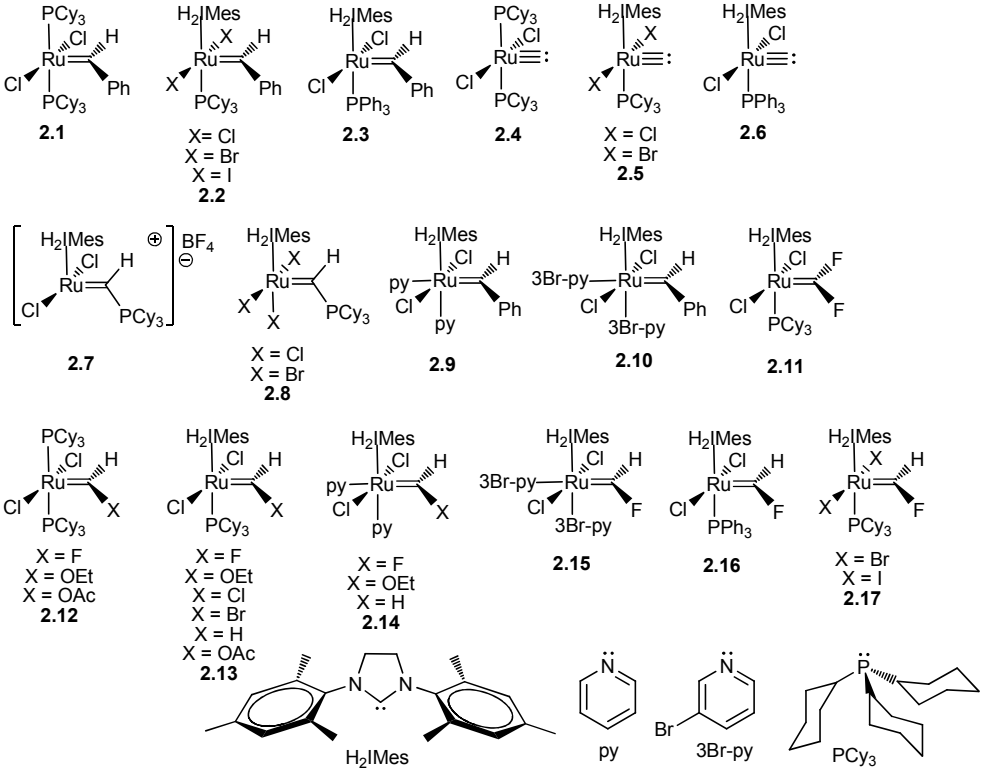

Chart 2.1. Important Carbene and Carbide Complexes

In particular, catalysts such as **2.1** and **2.2-Cl** (Chart 2.1) fail to mediate CM of vinyl halides. This is unfortunate since alkenyl halides are crucial building blocks in transition-metal catalyzed syntheses, particularly for palladium-catalyzed cross-coupling reactions.[3] As discussed in Chapter 1, there are a number of reasons why vinyl halides might fail to participate in CM. In order for vinyl halides to participate in CM, ruthenium monohalomethylidene complexes would most likely form during the catalytic cycle. We set out to synthesize monohalomethylidene complexes in order to test their stability and activity in CM reactions and ultimately determine why vinyl halides did not participate in CM reactions. Reasoning that a monofluoromethylidene complex would be the most stable of the monohalomethylidene species, we investigated potential syntheses of Ru(=CHF)(H_2IMes)(PCy_3)Cl_2 (**2.13-F**) and Ru(=CHF)(H_2IMes)$(py)_2Cl_2$ (**2.14-F**).[4]

2.2. Ruthenium Monofluoromethylidene Complexes

2.2.1. Synthesis and Isolation

Metathesis of **2.2-Cl** with 2 equivalents of β-fluorostyrene[5] in a pentane/benzene mixture affords **2.13-F** in 77% isolated yield after 2 d; stilbene is the byproduct (Scheme 2.1). A shorter reaction time can be achieved with greater excess of β-fluorostyrene, but obtaining large quantities of this reagent presented synthetic challenges.

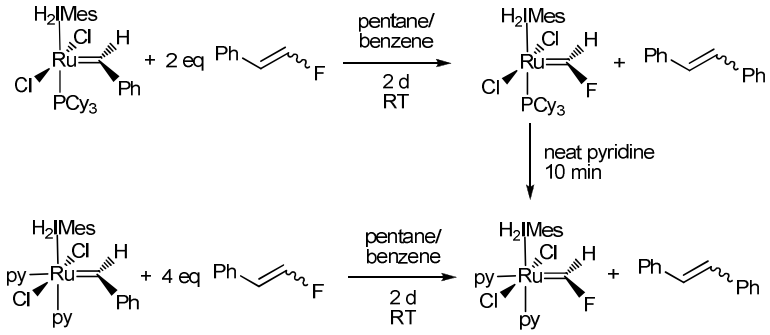

Scheme 2.1. Initial Syntheses of **2.13-F** and **2.14-F**

Complex **2.13-F** is unambiguously identifiable by NMR spectroscopy. The carbene α-proton is clearly visible as a doublet at 13.1 ppm ($^2J_{HF}$ = 106 Hz) in the ^{1}H NMR spectrum. Coupling to the ^{31}P nucleus is not observed, which suggests that the CHF fragment lies in a plane approximately perpendicular to the Ru-P bond.[6-8] The CHF fragment gives rise to a doublet at 283 ppm in the ^{13}C{^{1}H} NMR spectrum ($^1J_{CF}$ = 416 Hz). These ^{1}H and ^{13}C NMR signals occur at chemical shifts very similar to those in **2.13-OEt** (δ 276.8 ppm),[7] 6 and 11 ppm respectively upfield of their counterparts in **2.2-Cl** (δ 298 ppm). The resonance at 32.6 ppm in the ^{31}P{^{1}H} NMR spectrum is a poorly resolved doublet due to coupling to the ^{19}F nucleus. The latter nucleus gives rise to a doublet at 113.7 ppm in the ^{19}F NMR spectrum ($^2J_{HF}$ = 106 Hz); the P-F coupling is again poorly resolved. ^{19}F NMR chemical shift, and $^2J_{CF}$ coupling constants of **2.13-F** are very similar to those in difluorocarbene complex, **2.11** (δ 133 ppm; $^2J_{CF}$ = 432 Hz). The corresponding ^{13}C{^{1}H} NMR signal in **2.11** (δ 218 ppm) occurs well upfield of that in **2.13-F**.[9]

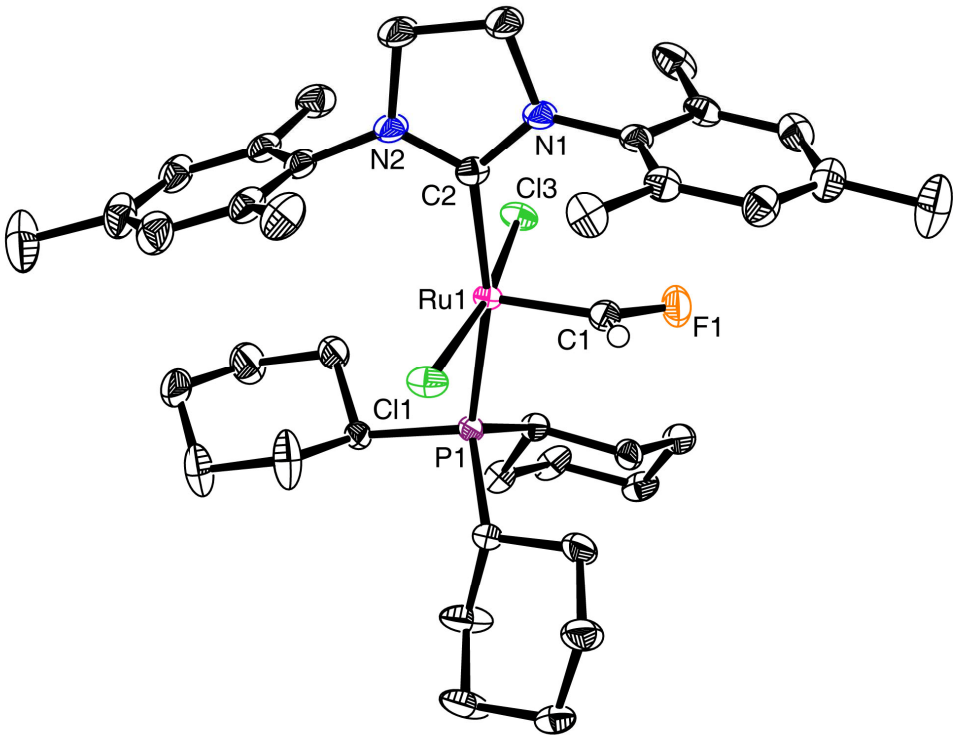

Figure 2.1. 50% thermal ellipsoid plot of [Ru(CHF)(H_2IMes)(PCy_3)Cl_2] (**2.13-F**). Selected crystallographic data are presented in Table 2.1 and selected bond distances and angles are presented in Table 2.2. Complete XRD data can be found in Appendix 1.

Orange prismatic crystals of **2.13-F** were grown from a saturated solution of pentane/benzene (20:1) at 28 °C. An ORTEP diagram of **2.13-F** is shown in Figure 2.1 and selected crystallographic data are presented in Table 2.1 with selected bond distances and angles presented in Table 2.2. The analysis reveals a slightly distorted square pyramid with an apical monofluoromethylene unit. The basal plane contains two mutually *trans* chlorides and an NHC ligand *trans* to a tricyclohexylphosphine ligand. The monoclinic unit cell contains 1 molecule of **2.13-F** and 0.5 molecules of benzene. Compound **2.13-F** is the first crystallographically characterized terminal

monohalomethylidene complex. The Ru=C distance in **2.13-F** (1.783(2) Å) is statistically indistinguishable from that of **2.11** (1.775(3) Å),[9] but is shorter than that of **2.2-Cl** (1.835(2) Å).[10] The CHF unit lies in the Cl-Ru-Cl plane. Unfortunately, disorder of the CHF moiety precludes precise determination of the C-F bond length and Ru-C-F angle.

Table 2.1. Crystallographic Data for Complexes **2.13-F**, **2.14-F** and **2.8-Cl**

	2.13-F	**2.14-F**	**2.8-Cl**
Formula	$C_{43}H_{63}Cl_2FN_2PRu$	$C_{32}H_{37}Cl_2FN_4Ru$	$C_{41.33}H_{62.67}Cl_3N_2O_{0.33}PRu$
FW	829.89	668.63	831.32
Crystal System	Monoclinic	Monoclinic	Hexagonal
Space group	$P2_1/n$	$P2_1/n$	$P6_1$
A (Å)	11.7509(9)	8.8643(6)	20.7728 (8)
B (Å)	21.2958(15)	17.115(1)	20.7728 (8)
C (Å)	17.7264(13)	20.147(1)	18.1437 (16)
α (deg)	90	90	90
β (deg)	95.055(4)	95.070(1)	90
γ(deg)	90	90	120
V ($Å^3$)	4418.7(6)	3044.5(3)	6780.3 (7)
Z	4	4	6
Rad. (Ka, Å)	0.71073	0.71073	0.71073
T (K)	108 (2)	85(2)	108 (2)
D_{calcd} (Mg m^{-3})	1.247	1.459	1.222
ρ_{calcd} (mm^{-1})	0.546	0.725	0.588
F_{000}	1748	1376	2624
R1	0.0341	0.0434	0.0440
wR2	0.0992	0.0991	0.0922
GOF	1.071	1.143	1.005

Table 2.2. Selected Bond Lengths and Angles for Complexes **2.13-F**, **2.14-F** and **2.8-Cl**

	2.13-F	**2.14-F**	**2.8-Cl**
Bond Distances (Å)			
Ru-C(1)	1.783(2)	1.857(11)	1.815(6)
Ru-C(H_2IMes)	2.0872(19)	2.069(3)	2.021(5)
C(1)-F(1)	n/a	1.358(11)	-
C(1)-P(1)	-	-	1.825(6)
Ru-Cl (*cis* to H_2IMes)	2.3853(5)	2.3995(8)	2.3590(15)
Ru-Cl (*cis* to H_2IMes)	2.3901(5)	2.4057(8)	2.3991(15)
Ru-Cl (*trans* to H_2IMes)	-	-	2.4038(14)
N(1)-C(H_2IMes)	1.342(3)	1.355(4)	1.348(7)
N(2)-C(H_2IMes)	1.346(3)	1.353(4)	1.363(7)
Ru-P	2.4238(5)	-	-
Ru-N(3) (*trans* to H_2IMes)	-	2.184(2)	-
Ru-N(4) [*trans* to C(1)]	-	2.288(8)	-
Bond Angles (deg)			
Ru-C(1)-F(1)	n/a	126.0(8)	-
Ru-C(1)-P(1)	-	-	129.3(3)
C(1)-Ru-C(H_2IMes)	97.36(8)	93.3(3)	97.4(2)
C(1)-Ru-Cl (*cis* to H_2IMes)	95.63(8)	95.5(3)	105.92(19)
C(1)-Ru-Cl (*cis* to H_2IMes)	93.71(8)	85.0(3)	85.48(19)
C(H_2IMes)-Ru-X	167.08(6) (X = P)	-	155.79(16) (X = Cl_{trans}
Cl-Ru-Cl *trans*	170.63(2)	176.27(3)	168.57(6)
C(H_2IMes)-Ru-Cl *cis*	91.49(6)	89.06(8)	94.24(16)
C(H_2IMes)-Ru-Cl *cis*	87.98(5)	94.60(8)	83.11(16)
C(1)-Ru-N(3)	-	87.9(3)	-
N(3)-Ru-N(4)	-	76.97(18)	-
N(1)-C(H_2IMes)-N(2)	108.03(18)	106.1(2)	107.0(5)

Compound **2.14-F,** Ru(=CHPh)(H_2IMes)(py)$_2$Cl$_2$, was synthesized in two ways (Scheme 2.1). Dissolution of **2.13-F** in pyridine afforded rapid conversion to **2.14-F** in 91% isolated yield. Alternatively, Ru(=CHPh)(H_2IMes)(py)$_2$Cl$_2$ (**2.9**) was treated with 4 equiv of β-fluorostyrene, affording **2.14-F** in 75% isolated yield. Doublets at 13.3 ($^2J_{HF}$ = 95 Hz), 298.3 ($^1J_{CF}$ = 409 Hz), and 130.3 ppm ($^2J_{FH}$ = 91 Hz) in the ^{1}H, ^{13}C{^{1}H}, and ^{19}F NMR spectra respectively are diagnostic of the CHF ligand in this complex, which retains two pyridine ligands that are equivalent on the ^{1}H NMR timescale at 23 °C.

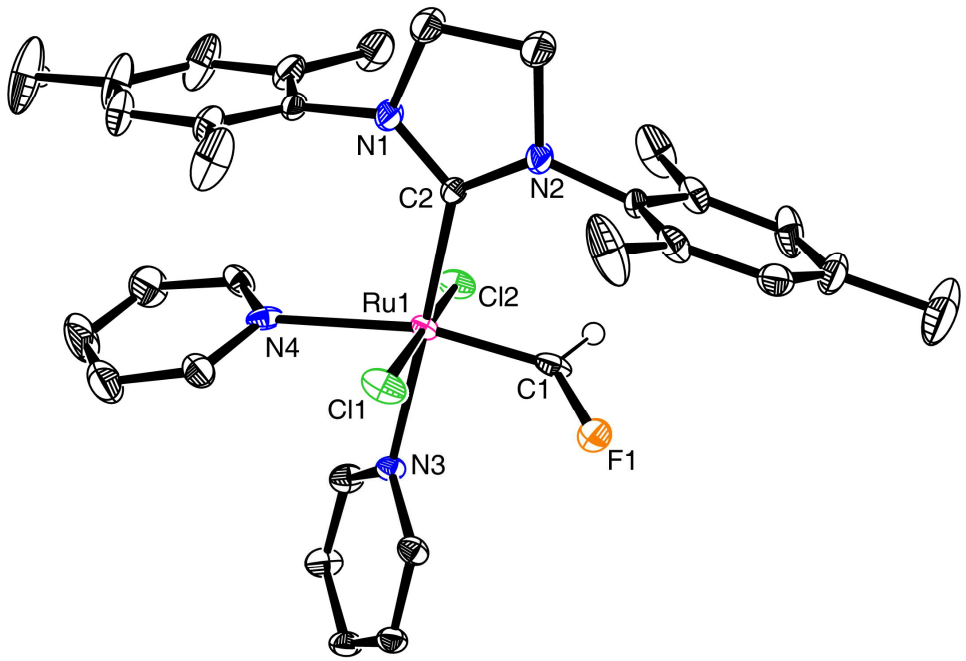

Figure 2.2. 50% thermal ellipsoid plot of [Ru(CHF)(H_2IMes)(py)$_2$Cl$_2$] (**2.14-F**). Selected crystallographic data are presented in Table 2.1 and selected bond distances and angles are presented in Table 2.2. Complete XRD data can be found in Appendix 2.

Orange plates of **2.14-F** were grown from slow diffusion of pentane into a pyridine solution at 25 °C. An ORTEP diagram is shown in Figure 2.2 and selected

crystallographic data are presented in Table 2.1 with selected bond distances and angles presented in Table 2.2. The analysis reveals a distorted octahedral arrangement with two mutually *trans* chloride ligands, a pyridyl ligand *trans* to the NHC ligand, and a second pyridyl ligand *trans* to the monofluoromethylidene ligand. The pyridyl ligand *trans* to the CHF ligand is significantly longer (0.1Å) than the pyridyl ligand *trans* to the H_2IMes ligand indicating that CHF is a stronger *trans*-influence ligand. The monofluoromethylidene ligand and one pyridyl ligand were disordered 50/50 over two coordination sites in the equatorial plane containing the ruthenium and two chlorides. The monoclinic unit cell contains 4 molecules of **2.14-F**. The C-F bond length (1.358Å) is typical of a C-F single bond.[11-13]

A second method of synthesis for the monofluoromethylidene complexes employs vinyl fluoride gas. This method generally gave higher yields of the monofluoromethylidene complexes over a shorter time frame with styrene as the byproduct. The benzylidene complexes (**2.1**-**2.3**, **2.9** and **2.10**) were dissolved in benzene and then treated with excess vinyl fluoride gas while in a high pressure reaction flask. Reactions typically gave 100% conversion within 1 hour. Using this method, a number of monofluoromethylidene complexes (**2.12-F** through **2.17**) were synthesized from ruthenium benzylidene complexes with varying ligand sets. (Table 2.3, Scheme 2.2)

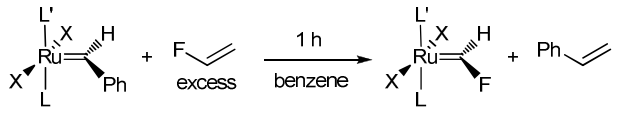

L = L' = PCy_3; X = Cl	**2.12-F**
L' = H_2IMes; L = PCy_3; X = Cl	**2.13-F**
L' = H_2IMes; L = PCy_3; X = Br	**2.17-Br**
L' = H_2IMes; L = PCy_3; X = I	**2.17-I**
L' = H_2IMes; L = PPh_3; X = Cl	**2.16**
L' = H_2IMes; L = 2 py; X = Cl	**2.14-F**
L' = H_2IMes; L = 2 (3Br-py); X = Cl	**2.15**

Scheme 2.2. Synthesis of Monofluoromethylidene Complexes

Table 2.3. NMR Data for Monofluoromethylidene Compounds

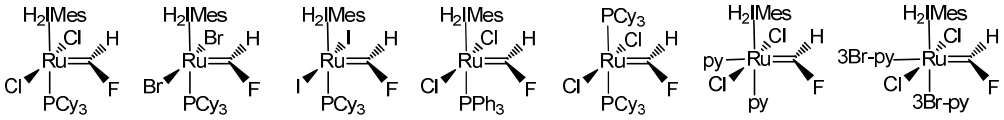

NMR[a]	^{1}H (ppm)	^{19}F (ppm)	$^{2}J_{HF}$ (Hz)	^{31}P (ppm)	$^{3}J_{PF}$ (Hz)	^{13}C (ppm)[b]	$^{1}J_{CF}$ (Hz)
2.13-F	13.1 (d)	+113.7 (d)	106	32.6 (s)	0	283 (d)	416
2.17-Br	13.0 (d)	+124.3 (dd)	105	31.0 (d)	7	286 (d)	423
2.17-I	12.4 (d)	+146.2 (dd)	105	31.2 (d)	10	*n/a*	*n/a*
2.16	12.9 (dd)[c]	+137.3 (dd)	110	34.3 (d)	54	291 (dd)[d]	421
2.12-F	14.2 (d)	+127.0 (dt)	110	34.1 (d)	14	284	419
2.14-F	13.3 (d)	+130.3 (d)	95	-	-	298 (d)	409
2.15	13.1 (d)	+131.9 (d)	92	-	-	*n/a*	*n/a*

[a] C_6D_6 was used as the NMR solvent for these data collections. [b] n/a = not available. [c] $^{3}J_{PH}$ = 2 Hz: this was the only example of PH coupling [d] $^{2}J_{CP}$ = 60 Hz: this was the only time CP coupling was observed.

A general trend was observed in these data. As the ligand set becomes less σ-donating (Cl > Br > I; PCy_3 > PPh_3; PCy_3 > H_2IMes; py > 3Br-py), the ^{1}H NMR signal shifts upfield and the ^{19}F NMR signal shifts downfield. Only compounds **2.13-F** and **2.14-F** were cleanly isolated.

2.2.2. Reactivity

2.2.2.1. Metathesis Activity

Both **2.13-F** and **2.14-F** exhibit olefin metathesis activity. Complex **2.13-F** effects complete RCM of the benchmark substrate diethyl diallylmalonate within 3 h, only slightly more rapidly than **2.13-OEt**[7] under the same conditions (0.10 M substrate, 3

mol% catalyst loading, C_6D_6, 60 °C) and much slower than **2.2-Cl** (Table 2.4). Low RCM activity of **2.13-OEt** and **2.13-F** can be contributed to slow initiation in both cases. A ^{31}P NMR magnetization transfer experiment reveals that PCy_3 dissociation from **2.13-F** is so slow that no exchange with free PCy_3 is observed even at 80 °C under standard conditions[14] in toluene-d_8 with up to 50 second mixing times. Thus, initiation via loss of PCy_3 is clearly problematic for **2.13-F**. ^{31}P NMR magnetization transfer experiments also indicated that phosphine dissociation for compound **2.11** was extremely slow. However, under ring-opening metathesis polymerization (ROMP) conditions (0.005 M cat., 300 equiv COD in CD_2Cl_2, 25 °C, 1.25 h) of 1,5-cyclooctadiene (COD), **2.11** effects the ROMP of COD to the extent of only 9%,[9] ROMP was complete with **2.13-F** (eq. 2.1).

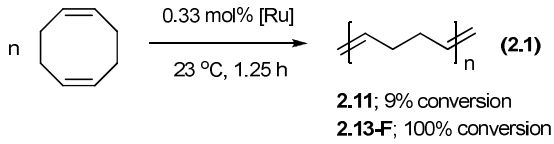

2.11; 9% conversion
2.13-F; 100% conversion

An alternative explanation to slow activation of the catalyst involves a thermodynamic preference for Ru=CHX (X = OEt, F) compared to $Ru=CH_2$ ligation, which would also account for the formation of only a small quantity of the active RCM catalyst, $Ru(=CH_2)(H_2IMes)(PCy_3)_2Cl_2$ (**2.13-H**). In this case, **2.11** would still be expected to be more thermodynamically stable compared to **2.13-F** as discussed previously in Chapter 1.

Table 2.4. Catalyzed RCM of Diethyldiallylmalonate

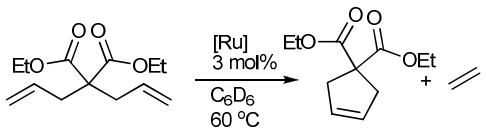

[Ru]	30 min	1 h	2 h	3 h
2.2-Cl	**92%**	100%	-	-
2.13-F	36%	75%	**95%**	100%
2.14-F	42%	82%	**93%**[a]	93%

[a] Catalyst **2.14-F** decomposed. Bolded percent conversions give a point of comparison.

RCM of diethyl diallylmalonate with **2.14-F** was initially slightly more rapid than with **2.13-F**, but ceased after 2 h due to catalyst decomposition at 60 °C (Table 2.4). When compared with 2nd gen. Grubbs catalyst, both **2.13-F** and **2.14-F** were sluggish.

Table 2.5. Catalyzed Self-CM of 1-Hexene

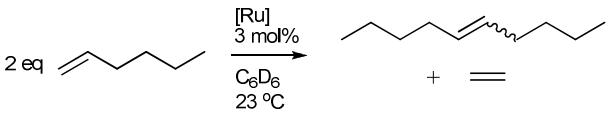

[Ru]	1 h	2 h	4 h	9 h	33 h	76 h
2.2-Cl	27%	33%	39%	48%	84%	-
2.13-F	-	14%	19%	23%	30%	39%
2.14-F	-	13%	19%	25%	37%	45%

Self-cross-metathesis of 1-hexene, a 'Type I' substrate in this system,[15] occurs with both **2.13-F** and **2.14-F** (0.10 M substrate, 3 mol% catalyst, C_6D_6, 23 °C) at similar rates; both are slow compared to **2.2-Cl**. At lower temperatures, **2.14-F** remains active even after 76 h (Table 2.5). If phosphine dissociation was the only rate inhibitor for **2.13-F**, the rate of RCM or CM with catalyst **2.14-F** should be much faster than that of **2.13-F** because pyridyl ligands dissociate more readily than tricyclohexylphosphine. No new alkylidene complexes are observed by ^{1}H NMR at any time, which indicates that either slow initiation or thermodynamic stability of **2.13-F** and **2.14-F** allow for only a small quantity of highly active catalyst, such as **2.13-H** or **2.14-H**, to form. No fluorinated olefins (vinyl fluoride, 1-fluoro-1-hexene) were observed in the reactions of self-CM of 1-hexene with **2.13-F**. However, a very small quantity (too small for accurate integration) of vinyl fluoride appeared over time in the self-CM reaction with **2.14-F**. This quantity of vinyl fluoride can be accounted for in two ways. Equilibrium formation of small quantities of vinyl fluoride and Ru(=CH-*n*-Bu)(H_2IMes)$(py)_2Cl_2$ upon reaction of **2.14-F** with 1-hexene is one explanation. A second possibility that can account for vinyl fluoride generation is bimolecular decomposition[16] of **2.14-F** with Ru(=CH_2)(H_2IMes)$(py)_2Cl_2$, **2.14-H**, which must be present at least in low concentration. It is important to note that **2.14-F** decomposes much more rapidly under the conditions of significantly higher concentration required for ^{13}C NMR spectrum acquisition. This suggests that at least one decomposition mechanism is second-order in [**2.14-F**].

2.2.2.2. Stoichiometic Metathesis with Ethyl Vinyl Ether.

When compound **2.14-F** is treated with 2 equivalents of ethyl vinyl ether, it undergoes conversion to > 95% Ru(=CHOEt)(H_2IMes)(py)$_2$Cl$_2$ (**2.14-OEt**) within hours at room temperature, with concomitant liberation of vinyl fluoride (Scheme 2.3; top). In contrast, conversion of **2.13-F** to **2.13-OEt** is not seen even after 3 days at 23 °C (10 equiv ethyl vinyl ether used). We propose that the dichotomy in the reactions of **2.13-F** and **2.14-F** with ethyl vinyl ether is due to slow phosphine dissociation of **2.13-F** under these conditions. Stoichiometric metathesis of **2.13-F** with ethyl vinyl ether at 80 °C liberates a small amount of vinyl fluoride, however, rapid decomposition of **2.13-F** to **2.5-Cl** precluded full evaluation of the effects of phosphine lability (Scheme 2.3; bottom).

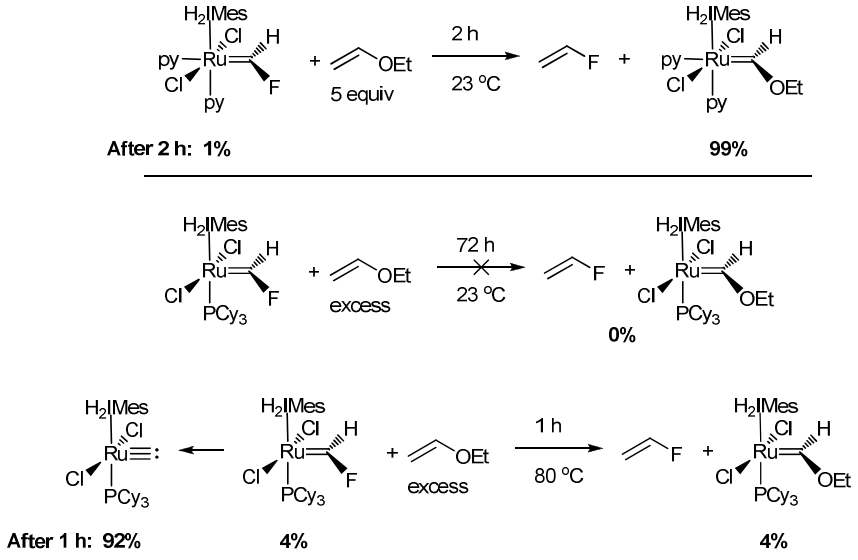

Scheme 2.3. Stoichiometric Metathesis with Ethyl Vinyl Ether

These reactions bear directly on the stability of α-fluoro-ruthenacyclobutane intermediates. Formation **2.13-F** and **2.14-F** in good yields from **2.2-Cl** and **2.9** require that the α-fluoro-β,α*-diphenylruthenacyclobutane intermediate must undergo cycloreversion to **2.13-F** or **2.14-F** and stilbene. The essentially quantitative reaction of ethyl vinyl ether with **2.14-F** requires that the α-fluoro-α*-ethoxyruthenacyclobutane intermediate must not decompose more rapidly compared to the rate of ring fragmentation to yield **2.14-OEt** and vinyl fluoride. Finally, the isolation of monofluoromethylidene complexes and their relative stability in solution indicates that productive metathesis should occur before decomposition takes place if there is no other thermodynamic barrier.

2.2.2.3. Decomposition

Compound **2.13-F** is stable in the solid state and in a THF solution (90% remains after 28 d at 23 °C). Under other conditions, it eventually undergoes conversion to the terminal carbide complex **2.5-Cl**. As measured by ^{1}H and ^{31}P NMR spectroscopy, conversion to **2.5-Cl** is complete any time between 5 to 16 h in CD_2Cl_2. This transformation occurs more slowly in benzene or toluene. The reaction has a long and variable induction period which is highly dependent on purity of the sample and the solvent. The conversion of **2.13-F** to **2.5-Cl** required approximately 5 days in C_6D_6. Decomposition of **2.13-F** in toluene-d_8 was observed after heating to 80 °C for 1 h, but in another case only 3% conversion to **2.5-Cl** was noted after being subjected to temperatures of 80 °C for 1 h followed by 55 °C for 4 h and finally 23 °C for 7 d.

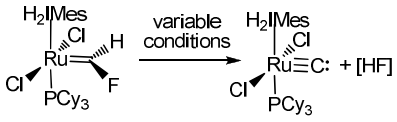

Scheme 2.4. Decomposition of **2.13-F**

Unlike the related formation of **2.4** from an acetoxycarbene complex, **2.12-OAc**,[17,18] decomposition of the monofluoromethylidene complex, **2.13-F**, does not display simple first-order kinetics, but evinces a long induction period during which time little or no **2.5-Cl** is observed, followed abruptly by relatively rapid formation of **2.5-Cl**. We propose that this is due to the slow formation of HF, that further initiates the decomposition of **2.13-F** to **2.5-Cl**. In order to test the competence of Brønsted and Lewis acids to mediate this process, we examined reactions of **2.13-F** with HCl and with Me_3SiCl. In the former case, we find that 1 equiv ethereal HCl consumes **2.13-F** in C_6D_6, affording 89% **2.5-Cl** and 11% of an unidentified side product within 1 h. Treatment of **2.13-F** with 2 equiv Me_3SiCl in CD_2Cl_2 yields quantitative formation of **2.5-Cl** within 30 min, along with 1 equiv Me_3SiF. Suitable Lewis or Brønsted acids are competent to promote the conversion of **2.13-F** to **2.5-Cl;** therefore, decomposition of **2.13-F** is perpetuated through liberation of HF.

Other ligand variations of the monofluoromethylidene complex (**2.12-F** and **2.16**) undergo decomposition to the cooresponding carbide. In the case of **2.14-F** and **2.15**, the final products are unknown. The bis-pyridine carbide complex is rare and based on results from Steve Caskey,[19] is unstable to further decomposition. The monofluoromethylidene complex (**2.12-F**) could not be isolated cleanly; there was always a small amount of carbide contamination. Overall, decomposition of the

monofluoromethylidene complexes, **2.13-F** and **2.14-F**, is too slow to affect CM. Therefore, thermodynamic stability of the CHF group accounts for problems with CM.

2.3. Ruthenium Monochloromethylidene Complexes

2.3.1. Decomposition

Unlike the cases of other vinyl-X reagents investigated earlier (X = O_2CR and F),[4, 17, 20] the analogous Fischer carbene intermediate [Ru(CHCl)H_2IMes(PCy_3)Cl_2], **2.13-Cl**, was not observed upon reaction of 2nd generation Grubbs catalyst (**2.2-Cl**) with vinyl chloride, although the metathesis byproduct, styrene, was seen (Scheme 2.5).[21] Furthermore, although the expected carbide decomposition product, **2.5-Cl** formed, it was not the major Ru-containing product. Instead, the new phosphoniomethylidene complex, [Ru(CHPCy_3)H_2IMesCl_3] (**2.8-Cl**) formed in a 2:1 ratio with **2.5-Cl**. The ratio of compounds **2.5-Cl** and **2.8-Cl** remained constant over the reaction time indicating that **2.5-Cl** and **2.8-Cl** do not interconvert during the reaction. Formation of the carbide complex, **2.5-Cl,** in reactions of **2.2-Cl** with vinyl chlorides implies loss of HCl from the initial intermediate [Ru(CHCl)H_2IMes(PCy_3)Cl_2], **2.13-Cl**. Therefore, the above reaction was performed in the presence of Hunig's base, NEt-*i*-Pr_2. Consumption of **2.2-Cl** occurred at the same rate as in the absence of the base, but the product distribution changed dramatically: **2.5-Cl** forms quantitatively. Hunig's base fails to convert the phosphoniomethylidene complex, **2.8-Cl** into the carbide, **2.5-Cl** under identical reaction conditions. Thus, formation of **2.8-Cl** does not precede formation of **2.5-Cl** on the reaction pathway. Along the same lines, liberation of HCl from the formation of **2.5-Cl** could then react with **2.5-Cl** forming **2.8-Cl**. However, addition of HCl gas to a reaction

mixture of the carbide compound, **2.5-Cl** in benzene showed no conversion to the phosphoniomethylidene complex, **2.8-Cl**. It is likely that both **2.5-Cl** and **2.8-Cl** form from a common intermediate (or transition state) such as a methylidyne complex of the form $[Ru(CH)(H_2IMes)(PCy_3)Cl_2]Cl$ (Scheme 2.6). Although a putative intermediate of this sort has not been observed in the Ru system, the closely related osmium complex, $[Os(CH)(PCy_3)_2Cl_2]OTf$ has been prepared.[22, 23]

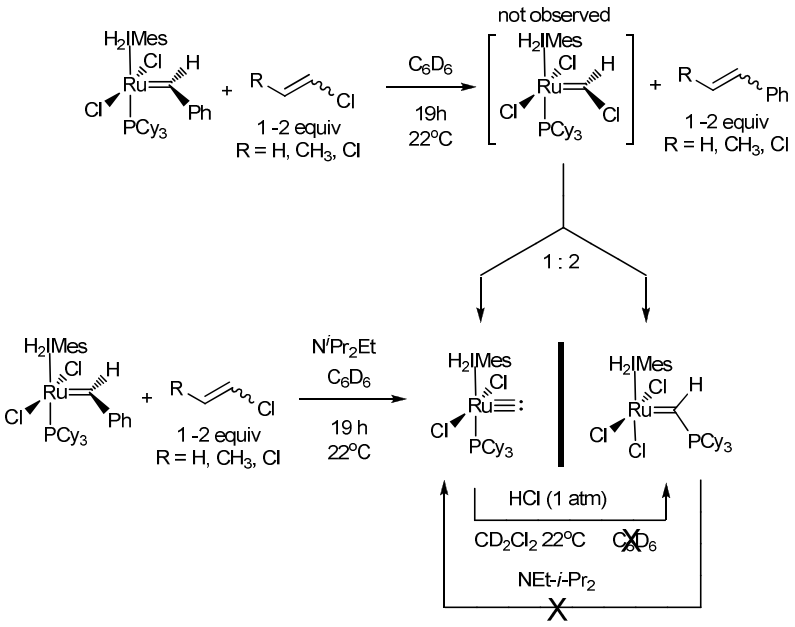

Scheme 2.5. Formation of Terminal Carbide and Phosphoniomethylidene Complexes

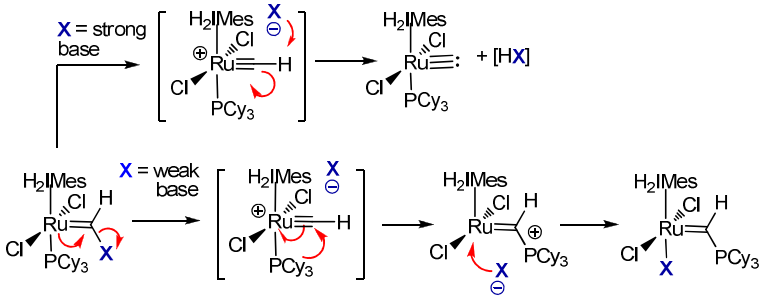

Scheme 2.6. Proposed Decomposition of the Monohalomethylidene Complexes

We attempted to access the monochloromethylidene complex, **2.13-Cl**, through other methods. Given that BCl_3 has been used to convert difluorocarbene complexes into the corresponding dichlorocarbene species,[24] the reaction of **2.13-F** with BCl_3 in benzene at 22 °C and in toluene at −40 °C was examined. Within 30 min this afforded **2.7[$BCl_{4-x}F_x$]** without observation of **2.13-Cl** even at low temperatures. Quantitative conversion of **2.7[$BCl_{4-x}F_x$]** to **2.8-Cl** occurred upon addition of THF (Scheme 2.7). Similarly, the reaction of **2.13-F** with BF_3•OEt_2 produced **2.7** directly in 70% isolated yield. In contrast, reaction of **2.13-F** with HCl or Me_3SiCl produces primarily **2.5-Cl** as discussed earlier.[4] Complex **2.8-Cl** can also be formed upon reaction of ionic **2.7** with [*n*-Bu_4N]Cl (eq. 2.2). Single-crystal X-ray diffraction confirmed the structure of **2.8-Cl** (Figure 2.3).

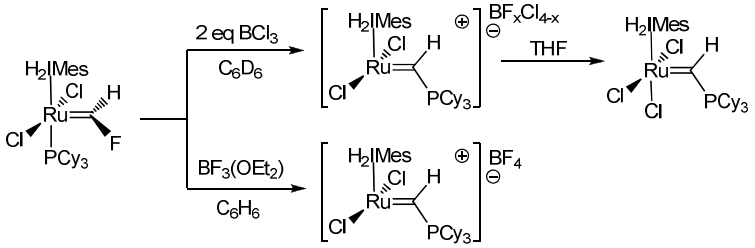

Scheme 2.7. Formation of the Phosphoniomethylidene Complex from **2.13-F**

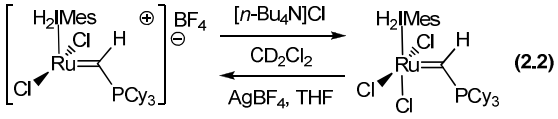

(2.2)

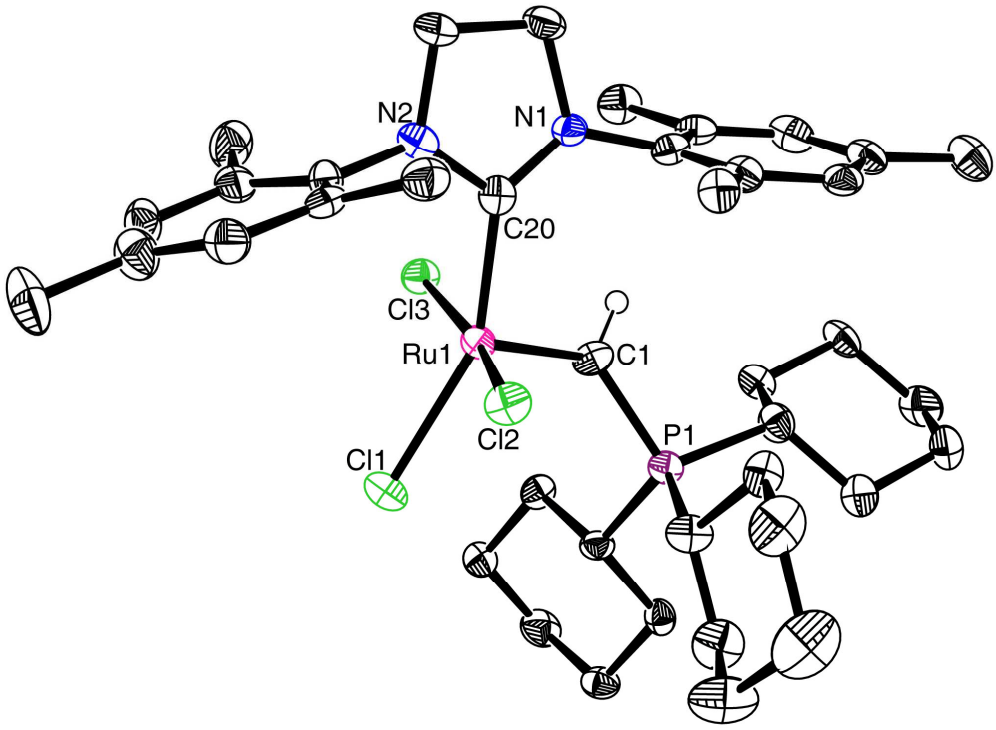

Figure 2.3. 50% thermal ellipsoid plot of [Ru(CHPCy$_3$)(H$_2$IMes)Cl$_3$] (**2.8-Cl**). Selected crystallographic data are presented in Table 2.1 and selected bond distances and angles are presented in Table 2.2. Complete XRD data can be found in Appendix 3.

Yellow needles of **2.8-Cl** were grown by diffusion of pentane into a THF-d_8 solution at 28 °C. An ORTEP diagram is shown in Figure 2.3, selected crystallographic data are presented in Table 2.1, and selected bond distances and angles are presented in Table 2.2. The coordination geometry is best described as distorted square pyramidal (τ = 0.213)[25] with the phosphoniomethylidene ligand at the apex. The basal plane contains two mutually *trans* chlorides, and an NHC ligand *trans* to the third chloride. The hexagonal unit cell contains 2 molecules of THF-d_8 and 6 molecules of **2.8-Cl.** Both the Ru1-C1 bond distance and the C1-Ru1-C20 bond angle are statistically indistinguishable

from the corresponding parameters in **2.7[B(C_6F_5)$_4$]**.[26] The Ru=C distance is in the usual range for 2nd Grubbs catalysts, **2.2**.[4, 9, 10]

The ratio of carbide, **2.5-Cl** to the phosphoniomethylidene complex **2.8-Cl** formed depends on the acidity of the reaction mixture. In the presence of Hunig's base, **2.13-Cl** forms only carbide. In a solution with no additives, **2.13-Cl** forms a 1:2 mixture of **2.5-Cl** and **2.8-Cl**. In contrast, **2.13-F** decomposes to form only the corresponding carbide **2.5-Cl**. Addition of boron trichloride or boron trifluoride·etherate to a solution of **2.13-F** yielded **2.7[$BF_{4-x}Cl_x$]**, a derivative of **2.8-Cl**. These Brønsted acids, acting as fluoride abstractors, make the reaction mixture more acidic favoring the formation of the phosphoniomethylidene complex. Synthesis of **2.7** requires the treatment of **2.5-Cl** with a strong acid such as H[BF_4]·etherate. In this reaction, the acid is strong enough to protonate the weakly basic carbide giving an intermediate (or transition state) methylidyne complex, [Ru(≡CH)H_2IMes(PCy_3)Cl_2][BF_4] which then goes through phosphine migration to give the 14-electron phosphoniomethylidene complex, **2.7**.[26] Combining this information and the consideration that halides are good leaving groups, we propose a decomposition process for the monohalomethylidene complexes in which the C-X bond breaks and electron density from the Ru is donated to the α-C to form an intermediate Ru-methylidyne complex which is quite unstable (Scheme 2.6). At this point, when X is a strong base such as fluoride, it abstracts the proton from the methylidyne unit to form the corresponding carbide (Scheme 2.6; top). When X is a weak base, such as chloride, the rate of phosphine migration is competitive with proton abstraction yielding a mixture of **2.5-Cl** and **2.8-Cl** (Scheme 2.6; bottom). Therefore, acidic or basic additives in the reaction mixture can dramatically alter the ratio of

products. Although other processes are possible for explaining the decomposition of these monohalomethylidene complexes, the pathway shown in Scheme 2.6 best explains all the data. Whether this decomposition process occurs in a step-wise manner or is concurrent is still a question to be answered.

2.3.2. Synthesis and Observation

Complex **2.8-Cl** can be formed by the reaction of **2.5-Cl** at 22 °C with HCl in CD_2Cl_2 but not in C_6D_6 (Eq. 2.3). Although direct metathesis reaction at low temperature failed to produce **2.13-Cl**, addition of excess HCl (1 atm) to the head space of a frozen solution of selectively ^{13}C-labeled **2.5-Cl(^{13}C)** in CD_2Cl_2 followed by warming to –70 °C elicited a rapid color change from the pale yellow of **2.5-Cl(^{13}C)** to bright red. Multinuclear NMR spectroscopy revealed complete consumption of **2.5-Cl(^{13}C)** and formation of a single new complex. Data for this compound include carbene resonances at δ 14.44 ppm ($^1J_{HC}$ = 201 Hz) and 268.1 ppm in the ^{1}H and ^{13}C NMR spectra, respectively. On the basis of the similarity of these data to those for isolable **2.13-OAc** (Table 2.6) and dissimilarity to cationic five-coordinate and neutral six-coordinate carbyne complexes,[27] we identify this compound as **2.13-Cl(^{13}C)**. Upon increasing the temperature to –20 °C and then to 0 °C, **2.13-Cl(^{13}C)** underwent conversion to **2.8-Cl(^{13}C)** cleanly and quantitatively over ~2 h; no other species were observed in the acidic solution (Eq. 2.3, Figure 2.4). In contrast, reaction of the carbide, **2.5-Cl(^{13}C)** with HO_3SCF_3 (HOTf) led directly to the formation of purple **2.7[OTf]** without any observable intermediate, even at –90 °C, ruling out the 5-coordinate cationic methylidyne complex, $[Ru(\equiv CH)H_2IMes(PCy_3)Cl_2][X]$ (X = Cl or OTf), as the observed intermediate

(Eq. 2.4). The other possible intermediate that could account for the doublet at δ 14.4 ppm is the 6-coordinate methylidyne complex, [Ru(≡CH)H_2IMes(PCy_3)Cl_3]; however, this intermediate is ruled out for steric reasons (see Chapter 6; Section 6.3.1) leaving **2.13-Cl** as the most likely option.

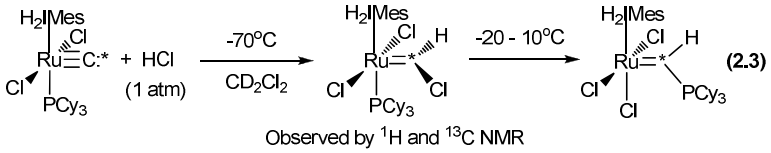

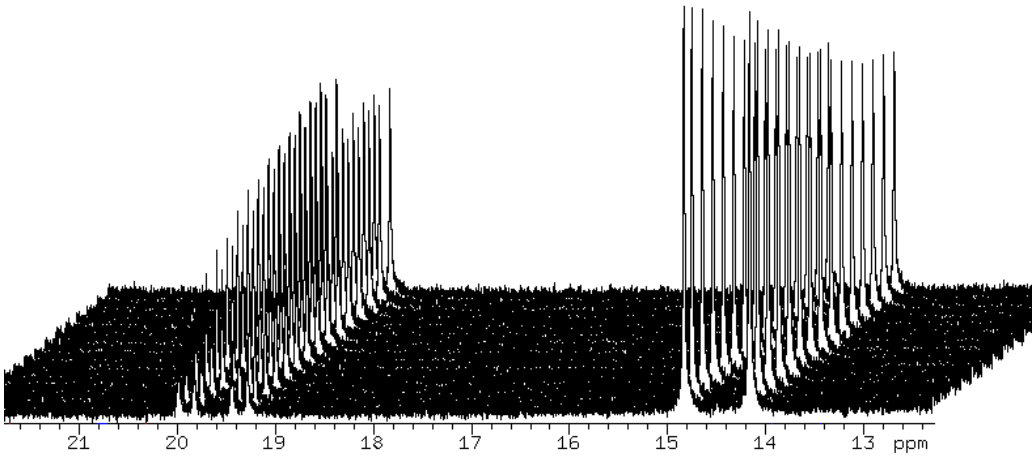

Figure 2.4. 1st order decay of **2.13-Cl(^{13}C)** (14.4 ppm) to **2.8-Cl(^{13}C)** (19.7 ppm)

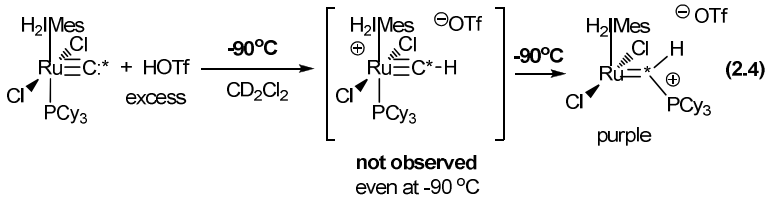

Table 2.6. Selected ^{1}H, ^{13}C, and ^{31}P NMR Data for Comparison with **2.13-Cl(^{13}C)**[a]

#	Compound	Ru(C_α) ^{13}C shift	Ru($C_\alpha H$) ^{1}H shift	$^{1}J_{CH}$ (Hz)	^{31}P shift
1[a]	**Ru(=^{13}CHCl)(H_2IMes)(PCy_3)Cl_2**	**268.1**	**14.4 (d)**	**201**	**25.8**
2	Ru(=^{13}CHOAc)(H_2IMes)(PCy_3)Cl_2	269.6	14.4 (d)	185	32.2
3	Ru(=CHF)(H_2IMes)(PCy_3)Cl_2[4]	283.0	13.1		32.6
4[b]	Ru(=CHOEt)(H_2IMes)(PCy_3)Cl_2[7]	276.8	13.6		32.6
5	Ru(=^{13}CHOAc)(H_2IMes)Cl_2[19]	n/a	11.7 (d)	207	–
6	Ru(=^{13}CHPCy_3)(H_2IMes)Cl_3	271.4	19.7(dd)	163	32.9
7	Ru(=^{13}CHPCy_3)(H_2IMes)Cl_2^+ OTf^-	263.4	17.8(dd)	173	N/A
8[c]	Ru(=CHPh)(H_2IMes)(PCy_3)Cl_2[28]	294.2	19.2 (s)		31.4
9[c]	Ru(=CHPh)(PCy_3)$_2Cl_2$[6]	294.7	20.0 (s)		36.6
10	Ru(≡^{13}C:)(H_2IMes)(PCy_3)Cl_2	478.7	–	–	34.6
11[d]	[Ru(≡CMe)(H_2IMes)(PCy_3)Cl_2]$^+$ OTf^- [19]	314.8	–	–	47.7
12[d]	Ru(≡C-*p*-C_6H_4Me)(PCy_3)$_2Cl_2^+$ BF_4 [27]	299.7	–	–	49.9
13[d]	Ru(≡C-*p*-C_6H_4Me)(PCy_3)$_2Cl_2F$ [27]	293.9	–	–	28.5
14	[Os(≡CH)(PCy_3)$_2Cl_2$]$^+$ OTf^- [23]	285.7	11.0	227	50.6

[a] All reactions were run in CD_2Cl_2. Shifts are quoted in ppm [b] Additional electron-rich Fischer carbene NMR data is available for comparison.[7] [c] Switching between the H_2IMes ligand and PCy_3 ligand does not seem to alter the ^{1}H and ^{13}C shift greatly [d] ^{13}C NMR shifts for C_α in 5- and 6- coordinate Ru-carbynes tend to fall in the δ = 290-320 range.[27]

In order to demonstrate that a monochloromethylidene intermediate was being formed in the metathesis reactions as well, we sought to intercept it via enyne metathesis.[29] Addition of excess vinyl chloride to the headspace above a frozen C_6D_6 solution of 2nd generation Grubbs catalyst, **2.2-Cl** and 10 equivalents of trimethylsilylacetylene in a J. Young tube, followed by heating to 60 °C for 1 h led to complete consumption of **2.2-Cl** and formation of the expected mixture of **2.5-Cl** and

2.8-Cl. More importantly, GC-MS and ^{1}H NMR analysis revealed that a mixture of the products of enyne metathesis (Eq. 2.5) had formed in ~30% yield based on the initial amount of alkyne used, indicating 3 turnovers. Although styrene was observed, no phenyl containing butadiene compounds were present indicating that initiation occurred by reaction of vinyl chloride with **2.2-Cl** not by reaction of alkyne with **2.2-Cl**. These findings are consistent with other known enyne metathesis reactions, in which olefin metathesis is rapid and reversible, whereas alkyne insertion is slow, irreversible, and responsible for product selectivity.[30] The major diene product obtained is best explained by alkyne insertion into the Ru=CHCl unit. Other paths that would lead to the same product are sterically disfavored, especially in the present case due to the presence of the bulky trimethylsilyl group.[30] Further details about vinyl chlorides in enyne metathesis reactions are given in Chapter 4.

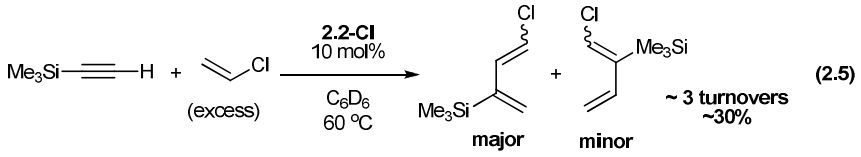

In summary, attempted CM of **2.2-Cl** with vinyl chloride yields styrene, the product of the initial metathesis cycle. However, the expected monochloromethylidene complex **2.13-Cl** is not observed at room temperature. Instead, in the absence of added base, both the terminal carbide complex **2.5-Cl** and the phosphoniomethylidene complex **2.8-Cl** are formed. In the presence of NEt-*i*-Pr$_2$, only **2.5-Cl** is produced. However, NEt-*i*-Pr$_2$, does not convert **2.8-Cl** into **2.5-Cl**.

2.4. Attempts with Vinyl Bromide

Reaction of 2nd generation Grubbs catalyst, **2.2-Cl**, with vinyl bromide was more complicated because of halogen exchange not only among the Ru-containing species (as expected)[27, 31-33] but also with the vinyl bromide and **2.2-Cl** (vinyl *chloride* was observed in the product mixture; Eq. 2.6).

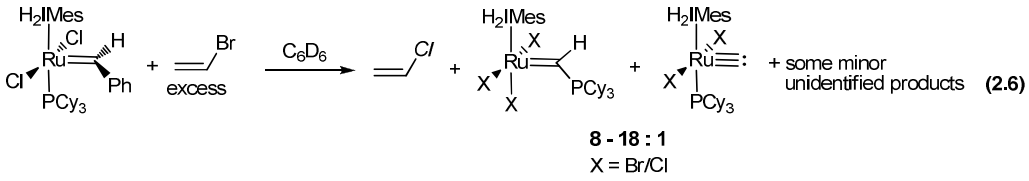

In order to simplify the reaction with vinyl bromide, we employed **2.2-Br**, whereupon the carbide, **2.5-Br** and **2.8-Br** formed in a 1:12 ratio along with some minor decomposition products that are not yet identified (Scheme 2.8; top). Addition of Hunig's base to the reaction mixture gave conversion to 82% carbide and an unidentified byproduct (Scheme 2.8; bottom). No phosphoniomethylidene complex was observed in this reaction supporting the proposed decomposition pathway (Scheme 2.6).

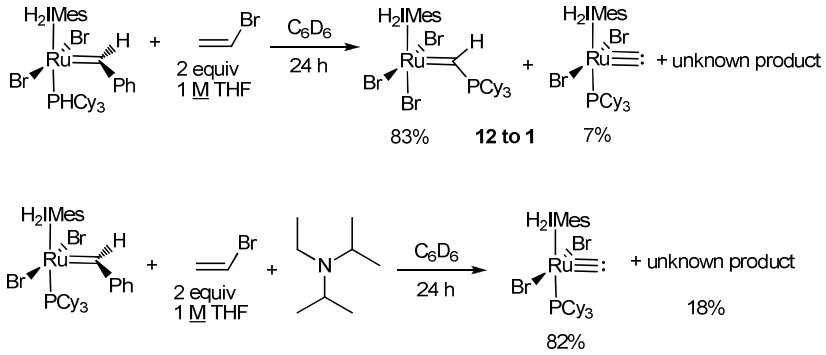

Scheme 2.8. Stoichiometric Metathesis with Vinyl Bromide

2.5. Conclusions

Cross-metathesis reactions of **2.2-Cl** and **2.9** with β-fluorostyrene or vinyl fluoride afford the first two isolated monofluoromethylidene complexes **2.13-F** and **2.14-F**, both of which slowly catalyze RCM and CM of benchmark alkenes. Thus, the failure to form a monofluoroalkylidene complex is ruled out as an explanation for the failure of CM reactions of vinyl fluoride. Quantitative formation of **2.13-F** and **2.14-F** upon reaction of **2.2-Cl** and **2.9** with 1 equivalent of β-fluorostyrene indicates a thermodynamic preference for the monofluoromethylidene ligand relative to the benzylidene moiety. Also, the reverse reaction of **2.13-F** and styrene yields no reaction. However, the CHF ligand in **2.14-F** is replaced quantitatively by the CHOEt moiety upon reaction with ethyl vinyl ether. Complex **2.14-F** is the more rapidly-initiating catalyst, but still only shows sluggish catalytic activity. Compound **2.13-F** also shows sluggish metathesis activity indicating thermodynamic stability of the CHF moiety. This is in agreement with DFT calaculations by Fomine (Chapter 1).[34] Complex **2.13-F** decomposes to form the stable terminal carbide complex **2.5-Cl**. Brønsted and Lewis acids facilitate carbide formation from **2.13-F**. Overall, decomposition rates of **2.13-F** and **2.14-F** are slow relative to metathesis rates, pointing towards thermodynamic stability of the CHF moiety with respect to further metathesis as the reason vinyl fluoride does not undergo CM. Reaction of 2nd generation Grubbs catalyst, **2.2-Cl**, with vinyl chloride did not give the expected monochloromethylidene complex, **2.13-Cl**. Products of this reaction included the expected metathesis byproduct styrene, indicating that **2.13-Cl** must have formed but was unstable. The decomposition products of **2.13-Cl** included the phosphoniomethylidene complex, **2.8-Cl**, and the carbide, **2.5-Cl**, in a 2 to 1 ratio

respectively. Attempted synthesis of **2.13-Cl** via reaction of the monofluoromethylidene complex, **2.13-F**, with BCl_3 instead produces **2.7[BF_xCl_{4-x}]** without observation of **2.13-Cl**. Low-temperature reaction of **2.5-Cl** with HCl in CD_2Cl_2 produces **2.13-Cl** as a thermally sensitive compound that undergoes conversion to **2.8-Cl** upon warming to –20 °C. Instability of **2.13-Cl**, not failure to form **2.13-Cl**, accounts for the failure of attempted cross-metathesis reactions of vinyl chloride using catalysts such as **2.2-Cl**. Reactions with vinyl bromide and 2nd generation Grubbs catalyst, **2.2-Cl**, afforded similar results to those with vinyl chloride; however, halogen exchange complicated the analysis of the results. Stoichiometric metathesis of **2.2-Br** with vinyl bromide yielded complexes **2.8-Br** and **2.5-Br** in a 12 to 1 ratio respectively. This was expected as the bromide anion is a weaker base than the chloride anion. We conclude that complexes **2.13-Cl** and **2.13-Br** are formed initially in stoichiometric CM with **2.2**, but they quickly undergo rapid conversion to a mixture of **2.8** and **2.5**.

2.6. Experimental

2.6.1. General Procedures. All reactions were carried out in a nitrogen-filled MBRAUN Labmaster 130 glove box, unless otherwise specified. ^{1}H, ^{13}C, ^{19}F, and ^{31}P NMR spectra were acquired on a Varian Mercury 300 MHz, Inova 400 MHz, or Inova 500 MHz NMR spectrometer. ^{1}H and ^{13}C spectra were referenced to solvent signals.[35] ^{19}F NMR spectra and ^{31}P NMR spectra were referenced to external $CFCl_3$ in $CDCl_3$ (δ=0) and external 85% H_3PO_4 (δ=0) respectively. Reactions were integrated against a known quantity of 1,3,5-trimethoxybenzene or 1-bromo-3,5-bis(trifluoro)benzene within the reaction mixture as the internal standard (IS).

2.6.2. Materials. Hydrogen chloride (anhydrous, 2 M solution in diethyl ether), vinyl bromide (1.0 M solution in tetrahydrofuran), boron trichloride (1.0 M solution in heptane), triphenylphosphine, and 1,3,5-trimethoxybenzene were purchased from Aldrich Chemical. Diisopropylethylamine, vinyl acetate, chlorotrimethylsilane, boron trifluoride etherate (*ca.* 48% BF_3), aluminum oxide (neutral, 50-200 micron), trifluoromethanesulfonic acid (HOTf), anhydrous sodium iodide, anhydrous lithium bromide, and 1-hexene were purchased from Acros Organics. Ethyl vinyl ether and diethyl diallylmalonate were purchased from Alfa Aesar. Sulfur, sublimed powder, and pyridine were purchased from J. T. Baker Inc. Trimethylsilylacetylene was purchased from GFS. Vinyl chloride (gas), 1-bromo-3,5-bis(trifluoro)benzene and tetrabutylammonium chloride were purchased from Fluka. Vinyl fluoride (gas) was purchased from SynQuest. Triethylamine was purchased from Fisher Scientific. All bulk solvents were obtained from VWR Scientific and dried by passage through solvent purification columns according to the method of Grubbs.[36] Deuterated solvents were purchased from CIL and dried over 4 Å molecular sieves. All liquid reagents were degassed and then dried over sieves or passed through activated alumina. Solid reagents were used as received. The compounds $Ru(CHPh)(H_2IMes)(PCy_3)Cl_2$ (**2.2-Cl**),[8] $Ru(CHPh)(H_2IMes)(py)_2Cl_2$ (**2.9**),[14] $Ru(=CHPh)(H_2IMes)(PCy_3)_2Br_2$ (**2.2-Br**),[14, 19] $Ru(CHPh)(PCy_3)_2Cl_2$ (**2.1**),[6] $Ru(=CHPh)(H_2IMes)(PCy_3)_2I_2$ (**2.2-I**),[14, 19] $[Ru(=CHPCy_3)(H_2IMes)Cl_2][BF_4]$ (**2.7**),[26] $Ru(\equiv{}^{13}C:)(H_2IMes)(PCy_3)Cl_2$ (**2.5-Cl(**^{13}**C)**),[18] $Ru(\equiv C:)(H_2IMes)(PCy_3)Cl_2$ (**2.5-Cl**),[37] $Ru(CHPh)(H_2IMes)(PPh_3)Cl_2$ (**2.3**)[38] and β-fluorostyrene[5] were synthesized according to published procedures. Ruthenium catalysts

(Ru(CHPh)(H_2IMes)(PCy_3)Cl_2 (**2.2-Cl**), Ru(CHPh)(H_2IMes)(3Br-py)$_2Cl_2$ (**2.10**), and [Ru(=CHPCy_3)(H_2IMes)Cl_2][BF_4] (**2.7**) were also obtained from Materia, Inc. The compound Ru(≡C:)(PCy_3)$_2Cl_2$ (**2.4**),[37, 39] was referenced to published NMR data.

2.6.3. Synthetic Procedures.

[Ru(CHF)(H_2IMes)(PCy_3)Cl_2] (2.13-F) Method 1: A 0.084 M solution of β-fluorostyrene in pentane (5 mL, 0.4 mmol, 2 equiv) was added to [Ru(CHPh)(H_2IMes)(PCy_3)Cl_2] (**2.2-Cl**) (150 mg, 0.18 mmol). To this suspension, 20 μL of benzene was added. The reaction mixture was stirred for 48 hours then cooled at –35°C for 3 hours. Filtration and washing with 3 × 2mL of cold pentane afforded **2.13-F** as an orange powder (108 mg, 0.137 mmol) in 77.4% yield. This compound can be recrystallized from pentane/toluene or pentane/benzene in which case 1 equiv arene is retained. ^{1}H NMR (400 MHz, C_6D_6): δ = 13.1 (d, $^2J_{HF}$= 106 Hz, 1H, Ru=CF*H*), 6.8 (s, 2H, mesityl *meta*), 6.7 (s, 2H, mesityl *meta*), 3.3 (s, 4H, H_2IMes –CH_2CH_2-), 2.7 (s, 6H, mesityl *ortho*-CH_3), 2.6 (s, 6H, mesityl *ortho*-CH_3), 2.1 (s, 3H, mesityl *para*-CH_3), 2.0 (s, 3H, mesityl *para*-CH_3), 2.5 (broad q, 3H, PCy_3), 1.0 – 1.8 (PCy_3). ^{13}C{^{1}H} NMR (100.6 MHz, C_6D_6): δ = 283 (d, $^1J_{CF}$ = 416 Hz, Ru=*C*FH), 219 (d, $^3J_{CF}$ = 82 Hz, H_2IMes C_α), 139.2 (s, mesityl *meta/ortho*), 138.5 (s, mesityl *ipso/para*), 138.4 (s, mesityl *ipso/para*), 138.3 (s, mesityl *meta/ortho*), 137.3 (s, mesityl *ipso/para*), 134.9 (s, mesityl *ipso/para*), 130.1 (s, mesityl *meta/ortho*), 129.8 (s, mesityl *meta/ortho*), 51.9 (d, J ≅ 3 Hz, H_2IMes –*C*H_2*C*H_2-), 50.8 (d, J ≅ 2 Hz, H_2IMes –*C*H_2*C*H_2-) 31.8 (d, $^2J_{PC}$= 17.5 Hz, P*C*y_3), 29.5 (s, mesityl *ortho*-*C*H_3), 28.1 (d, $^3J_{PC}$ = 10.5 Hz, P*C*y_3), 26.6 (s, mesityl *para*-*C*H_3), 21.1 (d, $^4J_{PC}$= 3.0 Hz, P*C*y_3), 19.6 (d, $^1J_{PC}$=109.1 Hz, P*C*y_3). ^{31}P{^{1}H} NMR: (161.9 MHz, C_6D_6):

δ = 32.6 (d, J_{PF} unresolved). ^{19}F NMR: (376.3 MHz, C_6D_6) δ = 113.7 (dd, $^2J_{FH}$ = 106 Hz, J_{PF} = unresolved). Anal. Calcd. for **2.13-F** •C_7H_8. For $C_{40}H_{60}Cl_2FN_2PRu$•C_7H_8: C, 63.93%; H, 7.76%; N, 3.17%. Found C, 63.74%; H, 7.70%; N, 3.18%. Method 2: Compound **2.2-Cl** (1.01 g, 1.19 mmol) was dissolved in 50 mL of C_6H_6 and placed in a 600 mL bomb flask and removed from the glove box. The bomb flask was evacuated and filled with vinyl fluoride (10 psig). The solution was stirred at 50 °C for 3h. The solution was then concentrated to 20 mL total volume and 100 mL of pentane was added. A black precipitate was removed by filtration in air. The orange filtrate was then placed in a round-bottom flask, and volatiles were removed in vacuo. The resulting orange solid was dried *in vacuo* overnight giving compound **2.13-F** (0.92 g, 1.16 mmol) in a 97% isolated yield. Attempts to run this reaction with 2nd generation Grubbs catalyst from Materia failed to yield **2.13-F** but gave 100% conversion to the carbide **2.5-Cl**. The starting material must be pure in order for this reaction to work properly.

Stability of compound 2.13-F to air and water. Compound **2.13-F** (18.0 mg) was dissolved in 1 mL C_6D_6 and a drop of distilled H_2O was added while solution was open to air. The solution was shaken vigorously and monitored by NMR spectroscopy over 7 days. Excess H_2O was apparent in the solution by ^{1}H NMR spectroscopy. After 7 days, very little reaction was seen. ^{31}P NMR spectrum displayed 5% tricyclohexylphosphine oxide, 7% Ruthenium carbide **2.5-Cl**, 83% starting ruthenium **2.13-F**, and 5% of an unknown compound at 32.4 ppm.

[Ru(CHF)(H_2IMes)(py)$_2$Cl$_2$] (2.14-F) Method 1: A 0.32 M solution of β-fluorostyrene in pentane (1.0 mL, 0.27 mmol, 3.9 equiv) was added to a suspension of **2.9** (55 mg, 0.069 mmol) in 0.5 mL of benzene. The reaction mixture was stirred for 48 hours. The mixture was filtered and washed with 3 × 1mL of cold pentane to afford **2.14-F** as a yellow-orange powder (35 mg, 0.052 mmol) in 75% yield. Method 2: Compound **2.13-F** (76 mg, 0.096 mmol) was dissolved in 1 mL pyridine and stirred for 10 minutes. The solution was filtered through celite to remove an insoluble solid. Cold (–35°C) pentane (10 mL) was added to the red-orange filtrate and the solution was cooled at –35°C for 30 minutes. Filtration followed by 4 consecutive washes with 10 mL of cold pentane afforded **2.14-F** an orange-red solid (58 mg, 0.087 mmol) in 91% yield. ^{1}H NMR (400 MHz, C_6D_6 at 60°C): δ = 13.3 (d, $^2J_{HF}$ = 95.2 Hz, 1H, Ru=CF*H*), 8.9 (d, $^3J_{HH}$ = 5.2 Hz, 4H, pyridine *ortho*), 6.7 (s, broad, 6H, pyridine *para* and *meta*), 6.4 (s, broad, 4H, mesityl *meta*), 3.4 (s, 4H, H_2IMes –C*H*$_2$C*H*$_2$-), 2.7 (s, 12H, mesityl *ortho*-C*H*$_3$), 2.0 (s, 6H, mesityl *para*-C*H*$_3$). ^{13}C{^{1}H} NMR (100.6 MHz, C_6D_6): δ = 298.3 (d, $^1J_{CF}$ = 409.3 Hz Ru=*C*HF), 219.1 (s, H_2IMes C_α). Compound **2.14-F** decomposed to the extent of ~50% during data acquisition. It is not stable at the necessary concentration for this length of time. Decomposition products in solution prevented assignment of the aryl and alkyl resonances. ^{19}F NMR: (376.3 MHz, C_6D_6) δ = 130.3 (d, $^2J_{FH}$ = 90.7 Hz). Anal. Calcd. For $C_{32}H_{37}Cl_2FN_4Ru$: C, 57.48%; H, 5.58%; N, 8.38%. Found C, 57.79%; H, 5.77%; N, 8.17%.

[Ru(CHPh)(H_2IMes)(PCy$_3$)Br$_2$] (2.2-Br): Compound **2.2-Cl** (268.4 mg, 0.3261 mmol, 1.000 equiv) was dissolved in 25 mL of tetrahydrofuran along with dry LiBr

(640.4 mg, 7.374 mmol, 22.61 equiv) and stirred for 20 hours at room temperature. The THF was removed in vacuo and the solid was redissolved in cold toluene (20 mL) and filtered through celite. The celite was washed with additional cold toluene until all color passed through (4 × 10 mL). The solution was concentrated to 15 mL and placed in the freezer overnight at –35 °C. After which, the solution was again filtered through celite and washed through with cold toluene (4 × 10 mL). The toluene was removed in vacuo and the solid was redissolved in 10 mL of benzene, frozen, and lyophilized. Compound **2.2-Br** was isolated in 74.7% (222 mg, 0.243 mmol). The NMR spectra indicated that the solid was composed of 92% **2.2-Br** and 8% **2.2-Cl/Br.**

[Ru(CHF)(H_2IMes)(PCy_3)Br_2] (2.17-Br): Compound **2.2-Br** (21.2 mg, 0.0226 mmol, 1.00 equiv) was dissolved in 1 mL of C_6D_6 and placed in a J. Young tube and removed from the glovebox. The J. Young tube was evacuated and refilled with vinyl fluoride gas (5 psig, excess). The reaction mixture was placed in an oil bath at 35 °C for 2 hours. After which the reaction mixture was cooled and NMR data was acquired for **2.17-Br**. ^{1}H NMR (400 MHz, C_6D_6): δ(major product) = 12.97 (d, J = 105.2 Hz, 1H), 6.81 (s, H_2IMes aryls, 2H), 6.73 (s, H_2IMes aryls, 2H), 3.28 (H_2IMes backbone, 4H), 2.75 (s, 6H), 2.66 (s, 6H), 2.11 (s, 3H), 2.05 (s, 3H), 1.85-1.05 (m, PCy_3, 33H). δ(minor product) = 13.07 (d, J = 106 Hz, **2.17-Cl/Br**). ^{19}F NMR (376.353 MHz, C_6D_6): δ = 124.3 (dd, $^2J_{HF}$ = 105 Hz, $^3J_{FP}$ = 7 Hz, 93.2%), 118.5 (d, $^2J_{HF}$ = 108 Hz, 6.8%). ^{31}P NMR (161.914 MHz, C_6D_6): δ = 32.4 (broad s, very small), 31.5 (broad s, 6%), 31.0 (d, $^3J_{FP}$ = 7 Hz, 94%). ^{13}C NMR (100.6 MHz, C_6D_6): δ = 285.9 (d, $^1J_{CF}$ = 422.8 Hz), 219.1 (d, $^3J_{CF}$ = 81.4 Hz), 138.86, 138.50, 138.39, 138.17, 137.15, 134.92, 130.16, 129.95, 128.56, 52.1

(d, J = 3.6 Hz), 50.9 (d, J = 9.9 Hz), 32.4 (d, J = 18.2 Hz), 29.9, 28.1 (d, J = 9.9 Hz), 26.59, 21.16, 21.1 (d, J = 3.6 Hz), 19.8.

The volatiles were removed from the solution and the product was isolated as a bright orange powder (no yield was obtained).

[Ru(CHPh)(H_2IMes)(PCy_3)I_2] (2.2-I): Compound **2.2-Cl** (368 mg, 0.433 mmol, 1.00 equiv) was dissolved in 15 mL of tetrahydrofuran along with dry NaI (1.25 g, 8.24 mmol, 19.0 equiv) and stirred for 20 hours at room temperature. A white solid was filtered from the solution. The THF was removed *in vacuo* and the solid was redissolved in cold toluene (20 mL) and filtered through celite. The celite was washed with additional cold toluene until all color passed through (4 × 10 mL). The toluene was removed in vacuo and the solid was redissolved in 10 mL of benzene, frozen, and lyophilized. Compound **2.2-I** was isolated in 49.7% (221.5 mg, 0.215 mmol). The NMR spectra indicated that the solid was composed of only **2.2-I.**[19]

[Ru(CHF)(H_2IMes)(PCy_3)I_2] (2.17-I): Compound **2.2-I** (20 mg, 0.019 mmol, 1.0 equiv) was dissolved in 1 mL of C_6D_6, placed in a J. Young tube and removed from the glovebox. The J. Young tube was evacuated and refilled with vinyl fluoride gas (5 psig, excess). The reaction mixture was placed in an oil bath at 45 °C for 1 hour. After which the reaction mixture was cooled and NMR data was acquired for **2.17-I**. ^{1}H NMR (400 MHz, C_6D_6): δ = 18.57 (Ru(CHH), ~1%), 12.37 (d, $^2J_{HF}$ = 105.2 Hz, 1H), 9.56 (impurity, 3%), 6.75 (s, H_2IMes aryl), 6.69 (s, H_2IMes aryl), 3.31 (m, H2IMes backbone, 4H), 3.1 (m, PCy_3), 2.76 (s, H_2IMes-CH_3, overlapping), 2.75 (s, H_2IMes-CH_3,

overlapping, 12H total), 2.08 (s, H_2IMes-CH_3, 3H), 2.00 (s, H_2IMes-CH_3, 3H), 2.0-0.8 (PCy_3). ^{19}F NMR (376.4 MHz, C_6D_6): δ = 146.18 (dd, $^2J_{HF}$ = 103.9 Hz, $^3J_{FP}$ = 10.2 Hz). ^{31}P NMR (161.9 MHz, C_6D_6): δ = 47.97 (broad s, 26%), 31.15 (d, 74%). The product, **2.17-I**, was not isolated cleanly.

[Ru(CHPh)(H_2IMes)(PPh_3)Cl_2] (2.3): Compound **2.9** (154 mg, 0.212 mmol, 1.00 equiv) was dissolved in 10 mL of benzene and triphenylphosphine (93.4 mg, 0.356 mmol, 1.68 equiv) was added. The reaction mixture was stirred for 1 hour and the solution was held under vacuum for thirty seconds every 15 minutes. The mixture was concentrated to 5 mL and 15 mL of pentane was added. The solution was placed in the freezer at −35 °C overnight. A red precipitate was isolated by filtration and washed with 3 × 10 mL pentane. The product, **2.3**, was isolated in 95.4% yield (143.2 mg, 0.2021 mmol).[38]

[Ru(CHF)(H_2IMes)(PPh_3)Cl_2] (2.16) Method 1: Compound **2.3** (18.4 mg, 0.0260 mmol, 1.00 equiv.) was dissolved in 1 mL C_6D_6 and put in a J. Young tube. The reaction was removed from the glovebox and the J. Young tube was evacuated and refilled with vinyl fluoride gas (5 psig, 2 mL, excess). The reaction was allowed to sit at room temperature for one hour and then NMR data was acquired. ^{1}H NMR (400 MHz, C_6D_6): δ(major product) = 12.88 (dd, $^3J_{PF}$ = 2 Hz, $^2J_{FH}$ = 110.4 Hz, 1H), 7.85 (s, impurity, 0.4H) 7.58 (tt, PPh_3, 6H), 7.14 (s, overlapping with solvent peak), 6.94 (m, PPh_3, 9H), 6.69 (s, 4H), 6.56 (s, 1H), 3.99 (s, impurity, 1H), 3.54 (s, impurity, 0.2H), 3.27 (s, H_2IMes backbone, 4H), 2.54 (bs, 12H), 2.13 (bs, 3H), 2.03 (bs, 3H), 1.99 (s, impurity,

2H), 1.91 (bs, impurity, 6H). Based on proton NMR spectrum, **2.16** is the major product; however, there are two other ruthenium products containing an H_2IMes ligand. ^{13}C NMR (100.596 MHz, C_6D_6): δ = 290.8 (dd, $^1J_{CF}$ = 420.8 Hz, $^2J_{CP}$ = 60 Hz), 216.06 (d, $^3J_{CF}$ = 102.7 Hz), 163.1 (s), 137.9 (s), 136.5 (s), 134.9 (d, J = 10.3 Hz), 132.4 (d, J = 40.6 Hz), 130.1 (s), 129.4 (d, J = 1.9 Hz), 128.5 (s), 128.1 (s), 51.3 (bs), 46.6 (s, minor product), 44.2 (s), 21.0 (bs), 20.8 (s), 20.2 (bs), 18.8 (bs), 18.2 (s). ^{31}P NMR (121.476 MHz, C_6D_6): δ = 34.3 (d, $^3J_{PF}$ = 54.1 Hz). ^{19}F NMR (376.337 MHz, C_6D_6): δ = 137.33 (dd, $^1J_{FH}$ = 110.2 Hz, $^3J_{FP}$ = 54.2 Hz). Method 2: Compound **2.14-F** (12.2 mg, 0.0182 mmol, 1.00 equiv) was dissolved in C_6D_6 (1 mL). Triphenylphosphine (23.9 mg, 0.0911 mmol, 5.01 equiv) was added to the reaction mixture. After 30 minutes, the ^{1}H, ^{31}P, and ^{19}F NMR spectra showed 60% conversion to product (**2.16**). The volatiles were removed from the reaction mixture and the solids were redissolved in 1 mL of C_6D_6. At this point, one major product (**2.16,** 73%) was observed along with 2 minor products (^{31}P NMR δ = 34.4 (**2.6,** 16%) and 22.0 (unidentified, 11%)). All starting material, **2.14-F**, had been consumed.

[Ru(≡C:)(H_2IMes)(PPh_3)Cl_2] (2.6): The above reaction (Method 2) was left in solution for 3 hours over which time complete decomposition to **2.6** was observed by ^{31}P NMR spectroscopy. ^{31}P NMR: δ = 34.4 (99%), 27.8 (1%, unidentified). Decomposition rate varied depending on purity of solvent and **2.16**.

[Ru(CHF)(PCy_3)$_2Cl_2$] (2.12-F): Compound **2.1** (122.5 mg, 0.1488 mmol, 1.000 equiv) was dissolved in 20 mL of C_6H_6 and the solution was placed in a bomb flask. The

bomb flask was removed from the glovebox, evacuated and refilled with vinyl fluoride gas (5 psig, excess). The solution was stirred for 1 hour at 45 °C and the solution was then concentrated to dryness under vacuum. The solution was redissolved in 10 mL of benzene and lyophilized. An orange solid, **2.12-F**, was isolated in 97.4% yield. NMR data confirmed the formation of **2.12-F**; however, there was a small amount of carbide formation (6.7%). Attempts to separate the carbide (**2.4**) from the product, **2.12-F,** failed. ^{1}H NMR (300 MHz, C_6D_6): δ = 14.19 (d, $^{2}J_{HF}$ = 110.1 Hz, 1H), 7.92 (m, impurity, 0.4H), 7.73 (m, impurity, 0.4H), 2.77 (bs, 6H), 2.5-0.9 (PCy_3, 72H). ^{31}P NMR (121.476 MHz, C_6D_6): δ = 38.98 (s, 6.7%, **2.4**), 34.12 (d, $^{3}J_{PF}$ = 13.7 Hz, 93%). ^{19}F NMR (282.347 MHz, C_6D_6): δ = 127.0 (dt, $^{2}J_{FH}$ = 111.2 Hz, $^{3}J_{FP}$ = 13.8 Hz). ^{13}C NMR (100.596 MHz, C_6D_6): δ = 473.19 (s, carbide), 283.64 (d, $^{1}J_{CF}$ = 418.8 Hz), 135.22, 135.12, 130.06, 32.50 (t, J = 9.2 Hz), 32.15 (t, J = 9.9 Hz), 30.61, 30.41, 30.13, 28.12 (m), 27.00, 26.82. The solution was left overnight. At that point there was 13% **2.4** and 87% product. After 48h, there was 20% carbide (**2.4**) and 80% product (**2.12-F**).

[Ru(CHF)(H_2IMes)(3Br-py)$_2$$Cl_2$] (2.15) Method 1: Compound **2.10** (61.5 mg, 0.0695 mmol, 1.00 equiv) was dissolved in 3 mL of benzene and the solution was placed in a bomb flask. The bomb flask was evacuated and refilled with vinyl fluoride gas (5 psig, excess). The solution was stirred for 45 minutes at room temperature. The mixture changed from a yellow/green color to orange/red in the first five minutes. The solution was filtered and then frozen and the benzene was removed by lyophilization. The solid was then dissolved in a benzene/pentane mixture (1:5) and the red solution was decanted away from an unidentified yellow solid. The solvent was removed from the red solid and

the solid was dissolved in 5 mL of benzene, frozen and lyophilized. No yield was determined for this reaction. NMR data confirmed the formation of **2.15**. ^{1}H NMR (400 MHz, C_6D_6): δ = 13.14 (d, $^{2}J_{HF}$ = 92.4 Hz, 1H), 9.224 (s, 3Br-py, 2H), 8.90 (s, 3Br-py, 2H), 6.80 (s, H_2IMes aryls, overlapping) ~6.65 (bs, 3Br-py, overlapping), 6.46 (s, H_2IMes aryls, overlapping, 6H total), ~5.92 (bs, 3Br-py, 2H), 3.29 (s, H_2IMes backbone, 4H), 2.64 (s, H_2IMes methyls, 12H), 2.04 (bs, H_2IMes methyls, overlapping), 1.92 (bs, H_2IMes methyls, overlapping, 6H total). ^{19}F NMR (282.347 MHz, C_6D_6): δ = 131.85 ($^{2}J_{FH}$ = 91.8 Hz). Method 2: Compound **2.13-F** (120 mg, 0.15 mmol, 1.0 equiv) was dissolved in 5 mL of 3-bromopyridine and stirred for 10 minutes. To the solution, 15 mL of pentane was added and the solution was placed in the freezer overnight at –35 °C. The solution was then filtered and the orange/red solid, **2.15** was collected in a 36% yield (44 mg, 0.53 mmol). The solid was stirred in minimum benzene and an undissolved red solid was isolated for elemental analysis. Anal. Calcd. For $C_{32}H_{35}Cl_2Br_2FN_4Ru$•HF: C, 45.41%; H, 4.29%; N, 6.62%. Found C, 45.53%; H, 4.22%; N, 6.67%. Elemental analysis revealed that **2.15•HF** could be isolated cleanly. It appears that the actual product used for elemental analysis was [Ru(CHF)H_2IMes(3Br-py)Cl_2]•3-bromopyridinium fluoride indicating 50% decomposition of **2.15** to form the corresponding carbide and HF which then reacts with an equivalent of 3-bromopyridine. The corresponding carbide would decompose further in the benzene solution while the HF would react with one of two equivalents of the 3-bromopyridine, forming the pyridine salt and [Ru(CHF)H_2IMes(3Br-py)Cl_2]. [Ru(CHF)H_2IMes(3Br-py)Cl_2] would be less susceptible to decomposition because the Ru-center would be more electron deficient and therefore, less likely to undergo the formal oxidation step needed to form the carbide (Scheme 2.9).

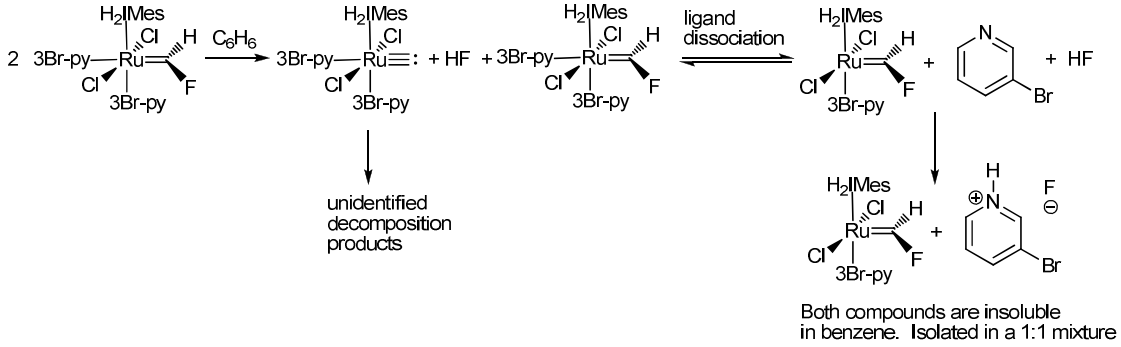

Scheme 2.9. Reactivity of **2.15** in Benzene

Formation of [Ru(≡C:)(H_2IMes)(PCy_3)Cl_2] (2.5-Cl) from 2.13-F

1) Compound **2.13-F** (10 mg, 0.013 mmol) was dissolved in 1 mL CD_2Cl_2. The resulting solution was stored in an air tight NMR tube at room temperature (23 ^oC). Complete conversion to **2.5-Cl** was observed by ^{31}P and ^1H NMR spectroscopy between 5 and 16 h.

2) Compound **2.13-F** (10 mg, 0.013 mmol) was dissolved in 1 mL C_6D_6. The resulting solution was stored in an air tight NMR tube at room temperature (23 ^oC). Complete conversion to **2.5-Cl** was observed by ^{31}P and ^1H NMR spectroscopy after 5 days.

3) Compound **2.13-F** (31.6 mg, 0.0400 mmol) was dissolved in 1 mL C_7D_8 with PCy_3 (16.8 mg, 0.0599 mmol, 1.50 equiv) for ^{31}P NMR magnetization transfer experiment. Decomposition to form 100% **2.5-Cl** in toluene-d_8 was observed after heating to 80 °C for 1 h. In another case under identical conditions, only 3% conversion to **2.5-Cl** was noted after being subjected to temperatures of 80 °C for 1 h followed by 55 °C for 4 h and finally 23 °C for 7 d.

4) Compound **2.13-F** (10 mg, 0.013 mmol) was dissolved in 1 mL CD_2Cl_2. Chlorotrimethylsilane (3.2 μL, 0.026 mmol, 2.0 equiv) was added to the solution of **2.13-**

F. Complete conversion to **2.5-Cl** was observed by ^{31}P and ^{1}H NMR spectroscopy after 30 minutes; 1 equiv Me_3SiF was also formed.

5) Compound **2.13-F** (10 mg, 0.013 mmol) was dissolved in 1 mL C_6D_6. Hydrogen chloride (anhydrous, 2M solution in diethyl ether; 6.3 μL, 0.013 mmol, 1.0 equiv) was added to the solution of **2.13-F**. After 1 h, observation by ^{1}H and ^{31}P NMR spectroscopy revealed that **2.13-F** had been completely consumed, and **2.5-Cl** was the major product (89%). An unidentified compound accounted for the remainder of the material (byproduct signal: $^{31}P\{^{1}H\}$ NMR (C_6D_6): δ = 27.1 ppm)

6) Compound **2.13-F** (10 mg, 0.013 mmol) was dissolved in 1 mL C_6D_6. Vinyl acetate (11.6 μL, 0.13 mmol, 10 equiv) was added to the solution of **2.13-F**. Complete conversion to **2.5-Cl** was observed by ^{31}P and ^{1}H NMR spectroscopy after 6 hours. There was no evidence of metathesis of **2.13-F** with vinyl acetate (no vinyl fluoride or acetic acid observed).

7) Compound **2.13-F** (10 mg, 0.013 mmol) was dissolved in 1 mL C_6D_6. Sulfur (3 mg, 0.13 mmol, 8 equiv S) was added to the solution of **2.13-F**. Complete conversion to **2.5-Cl** was observed by ^{31}P and ^{1}H NMR spectroscopy after 5 hours. Sulfur continued to react with **2.5-Cl** to form the thiocarbonyl compound, $[Ru(CS)(H_2IMes)PCy_3Cl_2]$ and then to trap released PCy_3 by formation of $S{=}PCy_3$, as is seen in the reaction of related $Ru(C)(PCy_3)_2Cl_2$ (**2.4**) with S_8.[19]

General method for ring-closing metathesis (RCM) reactions with diethyl diallylmalonate. Diethyl diallylmalonate (24.2 μL, 0.100 mmol) was added to 1.0 mL of stock solution of C_6D_6 containing 1,3,5-trimethoxybenzene (0.200 mmol, 33.6 mg in 4.0

mL of C_6D_6). A ^1H NMR spectrum of the solution was acquired. Compound **2.13-F** (2.4 mg, 0.0030 mmol, 3.0 mol%), **2.14-F** (2.0 mg, 0.0030 mmol, 3.0 mol%), and **2.2-Cl** (2.5 mg, 0.0030 mmol, 3.0 mol%) were each added to separate air tight NMR tubes containing the diethyl diallylmalonate solutions. NMR tubes were heated to 60 °C. NMR tubes were opened to N_2 on a Schlenk line for 30 seconds every 30 minutes. ^1H NMR spectra were obtained every hour for 4 consecutive hours.

General method for cross metathesis (CM) reactions with 1-hexene. 1-Hexene (12.4 μL, 0.100 mmol) was added to 1.0 mL of stock solution of C_6D_6 containing 1,3,5-trimethoxybenzene (0.200 mmol, 33.6 mg in 4.0 mL of C_6D_6). A ^1H NMR spectrum of the solution was acquired. Compound **2.13-F** (2.4 mg, 0.0030 mmol, 3 mol%), **2.14-F** (2.0 mg, 0.0030 mmol, 3 mol%), and **2.2-Cl** (2.5 mg, 0.0030 mmol, 3 mol%) were each added to an air tight NMR tube containing 1-hexene solutions. NMR tubes were opened to N_2 on a Schlenk line for 30 seconds every 30 minutes. ^1H NMR spectra were obtained every hour for 4 consecutive hours. Additional ^1H NMR spectra were acquired 9, 33, and 76 hours after the reaction was started.

Attempted reactions of ethyl vinyl ether with 2.13-F and 2.14-F. Compound **2.13-F** (10 mg, 0.013 mmol) was dissolved in 1 mL C_6D_6 and ethyl vinyl ether (12 μL, 0.13 mmol, 10 equiv) was added. No reaction was observed by NMR monitoring over three days.

Compound **2.13-F** (19.6 mg, 0.0245 mmol, 1 equiv), internal standard (17.8 mg, 0.0608 mmol) and ethyl vinyl ether (3.9 mg, 0.054 mmol, 2.2 equiv) were dissolved in 1

mL C_6D_6 and the solution was heated to 80 °C in a J. Young tube for 1 hour, after which time NMR data were collected. The ^{31}P NMR spectrum showed 92% Ru carbide (**2.5-Cl**), 4% Ru(=CHF) complex (**2.13-F**), and 4% Ru(=CHOEt) complex (**2.13-OEt**). Metathesis is in competition with decomposition of compound **2.13-F**. High temperatures are required because liberation of the tricyclohexylphosphine is slow.

Compound **2.14-F** (10 mg, 0.015 mmol) was dissolved in 1 mL C_6D_6 and ethyl vinyl ether (7 μL, 0.07 mmol, 5 equiv) was added. Within 2 hours, >99% conversion to the corresponding ethoxycarbene complex (**2.14-OEt**) and vinyl fluoride was observed by NMR spectroscopy.

Alternate Synthesis of [Ru(CHOEt)(H_2IMes)(py)$_2$Cl$_2$] (2.14-OEt). Ru(CHPh)(H_2IMes)(py)$_2$Cl$_2$ (**2.9**) (15 mg, 0.021 mmol) was dissolved in 1 mL C_6D_6 and ethyl vinyl ether (8μL, 0.084 mmol, 4 equiv) was added. An immediate color change from green to orange was observed. The ^1H NMR spectrum showed 100% conversion to **2.14-OEt;** 1 equivalent of styrene was also observed. ^1H NMR (400 MHz, C_6D_6): δ = 14.0 (s, 1H, Ru=C*H*), 9.2 (s, broad, 4H, pyridine *ortho*), 6.8, 6.7, 6.3 (three overlapping peaks, broad s, pyridine *meta and para*, mesityl *meta*), 3.4-3.3 (overlapping signals, H_2IMes –CH_2CH_2-, Ru=CHOCH_2CH$_3$, and excess ethyl vinyl ether), 2.7 (s, 12H, mesityl *ortho*-CH_3), 1.9 (2 overlapping peaks, broad s, 6H total, mesityl *ortho*-CH_3), 0.54 (t, 3H, Ru=CHOCH$_2$CH_3).

Alternative synthesis of [Ru(=CHPCy$_3$)(H_2IMes)Cl$_2$][BF$_4$] (2.7) Ru(=CHF)(H_2IMes)(PCy$_3$)Cl$_2$ (**2.13-F**) (100 mg, 0.126 mmol, 1.00 equiv) was dissolved

in 10 mL of C_6H_6 and placed in a 100 mL round-bottom flask with septum and removed from the glove box. BF_3•OEt_2 (20 µL, 0.158 mmol, 1.25 equiv) was added via syringe to the solution of **2.13-F** with stirring at 23 °C. The solution immediately began to darken to a brown/black color. A precipitate started to form within 30 minutes and the reaction mixture was left to stir for 3 hours to ensure completion. The precipitate was then filtered in air, rinsed with pentane (3 × 5 mL), dried, and transferred into the glove box. ^{31}P, ^{19}F, and ^{1}H NMR spectra indicated that [Ru(=CHPCy$_3$)(H_2IMes)Cl_2][BF_4] (**2.7**, 76 mg, 0.089 mmol) [26] had formed cleanly in a 70.3% isolated yield.

Conversion of Ru(=CHPCy$_3$)(H_2IMes)Cl_3 (2.8-Cl) to [Ru(=CHPCy$_3$)(H_2IMes)Cl_2][BF_4] (2.7). Compound **2.8-Cl** (10 mg, 0.010 mmol, 1.0 equiv) was dissolved in 1 mL of THF and $AgBF_4$ (2.6 mg, 0.013 mmol, 1.3 equiv) was added. After 30 min, a ^{31}P NMR spectrum showed about 50% conversion of starting material to **2.7.** More $AgBF_4$ (3.0 mg, 0.015 mmol, 1.5 equiv) was added to the reaction mixture. After an additional 30 min, a ^{31}P NMR spectrum indicated formation of **2.7** (60%) and a second unidentified product at 35.2 ppm (40%).

Synthesis and Properties of Ru(=CHPCy$_3$)(H_2IMes)Cl_3 (2.8-Cl) Method 1: Piers' compound, [Ru(=CHPCy$_3$)(H_2IMes)Cl_2][BF_4], (**2.7**), (11.0 mg, 0.0128 mmol, 1.00 equiv) was dissolved in 0.8 mL of CD_2Cl_2. The solution was added to 60 µL (3.0 mg, 0.012 mmol, 0.94 equiv) of a stock solution of $^{n}Bu_4NCl$ (20 mg in 400 µL). The reaction mixture turned yellow immediately. ^{31}P and ^{1}H NMR spectra indicated formation of **2.8-Cl** as the major product (>95%). The same result was observed with 5 equiv of $^{n}Bu_4NCl$.

Difficulty separating the product from the ionic byproduct made this an impractical synthesis for **2.8-Cl**. Method 2**:** Ru(=CHF)(H_2IMes)(PCy_3)Cl_2 (**2.13-F**) (90.0 mg, 0.114 mmol, 1.00 equiv) was dissolved in 10 mL of C_6H_6 and BCl_3 solution (1.0 M in heptane, 114 μL, 0.114 mmol, 1.00 equiv) was added. Over 20 minutes, a brown precipitate formed and the supernatant solution became colorless. ^{31}P and ^{1}H NMR spectra revealed consumption of all starting material. The precipitate was filtered and washed with toluene (2 × 3mL) and pentane (2 × 3mL). The ^{31}P and ^{1}H NMR spectra (CD_2Cl_2) indicated formation of a compound similar to Piers' complex ([Ru(=CHPCy_3)(H_2IMes)Cl_2][BCl_xF_y] where x + y = 4; 105 mg isolated): the ^{31}P and ^{1}H NMR spectra are identical to those of **2.7** but ^{19}F NMR spectroscopy indicates that fluorine is present. The solid turned yellow upon dissolution in THF (3mL) and pentane (10 mL) was added to the solution which was then cooled to –30 °C overnight. The yellow precipitate was then filtered, washed with pentane (3 × 5 mL), and dried in vacuo for 2 h giving a 43% yield of **2.8-Cl** (40 mg, 0.050 mmol). ^{1}H NMR spectroscopy showed that clean conversion to Ru(=CHPCy_3)(H_2IMes)Cl_3 (**2.8-Cl**) had occurred. Recrystallization of **2.8-Cl** involved slow diffusion of pentane into THF-d_8 at 28 °C. Yellow needlelike crystals were obtained for a single-crystal X-ray diffraction study. A solution of **2.8-Cl** in CD_2Cl_2 was left open to air and showed no decomposition even after 2 days. NMR data for **2.8-Cl:** ^{1}H NMR (400 MHz, CD_2Cl_2): δ = 19.8 (d, $^{2}J_{HP}$= 50.4 Hz, 1H, Ru=C*H*PCy_3), 7.0 (broad s, 4H, mesityl *meta*), 4.0 (broad s, 4H, H_2IMes –CH_2CH_2-), 3.0 (q, 3H, PCy_3 H_α), 2.3 (s, mesityl CH_3), 1.7 (s, mesityl CH_3), 1.0 – 2.5 (m, 51H, PCy_3, overlapping with mesityl CH_3). ^{13}C{^{1}H} NMR (100.6 MHz, CD_2Cl_2): δ = 269.7 (t, $^{1}J_{CP}$ = 14 Hz, Ru=*C*HPCy_3), 204.4 (d, $^{3}J_{CP}$ = 3.0 Hz, H_2IMes C_α), 139.3 (two broad overlapping

s, mesityl), 130.2 (broad s, mesityl), 128.8 (s, mesityl), 52.5 (broad s, H_2IMes -*C*H_2*C*H_2-), 34.5 (d, $^1J_{PC}$= 142.9 Hz, P*Cy*$_3$), 27.8 (d, $^3J_{PC}$ = 14.0 Hz, P*Cy*$_3$), 27.3 (d, $^2J_{PC}$= 47.6 Hz, P*Cy*$_3$), 26.2 (d, $^4J_{PC}$= 6 Hz, P*Cy*$_3$), 21.6 (broad s, mesityl *C*H_3), 20.5 (broad s, mesityl *C*H_3), 19.0 (broad s, mesityl *C*H_3). $^{31}P\{^1H\}$ NMR: (161.9 MHz, CD_2Cl_2): δ = 32.2 (d, J = 3.4 Hz).

Attempt to observe intermediate(s) at low temperature. Ru(=CHF)(H_2IMes)(PCy_3)Cl_2 (**2.13-F**) (10.0 mg, 0.0126 mmol, 1.00 equiv) was dissolved in 1 mL of toluene-d_8 and the solution was cooled to –40 °C. Chilled BCl_3 was added (12.6 µL, 0.0126 mmol, 1.00 equiv). The reaction was kept at –40 °C but NMR showed only consumption of starting material and no formation of new carbene peaks. The product precipitated from toluene-d_8 as it had from benzene. Dissolution of the brown solid in THF showed only **2.8-Cl** as the product. The above reaction was also run with 10 equiv of BCl_3 with the same result.

Stability of 2.8-Cl to Hunig's base. Compound **2.8-Cl** (10 mg, 0.012 mmol) was dissolved in 1 mL of C_6D_6 and three drop of diisopropylethylamine (> 10 equiv by ^1H NMR) was added. No reaction was seen up to five days.

Attempted ring-closing metathesis (RCM) with 2.8-Cl as a catalyst. Ru(=CHPCy_3)(H_2IMes)Cl_3 (**2.8-Cl**) (3 mg, 0.004 mmol, 10mol%, 1 equiv) was dissolved in 1 mL C_6D_6 and diallyl diethylmalonate (10 µL, 0.041 mmol, 10 equiv) was added. The solution was monitored for 47 hours. After 15 min, 4 hours, 24 hours, and 47 hours;

11%, 21%, 37% and 41% of the starting material had been converted to the ring-closed product respectively.

Stoichiometric Olefin Metathesis with Vinyl Halides

With Vinyl Chloride. Ru(=CHPh)(H_2IMes)(PCy_3)Cl_2 (**2.2-Cl**) (20.6 mg, 0.0243 mmol, 1.00 equiv) was dissolved in 1 mL of C_6D_6. The solution was added to a J. Young tube and frozen. The head space was evacuated, and then vinyl chloride (1 atm, 0.08 mmol, < 4 equiv) was added. The solution was thawed and mixed thoroughly. After 20 min, ^{1}H NMR showed about 1 equiv of vinyl chloride in solution and a small amount of styrene (< 5%) was observed indicating metathesis was taking place. Table 2.7 gives percentages of ruthenium products and starting material based on the relative integrations of the ^{31}P NMR spectra over time. After 19 hours, there was complete consumption of **2.2-Cl** and styrene formation (0.9 equiv relative to initial amount of **2.2-Cl**) was observed. The ruthenium products consisted of Ru(≡C:)(H_2IMes)(PCy_3)Cl_2 (**2.5-Cl**) and Ru(=CHPCy_3)(H_2IMes)Cl_3 (**2.8-Cl**) in a 1 to 2.2 ratio respectively by ^{31}P NMR spectroscopy. There was also one minor unidentified product (δ ^{31}P = 32.4 ppm, 9%; δ ^{1}H = 16.2 ppm). The ratio of products **2.5-Cl** and **2.8-Cl** is consistent within error throughout the reaction time indicating a common intermediate for both **2.5-Cl** and **2.8-Cl**.

Table 2.7. Stoichiometric Metathesis of **2.2-Cl** and Vinyl Chloride

Total time (h)	*2.5*	*16*	*19*
2.5-Cl (%)	9	27	63
2.8-Cl (%)	19	56	28
2.2-Cl (%)	71	10	0
32.4 ppm (%)	1	7	9
Ratio (**2.8-Cl/2.5-Cl**)	2.1	2.1	2.2

With 1,2-Dichloroethylene. $Ru(=CHPh)(H_2IMes)(PCy_3)Cl_2$ (**2.2-Cl**) (20 mg, 0.024 mmol) was dissolved in 1 mL of C_6D_6 and 1,2-dichloroethylene (1.8 μL, 0.024 mmol, 1.0 equiv) was added. After 2 h, very little reaction had taken place (< 2% by ^1H NMR spectroscopy). After 4 h, another 3.0 μL (0.040 mmol, 1.6 equiv) of 1,2-dichloroethylene was added. Table 2.8 gives percentages of ruthenium products and starting material based on the relative integrations of the ^{31}P NMR spectra over time.

Table 2.8. Stoichiometric Metathesis of **2.2-Cl** and 1,2-Dichloroethylene

Total time (h)	*6.5*	*9*	*21*	*33*	*46*	*73*
2.5-Cl (%)	5	7	15	22	n/a	26
2.8-Cl (%)	14	17	42	60	n/a	74
2.2-Cl (%)	81	76	43	18	6	0
Ratio (**2.8-Cl /2.5-Cl**)	2.8	2.4	2.8	2.7	n/a	2.8

After 73 hours, there was complete consumption of **2.2-Cl**. The ruthenium products consisted of $Ru(\equiv C:)(H_2IMes)(PCy_3)Cl_2$ (**2.5-Cl**) (26% by ^{31}P NMR) and $Ru(=CHPCy_3)(H_2IMes)Cl_3$ (**2.8-Cl**) (74% by ^{31}P NMR; 0.7 equiv with respect to the initial amount of **2.2-Cl** by ^1H NMR spectroscopy). Volatiles from the reaction mixture

were separated by vacuum transfer and the NMR and GC-MS were acquired. Both *cis* and *trans* isomers of β-chlorostyrene were seen in a 1 to 2 ratio by ^{1}H NMR in 92% yield with respect to the initial amount of **2.2-Cl**. *Cis*- and *trans*-β-chlorostyrene was the only styryl containing products observed by ^{1}H NMR and GC-MS. ^{1}H NMR (400 MHz, C_6D_6): δ = 7.3 – 7 (*Ph*HC=CHCl), 6.50 (d, *trans* PhHC=C*H*Cl, $^3J_{HH}$ = 13.6 Hz), 6.15 (d, *trans* Ph*H*C=CHCl, $^3J_{HH}$ = 13.6 Hz), 6.08 (d, *cis* PhHC=C*H*Cl, $^3J_{HH}$ = 8 Hz), 5.73 (d, *cis* Ph*H*C=CHCl, $^3J_{HH}$ = 8.4 Hz).

With 1-Chloro-1-propene. Ru(=CHPh)(H_2IMes)(PCy_3)Cl_2 (**2.2-Cl**) (20.7 mg, 0.0244 mmol) was dissolved in 1 mL of C_6D_6 along with 1,3,5-trimethoxybenzene (2.07 mg, 0.012 mmol). 1-chloro-1-propene (3.6 mg, 0.047 mmol, 1.9 equiv) was then added. ^{1}H and ^{31}P NMR spectra were acquired over 24 h. Table 2.9 shows the relative percentages of products over time based on integrations from ^{31}P NMR spectra.

Table 2.9. Stoichiometric Metathesis of **2.2-Cl** and 1-Chloro-1-propene

Total time (h)	*20 min*	*2*	*4*	*8.5*	*20.5*
2.5-Cl (%)	7	12	18	25	30
2.8-Cl (%)	n/a [a]	27	41	58	68
2.2-Cl (%)	85	59	40	16	0
32.4 ppm (%)	0	1	1	1	2
Ratio (**2.8-Cl/2.5-Cl**)	n/a	2.3	2.3	2.3	2.3

[a] overlap from **2.8-Cl** and **2.2-Cl** made integration unreliable

Reaction reached completion after 20.5 hours with a 1 to 2.3 ratio of **2.5-Cl** to **2.8-Cl**. Proton NMR spectroscopy indicated *trans* and *cis* 1-phenyl-1-propene as the major styryl containing products in a 6 to 1 ratio respectively.[40] ^{1}H NMR (400 MHz, C_6D_6): δ = 7.23-7 (*cis and trans* (CH_3)HC=CH*Ph*), 6.40 (dq, *cis* (CH_3)HC=C*H*Ph, $^3J_{HH}$ = 10 Hz, $^4J_{HH}$ =

unresolved), 6.28 (dq, *trans* (CH_3)HC=C*H*Ph, $^3J_{HH}$ = 15.6 -16 Hz, $^4J_{HH}$ = 1.6 - 2 Hz, quartet appears as broadened doublet), 6.01 (dq, *trans* (CH_3)*H*C=CHPh, $^3J_{HH}$ = 16 Hz, $^4J_{HH}$ = 6.8 Hz), 5.6 (*cis* (CH_3)*H*C=CHPh, obscured by 1-chloro-1-propene), 1.68 (dd, *cis* (C*H*$_3$)HC=CHPh, $^3J_{HH}$ = 6.8-7.6 Hz, $^4J_{HH}$ = 1.6-2.4 Hz), 1.62 (dd, *trans* (C*H*$_3$)HC=CHPh, $^3J_{HH}$ = 6.4-6.8 Hz, $^4J_{HH}$ = 1.2-1.6 Hz). A very small amount (< 1%) of *trans* 2-butene was observed in the ^{1}H NMR spectrum by comparison with independent samples of *cis* and *trans* 2-butene. GC-MS confirmed the presence of *trans* and *cis* 1-phenyl-1-propene.

Observation of Halogen Exchange. Ru(=CHPh)(H_2IMes)(PCy_3)Cl_2 (**2.2-Cl**) (11 mg, 0.013 mmol, 1.0 equiv) was dissolved in 1 mL of C_6D_6 and vinyl bromide (70.6 μL, 1M in THF, 0.0706 mmol, 5.4 equiv) was added. After 2 h, vinyl *chloride* was observed in the ^{1}H NMR spectrum (0.3 equiv) along with styrene (0.4 equiv), starting materials (**2.2-Cl**, 0.3 equiv) and expected decomposition products. Decomposition products consisted of multiple small peaks between 31.44 and 31.02 ppm in the ^{31}P NMR spectrum as well as a large singlet at 17.0 ppm. After 20h, the reaction mixture contained very little (< 0.1 equiv) of **2.2-Cl**, 0.7 equiv of vinyl chloride, and 0.7 equiv of styrene. The plethora of decomposition products precluded their positive identification.

With Vinyl Bromide (1 M solution in THF). Ru(=CHPh)(H_2IMes)(PCy_3)Br_2 (**2.2-Br**) (10.7 mg, 0.0125 mmol, 1.00 equiv) was dissolved in 1 mL of C_6D_6 and vinyl bromide (1 M solution in THF, 20.0 μL, 0.0200 mmol, 1.6 equiv) was added. The reaction was monitored by ^{1}H and ^{31}P NMR spectroscopy. The reaction reached completion with 2% starting material left (based on ^{1}H NMR); styrene was identified in ^{1}H NMR spectrum. At 8h, the ^{31}P NMR spectrum showed 4 products δ = 33.0 (**2.5-Br**, 6%), 31.3 (**2.8-Br**, 55%), 30.3 (**2.2-Br** or unidentified**,** 7.4%), 14.5 (unidentified, 31%)

(ratio 1 : 9.2 : 1.2 : 5.2 respectively). After 26h, a ^{31}P NMR spectrum showed 3 products δ = 33.0 (**2.5-Br**, 7%), 31.3 (**2.8-Br**, 83%), 30.3 (**2.2-Br** or unidentified, 9.4%) (ratio 1 : 11.9 : 1.3 respectively). The ^{1}H NMR spectrum indicated that two phosphoniocarbene complexes had formed δ = 19.3 ppm (d, J = 50.4 Hz, 60% with respect to the internal standard set to 1 equiv of **2.2-Br** initially) and 19.5 ppm (d, J = 50.4 Hz, 12%). One possibility for these two products is some residual chloride contamination in the ruthenium starting material.

With Gaseous Vinyl Bromide. Ru(=CHPh)(H_2IMes)(PCy_3)Br_2 (**2.2-Br**) (20.0 mg, 0.0213 mmol, 1.00 equiv) was dissolved in 1 mL of C_6D_6, the solution was frozen, the J. Young tube containing the solution was evacuated and vinyl bromide (1 atm, 0.08 mmol, < 4 equiv) was added to the headspace of the NMR tube. The solution was then thawed and mixed thoroughly. After about 5 minutes, a ^{1}H NMR spectrum showed that about 2 equiv of vinyl bromide had partitioned into the solution. After 2 h, **2.2-Br** had been completely consumed. The ^{1}H NMR spectrum displayed a large doublet in the carbene region (19.3 ppm, $^{2}J_{HP}$ = 50.4 Hz) indicative of **2.8-Br**. There was also a singlet at δ = 15.6 ppm as well as a few small peaks between 19.7 to 19.4 ppm (< 5%). Styrene was also apparent. Multiple products were observed in the ^{31}P NMR spectrum including **2.5-Br** (33.0 ppm, 2%), **2.8-Br** (31.5 ppm, d, 36%), (ratio of **2.5-Br:2.8-Br** was 1 to 18 respectively) and some unknown compounds (31.0 ppm, s, 2%; 30.4 ppm, d, 13%; 28.9 ppm, s, 2%) and a broad singlet at 14.6 ppm (45%). After 20 h, the ^{31}P NMR spectrum showed only 4 products: **2.5-Br** (6%), **2.8-Br** (51%), unknown products at δ = 31.0 (6%) and a broad singlet at 19.3 ppm (37%). The ratio of **2.5-Br** to **2.8-Br** was 1:8.5 respectively.

With β-bromostyrene. $Ru(CHPh)(H_2IMes)(PCy_3)Br_2$ (**2.2-Br**) (20 mg, 0.021 mmol, 1.0 equiv) and β-bromostyrene (4 mg, 0.02 mmol, 1 equiv) were dissolved in 1 mL of C_6D_6 and the reaction was monitored by ^1H and ^{31}P NMR over 11 days. After 11 days, **2.2-Br** was completely consumed and ^{31}P showed one major product, **2.8-Br** (93.3%) and one minor product, **2.5-Br** (6.7%) in a 14 to 1 ratio. ^1H NMR spectrum contains a doublet at 19.3 ppm (J = 50.4 Hz) corresponding with **2.8-Br**. Stilbene was observed as a byproduct by comparison with an independent source of stilbene.

Stoichiometric Olefin Metathesis with Vinyl Halides in the presence of Hunig's Base

With Vinyl Chloride. $Ru(=CHPh)(H_2IMes)(PCy_3)Cl_2$ (**2.2-Cl**) (20.6 mg, 0.0243 mmol, 1.00 equiv) was dissolved in 1 mL of C_6D_6. Hunig's Base (diisopropylethylamine) (5 μL, 0.029 mmol, 1.2 equiv) was added to the reaction mixture. The solution was added to a J. Young tube and frozen. The head space was evacuated and vinyl chloride (1 atm, 0.08 mmol) was added. The solution was thawed and mixed thoroughly. Free phosphine (up to 3%) was observed in the ^{31}P NMR spectra during the course of the experiment. After 20 min, ^1H NMR spectrum showed that about 1 equiv of vinyl chloride was dissolved in solution and the metathesis reaction had begun (15% of **2.2-Cl** consumed). After 2.5 hours, ^{31}P NMR spectroscopy confirmed the formation of **2.5-Cl** (38%) along with **2.2-Cl** (59%) and free phosphine (3%). ^1H NMR spectroscopy confirmed the formation of styrene and diisopropylethylammonium chloride. After 16 hours, **2.5-Cl** (97%) was still the only product observed by NMR along with **2.2-Cl** (3%) and free phosphine (< 1%). After 19 hours, there was complete consumption of **2.2-Cl** and styrene formation (1 equiv relative to initial amount of **2.2-**

Cl) was observed. The ruthenium products consisted only of Ru(≡C:)(H_2IMes)(PCy_3)Cl_2 (**2.5-Cl**) (100% by ^{31}P NMR; 1 equiv relative to initial amount of **2.2-Cl** by ^{1}H NMR spectroscopy).

With 1,2-Dichloroethylene. Ru(=CHPh)(H_2IMes)(PCy_3)Cl_2 (**2.2-Cl)** (20 mg, 0.024 mmol) and NEt_3 (3.3 μL, 0.024 mmol, 1.0 equiv) were dissolved in 1 mL of C_6D_6 along with 1,3,5-trimethoxybenzene (2 mg, internal standard). ^{1}H NMR spectrum was obtained. 1,2-dichloroethylene (1.8 μL, 0.024 mmol, 1.0 equiv) was added to the reaction mixture. ^{1}H NMR spectra were obtained over a period of 15 days as the metathesis was severely retarded by the presence of NEt_3 and free PCy_3 (up to 3%) was seen throughout the experiment in ^{31}P NMR. After 15 days, **2.5-Cl** (88% by ^{31}P NMR) was the major product. There was no evidence for the formation of **2.8-Cl**. Proton NMR spectroscopy indicated *cis* and *trans* β-chlorostyrene as the major styryl containing products. GC-MS confirmed the presence of *cis* and *trans* β-chlorostyrene.

With 1-Chloro-1-propene. Ru(=CHPh)(H_2IMes)(PCy_3)Cl_2 (**2.2-Cl**) (20.7 mg, 0.0244 mmol) was dissolved in 1 mL of C_6D_6 along with 1,3,5-trimethoxybenzene (internal standard 2.07 mg, 0.012 mmol), diisopropylethylamine (3.5 mg, 0.027 mmol, 1.1 equiv), and then 1-chloro-1-propene (3.6 mg, 0.047 mmol, 1.9 equiv) were added. ^{1}H and ^{31}P NMR spectra were acquired over 24 h. Table 2.10 shows the relative percents of products and starting material over time based on ^{31}P NMR spectroscopy. Reaction reached completion after 48 hours. Product **2.8-Cl** was not observed. Proton NMR spectroscopy indicated *cis* and *trans* 1-phenyl-1-propene as the major styryl containing products in a 1 to 4 ratio respectively based on integration. A very small amount (< 1%) of *trans* 2-butene was observed in the ^{1}H NMR spectrum. GC-MS confirmed the

presence of *cis* and *trans* 1-phenyl-1-propene. Diisopropylethylammonium chloride was also observed as a byproduct of the reaction.

Table 2.10. Stoichiometric Metathesis with **2.2-Cl** and 1-Chloro-1-propene in the presence of Diisopropylethylamine

Total time (h)	*20 min*	*2*	*4*	*8.5*	*20.5*	*29*	*48*
2.5-Cl (%)	8	26	38	57	85	90	97
2.2-Cl (%)	88	69	56	36	11	4	0
Free PCy_3 (%)	4	5	6	7	4	6	3

With Vinyl Bromide (1 M solution in THF). $Ru(=CHPh)(H_2IMes)(PCy_3)Br_2$ (**2.2-Br**) (10.7 mg, 0.0125 mmol, 1.00 equiv) was dissolved in 1 mL of C_6D_6 and vinyl bromide (1 M solution in THF, 20.0 μL, 0.0200 mmol, 1.6 equiv) and diisopropyethylamine (2.5 μL, 0.014 mmol, 1.1 equiv) were added. The reaction was monitored by ^1H and ^{31}P NMR spectroscopy. The reaction reached completion after 4 hours (all ruthenium starting material was consumed) and formation of styrene and diisopropylethylammonium chloride were observed. A ^{31}P NMR spectrum showed two products: δ = 33.8 (unknown, 14%), 33.0 (**2.5-Br**, 86%) but no evidence of **2.8-Br**.

With Gaseous Vinyl Bromide. $Ru(=CHPh)(H_2IMes)(PCy_3)Br_2$ (**2.2-Br**) (20 mg, 0.021 mmol, 1.0 equiv) was dissolved in 1 mL of C_6D_6 and Hunig's base (4.0 μL, 0.023 mmol, 1.1 equiv) was added. The solution was frozen, the head space in the J. Young tube containing the frozen solution was evacuated and vinyl bromide (1 atm, 0.08 mmol) was added. The solution was then thawed and mixed thoroughly. After 2 h, **2.2-**

Br had been completely consumed. Styrene was apparent in the ^{1}H NMR spectrum. Four products were observed in the ^{31}P NMR spectrum including an unknown peak at 33.9 ppm (9.2%), **2.5-Br** (33.0 ppm, 69%), a doublet at 30.3 (10%) and a broad singlet at 18 ppm (11%). After 20h, the ^{31}P NMR spectrum displayed an unknown peak at 33.9 ppm (9.2%), **2.5-Br** (33.0 ppm, 81%), **2.8-Br** (31.5ppm, 8%) and a singlet at 31.0 ppm (2%).

Low-temperature Observation of [Ru(=CHCl)(H_2IMes)(PCy_3)Cl_2] (2.13-Cl)

Compound 2.5-Cl and HCl (g) at Room Temperature in CD_2Cl_2. Ru(≡C:)(H_2IMes)(PCy_3)Cl_2 (**2.5-Cl**) (20 mg, 0.026 mmol, 1 equiv) was dissolved in 1 mL of CD_2Cl_2 and added to a J. Young tube. The solution was frozen and the head space in the J. Young tube was evacuated. The headspace was then filled with 1 atmosphere of HCl (gas) (0.08 mmol, < 4 equiv). Upon thawing, the reaction mixture turned bright red and then the color quickly (in less than 1 minute) faded to yellow. ^{31}P and ^{1}H NMR spectra displayed one major product corresponding to **2.8-Cl** (88%). Two minor unidentified products were observed in the ^{31}P NMR spectrum at δ = 79.2 (8%) and 32.0 (4%).

Compound 2.5-Cl and HCl (g) at Room Temperature in C_6D_6. Ru(≡C:)(H_2IMes)(PCy_3)Cl_2 (**2.5-Cl**) (20 mg, 0.026 mmol, 1.0 equiv) was dissolved in 1 mL of C_6D_6 and added to a J. Young tube. The solution was frozen and the head space of the J. Young tube was evacuated. The headspace was then filled with 1 atmosphere of HCl (gas) (0.08 mmol, < 4 equiv). Upon thawing, the reaction mixture turned slightly orange/yellow. After 30 min and 3h, ^{31}P and ^{1}H NMR spectra displayed mostly starting

material (90%). Two minor products appeared in the ^{31}P NMR spectrum at δ = 75.9 (3%) and 31.5 (5.3%). After 24 h, there was still a large amount of starting material (77%). The two minor products in the ^{31}P NMR spectrum at δ = 75.9 (7.2%) and 31.5 (16%) had increased slightly.

Compound 2.5-Cl and HCl (g) at –90 to 0 °C in CD_2Cl_2. Ru(≡C:)(H_2IMes)(PCy_3)Cl_2 (**2.5-Cl**) (10 mg, 0.013 mmol, 1.0 equiv) was dissolved in 1 mL of CD_2Cl_2 and added to a J. Young tube. The solution was frozen and the head space of the J. Young tube was evacuated. The headspace was then filled with 1 atmosphere of HCl (gas) (0.08 mmol, < 8 equiv). Upon thawing, the reaction mixture turned bright red and was immediately placed in the 300 MHz NMR spectrometer with a probe precooled to –90 °C. ^{1}H NMR spectra displayed one major product corresponding to **2.13-Cl**. The temperature was slowly ramped to 0 °C and ^{1}H NMR spectra were acquired periodically. Small amounts (< 5%) of decomposition to compound **2.8-Cl** were observed at –40 °C. After 1 h 15 min at –20 °C, only about half of **2.13-Cl** had decomposed to **2.8-Cl** and the temperature was ramped to –10 °C for 1 h and then to 0 °C whereupon complete decomposition to **2.8-Cl** was finally observed. NMR data for **2.13-Cl:** ^{1}H NMR (300 MHz, CD_2Cl_2, –60 °C): δ = 14.4 (s, Ru=C*H*Cl), 6.95 (s, mesityl *meta*), 6.90 (s, mesityl *meta*), 3.93 (s, H_2IMes –CH_2CH_2-), 2.51 (s, mesityl CH_3), 2.44 (s, mesityl CH_3), 2.39 (s, mesityl CH_3), 2.26 (q, PCy_3), 1.56 (broad s, PCy_3), 1.05 (broad s, PCy_3). ^{13}C{^{1}H} NMR (75.47 MHz, CD_2Cl_2, –40 °C): δ = 267.7 (s, Ru=*C*HCl (confirmed with ^{13}C-labeled carbene), 213.0 (d, $^3J_{CP}$ = 76.6 Hz, H_2IMes C_α), 138.8 (s, mesityl), 138.2 (s, mesityl), 137.3 (s, mesityl), 136.0 (s, mesityl), 129.5 (s, mesityl), 128.9 (s, mesity), 51.8 (s, H_2IMes –*C*H_2*C*H_2-), 51.1 (s, H_2IMes –*C*H_2*C*H_2-), 31.8 to 24.7 (P*Cy*$_3$), 20.8 (s, mesityl

CH_3), 19.1 (s, mesityl *C*H_3), 18.2 (s, mesityl *C*H_3) . See table S-1 for direct comparison of **8** with other ruthenium complexes.

$^{13}C_\alpha$-labeled Compound 2.5-Cl and HCl (g) at –90-0 °C in CD_2Cl_2. Ru(≡^{13}C:)(H_2IMes)(PCy_3)Cl_2 (**2.5-Cl[^{13}C]**) (20 mg, 0.026 mmol, 1.0 equiv) was dissolved in 1 mL of CD_2Cl_2 and added to a J. Young tube. The solution was frozen and the head space in the J. Young tube was evacuated. The headspace was then filled with 1 atm of HCl (gas) (0.08 mmol, < 4 equiv). Upon thawing, the reaction mixture turned bright red and was immediately placed in the 300 MHz NMR spectrometer with a probe precooled to –90 °C. ^{1}H NMR spectra displayed one major product corresponding to compound **2.13-Cl(^{13}C)**. NMR data for **2.13-Cl(^{13}C):** ^{1}H NMR (300 MHz, CD_2Cl_2, –40 °C): δ = 14.44 (d, $^1J_{C^{13}H}$ = 201 Hz, Ru=C^{13}*H*Cl), 6.94 (s, mesityl *meta*), 6.90 (s, mesityl *meta*), 3.93 (s, H_2IMes –CH_2CH_2-), 2.49 (s, mesityl CH_3), 2.37 (s, mesityl CH_3), 2.5 - 1.0 (PCy_3). ^{13}C{^{1}H} NMR (75.47 MHz, CD_2Cl_2, –40 °C): δ = 268.1 (Ru=*C*^{13}HCl)

$^{13}C_\alpha$-labeled Compound 2.5-Cl and Trifluoromethanesulfonic Acid (HO_3SCF_3) at –90 to 20 °C in CD_2Cl_2. Ru(≡^{13}C:)(H_2IMes)(PCy_3)Cl_2 (**2.5-Cl[^{13}C]**) (20 mg, 0.026 mmol, 1.0 equiv) was dissolved in 1 mL of CD_2Cl_2 and added to a regular NMR tube capped with a septum. The solution was frozen and triflic acid (HO_3SCF_3, HOTf) (5 µL, 0.0570 mmol, 2.2 equiv) was added. Upon thawing, the reaction mixture turned dark purple and was immediately placed in the 300 MHz NMR spectrometer with a precooled probe at –90 °C. ^{1}H NMR spectra revealed one major product corresponding to compound **2.7[OTf]**. No evidence for a discrete ruthenium-methylidyne complex was observed even at –90 °C, only the final product, **2.7[OTf]**, was seen. ^{1}H NMR (300 MHz, CD_2Cl_2, 20 °C): δ = 17.8 (dd, J = 172.8 Hz, 36 Hz, Ru=^{13}C*H*PCy_3) 14.4 (broad s,

excess TfO*H*), 7.12 (s, mesityl *meta*), 4.22 (s, H_2IMes –CH_2CH_2-), 2.41 (s, mesityl CH_3), 2.38 (s, mesityl CH_3), 2.4 – 1.1 (PCy_3). $^{13}C\{^1H\}$ NMR (75.47 MHz, CD_2Cl_2, 20°C): δ = 263.41 (Ru=^{13}CHPCy_3), 142.0 (s, mesityl), 139.5 (s, mesityl), 131.8 (s, mesityl), 32.1 – 20.3 (PCy_3 and mesityl CH_3), 0.63 (d, $^1J_{CF}$ = 50.5 Hz, -OS(O_2)CF_3).

Enyne Metathesis with Vinyl Halides and Trimethylsilylacetylene.

The major cycle proposed based on DFT calculations[30] is discussed further in Chapter 4. Note that this one cycle accounts for the observed initiation product as well as the major enyne metathesis products observed.

With Vinyl Chloride. Trimethylsilylacetylene (20.8 mg, 0.212 mmol, 1.00 equiv) was dissolved in 0.8 mL of C_6D_6 and the solution was frozen in a J. Young tube. Compound **2.2-Cl** (17.4 mg, 0.0205 mmol, 10 mol% to alkyne) was dissolved in 0.2 mL of C_6D_6 and added to the frozen solution. The solution was kept frozen, the head space in the J. Young tube was evacuated, and vinyl chloride was added to the solution by opening to the vinyl chloride gas and submerging the J. Young tube in liquid N_2 for 3 seconds. The solution was then thawed and placed in an oil bath at 60 °C. After 20 minutes, ^{1}H NMR analysis showed complete consumption of **2.2-Cl** and formation of the catalyst decomposition species **2.5-Cl** and **2.8-Cl**. The solution was heated for another 40 minutes to ensure completion of the metathesis reaction. The ruthenium-containing species were removed from the reaction by running the solution through alumina (neutral, 50-200 micron). GC-MS was utilized to discern metathesis products. Styrene (minor), *E* and *Z* isomers of 1-chloro-3-trimethylsilyl-1,3-butadiene (major), and *E* and *Z* isomers of 1-chloro-2-trimethylsilyl-1,3-butadiene (minor) were resolved. To obtain a cleaner ^{1}H

NMR spectrum of the diene products, the solution was also run through silica gel 60 (EM Science) and excess vinyl chloride was removed through three freeze/pump/thaw degassing cycles. ^{1}H NMR (400 MHz, C_6D_6): δ = 5.0 (d, J =10.7 Hz, 1H, styrene), 5.14 (d, J = 3.2 Hz, 1.4 H), 5.37 (d, J = 2.8 Hz, 1.5H), 5.5 (d, J = 4 Hz, overlapping with styrene), 5.64 (d, J = 8.4 Hz, 1.5H), 5.87 (m, 1.7 H), 6.0 (d, J = 13.6 Hz, 1.2 H), 6.47 (d, J = 13.6 Hz, 1.2 H), 0.316 (s, 2.3H), 0.0 (s, 7.8 H), -0.12 (s, 11.7 H), all other peaks are indiscernible. Integration of this ^{1}H NMR spectrum gives a ratio of approximately 3:1 for new diene products to styrene based on the (major product) *E* and *Z* 1-chloro-3-trimethylsilyl- diasteriotopic alkenyl proton shift integrations.

With Vinyl Bromide. Trimethylsilylacetylene (20.8 mg, 0.212 mmol, 1 equiv) was dissolved in 0.8 mL of C_6D_6 and the solution was frozen in a J. Young tube. Compound **2** (17.4 mg, 0.0205 mmol, 10 mol% to alkyne) was dissolved in 0.2 mL of C_6D_6 and added to the frozen solution. The solution was kept frozen, the head space in the NMR tube was evacuated, and vinyl bromide was added to the solution by opening to the vinyl bromide gas and submerging the J. Young tube in liquid N_2 for 3 seconds. The solution was then thawed and placed in an oil bath at 60 °C. After 20 minutes, a ^{1}H NMR spectrum showed complete consumption of **2.2-Cl**; the decomposition species of the catalyst could be identified as **2.5-Cl** and **2.8-Cl**. The solution was heated for another 40 minutes to ensure completion of the metathesis reaction. The ruthenium-containing species were removed from the reaction by running the solution through alumina (neutral, 50-200 micron). GC-MS was utilized to discern metathesis products: 2-trimethylsilyl-1,3-butadiene, styrene, *E* and *Z* isomers of 1-chloro-3-trimethylsilyl-1,3-butadiene (from halogen exchange between vinyl bromide and **2.2-Cl**), and *E* and *Z* isomers of 1-bromo-

3-trimethylsilyl-1,3-butadiene. Multiple products made the ^{1}H NMR spectrum very difficult to interpret and the small scale of the reaction made separation impractical.

2.7. References

1. Grubbs, R. H., *Handbook of Metathesis*. Wiley-VCH: Weinheim, 2003; Vol. 1-3.
2. Trnka, T. M.; Grubbs, R. H., The development of L2X2Ru = CHR olefin metathesis catalysts: An organometallic success story. *Accounts Chem. Res.* **2001,** *34* (1), 18-29.
3. Tsuji, J., Reactions of Organic Halides and Pseudohalides. In *Transition Metal Reagents and Catalysts: Innovations in Organic Synthesis*, Wiley: New York, 2000; pp 27-108.
4. Macnaughtan, M. L.; Johnson, M. J. A.; Kampf, J. W., Synthesis, Structure, and Olefin Metathesis Activity of Two Ruthenium Monofluoromethylidene Complexes. *Organometallics* **2007,** *26* (4), 780-782.
5. Petasis, N. A.; Yudin, A. K.; Zavialov, I. A.; Prakash, G. K. S.; Olah, G. A., Facile preparation of fluorine-containing alkenes, amides and alcohols via the electrophilic fluorination of alkenyl boronic acids and trifluoroborates. *Synlett* **1997,** (5), 606-&.
6. Schwab, P.; Grubbs, R. H.; Ziller, J. W., Synthesis and applications of RuCl2(=CHR')(PR(3))(2): The influence of the alkylidene moiety on metathesis activity. *J. Am. Chem. Soc.* **1996,** *118* (1), 100-110.
7. Louie, J.; Grubbs, R. H., Metathesis of Electron-Rich Olefins: Structure and Reactivity of Electron-Rich Carbene Complexes. *Organometallics* **2002,** *21*, 2153.
8. Trnka, T. M.; Morgan, J. P.; Sanford, M. S.; Wilhelm, T. E.; Scholl, M.; Choi, T. L.; Ding, S.; Day, M. W.; Grubbs, R. H., Synthesis and activity of ruthenium alkylidene complexes coordinated with phosphine and N-heterocyclic carbene ligands. *J. Am. Chem. Soc.* **2003,** *125* (9), 2546-2558.
9. Trnka, T. M.; Day, M. W.; Grubbs, R. H., Olefin metathesis with 1,1-difluoroethylene. *Angew. Chem.-Int. Edit.* **2001,** *40* (18), 3441-+.
10. Love, J. A.; Sanford, M. S.; Day, M. W.; Grubbs, R. H., Synthesis, structure, and activity of enhanced initiators for olefin metathesis. *J. Am. Chem. Soc.* **2003,** *125* (33), 10103-10109.
11. Love, I., Variation of Carbon-fluorine Spin-spin Coupling Constants with Carbon-substituted Bond Length. *Mol. Phys.* **1968,** *15* (1), 93.
12. Sutton, L. E., Bond Lengths and Hyperconjugation. *Tetrahedron* **1959,** *5* (2-3), 118-126.
13. Sutton, L. E., *Tables of lnteratomic Distances and Configuration in Molecules and Ions*. The Chemical Society: London, 1958.
14. Sanford, M. S.; Love, J. A.; Grubbs, R. H., Mechanism and activity of ruthenium olefin metathesis catalysts. *J. Am. Chem. Soc.* **2001,** *123* (27), 6543-6554.
15. Chatterjee, A. K.; Choi, T. L.; Sanders, D. P.; Grubbs, R. H., A general model for selectivity in olefin cross metathesis. *J. Am. Chem. Soc.* **2003,** *125* (37), 11360-11370.
16. Ulman, M.; Grubbs, R. H., Ruthenium carbene-based olefin metathesis initiators: Catalyst decomposition and longevity. *J. Org. Chem.* **1999,** *64* (19), 7202-7207.
17. Caskey, S. R.; Stewart, M. H.; Kivela, J. E.; Sootsman, J. R.; Johnson, M. J. A.; Kampf, J. W., Two Generalizable Routes to Terminal Carbido Complexes. *J. Am. Chem. Soc.* **2005,** *127*, 16750-16751.

18. Caskey, S. R.; Stewart, M. H.; Johnson, M. J. A.; Kampf, J. W., Carbon–Carbon Bond Formation at a Neutral Terminal Carbido Ligand: Generation of Cyclopropenylidene and Vinylidene Complexes. *Angew. Chem. Int. Ed.* **2006,** *45* (44), 7422-7424.
19. Caskey, S. R. Exploration of Ruthenium Carbon Multiple Bond Complexes: Carbenes, Carbynes, and Carbides. Ph.D., University of Michigan, Ann Arbor, 2007.
20. Caskey, S. R.; Ahn, Y. J.; Johnson, M. J. A.; Kampf, J. W., Terminal Carbide Formation from Acyloxycarbenes: Relevance to Olefin Metathesis. *submitted* **2007**.
21. Macnaughtan, M. L.; Johnson, M. J. A.; Kampf, J. W., Olefin Metathesis Reactions with Vinyl Halides: Formation, Observation, Interception, and Fate of the Ruthenium-Monohalomethylidene Moiety. *J. Am. Chem. Soc.* **2007,** *129* (25), 7708-7709.
22. Stewart, M. H.; Johnson, M. J. A.; Kampf, J. W., Terminal Carbido Complexes of Osmium: Synthesis, Structure, and Reactivity Comparison to the Ruthenium Analogues. *Organometallics* **2007,** *26*, accepted.
23. Stewart, M. H. Synthesis and Reactivity of Terminal Carbide Complexes Prepared by Chalcogen Atom Transfer. Ph.D., University of Michigan, Ann Arbor, 2007.
24. Brothers, P. J.; Roper, W. R., Transition-Metal Dihalocarbene Complexes. *Chemical Reviews* **1988,** *88* (7), 1293-1326.
25. Addison, A. W.; Rao, T. N.; Reedijk, J.; Vanrijn, J.; Verschoor, G. C., Synthesis, Structure, and Spectroscopic Properties of Copper(Ii) Compounds Containing Nitrogen Sulfur Donor Ligands - the Crystal and Molecular-Structure of Aqua[1,7-Bis(N-Methylbenzimidazol-2'-Yl)-2,6-Dithiaheptane]Copper(Ii) Perchlorate. *Journal of the Chemical Society-Dalton Transactions* **1984,** (7), 1349-1356.
26. Romero, P. E.; Piers, W. E.; McDonald, R., Rapidly Initiating Ruthenium Olefin-Metathesis Catalysts. *Angew. Chem. Int. Ed.* **2004,** *43*, 6161.
27. Caskey, S. R.; Stewart, M. H.; Ahn, Y. J.; Johnson, M. J. A.; Rowsell, J. L. C.; Kampf, J. W., Synthesis, Structure, and Reactivity of Four-, Five-, and Six-Coordinate Ruthenium Carbyne Complexes. *Organometallics* **2007,** *26*, 1912-1923.
28. Weskamp, T.; Kohl, F. J.; Hieringer, W.; Gleich, D.; Herrmann, W. A., Highly active ruthenium catalysts for olefin metathesis: The synergy of N-heterocyclic carbenes and coordinatively labile ligands. *Angew. Chem.-Int. Edit.* **1999,** *38* (16), 2416-2419.
29. Diver, S. T.; Giessert, A. J., Enyne metathesis (Enyne Bond Reorganization). *Chemical Reviews* **2004,** *104* (3), 1317-1382.
30. Lippstreu, J. J.; Straub, B. F., Mechanism of enyne metathesis catalyzed by Grubbs ruthenium - Carbene complexes: A DFT study. *J. Am. Chem. Soc.* **2005,** *127* (20), 7444-7457.
31. Tanaka, K.; Böhm, V. P. W.; Chadwick, D.; Roeper, M.; Braddock, D. C., Anionic Ligand Exchange in Hoveyda-Grubbs
Ruthenium(II) Benzylidenes. *Organometallics* **2006,** *25*, 5696-5698.
32. Sanford, M. S. Synthetic and Mechanistic Investigations of Ruthenium Olefin Metathesis Catalysts. Ph. D., California Institute of Technology, Pasadena, CA, 2001.
33. Wilhelm, T. E. Ph. D., California Institute of Technology, Pasadena, CA, 1997.
34. Fomine, S.; Ortega, J. V.; Tlenkopatchev, M. A., Metathesis of halogenated olefins - A computational study of ruthenium alkylidene mediated reaction pathways. *Journal Of Molecular Catalysis A-Chemical* **2007,** *263* (1-2), 121-127.

35. Gottlieb, H. E.; Kotlyar, V.; Nudelman, A., NMR chemical shifts of common laboratory solvents as trace impurities. *J. Org. Chem.* **1997,** *62* (21), 7512-7515.
36. Pangborn, A. B.; Giardello, M. A.; Grubbs, R. H.; Rosen, R. K.; Timmers, F. J., Safe and convenient procedure for solvent purification. *Organometallics* **1996,** *15* (5), 1518-1520.
37. Carlson, R. G.; Gile, M. A.; Heppert, J. A.; Mason, M. H.; Powell, D. R.; Vander Velde, D.; Vilain, J. M., The metathesis-facilitated synthesis of terminal ruthenium carbide complexes: A unique carbon atom transfer reaction. *J. Am. Chem. Soc.* **2002,** *124* (8), 1580-1581.
38. Sanford, M. S.; Love, J. A.; Grubbs, R. H., A versatile precursor for the synthesis of new ruthenium olefin metathesis catalysts. *Organometallics* **2001,** *20* (25), 5314-5318.
39. Hejl, A.; Trnka, T. M.; Day, M. W.; Grubbs, R. H., Terminal ruthenium carbido complexes as sigma-donor ligands. *Chem. Commun.* **2002,** (21), 2524-2525.
40. Kelly, J. F. D.; Kelly, J. M.; McMurry, T. B. H., Photochemistry of substituted cyclic enones. Part 12. Photocycloaddition of 3-phenylcyclopentenone and 3-phenylcyclohexenone to (E)- and (Z)-1-phenylpropene. *Journal Of The Chemical Society-Perkin Transactions 2* **1999,** (9), 1933-1941.

Chapter 3

Scope and Limitations of Ruthenium-Based Catalysts for Cross-Metathesis of Vinyl Halides.

3.1. Introduction

3.1.1. Reasons for the Failure of Vinyl Halides in CM

Ruthenium-catalyzed cross-metathesis (CM) of vinyl halides generally fails.[1] Given the usefulness of alkenyl halides in a number of metal-catalyzed cross-coupling reactions,[2] improvement of CM systems employing vinyl halides would be beneficial. Chapter 2 addresses the reasons vinyl halides fail to undergo CM. For the reactions of vinyl fluoride with Grubbs catalyst, **3.1-H_2IMes** (Chart 3.1), an initial metathesis cycle affords the expected Fischer carbene intermediate (**3.8-F,** Chart 3.1). Compound **3.8-F** is isolable; however, this complex show limited catalytic ability and is subject to deactivation via formation of the corresponding terminal carbide species **3.2-H_2IMes** (Chart 3.1 and Eq. 3.1).[3-5]

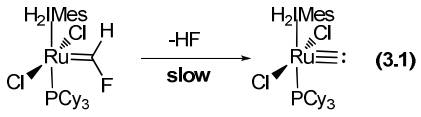

(3.1)

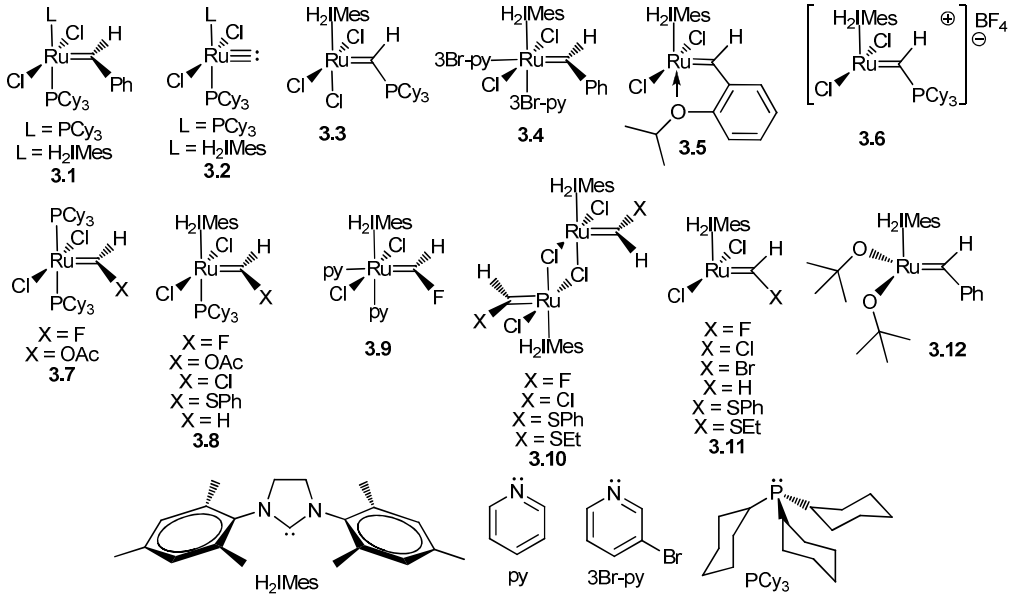

Chart 3.1. Important Ruthenium Complexes

Depending on conditions, reactions of vinyl chloride with **3.1-H_2IMes** form either the terminal carbide complex **3.2-H_2IMes** (Eq. 3.2) or a mixture of **3.2-H_2IMes** and the phosphoniomethylidene complex **3.3** (Eq. 3.3; Chapter 2).[5] Decomposition of the monochloromethylidene complex, **3.8-Cl**, is extremely rapid under all conditions and **3.8-Cl** is not observed at room temperature.

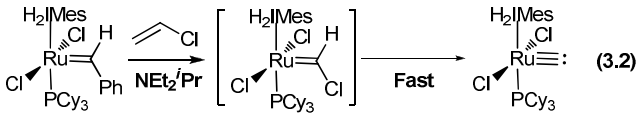

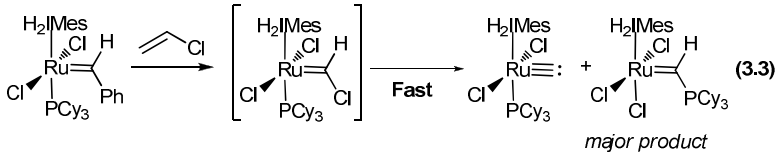

As discussed in Chapters 1 and 2, two independent factors are implicated in the failure to achieve CM with vinyl halides and related directly functionalized olefins. First, enhanced stability of the Fischer carbene complexes relative to their alkylidene counterparts increases the barrier to CM.[6] This is most severe in the case of CM with vinyl fluoride.[4,7,8] Second, the Fischer carbene complexes are subject to deactivation via formation of catalytically inactive **3.2-H_2IMes** and/or **3.3** (Eq. 3.1-3.3). Decomposition becomes more rapid relative to productive CM in systems employing vinyl chloride and especially vinyl bromide. As the halogen on the monohalomethylidene moiety becomes a better leaving group (X = Br > Cl >> F), the ruthenium monohalomethylidene intermediate becomes more sensitive to decomposition.[3-5,9]

3.1.2. The Decomposition Pathway of Monohalomethylidene Complexes

As indicated in Chapter 2, experimental studies indicate that the tricyclohexylphosphine-ligated monochloromethylidene intermediate, **3.8-Cl**, undergoes much more rapid decomposition than its monofluoromethylidene counterpart, **3.8-F**.[4,5] The formation of **3.2-H_2IMes** and **3.3** via decomposition of **3.8-Cl** proceeds through a common intermediate (or transition state) as shown in Scheme 3.1. To form either the carbide complex, **3.2-H_2IMes** (Scheme 3.1; top), or **3.3** (Scheme 3.1; bottom); the ruthenium center must undergo a formal oxidation. Electron density to form the Ru-C triple bond is released from the ruthenium center. Therefore, removal of one of the strong σ-donating ligands should impede decomposition of the monochloromethylidene complex by making the Ru center more electron-deficient.

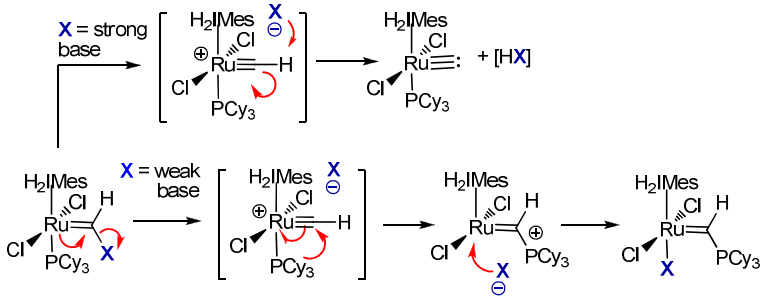

Scheme 3.1. Proposed Decomposition of the Monohalomethylidene Complexes

Furthermore, computational studies of the mechanism for carbide formation[10] and the factors that control the stability of the carbide unit[9] indicate that with strong σ-donating PCy_3 ligands, the formation of the terminal 1st generation carbide complex is barely energetically favorable (Scheme 3.2; $\Delta G_i = -2.7$ kcal/mol and $\Delta H_i = 8.8$ kcal/mol). Formation of **3.2-PCy$_3$** from the acetoxymethylidene complex, **3.7-OAc**, requires electron-density from the Ru-center to be transferred to the Ru-C triple bond. The stronger metal-ligand bond of **3.2-PCy$_3$** is demonstrated by the larger energy required to remove PCy_3 from the Ru-center of the carbide ($\Delta H_C = +36$ kcal/mol) compared to the acetoxymethylidene complex ($\Delta H_{OAc} = +26$ kcal/mol).[9] Experimentally, attempted phosphine and halide exchange at the Ru-center for **3.2-PCy$_3$** failed. However, ligand exchange of the acetoxymethylidene complex is relatively facile.[3,11] Together, these data suggest that terminal carbide formation from the acetoxymethylidene complex could be hindered by the use of catalysts in which the labile ligand is very weak or absent, i.e. by making the ruthenium center more electron-deficient. From Scheme 3.2, it can be inferred that decomposition of the 14-electron aectoxymethylidene complex would be 10 kcal/mol larger than the decomposition of the 16-electron acetoxymethylidene complex

and therefore, less energetically favored ($\Delta H \cong +18.8$ kcal/mol; $\Delta G \cong +7.3$ kcal/mol). This is expected to be applicable to other carbene complexes such as **3.8-F** and **3.8-Cl** which undergo similar decomposition to form the corresponding carbide complex, **3.2-H_2IMes**, and acid. In addition, the absence of PCy_3 ligands prevents the formation of the phosphoniomethylidene complex, **3.3** (Eq. 3.3). Therefore, phosphine-free catalysts **3.4-3.6** were examined for the metathesis of vinyl halides with reactive terminal and internal olefins. Grela and co-workers reached similar conclusions. Using catalyst **3.5** and closely related compounds, they describe CM in neat 1,2-dichloroethylene in good yields for four substrates and low to moderate yields in a few other cases.[12]

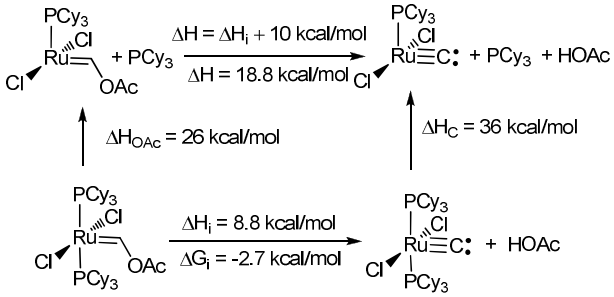

Scheme 3.2. Ligand Effect on Carbide Formation

3.1.3 Catalyst Selection

CM of vinyl halides was tested with phosphine-free catalysts **3.4-3.6** to determine if decomposition of the intermediates could be suppressed in order to allow for productive CM. Precatalyst **3.4**[13] has weakly donating 3-bromopyridine ligands. Weakly donating neutral ligands greatly enhance the initiation rate of the metathesis catalyst. The presence of neutral ligands in the reaction mixture increases the longevity of the ruthenium alkylidene intermediates through reassociation to form more stable 16-electron

ruthenium species. However, the presence of these neutral ligands may contribute to faster decomposition of the ruthenium monohalomethylidene intermediates as discussed earlier. The chelating ether group in **3.5**[14,15] renders **3.5** slow to initiate. This chelating ether donor is lost in the first metathesis cycle, generating the 14-electron active catalyst (Scheme 3.3, boxed). Moreover, the liberated isopropoxystryene may undergo metathesis with a ruthenium intermediate to regenerate **3.5**, thereby extending the lifetime of the catalyst without directly jeopardizing the monohalomethylidene intermediates. The same active species forms when the Piers complex, **3.6**,[16] irreversibly loses tricyclohexylvinylphosphonium ion in the first metathesis cycle (Scheme 3.3). Overall, monohalomethylidene complexes formed from catalysts **3.4**, **3.5** and **3.6** would be less likely to undergo conversion into terminal carbide species when compared with catalysts containing PCy_3 ligands.

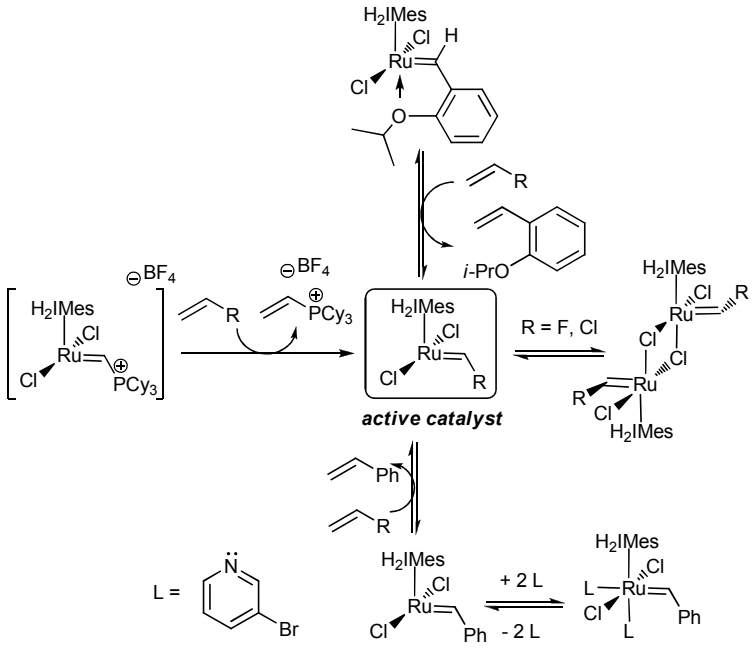

Scheme 3.3. Initiation of Precatalysts **3.4-3.6**

3.2. CM Results

3.2.1. CM with Vinyl Fluoride

Because monofluoromethylidene complexes such as **3.8-F** are more persistent than their monochloromethylidene analogues, **3.8-Cl**, with respect to ruthenium carbide formation,[3-5] metathesis reactions with vinyl fluoride in the presence of **3.1-H_2IMes** and **3.5** were examined. In the CM reaction of vinyl fluoride with 5-decene and catalyst **3.1-H_2IMes** at varying temperatures (Eq. 3.4), only 2.6 turnovers (TON) were observed independent of temperature (when T ≥ 65 °C) and the only new carbene intermediate observed was **3.8-F** which eventually decomposed to the corresponding carbide, **3.2-H_2IMes**, (Table 3.1, Entries 1-4). Reactions with **3.5** (Table 3.1, Entries 5 and 6) gave <2 turnovers. In these cases, the formation of 1-fluoro-1-alkene was limited by stability of the monofluoromethylidene unit with respect to continued metathesis. Although the yields are poor, these are the first successful CM reactions of vinyl fluoride. Full experimental data is available in Table 3.9 in section 3.7. CM attempts of vinyl fluoride with a number of other alkenes showed less than one TON. Examples are given in Table 3.1, Entries 7-10.

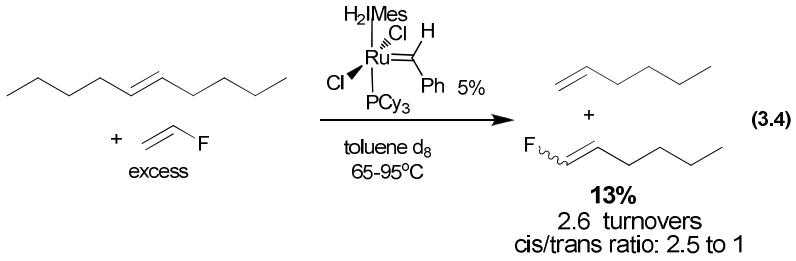

(3.4)

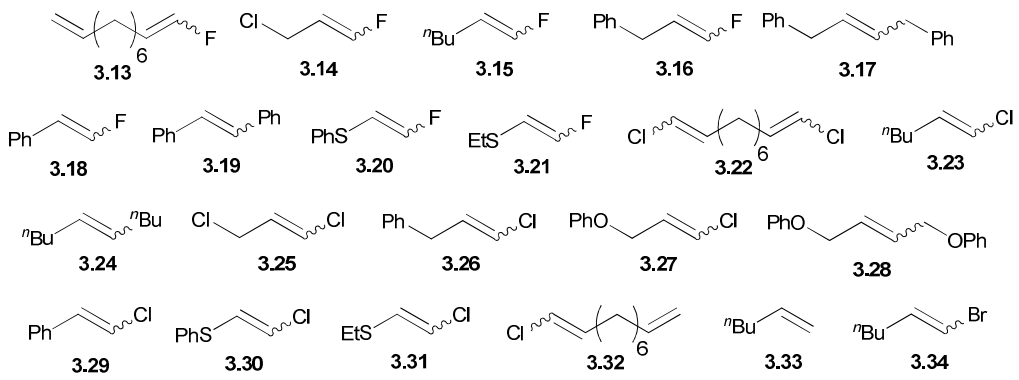

Chart 3.2. Possible CM Products (*E*/*Z*).[12,17-30]

Table 3.1. Olefin Cross-Metathesis with Vinyl Fluoride

#	Alkene	[Ru][a]	Solvent	Temp	%Yield[c]	products (Chart 3.2)	*Z*/*E* ratio[d]
1		**3.1**[f]	toluene-d_8	23 °C	0 0	**3.15** **3.33**	*n/a*
2	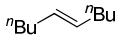	**3.1**[f]	toluene-d_8	65 °C	13 13	**3.15** **3.33**	*2.6*
3	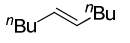	**3.1**[f]	toluene-d_8	80 °C	13 13	**3.15** **3.33**	*2.4*
4	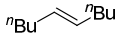	**3.1**[f]	toluene-d_8	95 °C	13 13	**3.15** **3.33**	*2.5*
5	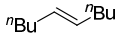	**3.5**	CD_2Cl_2	23 °C 50 °C	9	**3.15**	*3.7*
6	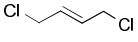	**3.5**	C_6D_6[b]	50 °C	11	**3.14**	*1.3*
7		**3.5**[e]	C_6D_6[b]	50 °C	<10 <10	**3.16** **3.17**	*n/a*
8		**3.5**	C_6D_6	50 °C	0 <5	**3.18** **3.19**	*n/a*
9		**3.5**	C_6D_6[b]	23 °C	0	**3.20**	*n/a*
10		**3.5**	C_6D_6[b]	23 °C	0	**3.21**	*n/a*

For Table 3.1: [a] 5 mol% catalyst used unless otherwise indicated. See Table 3.9 for more detail. [b] A mixture of C_6D_6 and CD_2Cl_2 in a 10 to 1 ratio was used. CD_2Cl_2 was added to ensure that all catalyst dissolved. [c] Alkenyl halide CM product based on internal standard with respect to starting alkene; determined by ^{1}H NMR/GCMS. [d] n/a = not determined or unavailable. [e] 10 mol% catalyst loading used. [f] For **3.1**, L = H_2IMes.

3.2.2. Synthesis of the Monohalomethylidene Dimer, 3.10.

Attempts to observe ruthenacyclobutane intermediates in the CM reactions of vinyl fluoride with **3.5** and **3.6** led to the discovery of a new monofluoromethylidene complex, **3.10-F**. Although no ruthenacycles were observed at low temperatures, the ^{1}H NMR spectrum of **3.10-F** was consistent with the four-coordinate 14-electron monomer **3.11-F**. However, this seemed unlikely given the absence of compounds of the form [Ru(=CHR)(H_2IMes)X_2] except in cases of bulky R groups (R = PCy_3, **3.6**[16]) or bulky, basic X groups (X = *t*-OBu, **3.12**[31]). Direct reaction of **3.6** with vinyl fluoride at low temperature slowly afforded **3.10-F**. However, separation of **3.10-F** from tricyclohexylvinylphosphonium tetrafluoroborate proved difficult. Complex **3.10-F** formed from **3.5** and vinyl fluoride in toluene as a yellow microcrystalline precipitate (Eq. 3.5, X = F) in 81% isolated yield. Similar treatment of **3.5** with vinyl chloride resulted in isolation of the thermally unstable compound **3.10-Cl** (Eq. 3.5, X = Cl) in 53% yield. Piers recently described a chloride-bridged heterodimer related to **3.10-F** and **3.10-Cl**.[32]

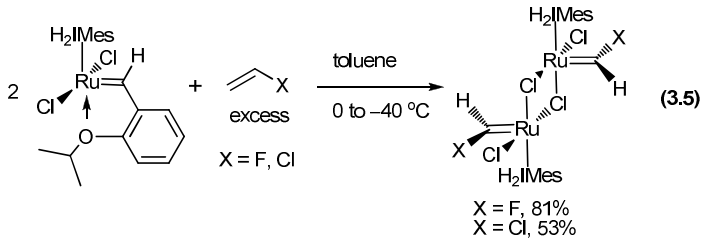

(3.5)

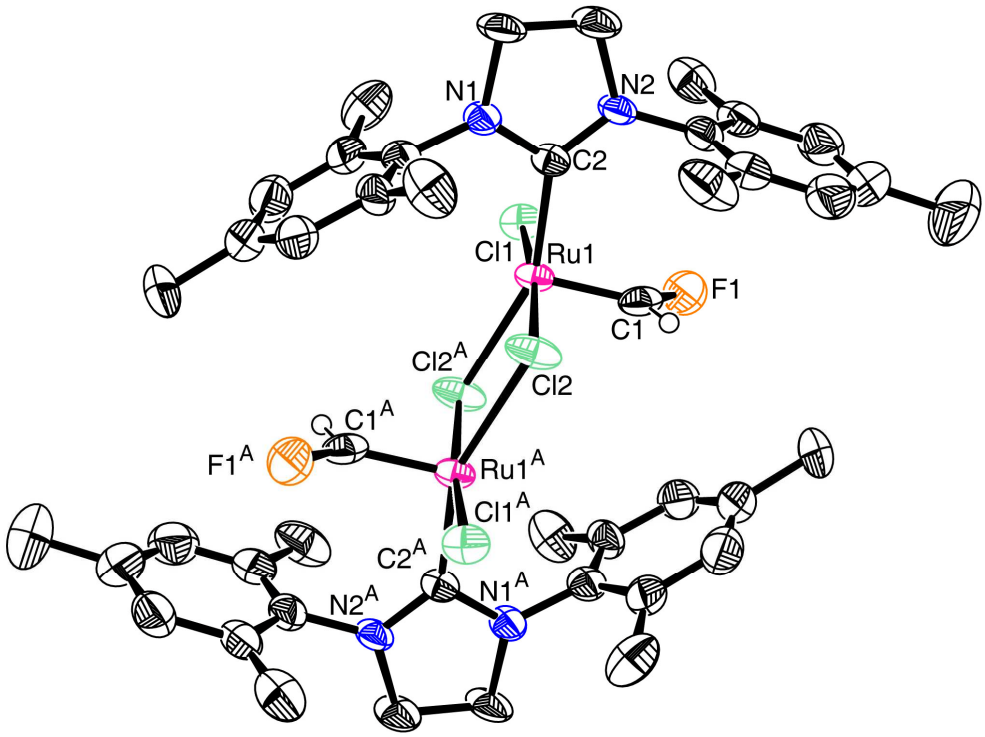

Figure 3.1. 50% thermal ellipsoid plot of [Ru(CHF)(H_2IMes)(μ-Cl)Cl]$_2$ (**3.10-F**). Selected crystallographic data are presented in Table 3.2 and selected bond distances and angles are presented in Table 3.3. Complete XRD data can be found in Appendix 4.

Orange single crystals of **3.10-F** suitable for X-ray diffraction study were recrystallized from diffusion of pentane into a saturated solution in chloroform at –35 °C. An ORTEP diagram is shown in Figure 3.1, selected crystallographic data are presented in Table 3.2, and selected bond distances and angles are presented in Table 3.3. The thermal ellipsoid plot of one of the two crystallographically independent but chemically equivalent molecules clearly shows that **3.10-F** is a chloride-bridged dimer in the solid state. Analysis reveals that the Ru(CHF)(H_2IMes)(μ-Cl_2)Cl unit forms a distorted square-pyramidal arrangement with the CHF unit in the apical position. The basal plane

contains two chlorines that are mutually *trans*. Each unit has one terminal chloride ligand and one bridging chloride between the Ru-centers. The bridging chloride ligands from each Ru unit are bound *trans* to the H_2IMes ligand to give the dimer complex. A crystallographic C_2 axis is centered between the two Ru units. The product is moderately soluble in CD_2Cl_2 or $CDCl_3$ but is thermally sensitive in solution; complete decomposition occurs within 20 min at 23 °C. The triclinic unit cell contains 4 molecules of chloroform and 2 molecules of **3.10-F**.

Table 3.2. Crystallographic Data for Complex **3.10-F**

Formula	$C_{46}H_{56}Cl_{10}F_2N_4Ru_2$	V (Å ^{3})	3027.0 (11)
FW	1259.59	*Z*	2
Crystal System	Triclinic	Rad. (Ka, Å)	0.71073
Space group	P-1	*T* (K)	230 (2)
A (Å)	12.896 (3)	D_{calcd} (Mg m^{-3})	1.382
B (Å)	14.961 (3)	ρ_{calcd} (mm^{-1})	0.978
C (Å)	16.779 (4)	F_{000}	1272
α (deg)	90.295 (4)	R1	0.0537
β (deg)	97.646 (4)	wR2	0.1005
γ(deg)	109.138 (3)	GOF	1.000

Table 3.3. Selected Bond Lengths and Angles for Complex **3.10-F**

Bond Distances (Å):		**Bond Angles (deg):**	
Ru(1)-C(1)	1.793 (4)	Ru(1)-C(1)-F(1)	126.8 (3)
Ru(1)-C(2)	2.007 (4)	C(1)-Ru(1)-C(2)	96.88 (16)
Ru(1)-Cl(2)	2.4078 (10)	C(1)-Ru(1)-Cl(2)	88.24 (14)
Ru(1)-Cl(2A)	2.4244 (11)	C(1)-Ru(1)-Cl(2A)	107.63 (12)
Ru(1)-Cl(1)	2.3551 (10)	C(1)-Ru(1)-Cl(1)	96.20 (16)
C(1)-F(1)	1.353 (4)	C(2)-Ru(1)-Cl(2A)	155.46 (12)
		Cl(2)-Ru(1)-Cl(1)	171.90 (4)

3.2.3. CM with 3.10-F.

The reaction of 5-decene with excess vinyl fluoride in the presence of **3.10-F** led to 12.5% conversion to 1-fluoro-1-hexene per [Ru] (Eq. 3.6), thus indicating the competence of **3.10-F** as an intermediate in reactions using either **3.5** or **3.6** as a catalyst. Although 10% catalyst loading was used, TON for these reactions could not be determined as **3.10-F** was only partially soluble in benzene.

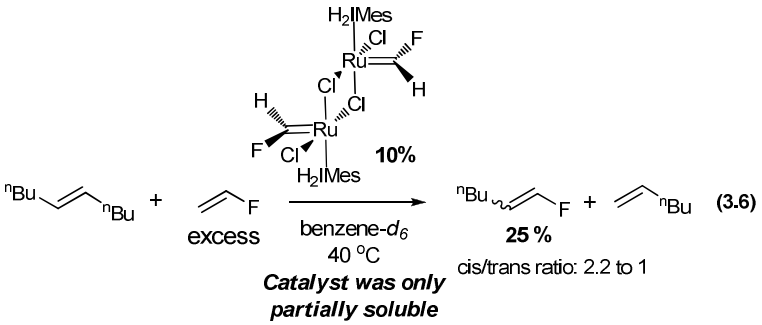

(3.6)

Overall, vinyl fluoride as a substrate for CM shows only low conversion to desired products. The thermodynamic stability of the 14-electron monofluoromethylidene

complex and the preference for the ruthenacycle to reform **3.11-F** severely hinders metathesis activity.

3.3. CM with Chlorinated Olefins

3.3.1. Results with 1,2-Dichloroethene.

Our previous results[4,5] and those of Grubbs,[8] Fomine,[6] and Grela[12] suggested that a monochloromethylidene complex would be less thermodynamically stable relative to analogous alkylidene complexes than were the monofluoromethylidene complexes. Therefore, the monochloromethylidene complexes should encounter a lower energy barrier to CM.

The CM reactivity of several olefins with vinyl chloride or 1,2-dichloroethene was investigated using precatalysts **3.4**-**3.6**, intentionally avoiding catalysts that contained PCy_3 ligands. Precatalyst **3.4** was unsuccessful in promoting CM of vinyl halides (Table 3.4, Entry 4; Table 3.5, Entry 3). Even weakly-donating neutral ligands appear to encourage decomposition of the monochloromethylidene intermediates before further metathesis can take place. In contrast, precatalysts **3.5** and **3.6** afford CM of 1,2-dichloroethylene in moderate to good yields with several substrates (Table 3.4, Entries 1, 6, 9, 11, and 18). As shown in Table 3.4, Entries 5 and 8, precatalyst **3.6** requires a terminal olefin for initiation. In general, precatalyst **3.5** gives slightly better yields of chlorinated product than precatalyst **3.6** (Table 3.4, Entries 7 and 8). This is most likely due to the slower initiation of **3.5**.

Table 3.4. Cross-Metathesis Results with 1,2-Dichloroethene

#	Alkene	[Ru][a]	Solvent	Temp	%Yield[c]	Products Chart 3.2	TON	Z/E ratio[d]
1	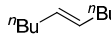	**3.5**	C_6D_6	23 °C	100	**3.23**	20	*2.4*
2	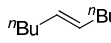	**3.5**[f]	C_6D_6	23 °C	99	**3.23**	28	*2.2*
3	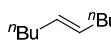	**3.5**	C_6D_6	45 °C	85	**3.23**	17	*2*
4	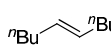	**3.4**	C_6D_6[b]	50 °C	<5	**3.23**	<1	*n/a*
5	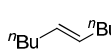	**3.6**	C_6D_6[b]	50 °C	0	**3.23**	0	
6		**3.5**[e]	C_6D_6	50 °C	>90	**3.23**	>9	*1.5*
7		**3.5**	C_6D_6	45 °C	60 10	**3.23** **3.24**	12	*1.3*
8		**3.6**	C_6D_6[b]	50 °C	43 13	**3.23** **3.24**	9	*1.6*
9	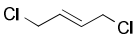	**3.5**[e]	C_6D_6	50 °C	78	**3.25**	8	*1*
10	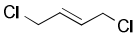	**3.5**	C_6D_6	45 °C	53	**3.25**	11	*1.3*
11		**3.6**[e]	C_6D_6[b]	50 °C	58 20	**3.26** **3.17**	6	*1*
12		**3.5**[e]	C_6D_6	50 °C	50 25	**3.26** **3.17**	5	*1*
13		**3.5**	C_6D_6	45 °C	50 10	**3.26** **3.17**	10	*1*
14		**3.5**	C_6D_6[b]	50 °C	20 10	**3.27** **3.28**	4	*1.3*
15		**3.5**	C_6D_6[b]	50 °C	5 48	**3.29**[h] **3.19**	1	*n/a*
16	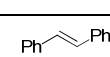	**3.5**	C_6D_6[b]	50 °C	0	**3.29**	0	-
17		**3.5**	C_6D_6	23 °C	50	**3.30**	10	*7.2*
18		**3.5**[g]	C_6D_6	23 °C	70	**3.30**	14	*4.4*

[a] 5 mol% catalyst was used unless otherwise indicated. See Table 3.10 for more detail. [b] A mixture of C_6D_6 and CD_2Cl_2 in a 10 to 1 ratio was used. CD_2Cl_2 was added to ensure that all catalyst dissolved. [c] Alkenyl halide CM product based on internal standard with respect to starting alkene; determined by ^{1}H NMR/GCMS [d] n/a = not determined or unavailable [e] 10 mol% catalyst loading used. [f] Slow addition of catalyst, 1mol% per hour, was used. 4 mol% catalyst loading was used. [g] Slow addition of catalyst, 1mol% per hour, was used. 5 mol% catalyst loading was used. [h] The addition products of HCl to

styrene (PhC_2H_4Cl) was observed in ≤ 5% yield, suggesting the liberation of HCl through the decomposition of the monohalomethylidene species (derivatives of **3.10-Cl**) with concomitant formation of carbide complexes. [4,5]

Alkene substrates that undergo CM with 1,2-dichloroethene must be unhindered and very reactive towards olefin metathesis catalysts. Rapid reactivity of the unhindered alkene with the monochloromethylidene intermediate (**3.11-Cl**) is necessary to compete with the decomposition of the monochloromethylidene complexes, **3.10-Cl** and **3.11-Cl**, as the intermediates do not survive long under the conditions employed (Scheme 3.4; $k_{prod} > k_{dec}$). Secondly, if the alkene is monosubstituted, its corresponding 1,2-disubstituted homodimer must also react rapidly with the catalytic intermediates. For example, both 1-hexene and 5-decene afford good yields of 1-chloro-1-hexene in reactions with 1,2-dichloroethene (Table 3.4, Entries 1-3 and 6-7; Scheme 3.5; left). These reactive alkenes comprise only a subset of the class of alkenes that Grubbs has designated "type I" in metathesis reactions catalyzed by **3.1-H_2IMes**.[33] If the CM homodimer is slow to react with the key monochloromethylidene intermediate, deactivation of the catalyst occurs before productive CM (Scheme 3.4, $k_{prod} < k_{dec}$; Scheme 3.5; right). In the case of styrene, formation of stilbene (which is unreactive in CM with 1,2-dichloroethene) by self-CM accounts for the very low yield (5%) of β-chlorostyrene under our conditions (Scheme 3.5; Table 3.4, Entries 15 and 16). Use of neat 1,2-dichloroethene as indicated by Grela[12] appears to be more effective for styrene derivatives, likely by intercepting styrene prior to its self-CM.

The exception to "type I" olefins is phenyl vinyl sulfide (Table 3.4, Entries 17 and 18) which forms the Fischer carbene complex (**3.11-SPh**). This directly functionalized olefin usually retards olefin metathesis reactions because it forms a stable Fischer carbene

complex.[8] Therefore, phenyl vinyl sulfide does not form its homodimer, 1,2-bis(phenylthio)ethene. The formation of the more thermodynamically stable **3.11-SPh** may help to decrease the amount of **3.11-Cl** in solution and thereby slow down catalyst deactivation. Unlike typical CM-active alkenes, the chloro-olefins will undergo metathesis to some extent with **3.11-SPh** because **3.11-Cl** is also thermodynamically stable with respect to other alkylidene compounds, such as **3.11-H**. Consumption of **3.11-Cl** via metathesis with phenyl vinyl sulfide should be relatively fast as formation of **3.11-SPh** is thermodynamically favored assuming no large kinetic barriers. It is likely that other olefins that form Fischer carbene compounds will show similar behavior; Grela has identified two others.[12] Note that use of more hindered substrates such as 2-chloro-1-alkenes and 1,1-dichloroalkenes remains a synthetic challenge.

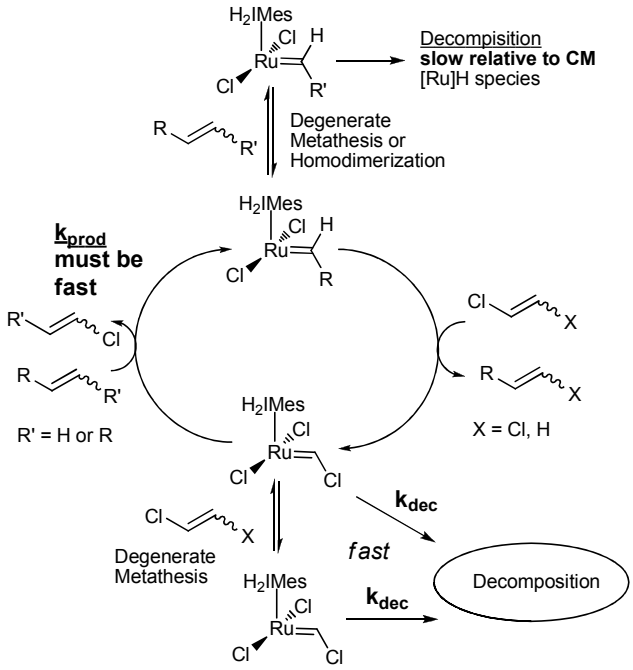

Scheme 3.4. Competition between CM and Decomposition of the Monohalomethylidene Intermediates

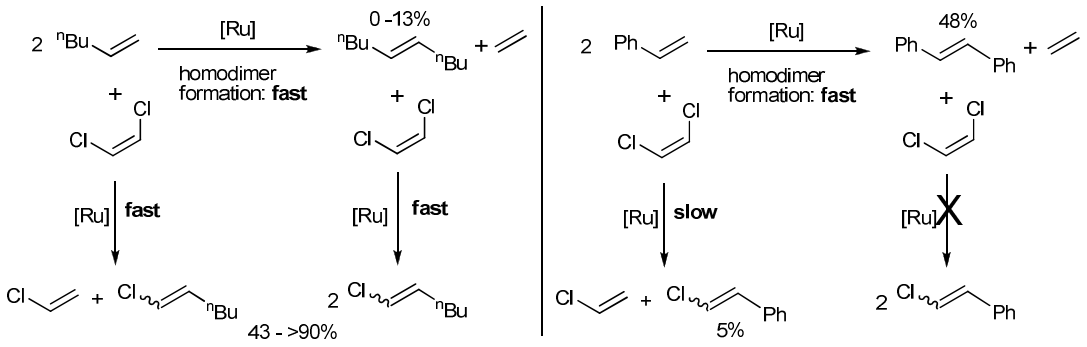

Scheme 3.5. Cross-Metathesis versus CM Homodimerization.

3.3.2. Vinyl Chloride versus 1,2-Dichloroethene

In general, we find that reactions involving 1,2-dichloroethene are superior to those employing vinyl chloride (Table 3.4, Entries 1-3 and 12 compared to Table 3.5, Entries 1-4). The sole exception involves the attempted CM of 5-decene with 1,2-dichloroethene using precatalyst **3.6** (Table 3.4, Entry 5; Table 3.5, Entry 2). In this case, initiation of the precatalyst does not occur, as neither substrate is a terminal olefin. One reasonable explanation for the superiority of 1,2-dichloroethene as a CM substrate involves "pseudopoisoning"[34] of the catalyst by excess vinyl chloride via degenerate metathesis exchange of intermediate **3.11-Cl** with vinyl chloride in preference to productive metathesis with the other substrate (Scheme 3.4). Degenerate metathesis would serve to trap the catalyst as **3.11-Cl**, in which form it is most susceptible to decomposition. Degenerate metathesis with 1,2-dichloroethene is less problematic because it is more sterically hindered with respect to vinyl chloride and therefore less reactive with the catalyst. Alternatively, the use of vinyl chloride permits the formation of the methylidene complex **3.11-H**; this species is also implicated in catalyst

decomposition.[35] The former explanation is more likely, good yields of 1-chloro-1-hexene can be obtained via reaction of 1-hexene with 1,2-dichloroethene (Table 3.4, Entries 6-8) in spite of the fact that **3.11-H** would form under these conditions as well. Comparison of Entries 1-3 in Table 3.5 and Entries 1-3 and 6-7 in Table 3.4 shows that of the potential methylidene sources, vinyl chloride is more deleterious to CM than is 1-hexene. All results to date are consistent with the proposal that the relative rates of two processes that occur for intermediate **3.11-Cl** – productive reaction with the substrate versus decomposition – are primarily responsible for determining the yield (Scheme 3.4). Only the most active substrates can intercept **3.11-Cl** before it undergoes irreversible deactivation.

Table 3.5. Cross-Metathesis with Vinyl Chloride

#	Alkene	[Ru][a]	solvent	temp	%Yield[c]	Products Chart 2	TON	*Z/E ratio*[d]
1	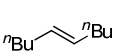	**3.5**	C_6D_6[b]	23 °C	29 29	**3.23** **3.33**	6	*Z only det'd*
2	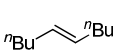	**3.6**	C_6D_6[b]	50 °C	25 22	**3.23** **3.33**	5	*7.4*
3	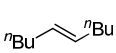	**3.4**	C_6D_6[b]	50 °C	0 0	**3.23** **3.33**	0	*n/a*
4		**3.5**[e]	C_6D_6[b]	50 °C	20 <10	**3.26** **3.17**	2	*3*
5		**3.5**	C_6D_6[b]	50 °C	<5 <5	**3.29**[f] **3.19**	<1	*n/a*

[a] conditions: 5 mol% catalyst unless otherwise indicated. See Table 3.11 for more detail. [b] A mixture of C_6D_6 and CD_2Cl_2 in a 10 to 1 ratio was used. CD_2Cl_2 was added to ensure that all catalyst dissolved. [c] Alkenyl halide CM product based on internal standard with respect to starting alkene; determined by ^{1}H NMR/GCMS [d] n/a = not determined or unavailable [e] 10 mol% catalyst loading used. [f] The addition products of HCl to styrene (PhC_2H_4Cl) were observed in ≤ 5% yield, suggesting the liberation of HCl through the decomposition of the monohalomethylidene species (derivatives of **3.10-Cl**) with concomitant formation of carbide complexes. [4,5]

3.3.3. Ruthenium Decomposition during CM

No new carbene complexes are observed by ^{1}H NMR spectroscopy during the course of the reactions under catalytic conditions, except in the cases of phenyl vinyl sulfide and ethyl vinyl sulfide, where **3.10-SPh, 3.10-SEt, 3.11-SPh** and/or **3.11-SEt** are the more thermodynamically stable carbene complexes. At present, the catalyst decomposition products are unknown, although minor haloalkane byproducts detected by GC-MS in cases where styrene was used suggest that loss of HCl is occurring (Table 3.4, Entry 15; Table 3.5, Entry 5). This suggests the formation of terminal carbide complexes that must then undergo further transformations. No four-coordinate terminal carbide complexes analogous to **3.11-Cl** have yet been reported; DFT calculations indicate that the absence of a strong σ-donor ligand *trans* to the *N*-heterocyclic carbene ligand is unfavorable (Scheme 3.2).[9] However, even weak donor ligands such as pyridine lead to terminal carbide complexes that decompose rapidly.[36] Thus, carbide complexes analogous to dimeric **3.10-F** and **3.10-Cl** likely undergo further decomposition to currently unknown species.

Since decomposition of monohalomethylidene ligands through loss of HX is more favorable in 16-electron species than in the active 14-electron species, decomposition is likely to occur when [Ru=CHCl] is in its dimeric form (**3.10-Cl**) than when the catalyst is in its active 14-electron form (**3.11-Cl**). A low catalyst concentration is desirable in order to limit formation of dimer **3.10-Cl**. Slow addition of precatalysts effectively lowers the concentration of active species in solution, results in higher yields of the CM products and in some cases permits lower catalyst loadings (Table 3.4, Entries 2 and 18).[12] This is the most logical explanation for the reasons that **3.5** is a better catalyst than **3.6**.

Hoveyda's catalyst, **3.5**, has a slower initiation step, effectively lowering catalyst concentrations.

In many cases, as the Ru-catalyst decomposes, small amounts of ruthenium hydrides are observed in solution. The specific identity of these ruthenium compounds is unknown. However, many Ru-hydrides are known to effect alkene isomerization and alkene isomerization has been shown with 2nd generation Grubbs catalyst, **3.1-H_2IMes**. [37]

3.3.4. Alkene Isomerization

In a few of the CM reactions above, alkene-isomerized byproducts are observed in small amounts. Some byproducts also form from alkene-isomerization (AI) followed by CM. The chain lengths of alkene isomerization/CM products observed were generally 1 carbon unit longer and shorter. For CM of 5-decene with chlorinated olefins, alkene-isomerization byproducts observed by GC-MS included: 4-nonene (0 to 10%), 5-undecene (0 to 10%), 1-chloro-1-heptene (0 to 2%), and 1-chloro-1-pentene (0 to 2%) (Scheme 3.6).

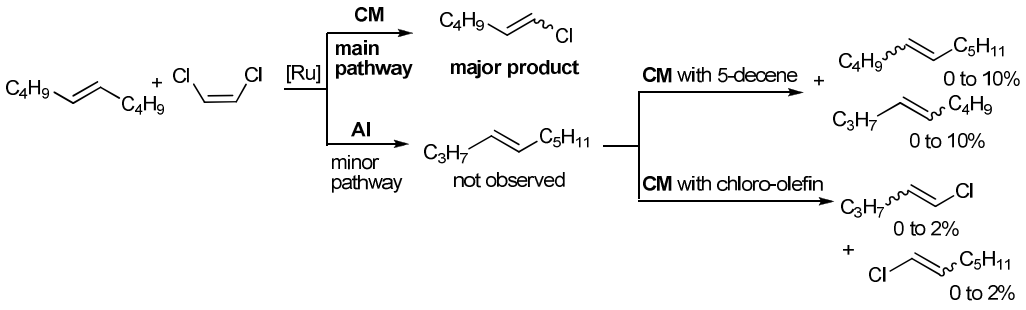

Scheme 3.6. Byproducts from Alkene Isomerization Processes

In the case of allylbenzene and allyloxybenzene, alkene isomerization was not generally observed during CM reactions. However, homodimerization of these terminal olefins seemed to hinder metathesis with chlorinated olefins, explaining why 5-decene was a better substrate for CM with chlorinated olefins then were allylbenzene or allyloxybenzene. Interestingly, control experiments with terminal alkenes and **3.5** gave CM homodimerization products as well as alkene isomerization products indicating that the Ru-hydride species must form through decomposition of the 14-electron alkylidene species (Scheme 3.7 and 3.8). Alkene isomerization was much more prominent in control reactions than in CM with chlorinated olefins.

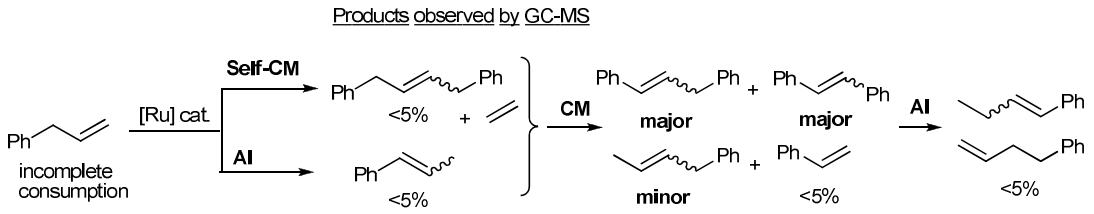

Scheme 3.7. CM of Allylbenzene under Standard Metathesis Conditions

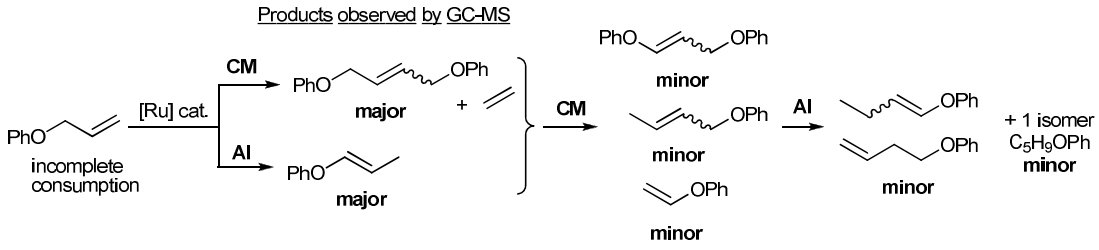

Scheme 3.8. CM of Allyloxybenzene under Standard Metathesis Conditions

3.4. CM with Vinyl Bromide

Attempted CM reactions of 1,2-dibromoethene afford only low yields of alkenyl bromide products even with 5-decene and 1-hexene (Table 3.6, Entries 1 and 2). Two factors can explain these low yields. First, more rapid decomposition of **3.11-Br** relative to its monochloromethylidene homologue **3.11-Cl** would make the rate ratio of productive metathesis to catalyst decomposition less favorable. Previous results indicate that the rate of terminal carbide formation from Fischer carbene complexes of the form $Ru(=CHX)(H_2IMes)(PCy_3)Cl_2$ is inversely related to typical C-X bond strengths,[3-5,38] so **3.11-Br** is similarly expected to undergo decomposition even more rapidly than **3.11-Cl**. Although the monochlorodimer, **3.10-Cl**, can be isolated by reaction of **3.5** and vinyl chloride, vinyl bromide under the same reaction condition yields only an intractable mixture. Second, slower reaction of the key monobromomethylidene intermediate **3.11-Br** with its metathesis partner would have a similar effect on the key ratio. This is expected on steric grounds. Futhermore, observation by GC-MS of *chlorinated* products such as 1-chloro-1-hexene indicates that considerable halogen exchange with the halide ancilliary ligands in **3.11-Br** occurs. Finally, minor side products, such as 1,1,2-tribromoethane and 1,1,2,2-tetrabromoethane, also suggest that HBr is formed, again pointing to the possibility of carbide formation (Table 3.6, Entry 1 and 2). As observed with the chlorinated olefins, 1,2-dibromoethene showed better yields in CM with 5-decene than did vinyl bromide (Table 3.6, Entries 1-3).

Table 3.6. Cross-Metathesis with Brominated Olefins

#	Alkene	Olefin	[Ru][a]	solvent	Temp	%Yield[c]	Products Chart 2	Z/E ratio[d]
1	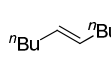	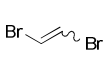	**3.5**	C_6D_6[b]	50 °C	22[e] 8[f]	**3.34** **3.23**	*n/a*
2		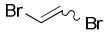	**3.6**	C_6D_6[b]	50 °C	16[e]	**3.34**	*0.5*
3	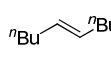		**3.5**	C_6D_6[b]	50 °C	5[e]	**3.34**	*n/a*

[a] conditions: 5 mol% catalyst unless otherwise indicated. See Table 3.12 for more detail. [b] A mixture of C_6D_6 and CD_2Cl_2 in a 10 to 1 ratio was used. CD_2Cl_2 was added to ensure that all catalyst dissolved. [c] Alkenyl halide CM product based on internal standard with respect to starting alkene; determined by ^{1}H NMR/GCMS [d] n/a = not determined or unavailable [e] In certain reactions, the addition products of HBr to 1,2-dibromoethylene (1,1,2-tribromoethane and 1,1,2,2-tetrabromoethane) were observed in ≤ 5% yield, suggesting the liberation of HBr through the decomposition of the monohalomethylidene species with concomitant formation of carbide complexes.[4,5] [f] Halogen exchange was observed when using brominated olefins for CM (**3.23** represents 1-*chloro*-1-hexene).

3.5. Ring-Opening Cross-Metathesis

3.5.1. Vinyl Fluoride

As discussed in Section 3.2.1, CM reactions of vinyl fluoride with simple alkenes are slowed as a result of the thermodynamic stability of the monofluoromethylidene intermediate (**3.10-F** and **3.11-F**). Attempts to overcome this heightened energy barrier by heating the reaction mixtures run afoul of decomposition processes. However, ring-opening CM of cyclooctene with vinyl fluoride is much more efficient. Release of ring strain provides an enthalpic driving force for return to the alkylidene form of the catalyst. In this case, 55% conversion of cyclooctene to fluorinated ring-opened products (Table 3.7, Entry 1) occurs, in spite of the low solubility of intermediate **3.10-F** formed during the reaction. This compares favorably to the 9% and 11% yields obtained in the respective CM reactions of 5-decene and 1,4-dichloro-2-butene with vinyl fluoride (Table 3.1, Entries 5 and 6). Heating the reaction mixture of cyclooctene with vinyl fluoride to

50 °C caused the intermediate **3.10-F** to decompose rapidly and prevented any formation of the desired product (Table 3.7, Entry 2). In addition to the RO-CM products, small amounts of polymerized cyclooctene were observed by GC-MS and ^{1}H NMR spectroscopy in most of the following reactions.

Table 3.7. RO-CM with Vinyl Fluoride

#	Alkene	[Ru][a]	Temp	% Yield[b]	Product Chart 2	TON	*Z/E* ratio[c]
1		**3.5**	23 °C sonicated	55	**3.13**	n/d[d]	2.6
2		**3.5**	50 °C	0	**3.13**	0	n/a

[a] 5 mol% catalyst in C_6D_6 was used unless otherwise indicated. See Table 3.13 for more detail. [b] Alkenyl halide CM product based on internal standard with respect to starting alkene; determined by ^{1}H NMR/GCMS [c] n/a = not determined or unavailable [d] Intermediate, **3.10-F**, precipitated from C_6D_6 during the course of the reaction; therefore, catalyst loading was <5%.

3.5.2. Chlorinated Olefins in RO-CM

Ring-opening CM of cyclooctene with 1,2-dichloroethene occurs with nearly quantitative conversion to 1,10-dichlorodeca-1,9-diene (Table 3.8, Entries 1-3), a fact that can again be explained by the effect of ring strain release on the rate of return to an alkylidene form of the catalyst and the speed by which intermediate **3.11-Cl** is consumed after formation (Scheme 3.4). Slow addition of **3.5** reveals that 97% conversion could be reached with only 3 mol% catalyst loading (Table 3.8, Entry 3) All three isomers of 1,10-dichloro-1,9-decadiene (*Z/Z, E/Z, E/E*) are observed. The *Z:E* ratio of 2:1 indicates that product formation is not under thermodynamic control. Owing to the rapid rate of catalyst decomposition, this is expected.

Ring-opening CM with vinyl chloride gave two products. The monosubstituted *E/Z*-1-chloro-1,9-decadiene as the major product and 1,10-dichloro-1,9-decadiene (3 isomers) as the minor product. Ratios of the two products could not be determined because of extensive overlapping of the alkene protons in the ^{1}H NMR spectrum. Overall conversion to products was 93% (Table 3.8, Entry 4).

Table 3.8. RO-CM with Chlorinated and Brominated Olefins

#	Alkene	Olefin	[Ru][a]	temp	%Yield[b]	Products Chart 2	TON	*Z/E* ratio[c]
1			**3.5**	23 °C	>95	**3.22**	>19	*2.1*
2			**3.5**	45 °C	>95	**3.22**	>19	*2.1*
3			**3.5**[e]	23 °C	97	**3.22**	32	*n/a*
4			**3.5**	23 °C	93	**3.22+3.32**	19	*n/a*
5[d]			**3.5**	23 °C	0	**n/a**	0	*n/a*

[a] Conditions: 5 mol% catalyst in C_6D_6 unless otherwise indicated. See Table 3.14 for more detail. [b] Alkenyl halide CM product based on internal standard with respect to starting alkene; determined by ^{1}H NMR/GCMS [c] n/a = not determined or unavailable [d] In certain reactions, the addition products of HBr to 1,2-dibromoethylene and cyclooctene (1,1,2-tribromoethane and 1,1,2,2-tetrabromoethane and 1-bromocyclootane, respectively) were observed in ≤ 5% yield, suggesting the liberation of HBr through the decomposition of the monohalomethylidene species with concomitant formation of carbide complexes.[4,5] [e] Slow addition of catalyst, 1mol% per hour, was used. 3 mol% catalyst loading was used.

3.5.3. Brominated Olefins in RO-CM

Ring-opening CM attempts with 1,2-dibromoethene failed to yield the desired products indicating that **3.11-Br** is to thermally unstable to undergo productive metathesis before decomposition occurs. Byproducts observed in this reaction included 1,1,2-tribromoethane, 1,1,2,2-tetrabromoethane, 1-bromo-octane and a small amount of

polymer (Table 3.8, Entry 5), again pointing to HBr as a decomposition product of **3.11-Br.**

3.6. Conclusions

In summary, commercial phosphine-free ruthenium-based catalysts **3.5** and **3.6** effect CM of vinyl chlorides such as 1,2-dichloroethene with terminal and internal olefins to yield alkenyl chlorides up to 99% yield (4% catalyst loading). Ring opening-CM is even more favorable, giving close to quantitative conversion to the chlorinated alkene products (97%, 3% catalyst loading) and 55% yield with vinyl fluoride. Yields in CM reactions of vinyl fluoride and 1,2-dibromoethene are low but catalysis occurs for these substrates as well. At present, only quite reactive olefins participate successfully in these CM reactions. Rapid catalyst decomposition precludes reactions with more challenging substrates for directly chlorinated and brominated olefins. With vinyl fluoride, the key intermediate, **3.11-F**, is too stable with respect to continued CM. More active or more robust catalysts may be needed in order to reduce the catalyst loading with sensitive substrates. The rational design of more robust catalysts will rely on the identification of the catalyst decomposition products under these conditions. In order for brominated olefins to be useful for CM reactions with other alkenes, more electron-withdrawing ligands are needed.

3.7. Experimental

3.7.1. General Procedures. All reactions were set up in a nitrogen-filled MBRAUN Labmaster 130 glove box, unless otherwise specified and run under a nitrogen

atmosphere. ^{1}H, ^{13}C, ^{19}F, ^{31}P, and two-dimensional GCOSY NMR spectra were acquired on a Varian Inova 300 MHz, 400 MHz, or 500 MHz NMR spectrometer. ^{1}H NMR spectra were referenced to solvent signals.[39] ^{19}F NMR spectra and ^{31}P NMR spectra were referenced to external $CFCl_3$ in $CDCl_3$ ($\delta = 0$) and external 85% H_3PO_4 ($\delta = 0$) respectively. Reactions were integrated against a known quantity of 1,3,5-trimethoxybenzene or 1-bromo-3,5-bis(trifluoromethyl)benzene within the reaction mixture as the internal standard (IS). All NMR scale reactions were filtered through activated alumina before GC-MS data were acquired. GC-MS data was acquired on a Shimadzu GC-MS-QP5000 Gas Chromatograph – Mass Spectrometer.

3.7.2. Materials. Vinyl bromide, allyl benzene, methyl acrylate, 1,4-dichloro-2-butene, allyl alcohol, 1,3,5-trimethoxybenzene, and allyl acetate were purchased from Aldrich Chemical Co. Styrene, 5-decene, aluminum oxide (neutral, 50-200 micron), 1-hexene, stilbene, 1-bromo-1-propene, allyl phenyl ether, cyclooctene, and ethyl vinyl ketone were purchased from Acros Organics. Vinyl fluoride, 1,1-difluoroethylene, and 1-bromo-3,5-bis(trifluoromethyl)benzene were purchased from Synquest Labs, Inc. Vinyl chloride was purchased from Fluka. Vinyl boronic acid *n*-butyl-ester, 1,2-dichloroethylene, and 1,2-dibromoethylene were purchased from TCI America. All bulk solvents were obtained from VWR Scientific, degassed, and dried over 4 Å molecular sieves. Deuterated solvents were purchased from CIL and dried over 4 Å molecular sieves. All liquid reagents were degassed. Vinyl fluoride, vinyl chloride, vinyl bromide and solid reagents were used as received. The starting compounds $[Ru(CHPCy_3)(H_2IMes)Cl_2][BF_4]$ (**3.6**);[16] α-fluorostyrene and β-fluorostyrene[22] were

synthesized according to published procedures. Ru(=CH(*i*-PrOC$_6$H$_4$)(H$_2$IMes)Cl$_2$ (**3.5**), Ru(=CHPh)(H$_2$IMes)(PCy$_3$)Cl$_2$ (**3.1**), and Ru(=CHPh)(H$_2$IMes)Cl$_2$(3-Brpy)$_2$ (**3.4**) were obtained from Materia, Inc.

3.7.3. Synthetic Procedures

General Procedure for Cross-Metathesis (CM) (Eq. 3.7) and Ring-opening Cross-Metathesis (ROCM) Reactions (Eq. 3.8)

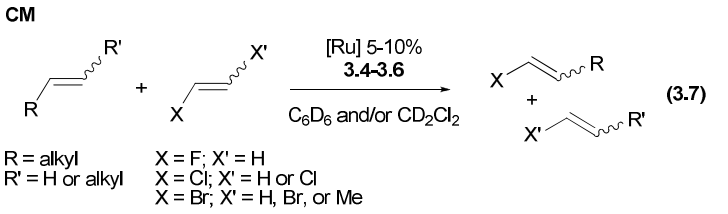

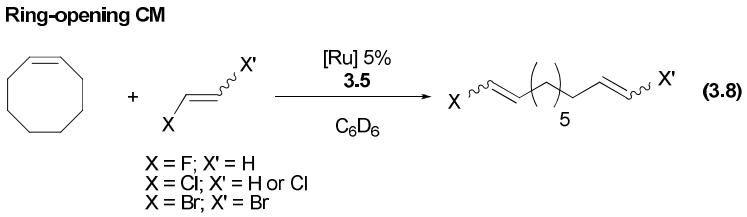

General preparative procedure for reactions involving only liquid/solid substrates. Internal standard (1,3,5-trimethoxybenzene or 1-bromo-3,5-bis(trifluoromethyl)benzene; 0.05 mmol, from a 0.10 M stock solution, 0.50 mL), the non-halogenated alkene, and the halogenated olefin were dissolved in 0.8 mL of C$_6$D$_6$ (and/or CD$_2$Cl$_2$ depending on reaction conditions; see Tables 3.9 through 3.14) and a standard NMR spectrum was acquired. The appropriate amount of **3.4, 3.5** or **3.6** (0.03 M stock solution) was added to the reaction mixture at 23 °C (5 mol% or 10 mol% relative

to limiting reagent; see Table 3.9-3.14 for quantities of starting materials). The reaction mixture was then heated to 40-50 °C or kept at room temperature (23 °C) for up to 24 h. NMR spectra were acquired at 1 h, 2 h, 3 h, 5 h, 16h, and 24 h. Most reactions required less than 3 h to reach the endpoint. After completion, the reaction mixture was passed through alumina and washed through with either pentane or C_6D_6. Finally, GC-MS and NMR data of the resulting catalyst-free solution was acquired to distinguish all products.

General preparative procedure for reactions with gaseous reagents. The appropriate amount of stock solution of the catalyst (**3.4, 3.5** or **3.6**) (0.03 M stock solution) in C_6D_6 (and/or CD_2Cl_2 depending on reaction conditions) was placed in a J. Young tube and the solution was frozen in the cold well of the glove box. Internal standard (0.05 mmol) and the non-halogenated alkene were dissolved in 0.8 mL of C_6D_6, the solution was added to the J. Young tube, and the reaction mixture was again frozen. The reaction mixture was removed from the glove box, the head space in the J. Young tube was evacuated, and vinyl halide was added either while the reaction mixture was submerged in liquid N_2 or while the solution remained frozen without submergence. Amounts of vinyl halide in the reaction mixture were then determined by integration against the internal standard in the ^{1}H NMR spectrum. The reaction mixture was heated to 40-50 °C or kept at room temperature (23 °C) for up to 40 h. NMR spectra were acquired after reaction times of 1 h, 2 h, 3 h, 5 h, 16 h, and 24 h and in some cases 40 h. Most reactions required less than 3 h to reach the endpoint. After completion, the reaction mixture was passed through alumina and washed through with either pentane or C_6D_6. Finally, GC-MS and NMR data of the resulting catalyst-free solution was acquired. Specific conditions for these reactions are collected in Tables 3.9 to 3.14.

Characterization data for alkenyl halide CM products was in agreement with reported data: **3.13,**[17] **3.14,**[18] **3.15,**[19] **3.16**,[20] **3.17**,[21] **3.18**,[22] **3.22**,[23] **3.25,**[24] **3.26**,[25] **3.27**,[26] **3.28**,[27] **3.29**,[25, 28] **3.30**,[12] **3.34,**[29, 30]. Compounds **3.19**, **3.24** and **3.33** can be purchased.

Table 3.9. Olefin Cross-Metathesis with Vinyl Fluoride

#	Olefin A Mmol	Olefin B mmol	[Ru][a]	Solvent	temp/ time	%Yield[c] (product Chart 2)	TON	*Z/E* ratio[d]
1	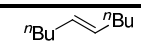 0.153	0.70	**3.1**[g]	C_7D_8	23°C/ 40h	0 (**3.15**)	0	-
2	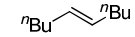 0.153	0.60	**3.1**[g]	C_7D_8	65°C/ 21h	13(**3.15**)[f]	2.6	*2.6*
3	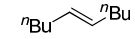 0.153	0.50	**3.1**[g]	C_7D_8	80°C/ 2h	13(**3.15**) [f]	2.6	*2.4*
4	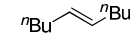 0.153	0.40	**3.1**[g]	C_7D_8	95°C/ 1h	13(**3.15**) [f]	2.6	*2.5*
4	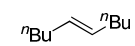 0.50	4.25	**3.5**	CD_2Cl_2	23 °C/ 0.5 h, 50 °C/ 3h	9 (**3.15**) [f]	2	3.7
3	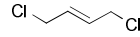 0.32	0.8	**3.5**	C_6D_6[b]	50 °C/ 24 h	11 (**3.14**) [f]	2	1.3
5	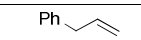 0.32	0.1	**3.5**[e]	C_6D_6[b]	50 °C/ 24 h	<10 (**3.16**) <10 (**3.17**)	<1	n/a
6	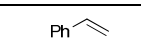 0.31	0.83	**3.5**	C_6D_6	50 °C/ 24 h	0 (**3.18**) <5 (**3.19**)	0	-
7	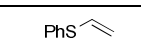 0.15	n/a	**3.5**	C_6D_6[b]	23 °C/ 24 h	0 (**3.20**)	0	-
8	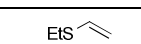 0.15	n/a	**3.5**	C_6D_6[b]	23 °C/ 24 h	0 (**3.21**)	0	-

[a] 5 mol% catalyst used unless otherwise indicated. [b] A mixture of C_6D_6 and CD_2Cl_2 in a 10 to 1 ratio was used. CD_2Cl_2 was added to ensure that all catalyst dissolved. [c] Alkenyl halide CM product based on internal standard with respect to starting alkene; determined by ^{1}H NMR/GCMS. [d] n/a = not determined or unavailable. [e] 10 mol% catalyst loading used. [f] Compound **3.33** was also formed with the same percent conversion. [g] Ruthenium catalyst was 2nd generation Grubbs catalyst, **3.1-H_2IMes**.

Table 3.10. Olefin Cross-Metathesis Results with 1,2-Dichloroethene

#	Olefin A mmol	Olefin B mmol	[Ru][a]	solvent	temp/ time	%Yield[c] (product Chart 2)	TON	Z/E ratio[d]
1	0.15	0.75	**3.5**	C_6D_6	23 °C/ 16 h	100 (**3.23**)	20	2.4
2	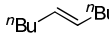 0.17	0.52	**3.5**[f]	C_6D_6	23 °C/ 40 h	99 (**3.23**)	28	2.2
3	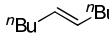 0.17	0.70	**3.5**	C_6D_6	45 °C/ 3 h	85 (**3.23**)	17	2
4	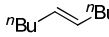 0.15	0.24	**3.4**	C_6D_6[b]	50 °C/ 3 h	<5 (**3.23**)	<1	n/a
5	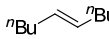 0.15	0.14	**3.6**	C_6D_6[b]	50 °C/ 24 h	0 (**3.23**)	0	-
6	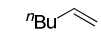 0.15	0.76	**3.5**[e]	C_6D_6	50 °C/3 h	>90 (**3.23**)	>9	1.5
7	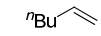 0.16	0.44	**3.5**	C_6D_6	45 °C/ 3 h	60 (**3.23**) 10 (**3.24**)	12	1.3
8	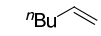 0.31	0.31	**3.6**	C_6D_6[b]	50 °C/ 3 h	43 (**3.23**) 13 (**3.24**)	9	1.6
9	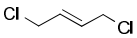 0.09	0.51	**3.5**[e]	C_6D_6	50 °C/ 3 h	78 (**3.25**)	8	1
10	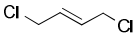 0.11	0.7	**3.5**	C_6D_6	45 °C/ 3 h	53 (**3.25**)	11	1.3
11	0.16	0.41	**3.6**[e]	C_6D_6[b]	50 °C/ 24 h	58 (**3.26**) 20 (**3.17**)	6	1
12	0.15	0.51	**3.5**[e]	C_6D_6	50 °C/ 3 h	50 (**3.26**) 25 (**3.17**)	5	1
13	0.18	0.57	**3.5**	C_6D_6	45 °C/ 3 h	50 (**3.26**) 10 (**3.17**)	10	1
14	0.30	0.32	**3.5**	C_6D_6[b]	50 °C/ 16 h	20 (**3.27**) 10 (**3.28**)	4	1.3
15	0.15	0.42	**3.5**	C_6D_6[b]	50 °C/ 3 h	5 (**3.29**)[h] 48 (**3.19**)	1	n/a
16	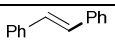 0.18	0.61	**3.5**	C_6D_6	40 °C/ 14h	0 (**3.29**)	-	-
17	0.15	0.9	**3.5**	C_6D_6	23 °C/ 24 h	50(**3.30**)	10	7.2

Table 3.10. Olefin Cross-Metathesis Results with 1,2-Dichloroethene (*continued)*

#	Olefin A mmol	Olefin B mmol	[Ru][a]	solvent	temp/ time	%Yield[c] (product Chart 2)	TON	Z/E ratio[d]
18	PhS 0.18	Cl Cl 0.694	**3.5**[g]	C_6D_6	23 °C/ 40 h	70(**3.30**)	14	4.4
19	EtS 0.16	Cl Cl 0.9	**3.5**	C_6D_6	23 °C/ 24 h	5 (**3.31**)	1	*Z* only det'd

[a] 5 mol% catalyst was used unless otherwise indicated. [b] A mixture of C_6D_6 and CD_2Cl_2 in a 10 to 1 ratio was used. CD_2Cl_2 was added to ensure that all catalyst dissolved. [c] Alkenyl halide CM product based on internal standard with respect to starting alkene; determined by ^{1}H NMR/GCMS [d] n/a = not determined or unavailable [e] 10 mol% catalyst loading used. [f] Slow addition of catalyst, 1 mol% per hour, was used. 4 mol% catalyst loading was used. [g] Slow addition of catalyst, 1 mol% per hour, was used. 5 mol% catalyst loading was used. [h] The addition products of HCl to styrene (PhC_2H_4Cl) was observed in ≤ 5% yield, suggesting the liberation of HCl through the decomposition of the monohalomethylidene species (derivatives of **3.10-Cl**) with concomitant formation of carbide complexes. [4,5]

Table 3.11. Olefin Cross-Metathesis with Vinyl Chloride

#	Olefin A mmol	Olefin B mmol	[Ru][a]	Solvent	temp/ time	%Yield[c] (product Chart 2)	TON	*Z/E ratio*[d]
1	^{n}Bu ^{n}Bu 0.15	Cl 1.2	**3.5**	C_6D_6[b]	23 °C / 24 h	29 (**3.23**) 29 (**3.33**)	6	*Z* only det'd
2	^{n}Bu ^{n}Bu 0.15	Cl 1.2	**3.6**	C_6D_6[b]	50 °C/ 3 h	25 (**3.23**) 22 (**3.33**)	5	7.4
3	^{n}Bu ^{n}Bu 0.15	Cl 0.88	**3.4**	C_6D_6[b]	50 °C/ 3 h	0 (**3.23**) 0 (**3.33**)	0	-
4	Ph 0.32	Cl 2.4	**3.5**[e]	C_6D_6[b]	50 °C/ 24 h	20(**3.26**) <10 (**3.17**)	2	3
5	Ph 0.15	Cl 1.8	**3.5**	C_6D_6[b]	50 °C/ 3 h	<5 (**3.29**)[f] <5 (**3.19**)	<1	n/a

[a] 5 mol% catalyst was used unless otherwise indicated. [b] A mixture of C_6D_6 and CD_2Cl_2 in a 10 to 1 ratio was used. CD_2Cl_2 was added to ensure that all catalyst dissolved. [c] Alkenyl halide CM product based on internal standard with respect to starting alkene; determined by ^{1}H NMR/GCMS [d] n/a = not determined or unavailable [e] 10 mol% catalyst loading used. [f] The addition products of HCl to styrene (PhC_2H_4Cl) was observed in ≤

5% yield, suggesting the liberation of HCl through the decomposition of the monohalomethylidene species (derivatives of **3.10-Cl**) with concomitant formation of carbide complexes. [4,5]

Table 3.12. Olefin Cross-Metathesis with Vinyl Bromide

#	Olefin A mmol	Olefin B mmol	[Ru][a]	solvent	temp/ time	%Yield[c] (product Chart 2)	TON	Z/E ratio[d]
1	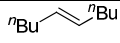 0.15	0.30	**3.5**	C_6D_6[b]	50 °C/ 24 h	22 (**3.34**)[e] 8 (**3.23**)[f]	4 2	n/a
2	0.31	0.33	**3.6**	C_6D_6[b]	50 °C/ 3 h	16(**3.34**)[e]	3	0.5
3	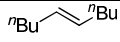 0.15	1.2	**3.5**	C_6D_6[b]	50 °C/ 3 h	5(**3.34**)[e]	1	n/a

[a] 5 mol% catalyst was used unless otherwise indicated. [b] A mixture of C_6D_6 and CD_2Cl_2 in a 10 to 1 ratio was used. CD_2Cl_2 was added to ensure that all catalyst dissolved. [c] Alkenyl halide CM product based on internal standard with respect to starting alkene; determined by ^{1}H NMR/GCMS [d] n/a = not determined or unavailable [e] In certain reactions, the addition products of HBr to 1,2-dibromoethylene (1,1,2-tribromoethane and 1,1,2,2-tetrabromoethane) were observed in ≤ 5% yield, suggesting the liberation of HBr through the decomposition of the monohalomethylidene species with concomitant formation of carbide complexes.[4,5] [f] Halogen exchange was observed when using brominated olefins for CM (**3.23** represents 1-*chloro*-1-hexene).

Table 3.13. Olefin RO-CM with Vinyl Fluoride

#	Olefin A Mmol	Olefin B mmol	[Ru][a]	solvent	temp/ time	%Yield[b] (product Chart 2)	TON[c]	*Z/E* ratio
1	0.15	0.45	**3.5**[d]	C_6D_6	23 °C/ 48 h	55 (**3.13**)	n/d	2.6
2	0.15	2.7	**3.5**	C_6D_6	50 °C/ 24 h	0 (**3.13**)	0	-

[a] 5 mol% catalyst in C_6D_6 was used unless otherwise indicated. [b] Alkenyl halide CM product based on internal standard with respect to starting alkene; determined by ^{1}H NMR/GCMS [c] n/a = not determined or unavailable [d] Intermediate, **3.10-F**, precipitated from C_6D_6 during the course of the reaction; therefore, catalyst loading was <5%. Mixture was sonicated.

Table 3.14. Olefin RO-CM with Chlorinated and Brominated Olefins

#	Olefin A Mmol	Olefin **3.** mmol	[Ru][a]	solvent	temp/ time	%Yield[b] (product Chart 2)	TON	*Z/E* ratio[c]
1	0.15	0.82	**3.5**	C_6D_6	23 °C/ 24 h	>95 (**3.22**)	>19	*2.1*
2	0.15	0.82	**3.5**	C_6D_6	45 °C/ 1 h	>95 (**3.22**)	>19	*2.1*
3	0.17	0.69	**3.5**[e]	C_6D_6	23 °C/ 44 h	97 (**3.22**)	32	*n/a*
4	0.17	1.8	**3.5**	C_6D_6	23 °C/ 24 h	93 (**3.22**+**3.32**)	19	*n/a*
5	0.15	0.833	**3.5**	C_6D_6	23 °C/ 24 h	0[d]	0	*n/a*

[a] Conditions: 5 mol% catalyst in C_6D_6 unless otherwise indicated. [b] Alkenyl halide CM product based on internal standard with respect to starting alkene; determined by ^{1}H NMR/GCMS [c] n/a = not determined or unavailable [d] The addition products of HBr to 1,2-dibromoethylene and cyclooctene (1,1,2-tribromoethane and 1,1,2,2-tetrabromoethane and 1-bromocyclootane, respectively) were observed in ≤ 5% yield, suggesting the liberation of HBr through the decomposition of the monohalomethylidene species with concomitant formation of carbide complexes.[4,5] [e] Slow addition of catalyst, 1 mol% per hour, was used. 3 mol% catalyst loading was used.

CM Attempts with other Olefins. Multiple CM reactions were attempted using the general preparative procedures detailed above with several combinations of reagents in which no catalytic reaction was seen. The following substrates proved unreactive in reactions with vinyl fluoride, vinyl chloride, and 1,2-dichloroethylene: stilbene, allyl alcohol, allyl acetate, ethyl vinyl ketone, methyl acrylate, vinyl boronic acid *n*-butylester. Multiple CM reactions of α-fluorostyrene, β-fluorostyrene, and 1,1-difluoroethylene (separately) with 5-decene or 1-hexene yielded <5% CM products.

Synthesis of the Monofluoromethylidene Dimer 3.10-F (Eq. 3.5, X = F)**.** Compound **3.5** (154.2 mg, 0.246 mmol) was dissolved in 6 mL of toluene and the solution was transferred to a 25 mL bomb flask. The bomb flask was evacuated and refilled with vinyl fluoride gas (5 psig). The solution was cooled in an ice/sodium chloride bath (–4 °C) and stirred for 3 hours. Over this time period, an orange-yellow precipitate formed in solution. The solution was cooled to –35 °C for 30 minutes and then the precipitate was filtered, rinsed with pentane (3 × 2 mL) and dried in vacuo for 30 minutes. The product was then stirred in benzene (5 mL) for 5 min and dried in vacuo for 5 h. The product (**3.10-F**) was isolated in 81.3% yield as an orange-yellow solid (102.3 mg, 0.100 mmol). Single crystals suitable for X-ray diffraction study were obtained upon recrystallization from chloroform at –35 °C. The thermal ellipsoid plot of one of the two crystallographically independent but chemically equivalent molecules clearly shows that **3.10-F** is a chloride-bridged dimer in the solid state. The product is moderately soluble in CD_2Cl_2 or $CDCl_3$ but is thermally sensitive in solution; complete decomposition occurs within 20 min at 23 °C. ^{1}H NMR (400 MHz, CD_2Cl_2, –20 °C): δ = 12.75 (d, Ru=C*H*F, $^2J_{HF}$ = 95.2 Hz, 1H), 6.98 (s, Mes aryl, 1H), 6.93 (s, Mes aryl, 1H), 6.89 (s, Mes aryl, 2H), 3.98 (m, *H*$_2$IMes backbone, 5H), 2.38 (s, Mes C*H*$_3$, 3H), 2.28 (s, Mes C*H*$_3$, 4H), 2.19, 2.18, 2.16 (overlapping s, Mes C*H*$_3$, 9H), 1.96 (s, Mes C*H*$_3$, 3H), minor products or isomers include: 13.10 (d, overlaps with major product), 12.34 (d, overlaps with major product). ^{13}C NMR (100.489 MHz, CD_2Cl_2, –20 °C, 50,000 scans): δ = 213.48 (H_2IMes carbene *C*), 140.08, 139.61, 139.20, 138.26, 137.52, 134.83, 131.215, 129.90, 129.71, 129.59, 129.36, 129.23, 51.12, 50.99, 21.16, 20.84, 19.96, 19.60, 18.16, 17.99. ^{19}F NMR (376.344 MHz, CD_2Cl_2, 23 °C): δ = 124.30 (d, Ru=CH*F*, $^2J_{HF}$ = 96.3 Hz, 84%), minor

products or isomers: 130.92 (d, $^2J_{HF}$ = 96.3 Hz, 7%), 121.36 ($^2J_{HF}$ = 101.6 Hz, 9%) Anal. Calcd. for $C_{44}H_{54}Cl_4F_2N_4Ru_2$: C, 51.77 %; H, 5.33 %; N, 5.49 %. Found C, 51.79 %; H, 5.41 %; N, 5.40 %

Attempts to Observe a Fluorinated Ruthenacycles. Treatment of **3.6** (20 mg, 0.023 mmol) with excess vinyl fluoride gas at –20 °C in 1 mL of dichloromethane in a J. Young tube for 12 hours afforded vinyltricyclohexylphosphonium tetrafluoroborate and a single new monofluoromethylidene complex (**3.10-F**), but there was no evidence for the presence of any fluorinated metalacycles . Furthermore, initial low-temperature treatment of **3.6** (20 mg, 0.023 mmol) in 1 mL of dichloromethane with excess ethene added into a J. Young tube containing the reaction mixture at –60 °C afforded the ruthenacyclobutane complex as described by Piers.[40] Subsequent evacuation of the J. Young tube followed by addition of vinyl fluoride gas at –60 °C resulted in liberation of ethene and complete conversion over 3 hours to the same new monofluoromethylidene complex that was formed in the absence of ethene with no evidence of the metallocyclic intermediates.

Reaction of 3.10-F with excess pyridine-*d*$_5$. Compound **3.10-F** (20 mg, 0.020 mmol) was dissolved in 1 mL of pyridine-*d*$_5$. After a short mixing time (5 minutes), all solid dissolved and turned red/orange. ^{1}H and ^{19}F NMR confirmed the formation of compound **3.9-py-*d*$_5$** (Eq. 3.9). ^{1}H NMR (400 MHz, pyridine *d*$_5$): δ = 13.38 (d, $^2J_{HF}$ = 89.6 Hz, [Ru]=C*H*F, 1H), 6.99 and 6.371 (broad s, overlapping, Mes aryls, 4H), 3.89 (s, *H*$_2$IMes backbone, 4H), 2.77 (broad s, Mes C*H*$_3$, 12H), 2.20 and 2.00 (broad s, overlapping, Mes C*H*$_3$, 6H). ^{19}F NMR (376.356 MHz,pyridine *d*$_5$): δ = 127.35 (d, $^2J_{HF}$ = 89.6 Hz, [Ru]=CH*F*)

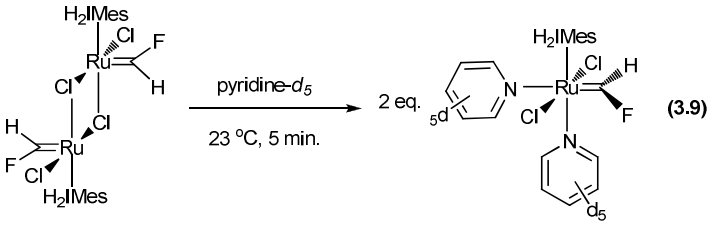

(3.9)

CM involving Vinyl Fluoride, with Compound 3.10-F as a Catalyst (Eq. 3.6). A suspension of compound **3.10-F** (16.8 mg, 0.0165 mmol) and 1-bromo-3,5-bis(trifluoromethyl)benzene (14.4 mg, 0.049 mg) in 0.5 mL of C_6D_6 was frozen. A solution of 5-decene (23.7 mg, 0.169 mmol) in 0.5 mL C_6D_6 was added to the frozen solution in a J. Young tube. The reaction mixture was again frozen and the J. Young tube was evacuated and refilled with vinyl fluoride while the J. Young tube was submerged in liq. N_2. ^{19}F NMR spectroscopy indicated that there was 0.696 mmol of vinyl fluoride in solution. The reaction mixture was thawed and heated at 40 °C and NMR data were collected over 22 h. Compound **3.10-F** did not fully dissolve in the solution. However, 1-fluoro-1-hexene formed (0.0414 mmol) indicated that there were at least 1.25 turnovers based on the total amount of dimer **3.10-F** added. Although the yield was low, **3.10-F** is catalytically competent. Formation of 1-fluoro-1-hexene was monitored by ^{19}F NMR spectroscopy. ^{19}F NMR (376.302 MHz, C_6D_6): δ = -130.2 (dd, $^3J_{HF}$ = 19.2 Hz, $^2J_{HF}$ = 86.2 Hz, *E*): -130.7 (dd, $^3J_{HF}$ = 42.5 Hz, $^2J_{HF}$ = 86.2 Hz, *Z*).

Synthesis of the Monochloromethylidene Dimer 3.10-Cl (Eq. 3.5; X = Cl)**.** A 50 mL bomb flask containing 10 mL toluene was cooled in liquid nitrogen, evacuated, and repressurized with vinyl chloride gas. The solution was allowed to warm to room temperature and taken into the glove box and cooled in the cold well for 30 minutes. The

toluene/vinyl chloride solution was added to compound **3.5** (107.7 mg, 0.172 mmol), stirred briefly (2 min) to ensure that all of compound **3.5** dissolved and placed in the freezer at –35 °C for 6 days. The solution turned brown-orange with an orange precipitate. The solution was filtered and the solid was washed with cold pentane (20 mL). Compound **3.10-Cl** was isolated in 53% yield as an elementally pure orange powder (48 mg, 0.045 mmol). Despite elemental purity, the compound is very sensitive in solution. Although compound **3.10-Cl** was dissolved in solvent that was precooled to –75 °C, small amounts of decomposition and/or isomers of the dimer are present, as determined via ^{1}H NMR spectroscopy. ^{1}H NMR (400 MHz, CD_2Cl_2, –75 °C): Major product: δ = 14.32 (major s, 1H); overlapping signals 7.00 (major s) 6.98 (major s) totaling 2H; 6.89 (major s), 6.87 (major, s) totaling 3H; 3.96 (m, 6H); 2.6-0.8 (alkyls, 20H). Minor products [relative to major component]: δ = 20.48 (s, 0.04H), 20.29 (s, 0.03H), 16.29 (s, 0.05H), 14.77 (s, 0.07H), 14.57 (s, 0.14H), 14.44 (s, 0.13H), 13.92 (s, 0.22H), 13.01 (d, J = 12 Hz, 0.16H), 12.89 (d, J = 12.3Hz, 0.20H), 7.5-6.5 (aryls). ^{13}C NMR (100.489 MHz, CD_2Cl_2, –75 °C): Major product: δ = 274.74, 209.26, 139.34, 139.19, 138.58, 137.70, 137.26, 136.51, 134.02, 130.71, 129.40, 129.23, 128.89, 128.75, 50.63, 50.40, 33.85, 22.37, 20.72, 20.59, 19.44, 19.10, 17.46, 17.41, 13.89. Anal. Calcd. for $C_{44}H_{54}Cl_6N_4Ru_2$: C, 50.15 %; H, 5.17 %; N, 5.32 %. Found C, 50.49 %; H, 5.30 %; N, 5.33 %

Temperature Study of Cross-Metathesis with Vinyl Fluoride. In 1 mL of toluene-d_8, 5-decene (23.2 mg, 0.165 mmol) was dissolved along with an internal standard (1-bromo-3,5-trifluoromethylbenzene, 12.7 mg, 0.043 mmol). A ^{1}H NMR spectrum was acquired (d_1 = 10 s). The J. Young tube was cooled in the glove box cold

well and compound **3.1-H_2IMes** (7.3 mg, 0.0086 mmol, 5.2 mol%) was added. The reaction mixture was removed from the glove box and frozen in liquid N_2. The J. Young tube was evacuated and was refilled with vinyl fluoride (7 psig). The reaction mixture was then heated in an oil bath to 100°C. ^{19}F NMR spectroscopy indicated that there was 0.406 mmol of vinyl fluoride present in solution. NMR data after 45 minutes indicated that 1-fluoro-1-hexene and 1-hexene had formed. Integration relative to the internal standard in the ^{19}F NMR spectrum (d_1 = 10 sec) indicated a 12% conversion to 1-fluoro-1-hexene (2.3 turnovers). *E*/*Z* isomer ratio = 1:3. ^{19}F NMR (376.302 MHz, CD_2Cl_2, d_1=1 sec): δ = -130.2 (dd, $^3J_{HF}$ = 19.2 Hz, $^2J_{HF}$ = 86.2 Hz, *E*): -130.7 (dd, $^3J_{HF}$ = 42.5 Hz, $^2J_{HF}$ = 86.2 Hz, *Z*)

A stock solution of 5-decene (86.0 mg, 0.613 mmol), internal standard (1-bromo-3,5-bis(trifluoromethyl)-benzene) (25.8 mg, 0.0881 mmol), and compound **3.1-H_2IMes** (24.0 mg, 0.0303 mmol) in 4.0 mL toluene-d_8 was prepared. This stock solution was split into four J. Young tubes. Each NMR tube contained 5-decene (0.153 mmol), internal standard (0.0220 mmol), and compound **3.1-H_2IMes** (0.0076 mmol, 5 mol%). The NMR tubes were evacuated and refilled with vinyl fluoride (0.7, 0.6, 0.5, 0.4 mmol corresponding to 23 °C, 65 °C, 80 °C, 95 °C respectively) while being frozen in liquid N_2 for three seconds. The NMR tubes were kept at room temperature, and heated to 23 °C, 65 °C, 80 °C, 95 °C and monitored over time. At 65 °C, 13% conversion to metathesis products was seen between 4.5 h and 21 h (0.02 mmol of 1-fluoro-1-hexene and 0.02 mmol 1-hexene), at which point metathesis no longer occurred and all catalyst had decomposed to carbide. The *E/Z* ratio of 1-fluoro-1-hexene was 1:2.6. At 80 °C, 13% conversion to metathesis products was seen between 1 and 2 h (0.02 mmol of 1-fluoro-1-

hexene and 0.02 mmol of 1-hexene) at which point metathesis no longer occurred and all catalyst had decomposed to carbide. The *E/Z* ratio of 1-fluoro-1-hexene was 1:2.4. At 95 °C, 13% conversion to metathesis products was seen at 1 h (0.02 mmol of 1-fluoro-1-hexene and 0.02 mmol of 1-hexene) at which point metathesis no longer occurred and all catalyst had decomposed to carbide. The *E/Z* ratio of 1-fluoro-1-hexene was 1:2.5. No reaction was observed at room temperature even after 21 hours.

Alkene Isomerization Reactions. Allylbenzene (35.5 mg, 0.300 mmol, 1.00 equiv) was dissolved in 1 mL of C_6D_6. A solution of **3.5** (9.4 mg, 0.015 mmol, 5 mol%) in 0.1 mL of CD_2Cl_2 was added to the reaction mixture. The reaction mixture was placed in an NMR tube and removed from the glove box. The reaction was heated to 50 °C for 16 h and then ^{1}H NMR data and GC-MS data were acquired. The major products in the reaction mixture were stilbene and 1,3-diphenyl-1-propene One minor product, 1-phenyl-2-butene, was observed. Products in less than 5% yield included styrene, 1-phenyl-3-butene, 1-phenyl-1-butene, 1-phenyl-1-propene, and 1,4-diphenyl-2-butene. Allylbenzene had not been completely consumed (Scheme 3.7).

Allyloxybenzene (40.2 mg, 0.300 mmol, 1.00 equiv) was dissolved in 1 mL of C_6D_6. A solution of **3.5** (9.4 mg, 0.015 mmol, 5 mol%) in 0.1 mL of CD_2Cl_2 was added to the reaction mixture. The reaction mixture was placed in an NMR tube and removed from the glove box. The reaction was heated to 50 °C for 16 h and then ^{1}H NMR data and GC-MS data were acquired. The major products in the reaction mixture were 1,4-diphenoxy-2-butene, and 1-propenyloxybenzene. Minor products included vinyloxybenzene, 2-butenyloxybenzene, 3-butenyloxybenzene, 1-butenyloxybenzene,

1,3-bis(phenoxy)-1-propene, and one isomer of C_5H_9OPh. Allyloxybenzene had not been completely consumed (Scheme 3.8).

3.8. References

1. Morrill, C.; Grubbs, R. H., Synthesis of functionalized vinyl boronates via ruthenium-catalyzed olefin cross-metathesis and subsequent conversion to vinyl halides. *J. Org. Chem.* **2003,** *68* (15), 6031-6034.
2. Tsuji, J., Reactions of Organic Halides and Pseudohalides. In *Transition Metal Reagents and Catalysts: Innovations in Organic Synthesis*, Wiley: New York, 2000; pp 27-108.
3. Caskey, S. R.; Stewart, M. H.; Kivela, J. E.; Sootsman, J. R.; Johnson, M. J. A.; Kampf, J. W., Two Generalizable Routes to Terminal Carbido Complexes. *J. Am. Chem. Soc.* **2005,** *127*, 16750-16751.
4. Macnaughtan, M. L.; Johnson, M. J. A.; Kampf, J. W., Synthesis, Structure, and Olefin Metathesis Activity of Two Ruthenium Monofluoromethylidene Complexes. *Organometallics* **2007,** *26* (4), 780-782.
5. Macnaughtan, M. L.; Johnson, M. J. A.; Kampf, J. W., Olefin Metathesis Reactions with Vinyl Halides: Formation, Observation, Interception, and Fate of the Ruthenium-Monohalomethylidene Moiety. *J. Am. Chem. Soc.* **2007,** *129* (25), 7708-7709.
6. Fomine, S.; Ortega, J. V.; Tlenkopatchev, M. A., Metathesis of halogenated olefins - A computational study of ruthenium alkylidene mediated reaction pathways. *Journal Of Molecular Catalysis A-Chemical* **2007,** *263* (1-2), 121-127.
7. Trnka, T. M.; Day, M. W.; Grubbs, R. H., Olefin metathesis with 1,1-difluoroethylene. *Angew. Chem.-Int. Edit.* **2001,** *40* (18), 3441-+.
8. Louie, J.; Grubbs, R. H., Metathesis of Electron-Rich Olefins: Structure and Reactivity of Electron-Rich Carbene Complexes. *Organometallics* **2002,** *21*, 2153.
9. Gary, J. B.; Buda, C.; Johnson, M. J. A.; Dunietz, B. D., Accessing Metal−Carbide Chemistry. A Computational Analysis of Thermodynamic Considerations. *Organometallics* **2008,** *27* (5), 814-826.
10. Buda, C.; Caskey, S. R.; Johnson, M. J. A.; Dunietz, B. D., Metathesis-Enabled Formation of a Terminal Ruthenium Carbide Complex: A Computational Study. *Organometallics* **2006,** *25*, 4756-4762.
11. Stewart, M. H.; Johnson, M. J. A.; Kampf, J. W., Terminal Carbido Complexes of Osmium: Synthesis, Structure, and Reactivity Comparison to the Ruthenium Analogues. *Organometallics* **2007,** *26*, accepted.
12. Sashuk, V.; Samojlowicz, C.; Szadkowska, A.; Grela, K., Olefin cross-metathesis with vinyl halides. *Chem. Commun.* **2008,** (21), 2468-2470.
13. Love, J. A.; Morgan, J. P.; Trnka, T. M.; Grubbs, R. H., A practical and highly active ruthenium-based catalyst that effects the cross metathesis of acrylonitrile. *Angew. Chem.-Int. Edit.* **2002,** *41* (21), 4035-4037.
14. Garber, S. B.; Kingsbury, J. S.; Gray, B. L.; Hoveyda, A. H., Efficient and recyclable monomeric and dendritic Ru-based metathesis catalysts. *J. Am. Chem. Soc.* **2000,** *122* (34), 8168-8179.
15. Gessler, S.; Randl, S.; Blechert, S., Synthesis and metathesis reactions of a phosphine-free dihydroimidazole carbene ruthenium complex. *Tetrahedron Lett.* **2000,** *41* (51), 9973-9976.

16. Romero, P. E.; Piers, W. E.; McDonald, R., Rapidly Initiating Ruthenium Olefin-Metathesis Catalysts. *Angew. Chem. Int. Ed.* **2004,** *43*, 6161.
17. Alami, M.; Crousse, B.; Ferri, F., Weakly ligated palladium complexes PdCl2(RCN)(2) in piperidine: versatile catalysts for Sonogashira reaction of vinyl chlorides at room temperature. *Journal Of Organometallic Chemistry* **2001,** *624* (1-2), 114-123.
18. Ochran, R. A.; Uggerud, E., S(N)2 reactions with allylic substrates - Trends in reactivity. *International Journal Of Mass Spectrometry* **2007,** *265* (2-3), 169-175.
19. Dolbier, W. R.; Rong, X. X.; Bartberger, M. D.; Koroniak, H.; Smart, B. E.; Yang, Z. Y., Cyclization reactivities of fluorinated hex-5-enyl radicals. *Journal Of The Chemical Society-Perkin Transactions 2* **1998,** (2), 219-231.
20. Uno, H.; Sakamoto, K.; Semba, F.; Suzuki, H., Behaviors Of Alpha-Fluorocarbenoids Derived From The Nucleophilic Desulfinylation Of Alpha-Chloro-Alpha-Fluoroalkyl Sulfoxides. *Bulletin Of The Chemical Society Of Japan* **1992,** *65* (1), 210-217.
21. Blackwell, H. E.; O'Leary, D. J.; Chatterjee, A. K.; Washenfelder, R. A.; Bussmann, D. A.; Grubbs, R. H., New approaches to olefin cross-metathesis. *J. Am. Chem. Soc.* **2000,** *122* (1), 58-71.
22. Petasis, N. A.; Yudin, A. K.; Zavialov, I. A.; Prakash, G. K. S.; Olah, G. A., Facile preparation of fluorine-containing alkenes, amides and alcohols via the electrophilic fluorination of alkenyl boronic acids and trifluoroborates. *Synlett* **1997,** (5), 606-&.
23. Mauze, B.; Ongoka, P.; Miginiac, L., Study Of The Alkylation Of Monochloroallyllithium Compounds - 1-Step Synthesis Of Secondary Or Tertiary Allyl Chlorides And Or Vinyl Chlorides Of Z-Configuration. *Journal Of Organometallic Chemistry* **1984,** *264* (1-2), 1-7.
24. Mortimer, F. S., The Nmr Spectra Of Some Halogenated Propenes - Abx2 Systems. *Journal Of Molecular Spectroscopy* **1959,** *3* (4), 335-348.
25. Liu, M. T. H.; Subramanian, R., Reaction Of Benzylchlorocarbene With Hydrogen-Chloride. *J. Org. Chem.* **1985,** *50* (17), 3218-3220.
26. Gomez, C.; Huerta, F. F.; Yus, M., DTBB-catalysed lithiation of 3-functionalised 1-chloropropenes. *Tetrahedron* **1998,** *54* (22), 6177-6184.
27. Bigi, F.; Casiraghi, G.; Casnati, G.; Sartori, G., Modification Of The Nickel Reaction - A General Synthetic Approach To 2-Vinyl-2,3-Dihydrobenzofurans. *Tetrahedron* **1983,** *39* (1), 169-174.
28. Merrer, D. C.; Moss, R. A.; Liu, M. T. H.; Banks, J. T.; Ingold, K. U., Benzylchlorocarbene: Origins of Arrhenius curvature in the kinetics of the 1,2-H shift rearrangement. *J. Org. Chem.* **1998,** *63* (9), 3010-3016.
29. Nelson, D. J.; Brown, H. C., Hydroboration Kinetics .4. Kinetics And Mechanism Of The Reaction Of 9-Borabicyclo[3.3.1]Nonane With Representative Haloalkenes - The Effect Of Halogen Substitution Upon The Rate Of Hydroboration. *J. Am. Chem. Soc.* **1982,** *104* (18), 4907-4912.
30. Dieck, H. A.; Heck, R. F., Palladium-Catalyzed Conjugated Diene Synthesis From Vinylic Halides And Olefinic Compounds. *J. Org. Chem.* **1975,** *40* (8), 1083-1090.

31. Sanford, M. S.; Henling, L. M.; Day, M. W.; Grubbs, R. H., Ruthenium-based four-coordinate olefin metathesis catalysts. *Angew. Chem.-Int. Edit.* **2000,** *39* (19), 3451-+.
32. vanderEide, E. F.; Romero, P. E.; Piers, W. E., Generation and Spectroscopic Characterization of Ruthenacyclobutane and Ruthenium Olefin Carbene Intermediates Relevant to Ring Closing Metathesis Catalysis. *J. Am. Chem. Soc.* **2008,** *130* (13), 4485-4491.
33. Chatterjee, A. K.; Choi, T. L.; Sanders, D. P.; Grubbs, R. H., A general model for selectivity in olefin cross metathesis. *J. Am. Chem. Soc.* **2003,** *125* (37), 11360-11370.
34. Zhang, W.; Moore, J. S., Reaction pathways leading to arylene ethynylene macrocycles via alkyne metathesis. *J. Am. Chem. Soc.* **2005,** *127* (33), 11863-11870.
35. Hong, S. H.; Wenzel, A. G.; Salguero, T. T.; Day, M. W.; Grubbs, R. H., Decomposition of Ruthenium Olefin Metathesis Catalysts. *J. Am. Chem. Soc.* **2007,** *129*, 7961.
36. Caskey, S. R. Exploration of Ruthenium Carbon Multiple Bond Complexes: Carbenes, Carbynes, and Carbides. Ph.D., University of Michigan, Ann Arbor, 2007.
37. Lehman, S. E.; Wagener, K. B., Synthesis of ruthenium olefin metathesis catalysts with linear alkyl carbene complexes. *Organometallics* **2005,** *24* (7), 1477-1482.
38. Caskey, S. R.; Ahn, Y. J.; Johnson, M. J. A.; Kampf, J. W., Terminal Carbide Formation from Acyloxycarbenes: Relevance to Olefin Metathesis. *submitted* **2007**.
39. Gottlieb, H. E.; Kotlyar, V.; Nudelman, A., NMR chemical shifts of common laboratory solvents as trace impurities. *J. Org. Chem.* **1997,** *62* (21), 7512-7515.
40. Romero, P. E.; Piers, W. E., Direct Observation of a 14-Electron Ruthenacyclobutane Relevant to Olefin Metathesis. *J. Am. Chem. Soc.* **2005,** *127*, 5032-5033.

Chapter 4

Enyne Metathesis with Vinyl Halides

4.1. Introduction

Until recently, the reasons for the failure of ruthenium-catalyzed cross-metathesis (CM) reactions involving alkenyl halides were not well understood. Two factors are responsible for this failure. First, the Fischer carbene complexes that form upon initial reaction of vinyl halides, vinyl ethers, or vinyl esters with the Grubbs-type catalysts, Ru(=CHX)(H_2IMes)(L')Cl_2 (Chart 4.1: **4.2-4.6, 4.10-4.12, 4.19,** and **4.20**), are thermodynamically stable with respect to the corresponding benzylidene complexes from which they form, Ru(=CHPh)(H_2IMes)(L')Cl_2 (Chart 4.1: **4.1, 4.9,** and **4.13**).[1-4] Second, complexes of the form Ru(=CHX)(H_2IMes)(PCy_3)Cl_2 (X = F, OAc, Cl, Br) (Chart 4.1: **4.2-4.4** and **4.6**) rearrange to form the corresponding terminal carbide and/or phosphoniomethylidene complexes (Chart 4.1: **4.**7 and **4.8**).[1,2,5] Nevertheless, monofluoromethylidene complexes (Chart 4.1: **4.2**, **4.10** and **4.19**) prepared by metathesis are often persistent in solution and isolable.[2,6] Even certain acyloxycarbene complexes such as **4.6** and can be isolated under some conditions.[5] However, the monochloro- and monobromomethylidene complexes **4.3, 4.4** and **4.11** are not isolable intermediates in reactions of vinyl halides with **4.1** or **4.9**.[2]

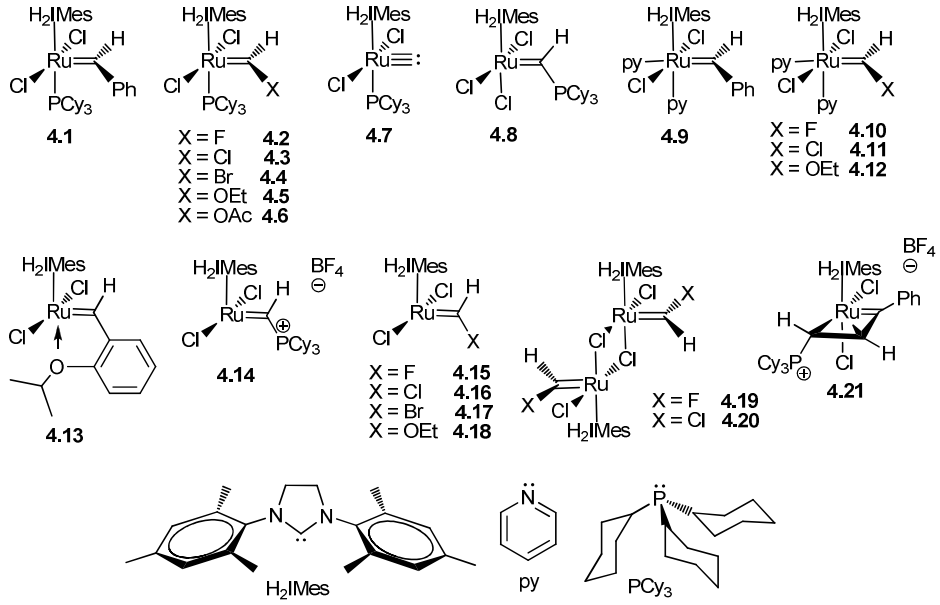

Chart 4.1. Important Ruthenium Compounds

In Chapter 3, we demonstrated that catalysts which lack a fifth recoordinating ligand *trans* to the *N*-heterocyclic carbene ligand (H_2IMes = 4,5-dihydro-1,3-bis-(2,4,6-trimethylphenyl)imidazol-2-ylidene) such as **4.13**[7,8] or **4.14**[9] (Chart 4.1) permit successful CM of vinyl halides and simple alkenes.[6] Grela and co-workers report similar findings.[10] However, the isolable monofluoromethylidene dimer, **4.19**, formed from these catalysts was too thermodynamically stable with respect to the Ru-alkylidene intermediate to afford efficient catalytic turnover in CM reactions. CM with vinyl fluoride therefore gave low yields (9 to 11%; ~2 TON).[6] When cyclooctene was used in ring-opening CM with vinyl fluoride, yields of the metathesis product (1-fluoro-1,9-decadiene) were significantly higher (55%; 11 TON). This indicated that the added enthalpic driving force from release of ring strain allowed for a higher catalytic turnover.[6] Formation of the isolable monochloromethylidene dimer, **4.20**, was also observed; however, this

substrate was more active in CM with simple alkenes, affording alkenyl chloride products in yields up to 98% (4 mol% catalyst loading, 24 TON). This indicated that the 14-electron monochloromethylidene intermediate (Chart 4.1: **4.16**) was less thermodynamically stable than the monofluoromethylidene intermediate (Chart 4.1: **4.15**). These findings agree well with DFT calculations reported by Fomine describing the thermodynamics of metathesis of a model Ru-alkylidene complex with 1,2-dichloroethene and 1,2-difluoroethene as discussed in Chapter 1.[3]

4.2. Enyne Metathesis (EyM) with Vinyl Halides

4.2.1. EyM with Vinyl Fluoride

Given the similar metathesis activity of **4.2** and **4.5** and the similar reactivity and decomposition modes of **4.2** and **4.6**,[1] we reasoned that enyne metathesis (EyM) reactions with vinyl halides (Eq. 4.1) should be feasible under the same mild conditions as EyM with ethyl vinyl ether and vinyl acetate.[11] In fact, EyM of vinyl fluoride with a number of alkynes proceeds to give high percent conversion to the fluorinated butadiene products (Chart 4.2: **4.22-4.29**). EyM with vinyl fluoride generally yielded 70-100% conversion of starting materials to products with catalysts **4.1, 4.2, 4.9, 4.13,** or **4.14**. Both terminal and internal alkynes were tolerated as substrates. Alkyl-, aryl-, and silyl-substituted alkynes as well as propargyl benzoate were successful substrates for EyM with vinyl fluoride. In general, benzene was the optimal solvent for these reactions; however, some butadiene products, **4.23** and **4.27**, had relatively low boiling points (100-150 °C). In these cases, dichloromethane was the preferred solvent for isolation purposes (Tables 4.1 and 4.2).

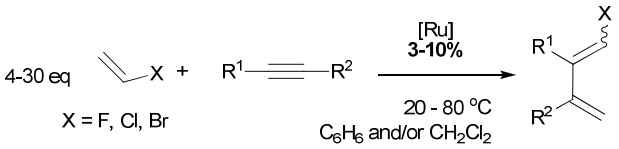

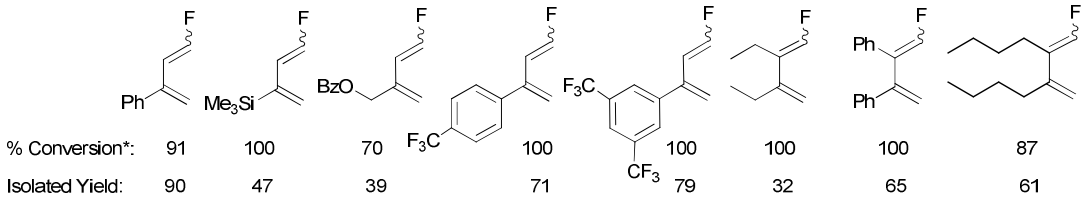

	4.22	4.23	4.24	4.25	4.26	4.27	4.28	4.29
% Conversion*:	91	100	70	100	100	100	100	87
Isolated Yield:	90	47	39	71	79	32	65	61

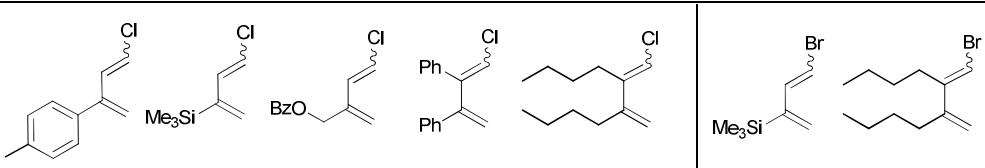

	4.30	4.31	4.32	4.33	4.34	4.35	4.36
% Conversion*:	90	100	78	75	100	58	10-30
Isolated Yield:	45	52	41	n/a	83	25	n/a

* Percent conversion based on NMR scale reactions with internal standard

Chart 4.2: EyM Products

4.2.2. EyM with Vinyl Chloride

Vinyl chlorides likewise gave excellent conversion to the chlorinated butadiene products in EyM with an assortment of alkynes (Chart 4.2: **4.30-4.34;** Table 4.3). In these cases, the choice of catalyst was restricted. Only catalysts **4.13** and **4.14** were productive for EyM with vinyl chloride. EyM of vinyl chloride with trimethylsilylacetylene using catalyst **4.1** gave only 30% yield of **4.31** with 10 mol% catalyst loading as seen in Chapter 2. Of the 1-chloro-(2,)3-substituted-1,3 butadienes synthesized by this method, only two had been previously reported (**4.33** and **4.34**).[12] For reactions with vinyl chloride and aryl alkynes, the corresponding chlorinated aryl alkene

and dichlorinated aryl alkane were detected in less than 5% conversion with respect to the initial alkyne (Scheme 4.2). The formation of these products is attributed to decomposition of the catalytic intermediates (**4.16** and/or **4.20**) through loss of HCl followed by the addition of HCl across the aryl alkyne.

4.2.3. EyM with Vinyl Bromide

Vinyl bromide gave much lower percent conversions for EyM (Chart 4.2: **4.35** and **4.36**[12]; Table 4.4). Reasonable conversion was achieved only with the most active alkyne substrate, trimethylsilylacetylene. Failure to achieve adequate EyM with vinyl bromide can be attributed to the weak C-Br bond in the key Ru intermediate, **4.17**, and therefore very rapid catalyst decomposition. Formation of brominated alkenes and dibrominated alkanes from the starting alkynes was observed in up to 10% conversion with respect to the initial amount of alkyne when 10 mol% catalyst loading was used (Scheme 4.3). This strongly suggests that decomposition of the monobromomethylidene intermediate occurs through loss of HBr. In addition, halogen exchange with the chloride ancilliary ligands on the ruthenium intermediates was noted.[2] In these cases, 1-chloro-(2,)3-substituted-1,3-butadiene was observed as a byproduct along with small amounts of the desired product, 1-bromo-(2,)3-substituted-1,3-butadiene. Variable temperature studies with vinyl bromide and trimethylsilylacetylene showed little variation in percent conversion to the desired products over the temperature range –20 to 45 °C (Table 4.4: Entries 1-4). As temperature was decreased, both decomposition and metathesis were slowed.

4.3. Regiochemistry

In general, terminal alkynes and vinyl halides afforded the 1-halo-3-substituted isomer with > 95% regioselectivity (compounds **4.22**, **4.24-4.26**, **4.30**, **4.32**). The only exception to high regioselectivity was the EyM reaction of vinyl halides with trimethylsilylacetylene. In the case of vinyl fluoride, 13% of the (*E/Z*) 1-fluoro-2-trimethylsilyl-1,3-butadiene isomers was detected as well as other more common side products, including 1,4-difluoro-2-trimethylsilyl-1,3-butadiene (1%) and 2-trimethylsilyl-1,3-butadiene (~1%). Generally, the byproducts, 1,4-dihalo-2-substituted-1,3-butadiene and 2-substituted-1,3-butadiene were seen in less than 5% yield and were identified via gas chromatography-mass spectrometry (GC-MS) (Schemes 4.1-4.3).

The *E/Z* ratio for the desired products was typically close to unity, as was commonly observed in previously published EyM reactions.[11, 13] The only exceptions to the *E/Z* ratio were 1-fluoro-2,3-diphenyl-1,3-butadiene (Chart 4.2: **4.28**) and 1-chloro-2,3-diphenyl-1,3-butadiene (Chart 4.2: **4.33**), in which the *E/Z* ratios were 5 and 18 respectively. As a substrate, diphenylacetylene required anomalously long reaction times. As steric bulk on the alkyne was increased, metathesis was slowed and could be completely shut down as noted in the case with bis(trimethylsilyl)acetylene, for which no reaction was observed.

4.4. Reaction Conditions

As is customary, excess olefin was used in order to suppress alkyne homodimerization of terminal alkynes (Eqs. 4.2 and 4.3).[14] Under conditions where excess vinyl halide was used, we did not observe alkyne dimerization; however, alkyne

dimerization with terminal alkynes was observed when insufficient amounts of vinyl halide (< 2 equivalents) were used. Control reactions of terminal alkynes with catalysts **4.1** and **4.13** in the absence of vinyl halides yielded the alkyne homodimers.[15] Catalyst loadings were 4-5 mol% with respect to the alkyne. For phenylacetylene and catalyst **4.1**, 61% conversion to (*Z*)-1,4-diphenyl-but-1-en-3-yne[15] and 7% conversion to 1,3-diphenyl-but-3-en-1-yne[15] was observed after 24 hours at 40 °C (Eq. 4.2). Trimethylsilylacetylene was dimerized with catalyst **4.13** (5 mol% catalyst loading). After 44 hours at room temperature, 22% conversion to 1,3-bistrimethylsilyl-but-3-en-1-yne[15] and 7% conversion to a second isomer was observed (Eq. 4.3).

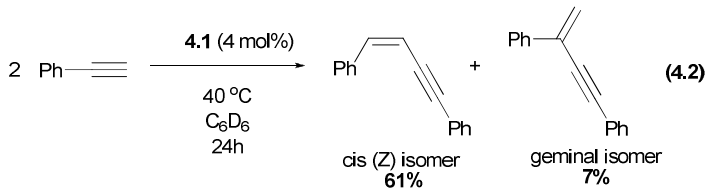

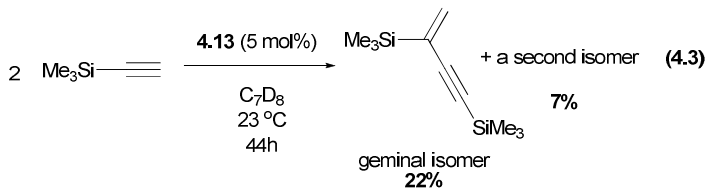

4.5. Catalyst Selection

4.5.1. Vinyl Fluoride

As seen in Tables 4.1, 4.3 and 4.4, the observed percent conversion to products for certain alkynes depended on the catalyst. In the case of vinyl fluoride, catalysts **4.1**, **4.9**, **4.13** and **4.14** were viable with catalyst loadings as low as 4 mol%. For the

formation of 1-fluorobutadienes **4.22**, **4.23**, **4.25**, **4.26**, and **4.28** (Chart 4.2), complex **4.1** was an effective catalyst (Table 4.1: entries 1, 7, 11, 12, 16 respectively). For the formation of 1-fluorobutadienes **4.24**, **4.27**, and **4.29** (Chart 4.2), catalysts **4.13** and **4.14** were more efficient than other catalysts (Table 4.1: entries 8-10, 14, and 18 respectively). Overall, compound **4.13** was the most indiscriminate catalyst with respect to alkyne functionality. Catalysts **4.1**, **4.9** and **4.13** afforded much higher yields of 1-fluoro-3-phenyl-1,3-butadiene (**4.22**, Table 4.1: entries 1-3) than did **4.14** (Table 4.1: entry 4), which gave an unexpectedly low conversion. The low conversion arose from the presence of a competing reaction whereby phenylacetylene reacted within 5 minutes at room temperature with **4.14** to form a "side-on" η^3-vinylcarbene complex (Eq. 4.4). The structure of complex **4.21** (Chart 4.1) was determined by two-dimensional COSY and HSQC NMR experiments as well as $^1H\{^{31}P\}$ NMR spectroscopy. Grubbs has reported the formation of related η^3-vinylcarbene complexes in reactions of **4.1** with an alkyne at 80 °C for 5 hours (Eq. 4.5).[16] Compound **4.21** was found to be unreactive even towards excess vinyl fluoride at 60 °C in benzene over 48 h and therefore inactive for EyM under our conditions.

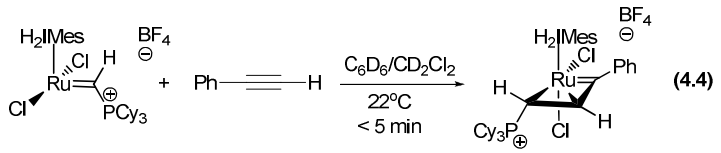

(4.4)

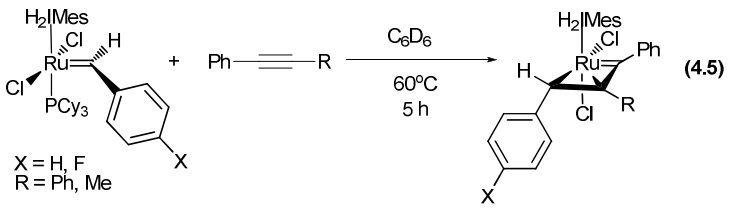

(4.5)

Table 4.1. Reaction Details for NMR Scale Reactions with Vinyl Fluoride.

#	R^{1a}	R^{2a}	Vinyl fluoride (mmol)	Solvent	Temp	[Ru][b]	Product: % conversion[c]	time (h)[d]
1	Ph	H	4.8	C_6D_6	65°C	**4.1**	**4.22:** 91 (100)	1.5
2	Ph	H	2.1	C_6D_6	45°C	**4.13**[e]	**4.22:** 80 (100)	0.5
3	Ph	H	2.2	CD_2Cl_2	45°C	**4.9**[e]	**4.22:** 62	1.5
4	Ph	H	1.6	C_6D_6/ CD_2Cl_2	23°C	**4.14**[e]	**4.22:** 22	49
5	$Si(CH_3)_3$	H	1.4	CD_2Cl_2	45°C	**4.9**	**4.23:** 78 (95)	1.5
6	$Si(CH_3)_3$	H	1.7	C_6D_6	23°C	**4.9**[f]	**4.23:** 87	24
7	$Si(CH_3)_3$	H	1.6	C_6D_6	50°C	**4.1**[g]	**4.23:** (100)	6
8	CH_2OBz	H	2.6	C_6D_6	45°C	**4.13**	**4.24:** 70 (100)	0.5
9	CH_2OBz	H	1.3	C_6D_6/ CD_2Cl_2	45°C	**4.14**	**4.24:** 56 (>90)	24
10	CH_2OBz	H	2.1	C_6D_6	70°C	**4.1**	**4.24:** 37	31
11	$(CF_3)Ph$	H	1.0	C_6D_6	80°C	**4.1**	**4.25:** (100)	0.5
12	$(CF_3)_2Ph$	H	1.5	C_6D_6	60°C	**4.1**	**4.26:** (100)	0.5
13	$(CF_3)_2Ph$	H	3.2	C_6D_6	80°C	**4.1**	**4.26:** (100)	0.5
14	C_2H_5	C_2H_5	2.3	CD_2Cl_2	23°C	**4.14**[e]	**4.27:** 100	0.5
15	C_2H_5	C_2H_5	1.0	C_6D_6	23°C	**4.14**[e]	**4.27:** 100	0.5
16	Ph	Ph	0.9	C_6D_6	80°C	**4.1**	**4.28:** 100	12
17	Ph	Ph	3.3	C_6D_6/ CD_2Cl_2	23°C	**4.14**[e]	**4.28:** 48.8	72
18	C_4H_9	C_4H_9	1.2	CD_2Cl_2	40°C	**4.14**[e]	**4.29:** 87 (100)	1.5

[a] R^1 and R^2 indicate substitution on the alkyne; see Eq. 4.1. [b] Catalyst loading was 5 mol% based on the amount of alkyne unless otherwise indicated. [c] Percent conversion was determined based on the amounts of fluorine-containing products in the ^{19}F NMR spectrum with respect to an internal standard. Percentages in parentheses represent the amount of starting alkyne that was consumed. [d] Reaction times generally represent the point at which the reaction reached completion, however, in some cases where low yields were observed, the reaction was run longer than necessary to be sure of completion. [e] 4

mol% catalyst loading was used. [f] 7.5 mol% catalyst loading was used. [g] 10 mol% catalyst loading was used.

Table 4.2. Larger Scale EyM Reactions with Vinyl Fluoride

#	R^{1a}	R^{2a}	alkyne (mmol)	Solvent	Temp	[Ru][b]	Isolated %Yield[c]	time (h)
1	Ph	H	1.2	CH_2Cl_2	45 °C	**4.9**	**4.22:** 90%	5
2	$Si(CH_3)_3$	H	1.5	CH_2Cl_2	40 °C	**4.9**	**4.23:** 47%[e]	3
3	CH_2OBz	H	1.5	C_6H_6	45 °C	**4.13**	**4.24:** 39% (76%) [f]	24
4	CF_3Ph	H	0.622	CH_2Cl_2	45 °C	**4.9**	**4.25:** 67%	3
5	CF_3Ph	H	0.622	C_6H_6	65 °C	**4.1**	**4.25:** 71%	3
6	$(CF_3)_2Ph$	H	0.420	CH_2Cl_2	45 °C	**4.9**	**4.26:** 79%	3
7	$(CF_3)_2Ph$	H	0.466	C_6H_6	65 °C	**4.1**	**4.26:** 79%	3
8	C_2H_5	C_2H_5	1.5	CH_2Cl_2	22 °C	**4.14**[d]	**4.27:** 32% [e]	3
9	Ph	Ph	1.5	C_6H_6	80 °C	**4.1**	**4.28:** 65%	24
10	C_4H_9	C_4H_9	1.15	CH_2Cl_2	40 °C	**4.14**[d]	**4.29:** 61%	3

[a] R^1 and R^2 indicate substitution on the alkyne; see Eq. 4.1. [b] Catalyst loading was 5 mol% based on the amount of alkyne unless otherwise indicated. [c] Isolation procedures were dependent on diene synthesized and are given in the next section along with characterization data. [d] 3 mol% catalyst loading used. [e] Although 100% conversion was seen, volatility of the product caused lower yields during isolation. [f] Yield in parentheses was the product yield based on ^{1}H NMR spectroscopy before column chromatography.

Byproducts for EyM with vinyl fluoride confirmed by GC-MS (0 to ≤ 12%) included 1,4-difluoro-2,3-substituted-1,3-butadiene and 2,3-substituted-1,3-butadiene and 1-fluoro-2-substituted-1,3-butadiene (Scheme 4.1).

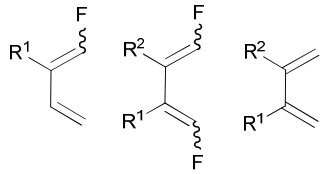

Scheme 4.1. Byproducts of EyM with Vinyl Fluoride

4.5.2. Vinyl Chloride and Vinyl Bromide

For reactions involving vinyl chloride and vinyl bromide, catalysts **4.13** or **4.14** were required in order to minimize catalyst decomposition.[2,6] In these cases, **4.13** was the more efficient catalyst, requiring 5-10 mol% catalyst loadings (Tables 4.3 and 4.4). Generally, EyM with vinyl chloride or vinyl bromide required higher catalyst loadings than with vinyl fluoride.

Table 4.3. Reaction Details for NMR Scale Reactions with Vinyl Chloride.

#	R^{1a}	R^2	Vinyl Chloride (mmol)	solvent	Temp	[Ru][b]	Product: % conversion[c]	time (h)[d]
1	Tolyl	H	2.5	C_6D_6	23°C	**4.13**	**4.30:** 90	1.5
2	$Si(CH_3)_3$	H	0.92	C_6D_6	45°C	**4.13**	**4.31:** 100	0.5
3	$Si(CH_3)_3$	H	1.5	C_6D_6	23°C	**4.13**	**4.31:** 89	1.5
4	CH_2OBz	H	2.5	C_6D_6	23°C	**4.13**	**4.32:** 78(100)	1
5	Ph	Ph	1.9	C_6D_6	23°C	**4.13**[f]	**4.33**[g]**:** 59	22
6	Ph	Ph	0.62	C_6D_6	40°C	**4.13**[f]	**4.33**[g]**:** 75	17
7	C_4H_9	C_4H_9	4.5	C_6D_6	23°C	**4.13**	**4.34**[g]**:** 80	1
8	C_4H_9	C_4H_9	1.3	C_6D_6	23°C	**4.13**[e]	**4.34**[g]**:** 100	17

[a] R^1 and R^2 indicate substitution on the alkyne; see Eq. 4.1. [b] Catalyst loading was 5 mol% based on the amount of alkyne unless otherwise indicated. [c] Percent conversion was determined based on the amounts of products in the ^1H NMR spectrum with respect to an internal standard. Percentages in parentheses represent the amount of starting alkyne that was consumed. [d] Reaction times generally represent the point at which the reaction reached completion, however, in some cases where low yields were observed, the reaction was run longer than necessary to be sure of completion. [e] 7.5 mol% catalyst loading was used. [f] 10 mol% catalyst loading was used. [g] reference for products **4.33** and **4.34.**[12]

Byproducts in EyM with vinyl chloride (0 to ≤ 5%) included 1,4-dichloro-2,3-substituted-1,3-butadiene, 2,3-substituted-1,3-butadiene, 1-chloro-1,2-substituted-alkene, $C_2H_2R^1R^2Cl_2$, and 1-chloro-2-substituted-1,3-butadiene (Scheme 4.2).

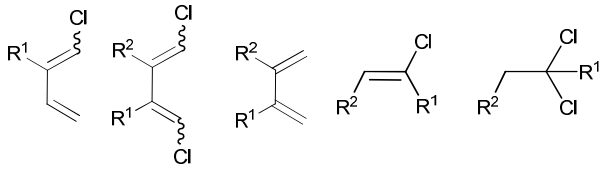

Scheme 4.2. Byproducts of EyM with Vinyl Chloride

Table 4.4. Reaction Details for NMR Scale Reactions with Vinyl Bromide

#	R^{1a}	R^{2a}	Vinyl Bromide mmol	Solvent	Temp	[Ru][b]	Products: % conversion[c]	time (h)[d]
1	$Si(CH_3)_3$	H	0.71	C_6D_6	45°C [e]	**4.13**	**4.35:** 25	0.5
2	$Si(CH_3)_3$	H	0.9	C_7D_8	20°C [e]	**4.13**	**4.35:** 31	1
3	$Si(CH_3)_3$	H	1.2	C_7D_8	0°C [e]	**4.13**	**4.35:** 35	3.5
4	$Si(CH_3)_3$	H	1.2	C_7D_8	-20°C [e]	**4.13**	**4.35:** 30	44
5	$Si(CH_3)_3$	H	1.0	C_6D_6	23°C	**4.13** [f]	**4.35:** 50	1
6	$Si(CH_3)_3$	H	0.90	CD_2Cl_2	23°C	**4.13** [f]	**4.35:** 58 (76)	1
7	C_4H_9	C_4H_9	1.3	C_6D_6	45°C	**4.13**	**4.36**[g]**:** 15	1.5
8	C_4H_9	C_4H_9	1.5	C_6D_6	23°C	**4.13**	**4.36**[g]**:** 15	1.5
9	C_4H_9	C_4H_9	1.2	C_6D_6	23°C	**4.13** [f]	**4.36**[g]**:** 30	1.5

[a] R^1 and R^2 indicate substitution on the alkyne; see Eq. 4.1. [b] Catalyst loading was 5 mol% based on the amount of alkyne unless otherwise indicated. [c] Percent conversion was determined based on the amount of products in the ^{1}H NMR spectrum with respect to an internal standard. Percentages in parentheses represent the amount of starting alkyne that was consumed. [d] Reaction times generally represent the point at which the reaction reached completion, however, in some cases where low yields were observed, the reaction was run longer than necessary to be sure of completion. [e] Temperature study [f] 10 mol% catalyst loading was used. [g] reference for product **4.36.**[12]

Byproducts with vinyl bromide (0 to ≤ 10 %) included 1-chloro-2,3-substituted-1,3-butadiene, 1-bromo-1,2-substituted-alkene, $C_2H_2R^1R^2Br_2$, and for trimethylsilylacetylene, 1-bromo-2-trimethylsilyl-1,3-butadiene. A number of other alkynes were tried with vinyl bromide but percent conversions were < 20% (Scheme 4.3).

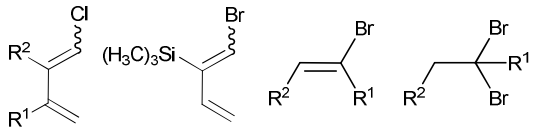

Scheme 4.3. Byproducts of EyM with Vinyl Bromide

Table 4.5. Larger Scale EyM Reactions with Vinyl Chloride and Vinyl Bromide

#	R^{1a}	R^{2a}	substrate (mmol)	solvent	Temp	[Ru][b]	Isolated %Yield[c]	time (h)
1	Tolyl	H	1.53	C_6H_6	23°C	**4.13**[e]	**4.30:** 45% (78%) [h,i]	24
2	$Si(CH_3)_3$	H	1.52	CH_2Cl_2	23°C	**4.13**	**4.31:** 52%	3
3	CH_2OBz	H	1.06	C_6H_6	23°C	**4.13**[d]	**4.32:** 41% (66%) [h,i]	24
4	C_4H_9	C_4H_9	1.52	C_6H_6	23°C	**4.13** [f]	**4.34:** 83%	24
5[g]	$Si(CH_3)_3$	H	1.53	CH_2Cl_2	23°C	**4.13** [e]	**4.35:** 25%	3

[a] R^1 and R^2 indicate substitution on the alkyne; see Eq. 4.1. [b] Catalyst loading was 5 mol% based on the amount of alkyne unless otherwise indicated. [c] Isolation procedures were dependent on diene synthesized and are given in the next section along with characterization data. [d] 7 mol% catalyst loading used. [e] 8 mol% catalyst loading used. [f] 10 mol% catalyst loading was used. [g] Vinyl bromide was used to make 1-bromo-3-trimethylsilyl-1,3-butadiene. [h] Butadiene decomposes quickly when warm and/or neat. A small amount (100 ppm) of 4-tertbutylcatechol was added to the reaction mixture and final product to slow decomposition. [i] Yield in parentheses was the product yield based on ^{1}H NMR spectroscopy before column chromatography.

4.6. Stability of the Butadiene Products

Although the synthesized butadienes were isolable (Chart 4.2), most were thermally sensitive and decomposed readily when neat, making purification difficult. Addition of 10 to 100 ppm of 4-tert-butylcatechol helped stabilize the most sensitive butadienes (Chart 4.2: **4.30** and **4.32**). The fluorinated butadienes are more stable than the chlorinated butadienes. Butadiene products were often stored as 0.15 M solutions in pentane at −10 °C with 100 ppm of 4-tertbutylcatechol to minimize decomposition with

the exception of **4.28** which was a solid at room temperature and was stored in solid form at −10 °C.

4.7. Mechanism

Mechanistic details for EyM have been thoroughly discussed in the literature.[13, 17] Following initiation via the formation of a four-coordinate 14-electron benzylidene complex from the precatalyst, both insertion of the olefin (Scheme 4.4) and insertion of the alkyne have been proposed as possible activation steps for the catalytic cycle of EyM.[13] In the case of EyM with vinyl fluoride, the only styryl-containing product observed by ^{1}H NMR spectroscopy and gas chromatography-mass spectrometry (GC-MS) was styrene. Additionally, the monofluoromethylidene complexes **4.2** and **4.10** were observed directly by ^{1}H NMR spectroscopy during the course of the reaction when catalysts **4.1** and **4.9**, respectively, were used. This suggests that the operant EyM mechanism begins with initial loss of a neutral ligand, followed by metathesis with vinyl fluoride to form a 14-electron ruthenium monofluoromethylidene complex, **4.15**, as depicted in Scheme 4.4. Subsequent irreversible insertion of the alkyne followed by reaction with a second equivalent of vinyl fluoride completes the cycle and accounts for the observed regiochemistry, i.e., the formation of 1-fluoro-*3*-substituted-1,3-butadiene products in the case of terminal alkynes (Figure 4.1). Although multiple pathways are possible,[18] this single pathway can account for both the sole observed initiation product and the 1-halo-3-substituted-1,3-butadiene products from terminal alkynes. Fischer carbene complexes such as **4.2**, **4.5**, **4.6**, **4.10**, **4.12**, **4.15**, and **4.18** are thermodynamically stable with respect to formation of their methylidene analogues by CM. Moreover,

methylidene complexes are generally not observed in the stoichiometric reactions of precursors **4.1**, **4.9**, **4.13**, and **4.14** with the appropriate directly functionalized olefins.[1,2,4] Finally, compound **4.2** is catalytically competent (Scheme 4.5). Starting with the monofluoromethylene complex (**4.2**) as a metathesis catalyst affords the EyM products in the same yield as catalyst **4.1** (Scheme 4.5); byproduct yields were also identical. This indicates that the monofluoromethylidene complex enters efficiently into the catalytic cycle, supporting the validity of the proposed major pathway (Scheme 4.4). The byproducts 1,4-difluoro-2,3-substituted-1,3-butadiene, 2,3-substituted-1,3-butadiene, and 1-fluoro-2-substituted-1,3-butadiene may arise via minor pathways.

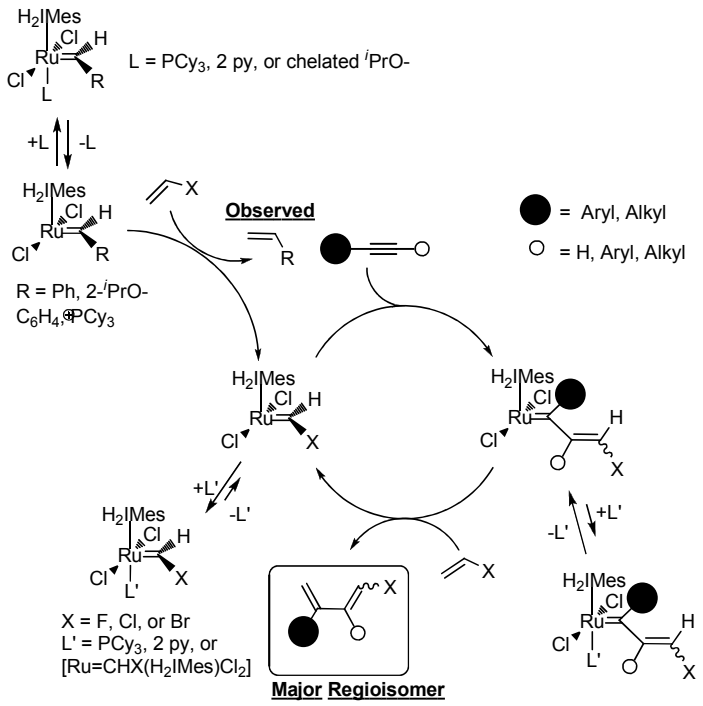

Scheme 4.4. Proposed Mechanism for EyM with Vinyl Halides: "Alkylidene First" [13,18]

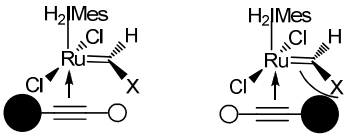

Figure 4.1. Steric Effects of Alkyne Binding at the Ru-center: Regiocontrol for the Formation of 1-X-*3*-substituted-1,3-butadienes.

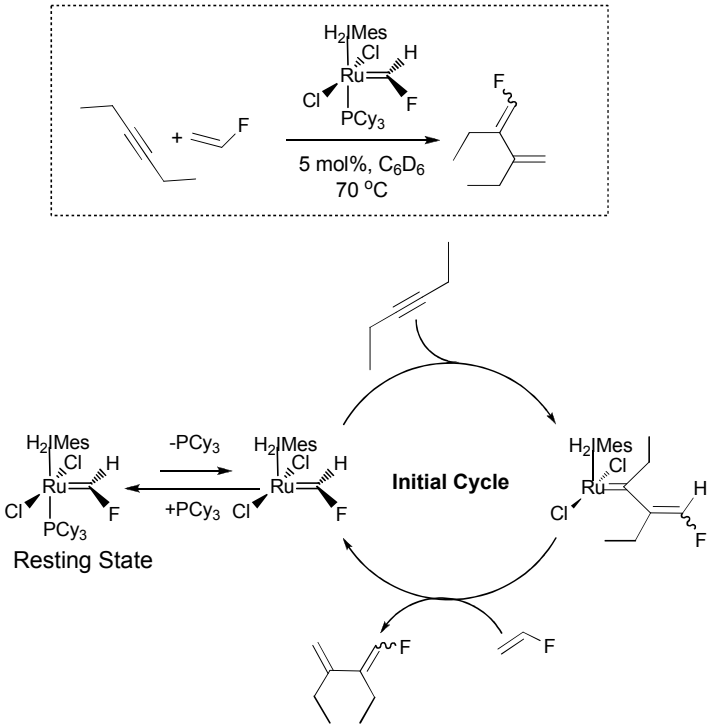

Scheme 4.5. EyM Catalyzed with Compound **4.2**

4.8. Conclusions

Enyne metathesis with vinyl fluoride and a variety of substituted alkynes allows for early installation of a fluorine substituent into organic compounds. A number of previously unreported 1-fluoro- and 1-chloro-2,3-substituted butadienes have been synthesized via Ru-catalyzed enyne metathesis in moderate to high yields. Both terminal

and internal alkynes were tolerated as substrates. Compatible functionalities on the alkyne substrate include but are not limited to alkyl, aryl, and silyl groups; propargyl benzoate was also tolerated. Based on the observed regioselectivity of the products, the formation of styryl-containing side products, previously reported data [13,17] and enyne metathesis using the monofluoromethylidene complex (**4.2**) as a catalyst, it appears that the mechanism goes through the appropriate monohalomethylidene intermediate. Catalysts **4.1, 4.9, 4.13,** and **4.14** are all effective catalysts for EyM with vinyl fluorides. For vinyl chlorides and vinyl bromides, only **4.13** and **4.14** catalyze EyM reactions. Overall, **4.13** tended to give the highest percent conversions to desired products. However, 1-isopropoxy-2-vinylbenzene liberated from **4.13** must then be removed via column chromatography in order to isolate the butadiene products cleanly, whereas **4.14** liberates vinyltricyclohexylphosphonium tetrafluoroborate which can be removed by filtration, allowing for easier isolation of the diene products. When using aryl alkynes, the Piers catalyst, **4.14**, forms a side-on η^3-vinylcarbene complex (**4.21**) which is inactive in enyne metathesis under the conditions assayed. Regioselectivity and *E/Z* ratio are similar to previously reported EyM reactions with a variety of olefins.[13]

4.9. Experimental

4.9.1. General Procedures. All reactions were set-up in a nitrogen-filled MBRAUN Labmaster 130 glove box, unless otherwise specified and run under a nitrogen atmosphere. ^{1}H, ^{13}C, ^{19}F, ^{31}P, 2 dimensional gradient COSY, 2 dimensional gradient HSQC, and 1 dimensional NOESY NMR spectra were acquired on a Varian Inova 400 MHz or 500MHz NMR spectrometer. ^{1}H spectra were referenced to solvent signals.[19]

^{19}F NMR spectra and ^{31}P NMR spectra were referenced to external $CFCl_3$ in $CDCl_3$ (δ=0) and external 85% H_3PO_4 (δ=0) respectively. Exact mass electrospray ionization data (EI) was collected on a VG (Micromass) 70-250-S magnetic sector mass spectrometer (error within 5 ppm). All NMR scale reactions were filtered through activated alumina before gas chromatography-mass spectroscopy (GC-MS) data were acquired. GC-MS data were acquired on a Shimadzu GC-MS-QP5000 Gas Chromatograph – Mass Spectrometer.

4.9.2. Materials. Vinyl chloride was purchased from Fluka. Phenylacetylene, vinyl bromide, 5-decyne, propargyl benzoate, 4-ethynyl-α,α,α-trifluorotoluene, and 1-ethynyl-3,5-bis(trifluoromethyl)benzene were purchased from Aldrich and phenylacetylene was purified by filtration through alumina. Diphenylacetylene, propargyl alcohol, bis(trimethylsilyl)acetylene, aluminium oxide (neutral, Brockmann 1) and 3-hexyne were purchased from Acros Organics. Trimethylsilylacetylene and 4-ethynyltoluene were purchased from G. Fredrick Smith Chemicals Inc (GFS). Vinyl fluoride and 1-bromo-3,5-bis(trifluoromethyl)benzene were purchased from Synquest Labs Inc. Silica gel 60 was purchased from EM Science. All bulk solvents were obtained from VWR Scientific and were degassed and dried over 4 Å molecular sieves. Deuterated solvents were purchased from CIL and dried over 4 Å molecular sieves. All liquid reagents were degassed. Vinyl halides and solid reagents were used as received. The starting compounds $[Ru(CHPh)(H_2IMes)(PCy_3)Cl_2]$,[20,21] $[Ru(CHPh)(H_2IMes)(py)_2Cl_2]$,[22] $[Ru(CHPCy_3)(H_2IMes)Cl_2][BF_4]$,[2,9] and $[Ru(CHF)(H_2IMes)(PCy_3)Cl_2]$[1] were synthesized according to published procedures. All ruthenium catalysts (**4.1, 4.9, 4.13**, and **4.14**) were also obtained from Materia, Inc.

4.9.3. Synthetic Procedures

General Procedure for Enyne Metathesis (EyM) Reactions

NMR studies

The substituted alkyne (0.150 ± 0.04 mmol) was dissolved in 0.8 mL of C_6D_6 or CD_2Cl_2 along with 1-bromo-3,5-bis(trifluoromethyl)benzene (internal standard for all procedures, 0.050 ± 0.005 mmol) and the solution was transferred to a J. Young tube. Stock solutions were prepared as needed for reactions. A ^{1}H NMR spectrum was then acquired. The reaction was frozen in the glove box cold well and a ruthenium catalyst (4-10 mol%: **4.1**, **4.9**, **4.13**, or **4.14**; See Tables 4.1, 4.3 and 4.4 for specific details) was dissolved in 0.2 mL C_6D_6 or CD_2Cl_2 and added to the frozen solution. The J. Young tube was removed from the glove box, the solution was frozen completely in liquid N_2, and the J. Young tube was evacuated. The J. Young tube containing the reaction mixture was then submerged in liquid nitrogen and opened (for approx. 2 seconds) to a lecture bottle containing vinyl halide (5-10 psig). This method afforded an excess of vinyl halide in the reaction mixture (between 4 to 30 equivalents based on integration to internal standard in the ^{1}H NMR spectra; see Tables 4.1, 4.3 and 4.4 for specific amounts). The J. Young tube was placed in an oil bath at a predetermined temperature (see Tables 4.1, 4.3 and 4.4 for details). Reactions often underwent a color change within the first 10 minutes. Color change varied depending on substrate and catalyst. Catalyst loadings for all reactions were based on amount of alkyne used and are given in mol% in Tables 4.1, 4.3 and 4.4. Percent conversion of NMR scale reactions were based on halogen-containing diene products seen in the ^{1}H and/or ^{19}F NMR spectrum and their integration with respect to the internal standard. The amount of vinyl halide in each reaction was monitored by ^{1}H

and/or ^{19}F NMR spectroscopy. When the diene product integration remained unchanged in the NMR spectra for greater than 2 hours, the reaction mixture was filtered through a small plug of alumina gel and/or silica gel (elusion with pentane or benzene) to remove the ruthenium complexes and the products were farther identified by GC-MS. The reaction solutions were concentrated to products and analyzed by NMR spectroscopy.

Scaled Reactions (100 to 300 mg)

The catalyst was dissolved in 5 mL of solvent (C_6H_6 or CH_2Cl_2 depending on volatility of products and optimization of NMR studies; Tables 4.2 and 4.5), added to a bomb flask and placed in a cold well in the glove box. The alkyne was dissolved in 10 mL of solvent and added on top of the frozen catalyst solution. The reaction mixture was removed from the glove box and the solution was refrozen in liquid N_2. The bomb flask was evacuated and then repressurized with vinyl halide gas for about five seconds (7-10 psig), cooled in liq. N_2 and repressurized a second time. The solution was then thawed, placed in an oil bath at the appropriate temperature and stirred for a specified amount of time (Tables 4.2 and 4.5). The reaction was then allowed to cool to room temperature and the mixture was run through a short column of dry alumina and/or silica gel in order to remove ruthenium catalyst decomposition products. The solution was flushed through with 50 to 100 mL of pentane or benzene (in cases where propargyl benzoate was used) and solvents were then removed via rotatory evaporation or *in vacuo* depending on volatility of the product. In some cases, column chromatography was used to purify the products. Products were massed and characterized by ^{1}H, ^{13}C, and ^{19}F NMR data and EI (Electron Impact Ionization). Olefinic proton nuclei on 1,3-butadienes were

often slow to relax on an NMR timescale. Connectivity and *E/Z* isomers were distinguished using 2-dimensional gradient COSY, 2-dimensional gradient HSQC, and 1D NOESY NMR spectroscopy. See further isolation details for individual compounds along with characterization data below.

Characterization Data for Isolated Butadienes

4.22: (*E/Z*)-1-fluoro-3-phenyl-1,3-butadiene 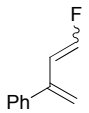

For reaction conditions, see Table 4.2: Entry 1. After stirring at 45 °C for 5 hours, the reaction mixture was cooled and filtered through a short column of alumina and flushed through with pentane (100 mL) to remove ruthenium impurities. All alkyne was consumed and volatiles were removed *in vacuo*. Products were isolated in a 90% yield. High resolution EI+ molecular ion calcd for $C_{10}H_9F$ 148.0688, found 148.0689 (M+). *E/Z* ratio was 1 to 1. ^{19}F NMR (282.320 MHz, CD_2Cl_2, d_1=2 sec): δ = -120.74 (dd, $^2J_{HF}$ = 83.6 Hz, $^3J_{HF}$ = 43.2 Hz, *Z*, 1F), -128.61 (dd, $^2J_{HF}$ = 83.6 Hz, $^3J_{HF}$ = 19.7 Hz, *E*, 1F). ^{1}H NMR (400MHz, CD_2Cl_2, d_1 = 10 sec): δ = 7.51-7.18 (m, aryl, *Z/E*, 10H), 6.75 (dd, $^2J_{HF}$ = 84 Hz, $^3J_{HH}$ = 11.5 Hz, -C*H*F, *E*, 1H), 6.69 (dd, $^2J_{HF}$ = 83.2 Hz, $^3J_{HH}$ = 5.6 Hz, -C*H*F, *Z*, 1H), 6.32 (ddd, $^3J_{HF}$ = 19.2 Hz, $^3J_{HH}$ = 11.2 Hz, $^4J_{HH}$ = 0.8 Hz, -C*H*=CHF, *E*, 1H), 5.78 (d, $^4J_{HH}$ = 0.8 Hz, -C*H*H, 1H), 5.59 (bs, -C*H*H, 1H), 5.52 (ddd, $^3J_{HF}$ = 43.6 Hz, $^3J_{HH}$ = 5.2 Hz, $^4J_{HH}$ = 0.8 Hz, -C*H*=CHF, *Z*, 1H), 5.26 (d, $^4J_{HH}$ = 0.8 Hz, -CH*H*, 1H), 5.16 (bs, -CH*H*, 1H). ^{13}C NMR (100.582 MHz, CD_2Cl_2): δ = 154.2 (d, $^1J_{CF}$ = 260.7 Hz, -*C*FH), 150.8 (d, $^1J_{CF}$ = 270.8 Hz, -*C*FH), 143.9, 143.8, 142.4, 141.3, 141.1, 129.96, 129.83,

129.51, 129.27, 129.23, 128.06, 119.34 (d, $^4J_{CF}$ = 8.4 Hz, -*C*HH, *Z*), 117.4 (d, $^4J_{CF}$ = 7.5 Hz, -*C*HH, *E*), 117.0 (d, $^2J_{CF}$ = 15.6 Hz, -*C*H=CHF, *E*), 111.88 (s, -*C*H=CHF, *Z*).

4.23: (*E/Z*)-1-fluoro-3-trimethylsilyl-1,3-butadiene 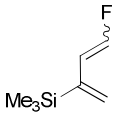

For reaction conditions, see Table 4.2: Entry 2. After stirring at 40 °C for 3 hours, the reaction mixture was cooled, filtered through a short column of alumina and flushed through with pentane (100 mL) to remove ruthenium impurities. The volatiles were removed by rotator evaporation and the residue is then purified by column chromatography (silica gel, eluted with pentane). Pentane was then removed by rotatory evaporation. Yield after column chromatography was 47%. High resolution EI+ molecular ion calcd for $C_7H_{13}SiF$ 144.0771, found 144.0774 (M+). *E/Z* ratio was 1.3 to 1 based on ^{1}H NMR data. ^{19}F NMR (376.353 MHz, CD_2Cl_2): δ = major; -121.14 (dd, $^3J_{HF}$ = 48 Hz, $^2J_{HF}$ = 85 Hz, *Z*, 0.97F) -128.8 (dd, $^3J_{HF}$ = 20 Hz, $^2J_{HF}$ = 85 Hz, *E*, 1.00F); minor; -124.0 (dt, $^2J_{HF}$ = 84 Hz, $^3J_{HF}$ = $^5J_{FF}$ = 19 Hz, 1,*4(E)*-di*fluoro*-2-trimethylsilyl-1,3-butadiene, 0.06F), -117.4 (ddd, $^3J_{HF}$ = 50 Hz, $^2J_{HF}$ = 87 Hz, $^5J_{FF}$ = 8 Hz, 1,*4(Z)*-di*fluoro*-2-trimethylsilyl-1,3-butadiene, 0.10F), -103.1 (dd, $^5J_{FF}$ = 19 Hz, $^2J_{HF}$ = 89 Hz, *1*,4(*E*)-di*fluoro*-2-trimethylsilyl-1,3-butadiene, 0.06F), -100.8 (dd, $^5J_{FF}$ = 8 Hz, $^2J_{HF}$ = 90 Hz, *1*,4(*Z*)-di*fluoro*-2-trimethylsilyl-1,3-butadiene, 0.10F), -105.3 (d, $^2J_{HF}$ = 89 Hz, 1-fluoro-2-trimethylsilyl-1,3-butadiene isomer, 0.07F), -107.9 (d, $^2J_{HF}$ = 92 Hz, 1-fluoro-2-trimethylsilyl-1,3-butadiene isomer, 0.19F). ^{1}H NMR (500MHz, CD_2Cl_2, major products only, d_1 = 10 sec): δ = 6.84 (dd, $^2J_{HF}$ = 85 Hz, $^3J_{HH}$ = 11.5 Hz, *E*, -C*H*F, 1.3H), 6.43 (ddt, $^2J_{HF}$ = 85 Hz, $^3J_{HH}$ = 5.5 Hz, $^4J_{HH}$ = 1 Hz, *Z*, -C*H*F, 1.0H), 6.16 (dd, $^2J_{HF}$ = 20.5 Hz, $^3J_{HH}$ = 11.5 Hz, *E*, -C*H*=CHF, 1.3H), 5.84(dd, $^2J_{HH}$ = 3.5 Hz, $^4J_{HH}$ = 1 Hz, *Z*, -C*H*H, 1.0H), 5.70

(dd, $^{2}J_{HH}$ = 3 Hz, $^{4}J_{HH}$ = 0.5 Hz, *E*, -C*H*H, 1.3H), 5.54 (pseudo dd, $^{2}J_{HH}$ = 3.5 Hz, $^{4}J_{HH}$ = 0.5 Hz, *Z*, -CH*H*, 1.0H), 5.39 (dd, $^{2}J_{HF}$ = 48 Hz, $^{3}J_{HH}$ = 5.5 Hz, *Z*, -C*H*=CHF, 1.0H), 5.38 (d, $^{2}J_{HH}$ = 3 Hz, , *E*, -CH*H*, 1.3H), 0.18 (s, *E*, -CH_3, 12 H), 0.16 (d, J = 1.5 Hz, *Z*, -CH_3, 9H). ^{13}C NMR (125.714 MHz, CD_2Cl_2, major products only): δ = 150.57 (d, $^{1}J_{CF}$ = 257.7 Hz, -*C*FH), 146.84 (d, $^{1}J_{CF}$ = 266.1 Hz, -*C*FH), 143.50 (s) 143.44 (s), 130.14 (d, $^{4}J_{CF}$ = 4.5 Hz, *Z*, -*C*HH), 128.04 (d, $^{4}J_{CF}$ = 7.3 Hz, *E*, -*C*HH), 118.49 (d, $^{2}J_{CF}$ = 13.8 Hz, *E*, -*C*=CHF), 114.67 (d, $^{1}J_{CF}$ = 2.3 Hz, *Z*, -*C*=CHF), -0.92 (s, -*C*H_3), -1.12 (d, $^{5}J_{CF}$ = 4.1 Hz, -*C*H_3)

4.24: (*E/Z*)-4-fluoro-2-methylene-3-butenyl benzoate 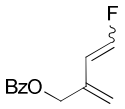

For reaction conditions, see Table 4.2: Entry 3. After stirring at 45 °C for 24 hours, the reaction mixture was cooled, filtered through a short column of alumina, and flushed through with 150 mL benzene to remove ruthenium impurities and to ensure all products were washed through. The crude products were obtained in a 76% yield (based on integration of products in the ^{1}H NMR spectrum with respect to an internal standard). The volatiles were removed and the residue is then purified by column chromatography (silica gel, eluted with 40:1 pentane-diethyl ether mixture: early fractions contained 1-isopropoxy-2-vinylbenzene, which is a byproduct from Hoveyda's catalyst; later fractions contained products). The purified products were obtained in 39% yield. High resolution EI+ molecular ion calcd for $C_{12}H_{11}FO_2$ 206.07431, found 206.0741 (M+). *E/Z* ratio was 1 to 1.2. ^{19}F NMR (376.302 MHz, CD_2Cl_2, d_1 = 1 sec): δ = -120.4 (dd, $^{2}J_{HF}$ = 83.2 Hz, $^{3}J_{HF}$ = 46.7 Hz, -CH*F*, *Z*, 1.2F), -128.5 (dd, $^{2}J_{HF}$ = 82.8 - 83.5 Hz, $^{3}J_{HF}$ = 20.7 – 19.9 Hz, -CH*F*, *E*, 1.0F). ^{1}H NMR (400MHz, CD_2Cl_2, d_1 = 10 sec): δ = 8.01 (bt, *ortho-H*, *E/Z*, J =

8.4 Hz, 4.4H), 7.54 (m, *para-H, E/Z*, 2.2H), 7.42 (bt, *meta-H, E/Z*, 4.4H), 6.95 (dd, $^{2}J_{HF}$ = 82.8 Hz – 83.2 Hz, $^{3}J_{HH}$ = 11.2 – 11.6 Hz, -C*H*F, *E*, 1H), 6.48 (dd, $^{2}J_{HF}$ = 83.2 – 83.6 Hz, $^{3}J_{HF}$ = 5.2 – 5.6 Hz, -C*H*F, *Z*, 1.2H), 6.10 (ddd, $^{3}J_{HF}$ = 20.8 – 20.4 Hz, $^{3}J_{HH}$ = 11.2 – 11.6 Hz, $^{4}J_{HH}$ = 0.4 – 0.8 Hz, -C*H*=CHF, *E*, 1H), 5.33 (dd, $^{3}J_{HF}$ = 46.8 Hz, $^{3}J_{HH}$ = 5.6 Hz, -C*H*=CHF, *Z*, 1.2H), 5.32 (bs, -C*H*H, overlapping), 5.31 (bs, -C*H*H, overlapping), 5.26 (s, -CH*H*, overlapping), 4.85 (s, -CH_2OBz, 2H), 5.19 (s, -CH*H*, 1.2H), 4.98 (s, -CH_2OBz, 2.4H). ^{13}C NMR (100.582 MHz, $CDCl_3$): δ = 166.06 (s, Ph(O)*C*O-), 166.04 (s, Ph(O)*C*O-), 150.68 (d, $^{1}J_{CF}$ = 259 Hz, -*C*FH), 148.04 (d, $^{1}J_{CF}$ = 270 Hz, -*C*FH), 136.28 (d, $^{3}J_{CF}$ = 2.9 Hz, -*C*=CH_2), 135.81 (d, $^{3}J_{CF}$ = 10.4 Hz, -*C*=CH_2), 133.175 (s, *para-C*), 132.98 (s, *para-C*), 130.19 (s, *ipso-C*), 129.86 (s, *ipso-C*), 129.67 (s, *ortho-C's, both isomers*), 128.45 (s, *meta-C*), 128.36 (s, *meta-C*), 117.89 (d, $^{4}J_{CF}$ = 9.6 Hz, -*C*HH, *E*), 117.63 (d, $^{4}J_{CF}$ = 6.6 Hz, -*C*HH, *Z*), 113.40 (d, $^{2}J_{CF}$ = 17.0 Hz, -*C*H=CHF, *E*), 109.32 (s, -*C*H=CHF, *Z*), 66.10 (d, $^{4}J_{CF}$ = 5.9 Hz, -O*C*H_2-, *Z*), 64.65 (s, -O*C*H_2-, *E*)

4.25: (*E/Z*)-1-fluoro-3-(4-trifluoromethyl)phenyl-1,3-butadiene 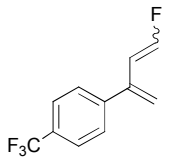

For reaction conditions, see Table 4.2: Entry 5. Ru carbide byproduct (**4.**7) from catalyst **4.1** can be removed by running the reaction mixture through a silica plug followed by elusion with pentane. Styrene, which is a byproduct from the ruthenium catalyst, is removed *in vacuo* along with solvents. Isolated yield was 71%. High resolution EI+ molecular ion calcd for $C_{11}H_8F_4$ 216.0562, found 216.0566 (M+). *E/Z* ratio was 1.6 to 1. ^{19}F NMR (376.302 MHz, CD_2Cl_2, d_1=1 sec): δ = major: -119.4 (dd, $^{3}J_{HF}$ = 41.8 Hz, $^{2}J_{HF}$ = 82.4 Hz, *Z*, 1F), -63.70 (s, -CF_3, *Z*, 3F); -127.6 (dd, $^{3}J_{HF}$ = 19.6 Hz, $^{2}J_{HF}$ = 83.5 Hz, *E*, 1.6F), -63.74 (s, -CF_3, *E*, 5.2H); minor: -118.8 (dd, $^{3}J_{HF}$ = 41.0 Hz, $^{2}J_{HF}$

= 81.7 Hz, *Z*, 0.35F), -63.23 (s, -CF_3), -126.0 (dd, *E*, 0.03F), -63.5 (s, -CF_3). ^{1}H NMR (400MHz, CD_2Cl_2, major products only): δ = 7.65-7.61 (m, aryl, *E/Z*, 7H), 7.54-7.48 (m, aryl, *E/Z*, 4H), 6.70 (dd, $^2J_{HF}$ = 83.6 Hz, $^3J_{HH}$ = 11.2, -C*H*F, *E*, 1.6H overlapping), 6.68 (dd, $^2J_{HF}$ = 82.4 Hz, $^3J_{HH}$ = 5.2 Hz, -C*H*F, *Z*, 1H), 6.32 (ddd, $^3J_{HF}$ = 18.8 Hz, $^3J_{HH}$ = 11.2 Hz, $^4J_{HH}$ = 0.8 Hz, -C*H*=CHF, *E*, 1.6H), 5.65 (s, -C*H*H, *Z*, 1H), 5.62 (s, -C*H*H, *Z*, 1H), 5.53 (ddd, $^3J_{HF}$ = 42.4 Hz, $^3J_{HH}$ = 5.6 Hz, $^4J_{HH}$ = 0.8 Hz, -C*H*=CHF, *Z*, 1H), 5.35 (s, C*H*H, *E*, 1.6H), 5.21 (s, -CH*H*, *E*, 1.6H). ^{13}C NMR (100.582 MHz, CD_2Cl_2, major products only): δ = 153.3 (d, $^1J_{CF}$ = 261.5 Hz, -*C*HF), 150.1 (d, $^1J_{CF}$ = 271.9 Hz, -*C*HF), 133.05 (aryl), 130.48, 129.86, 128.90 (aryl), 128.71 (aryl), 128.18, 128.07, 127.58 (aryl), 125.89 (m, -*C*F_3), 125.70 (m, -*C*F_3), 120.14 (d, $^4J_{CF}$ = 8.2 Hz, Z, -*C*HH), 117.82 (d, $^4J_{CF}$ =8.2 Hz, -*C*HH, E), 115.55 (d, J_{CF} = 16.9Hz), 110.30 (s)

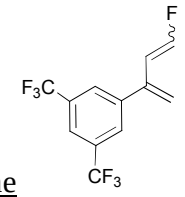

4.26: (*E/Z*)-1-fluoro-3-(3,5-bis(trifluoromethyl))phenyl-1,3-butadiene

For reaction conditions, see Table 4.2: Entry 7. Ru carbide impurity (**4.7**) in product can be removed by running the reaction mixture through a silica plug followed by elusion with pentane. Styrene, which is a byproduct from the ruthenium catalyst, is removed *in vacuo* along with solvents. Isolated yield was 79%. *E/Z* ratio is 1.3 to 1. High resolution EI+ molecular ion calcd for $C_{12}H_7F_7$ 284.0436, found 284.0437 (M+). ^{19}F NMR (376.302 MHz, CD_2Cl_2, d_1=1 sec): δ = major products: -117.6 (dd, $^3J_{HF}$ = 42.1 Hz, $^2J_{HF}$ = 82.0 Hz, *Z*, 1F), -63.38 (s, -CF_3, *Z*, 6F); -125.6 (dd, $^3J_{HF}$ = 17.7 - 18.4 Hz, $^2J_{HF}$ = 82.0 – 82.8 Hz, *E*, 1.3F), -63.74 (s, -CF_3, *E*, 8F); minor products: -116.74 (dd, $^3J_{HF}$ = 40.6 Hz, $^2J_{HF}$ = 81.3 Hz, *Z*, 0.22F), -124.9 (dd, $^3J_{HF}$ = 19.9 Hz, $^2J_{HF}$ = 84.8 Hz, *E*, 0.14F),

-63.8 (bs, -C*F*$_3$, overlapping, 3H). ^{1}H NMR (400MHz, CD_2Cl_2, major products only): δ =7.88 (bs, *para-H*, overlapping), 7.86 (bs, ortho-H, overlapping), 7.85 (para-H, overlapping), 7.84 (bs, ortho-H, overlapping), 6.70 (dd, $^2J_{HF}$ = 82.0 Hz, $^3J_{HH}$ = 5.6 Hz, -C*H*F, *Z*, 1H, overlapping), 6.69 (dd, $^2J_{HF}$ = 82.8 Hz, $^3J_{HH}$ = 11.2 Hz, -C*H*F, *E*, 1.3H, overlapping), 6.34 (ddd, $^3J_{HF}$ = 18.4 Hz, $^3J_{HH}$ = 11.2 Hz, $^4J_{HH}$ = 0.8 Hz, -C*H*=CFH, *E*, 1.3H), 5.70 (s, -C*H*H, Z, 1H), 5.63 (s, -CH*H, Z*, 1H), 5.59 (ddd, $^3J_{HF}$ = 41.6 Hz, $^3J_{HH}$ = 5.2 Hz, $^4J_{HH}$ = 0.8 Hz, -C*H*=CFH, *Z*, 1H), 5.45 (s, -C*H*H, *E*, 1.3H), 5.29 (s, -CH*H*, *E*, 1.3H). ^{13}C NMR (125.714 MHz, CD_2Cl_2, major products only): δ = 154.5 (d, $^1J_{CF}$ = 263.4 Hz, -*C*HF), 151.4 (d, $^1J_{CF}$ = 272.5 Hz, -*C*HF), 143.5, 142.4, 140.4 (d, J = 11.4 Hz), 138.7, 133.22 (d, J = ~40Hz), 133.0 (d, J = ~40 Hz), 129.56 (bd, aryl), 129.47 (d, J = 38 Hz), 128.63 (bd, aryl), 128.3, 125.1 (d, J = 14.3 Hz), 122.42 (m, -*C*F$_3$), 121.97 (m, -*C*F$_3$), 121.30 (d, $^4J_{CF}$ =6.7 Hz , -*C*HH, *Z*), 118.93 (d, $^4J_{CF}$ = 7.3 Hz, -*C*HH, *E*),115.17 (d, $^2J_{CF}$ = 17.1 Hz, -*C*H=CFH, *E*), 109.9 (s, -*C*H=CFH, *Z*).

4.27: (*E/Z*)-3-(fluoromethylene)-4-methylenehexane 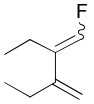

For reaction conditions, see Table 4.2: Entry 8. After 3 h of stirring at room temperature, the reaction mixture was filtered through a short column of alumina (eluded with 100 mL pentane). All alkyne was consumed and the vinyl tricyclohexylphosphonium tetrafluoroborate generated by Piers catalyst was removed on the alumina plug along with other Ru decomposition products. After rotatory evaporation, the products were isolated in a 32% yield. High resolution EI+ molecular ion calcd for $C_8H_{13}F$ 128.1001, found 128.0995 (M+). *E/Z* ratio was ~1 to 1. ^{19}F NMR (376.302 MHz, CD_2Cl_2, d_1=1 sec): δ = -133.0 (d, $^2J_{HF}$ = 86 Hz, 1F), -135.5 (d, $^2J_{HF}$ = 87

Hz, 1F); minor products: -131.7 (dq, 0.06F), -132.1 (db, 0.01F), -133.4 (d bq, 0.1F). ^{1}H NMR (500 MHz, CD_2Cl_2, major products only, d_1 = 10 sec): δ = 6.74 (d, $^{2}J_{HF}$ = 86.0 Hz, -C*H*F, *A*, 1H), 6.47 (d, $^{2}J_{HF}$ = 86.0 Hz, -C*H*F, *B*, 1H), 5.10 (d, $^{2}J_{HH}$ = 1.5 Hz, -C*H*H, *B*,1H), 5.02 (bd, -C*H*H, *A*, 1H), 4.97 (b, -CH*H*, *B*, 1H), 4.94 (b pseudo-quintet, $^{2}J_{HH}$ = $^{4}J_{HH}$ =1.5 Hz, -CH*H*, *A*, 1H), 2.32 (qdd, $^{3}J_{HH}$ = 7.5 Hz, $^{4}J_{HF}$ = 3 Hz, $^{4}J_{HH}$ = 1 Hz, 2-ethyl, *A*, 2H), 2.26 (bq, $^{3}J_{HH}$ = 7.5 Hz, 3-ethyl, *B*, 2H), 2.18 (bq, $^{3}J_{HH}$ = 7.5 Hz, 3-ethyl, *A*, 2H), 2.07 (qdd, $^{3}J_{HH}$ = 7.5 Hz, $^{4}J_{HF}$ = 4 Hz, $^{4}J_{HH}$ = 1-1.5 Hz, 2-ethyl, *B*, 2H), 1.08 (t, $^{3}J_{HH}$ = 7.5 Hz, C*H*$_3$, 3H), 1.06 (t, $^{3}J_{HH}$ = 7.5 Hz, C*H*$_3$, 3H), 1.03 (t, $^{3}J_{HH}$ = 7.5 Hz, -C*H*$_3$, 3H), 1.01 (t, $^{3}J_{HH}$ = 7.5 Hz, -C*H*$_3$, 3H). ^{13}C NMR (125.714 MHz, CD_2Cl_2, major products only): δ =147.22 (d, $^{1}J_{CF}$ = 257 Hz, -*C*HF, *A*), 146.62 (-*C*=CHF), 146.46 (-*C*=CHF), 144.90 (d, $^{1}J_{CF}$ = 258 Hz, -*C*HF, *B*), 128.35 (s, -*C*=CHH), 126.63 (s, -*C*=CHH), 114.40 (bs, -*C*HH), 112.25 (d, $^{4}J_{CF}$ = 7 Hz, -*C*HH), 29.89 (s, 3-ethyl, *B*), 28.04 (s, 3-ethyl, *A*), 24.52 (s, 2-ethyl, *B*), 19.31 (s, 2-ethyl, *A*) 15.81 (s, -*C*H$_3$), 15.42 (s, -*C*H$_3$), 14.32 (s, -*C*H$_3$), 14.05 (s, -*C*H$_3$). *A* and *B* represents *E/Z* isomers – the connectivity of the 2 products was distinguished with GCOSY NMR spectroscopy and GHSQC NMR spectroscopy but *E/Z* isomers could not be assigned definitively.

4.28: (*E/Z*)-1-fluoro-2,3-diphenyl-1,3-butadiene 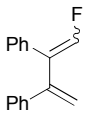

For reaction conditions, see Table 4.2: Entry 9. The cooled reaction mixture was filtered through a short plug of silica (elusion with 100 mL pentane). After solvents are removed *in vacuo*, diene products were purified by recyrstallization at -10°C from minimum warm methanol. Three crops of crystals gave an isolated yield of 65%. High resolution EI+ molecular ion calcd for $C_{14}H_{13}F$ 224.1001, found 224.1005 (M+). *E/Z* ratio

was 5 to 1 based on ^{1}H NMR data. ^{19}F NMR (282.320 MHz, CD_2Cl_2, d_1 = 2 sec): δ = -126.9 (d, $^{2}J_{HF}$ = 83.6 Hz, *Z*, 1H), -127.3 (d, $^{2}J_{HF}$ = 84.4 Hz, *E*, 7.3F). ^{1}H NMR (500MHz, CD_2Cl_2): δ = 7.57-7.23 (m, aryl, *E/Z*, 12H), 7.15 (d, overlapping with aryls, -C*H*F, *Z*, 0.2H), 6.95 (d, $^{2}J_{HF}$ = 84.5 Hz, -C*H*F, *E*, 1H), 5.93 (d, $^{2}J_{HH}$ = 1 Hz, -C*H*H, *Z*, 0.2H), 5.57 (d, $^{2}J_{HH}$ = 1.5 Hz, -C*H*H, *E*, 1H), 5.42 (d, $^{2}J_{HH}$ = 1 Hz, -CH*H*, *Z*, 0.2H), 5.36 (d, $^{2}J_{HH}$ = 1.5 Hz, -CH*H*, *E*, 1H). ^{13}C NMR (100.582 MHz, CD_2Cl_2): δ = 148.8 (d, $^{1}J_{CF}$ = 271.9 Hz, -*C*HF, *E*), 148.4 (d, $^{1}J_{CF}$ = 263.7 Hz, -*C*HF, *Z*), 146.10, 146.02 (J = 8.1 Hz), 140.97, 140.95 (J = 2.2 Hz), 135.25, 133.16, 130.82 (aryl), 130.78 (aryl), 130.21 (aryl), 130.05 (aryl), 129.99 (aryl), 129.97 (aryl), 129.89 (aryl), 129.832 (aryl), 129.46 (aryl), 129.35 (aryl), 129.01 (aryl), 128.55, 128.51, 128.06, 124.9, 119.68 (d, J = 3.0 Hz, -*C*HH, *Z*), 118.68 (d, J = 3.72 Hz, -*C*HH,*E*), 90.91.

4.29: (*E/Z*)-5-(fluoromethylene)-6-methylenedecane 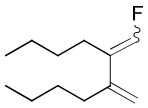

For reaction conditions, see Table 4.2: Entry 10. The reaction mixture was filtered through a short column of alumina and flushed through with pentane (100 mL). All alkyne was consumed and the vinyl tricyclohexylphosphonium tetrafluoroborate generated by Piers catalyst was removed on the alumina plug along with other Ru decomposition byproducts. After rotatory evaporation, the products were isolated cleanly. Isolated yield was 61%. High resolution EI+ molecular ion calcd for $C_{12}H_{21}F$ 184.1627, found 184.1630 (M+). *E/Z* ratio was 1 to 1. ^{19}F NMR (376.302 MHz, CD_2Cl_2, d_1 = 1 sec): δ = -131.3 (d, $^{2}J_{HF}$ = 86.6 Hz); -134.5 (d, $^{2}J_{HF}$ = 86.6 Hz). ^{1}H NMR (400MHz, CD_2Cl_2, d_1 = 10 sec): δ = 6.78 (d, $^{2}J_{HF}$ = 86.8 Hz, -C*H*F, *E*, 1H), 6.47 (d, $^{2}J_{HF}$ = 86.4 Hz, -C*H*F, *Z*, 1H), 5.13 (d, $^{2}J_{HH}$ = 1.6 Hz, -C*H*H, *Z*, 1H), 5.04 (d, $^{2}J_{HH}$ = 2 Hz, -

C*H*H, *E*, 1H), 5.02 (d, $^{2}J_{HH}$ = 1.6 Hz, -CH*H*, *Z*, 1H), 4.94 (pt, $^{2}J_{HH}$ = 1.2 Hz, -CH*H*, *E*, 1H), 2.34 (td, $^{3}J_{HH}$ = 7.2 Hz, $^{4}J_{HH}$ = 3.2 Hz, $CH_3(CH_2)_2CH_2$-C=CHF, *E*, 2H), 2.28 (bt, $^{3}J_{HH}$ = 7.2 Hz, $CH_3(CH_2)_2CH_2$-C=CH_2, *Z*, 2H), 2.20 (td, $^{3}J_{HH}$ = 6.8 Hz, $^{4}J_{HH}$ = 1.2 Hz, $CH_3(CH_2)_2CH_2$-C=CH_2, *E*, 2H), 2.04 (m, $CH_3(CH_2)_2CH_2$-C=CHF, *Z*, 2H), 1.3-1.5 (m, $CH_3(CH_2)_2CH_2$-C=CH_2, *E/Z*, 16H), 0.976 (t, $^{3}J_{HH}$ = 7.2 Hz, -CH_3, *E/Z*, 12H, overlapping). ^{13}C NMR (100.582 MHz, C_6D_6): δ = 146.7 (d, $^{1}J_{CF}$ = 256.4 Hz, *E*, -*C*HF), 144.5 (d, J = 8.1 Hz), 144.3 (d, $^{1}J_{CF}$ = 257.8 Hz, *Z*, -*C*HF), 144.1, 125.9 (d, J = 8.8 Hz), 124.1 (d, J = 1.5 Hz), 114.8 (d, J = 2.9 Hz, -*C*HH, *Z*), 112.5 (d, J = 6.6 Hz, -*C*HH, *E*), 35.8 (d, J = 4.0 Hz, 3-*n*-butyl, *Z*), 34.2 (s, 3-*n*-butyl, *E*), 31.3 (s, 2- and 3-*n*-butyl internal *C*H_2), 31.1 (s, 2- and 3-*n*-butyl internal *C*H_2), 31.05 (d, 2- and 3-*n*-butyl internal *C*H_2), 31.0 (d, J = 2.2 Hz, 2- and 3-*n*-butyl internal *C*H_2), 29.8 (d, J = 6.6Hz, 2-*n*-butyl, *Z*), 24.7 (d, J = 14.2 Hz, 2-*n*-butyl, *E*), 23.2 (s, 2- and 3-*n*-butyl internal *C*H_2), 23.17 (s, 2- and 3-*n*-butyl internal *C*H_2), 23.11 (s, 2- and 3-*n*-butyl internal *C*H_2), 22.97 (s, 2- and 3-*n*-butyl internal *C*H_2), 14.46 (s, 2- and 3-*n*-butyl *C*H_3), 14.44 (s, 2- and 3-*n*-butyl *C*H_3), 14.39 (s, 2- and 3-*n*-butyl *C*H_3), 14.35 (s, 2- and 3-*n*-butyl *C*H_3).

E/Z assignments for ^{1}H NMR data are based on 1D NOESY spectrum (through-space coupling between the -C=C*H*F proton and the –C=C*H*H proton in the *E* isomer). 2D COSY and 2D HQSC NMR spectroscopy was used to assign protons in the ^{1}H NMR data and the carbons in the ^{13}C NMR data.

4.30: (*E/Z*)-1-chloro-3-(4-methyl)phenyl-1,3-butadiene 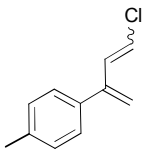

For reaction conditions, see Table 4.5: Entry 1. The reaction mixture was filtered through a short plug of alumina (elusion with 100 mL pentane). Crude yield before

column chromatography was 74% based on ^{1}H NMR integration for the crude mixture. Volatiles were removed *in vacuo*. 1-isopropoxy-2-vinylbenzene, which is a byproduct from Hoveyda-Grubbs catalyst (**4.13**), was separated from the products by column chromatography (silica gel, eluted with pentane; early fractions contained the desired products, later fractions contained 1-isopropoxy-2-vinylbenzene). Pentane was then removed *in vacuo*. Yield after column chromatography was 45%. *E/Z* 1-chloro-3-tolyl-1,3-butadiene is very sensitive to decomposition especially when neat. After any filtration through alumina or column chromatography, approximately 1 mg of 4-*t*-butylcatechol was added to the mixture to help stabilize the products. However, even with the addition of a radical stabilizer, removal of the pentane from the product in preparation for the column chromatography leads to a yellowing of the product indicating slight decomposition. *E/Z* ratio was 1.6 to 1. High resolution EI+ molecular ion calcd for $C_{11}H_{11}Cl$ 178.0549, found 178.0548 (M+). ^{1}H NMR (400MHz, CD_2Cl_2): δ = 7.30 (m, aryl, 2.6H), 7.19 (m, aryl, 7.8H), 6.75 (dd, $^{3}J_{HH}$ = 13.2 Hz, $^{4}J_{HH}$ = 0.8 Hz, -C*H*=CHCl, *E*, 1.6H), 6.49 (dd, $^{3}J_{HH}$ = 8.0 Hz, $^{4}J_{HH}$ = 0.8 Hz, -C*H*=CHCl, *Z*, 1H), 6.36 (d, $^{3}J_{HH}$ = 8.0 Hz, -C*H*Cl, *Z*, 1H), 6.19 (d, $^{3}J_{HH}$ = 13.2 Hz, -C*H*Cl, *E*, 1.6H), 5.74 (broad d, $^{2}J_{HH}$ = 1.2 Hz, -C*H*H, *Z*, 1H), 5.60 (broad pseudo t, $^{2}J_{HH}$ = $^{4}J_{HH}$ = 1.2Hz, -CH*H*, *Z*, 1H), 5.28 (dd, $^{2}J_{HH}$ = 1.6 Hz, $^{4}J_{HH}$ = 0.8Hz, -CH*H*, *E*, 1.6H), 5.20 (d, $^{2}J_{HH}$ = 1.6 Hz, -C*H*H, *E*, 1.6H), 2.363 (s, -C*H*$_3$, *E*, overlapping), 2.356 (s, -C*H*$_3$, *Z*, overlapping). ^{13}C NMR (100,582 MHz, CD_2Cl_2): δ = 145.7, 141.67, 138.44, 138.38, 137.32, 136.60, 135.48 (-*C*H=CHCl, *E*), 130.25 (-*C*H=CHCl, *Z*), 122.24, 120.43, 117.39 (-*C*HH, *Z*), 117.30 (-*C*HH, *E*), 21.43 (-*C*H$_3$), 21.41 (-*C*H$_3$).

4.31: (*E/Z*)-1-chloro-3-trimethylsilyl-1,3-butadiene[2] 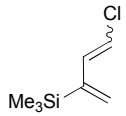

For reaction conditions, see Table 4.5: Entry 2. The reaction mixture was filtered through a short column of alumina and flushed through with pentane (100 mL) to remove ruthenium impurities. The volatiles were removed and the residue is then purified by column chromatography (silica gel, eluted with pentane) to remove 1-isopropoxy-2-vinylbenzene, which is a byproduct from Hoveyda-Grubbs catalyst (**4.13**). (silica gel, eluted with pentane; early fractions contained the desired product, later fractions contained 1-isopropoxy-2-vinylbenzene). Pentane was then removed by rotatory evaporation. Yield after column chromatography was 52%. High resolution EI+ molecular ion calcd for $C_7H_{13}SiCl$ 160.0475, found 160.0478 (M+). *E/Z* ratio was 1.6 to 1. ^{1}H NMR (500MHz, CD_2Cl_2): δ = 6.63 (dt, $^3J_{HH}$ = 13.5 Hz, $^4J_{HH}$ = 1 Hz, -C*H*=CHCl, *E*, 1.6H), 6.36 (dt, $^3J_{HH}$ = 8.0 Hz, $^4J_{HH}$ = 2 Hz, -C*H*=CHCl, *Z*, 1 H), 6.27 (d, $^3J_{HH}$ = 13.5 Hz, -C*H*Cl, *E*, 1.6H), 6.12 (d, $^3J_{HH}$ = 7.5 Hz, -C*H*Cl, *Z*, 1H), 5.95 (m, -C*H*H, *E*, 1.6H), 5.77 (d, J = 3 Hz, -C*H*H, *Z*, 2.5 H), 5.71 (dm, J = 1.5 Hz, -C*H*H, *E*, 1.6H), 5.48 (d, J = 3 Hz, -C*H*H, 2H), 0.21 (s, -Si(CH_3)$_3$, 21 H), 0.18 (s, -Si(CH_3)$_3$, 21 H). ^{13}C NMR (100.582 MHz, $CDCl_3$): δ = 146.36, 146.01, 138.03 (-*C*H=CHCl, *E*), 132.12 (-*C*H=CHCl, *Z*), 129.14 (-*C*HH, *Z*), 128.69 (-*C*HH, *E*), 118.72, 116.37, -1.21 (-Si(CH_3)$_3$), -1.74 (-Si(CH_3)$_3$).

4.32: (E/Z)-4-chloro-2-methylene-3-butenyl benzoate 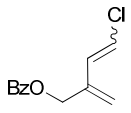

For reaction conditions, see Table 4.5: Entry 3. Crude yield before column chromatography was 66% based on NMR integration of products and internal standard.

Benzene must be used for the filtration through a short alumina plug followed by removal of volatiles *in vacuo*. 1-isopropoxy-2-vinylbenzene, which is a byproduct from Hoveyda-Grubbs catalyst (**4.13**) was separated from the products by column chromatography (silica gel, eluted with pentane until all 1-isopropoxy-2-vinylbenzene is removed, and then elusion with methylene chloride or benzene to isolate products). Solvents were removed *in vacuo*. Yield after column chromatography was 41%. High resolution EI+ molecular ion calcd for $C_{12}H_{11}O_2Cl$ 222.0447, found 222.0447 (M+). *E/Z* ratio was 1.1 to 1. ^{1}H NMR (500MHz, $CDCl_3$, d_1 = 10 sec): δ = 8.07 (m, *ortho-H*, 4.5H), 7.57 (m, *para-H*, 2.3H), 7.46 (m, *meta-H*, 4.5H), 6.57 (d, $^3J_{HH}$ = 13.5 Hz, *E*, 1.1H), 6.40 (d, $^3J_{HH}$ = 14 Hz, *E*, 1.1H), 6.26 (d, $^3J_{HH}$ = 8.5 Hz, *Z*, 1.0H), 6.17 (d, $^3J_{HH}$ = 8 Hz, *Z*, 1.0H), 5.62 (s, -CH*H*, *Z*, 1.0H), 5.57 (s, -C*H*H, *Z*, 1.0H), 5.39 (s, -C*H*H, *E*, 1.1H), 5.29 (s, -CH*H*, *E*, 1.1H), 5.05 (s, *Z*, -CH_2OBz, 2.0H), 4.96 (s, *E*, -CH_2OBz, 2.2H). ^{13}C NMR (125.714 MHz, $CDCl_3$): δ = 166.28 (s, -O*C*(O)Ph), 166.22 (s, -O*C*(O)Ph), 138.32 (s, -*C*=CH_2), 137.79 (s, -*C*=CH_2), 133.40 (s, *para-C*), 133.25 (s, *para-C*), 132.85 (s, *E*, -CH=CHCl), 130.22 (s, *ipso-C*), 129.95 (s, *ipso-C*), 129.84 (s, *ortho-C*, both isomers), 128.65 (s, *meta-C*), 128.59 (s, *meta-C*), 127.84 (s, *Z*, -CH=CHCl), 120.71 (s, *Z*, -*C*HH), 120.08 (s, *E*, -CH=CHCl), 119.37 (s, *E*, -*C*HH), 118.93 (s, *Z*, -*C*HH), 66.52 (s, -*C*H_2-), 64.32 (s, -*C*H_2-).

4.34: (*E/Z*)-5-(chloromethylene)-6-methylenedecane[12] 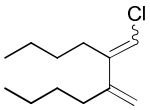

For reaction conditions, see Table 4.5: Entry 4. After filtration through a short alumina plug and removal of volatiles *in vacuo*, 1-isopropoxy-2-vinylbenzene, which is a byproduct from Hoveyda-Grubbs catalyst (**4.13**) was separated from the products by column chromatography (silica gel, eluted with pentane; early fractions contained the

desired product, later fractions contained 1-isopropoxy-2-vinylbenzene). Pentane was then removed *in vacuo*. Yield after column chromatography was 83%. *E/Z* ratio was 1.3 to 1. High resolution EI+ molecular ion calcd for $C_{12}H_{21}Cl$ 200.1332, found 200.1340 (M+). ^{1}H NMR (500MHz, CD_2Cl_2): δ = 6.15 (s, -C*H*Cl, *Z*, 1H), 5.88 (t, $^{4}J_{HH}$ = 1 Hz, -C*H*Cl, *E*, 1.3H), 5.12 (pseudo q, $^{4}J_{HH} = {}^{2}J_{HH}$ = 1.5-2 Hz, -C*H*H, *E*, 1.3H), 5.03 (d, $^{2}J_{HH}$ = 2 Hz, -C*H*H, *Z*, 1H), 4.93 (pseudo q, $^{4}J_{HH} = {}^{2}J_{HH}$ = 1-1.5 Hz, -CH*H*, *Z*, 1H), 4.88 (pseudo m, J = 1 Hz, -CH*H*, *E*, 1.3H), 2.40 (broad t, J = 7-8Hz, 2-CH_2(CH$_2$)$_2$CH$_3$, *E*, 2.6H) 2.20 – 2.12 (m, 2- and 3-CH_2(CH$_2$)$_2$CH$_3$, *E/Z*, 7H), 1.45 – 1.25 (m, 2- and 3-CH$_2$(CH_2)$_2$CH$_3$, *E/Z*, 18H), 0.88 – 0.94 (overlapping t's, -CH_3, *E/Z*, 14H). ^{13}C NMR (125.714 MHz, CD_2Cl_2): δ = 147.38 (alkenyl) 146.44 (alkenyl), 145.54 (alkenyl), 144.25 (alkenyl), 115.67 (alkenyl), 114.66 (alkenyl), 113.19 (alkenyl), 112.16 (alkenyl), 35.44 (alkyl), 35.09 (alkyl), 34.35 (alkyl), 31.19 (alkyl), 30.49 (alkyl), 30.43 (alkyl), 30.38 (alkyl), 28.72 (alkyl), 23.19 (alkyl), 23.08 (alkyl), 23.02 (alkyl), 22.70 (alkyl), 14.35 (-*C*H$_3$), 14.32 (-*C*H$_3$), 14.30 (-*C*H$_3$), 14.23 (-*C*H$_3$). *E/Z* assignments for ^{1}H NMR data are based on 1D NOESY spectroscopy and the through-space coupling of the -C=C*H*F proton and the –C=C*H*H proton for the *E* isomer. 2D COSY spectroscopy was used to assign the protons in the ^{1}H NMR data.

4.35: (*E/Z*)-1-bromo-3-trimethylsilyl-1,3-butadiene 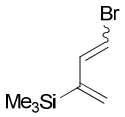

For reaction conditions, see Table 4.5: Entry 5. The reaction mixture was filtered through a short column of alumina and flushed through with pentane (100 mL) to remove ruthenium impurities. The volatiles were removed and the residue is then purified by column chromatography (silica gel, eluted with pentane) to remove 1-isopropoxy-2-

vinylbenzene, which is a byproduct from Hoveyda-Grubbs catalyst (**4.13**). (silica gel, eluted with pentane; early fractions contain the desired product, later fractions contain 1-isopropoxy-2-vinylbenzene). Pentane was then removed by rotatory evaporation. Yield after column chromatography was 25%. High resolution EI+ molecular ion calcd for $C_7H_{13}Br$ 203.9970, found 203.9972 (M+). *E/Z* ratio is 3 to 1. ^{1}H NMR (500MHz, CD_2Cl_2): δ = major: 6.90 (d broadened, $^3J_{HH}$ = 8 Hz, *Z*, overlapping), 6.87 (dt, $^3J_{HH}$ = 14 Hz, J =0.5-1 Hz, *E*, overlapping), 6.37 (d, $^3J_{HH}$ = 14 Hz, *E*, 3H), 6.24 (d, $^3J_{HH}$ = 7.5 Hz, *Z*, 1H), 5.76 and 5.75 (broadened, -C*HH*, 4.2H, overlapping), 5.46 and 5.45 (broadened, -C*HH*, 3.9H, overlapping) 0.17 (s, Si(C*H*$_3$)$_3$, 27H), 0.14 (s, Si(C*H*$_3$)$_3$, 9H).

Several EyM reactions were tested with α-fluorostryene, 1,1-difluoroethylene, 1,1-dichloroethylene and 1,2-dichloroethylene and a variety of alkynes. None of these substrates yielded the expected 1,3-butadiene products. Both bis(trimethylsilyl)acetylene and propargyl alcohol were tested for EyM with vinyl fluoride but no fluorinated diene products were observed.

Deciphering the Mechanism

In C_6D_6, 3-hexyne (12.3 mg, 0.150 mmol, 1.00 equiv) was dissolved along with compound **4.2** (5.9 mg, 0.0075 mmol, 5 mol%). The solution was frozen and the J. Young tube was evacuated. Vinyl fluoride gas was added to the head space of the J. Young tube and the solution was thawed and mixed. After 30 minutes, formation of *E/Z* 3-fluoromethylene-4-methylenehexane was observed. After 2 hours, complete consumption of 3-hexyne and compound **4.2** was observed by ^{1}H NMR spectroscopy.

This indicates that at least the initial cycle must go through the 14-electron monofluoromethylidene intermediate (Scheme 4.5), demonstrating that the monofluoromethylidene complexes can participate in EyM reactions.

Terminal Alkyne Dimerization with Olefin Metathesis Catalysts (Eq. 4.2)

Phenylacetylene (17.1 mg, 0.167 mmol, 1.00 equiv.), an internal standard, 1-bromo-3,5-bis(trifluoromethyl)benzene (10.9 mg, 0.0372 mmol) and catalyst **4.1** (6.2 mg, 0.0073 mmol, 4.4 mol%) were dissolved in 1 mL C_6D_6 and mixed thoroughly. The mixture was heated to 40 °C over 24 h. ^{1}H NMR spectroscopy indicated complete consumption of catalyst **4.1** after 1.5h but at that time very little product is observed. After 24h, ^{1}H NMR spectroscopy showed (Z)-1,4-diphenyl-but-1-en-3-yne (*cis*-PhHCH=CHC≡CPh)[15] in a 61% conversion, 1,3-diphenyl-but-3-en-1-yne (H_2C=C(Ph)(C≡CPh))[15] in a 7% conversion and leftover phenylacetylene (32%). GC-mass spectroscopy indicated the presence of the *cis* isomer in high yield and the germinal isomer along with (E)-1,4-diphenyl-but-1-en-3-yne (*trans*-PhHCH=CHC≡CPh) in less than 5% and trace amounts of 1,4-diphenylbuta-1,2,3-triene (HPhC=C=C=CPhH). These isomers were not observable by NMR spectroscopy. Ratios of isomers were similar to those seen by Caulton and Lee when using a ruthenium catalyst for alkyne dimerization.[15]

Trimethylsilylacetylene (15.3 mg, 0.156 mmol, 1.00 equiv.), an internal standard, 1-bromo-3,5-bis(trifluoromethyl)benzene (16.1 mg, 0.055 mmol) and catalyst **4.13** (4.6 mg, 0.0074 mmol, 4.7 mol%) were dissolved in 1 mL C_7D_8 and mixed thoroughly. The mixture was left at 23 °C over 44 h. ^{1}H NMR spectroscopy after 30 minutes indicated that all of **4.13** had been consumed. After 44h, only 30% of the trimethylsilylacetylene

had been consumed and one major dimer product was observed. The NMR data indicated that the major product was 1,3-bistrimethylsilyl-but-3-en-1-yne ($H_2C=C(SiMe_3)(C\equiv CSiMe_3)$ [15] in 22% conversion. A second isomer was observed in 7% yield but the identity of this isomer was unclear by NMR spectroscopy. GC-MS indicated one major isomer and one minor isomer in agreement with the NMR data.

An η^3-vinylcarbene complex (4.21)

An enyne metathesis reaction with vinyl fluoride and phenylacetylene, using 4 mol% of Piers catalyst was set up following the NMR scale procedure for EyM given above (Table 4.1: entry 4). An immediate color change of the solution from green/brown to red was observed upon addition of the phenyl acetylene. After three days at room temperature, only 22.4% conversion to the (E/Z)-1-fluoro-3-phenyl-1,3-butadiene (**4.22**) was observed by ^{19}F NMR spectroscopy. Upon farther exploration, the red compound was determined to be a stable side-on η^3 vinylcarbene complex that is unreactive to vinyl fluoride (Eq. 4.3). [16] Formation of compounds such as **4.21** with Piers catalyst was only a problem with aryl-substituted alkynes.

Piers catalyst, **4.14** (24.1 mg, 0.0281 mmol, 1.00 equiv.) was dissolved in 1 mL CH_2Cl_2. Phenylacetylene (54.8 mg, 0.536 mmol, 19.0 equiv.) was dissolved in 0.5 mL CH_2Cl_2. The two solutions were stirred for ten minutes and a color change from brown/green to deep red was observed. Cold pentane (15 mL) was added to the solution and the solution was placed in the freezer at – 35 °C overnight. A dark red precipitate (**4.21**) was isolated (14 mg, 0.0145 mmol, 52% yield). ^{31}P NMR (161.914 MHz, $CDCl_3$): δ = 47.08 ppm. ^1H NMR (400MHz, $CDCl_3$): δ = 8.85 (d, J = 7.6 Hz, phenyl, 1H), 7.60 (bt, J = 7.6 Hz, phenyl, 1H), 7.43 (m, J = 6.0 Hz, phenyl, 2H), 7.32 (t, J = 6.0 Hz, phenyl,

1H), 6.96 (s, H_2IMes-aryl, 1H), 6.81, 6.80 (s, overlapping, H_2IMes-aryl, 2H), 5.91 (s, H_2IMes-aryl, 1H), 4.38 (dd, $^2J_{PH}$ = 13.6 Hz, $^3J_{HH}$ = 7.6 Hz, Ru-*H*PCy$_3$, 1H), 3.9 – 3.7 (m, H_2IMes-backbone, 4H), 3.26 (pseudo-t, $^3J_{PH}$ = 7.6 Hz, $^3J_{HH}$ = 7.6 Hz, beta-C*H*, 1H), 2.44 (s, H_2IMes, -C*H*$_3$, 3H), 2.34 (s, H_2IMes, -C*H*$_3$, 3H), 2.23 (s, H_2IMes, -C*H*$_3$, 3H), 2.17, 2.15 (s, overlapping, H_2IMes, -C*H*$_3$, 6H), 1.89 (s, H_2IMes, -C*H*$_3$, 3H), 2 – 0.5 (broad, 30H, PCy$_3$). $^1H\{^{31}P\}$ NMR (400MHz, $CDCl_3$): δ = identical to above proton except for: 4.38 (d, $^3J_{HH}$ = 7.6 Hz, Ru-*H*PCy$_3$, 1H), 3.26 (d, $^3J_{HH}$ = 7.6 Hz, beta-C*H*, 1H). ^{13}C NMR (100.596 MHz, $CDCl_3$): δ = 280.55 (alpha-*C*(Ph)=Ru), 197.83 (H_2IMes carbene *C*), 140.56, 139.2 (d), 138.5, 137.8, 136.3, 135.84, 135.48, 134.42, 133.19, 131.1, (130.0, 129.85, 129.69), 129.54, (128.49, 128.41), 128.1, 57.16, 52.69, 51.23, 33.39, 32.71, 28.24, 27.77, 26.42, 26.24, 26.12, 25.36, 21.40, 20.86, 19.94, 19.62, 18.79, 18.50.

Compound **4.21** (20 mg, 0.021 mmol) was dissolved in C_6D_6 and vinyl fluoride gas was added to the J. Young tube by first evacuating the tube and then refilling with vinyl fluoride. The solution was heated to 60 °C over two days, no reaction with vinyl fluoride and only slow decomposition of compound **4.21** was observed.

4.10. References

1. Macnaughtan, M. L.; Johnson, M. J. A.; Kampf, J. W., *Organometallics* **2007,** *26* (4), 780-782.
2. Macnaughtan, M. L.; Johnson, M. J. A.; Kampf, J. W., *J. Am. Chem. Soc.* **2007,** *129* (25), 7708-7709.
3. Fomine, S.; Ortega, J. V.; Tlenkopatchev, M. A., *Journal Of Molecular Catalysis A-Chemical* **2007,** *263* (1-2), 121-127.
4. Louie, J.; Grubbs, R. H., *Organometallics* **2002,** *21*, 2153.
5. Caskey, S. R.; Stewart, M. H.; Kivela, J. E.; Sootsman, J. R.; Johnson, M. J. A.; Kampf, J. W., *J. Am. Chem. Soc.* **2005,** *127*, 16750-16751.
6. Macnaughtan, M. L.; Gary, J. B.; Gerlach, D. L.; Johnson, M. J. A.; Kampf, J. W., *Organometallics* **2009,** *ASAP*.
7. Garber, S. B.; Kingsbury, J. S.; Gray, B. L.; Hoveyda, A. H., *Journal of the American Chemical Society* **2000,** *122* (34), 8168-8179.
8. Gessler, S.; Randl, S.; Blechert, S., *Tetrahedron Lett.* **2000,** *41* (51), 9973-9976.
9. Romero, P. E.; Piers, W. E.; McDonald, R., *Angew. Chem. Int. Ed.* **2004,** *43*, 6161.
10. Sashuk, V.; Samojlowicz, C.; Szadkowska, A.; Grela, K., *Chem. Commun.* **2008,** (21), 2468-2470.
11. Giessert, A. J.; Snyder, L.; Markham, J.; Diver, S. T., *Organic Letters* **2003,** *5* (10), 1793-1796.
12. Xi, Z. F.; Song, Z. Y.; Liu, G. Z.; Liu, X. Z.; Takahashi, T., *Journal of Organic Chemistry* **2006,** *71* (8), 3154-3158.
13. Diver, S. T.; Giessert, A. J., *Chemical Reviews* **2004,** *104* (3), 1317-1382.
14. Melis, K.; De Vos, D.; Jacobs, P.; Verpoort, F., *Journal of Organometallic Chemistry* **2003,** *671* (1-2), 131.
15. Lee, J.-H.; Caulton, K. G., *Journal of Organometallic Chemistry* **2008,** *693* (8-9), 1664.
16. Trnka, T. M.; Day, M. W.; Grubbs, R. H., *Organometallics* **2001,** *20* (18), 3845-3847.
17. Lippstreu, J. J.; Straub, B. F., *Journal of the American Chemical Society* **2005,** *127* (20), 7444-7457.
18. Galan, B. R.; Giessert, A. J.; Keister, J. B.; Diver, S. T., *Journal of the American Chemical Society* **2005,** *127* (16), 5762-5763.
19. Gottlieb, H. E.; Kotlyar, V.; Nudelman, A., *Journal of Organic Chemistry* **1997,** *62* (21), 7512-7515.
20. Trnka, T. M.; Morgan, J. P.; Sanford, M. S.; Wilhelm, T. E.; Scholl, M.; Choi, T. L.; Ding, S.; Day, M. W.; Grubbs, R. H., *J. Am. Chem. Soc.* **2003,** *125* (9), 2546-2558.
21. Scholl, M.; Ding, S.; Lee, C. W.; Grubbs, R. H., *Organic Letters* **1999,** *1* (6), 953-956.
22. Sanford, M. S.; Love, J. A.; Grubbs, R. H., *J. Am. Chem. Soc.* **2001,** *123* (27), 6543-6554.

Chapter 5

Fischer to Fischer Carbene Olefin Metathesis: Tricking the Ruthenium Catalyst

5.1. Introduction

The ongoing development of olefin metathesis (OM) catalysts through metal and ligand alterations has lead to an ever expanding suite of tolerated functional groups. Initially, the synthesis of Ru-based OM catalysts such as 1st generation Grubbs catalyst, **5.1** (Chart 5.1), allowed for tolerance of oxygenated and protic functional groups as opposed to previously known W- and Mo-catalysts.[1] Upon replacing the tricyclohexylphosphine with an *N*-heterocyclic carbene (NHC) ligand (Chart 5.1: **5.2**), general reactivity with all olefins increased.[1] However, even with the large number and variety of OM catalysts now known, none will promote metathesis of alkenes with certain directly-functionalized olefins.[2] For the purposes of this chapter, "directly-functionalized" and "electron-rich" olefins will be defined as olefins containing α-heteroatom-substitution with lone-pair electron density on the heteroatom; (*e.g.* vinyl halides, ethyl vinyl ether, or phenyl vinyl sulfide). Chapters 2 through 4 focused on vinyl halides as substrates for olefin metathesis. Here, we will discuss a broader range of directly-functionalized olefins.

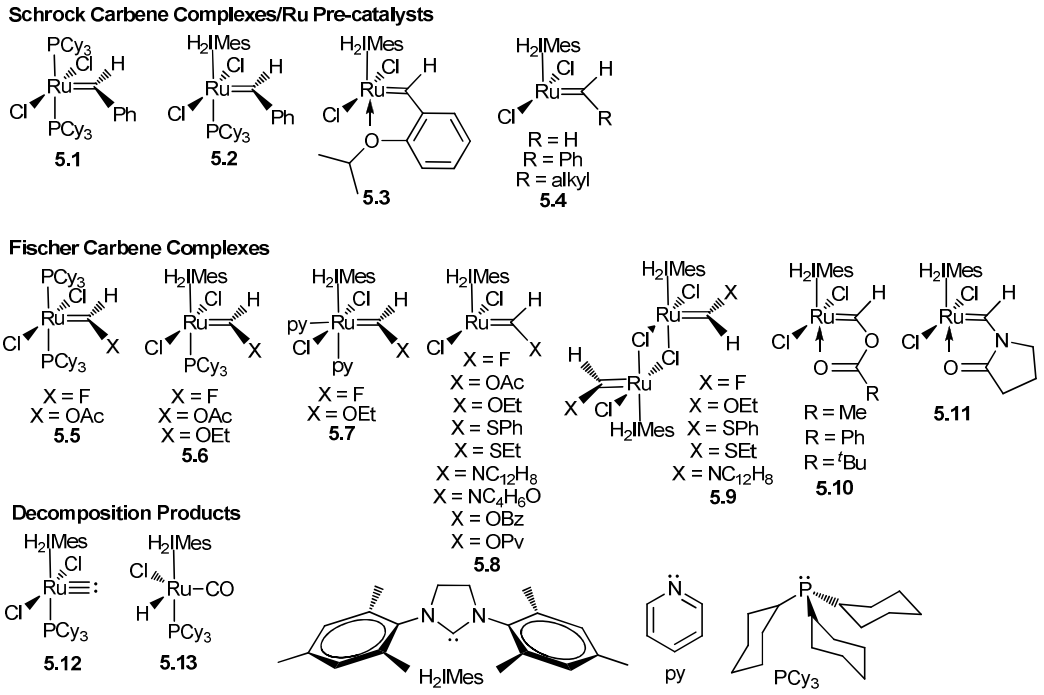

Chart 5.1. Important Ruthenium Compounds

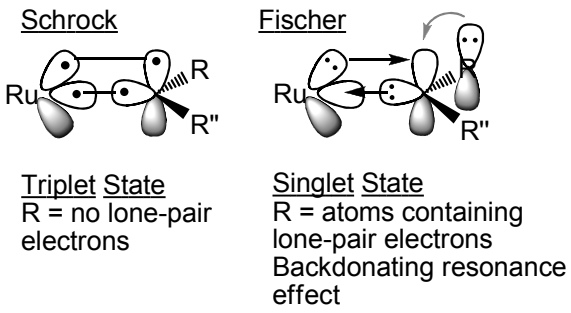

Figure 5.1. Definitions of Schrock and Fischer Carbene Complexes.[3]

Two distinct forms of carbene ligands have been distinguished as Fischer and Schrock carbene complexes. These complexes are usually defined by a number of properties including the nature of the carbene ligand, the metal identity, oxidation state and the ligand set on the metal center. For our purposes, all things are equal except for

the carbene ligand; therefore, Schrock carbene complexes will be defined as ruthenium carbene complexes in which R is an atom with no lone-pair electron density (Figure 5.1; left, Chart 5.1; first row). Fischer carbene complexes will be defined as ruthenium carbene complexes in which R is a hetero-atom that contains lone-pair electron density and can act as a π-donor substituent. (Figure 5.1; right, R = NR'_2, OR', SR', F, Cl; Chart 5.1; second row). In the case of Fischer carbene complexes, the electron density on the α-heteroatom can donate into the α-C(p) orbital (Figure 5.1) causing a redistribution of electron density around the ruthenium-carbon double bond. This has two effects; first, the singlet form of the carbene ligand directly affects the binding mode and reactivity of the Ru-complex. Second, the electron-deficient 14-electron Ru-carbene complex is stabilized through resonance effects at the α-carbon.[3] Certain carbene ligands with strong π-donating R groups have been found to lower the Gibbs free energy of their 14-electron ruthenium carbene complexes. This was demonstrated through DFT calculations by Fomine and through experimentation by Grubbs previously discussed in Chapter 1.[2, 4] The energetic difference between 14-electron Schrock carbene complexes and 14-electron Fischer carbene complexes prevents productive cross-metathesis of electron-rich olefin with more conventional alkenes (Scheme 5.1 and 5.2). Each turnover in the metathesis cycle would require conversion from a Fischer carbene complex to a Schrock carbene complex and the relative rate of this conversion is extremely slow when olefinic starting materials and products are thermoneutral. This behavior has made electron-rich olefins such as ethyl vinyl ether useful as capping agents to terminate metathesis polymerization reactions but not as active reagents in cross-metathesis reactions.

Methods to use directly-functionalized olefins in cross-metathesis reactions would further increase the breadth of OM.

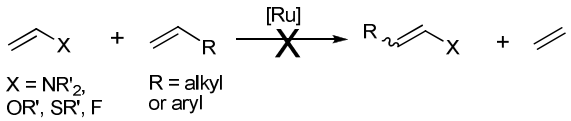

Scheme 5.1. CM with Electron-Rich Olefins.

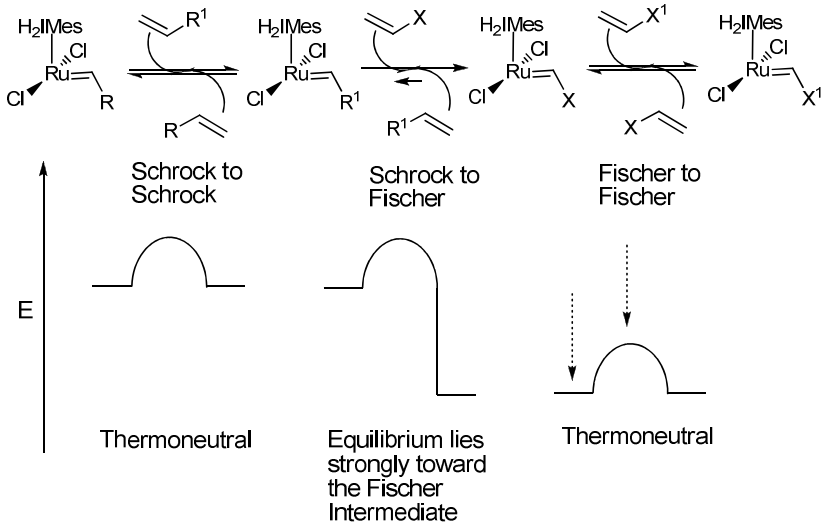

Scheme 5.2. Qualitative Energetic Comparison of Schrock and Fischer Carbene Complexes

A catalyst that could easily convert between Schrock and Fischer carbene moieties allowing for cross-metathesis of alkenes with electron-rich olefins would be ideal. However, with ruthenium catalysts, the energy difference for Schrock and Fischer carbene complexes comes directly from the carbene moiety; it becomes difficult to reliably predict a ligand system that would destabilize the Fischer carbene complex while

stabilizing the Schrock carbene complex. Conversion from a Fischer carbene complex to a Schrock carbene complex only occurs in the presence of a strong driving force;[5, 6] however, interconversion between Fischer carbene complexes has been shown to be predominantly energetically neutral.[2] The energy barrier between Fischer carbene complexes should be comparable to that of Schrock carbene interconversion.[7]

5.2. Stoichiometric Fischer Carbene Metathesis

5.2.1. 2nd Generation Grubbs Catalyst

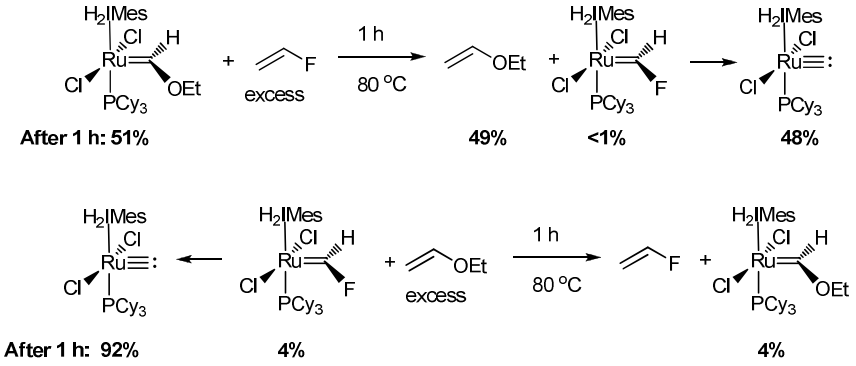

Scheme 5.3. Stoichiometric Fisher Carbene Metathesis (**5.6**)

Inspired by Grubbs' work,[2] we tested the interconversion of the monofluoromethylidene complex, **5.6-F**, and the ethoxymethylidene complex, **5.6-OEt**. Treatment of **5.6-OEt** with vinyl fluoride gave 49% conversion to **5.12** through initial formation of **5.6-F** and liberation of ethyl vinyl ether (Scheme 3.5, top). Liberation of vinyl fluoride was possible to a small extent upon treatment of **5.6-F** with ethyl vinyl ether at 80 °C; however, decomposition of the **5.6-F** occurred more rapidly (Scheme 5.3,

bottom). High temperatures are required for phosphine dissociation as the Fischer carbene complexes tend to coordinate phosphine ligands more tightly than Schrock carbene complexes.[2, 8] Therefore, Fischer carbene interconversion was further explored using the phosphine-free complexes, **5.7-F** and **5.7-OEt**.

5.2.2. 3rd Generation Grubbs Catalyst

Treatment of the monofluorocarbene complex, **5.7-F**, with ethyl vinyl ether confirmed that **5.7-F** would undergo metathesis with ethyl vinyl ether to give **5.7-OEt** and vinyl fluoride (Scheme 5.4, bottom). Treatment of **5.7-OEt** with excess vinyl fluoride yielded 90% consumption of **5.7-OEt** in 2 hours at room temperature (Scheme 5.6, top). Decomposition of **5.7-F** still hindered full evaluation of the equilibrium; however, the ability to perform these reactions at lower temperature did allow for the definitive finding that the energy barrier between Fischer carbene complexes was no greater than that between Schrock carbene complexes.

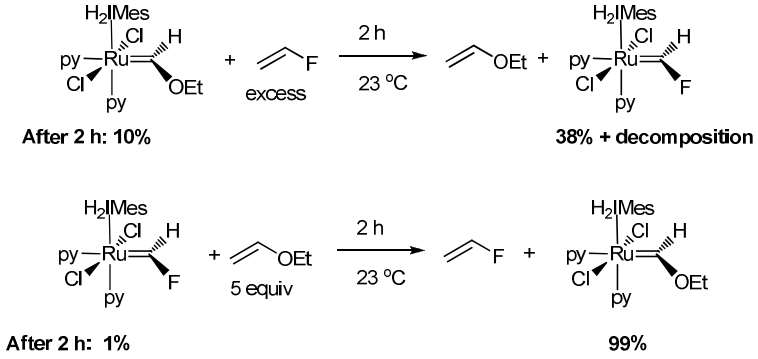

Scheme 5.4. Stoichiometric Fischer Carbene Metathesis (**5.7**)

Based on the success of the stoichiometric Fischer carbene metathesis, we hypothesized that addition of an electron-rich group (Eq 5.1, Y; Scheme 5.5) in the *beta* position of a desired alkene would allow for catalytic CM with electron-rich olefins. This system would bypass the need to form a Schrock carbene intermediate from a Fischer carbene intermediate. Only Fischer to Fischer carbene interconversion would be required to give the desired cross-product.

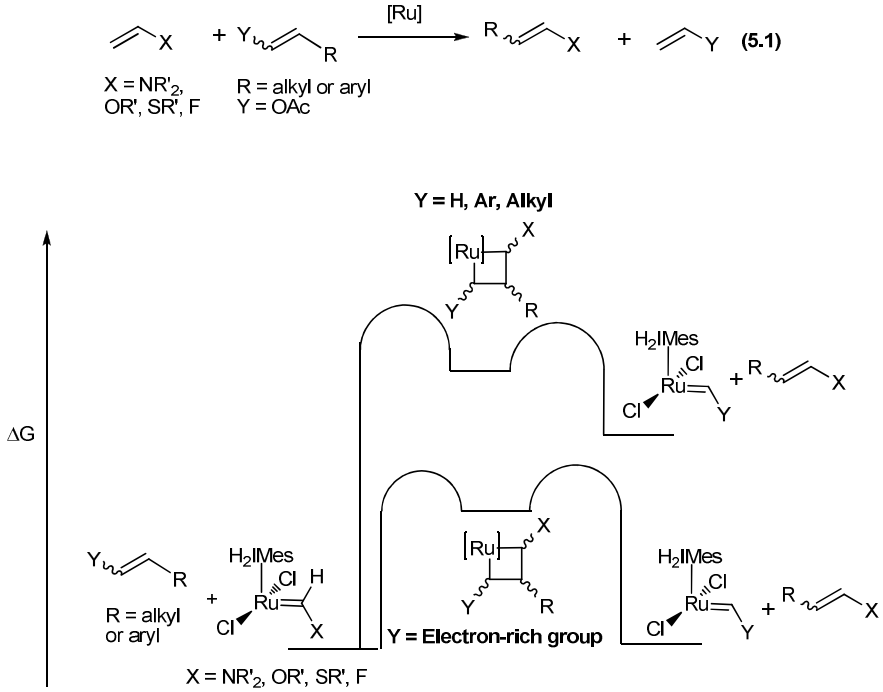

Scheme 5.5. General Fischer CM Reaction.

5.3. Chelated Ruthenium Acetoxycarbene Complex

As discussed earlier, phosphine lability of Fischer carbene complexes requires high temperatures. In addition, certain Fischer carbene complexes are more likely to decompose in the presences of a second neutral ligand such as PCy_3 (**5.5-F, 5.5-OAc, 5.6-F,** and **5.6-OAc**) or pyridine (**5.7-F**).[8-10] By using the Blechert/Hoveyda-Grubbs catalyst (Chart 5.1: **5.3**), the presence of a second neutral ligand can be eliminated. One difficulty presented by using **5.3** as a catalyst for CM is the lack of a 16-electron catalytic resting state after the initial metathesis cycle. This can lead to premature catalyst deactivation. Using an ester functional group in the Y position (Eq. 5.1) would allow access to the chelated acyloxycarbene complex, **5.10**, which could serve as an accessible 16-electron resting state for the catalyst. The acetate group was chosen as the Y group for a few reasons. The acetoxycarbene complex, **5.10-Me**, is a Fischer carbene complex and will readily interconvert with other Fischer carbene complexes and has already been well-characterized by our group.[9, 10] Treatment of the monofluoromethylidene dimer, **5.9-F**, with excess vinyl acetate readily forms **5.10-Me** and vinyl fluoride (Scheme 5.6). Furthermore, alkenyl acetates are easily accessible through *anti*-Markovnikov addition of glacial acetic acid across a terminal alkyne *via* a Re-catalyst (Scheme 5.7).[11] Finally, the metathesis product, vinyl acetate, can be removed *in vacuo* if needed.

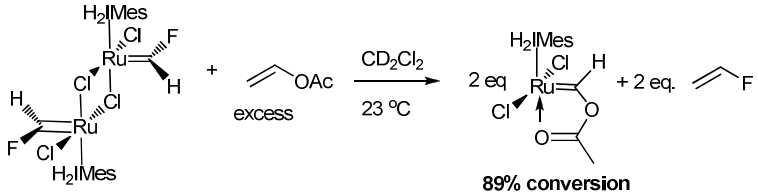

Scheme 5.6. Reaction of **5.9-F** with Vinyl Acetate

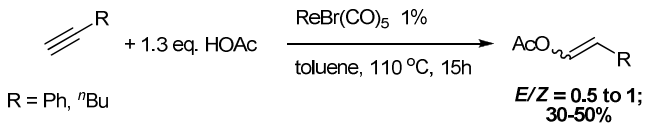

Scheme 5.7. Synthesis of Alkenyl Acetate

5.4. CM with Electron-rich Olefins

5.4.1. Styryl Acetate

5.4.1.1. Synthesis

Styryl acetate was prepared in a 49.5% isolated yield in one step from acetic acid and phenyl acetylene using $ReBr(CO)_5$ (1 mol%) as a catalyst on a gram scale. The *E/Z* ratio was around 0.5. Other acids such as benzoic acid or trifluoroacetic acid could also be employed in this reaction.[11]

5.4.1.2. Substrate Scope and Yield

Fischer to Fischer cross-metathesis (FCM) of an electron-rich olefin with styryl acetate in benzene-d_6 using Blechert/Hoveyda-Grubbs catalyst (**5.3**; 5 mol% catalyst loading) successfully afforded the cross-metathesis product in 2 to 72 hours depending on the identity of the electron-rich olefin (Eq 5.1, Table 5.1). Electron-rich olefins, ethyl vinyl ether, phenyl vinyl sulfide, and ethyl vinyl sulfide reached equilibrium relatively quickly (Table 5.1). Electron-rich olefins, vinyl benzoate, vinyl pivalate, and *N*-vinyl pyrrolidinone were slower to form the cross-product (24 to 72 hours) because of the

formation of a second catalytic resting state (Chart 5.1: **5.10-Ph**, **5.10-^{t}Bu**, **5.11**). Vinyl fluoride presented a unique case. Addition of vinyl fluoride gas by freezing the reaction mixture in liquid nitrogen while the system was open to vinyl fluoride gas afforded a large excess of vinyl fluoride (17 equivalents). The large excess of terminal olefin shut down productive metathesis through trapping of the catalyst as the monofluoromethylidene complex (**5.8-F** and **5.9-F**) via degenerate metathesis exchange. Making a solution of vinyl fluoride in benzene or toluene or evacuating the reaction vessel and then refilling with vinyl fluoride gas at ambient temperatures allowed for a lower concentration of vinyl fluoride in the reaction mixture. Lower concentrations of vinyl fluoride afforded the desired cross-product; however, a second addition of vinyl fluoride gas to the system was required to increase the yield of the desired products from 26% to around 42%. Vinyl chloride gave 22% conversion to desired products. Low yields are most likely due to competition between productive metathesis and decomposition of the monochloromethylidene intermediates. 1,2-dichloroethene and 9-vinylcarbazole did not afford the expected cross-product or the percent conversion was extremely low.

Table 5.1. Preliminary Substrate Scope Study for Styryl Acetate

	Reagent[a]	**Equiv**[b]	**Time (h)**[c]	**% Conversion**[d]	**Products (Chart 5.2)**	**E/Z**[f]
1		6.3	24	**75**	**5.14**	1.7
2	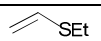	0.53	1.5	**73**	**5.15**	6.5
3		0.47	1.5	**51.2 (88[e])**	**5.16**	n/a
4		1.0	4.5	**60**	**5.16**	n/a
5		5.0	3	**66**	**5.16**	n/a
6		4.6	42	**38**	**5.17**	1.4
7		4.3	42	**14**	**5.18**	0.73
8	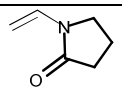	1.2	43	**10**	**5.19**	3.4
9		0.73	n/a	**42**	**5.21**	0.73
10		n/a	64	**22[g]**	**5.22**	-
11		1.0	48	**0**	**5.22**	-

[a] Conditions: 5 mol % **5.3** (0.0075 mmol), 1 mL C_6D_6, styryl acetate, 0.05 mmol IS (1-bromo-3,5-bis(trifluoromethyl)benzene, 45°C. [b] Equivalents of the electron-rich olefin are given with respect to the initial amount of styryl acetate. [c] NMR reactions were monitored until the percent conversion observed had not changed for 4 hours. In some cases, the time given is longer than was necessary for the reaction to reach equilibrium. [d] Percent conversion is based on the internal standard and the initial amount of styryl acetate as determined by NMR integration. [e] Percent conversion based on limiting reagent. [f] n/a = not available. In the case of ethyl vinyl sulfide and phenyl vinyl sulfide, the *E* and *Z* isomers overlapped in the ^{1}H NMR spectrum and therefore the *E/Z* ratio could not be determined. [g] An additional 5 mol% of **5.3** was added after 16.5 h. At that point, 16% conversion was observed.

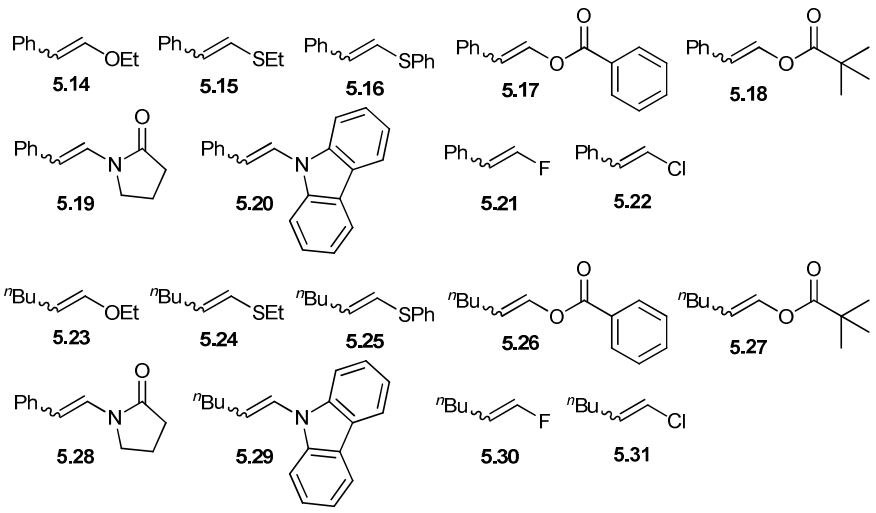

Chart 5.2. Cross-Products of FCM. [12-25]

5.4.2. Hexenyl Acetate

5.4.2.1. Synthesis

The starting material, 1-hexenyl acetate, was prepared in one step from acetic acid and 1-hexyne using $ReBr(CO)_5$ as a catalyst in 59% isolated yield on a gram scale. The *Z/E* ratio was around unity.[11]

5.4.2.2. Substrate Scope and Yield

Cross-metathesis with 1-hexenyl acetate generally afforded higher percent conversions to the cross product than did styryl acetate in the preliminary assay. Ethyl vinyl ether, ethyl vinyl sulfide, vinyl fluoride and phenyl vinyl sulfide gave high percent conversions in only 2 hours. Electron-rich olefins with chelating groups were slower to

react but overall gave much higher percent conversions to the desired products than they did with styryl acetate (Table 5.2).

Table 5.2. Preliminary Substrate Scope Study for 1-Hexenyl Acetate

	Reagent[a]	**Equiv**[b]	**Time (h)**[c]	**% Conversion**[d]	**Products (Chart 5.2)**	**E/Z**[e]
1		5.7	2	**60**	**5.23**	1.1
2	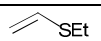	2.3	2	**70**	**5.24**	0.98
3		4.7	2	**82**[f]	**5.25**	n/a
4		5.3	40	**85**	**5.26**	0.67
5		4.9	40	**70**	**5.27**	n/a
6	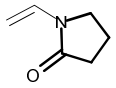	5	48	**10**	**5.28**	n/a
7	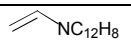	5	48	**6**	**5.29**	-
8		0.56	18	**43**	**5.30**	2.6
9	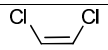	2.6	n/a	**0**	**5.31**	-

[a] Conditions: 5 mol% of **5.3**, 1 mL C_6D_6, 1-hexenyl acetate, 0.05 mmol IS (1-bromo-3,5-bis(trifluoromethyl)benzene, 45 °C or 23 °C. [b]Equivalents of the electron-rich olefin with respect to the amount of 1-hexenyl acetate. [c] NMR reactions were monitored until the percent conversion observed had not changed for 4 hours. In some cases, the time given is longer than was necessary to reach equilibrium. [d] Percent conversion is based on the internal standard and the initial amount of 1-hexenyl acetate as determined by NMR integration. [e] n/a = not available. [f] Very little starting material was left in solution.

5.4.3. Equilibrium

Initial studies indicated that the Fischer carbene cross-metathesis system is in equilibrium. This would not be surprising as most CM systems display an equilibrium

between the products and reactants when there is no driving force present.[26] In many cases, the equilibrium endpoint was reached before catalyst deactivation occurred. Addition of more catalyst did not alter the percent conversion to product. The equilibrium was tested by altering the concentration of ethyl vinyl ether in the reaction system while holding the amount of styryl acetate constant. Although the expected qualitative trend in which the amount of desired products increased with increasing concentration of ethyl vinyl ether, a quantitative assessment of this equilibrium proved extremely difficult (Table 5.3). The overall rate of product formation was not consistent between Entries 1-4 in Table 5.3. The effect of the relative rates of competing metathesis processes were each independently altered by the concentration of starting materials, products and catalyst affecting the overall rate of product formation. The relative rates of these competing processes are too convoluted to separate. For example, a large excess of the terminal olefin would engage the catalyst in a degenerate metathesis suppressing other catalytic pathways while a system with a lower concentration of terminal olefin would equilibrate at a lower percent conversion of products. Also, the *Z* isomer for both the starting materials and products is undergoing degenerate metathesis and *Z* to *E* isomerization occurs through this metathesis (Scheme 5.11).[27] Although the *Z* isomer is kinetically favored for CM, the *E* isomer is more thermodynamically favored; therefore, the *E/Z* ratio for both starting materials and products increases over time. Furthermore, the relative rate of productive metathesis for the *Z*-alkenyl acetate is much faster than for the *E* isomer ($k_Z > k_E$) so as the *E/Z* isomer ratio increases, the overall rate of productive metathesis decreases.[27] Similar trends were also observed with phenyl vinyl sulfide (Table 5.4).

Table 5.3. Altering the Concentration of Ethyl Vinyl Ether

	mmol[a]	**Equiv**[b]	**1.5 h**[b]	***E:Z***[c]	**19 h**[b]	***E:Z***[c]
1	0.097	0.4	26%	*1.0*	29%	*1.4*
2	0.35	1.3	41%	*1.3*	60%	*1.5*
3	0.84	3	42%	*1.3*	72%	*1.5*
4	1.6	6.3	45%	*1.6*	72%	*1.6*

[a] Reaction mixture in 1 mL of C_6D_6 using 5 mol% catalyst loading of **5.3** [b] Equivalents of ethyl vinyl ether and percent conversion to products were determined with respect to initial amount of styryl acetate and the internal standard. [c] *E/Z* ratio of products (*E/Z*-β-ethoxystyrene, **5.14**).

Table 5.4. Altering the Concentration of Phenyl Vinyl Sulfide

	mmol [a]	**Equiv** [b]	**0.5h**[b]	***E/Z***[c]	**1 h**[b]	***E/Z***[c]	**2.5 h**[b]	***E/Z***[c]	**3.5 h**[b]	***E/Z***[c]	**4.5h**[b]	***E/Z***[c]
1	0.12	1.0	33%	*0.6*	49%	*1.2*	54%	*1.8*	57%	*2.0*	60%	*2.4*
2	0.25	2.0	45%	*0.8*	52%	*1.4*	68%	*3.3*	66%	*3.3*	69%	*3.0*
3	0.62	5.0	41%	*0.7*	49%	*1.2*	66%	*2.5*	64%	*2.5*	64%	*2.6*
4	1.24	10.0	49%	*0.9*	50%	*1.3*	n/a	*n/a*	66%	*3.4*	66%	*3.6*

[a] Reaction mixture in 1 mL of C_6D_6 using 5 mol% catalyst loading of **5.3**. [b] Equivalents of phenyl vinyl sulfide and percent conversion to products were determined with respect to initial amount of styryl acetate and the internal standard. [c] *E/Z* ratio of starting material *E/Z*-styryl acetate. Initial *E/Z* ratio of styryl acetate is 0.4. For full experimental conditions see Table 5.6 entries 4-7.

5.4.4. Optimization

The preliminary reactions were run with the standard 5 mol% catalyst loadings of **5.3** in benzene-d_6. We decided to test whether lower catalyst loadings would have any adverse affects on the amount of products formed. Catalyst loadings as low as 1 mol% yielded the same percent conversion to product as 5 mol% loadings. Interestingly, when only 1 mol% catalyst loading was employed, less *E/Z* isomerization of styryl acetate was observed (Table 5.5).

Table 5.5. Altering Catalyst Loading

	5.3[a]	**4h**[c]	**48h**[c]
1	*5%*[b]	54%	54%
2	*2.5%*[b]	56%	58%
3	*1%*[b]	50%	57%

[a] Metathesis of 1-hexenyl acetate and phenyl vinyl sulfide (1:1 ratio), 1 mL C_6D_6. [b] mol% catalyst loading [c] Percent conversion based on internal standard with respect to the initial amount of 1-hexenyl acetate.

Also, acetone was tested as a solvent for these reactions and it was demonstrated that in some cases, benzene could be replaced by acetone with no detrimental effects to product formation (see Tables 5.6 through 5.10 in Experimental section).

5.4.5. Mechanism

Cross-metathesis with electron-rich olefins appears to follow the same mechanism as other cross-metathesis processes (Scheme 5.8).[28, 29] Initially, the terminal olefin,

which is more active towards metathesis catalysts than internal olefins, reacts with the catalyst **5.3** to form a new 14-electron Fischer carbene species, **5.8-X**, and 2-isopropoxystryene. At this point, a number of reactions can occur. For productive metathesis, the Fischer carbene complex (**5.8-X**) must coordinate with the alkenyl acetate and undergo cycloaddition to form a new metallocycle. If the metallocycle contains the R-group (R = Ph, ^{n}Bu) in the β-position, productive cycloreversion can take place and the Ru-acetoxycarbene (**5.8-OAc**) forms along with one equivalent of product (Scheme 5.9; top). If the metallocycle formed contains the R-group in an α-position, productive cycloreversion cannot occur because the energetic barrier is too large to form **5.4-R** (R = Ph or ^{n}Bu) and the metallocycle cycloreverts back to **5.10-X** and the starting olefin. One question to be answered is whether the α-R-metallocycle forms at all (Scheme 5.9; bottom). The reaction of **5.8-OAc** with a second equivalent of the electron-rich olefin generates vinyl acetate and **5.8-X**. The chelated acetoxycarbene complex (**5.10-Me**) can also form from **5.8-OAc** and acts as a resting state for the catalyst, prolonging the lifetime of the catalyst. A secondary resting state, which is sometimes observed, is the dimer complex, **5.9-X**, as discussed in Chapter 3. Neither **5.4-R** (R = Ph or ^{n}Bu) nor **5.4-H** form as both are Schrock carbene complexes and are higher energy than Fischer carbene complexes (Scheme 5.10). Because it is not possible for **5.4-R** to form in these reactions, the mechanism and product formation is simpler than other CM reactions. Degenerate metathesis reactions still occur during productive metathesis. The degenerate metathesis of alkenyl acetates causes *Z* to *E* isomerization. Initially, *E/Z* ratios of the starting materials are around 0.5 to 1. As metathesis occurs, the *Z* isomer is converted to the *E* isomer as the *E* isomer is more thermodynamically favored. Build up of the *E*

isomer is also observed because the *E* isomer is less reactive towards the OM catalyst than the *Z* isomer (Scheme 5.11).[27]

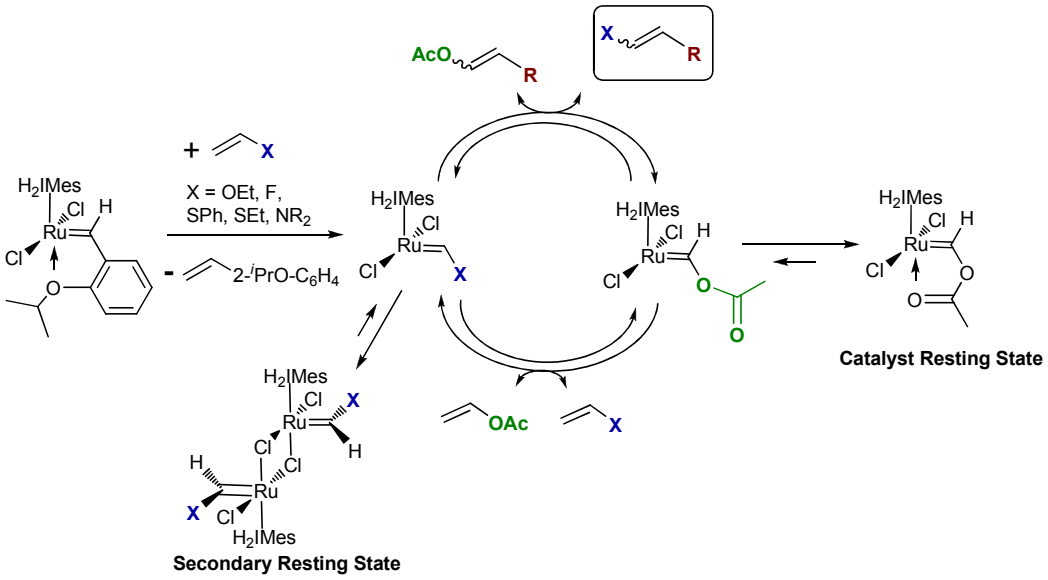

Scheme 5.8. Mechanism for Fischer Carbene Cross-Metathesis

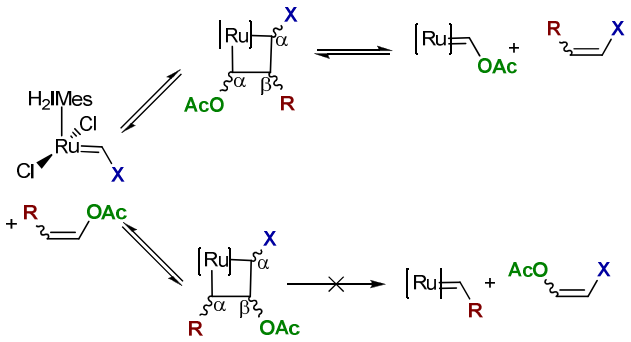

Scheme 5.9. Cycloaddition and Cycloreversion Processes

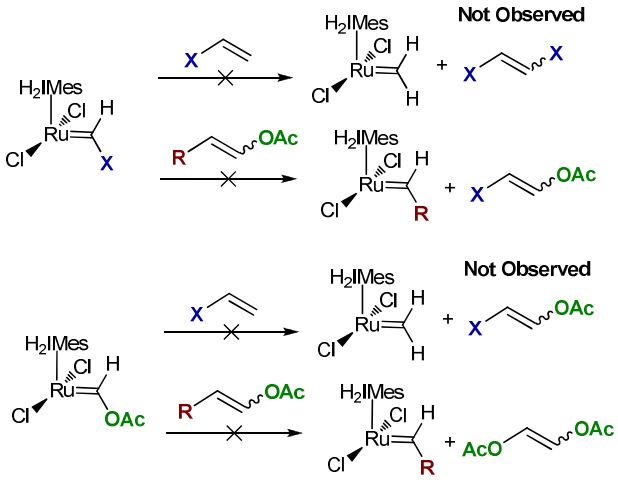

Scheme 5.10. Other Pathways: Fischer to Schrock Conversion

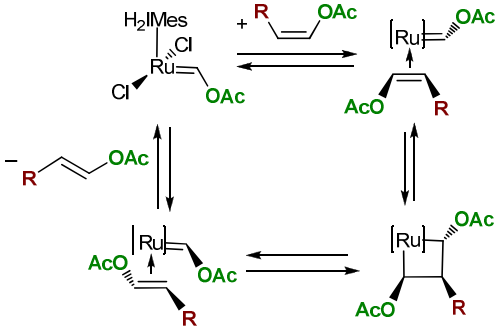

Scheme 5.11. Degenerate Metathesis; *E/Z* Isomerization

5.5. Conclusions

We have demonstrated that catalytic CM with electron-rich olefins is possible through modification of the second olefinic substrate to allow for a Fischer carbene metathesis pathway. This is the first demonstration of productive CM with ethyl vinyl ether as well as other electron-rich olefins. This CM system appears to be under equilibrium control as are other CM systems; however, quantitative assessment of the

equilibrium will require further experimental studies. CM of styryl acetate or 1-hexenyl acetate with electron-rich olefins works well. In general, 1-hexenyl acetate gave higher yields of desired products. Ethyl vinyl ether, ethyl vinyl sulfide, phenyl vinyl sulfide and vinyl fluoride were all competent reactants for this process. Vinyl benzoate, vinyl pivalate, *N*-vinyl pyrrolidinone and 9-vinylcarbazole required longer reaction times and for the most part, produced lower percent conversions to desired products than did electron-rich olefins without chelating functional groups. Both benzene and acetone were effective solvents for CM with electron-rich olefins. Catalyst loadings as low as 1 mol % were viable. In addition to broadening the substrate scope for cross-metathesis, Fischer carbene cross-metathesis (FCM) opens uncharted territories in olefin metathesis chemistry (see Chapter 7; Future Directions).

5.6. Experimental

5.6.1. General Procedures. All reactions were set-up in a nitrogen-filled MBRAUN Labmaster 130 glove box, unless otherwise specified and run under a nitrogen atmosphere. ^{1}H, ^{13}C, ^{19}F NMR data were acquired on a Varian Inova 400 MHz or 500MHz NMR spectrometer. ^{1}H spectra were referenced to solvent signals. [30] ^{19}F NMR spectra was referenced to external $CFCl_3$ in $CDCl_3$ (δ=0). NMR scale reactions were filtered through activated alumina before gas chromatography-mass spectroscopy (GC-MS) data were acquired. GC-MS data was acquired on a Shimadzu GC-MS-QP5000 Gas Chromatograph – Mass Spectrometer.

5.6.2. Materials. Vinyl chloride gas was purchased from Fluka. Phenylacetylene, ethyl vinyl ether, ethyl vinyl sulfide, phenyl vinyl sulfide, 9-vinylcarbazole, vinyl benzoate, 1,3,5-methoxybenzene, vinyl bromide, 4-fluorotoluene and vinyl pivalate were purchased from Aldrich and phenylacetylene was purified by filtration through alumina. Vinyl acetate and *N*-vinyl pyrrolidinone were purchased from Acros Organics. Vinyl fluoride gas and 1-bromo-3,5-bis(trifluoromethyl)benzene were purchased from Synquest Labs Inc. 1-Hexyne was purchased from Lancaster Synthesis Inc. Glacial acetic acid was purchased from Fischer Scientific. Rhenium carbonyl (Re_2CO_{10}) was purchased from Strem Chemicals, Inc. 1,2-dichloroethylene was purchased from TCI America. All bulk solvents were obtained from VWR Scientific and were degassed and dried over 4 Å molecular sieves. Deuterated solvents were purchased from CIL and dried over 4 Å molecular sieves. All liquid reagents were degassed. Gaseous vinyl halides and solid reagents were used as received. Ruthenium catalyst, **5.3,** was obtained from Materia, Inc. Compound **5.6-F**, **5.7-F**, and **5.6-OEt** were synthesized according to published procedures.[2, 8]

5.6.3. Synthetic Procedures

Metathesis Exchange between Fisher Carbene Complexes (Scheme 5.3)

Starting from 5.6-OEt. Compound **5.6-OEt** (20.0 mg, 0.0245 mmol) was dissolved in 1 mL C_6D_6 along with an internal standard (15.2 mg, 0.0519 mmol) and put in a J. Young tube. The tube was evacuated and refilled with vinyl fluoride (5 psig) while the tube was kept at room temperature. The solution was mixed and a ^{1}H NMR spectrum confirmed that 2 equiv of vinyl fluoride were present in the reaction mixture. The

reaction was then heated at 80 °C for 1 hour, after which time NMR data were collected. The ^{31}P NMR spectrum showed 48% Ru carbide (**5.12**),[31] <1 % Ru(=CHF) complex (**5.6-F**), and 51% starting material (**5.6-OEt**). After heating overnight, the ^{31}P NMR spectrum showed < 1 % hydride (**5.13**),[2] 84% carbide (**5.14**), 10% Ru(=CHF) complex (**5.6-F**), and 5% of an unknown decomposition product at 27.7 ppm.

Starting from 5.6-F. Compound **5.6-F** (19.6 mg, 0.0245 mmol, 1 equiv), internal standard (17.8 mg, 0.0608 mmol) and ethyl vinyl ether (3.9 mg, 0.054 mmol, 2.2 equiv) were dissolved in 1 mL C_6D_6 and the solution was heated to 80 °C in a J. Young tube for 1 hour, after which time NMR data were collected. The ^{31}P NMR spectrum showed 92% Ru carbide (**5.12**), 4% Ru(=CHF) complex (**5.6-F**), and 4% Ru(=CHOEt) complex (**5.6-OEt**). Metathesis is in competition with decomposition of compound **5.6-F**. High temperatures are required because liberation of the tricyclohexylphosphine is slow.

Decomposition of Compound 5.6-OEt. Compound **5.6-OEt** (20.0 mg, 0.0245 mmol) was dissolved in 1 mL C_6D_6 along with an internal standard (15.2 mg, 0.0519 mmol) and the solution was transferred to a J. Young tube. The reaction mixture was heated at 80 °C until decomposition of compound **5.6-OEt** was seen. Formation of the corresponding hydride complex (**5.13**) was observed by ^{31}P NMR spectroscopy. After 28 h, 59% decomposition had occurred. After 48 h, 85% decomposition had occurred.

Metathesis Exchange between Fischer Carbene Complexes (Scheme 5.4)

Starting from 5.7-F. Compound **5.7-F** (10.0 mg, 0.0150 mmol) was dissolved in 1 mL C_6D_6 and ethyl vinyl ether was added (7.16 μL, 0.0748 mmol, 5.0 equiv). After 2 h at 23 °C, NMR spectroscopy showed almost complete conversion to compound **5.7-OEt** and liberation of vinyl fluoride.

Starting from 5.7-OEt. Compound **5.7-OEt** (29.0 mg, 0.0417 mmol) and 1-bromo-3,5-bis(trifluoromethyl)benzene (23.2 mg, 0.0792 mmol) were dissolved in 1 mL C_6D_6. The solution was added to a J. Young tube, frozen in liquid N_2 and vinyl fluoride gas was added while the J. Young tube was submerged in liq. N_2. The reaction mixture was then thawed. ^{1}H and ^{19}F NMR spectra were acquired. After 10 min, the ^{19}F NMR spectrum showed 2.95 mmol of vinyl fluoride in the reaction mixture and 22% conversion to the monofluoromethylidene complex (**5.7-F**) but the ^{1}H NMR spectrum showed 58% consumption of compound **5.7-OEt**, thus indicating that some decomposition is taking place along with metathesis. After 2 hours, 90% of compound **5.7-OEt** had been consumed and 38% of compound **5.7-F** was observed.

Alternative Synthesis of 5.7-OEt.[2] $Ru(CHPh)(H_2IMes)(py)_2Cl_2$ (15 mg, 0.021 mmol) was dissolved in 1 mL C_6D_6 and ethyl vinyl ether (8μL, 0.084 mmol, 4 equiv) was added. An immediate color change from green to orange was observed. The ^{1}H NMR spectrum showed 100% conversion to **5.7-OEt;** 1 equivalent of styrene was also observed. ^{1}H NMR (400 MHz, C_6D_6): δ = 14.0 (s, 1H, Ru=C*H*), 9.2 (s, broad, 4H, pyridine *ortho*), 6.8, 6.7, 6.3 (three overlapping peaks, broad s, pyridine *meta and para*, mesityl *meta*), 3.4-3.3 (overlapping signals, H_2IMes –C*H*$_2$C*H*$_2$-, Ru=CHOC*H*$_2$CH$_3$, and excess ethyl vinyl ether), 2.7 (s, 12H, mesityl *ortho*-C*H*$_3$), 1.9 (2 overlapping peaks, broad s, 6H total, mesityl *ortho*-C*H*$_3$), 0.54 (t, 3H, Ru=CHOCH$_2$C*H*$_3$).

Metathesis Exchange of Compound 5.9-F with Vinyl Acetate (Scheme 5.6). Vinyl acetate (7.0 mg, 0.081 mmol) and 1-bromo-3,5-bis(trifluoromethyl)benzene (3.4 mg, 0.012 mmol; integration standard) were dissolved in 1 mL CD_2Cl_2 and mixed with

compound **5.9-F** (9.7 mg, 0.0095 mmol) until all compounds dissolved. After 30 min, 75% conversion to product was observed by ^{1}H and ^{19}F NMR spectroscopies. After 3 h, 89% conversion to compound **5.10-Me** was observed and all starting material had been consumed. ^{1}H NMR (400 MHz, $CDCl_3$): major product: δ = 11.79 (s, 1H), 7.37 (s, 2H), 7.02 (s, 4H), 4.13 (s, 5H), 2.47 (s, overlapping), 2.46 (s, overlapping total 17H), 2.35 (s, 7H). Minor product [relative to major component]: δ = 12.66 (s, 0.11H)

Synthesis of $ReBr(CO)_5$.[32, 33] In 20 mL of dry CH_2Cl_2 was dissolved $Re_2(CO)_{10}$ (510 mg, 0.766 mmol, 1.00 equiv). The solution was placed in a round bottom flask with a septum and removed from the glove box. Liquid bromine (134.6 mg, 0.8426 mmol, 1.100 equiv) was added via syringe. The solution turned light orange. The solution was allowed to stir for 30 minutes at room temperature and then volatiles were removed. The white/orange solid was then dissolved in 25 mL of acetone and 50 mL of methanol was added. The solution was cooled to -10 C for two days, after which time a colorless crystalline solid was isolated by filtration and washed with 3 × 10 mL of cold methanol. $ReBr(CO)_5$ was isolated in 77% yield (477 mg, 1.17 mmol).

Synthesis of the Styryl Acetate.[11] Phenylacetylene (900 μL, 837 mg, 8.20 mmol, 1.00 equiv) and glacial acetic acid (600 μL, 10.5 mmol, 1.28 equiv) were dissolved in 4 mL of toluene. $ReBr(CO)_5$ (35.8 mg, 0.0881 mmol, 1.08 mol% loading) was added to the toluene solution and placed in a 10 mL bomb flask and heated to 110 °C with vigorous stirring for 16 hours. Volatiles were removed *via* rotatory evaporation. The remaining solution was run on a silica gel column (elusion with pentane followed by 10 to 1 pentane to diethyl ether). Byproducts included (*Z*)-1,4-diphenyl-but-1-en-3-yne

(*cis*-PhHCH=CHC≡CPh)[34], 1,3-diphenyl-but-3-en-1-yne (H_2C=C(Ph)(C≡CPh))[34], and (*E*)-1,4-diphenyl-but-1-en-3-yne (*trans*-PhHCH=CHC≡CPh) [34] (<60 mg). *E/Z* styryl acetate was isolated as a yellow oil (658.0 mg, 4.057 mmol, 49.5 % isolated yield). *E/Z* ratio was 0.5. Reaction could be scaled by a factor of 2.

Synthesis of the 1-Hexenyl Acetate.[11] In 8 mL of toluene, 1-hexyne (1.9 mL, 16 mmol, 1.0 equiv) and glacial acetic acid (1.4 mL, 24 mmol, 1.5 equiv) were dissolved. $ReBr(CO)_5$ (71.2 mg, 0.175 mmol, 1.10 mol% loading) was added to the toluene solution and placed in a 25 mL bomb flask and heated to 110 °C with stirring for 24 hours. Volatiles were removed *via* rotatory evaporation. The remaining solution was run on a silica gel column (elusion with pentane followed by 60 to 1 pentane to ethyl acetate). *E/Z* 1-hexenyl acetate was isolated as a yellow oil (1.38 g, 9.7 mmol, 59% isolated yield). *E/Z* ratio was unity.

General Procedure for Cross Metathesis (CM) Reactions

NMR studies (all liquid and solid reagents)

Alkenyl acetate (0.10 to 0.20 mmol) and 1-bromo-3,5-bis(trifluoromethyl)benzene or 1,3,5-trimethoxybenzene as an internal standard (0.02 to 0.05 mmol) were dissolved in 0.8 mL of C_6D_6 or acetone-d_6 and varying amounts of the electron-rich olefin were added (see Tables 5.6-5.10 for details). A solution of **5.3** (1-5 mol% catalyst loading) in 0.2 mL of C_6D_6 or acetone-d_6 was added and the reaction mixture was placed in an NMR tube. The NMR tube was either left at room temperature or heated to 45 °C. The reactions were monitored by ^{1}H NMR spectroscopy.

NMR studies with vinyl fluoride

Excess Vinyl Fluoride. Styryl acetate (24.3 mg, 0.153 mmol, 1 equiv) and an internal standard, 4-fluorotoluene (5.5 mg, 0.056 mmol, 2.8 equiv) were dissolved in 0.4 mL of benzene-d_6. The solution was placed in a J. Young NMR tube and frozen. A solution of Blechert/Hoveyda-Grubbs catalyst, **5.3**, (4.7 mg, 0.0085 mmol, 5.5 mol%) in 0.6 mL benzene-d_6 was added to the J. Young tube and frozen. The reaction mixture was removed from the glovebox and refrozen. The J. Young tube was then evacuated and refilled with vinyl fluoride while submerged in liquid N_2. This method afforded 2.6 mmol (17 equiv) of vinyl fluoride in the reaction mixture. The J. Young tube was thawed and allowed to sit at room temperature. No product formation was observed by ^1H or ^{19}F NMR spectroscopy although all Hoveyda's catalyst, **5.3**, was consumed through stoichiometric metathesis with vinyl fluoride to give the monofluoromethylidene dimer, **5.9-F**. Catalyst deactivation occurred after 2 hours. A very small amount of β-fluorostyrene was observed by GC-MS; however, the majority of styrene-containing material was styryl acetate.

Vinyl Fluoride: <1 equivalent. A bombflask containing 4 mL of toluene was frozen and evacuated. The bomb flask was repressurized with vinyl fluoride gas while submerged in liquid N_2. The bomb flask was brought into the glove box. Styryl acetate (27.3 mg, 0.168 mmol, 1 equiv) and 4-fluorotoluene (17.6 mg, 0.160 mmol, 1.05 equiv) was dissolved in 1.2 mL of the vinyl fluoride/toluene solution. Hoveyda's catalyst, **5.3**, (4.7 mg, 0.0075 mmol, 4.5 mol%) was added to the reaction mixture. The mixture was placed in an NMR tube, parafilmed and placed in an oil bath at 45 °C. The solution turned from green to yellow in less than 5 minutes. The vinyl fluoride/toluene solution

(0.5 mL) was separately placed in an NMR tube with an internal standard, 4-fluorotoluene (17.6 mg, 0.160 mmol) to determine the concentration of vinyl fluoride in the toluene solution. The concentration of vinyl fluoride in toluene was determined to be 0.117 M (for 1.2 mL: 0.140 mmol, 0.836 equiv). After 2 hours at 45 °C, ^{19}F NMR spectroscopy indicated the formation of both *E/Z*-β-fluorostyrene with an *E/Z* ratio close to unity. Percent conversion to the desired products was 27.1 % with respect to the initial concentration of styryl acetate; however, integration of the ^{19}F NMR spectrum indicated that there was only 0.0694 mmol of vinyl fluoride in the reaction mixture. The amount of β-fluorostyrene and vinyl fluoride totaled only 0.115 mmol, indicating loss of vinyl fluoride gas from the reaction mixture. After 4 hours, percent conversion to the desired products was 32.0 % with respect to the initial amount of styryl acetate and the amount of vinyl fluoride left was 0.572 mmol. Total amount of fluorine-containing compounds indicated 0.111 mmol in solution. After 19 h, percent conversion to the desired products was 37.5 % with respect to the initial amount of styryl acetate and total amount of fluorinated compounds added to 0.102 mmol. After 28 h, percent conversion to the desired products was 38.3 % with respect to the initial amount styryl acetate and 0.099 mmol of fluorinated compounds were observed. Over the reaction time, the amount of vinyl fluoride in the reaction mixture decreased more rapidly than expected for the amount consumed for product formation. Gaseous vinyl fluoride may have been lost slowly through the NMR tube and cap during the long reaction time. Percent conversion to products based on the amount of vinyl fluoride left was 64.9%.

Slow addition of vinyl fluoride. Styryl acetate (24.9 mg, 0.154 mmol, 1 equiv) was dissolved in 0.5 mL of benzene-d_6 along with 1-bromo-3,5-

bis(trifluoromethyl)benzene (14.2 mg, 0.0485 mmol, 0.315 equiv) as an internal standard. The solution was placed in a J. Young tube and frozen. A solution of Hoveyda's catalyst, **5.3** (4.8 mg, 0.0076 mmol, 4.9 mol%) was dissolved in 0.5 mL benzene-d_6 and added to the J. Young tube. The reaction mixture was frozen and removed from the glove box. The reaction mixture was refrozen in liquid N_2, evacuated and refilled with vinyl fluoride gas (at room temperature). The initial ^{19}F NMR spectrum indicated that 0.051 mmol of vinyl fluoride (0.331 equiv) was present in the reaction mixture. The reaction mixture was fully thawed and placed in an oil bath at 45 °C. After 2 hours, more vinyl fluoride was added (0.745 mmol, 4.8 equiv). After 4.5 hours at 45 °C, there was 25% conversion to desired *E/Z*-β-fluorostyrene. After 16 hours, percent conversion to desired products was 26%. All catalyst had been deactivated. More catalyst was added (4.86 mg, 0.00776 mmol, 5.03 mol%). The reaction mixture was heated to 45 °C for 7 hours, after which, percent conversion to desired products was 42%.

Vinyl chloride. Styryl acetate (24.9 mg, 0.154 mmol, 1 equiv) was dissolved in 0.5 mL of benzene-d_6 along with 1-bromo-3,5-bis(trifluoromethyl)benzene (14.2 mg, 0.0485 mmol, 0.315 equiv) as an internal standard. The solution was placed in a J. Young tube and frozen. A solution of Hoveyda's catalyst, **5.3** (4.8 mg, 0.0076 mmol, 4.9 mol%) was dissolved in 0.5 mL benzene-d_6 and added to the J. Young tube. The reaction mixture was frozen and removed from the glove box. The reaction mixture was refrozen in liquid N_2, evacuated and refilled with vinyl chloride gas (at room temperature). The reaction mixture was fully thawed and placed in an oil bath at 45 °C. The ^1H NMR spectrum indicated 0.433 mmol of vinyl chloride (2.81 equiv) in solution. After 4.5h, 15% conversion to desired products had occurred and the *E/Z* ratio of the styryl acetate

was 0.75. After 16.5 h, 16% conversion to desired products was observed and the *E/Z* ratio of styryl acetate was 0.77. At this point, another 5 mol % of **5.3** was added to the reaction mixture. After 7 additional hours at 45 °C, the NMR data indicated 21% conversion to desired products and the *E/Z* ratio of the styryl acetate was 0.89. After an additional 48h, 22% conversion to products had occurred and the *E/Z* ratio of styryl acetate was 1.0.

Table 5.6. FCM with Styryl Acetate in Benzene-d_6.

	Alkene	**mmol**	**Equiv**[a]	**Temp**	**[Ru]**[c]	**Product: %conversion**[d]	**E/Z Ratio**[e]	**time (h)**[f]
1		0.18	1.2	50 °C	5% [b]	42	n/a	16
2		0.155	0.53	45 °C	5%	73	6.5	1.5
3		0.193	~1	45 °C	5%	54	n/a	1.5
4		0.124	1	23 °C	5%	60	n/a	4.5
5		0.247	2	23 °C	5%	69	n/a	3
6		0.617	5	23 °C	5%	66	n/a	3
7		1.235	10	23 °C	5%	66	n/a	n/a
8		0.749	4.6	45 °C	5%	38	1.41	42
9		0.762	4.4	45 °C	5%	14	0.73	42
10	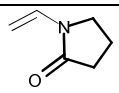	0.175	1.2	45 °C	5%	~10	3.4	43
11		0.150	1.0	45 °C	5%	0	-	48

[a] Equivalents of the electron-rich olefin with respect to initial amount of styryl acetate. [b] At 16 h, an additional 5% of **5.3** was added to the reaction mixture. No change in percent conversion was observed although *Z* to *E* isomerization continued to occur. [c] The mol% catalyst loading was always determined with respect to the amount of styryl acetate. [d]

Percent conversion to products was determined by NMR integration with respect to the internal standard and the initial amount of styryl acetate. [e] n/a = not available. [f] Reaction times generally represent the point at which the reaction reached completion, however, in some cases where low yields were observed, the reaction was run longer than necessary to be sure of completion.

Variable Ethyl Vinyl Ether Concentration and Addition of More Catalyst. A stock solution containing styryl acetate (284 mg, 1.75 mmol) and 1-bromo-3,5-bis(trifluoromethyl)benzene (104.0 mg, 0.3549 mmol) dissolved in 2.8 mL of C_6D_6 was used. For each reaction, 0.4 mL of the stock solution above was mixed with the appropriate amount of ethyl vinyl ether (see Table 5.7) diluted in 0.4 mL C_6D_6 and a standard ^{1}H NMR spectrum was taken. A stock solution of **5.3** (34.5 mg, 0.0551 mmol, 3.1 mol% cat. loading) was dissolved in 1.4 mL of C_6D_6 and 0.2 mL of that stock solution was added to the reaction mixture in an NMR tube and the mixture was shaken. A ^{1}H NMR spectrum was acquired at 1.5 hours and 19.5 hours. At 20 hours, a second stock solution of **5.3** (14.6 mg, 0.0232 mmol) in 0.8 mL of C_6D_6 was made and 0.2 mL of the solution (0.0059 mmol) was added to the reaction mixture. NMR data was collected at 22 hours and 25 hours. Table 5.7 gives percent conversion to products (*E/Z*-β-ethoxystyrene) and the *E/Z* ratios of both leftover starting material (*E/Z*-styryl acetate) and *E/Z* ratios of products at each time interval. The initial *E/Z* ratio of styryl acetate was 0.42.

Table 5.7. Varying the Concentration of Ethyl Vinyl Ether

	Equiv[a]	mmol[b]	1.5h[c]	19.5h	22h[d]	25h
1	**0.4 equiv**	**0.097**	**26%**	**29%**	**33%**	**35%**
		***E/Z* SM[e]**	*0.54*	*0.85*	*0.99*	*1.1*
		***E/Z* P[f]**	*0.96*	*1.44*	*1.50*	*1.8*
2	**1.3 equiv**	**0.35**	**41%**	**60%**	**61%**	**62%**
		***E/Z* SM**	*0.88*	*1.41*	*1.48*	*1.56*
		***E/Z* P**	*1.26*	*1.53*	*1.68*	*1.79*
3	**3 equiv**	**0.84**	**42%**	**72%**	**72%**	**74%**
		***E/Z* SM**	*0.96*	*2.04*	*2.05*	*2.9*
		***E/Z* P**	*1.27*	*1.46*	*1.70*	*1.62*
4	**6.3 equiv**	**1.6**	**45%**	**72%**	**76%**	**n/a**
		***E/Z* SM**	*0.81*	*1.71*	*2.34*	*n/a*
		***E/Z* P**	*1.60*	*1.60*	*1.67*	*n/a*

[a] The equivalents of ether vinyl ether used with respect to the initial amount of styryl acetate. [b] mmol of ethyl vinyl ether used [c] Percent conversions were based on internal standard with respect to initial amount of styryl acetate. [d] Additional catalyst added to reaction mixture 2 hours before data point. [e] *E/Z* ratio of styryl acetate. [f] *E/Z* ratio of β-ethoxystyrene.

Table 5.8. FCM with 1-Hexenyl Acetate in Benzene-d_6.

	Alkene	**mmol**	**Equiv**[a]	**Temp**	**[Ru]**[b]	**Product: % conversion**[d]	**E/Z Ratio**[e]	**time (h)**[f]
1		0.84	5.7	45 °C	5%	60	1.10	2
2		0.787	5.3	45 °C	5%	85	0.67	40
3	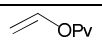	0.731	4.9	45 °C	5%	70	n/a	40
4		0.340	2.3	45 °C	5%	70	0.978	2
5		0.697	4.7	45 °C	5%	82	n/a	2
6		0.10	1.0	23 °C	5%	54	n/a	48[g]
7		0.10	1.0	23 °C	2.5%	58	n/a	48[g]
8		0.10	1.0	23 °C	1%	57	n/a	48[g]
9	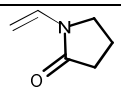	0.500	5.0	23 °C	5%	10[c]	n/a	48
10	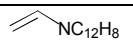	0.500	5.0	23 °C	5%	6[c]	n/a	48
11	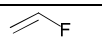	0.56	3.7	45 °C	5%	43	2.6	18
12	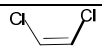	0.403	2.6	45 °C	5%	0	-	-

[a] Equivalents of the electron-rich olefin with respect to initial amount of 1-hexenyl acetate. [b] The mol% catalyst loading (**5.3**) was always determined with respect to the amount of 1-hexenyl acetate. [c] Reaction may not have reached the end point. Active catalyst was still present. [d] Percent conversion to products was determined by NMR integration with respect to the internal standard and the initial amount of 1-hexenyl acetate. [e] n/a = not available. [f] Reaction times generally represent the point at which the reaction reached completion, however, in some cases where low yields were observed, the reaction was run longer than necessary to be sure of completion. [g] run for 48 h to ensure that the end point was reached. 5% loading reached the end point at by 4h, 2.5% was at 56% conversion at 4h and 1% was at 50% conversion at 4h.

Table 5.9. FCM with 1-Hexenyl Acetate in Acetone-d_6.

	Alkene	**mmol**	**Equiv**[a]	**Temp**	**[Ru]**[b]	**Product: % conversion**[c]	**E/Z Ratio**[d]	**time (h)**[e]
1		0.10	1.0	23 °C	1%	30	1.0	24
2		0.10	1.0	23 °C	1%	52	n/a	22
3		0.20	2.0	23 °C	1%	49	n/a	24
4		0.50	5.0	23 °C	1%	6	n/a	24
5		0.10	1.0	23 °C	1%	54	n/a	24
6		0.10	1.0	23 °C	1%	61	0.9	24
7		0.20	2.0	23 °C	1%	>95	~1	48[f]
8		0.50	5.0	23 °C	1%	>95	1.1	4
9		1.0	10.0	23 °C	1%	>95	1.0	4
10		4.0	40.0	23 °C	1%	61	1	46
11	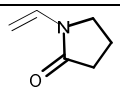	0.100	1.0	23 °C	1%	0	-	2
12		0.100	1	23 °C	1%	4	n/a	48

[a] Equivalents of the electron-rich olefin with respect to initial amount of 1-hexenyl acetate. [b] The mol% catalyst loading (**5.3**) was always determined with respect to the amount of 1-hexenyl acetate. [c] Percent conversion to products was determined by NMR integration with respect to the internal standard and the initial amount of 1-hexenyl acetate. [d] n/a = not available. [e] Reaction times generally represent the point at which the reaction reached completion, however, in some cases where low yields were observed, the reaction was run longer than necessary to be sure of completion. [f] Reaction had reached 68% completion at 30 min. The next NMR data point was taken at 48h.

Table 5.10. FCM with Styryl Acetate in Acetone-d_6.

	Alkene	**mmol**	**Equiv**[a]	**Temp**	**[Ru]**[b]	**Product: % conversion**[c]	**E/Z Ratio**[d]	**time (h)**[e]
1		0.10	1.0	23 °C	1%	7	n/a	44
2		0.10	1.0	23 °C	1%	22	n/a	44
3		0.10	1.0	23 °C	1%	49	n/a	22
4		0.50	5.0	23 °C	1%	50	n/a	44

[a] Equivalents of the electron-rich olefin with respect to initial amount of styryl acetate. [b] The mol% catalyst loading (**5.3**) was always determined with respect to the amount of styryl acetate. [c] Percent conversion to products was determined by NMR integration with respect to the internal standard and the initial amount of styryl acetate. [d] n/a = not available. [e] Reaction times generally represent the point at which the reaction reached completion, however, in some cases where low yields were observed, the reaction was run longer than necessary to be sure of completion.

5.7. References

1. Grubbs, R. H., *Handbook of Metathesis*. Wiley-VCH: Weinheim, 2003; Vol. 1-3.
2. Louie, J.; Grubbs, R. H., Metathesis of Electron-Rich Olefins: Structure and Reactivity of Electron-Rich Carbene Complexes. *Organometallics* 2002, *21*, 2153.
3. Crabtree, R. H., *The Organometallic Chemistry of the Transition Metals*. 3rd ed.; John Wiley & Sons, Inc.: New York, 2001; p 534.
4. Fomine, S.; Ortega, J. V.; Tlenkopatchev, M. A., Metathesis of halogenated olefins - A computational study of ruthenium alkylidene mediated reaction pathways. *Journal Of Molecular Catalysis A-Chemical* 2007, *263* (1-2), 121-127.
5. Diver, S. T.; Giessert, A. J., Enyne metathesis (Enyne Bond Reorganization). *Chemical Reviews* 2004, *104* (3), 1317-1382.
6. Macnaughtan, M. L.; Gary, J. B.; Gerlach, D. L.; Johnson, M. J. A.; Kampf, J. W., Cross-Metathesis of Vinyl Halides. Scope and Limitations of Ruthenium-based Catalysts. *Organometallics* 2009, *ASAP*.
7. Hammond, G. S., A Correlation Of Reaction Rates. *J. Am. Chem. Soc.* 1955, *77* (2), 334-338.
8. Macnaughtan, M. L.; Johnson, M. J. A.; Kampf, J. W., Synthesis, Structure, and Olefin Metathesis Activity of Two Ruthenium Monofluoromethylidene Complexes. *Organometallics* 2007, *26* (4), 780-782.
9. Caskey, S. R.; Stewart, M. H.; Kivela, J. E.; Sootsman, J. R.; Johnson, M. J. A.; Kampf, J. W., Two Generalizable Routes to Terminal Carbido Complexes. *J. Am. Chem. Soc.* 2005, *127*, 16750-16751.
10. Caskey, S. R. Exploration of Ruthenium Carbon Multiple Bond Complexes: Carbenes, Carbynes, and Carbides. Ph.D., University of Michigan, Ann Arbor, 2007.
11. Hua, R. M.; Tian, X., Re(CO)(5)Br-catalyzed addition of carboxylic acids to terminal alkynes: A high anti-Markovnikov and recoverable homogeneous catalyst. *J. Org. Chem.* 2004, *69* (17), 5782-5784.
12. Petasis, N. A.; Yudin, A. K.; Zavialov, I. A.; Prakash, G. K. S.; Olah, G. A., Facile preparation of fluorine-containing alkenes, amides and alcohols via the electrophilic fluorination of alkenyl boronic acids and trifluoroborates. *Synlett* 1997, (5), 606-&.
13. Datta, G. K.; von Schenck, H.; Hallberg, A.; Larhed, M., Selective terminal heck arylation of vinyl ethers with aryl chlorides: A combined experimental-computational approach including synthesis of betaxolol. *J. Org. Chem.* 2006, *71* (10), 3896-3903.
14. Lee, J. Y.; Lee, P. H., Palladium-catalyzed carbon-sulfur cross-coupling reactions with indium tri(organothiolate) and its application to sequential one-pot processes. *J. Org. Chem.* 2008, *73* (18), 7413-7416.
15. Mitsudo, T.; Hori, Y.; Yamakawa, Y.; Watanabe, Y., Ruthenium Complex Catalyzed Selective Addition of Carboxylic-acids to Acetylenes Giving Enol Esters. *Tetrahedron Lett.* 1986, *27* (19), 2125-2126.
16. Mitsudo, T.; Hori, Y.; Yamakawa, Y.; Watanabe, Y., Ruthenium Catalyzed Selective Synthesis of Enol Carbamates by Fixation of Carbon-dioxide. *Tetrahedron Lett.* 1987, *28* (38), 4417-4418.

17. Mitsudo, T.; Hori, Y.; Yamakawa, Y.; Watanabe, Y., Ruthenium-catalyzed Selective Addition of Carboxylic-acids to Alkynes - A Novel Synthesis of Enol Esters. *J. Org. Chem.* 1987, *52* (11), 2230-2239.
18. Ochiai, M.; Hirobe, M.; Miyamoto, K., Silver technology for stabilization of simple (Z)-enethiols: Stereoselective synthesis and reaction of silver (Z)-enethiolates. *J. Am. Chem. Soc.* 2006, *128* (28), 9046-9047.
19. Russell, G. A.; Ngoviwatchai, P.; Tashtoush, H. I.; Pladalmau, A.; Khanna, R. K., Reactions of Alkylmercurials with Heteroatom-centered Acceptor Radicals. *J. Am. Chem. Soc.* 1988, *110* (11), 3530-3538.
20. Subramanyam, V.; Silver, E. H.; Soloway, A. H., Reaction of Phosphoranes with Formate Esters = New Method for Synthesis of Vinyl Ethers. *J. Org. Chem.* 1976, *41* (7), 1272-1273.
21. Yatsumonji, Y.; Okada, O.; Tsubouchi, A.; Takeda, T., Stereo-recognizing transformation of (E)-alkenyl halides into sulfides catalyzed by nickel(0) triethyl phosphite complex. *Tetrahedron* 2006, *62* (42), 9981-9987.
22. Ye, S. M.; Leong, W. K., Regio- and stereoselective addition of carboxylic acids to phenylacetylene catalyzed by cyclopentadienyl ruthenium complexes. *J. Organomet. Chem.* 2006, *691* (6), 1117-1120.
23. Miller, R. B.; McGarvey, G., Highly Stereoselective Synthesis of Vinyl Bromides and Vinyl Chlorides via Disubstituted Vinylsilanes. *J. Org. Chem.* 1978, *43* (23), 4424-4431.
24. On, H. P.; Lewis, W.; Zweifel, G., Stereoselective Syntheses of (E)-1-halo-1-alkenes and (Z)-1-halo-1-alkenes from 1-alkynylsilanes. *Synthesis* 1981, (12), 999-1001.
25. Zweifel, G.; Lewis, W.; On, H. P., Alpha-chloroalkenylalanates - Their Preparation and Conversion into (E)-1-chloro-1-alkenes and Mixed 1,1-dihalo-1-alkenes. *J. Am. Chem. Soc.* 1979, *101* (17), 5101-5102.
26. Grubbs, R. H., Olefin-metathesis catalysts for the preparation of molecules and materials (Nobel lecture). *Angew. Chem.-Int. Edit.* 2006, *45* (23), 3760-3765.
27. Anderson, D. R.; Ung, T.; Mkrtumyan, G.; Bertrand, G.; Grubbs, R. H.; Schrodi, Y., Kinetic selectivity of olefin metathesis catalysts bearing cyclic (alkyl)(amino)carbenes. *Organometallics* 2008, *27* (4), 563-566.
28. Sanford, M. S.; Love, J. A.; Grubbs, R. H., Mechanism and activity of ruthenium olefin metathesis catalysts. *J. Am. Chem. Soc.* 2001, *123* (27), 6543-6554.
29. Sanford, M. S.; Ulman, M.; Grubbs, R. H., New insights into the mechanism of ruthenium-catalyzed olefin metathesis reactions. *J. Am. Chem. Soc.* 2001, *123* (4), 749-750.
30. Gottlieb, H. E.; Kotlyar, V.; Nudelman, A., NMR chemical shifts of common laboratory solvents as trace impurities. *J. Org. Chem.* 1997, *62* (21), 7512-7515.
31. Carlson, R. G.; Gile, M. A.; Heppert, J. A.; Mason, M. H.; Powell, D. R.; Vander Velde, D.; Vilain, J. M., The metathesis-facilitated synthesis of terminal ruthenium carbide complexes: A unique carbon atom transfer reaction. *J. Am. Chem. Soc.* 2002, *124* (8), 1580-1581.
32. Jolly, P. W.; Stone, F. G. A., Chemistry of Metal Carbonyls .30. Trans-bromotetracarbonyl(triphenylphosphine)rhenium. *Journal of the Chemical Society* 1965, (OCT), 5259.

33. Zingales, F.; Sartorel.U; Canziani, F.; Raveglia, M., Kinetic Studies of Group 7 Metal Carbonyls .I. Substitution Reactions of Tetracarbonyl Halide Dimers of Rhenium. *Inorg. Chem.* 1967, *6* (1), 154-&.
34. Lee, J.-H.; Caulton, K. G., Coupling of terminal alkynes by RuHXL2 (X = Cl or N(SiMe3)2, L = PiPr3). *J. Organomet. Chem.* 2008, *693* (8-9), 1664.

Chapter 6

Synthesis and Reactivity of Ruthenium Benzylidyne Complexes

6.1. Introduction

Alkyne metathesis (AM) has been restricted for the most part to W and Mo alkylidyne catalysts although some Re alkylidyne complexes will participate in alkyne metathesis.[1-4] Alkyne metathesis with a ruthenium alkylidyne catalyst is desirable because ruthenium is less oxophilic than tungsten and molybdenum. This would expand functional group tolerance and solvent choices for alkyne metathesis systems. A less oxophilic catalyst would also allow for easier handling techniques as the requirements for a water-free/air-free atmosphere would not need to be as rigorous.[5, 6] As discussed in Chapter 1, a number of Ru alkylidyne complexes are presented in the literature but none have displayed productive alkyne metathesis.[7-30] Steve Caskey in our group synthesized a number of four-, five-, and six-coordinate Ru-benzylidyne complexes from the common intermediate, **6.1-OAr`**, and also demonstrated a second method to access **6.1-Cl** through treatment of first-generation Grubbs catalyst with an alkyl germylene (Chart 6.1, Scheme 6.1).[31, 32] The first evidence of alkyne metatehsis was shown with these 1st generation Ru benzylidyne complexes. Cyclooctyne polymerization could be effected with **6.3-I** (Chart 6.1) when activated with thallium(I)trifluoromethanesulfonate. Beyond this, no alkyne metathesis activity was observed, although other types of reactivity with alkynes was noted such as

alkyne ligation with the square-planar complexes, **6.1**, and alkyne isomerization with **6.2-F/F**. [31] The goal of this chapter is to develop a library of accessible Ru-benzylidyne complexes and to test ligand substitution at the Ru-center to develop a better understanding of what types of Ru-benzylidyne complexes can be synthesized. Future work on this project will involve screening Ru-benzylidyne complexes for alkyne metathesis. Based on successful Mo- and W-based alkynidyne catalysts,[1-4] we predict that a stable $Ru(CR)X_3$ complex where X is a bulky, anionic ligand will be the best candidate for the catalysis of alkyne metathesis. Unfortunately, a Ru alkylidyne complex of this type has not been isolated.

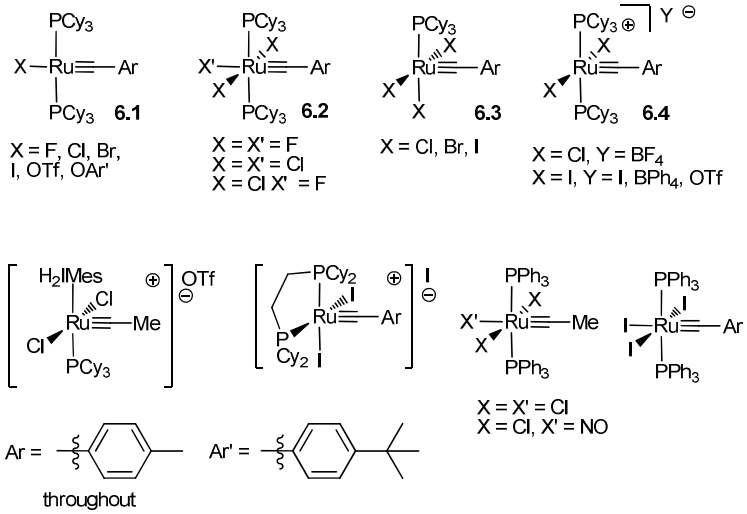

Chart 6.1. Previously Synthesized Ru-Benzylidyne Complexes in the Johnson Group

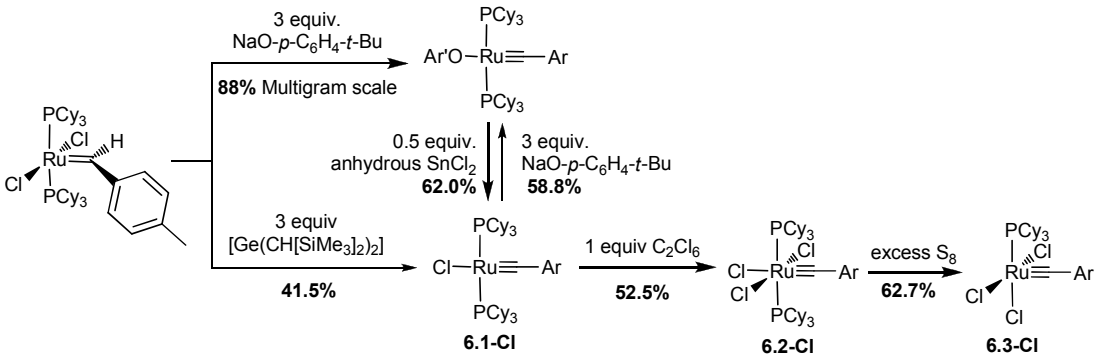

Scheme 6.1. Synthetic Pathway to [Ru(C-*p*-C_6H_4Me)(PCy_3)Cl_3] (**6.3-Cl**).

Synthetic procedures to make the 5-coordinate benzylidyne complexes in Figure 6.1 are multistep. The overall yield for **6.3-Cl** was 18%.[31] A more facile and higher yielding route to these 5-coordinate benzylidyne complexes was desired since these compounds have displayed ring-opening alkyne polymerization. Observations of carbon-halogen bond cleavage at the RuCHX moiety on the monohalomethylidene complexes discussed in Chapter 2 led to research into the synthesis and reactivity of RuCArX complexes.[33, 34] The propensity of the carbon-halogen bond on the Ru-carbene moiety to cleave allows for direct access to new Ru-benzylidyne species. This route also allows for the synthesis of Ru benzylidyne complexes with an *N*-heterocyclic carbene (NHC) ligand which could prove beneficial to alkyne metathesis in the same manner as olefin metathesis (see Chapter 1).

6.2. Synthesis of Ruthenium Benzylidyne Complexes

Metathesis of 2nd generation Grubbs catalyst, **6.6**, with α-chloro-*p*-methylstyrene allowed for the facile synthesis of a 5-coordinate benzylidyne complex, **6.8-Cl**, in 30%

yield (Chart 6.2). Further exploration led to the metathesis of 2nd generation Blechert/Hoveyda-Grubbs catalyst, **6.7**, with 5-decene and excess α-chloro-*p*-methylstyrene to yield **6.8-Cl** in >90% (Scheme 6.2; Chart 6.2). Treatment of **6.8-Cl** with excess iodotrimethylsilane (TMSI) forms the 5-coordinate triiodo-Ru-benzylidyne complex, **6.8-I** (Scheme 6.3).

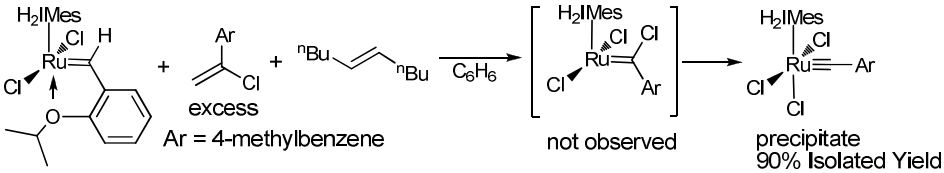

Scheme 6.2. Synthesis of [Ru(C-*p*-C_6H_4Me)(H_2IMes)Cl_3] (**6.8-Cl**).

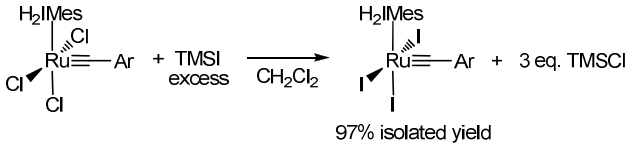

Scheme 6.3. Conversion to [Ru(C-*p*-C_6H_4Me)(H_2IMes)I_3] (**6.8-I**).

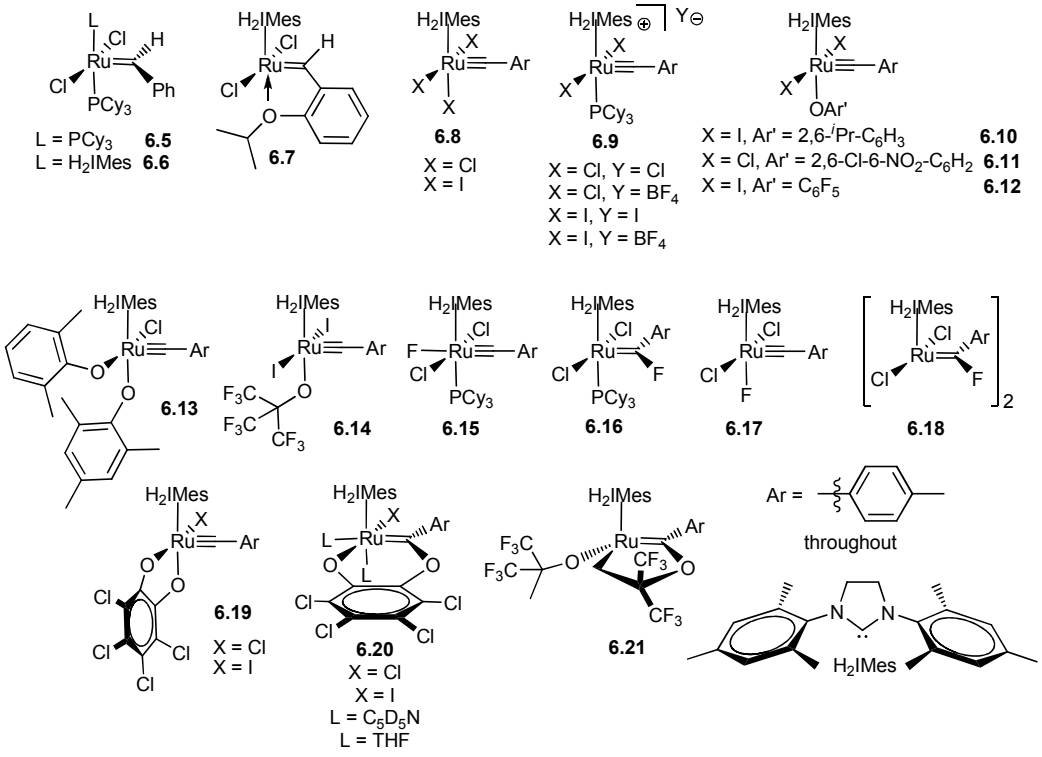

Chart 6.2. Numbered Complexes throughout Chapter 6.

Pink needles of **6.8-Cl** were grown from vapor diffusion of pentane into a saturated methylene chloride solution at −35 °C. An ORTEP diagram is shown in Figure 6.1, selected crystallographic data are presented in Table 6.1, and selected bond distances and angles are presented in Table 6.2. Analysis reveals a distorted square-pyramidal arrangement with an apical *p*-methylbenzylidyne unit, two mutually *trans* chlorides, and an NHC ligand *trans* to the third chloride in the basal plane. The H_2IMes ligand is locked parallel to the Ru-benzylidyne unit. The *p*-methylbenzylidyne unit is slightly bent due to steric pressure of the mesityl group attached to the NHC ligand. The monoclinic unit cell contains one molecule of methylene chloride and one molecule of **6.8-Cl**.

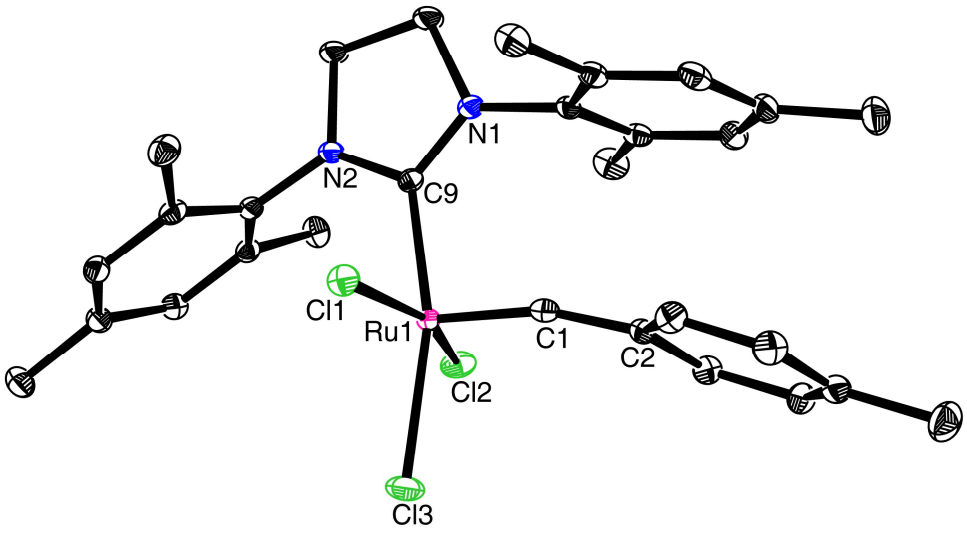

Figure 6.1. 50% thermal ellipsoid plot of [Ru(C-*p*-C_6H_4Me)(H_2IMes)Cl_3] (**6.8-Cl**). Selected crystallographic data are presented in Table 6.1 and selected bond distances and angles are presented in Table 6.2. Complete XRD data can be found in Appendix 5.

Dark red crystals of **6.8-I** were grown from vapor diffusion of pentane into a saturated chloroform solution at –35 °C. An ORTEP diagram is shown in Figure 6.2, selected crystallographic data are presented in Table 6.1, and selected bond distances and angles are presented in Table 6.2. Analysis reveals a distorted square-pyramidal arrangement with an apical *p*-methylbenzylidyne unit, two mutually *trans* iodides, and an NHC ligand *trans* to the third iodide in the basal plane. The triclinic unit cell contains one molecule of chloroform and one molecule of **6.8-I**.

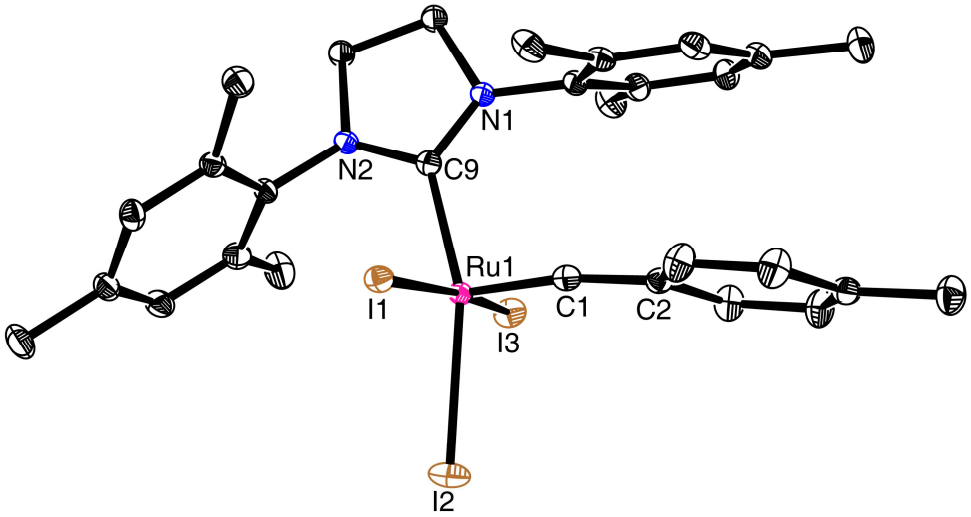

Figure 6.2. 50% thermal ellipsoid plot of [Ru(C-*p*-C_6H_4Me)(H_2IMes)I_3] (**6.8-I**). Selected crystallographic data are presented in Table 6.1 and selected bond distances and angles are presented in Table 6.2. Complete XRD data can be found in Appendix 6.

Table 6.1. Crystallographic Data for Complexes **6.8-Cl**, **6.8-I**, and **6.19-I**

	6.8-Cl	**6.8-I**	**6.19-I**
Formula	$C_{30}H_{35}Cl_5N_2Ru$	$C_{30}H_{34}Cl_3I_3N_2Ru$	$C_{39}H_{41}C_{l6}IN_2O_2Ru$
FW	701.92	1010.71	1010.41
Crystal System	Monoclinic	Triclinic	Triclinic
Space group	$P2_1/c$	P-1	P-1
A (Å)	8.2992(6)	8.6389(6)	8.9890(12)
B (Å)	22.0834(15)	12.9632(9)	12.2431(17)
C (Å)	17.2123(12)	16.5451(12)	19.494(3)
α (deg)	90	103.322(1)	86.304(2)
β (deg)	101.869(1)	103.899(1)	86.557(2)
γ(deg)	90	97.880(1)	81.653(2)
V ($Å^3$)	3087.1(4)	1713.5(2)	2115.5(5)
Z	4	2	2
Rad. (Ka, Å)	0.71073	0.71073	0.71073
T (K)	85(2)	85(2)	225(2)
D_{calcd} (Mg m^{-3})	1.510	1.959	1.586
ρ_{calcd} (mm^{-1})	0.963	3.416	1.514
F_{000}	1432	964	1008
R1	0.0317	0.0244	0.0324
wR2	0.0776	0.0643	0.0860
GOF	1.121	1.100	1.044

Table 6.2. Selected Bond Lengths and Angles for Complexes **6.8-Cl**, **6.8-I**, and **6.19-I**

	6.8-Cl	**6.8-I**	**6.19-I**
Bond Distances (Å):			
Ru-C(1)	1.669(2)	1.664(3)	1.681(2)
Ru-C(H_2IMes)	2.0543(19)	2.067(3)	2.045(2)
Ru-X (*cis* to H_2Imes)	Cl(1): 2.3319(5)	I(1): 2.6941(3)	2.6610(4); X = I(1)
Ru-X (*cis* to H_2Imes)	Cl(2): 3.3282(5)	I(3): 2.6702(3)	1.9854(14); X = O(2)
Ru-X (*trans* to H_2Imes)	Cl(3): 2.3764(5)	I(2): 2.6802(3)	2.0249(14); X = O(1)
N(1)-C(H_2IMes)	1.333(2)	1.336(3)	1.341(3)
N(2)-C(H_2IMes)	1.341(2)	1.333(4)	1.340(3)
Bond Angles (deg):			
Ru-C(1)-C(2)	164.21(16)	170.3(2)	163.75(18)
C(1)-Ru-C(H_2IMes)	97.83(8)	100.08(12)	98.14(9)
C(1)-Ru-X *cis*	Cl(1): 99.93(7)	I(1): 94.40(9)	92.01(7); X = I(1)
C(1)-Ru-X *cis*	Cl(2): 97.76(7)	I(3): 93.86(9)	111.83(9); X = O(2)
C(1)-Ru-X *trans*	97.25(7)	99.76(10)	104.41; X = O(1)
X-Ru-X *cis*	Cl(1): 87.444(19)	I(1): 89.529(10)	81.70(6); X = O(1), O(2)
X-Ru-X *cis*	Cl(2): 88.00(2)	I(3): 87.823(10)	87.18(4); X = O(1), I(1)
X-Ru-X *trans*	162.15(2)	171.642(11)	155.52(5); X = O(2), I(1)
C(H_2IMes)-Ru-X *cis*	Cl(1): 89.28(5)	I(1): 93.75(7)	98.14(6); X = I(1)
C(H_2IMes)-Ru-X *cis*	Cl(2): 90.66(5)	I(3): 86.04(7)	84.39(7); X = O(2)
C(H_2IMes)-Ru-X *trans*	164.90(6)	159.58(8)	156.65(7); X = O(1)
N(1)-C(H_2IMes)-N(2)	108.98(16)	109.2(2)	108.50(18)

6.3. Ligand Substitutions

6.3.1. Neutral Ligands

Steve Caskey found that addition of tricyclohexylphosphine to the 1st generation Ru benzylidyne complex, **6.3-Cl**, yields a new six-coordinate Ru-benzylidyne complex (Scheme 6.4, **6.2-Cl/PCy$_3$**).[31, 32] Treatment of **6.2-Cl/PCy$_3$** with trityl tetrafluoroborate leads to a cationic five-coordinate compound (**6.4-Cl**). Addition of tricyclohexylphosphine to **6.3-I** gave an equilibrium between the starting material, **6.3-I** and a new cationic five-coordinate benzylidyne compound, **6.4-I/I** (Scheme 6.5). Further treatment of the reaction mixture with sodium tetraphenylborate allowed for isolation of the cationic five-coordinate benzylidyne compound (**6.4-I/BPh$_4$**). The analogous reactions with 2nd generation Ru benzylidyne complexes lead to slightly different results because of the different steric bulk distribution of the NHC ligand compared with tricyclohexylphosphine. Treatment of [Ru(CAr)(H_2IMes)Cl_3], **6.8-Cl,** with tricyclohexylphosphine yielded a new phosphine-containing Ru species within 10 minutes in methylene chloride. Unlike the 6-coordinate **6.2-Cl/PCy$_3$** which has a ^{31}P NMR resonance shift of δ 18.2 ppm, the ^{31}P NMR shift for the new 2nd generation phosphine-containing Ru benzylidyne complex was δ 39.7 ppm, indicating a 5-coordinate Ru-benzylidyne species (**6.9-Cl/Cl)**. The ^{31}P NMR shift for **6.4-Cl/BF$_4$** is δ 49.9 ppm for comparison. Treatment of **6.9-Cl/Cl** with $LiBF_4$ produced identical ^{1}H and ^{31}P NMR spectra; however, the presence of tetrafluoroborate was observed in the ^{19}F NMR spectrum after isolation and purification indicated that **6.9-Cl/BF$_4$** had formed (Scheme

6.4). The crystal structure for **6.8-Cl** (Figure 6.1) indicates that the mesityl group on the NHC ligand sterically blocks the coordination site *trans* to the carbyne ligand explaining the outer-sphere coordination of one of the chloride ligand in **6.9-Cl/Cl**.

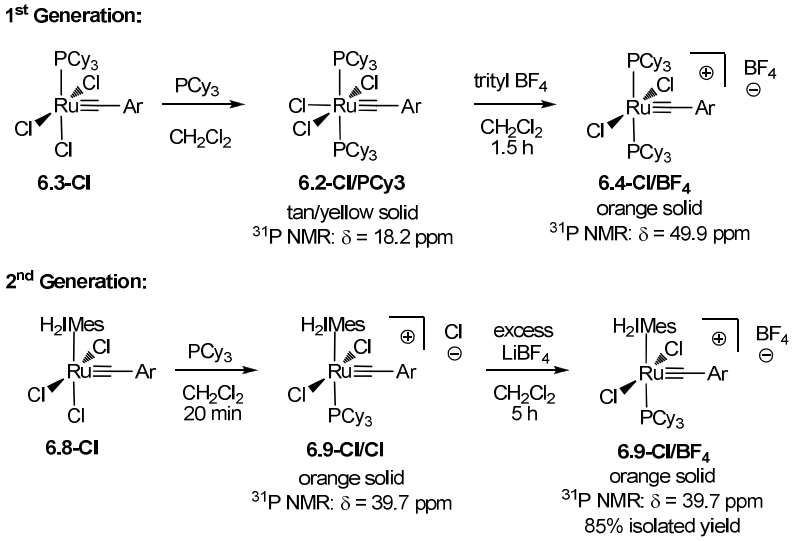

Scheme 6.4. Addition of PCy_3 to Chlorinated Benzylidyne Complexes

Treatment of **6.8-I** with tricyclohexylphosphine formed the five-coordinate cationic Ru benzylidyne complex, **6.9-I/I**, quantitatively. Unlike the corresponding reaction with the 1st generation Ru-benzylidyne compound (**6.4-I/I**), no equilibrium between the starting material, **6.8-I,** and product, **6.9-I/I** is observed (Scheme 6.5). The phenomenon of lower lability of the tricyclohexylphosphine ligand is similarly observed upon moving from 1st generation Grubbs catalyst, **6.5** to 2nd generation Grubbs catalyst, **6.6**.[35-37]

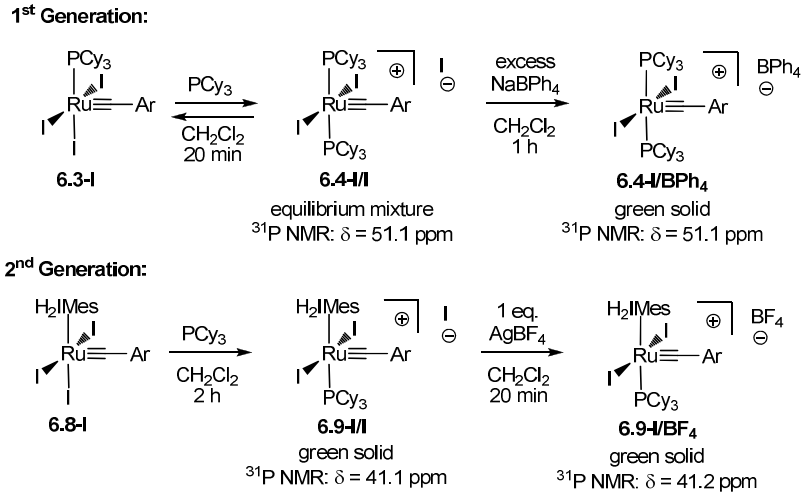

Scheme 6.5. Addition of PCy_3 to Iodo-Benzylidyne Complexes

6.3.2. Aryloxide and Alkoxide Ligands

Previous attempts to exchange aryloxide and alkoxide ligands for halides on the 1st generation 5- and 6-coordinate benzylidyne complexes were unsuccessful.[31] Aryloxide substitutions on 2nd generation 5-coordinate benzylidyne complexes, **6.8**, are more promising. A number of aryloxide salts were tested for substitution at the ruthenium center of complexes **6.8-Cl/I**. Most aryloxide salts tested gave at least one substitution *trans* to the H_2IMes ligand (C_s symmetry was retained) and in some cases, two substitutions forming a chiral ruthenium center with C_1 symmetry were observed (Scheme 6.6). Attempts to obtain trisubstitution at the Ru-center failed even when a large excess of aryloxide salts was used. A single equivalent of thallium(I)2,6-diisopropylphenoxide substituted cleanly onto **6.8-I** to give **6.10,** and a single equivalent of thallium(I)2,6-dichloro-4-nitrophenoxide substituted cleanly onto **6.8-Cl** to give **6.11** (Chart 6.2). Addition of excess thallium aryloxides to these reaction mixtures did not

yield further substitution even over extended periods of time (>72 h). Decomposition of the monosubstituted complexes, **6.10** and **6.11**, occurred instead. In the case of sodium perfluorophenoxide, only 66% substitution to **6.12** was observed along with 34% of the starting material. This was independent of the amount of sodium perfluorophenoxide used. Longer reaction times and higher temperatures caused **6.12** to decompose before further substitution was observed. Addition of bisthallium(I)tetrachlorocatecholate to **6.8-X** produced **6.19-X** cleanly (X = Cl or I). This reaction will be further discussed in section 6.4.1.1. Attempts to exchange the halide ligands for other types of catecholate salts were unsuccessful. Two substitutions at the Ru-center of **6.8-Cl** occurred with thallium(I)2,4,6-trimethylphenoxide to yield the disubstituted compound **6.13**. Steric bulk of the methyl groups on 2,4,6-trimethylphenoxide was not large enough to prevent disubstitution; however, upon moving to 2,6-diisopropylphenoxide, steric bulk appears to prevent disubstitution. Attempts at substitution reactions with thallium(I)4-methyl-2,6-tert-butylphenoxide failed because the steric bulk of the *t*-butyl groups prevented the oxide from binding at the Ru-center. It is unclear as to why thallium(I)2,6-dichloro-4-nitrophenoxide will only substitute once at the ruthenium center although insolubility of thallium(I)2,6-dichloro-4-nitrophenoxide in methylene chloride may play a role. Reactions with thallium(I)4-nitrophenoxide and sodium 4-methylbenzenethiolate afforded multiple products on an NMR scale and were not further pursued.

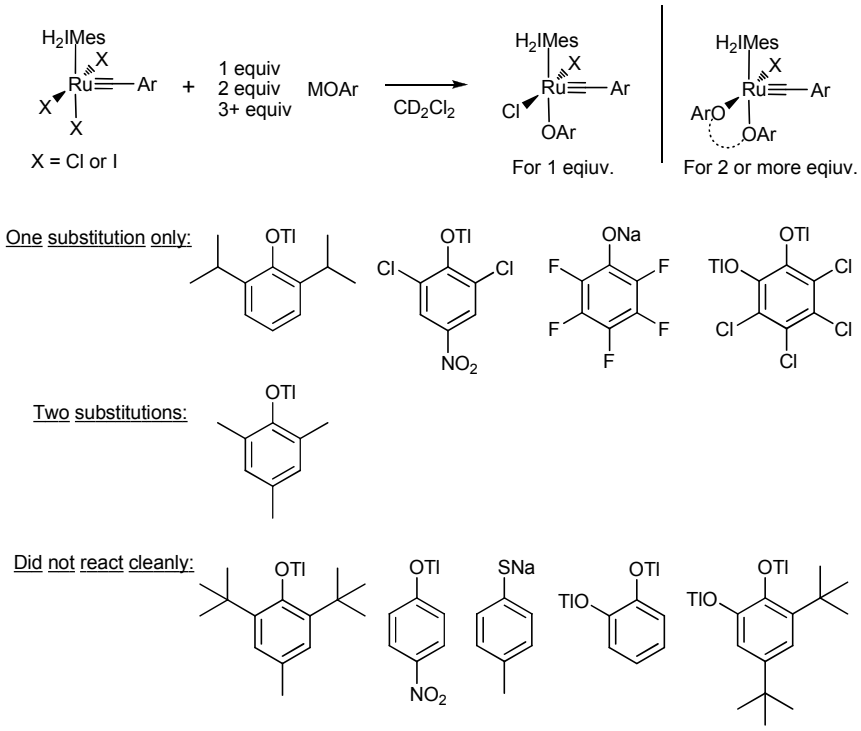

Scheme 6.6. Substitutions of Aryloxide Ligands

Compound **6.10** was isolated. The ^{1}H NMR data of **6.10** indicated that the 2,6-diisopropylphenoxide group was *trans* to the H_2IMes ligand based on the symmetry of the mesityl protons of the H_2IMes ligand. The phenoxide was locked on an NMR timescale so that the isopropyl groups in the 2 and 6 positions were chemically inequivalent with respect to each other. Each isopropyl group was bisected by the mirror plane of the molecule so that the methyl groups within an isopropyl group were chemically equivalent. The *meta*-protons on the phenyl ring were also chemically inequivalent. Based on this analysis, compound 6.10 is locked as the structure shown in Figure 6.3. It appears that the steric pressure of the isopropyl groups and iodide holds **6.10** in this conformation.

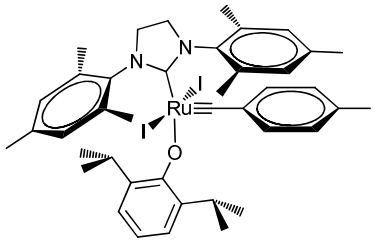

Figure 6.3. Conformation of **6.10**; Locked on an NMR Timescale.

Salt metathesis of **6.8-X** and a number of alkoxide salts was attempted. The majority of alkoxide salts tested lead to formation of multiple products or decomposition of the Ru compounds formed. Nonafluoro-*t*-butoxide underwent a single substitution *trans* to the H_2IMes ligand to form **6.14** respectively from **6.8-I**. Compound **6.14** was isolated from the reactions of complex **6.8-I;** however, a few impurities could not be removed. In order to isolate **6.14**, 1.1 equiv of **6.8-I** is treated with 1 equiv of the thallium(I)alkoxide salt because the solubility of the thallium(I)alkoxide is similar to the product, **6.14** but **6.8-I** is relatively insoluble compared to **6.14**. Proton NMR data indicated that the perfluorobutoxide ligand was bound *trans* to the H_2IMes ligand based on the mirror-plane symmetry of mesityl protons. For further discussion on alkoxide substitutions, see section 6.4.2.

6.4. Ligand Migration

6.4.1. Reversible

6.4.1.1. Tetrachlorocatecholate

The reaction of either **6.8-Cl** or **6.8-I** with bisthallium(I)tetrachlorocatecholate lead to a new chiral Ru-benzylidyne product (**6.19-X**; point group = C_1). Tetrachlorocatecholate substitutes η^2 at the ruthenium center, forming a new dark red compound (Scheme 6.7). Lower symmetry and a locked Ru-H_2IMes bond is confirmed by the distinction of all six mesityl methyl groups and four mesityl aryl protons in the ^{1}H NMR spectrum. The crystal structure of **6.19-I** confirmed the η^2-binding mode of tetrachlorocatecholate to the Ru-center (Figure 6.3). Addition of thallium(I)tetrachlorocatecholate to a solution of **6.8-Cl** in a ligating solvent such as tetrahydrofuran (THF) affords a new dark green product (Scheme 6.8). ^{1}H NMR spectroscopy reveals broadened H_2IMes protons which are no longer distinct, indicating slow rotation of the H_2IMes unit on an NMR timescale. ^{13}C NMR data for the dark green compound revealed an α-carbon shift of δ 278 ppm which is indicative of a ruthenium carbene complex (**6.20-Cl/THF**). Addition of pyridine-d_5 to **6.19-Cl** yielded a similar color change to green and peak broadening in the ^{1}H NMR spectrum (Scheme 6.9). The crystal structure of **6.20-Cl/C_5D_5N** confirmed that the binding mode of the tetrachlorocatecholate had changed from η^2-Ru to η^1-Ru/η^1-α-carbon (Figure 6.4). Treatment of **6.19-Cl** with THF yields **6.20-Cl/THF**. The coordinated THF ligands can be removed by dissolving **6.20-Cl/THF** in benzene and then concentrating the solution *in vacuo*. As **6.19-Cl** reforms, it precipitates from the benzene solution.

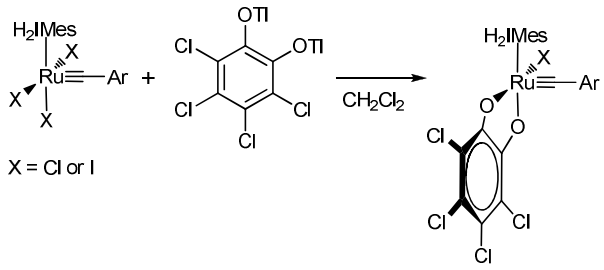

Scheme 6.7. Synthesis of **6.19-X**

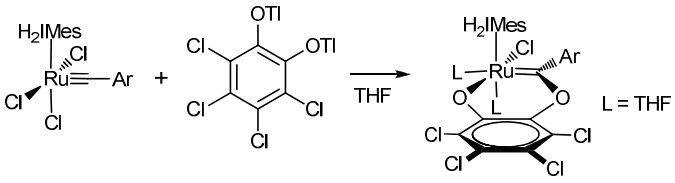

Scheme 6.8. Synthesis of **6.20-Cl/THF** in THF

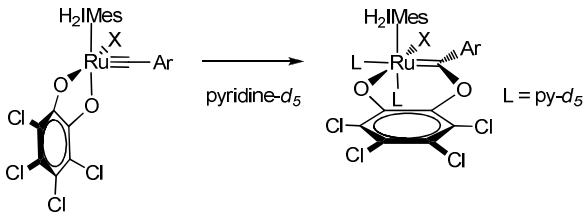

Scheme 6.9. Synthesis of **6.20-X/C_5D_5N**

Red x-ray quality crystals of **6.19-I** were grown from a solution of hexanes and methylene chloride-d_2 (15 to 1) at –35 °C. After 48 h, red crystalline plates had formed.

After 96 h, a second morphology of dark red block-like crystals was observed. The plates contained half an equivalent of CD_2Cl_2 and one equivalent of hexanes to one equivalent of **6.19-I** while the block-like crystals contained one equivalent of CD_2Cl_2 and half an equivalent of hexane to one equivalent of **6.19-I**. An ORTEP diagram for the block-like crystals is shown in Figure 6.4, selected crystallographic data are presented in Table 6.1, and selected bond distances and angles are presented in Table 6.2. The analysis reveals a distorted square-pyramidal arrangement with an apical *p*-methylbenzylidyne unit. The basal plane contains a chloride *trans* to one of the two Ru-bound oxygens and the second oxygen *trans* to the H_2IMes ligand. The unit cell was triclinic.

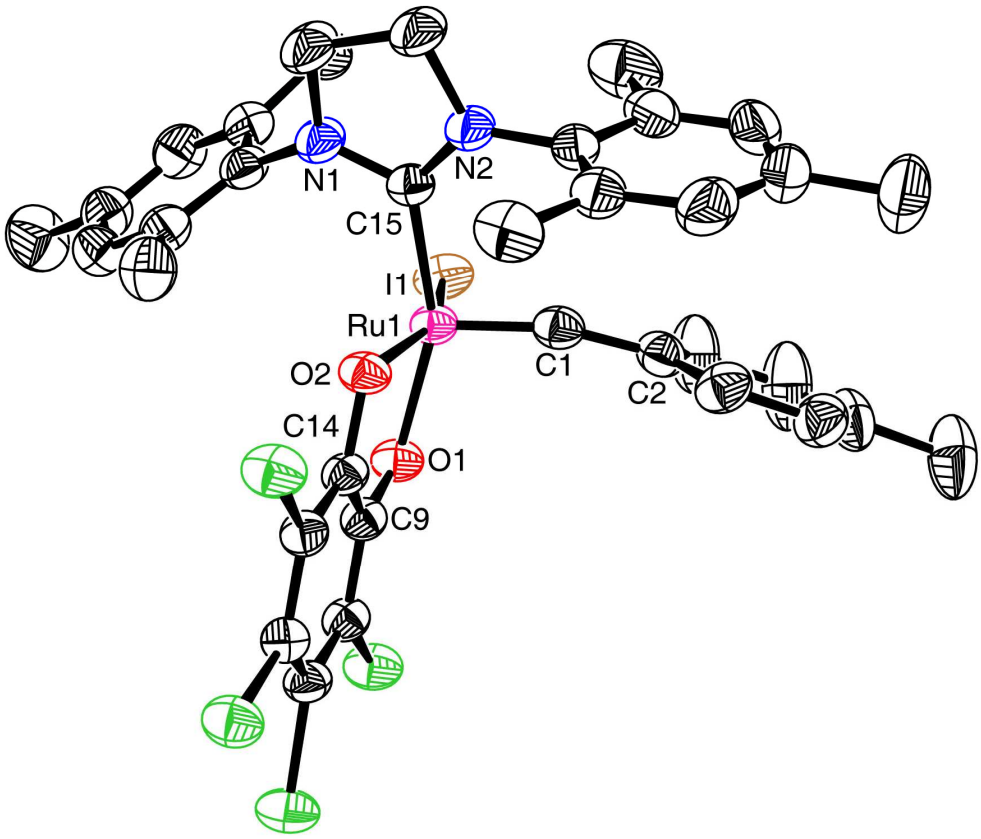

Figure 6.4. 50% thermal ellipsoid plot of [Ru(≡C-*p*-C_6H_4Me)(H_2IMes)($O_2C_6Cl_4$)I] (**6.19-I**). Selected crystallographic data are presented in Table 6.1 and selected bond distances and angles are presented in Table 6.2. Complete XRD data can be found in Appendix 7.

Green x-ray quality crystals of **6.20-Cl/C_5D_5N** were grown from a solution of hexane, methylene chloride, and pyridine (2000:200:1) at –35 °C. An ORTEP diagram is shown in Figure 6.5, selected crystallographic data are presented in Table 6.3, and selected bond distances and angles are presented in Table 6.4. The analysis reveals an octahedral arrangement with a ruthenadioxine consisting of Ru, the α-carbon, and the tetrachlorocatecholate of which, one oxygen is bound to the Ru and the other oxygen is bound through the α-carbon forming a *p*-methylbenzylidene unit. A pyridine-d_5 is bound *trans* to the H_2IMes ligand, the second pyridine-d_5 is bound *trans* to the *p*-methylbenzylidene unit, and the chloride is bound *trans* to the Ru-bound tetrachlorocatecholate oxygen. The monoclinic unit cell contains four molecules of methylene chloride, two molecules of hexane and four molecules of **6.20-Cl/C_5D_5N**.

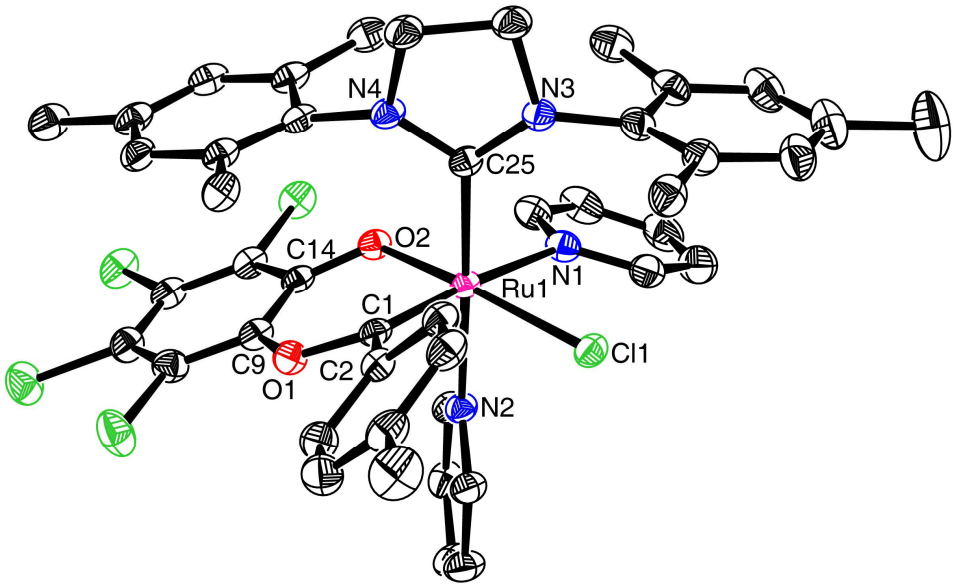

Figure 6.5. 50% thermal ellipsoid plot of [Ru(=C(OC_6Cl_4O)(*p*-C_6H_4Me))(H_2IMes)(C_5D_5N)$_2$Cl] (**6.20-Cl/C_5D_5N**). Selected crystallographic data are presented in Table 6.3 and selected bond distances and angles are presented in Table 6.4. Complete XRD data can be found in Appendix 8.

Table 6.3. Crystallographic Data for Complexes **6.20-Cl/C_5D_5N** and **6.22**

	6.20-Cl/C_5D_5N	**6.22**
Formula	$C_{49}H_{52}Cl_7N_4O_2Ru$	$C_{39.5}H_{44}F_{12}N_2O_2Ru$
FW	1078.17	907.84
Crystal System	Monoclinic	Monoclinic
Space group	P2(1)/c	P2(1)/c
A (Å)	10.6967(8)	12.6365(10)
B (Å)	25.3195(18)	17.5776(14)
C (Å)	19.9332(14)	18.7633(15)
α (deg)	90	90
β (deg)	104.088(1)	108.816(1)
γ(deg)	90	90
V ($Å^3$)	5236.2(7)	3941.8(5)
Z	4	4
Rad. (Ka, Å)	0.71073	0.71073
T (K)	85(2)	85(2)
D_{calcd} ($Mg\ m^{-3}$)	1.368	1.530
ρ_{calcd} (mm^{-1})	0.697	0.492
F_{000}	2212	1852
R1	0.0478	0.0428
wR2	0.1300	0.1107
GOF	1.093	1.072

Table 6.4. Selected Bond Lengths and Angles for Complexes **6.20-Cl/C_5D_5N** and **6.22**

	6.20-Cl/C_5D_5N	**6.22**
Bond Distances (Å):		
Ru-C(1)	1.876(3)	1.820(3)
Ru-C(H_2IMes)	2.068(3)	1.990(3)
Ru-X (*cis* to H_2Imes)	2.3981(7) X = Cl(1)	2.045(3), X = C(10)
Ru-O(2)	2.051(2)	1.986(2)
Ru-N(1)	2.288(3)	-
Ru-N(2)	2.176(2)	-
N(X)-C(H_2IMes)	1.366(4) ; X = 3	1.351(4); X = 1
N(Y)-C(H_2IMes)	1.367(4) ; Y = 4	1.364(3); Y = 2
C(1)-O(1)	1.371(4)	1.392(3)
O(1)-C(9)	1.370(3)	1.424(3)
C(9)-C(X)	1.419(4); X = 14	1.538(4); X = 10
C(14)-O(2)	1.294(4)	-
Bond Angles (deg):		
Ru-C(1)-C(2)	131.0(2)	128.6(2)
C(1)-Ru-C(H_2IMes)	90.37(12)	96.40(12)
O(1)-C(1)-C(2)	104.7(2)	108.2(2)
C(1)-Ru-X *cis*	93.02(9); X = Cl(1)	82.10(12), X = C(10)
C(H_2IMes)-Ru-X *cis*	94.13(8); X = Cl(1)	92.6(12), X = C(10)
C(1)-Ru-X	93.00(11); X = O(2)	116.05(11), X = O(2)
C(H_2IMes)-Ru-X	94.87(10); X = O(2)	143.97(10), X = O(2)
C(10)-Ru-O(2)	-	106.34(11)
Ru-C(1)-O(1)	123.9(2)	122.6(2)
C(1)-O(1)-C(9)	125.6(2)	113.2(2)
O(1)-C(9)-C(X)	125.3(3); X = 14	111.6(2); X =10
C(9)-C(10)-Ru	-	109.56(19)
C(X)-O(2)-Ru	121.83(19); X = 14	146.1(2); X = 13

6.4.1.2. Fluoride

Attempts to replace one of the chloride ligands on **6.8-Cl** with a fluoride resulted in mixtures of products, **6.17** and **6.18** (Scheme 6.10). A mixture of 1 equiv. of TAS-F, $[S(NMe_2)_3][F_2SiMe_3]$, and **6.8-Cl** in methylidene chloride-d_2 displayed a ^{19}F NMR singlet peak shift for one major product at δ –272.0 ppm (**6.17**), and two minor products at δ +133.7 ppm and +119.6 ppm (dimeric isomers of **6.18**). Based on the ^{19}F NMR chemical shifts seen for the monofluoromethylidene complexes (Chapter 2), NMR data for fluorinated Ru-benzylidyne complexes,[31, 32] and the μ-chloro bridging of 14-electron Ru complexes, the minor products were assigned as Ru monofluorobenzylidene complexes (**6.18**). The major product was assigned as complex **6.17**. Attempts to isolate compound **6.17** lead to decomposition products that were intractable.

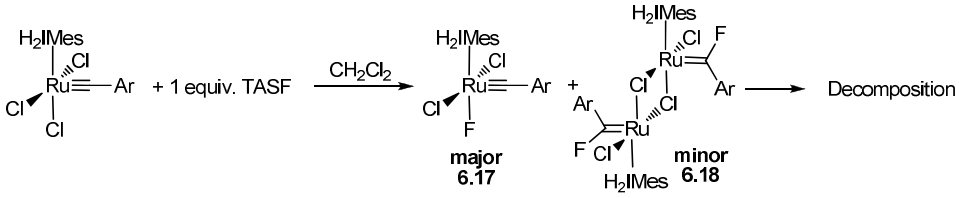

Scheme 6.10. Attempted Synthesis of **6.17**.

Running the above reaction in the presence of tricyclohexylphosphine gives two products cleanly in a 2.4 to 1 ratio. The ^{19}F NMR spectrum displays a doublet at δ –197.8 ppm ($^2J_{FP}$ = 53.4 Hz, 71%) and a singlet at δ +131.0 ppm (29%). NMR

assignments for **6.15** and **6.16** are given in Table 6.5 along with comparative NMR data of compounds **6.2-Cl/F** and **6.2-F/F** (Chart 6.1).[31, 32] Based on similar ^{19}F and ^{31}P NMR shifts, compound **6.15** was assigned as the 6-coordinated Ru-benzylidyne and compound **6.16** was assigned as the fluorobenzylidene complex shown in Scheme 6.11.

Table 6.5. NMR Data to Identify **6.16** and **6.15**

	6.15	**6.16**	**6.2-Cl/F**	**6.2-F/F**	**Ru(CHF)(H_2IMes)(PCy_3)Cl_2**
^{19}F NMR shifts	-197.8 (d, $^2J_{FP}$ = 53.4 Hz)	+131.0 (s)	-219.4	-191.0[a]	113.7
^{31}P NMR shifts	24.3 (d, $^2J_{FP}$ = 51.5 Hz)	24.3 (s)	28.5[b]	25.3	32.6

[a] ^{19}F NMR shift of the fluorine *trans* to PCy_3. [b] ^{31}P NMR shifts for 1st generation complexes tend to shift downfield with respect to the corresponding 2nd generation complex.[38-40]

When 2nd generation Grubbs catalyst (**6.6**) is treated with excess α-fluoro-*p*-methylstyrene, the same two products were observed in the ^{19}F NMR spectrum in the same ratio. The ability to synthesize the same mixture of **6.15** and **6.16** through two alternative methods indicates that these two compounds are in equilibrium. Both **6.15** and **6.16** are stable in solution over 2 weeks at room temperature (Scheme 6.11). Interestingly, the 1st generation Ru-benzylidyne complexes, **6.2-Cl/F** and **6.2-F/F** did not show migration of the fluoride ligand onto the α-carbon.[31, 32] Since **6.15** and **6.16** interconvert in solution, isolation of either species cleanly was not possible. Addition of 2 equiv of TASF to **6.8-Cl** leads to the disappearance of **6.15** and further conversion to

6.16. Addition of 3 equiv of TASF leads to further reaction of **6.15** and **6.16** to form a second unidentified product at ^{31}P δ 18.0 ppm and ^{19}F δ -204.3 ppm (d).

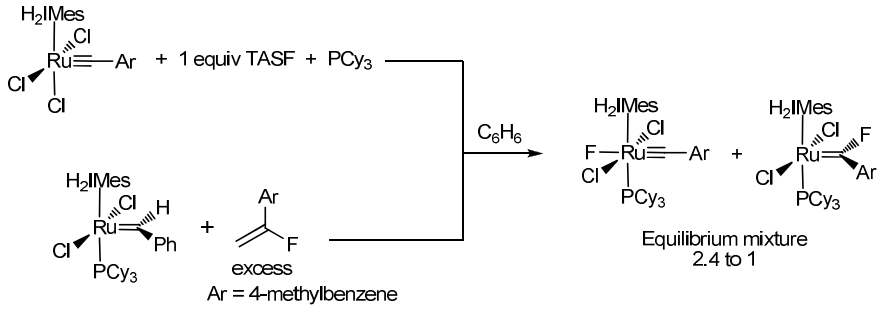

Scheme 6.11. Observation of the Equilibrium of **6.15** and **6.16**.

6.4.2. Migration followed by C-H Activation

Earlier in section 6.3.3, monosubstituted alkoxy-Ru benzylidyne complexes were discussed. Here, we address trisubstitution attempts of alkoxide salts at the Ru center. Attempts at trisubstitution reactions with $NaOC(CH_3)_3$ and $TlOC(CH_3)_2CF_3$ resulted in an intractable mixture; however, upon moving to $TlOC(CH_3)(CF_3)_2$, a clean new product, **6.21**, was observed *via* ^1H NMR spectroscopy (Scheme 6.12). Interestingly, ^{19}F NMR data indicated that only two hexafluoro-*t*-butoxide groups were present on Ru; nevertheless, liberation of 3 equiv. of TlI was observed. Another anomally was that each of the four CF_3 groups was locked on an NMR timescale in a different chemical environment as indicated by 4 quartet peaks seen in the ^{19}F NMR spectrum. Also, both

^{1}H NMR and ^{13}C NMR data showed significant signal broadening for the H_2IMes ligand peaks. The structure of **6.21** was discerned by X-ray crystallography.

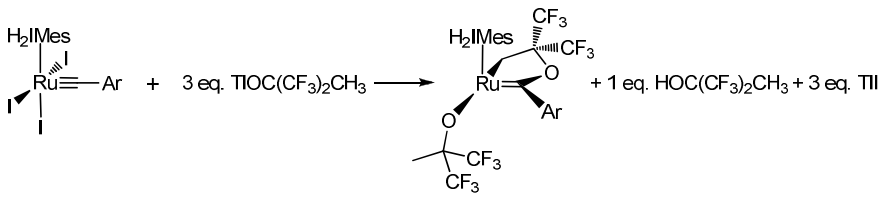

Scheme 6.12. Synthesis of **6.21**.

Dark red crystals of **6.21** were grown from a saturated hexanes solution at −35 °C. An ORTEP diagram is shown in Figure 6.6 selected crystallographic data are presented in Table 6.3, and selected bond distances and angles are presented in Table 6.4. Analysis reveals migration of one of two hexafluoro-*t*-butoxide ligands from the Ru center to the α-carbon followed by C-H activation at the Ru center to form a ruthena-2,2-bis(trifluoromethyl)-2,3-dihydrofuran complex. Complex **6.21** is a distorted tetrahedral complex; in which, the NHC ligand is *cis* to the α-carbene (C17-Ru-C1: 96.40(12)°), the α-carbane (C17-Ru-C10: 92.61(12)°), and C1-Ru-C10 is 82.10(12)°. The hexafluoro-*t*-butoxide ligand on Ru is positioned so that it is not directly *trans* to any one of the three carbon-based ligands as they are all strong trans influence ligands.

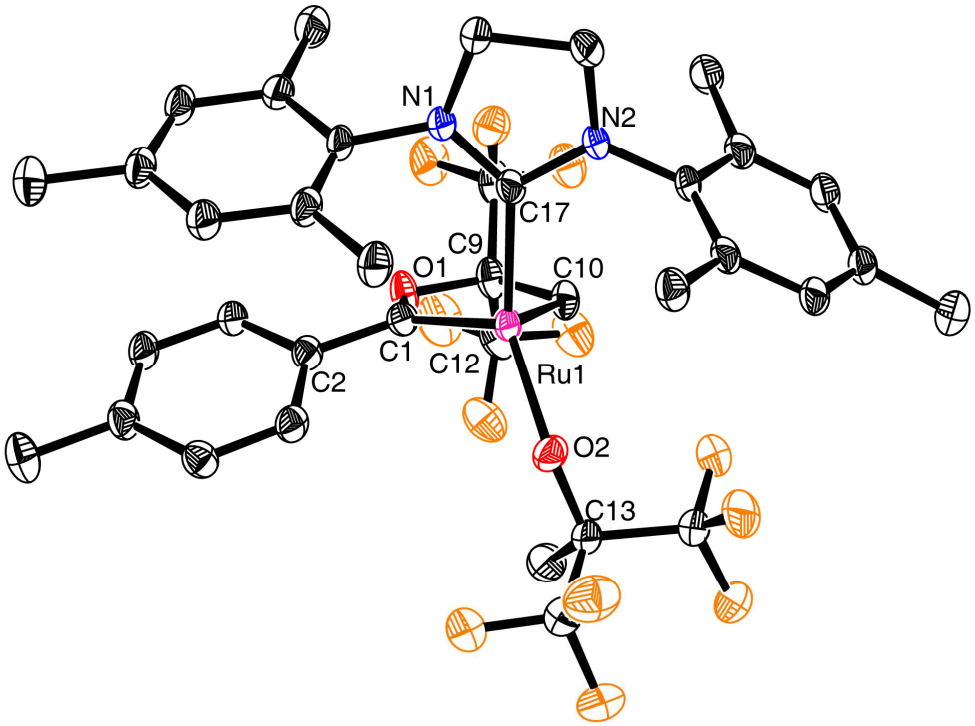

Figure 6.6. 50% thermal ellipsoid plot of [Ru(=C(OC(CF_3)$_2$$CH_2$) (*p*-$C_6H_4$Me) ($H_2$IMes)(OC($CF_3$)$_2$$CH_3$)] (**6.21**). Selected crystallographic data are presented in Table 6.3 and selected bond distances and angles are presented in Table 6.4. Complete XRD data can be found in Appendix 9.

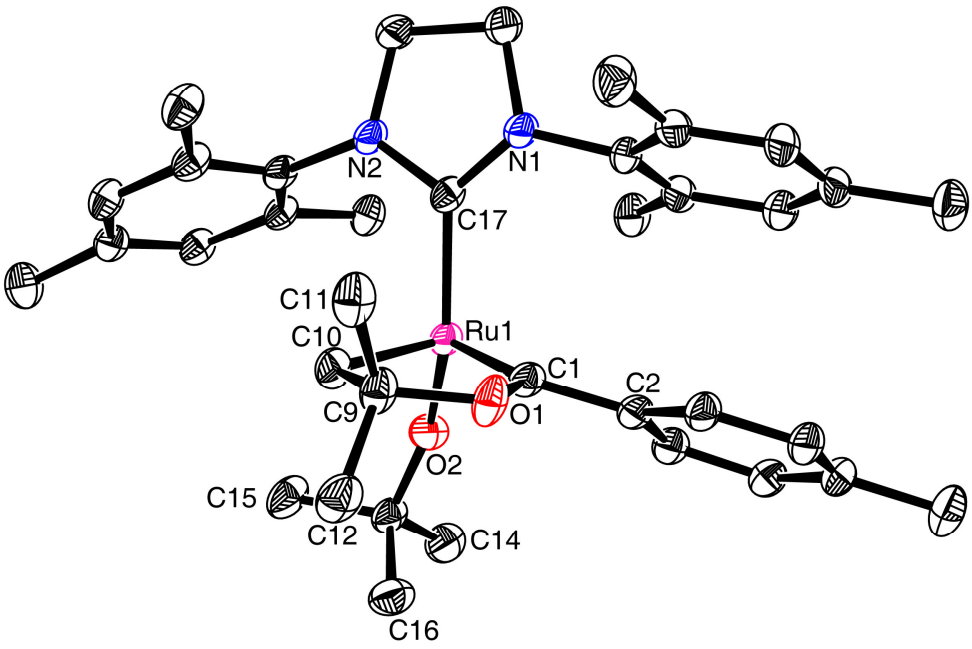

Figure 6.7. 50% thermal ellipsoid plot of [Ru(=C(OC(CF_3)$_2$$CH_2$) (*p*-$C_6H_4$Me) ($H_2$IMes)(OC($CF_3$)$_2$$CH_3$)] (**6.21**). Alternate view: fluorine atoms are omitted from C11, C12, C14 and C15 for clarity

This type of migration would be undesirable for Ru-alkylidyne catalysts as it is irreversible and would be detrimental to alkyne metathesis. Ligand choice for the alkyne metathesis catalyst will be very important for this reason as well as more obvious reasons such as activity of the catalyst. One possible way to prevent this type of migration is to use tridentate trianion ligands. Tethering the ancilliary ligands together will help to prevent migration through steric constraints.

6.5. Conclusion

A number of Ru-benzylidyne and Ru-benzylidene complexes with *N*-heterocyclic carbene ligands have been synthesized and characterized through salt metathesis with a common intermediate, **6.8-Cl**. Compound **6.8-Cl** is easily accessed in high yield through treatment of the Blechert/Hoveyda Grubbs catalyst, **6.7**, with 5-decene and excess α-chloro-*p*-methylstyrene. The halide-substituted 5-coordinate Ru-benzylidyne complexes (**6.8-X**) are extremely stable in solution under an inert atmospheres. They are also relatively air-stable in solution (4-16h). The cationic 5-coordinate Ru-benzylidyne complex **6.9-Cl/Cl** is remarkably stable to air (>48h) and once tricyclohexylphosphine is coordinated, it does not show any degree of lability.

Mono- and disubstitution of aryloxide salts was observed at the Ru-center; however, attempts at trisubstitution failed. Generally, in these cases, no further substitution was observed and the disubstituted complex persisted in solution. Treatment of compound **6.8-X** with bisthallium(I)tetrachlorocatecholate yielded a new compound, **6.19-X**, cleanly. When **6.19-X** was exposed to coordinating solvents such as THF or pyridine, migration of one of the oxides of the tetrachlorocatecholate from Ru to the α-carbon was observed to form **6.20-X/L**. The coordinating solvents ligated to the Ru-center could be easily removed by dissolving **6.20-Cl/THF** in benzene and then concentrating the solution *in vacuo*. Compound **6.19-Cl** could be isolated as it precipitated from benzene. The reversibility of the catecholate migration may prove useful in further attempts to remove or exchange the NHC ligand. Attempts to exchange the chlorides of **6.8-Cl** with fluorides proved difficult as the fluoride ancilliary ligand would migrate back to the α-carbon, forming a monofluorobenzylidene species (**6.16** and

6.18) along with the desired benzylidyne species (**6.15** and **6.17**). With alkoxide salts, one substitution with either hexa- or nonafluoro-*t*-butoxide was observed. However, attempts at two or three substitutions with alkoxides generally lead to an intractable mixture in the NMR spectra. One exception was the trisubstitution of hexafluoro-*t*-butoxide at the Ru-center. In this case, a new ruthena-2,2-bis(trifluoromethyl)-2,3-dihydrofuran, **6.21**, was isolated. It appears that during the second or third substitution, one of the hexafluoro-*t*-butoxide ligands migrates from the Ru to the α-carbon and then C-H activation of the methyl group at the Ru-center takes place. One of the other two hexafluoro-*t*-butoxide ligands stays on the Ru-center while the third abstracts the C-H activated proton and forms hexafluoro-*t*-butanol. We speculate that treatment of **6.8** with other alkoxide salts such as sodium-*t*-butoxide and thallium(I)ethoxide results in similar behavior but then these complexes undergo further decomposition processes. Irreversible migration will be important in the design of Ru-alkylidyne catalysts for alkyne metathesis as this process will deactivate Ru-based AM catalysts.

6.6. Experimental

6.6.1. General Procedures. All reactions were carried out in a nitrogen-filled MBRAUN Labmaster 130 glove box, unless otherwise specified. ^{1}H, ^{13}C, ^{19}F, and ^{31}P NMR spectra were acquired on a Varian Mercury 300 MHz, Inova 400 MHz, MR 400 MHz, or Inova 500 MHz NMR spectrometer. ^{1}H and ^{13}C spectra were referenced to solvent signals.[41] ^{19}F NMR spectra and ^{31}P NMR spectra were referenced to external $CFCl_3$ in $CDCl_3$ ($\delta = 0$) and external 85% H_3PO_4 ($\delta = 0$) respectively.

6.6.2. Materials. Lithium tetrafluoroborate, pyridine, and tris(dimethylamino)sulfur (trimethyl-silyl)difluoride (TAS-F) were purchased from Aldrich Chemical. Trans-5-decene, iodotrimethylsilane, 1,1,1,3,3,3-hexafluoro-2-propanol, sodium methoxide (anhydrous powder) and pentafluorophenol were purchased from Acros Organics. 1-Bromo-3,5-bis(trifluoromethyl)benzene was purchased from Fluka. 2,6-Dichloro-4-nitrophenol was purchased from TCI America. Tetrachlorocatechol was purchased from Alfa Aesar. 2,6-Diisopropylphenol and 2,4,6-trimethylphenol were purchased from Lancaster Synthesis Inc. Nonafluoro-tert-butanol was purchased from Apollo Scientific Ltd. Tricyclohexylphosphine, thallium(I)ethoxide and silver tetrafluoroborate were purchased from Strem Chemicals Inc. All bulk solvents were obtained from VWR Scientific and dried by passage through solvent purification columns according to the method of Grubbs.[42] Deuterated solvents were purchased from CIL and dried over 4 Å molecular sieves. All liquid reagents were degassed and then dried over sieves or passed through activated alumina. Solid reagents were used as received. The starting compounds Ru(=CHPh)(H_2IMes)(PCy_3)Cl_2 (**6.6**),[39] α-chloro-*p*-methylstyrene[43] and α–fluoro-*p*-methylstyrene[44] were synthesized according to published procedures. Ruthenium catalysts **6.6** and Ru(*o*-O-*i*-PrC_6H_4)H_2IMesCl_2 (**6.7)** were also obtained from Materia, Inc.

6.6.3. Synthetic Procedures

[Ru(C-*p*-C_6H_4Me)(H_2IMes)Cl_3] (6.8-Cl). Method 1: A solution of second-generation Grubbs catalyst [Ru(CHPh)(H_2IMes)PCy_3Cl_2] (**6.6**; 150.3 mg, 0.1770 mmol,

1.000 equiv) in 10 mL of benzene was placed in a 60 mL bomb flask. A solution of α-chloro-*p*-methyl-styrene (300 mg, 1.97 mmol, 11.1 equiv) in 1 mL benzene was added to the reaction mixture. The solution was heated to 50 °C for 48h with stirring. The solution was cooled and concentrated *in vacuo* to 2 mL. In the glove box, the 2 mL benzene solution was thawed and filtered. The pink solid, **6.8-Cl**, was isolated in 33.9% yield (37.0 mg, 0.0600 mmol). Pure **6.8-Cl** was obtained after drying overnight. Recrystallization of **6.8-Cl** involved slow diffusion of pentane into a methylene chloride solution at −35 °C. Orange/red needlelike crystals were obtained for a single-crystal X-ray diffraction study. Method 2: Blechert/Hoveyda-Grubbs catalyst, [Ru(*o*-O-*i*-PrC_6H_4)H_2IMesCl_2] (**6.7**; 1.623 g, 2.590 mmol, 1.000 equiv.) was weighed into a 60 mL bomb flask and 25 mL of benzene was added. A solution of α-chloro-*p*-methylstyrene (1.801 g, 11.80 mmol, 4.556 equiv.) and 5-decene (0.549 mg, 3.91 mmol, 1.51 equiv.) in 20 mL of benzene was added to the bomb flask. The bomb flask was sealed, removed from the glove box and heated in an oil bath at 45 °C for 48h *without* stirring. The solution was cooled and brought into the glovebox. The precipitate in the clear red reaction mixture was filtered and washed with 10 mL benzene and then 3 × 10 mL hexanes. The solid pink product, **6.8-Cl,** was redissolved in 15 mL of methylene chloride and added to 40 mL of hexanes to remove benzene from the microcrystalline product. The pale pink precipitate was filtered and collected in two crops. First crop yielded 1.188 g of **6.8-Cl**. The second crop yielded 0.375 g of product. The ^{1}H NMR spectrum indicated that for each mole of **6.8-Cl**, there was 0.5 moles of methylene chloride. Overall yield of **6.8-Cl** was 91.5% (1.563 g, 2.370 mmol). NMR data for **6.8-Cl:** ^{1}H NMR (400 MHz, CD_2Cl_2): δ = 7.36 (s, benzene, 2H), 7.32 (d, $^3J_{HH}$ = 8.0 Hz, 2H, *p*-

$C_6H_4CH_3$), 7.06 (d, $^3J_{HH}$ = 8.0 Hz, 2H, *p*-$C_6H_4CH_3$), 6.99 (s, 2H, mesityl), 6.45 (s, 2H, mesityl), 4.18 (m, H_2IMes backbone, 4H), 2.54 (s, mesityl –CH_3, 6H), 2.43 (s, mesityl –CH_3, 6H), 2.38 (s, mesityl –CH_3, 3H), 2.32 (s, mesityl –CH_3, 3H), 1.77 (s, *p*-$C_6H_4CH_3$, 3H). ^{1}H NMR (400 MHz, Method 2, $CDCl_3$): δ = 7.37 (s, benzene, 2H), 7.37 (d, $^3J_{HH}$ = 8.0 Hz, overlapping with benzene, *p*-$C_6H_4CH_3$), 7.01 (d, $^3J_{HH}$ = 8.4 Hz, 2H, *p*-$C_6H_4CH_3$), 6.96 (s, 2H, mesityl), 6.45 (s, 2H, mesityl), 4.21 (m, H_2IMes backbone, 4H), 2.57 (s, mesityl –CH_3, 6H), 2.46 (s, mesityl –CH_3, 6H), 2.37 (s, mesityl –CH_3, 3H), 2.28 (s, mesityl –CH_3, 3H), 1.80 (s, *p*-$C_6H_4CH_3$, 3H). $^{13}C\{^1H\}$ NMR (100.596 MHz, CD_2Cl_2): δ = 302.02 (Ru*C*-*p*-$C_6H_4CH_3$), 202.69 (H_2IMes carbene), 148.56, 140.91, 140.61, 139.18, 138.11, 138.09, 136.69, 131.17, 130.51, 130.23, 129.26, 129.13, 52.89, 51.86, 23.15, 21.42, 21.06, 20.41, 18.5. Anal. Calcd. for $C_{29}H_{33}Cl_3N_2Ru$: C, 56.45; H, 5.39; N, 4.54. Found C, 56.48; H, 5.63; N, 4.64. A solution of **6.8-Cl** in CD_2Cl_2 was left open to air and showed no decomposition after 4 hours; although complete decomposition was seen after 16h. Compound **6.8-Cl** was insoluble in benzene, toluene and hexanes and was only partially soluble in THF, chloroform and acetone.

[Ru(C-*p*-C_6H_4Me)(H_2IMes)I_3] (6.8-I). Compound **6.8-Cl** (512.4 mg, 0.8305 mmol, 1.000 equiv) was dissolved in 18 mL of methylene chloride and iodotrimethylsilane (793.9 mg, 3.968 mmol, 4.778 equiv) was added. The solution was stirred 20.5 h. Hexanes (50 mL) were added to the reaction mixture and the solution was allowed to stand for 30 min. The solution was filtered and compound **6.8-I** was isolated as a dark red precipitate (722.4 mg, 0.8034 mmol, 96.7%). ^{1}H NMR data showed that for every mole of **6.8-I**, there was 0.1 moles of benzene and 0.25 moles of methylene

chloride associated. Recrystallization of **6.8-I** involved slow diffusion of pentane into a chloroform solution at −35 °C. Red needlelike crystals were obtained for a single-crystal X-ray diffraction study. NMR data for **6.8-I:** ^{1}H NMR (400 MHz, CD_2Cl_2): δ = 7.52 (d, $^{3}J_{HH}$ = 8.4 Hz, -*p*-C_6H_4Me, 2H), 7.35 (s, benzene, 0.6H), 6.95 (d, $^{3}J_{HH}$ = 8.4 Hz, -*p*-C_6H_4Me, overlapping), 6.94 (s, mesityl aryl, overlapping 4H), 6.42 (s, mesityl aryl, 2H), 5.33(s, CH_2Cl_2, 0.50H), 4.15 (m, H_2IMes backbone, 4H), 2.61 (s, mesityl CH_3, overlapping), 2.60 (s, mesityl CH_3, overlapping, 12H), 2.34 (s, mesityl CH_3, 3H), 2.29 (s, mesityl CH_3, 3H), 1.79 (s, -*p*-$C_6H_4CH_3$, 3H). ^{1}H NMR (400 MHz, acetone-d_6): δ = 7.61 (d, $^{3}J_{HH}$ = 8.0 Hz, -*p*-C_6H_4Me, 2H), 7.34 (s, benzene), 7.08 (d, $^{3}J_{HH}$ = 8.0 Hz, -*p*-C_6H_4Me, 2H), 6.87 (s, mesityl aryl, 2H), 6.43 (s, mesityl aryl, 2H), 5.61 (s, CH_2Cl_2), 4.18 (m, H_2IMes backbone, 4H), 2.70 (s, mesityl CH_3, 6H), 2.65 (s, mesityl CH_3, 6H), 2.41 (s, mesityl CH_3, 3H), 2.26 (s, mesityl CH_3, 3H), 2.04 (ref: acetone-d_5), 1.78 (s, -*p*-$C_6H_4CH_3$, 3H). $^{13}C\{^{1}H\}$ NMR (100.738 MHz, E1333, CD_2Cl_2): δ = 290.07 (Ru*C*-*p*-$C_6H_4CH_3$), 207.04 (H_2IMes carbene), 147.69, 140.89, 139.88, 137.90, 137.73, 136.35, 133.53, 131.51, 130.58, 130.48, 130.31, 129.49, 128.84 (benzene), 53.31 (H_2IMes backbone), 52.47 (H_2IMes backbone), 23.06, 23.02, 21.35, 21.24, 20.98.

[Ru(C-*p*-C_6H_4Me)(H_2IMes)(PCy_3)Cl_2][BF_4](6.9-Cl/BF_4).

Tricyclohexylphosphine (51.0 mg, 0.182 mmol, 1.20 equiv) was dissolved in 4 mL methylene chloride and added to dry **6.8-Cl** (100.5 mg, 0.152 mmol, 1.00 equiv). The solution was stirred for 10 minutes and then $LiBF_4$ (70 mg, 0.46 mmol, 3.0 equiv) was added. The reaction mixture was then stirred vigorously for 5 hours; after which, the

solution was filtered and 15 mL of hexanes was added to the filtrate. The orange precipitate, **6.9-Cl/BF_4**, (123.0 mg, 0.130 mmol) was filtered and washed with 3 × 5 mL hexanes. Compound **6.9-Cl/BF_4** was isolated in 85% yield. Integration against an internal standard (1-bromo-3,5-bis(trifluoromethyl)benzene) to the NMR solution of **6.9-Cl/BF_4** indicated that it was free of LiCl and excess $LiBF_4$. Compound **6.9-Cl/BF_4** is air-stable in a solution of methylene chloride for >48 h. ^{1}H NMR (400 MHz, CD_2Cl_2): δ = 7.24 (d, $^3J_{HH}$ = 8.0 Hz, -*p*-C_6H_4Me, 2H), 7.12 (d, $^3J_{HH}$ = 8.0 Hz, -*p*-C_6H_4Me, 2H), 6.97 (s, mesityl aryl, 2H), 6.41 (s, mesityl aryl, 2H), 5.33(s, CH_2Cl_2, 0.19H), 4.09 (m, H_2IMes backbone, 4H), 2.55 (s, mesityl CH_3, overlapping), 2.52 (q, PCy_3, overlapping), 2.46 (s, mesityl CH_3, 12H), 2.42 (s, mesityl CH_3, 6H), 2.27 (s, mesityl CH_3, 3H), 1.80 (s, -*p*-$C_6H_4C H_3$, 3H), 1.7–0.9 (m, PCy_3, 30H). ^{1}H NMR (400 MHz, $CDCl_3$): δ = 7.23 (d, $^3J_{HH}$ = 8.4 Hz, -*p*-C_6H_4Me, 2H), 7.15 (d, $^3J_{HH}$ = 8.4 Hz, -*p*-C_6H_4Me, 2H), 6.93 (s, mesityl aryl, 2H), 6.39 (s, mesityl aryl, 2H), 5.30(s, CH_2Cl_2), 4.13 (m, H_2IMes backbone, 4H), 2.54 (s, mesityl CH_3, overlapping), 2.52 (q, PCy_3, overlapping) 2.49 (s, mesityl CH_3, overlapping, 12H), 2.40 (s, mesityl CH_3, 6H), 2.26 (s, mesityl CH_3, 3H), 1.80 (s, -*p*-$C_6H_4C H_3$, 3H), 1.7–0.9 (m, PCy_3, 30H). ^{19}F NMR (376.313 MHz, CD_2Cl_2): δ = –156.75 (s, BF_4). ^{31}P NMR (161.915 MHz, CD_2Cl_2): δ = 39.72. $^{13}C\{^1H\}$ NMR (100.596 MHz, E1407, CD_2Cl_2): δ = 299.98 (d, $^2J_{CPcis}$ = 8.7 Hz, Ru*C*-*p*-C_6H_4Me), 204.18 (d, $^2J_{CPtrans}$ = 90.8 Hz, H_2IMes carbene), 150.22, 140.90, 140.51, 138.68, 137.22, 136.62, 136.24, 132.53, 130.74, 130.64, 130.40, 129.44, 54.09 (d, $^4J_{CP}$ = 4.0 Hz, H_2IMes backbone), 52.58 (d, $^4J_{CP}$ = 2.3 Hz, H_2IMes backbone), 34.32, 34.12, 30.03, 30.00, 27.90, 27.79, 26.04, 23.33, 21.34, 21.22, 19.98, 18.41.

[Ru(C-*p*-C_6H_4Me)(H_2IMes)PCy_3I_2][I] (6.9-I/I). Compound **6.8-I** (100.5 mg, 0.1127 mmol, 1.000 equiv.) was dissolved in 5 mL methylene chloride and a solution of tricyclohexylphosphine (88.1 mg, 0.3142 mmol, 2.788 equiv) in 1 mL methylene chloride was added. The reaction mixture was stirred for 3 hours, poured into 45 mL of hexanes, and cooled to –35 °C for 2 hours. The solution was filtered to isolate an olive green solid (**6.9-I/I•0.8CH_2Cl_2**; 132.2 mg, 0.1066 mmol, 94.6%). ^{1}H and ^{31}P NMR spectroscopy displayed one major product and one minor product. ^{31}P NMR (161.922 MHz, CD_2Cl_2): δ = 42.66 (s, 7.5%), 41.15 (s, 92.5%). ^{1}H NMR (400 MHz, CD_2Cl_2) major product: δ = 7.37 (d, $^3J_{HH}$ = 8.4 Hz, -*p*-C_6H_4Me, 2H), 6.98 (d, $^3J_{HH}$ = 8.0 Hz, -*p*-C_6H_4Me, 2H), 6.92 (s, mesityl aryl, 2H), 6.32 mesityl aryl, 2H), 5.33 (s, CH_2Cl_2, 0.8H), 4.13 (m, H_2IMes backbone, 4H), 3.15 (q, PCy_3, 3H), 2.62 (s, mesityl CH_3, 6H), 2.60 (s, mesityl CH_3, 6H), 2.44 (s, mesityl CH_3, 3H), 2.24 (s, mesityl CH_3, 3H), 1.76 (s, -*p*-$C_6H_4CH_3$, 3H), 1.7–0.8 (m, PCy_3, 30H). Attempted purifications of **6.9-I/I** failed.

[Ru(C-*p*-C_6H_4Me)(H_2IMes)PCy_3I_2][BF_4] (6.9-I/BF_4). Tricyclohexylphosphine (13.1 mg, 0.0467 mmol, 2.05 equiv) was dissolved in 1 mL of CD_2Cl_2. Compound **6.8-I** (20.3 mg, 0.0228 mmol, 1.00 equiv) was added to the reaction mixture and the solution was stirred for 2 hours. One new major product and two minor products were observed in the 31P NMR spectrum. ^{31}P NMR (161.922 MHz, CD_2Cl_2): δ = 48.9 (s, 2.4%), 42.66 (s, 4.6%), 41.15 (s, 46.8%), and 10.7(46.0%, free PCy_3). The solution was added to 10 mL of hexanes and allowed to sit for 20 minutes. A green solid, 6.9-I/I was isolated by filtration and redissolved in 1 mL of CD_2Cl_2 containing $AgBF_4$ (4.4 mg, 0.023 mmol, 1.0

equiv). The solution was stirred for 30 minutes and the solution stayed a green color and formed a white precipitate. The solution was filtered and NMR data was collected. ^{31}P NMR data indicated the presence of only one product. ^{31}P NMR (161.922 MHz, CD_2Cl_2): δ = 41.18 (s). ^{19}F NMR data confirmed the presence of tetrafluoroborate. ^{1}H NMR (400 MHz, CD_2Cl_2) major product: δ = 7.37 (d, $^{3}J_{HH}$ = 8.4 Hz, -*p*-C_6H_4Me, 2H), 6.98 (d, $^{3}J_{HH}$ = 8.8 Hz, -*p*-C_6H_4Me, 2H), 6.92 (s, mesityl aryl, 2H), 6.33 mesityl aryl, 2H), 5.33 (s, CH_2Cl_2), 4.11 (m, H_2IMes backbone, 4H), 3.15 (q, PCy_3, 3H), 2.63 (s, mesityl CH_3, 6H), 2.60 (s, mesityl CH_3, 6H), 2.43 (s, mesityl CH_3, 3H), 2.25 (s, mesityl CH_3, 3H), 1.76 (s, -*p*-$C_6H_4CH_3$, 3H), 1.7–0.8 (m, PCy_3, 30H). Crystallization attempts of **6.9-I/BF$_4$** failed.

[Ru(C-*p*-C$_6$H$_4$Me)(H$_2$IMes)(O-2,6-*i*-propyl-C$_6$H$_3$)I$_2$] (6.10). Dissolved (**6.8-I**) (90.0 mg, 0.101 mmol, 1.00 equiv) in 5 mL methylene chloride and a solution of thallium(I)-2,6-diisopropylphenoxide (39.9 mg, 0.105 mmol, 1.04 equiv) was added. The mixture was stirred for 2 hours and then filtered through celite wetted with benzene to remove yellow Tl(I)I precipitate. The celite was washed with 3 × 5 mL of benzene. Volatiles were removed from the reaction solution. The solid was dissolved in a minimum amount of methylene chloride needed to dissolve the product (2 mL) and 15 mL of pentane was added. The solution was cooled at –35 °C for 24 h. A purple microcrystalline solid (**6.10**; 67.6 mg, 70.2%) was filtered and washed 3 × 5 mL pentane. ^{1}H NMR indicated that thallium(I)-2,6-diisopropylphenoxide was still an impurity in the purple solid. The salt impurity was taken into consideration when determining the above

isolated yield. Attempts to isolate **6.10** cleanly failed; however, if the reaction is run with < 1 equiv of the aryloxide salt, compound **6.10** should be easily isolated from **6.8-I** by solvation in minimum benzene. ^{1}H NMR (400 MHz, CD_2Cl_2): δ = 7.66 (d, $^{3}J_{HH}$ = 8.0 Hz, -*p*-C_6H_4Me, 2H), 7.05 (s, mesityl aryl, 2H), 7.00 (d, $^{3}J_{HH}$ = 7.6 Hz, -*p*-C_6H_4Me, 2H), 6.79 (dd, $^{3}J_{HH}$ = 7.6 Hz, $^{4}J_{HH}$ = 2.0 Hz, -O-2,6-di^{i}PrC_6H_3, 1H), 6.67 (dd, $^{3}J_{HH}$ = 7.6 Hz, $^{4}J_{HH}$ = 2.0 Hz, -O-2,6-di^{i}PrC_6H_3, 1H), 6.46 (t, $^{3}J_{HH}$ = 7.6 Hz, -O-2,6-di^{i}PrC_6H_3, 1H), 6.41 (s, mesityl aryl, 2H), 4.09 (m, H_2IMes backbone, 4H), 2.71 (s, mesityl CH_3, overlapping), ~2.71 (septet, -O-2,6-di^{i}*Pr*C_6H_3, overlapping 7H total), 2.59 (s, mesityl CH_3, 6H), 2.38 (s, mesityl CH_3, 6H), 2.07 (septet, -O-2,6-di^{i}*Pr*C_6H_3, 1H), 1.76 (s, -*p*-C_6H_4CH_3, 3H), 1.25 (d, $^{3}J_{HH}$ = 6.8 Hz, TlO-2,6-di^{i}*Pr*C_6H_3, all other peaks are buried, 5%), 0.89 (d, $^{3}J_{HH}$ = 6.8 Hz, -O-2,6-di^{i}*Pr*C_6H_3, 6H), 0.46 (d, $^{3}J_{HH}$ = 6.8 Hz, -O-2,6-di^{i}*Pr*C_6H_3, 6H).

[Ru(C-*p*-C_6H_4Me)(H_2IMes)(O-2,6-Cl-6-NO_2-C_6H_2)Cl_2] (6.11). Compound **6.8-Cl** (20.2 mg, 0.0327 mmol, 1.00 equiv) was dissolved in 1 mL CD_2Cl_2 and the solution was added to dry thallium(I)2,4dichloro-6-nitrophenoxide (13.1 mg, 1.01 equiv). The thallium salt was only sparingly soluble in methylene chloride. The reaction was stirred for 1 hour and then a ^{1}H NMR spectrum was acquired and all **6.8-Cl** had been consumed and one new product had formed. A second equivalent of thallium(I)2,4dichloro-6-nitrophenoxide (12.2 mg, 0.94 equiv) was added to the reaction mixture. After 1 h stirring, a 1H NMR was acquired and was identical to the initial NMR spectrum with the exception of two new peaks at 8.15 ppm and 6.65 ppm. The integration of these peaks was small with respect to the other peaks representing compound **6.11**. The reaction mixture was allowed to stir overnight and an NMR spectrum was acquired the next day.

A number of new peaks were observed and it appeared that the Ru species had decomposed. ^{1}H NMR (400 MHz, CD_2Cl_2, after the first hour): δ = 8.33 (s, thallium salt, 10%), 7.89 (s, -O-2,6-Cl-6-NO_2-C_6H_2, 2H) 7.41 (d, $^{3}J_{HH}$ = 8.4 Hz, -*p*-C_6H_4Me, 2H), 7.35 (C_6H_6), 7.09 (d, $^{3}J_{HH}$ = 8.4 Hz, -*p*-C_6H_4Me, 2H), 7.02 (s, mesityl aryl, 2H), 6.44 (s, mesityl aryl, 2H), 4.17 (m, H_2IMes backbone, 4H), 2.57 (s, mesityl CH_3, 6H), 2.42 (s, mesityl CH_3, 3H), 2.39 (s, mesityl CH_3, 6H), 2.35 (s, mesityl CH_3, 3H),1.76 (s, -*p*-C_6H_4CH_3, 3H).

[Ru(C-*p*-C_6H_4Me)(H_2IMes)(O-C_6F_5)I_2] (6.12). Compound **6.8-I** (19.9 mg, 0.0223 mmol, 1.00 equiv) was dissolved in 1 mL of CD_2Cl_2 along with sodium perfluorophenoxide (5.1 mg, 0.025 mmol, 1.1 equiv). The solution was stirred in the glove box overnight. A ^{1}H NMR spectrum was acquired the next day indicating that about 50% of the starting material, **6.8-I** had been consumed and 38% of a single new product had appeared. Excess sodium perfluorophenoxide (14.9 mg, 0.0723 mmol, 3.24 equiv) was added to the reaction mixture and it was allowed to stir for another 24 hours. The ^{1}H NMR spectrum indicated that the Ru species had decomposed. ^{1}H NMR (400 MHz, CD_2Cl_2, after the first hour): δ = 7.69 (d, $^{3}J_{HH}$ = 8.0 Hz, -*p*-C_6H_4Me, **6.12,** 1.2H), 7.52 (d, $^{3}J_{HH}$ = 8.4 Hz, -*p*-C_6H_4Me, **6.8-I,** 2H), 7.35 (s, benzene, 0.6H), 7.03 (s, mesityl aryl, **6.12**, overlapping), 7.02 (d, -*p*-C_6H_4Me, **6.12**, overlapping) 6.95 (d, $^{3}J_{HH}$ = 8.4 Hz, -*p*-C_6H_4Me, **6.8-I,** overlapping), 6.94 (s, mesityl aryl, **6.8-I,** overlapping), 6.42 (s, mesityl aryl, **6.12**, overlapping), 6.42 (s, mesityl aryl, **6.8-I,** overlapping, 3.2H total), 5.33(s, CH_2Cl_2), 4.15 (m, H_2IMes backbone, **6.8-I,** overlapping), 4.14 (m, H_2IMes backbone, **6.12,** overlapping), 2.65 (s, mesityl CH_3, **6.12**), 2.61 (s, mesityl CH_3, **6.8-I**), 2.60 (s,

mesityl CH_3, **6.8-I**), 2.55 (s, mesityl CH_3, **6.12**), 2.40 (s, mesityl CH_3, **6.12**), 2.36 (s, mesityl CH_3, **6.12**), 2.34 (s, mesityl CH_3, **6.8-I,** 3H), 2.29 (s, mesityl CH_3, **6.8-I,** 3H), 1.80 (s, -*p*-$C_6H_4CH_3$, **6.12,** overlapping), 1.79 (s, -*p*-$C_6H_4CH_3$, **6.8-I,** overlapping, 5.1H total).

[Ru(C-*p*-C_6H_4Me)(H_2IMes)(O-2,4,6-CH_3-C_6H_2)$_2$Cl] (6.13). Compound **6.8-Cl•0.5CH_2Cl_2** (19.8 mg, 0.0300 mmol, 1.00 equiv) was dissolved in 1 mL of CD_2Cl_2 and added to solid thallium(I)-2,4,6-trimethylphenoxide (21.6 mg, 0.0636 mmol, 2.12 equiv). The mixture was stirred for 1 hour and then a ^{1}H NMR spectrum was acquired. ^{1}H NMR (400 MHz, CD_2Cl_2, after the first hour): δ = 6.97 (s, -O-2,4,6-CH_3-C_6H_2, 2H), 6.68 (s, -O-2,4,6-CH_3-C_6H_2, 3H, overlapping with one H_2IMes mesityl aryl), 6.53 (d, $^3J_{HH}$ = 7.6 Hz, -*p*-C_6H_4Me, 2H), 6.44 (s, H_2IMes mesityl aryl, 1H), 6.34 (d, $^3J_{HH}$ = 7.6 Hz, -*p*-C_6H_4Me, overlapping), 6.32 (s, H_2IMes mesityl aryl, overlapping, 3H total), 5.90 (s, H_2IMes mesityl aryl, 2H), 4.03 (s, H_2IMes backbone, 4H), 2.68 (s), 2.35 (s), 2.07 (s), 1.97 (s), 1.94 (s), 1.88 (s), 1.87 (s), 1.55 (s), 1.14 (s).

[Ru(C-*p*-C_6H_4Me)(H_2IMes)(OC(CF_3)$_3$)I_2] (6.14). Compound **6.8-I** (100.1 mg, 0.1123 mmol, 1.156 equiv) was dissolved in 5 mL of CH_2Cl_2 and thallium(I)nonafluoro-tert-butoxide (42.7 mg, 0.0972 mmol, 1.00 equiv) was added and washed in with 1 mL of CH_2Cl_2. The reaction was stirred for 1.5 h and then filtered through celite which had been wetted with 5 mL of benzene. The solution was washed through the celite with an

additional 10 mL of benzene. The volatiles were removed from the reaction mixture *in vacuo*. ^{1}H NMR data revealed one major product and two minor products. Attempts to isolate the major product through solvation and recrystallization were unsuccessful. ^{1}H NMR (400 MHz, C_6D_6, partially soluble) major product: δ = 7.89 (d, $^{3}J_{HH}$ = 8.4 Hz, -*p*-C_6H_4Me, 2H), 6.91 (s, mesityl aryl, 2H), 6.24 (d, $^{3}J_{HH}$ = 8.0 Hz, -*p*-C_6H_4Me, 2H), 6.09 (s, mesityl aryl, 2H), 3.23 (m, H_2IMes backbone, 4H), 2.64 (s, mesityl CH_3, 6H), 2.50 (s, mesityl CH_3, 6H), 2.21 (s, mesityl CH_3, 3H), 1.70 (s, mesityl CH_3, 3H), 1.48 (s, -*p*-C_6H_4CH_3, 3H). ^{19}F NMR (376.313 MHz, C_6D_6, partially soluble): δ = -76.99 (s, 73%), -77.53 (s, 2%), -78.27 (s, 1%), -79.12 (bs, 18%), -79.97 (s, 4%).

[Ru(≡C-*p*-C_6H_4Me)(H_2IMes)(η^2-$O_2C_6Cl_4$)Cl] (6.19-Cl). Compound **6.8-Cl** (114.6 mg, 0.1857 mmol, 1.000 equiv) was dissolved in 3 mL of methylene chloride. Bisthallium(I)tetrachlorocatecholate (126.0 mg, 0.1925 mmol, 1.036 equiv) was added to the solution and the mixture was stirred for 40 min. at ambient temperature. The reaction mixture was then filtered through celite to remove thallium(I)chloride and washed through with 10 mL of methylene chloride until all color had passed through the celite. Hexanes (20 mL) were then added to the methylene chloride solution. The solution was then concentrated *in vacuo* to 5 mL. Hexanes (10 mL) were added to the concentrated reaction mixture and allowed to stand at –35 °C for 2 h. Red microcrystalline **6.19-Cl** (109.1 mg, 0.1378 mmol, 74.1%) was then isolated *via* filtration. NMR data for **6.19-Cl:** ^{1}H NMR (400 MHz, CD_2Cl_2): δ = 7.00 (d, J = 8.8 Hz, *p*-C_6H_4Me, overlapping), 6.97 (d, J = 8.4 Hz, *p*-C_6H_4Me, overlapping, 4H total), 6.94 (s, mesityl aryl, 1H), 6.70 (s, mesityl

aryl, 1H), 6.53 (s, mesityl aryl, 1H), 6.40 (s, mesityl aryl, 1H), 4.23 (m, H_2IMes backbone, 4H), 2.54 (s, mesityl CH_3, 3H), 2.47 (s, mesityl CH_3, 6H), 2.34 (s, mesityl CH_3, overlapping), 2.32 (s, mesityl CH_3, overlapping, 6H total), 2.19 (s, mesityl CH_3, 3H), 1.78 (s, *p*-C_6H_4CH_3, 3H) (Figure 6.7). $^{13}C\{^1H\}$ NMR (100.591 MHz, $CDCl_3$): δ = 309.59 (Ru*C*-*p*-$C_6H_4CH_3$), 205.22 (H_2IMes carbene), 157.27, 157.11, 146.11, 140.15, 139.86, 138.54, 138.22, 138.13, 137.29, 137.23, 136.68, 130.86, 130.10, 130.02, 129.91, 129.35, 128.51, 128.34 (benzene), 128.10, 119.86, 118.99, 117.13, 115.88, 51.97, 51.18, 22.66, 21.07, 20.76, 19.61, 18.60, 17.83, 17.67, 15.28, 14.13. Anal. Calcd. for $C_{35}H_{33}Cl_5N_2O_2Ru$: C, 53.08; H, 4.20; N, 3.54; Found C, 52.69; H, 4.22; N, 3.44. Attempts at recrystallization in a number of solvents yielded plate-like crystals that were too thin for X-ray diffraction.

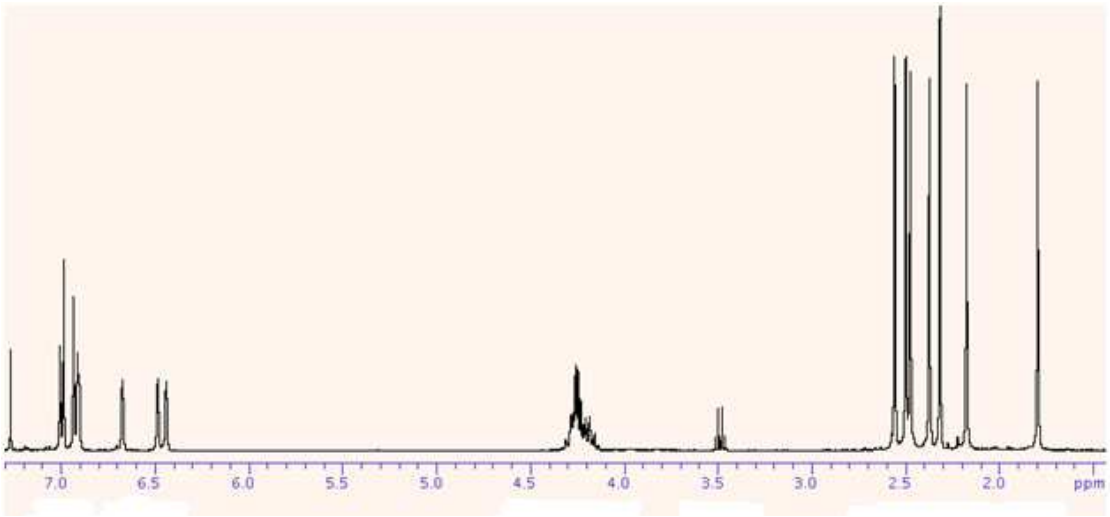

Figure 6.8. ^1H NMR spectrum for **6.19-Cl**

[Ru(=C(OC_6Cl_4O-)(*p*-C_6H_4Me)(H_2IMes)(C_4H_8O)$_2$Cl](6.20-Cl/THF).

Compound **6.8-Cl** (50.7 mg, 0.0822 mmol, 1.00 equiv) was suspended in 2 mL of tetrahydrofuran (THF). Bisthallium(I)tetrachlorocatecholate (50.0 mg, 0.0767 mmol, 0.933 equiv) was added with stirring. The solution turned dark green within 2 minutes. The solution was allowed to stir for 30 min. and then filtered. Solvent was removed *in vacuo* and the residue was redissolved in C_6D_6. NMR data for **6.20-Cl/THF:** ^{1}H NMR (400 MHz, CD_2Cl_2): δ = major aryl peaks: 7.39 (d, $^3J_{HH}$ = 8.8 Hz, *p*-C_6H_4Me, 2H), 6.81 (d, $^3J_{HH}$ = 8.8 Hz, *p*-C_6H_4Me, 2H), multiple broadened aryl peaks between 6–7.5 ppm, 3.56 (very broad s, H_2IMes backbone), 3.24 (broad s, THF), 2.18 (broad s, THF), multiple broad peaks between 1.4–2.6 ppm. $^{13}C\{^1H\}$ NMR (100.591 MHz, C_6D_6): δ = major peaks: 278.35 (Ru*C*(O-Cl_4Cat)-p-C_6H_4Me), 213.8 (H_2IMes carbene), 149.98, 144.99, 143.84, 140.14, 137.69, 137.61, 135.86, 128–127 (broadened peaks), 125.8, 123.9, 120.6, 114.4, 111.48, 67.37 (THF), 51.24 (bs, H_2IMes backbone), 25.34 (THF), 21.9–17.9 (multiple broadened peaks). Isolation and purification of compound **6.20-Cl/THF** was not attempted.

Conversion between 6.19-Cl and 6.20-Cl/THF. Compound **6.19-Cl** (20.0 mg, 0.0253 mmol) was dissolved in 2 mL of tetrahydrofuran (THF). The solution immediately turned green indicating **6.20-Cl/THF** had formed. Volatiles were removed *in vacuo* and the green solid was dissolved in 1 mL of C_6D_6. ^{1}H NMR data confirmed full consumption of **6.19** and formation of **6.20-Cl/THF**. The reaction mixture was then placed under vacuum. Over the next few minutes, **6.19-Cl** began to precipitate from solution. Redissolving the mixture in 5 mL of benzene and placing the solution under vacuum yielded further formation of **6.19-Cl** which was then isolated via filtration.

[Ru(=C(OC_6Cl_4O-)(*p*-C_6H_4Me)(H_2IMes)(C_6D_5N)$_2$Cl](6.20-Cl/C_6D_5N).

Compound **6.19-Cl** (11.7 mg, 0.0126 mmol, 1.00 equiv) was dissolved in CD_2Cl_2 and pyridine-d_5 (5 μL, 0.06 mmol, 5 equiv) was added. The color of the reaction mixture changed immediately from red to dark green. ^{1}H NMR (400 MHz, CD_2Cl_2): δ = 7.32 (d, $^3J_{HH}$ = 8.0 Hz, 2H), 6.94 (d, $^3J_{HH}$ = 8.0 Hz, 2H), 6.61 (bs, mesityl, overlapping), 6.40 (bs, mesityl, overlapping 4H total), 3.99 (bs, H_2IMes backbone, 4H), 2.55 (ss, mesityl CH_3, 6H), 2.34 (bs, mesityl CH_3, overlapping) 2.33 (ss, mesityl CH_3, overlapping), 2.30 (bs, mesityl CH_3, overlapping 9H total), 1.93 (bs, mesityl CH_3 and *p*-C_6H_4CH_3, 6H) (Figure 6.8).

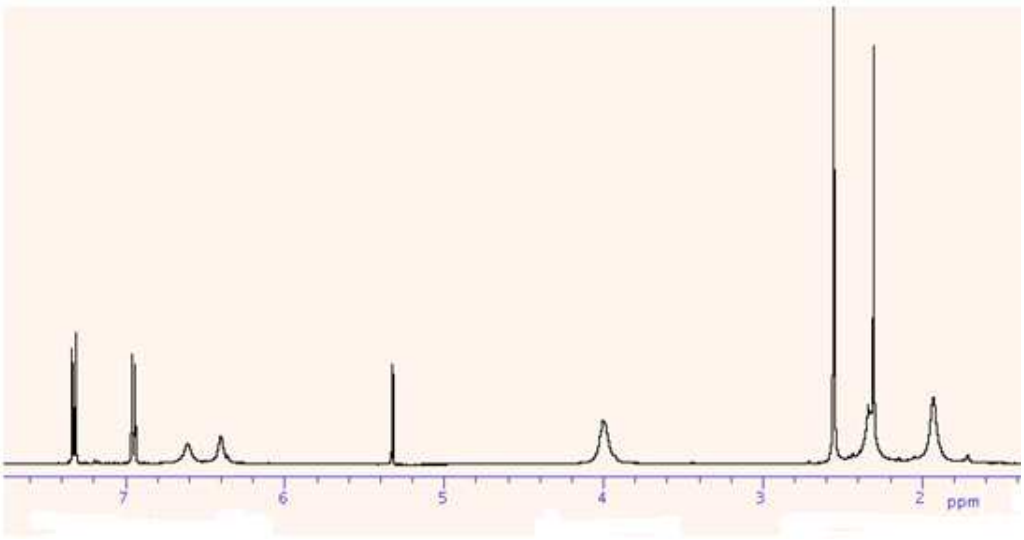

Figure 6.9. ^{1}H NMR spectrum of **6.20-Cl/C_5D_5N**

[Ru(≡C-*p*-C_6H_4Me)(H_2IMes)($O_2C_6Cl_4$)I (6.19-I). Compound **6.8-I** (50.5 mg, 0.0567 mmol, 1.00 equiv) and bisthallium(I)tetrachlorocatecholate (37.6 mg, 0.0574 mmol, 1.01 equiv) were dissolved in 2 mL of methylene chloride. The reaction mixture

was stirred for 1 h and filtered. Volatiles were removed *in vacuo* and the solids were redissolved in 1 mL of CD_2Cl_2 and a ^1H NMR spectrum was acquired. Hexanes (15 mL) was added to the NMR solution and placed in the freezer at –35 °C for 48 h. Large cubic crystals formed. Over the next 48 h, dark red rod-like crystals began to form. X-ray diffraction confirmed that the two types of crystals were **6.19-I**. NMR data for **6.19-I:** ^1H NMR (400 MHz, CD_2Cl_2): δ = 7.36 (s, C_6H_6, 6%) 7.15 (d, J = 8.0 Hz, *p*-C_6H_4Me, 2H), 6.93 (s, mesityl aryl, overlapping), 6.92 (d, J = 8.0 Hz, *p*-C_6H_4Me, overlapping, 3H total), 6.69 (s, mesityl aryl, 1H), 6.58 (s, mesityl aryl, 1H), 6.32 (s, mesityl aryl, 1H), 4.23 (m, H_2IMes backbone, 4H), 2.59 (s, mesityl CH_3, 3H), 2.57 (ss, mesityl CH_3, 3H), 2.43 (s, mesityl CH_3, 3H), 2.37 (s, mesityl CH_3, overlapping 6H), 2.31 (s, mesityl CH_3, 3H), 2.19(s, mesityl CH_3, 3H), 1.76 (s, *p*-$C_6H_4CH_3$, 3H).

Attempts to synthesize [Ru(C-*p*-C_6H_4Me)(H_2IMes)Cl_2F] (6.17). Compound **6.8-Cl** (22.1mg, 0.0358 mmol, 1.07 equiv) was dissolved in 1 mL of CD_2Cl_2 and dry TAS-F ([$S(NMe_2)_3$][F_2SiMe_3]; 9.2 mg, 0.0334, 1.00 equiv) was added. The solution was stirred for 30 minutes and then placed in an NMR tube. ^{19}F NMR (376.313 MHz, CD_2Cl_2): δ = 130.74 (s, small), 119.6 (bs, small), -158.4 (m, TMSF, 58%), -171.3 (m, TAS-F, 6.2%), -262 (d, J = 174.2 Hz, 3%), -270.5 (s, 30%), -308 (d, J = 174.9 Hz, 3%). The volatiles were removed *in vacuo*. The solids were dissolved in 1 mL of C_6H_6 and the solution was filtered to remove the insoluble salts. Benzene was removed *in vacuo* and the solids were redissolved in CD_2Cl_2. ^{19}F NMR (376.313 MHz, CD_2Cl_2): δ = -269.8 (s).

Attempts to precipitate the product using pentane did not yield a solid. Attempts to scale-up the reaction and isolate **6.17** failed.

Attempts to synthesize [Ru(C-*p*-C_6H_4Me)(H_2IMes)ClF_2]. A stock solution of **6.8-Cl** (101.7 mg, 0.1648 mmol) was dissolved in 4.0 mL of CD_2Cl_2 and split into 0.8 mL portions (20.34 mg, 0.0330 mmol, 1.00 equiv). The reaction mixture was added to dry TAS-F ([$S(NMe_2)_3$][F_2SiMe_3]; 17.3 mg, 0.0628, 1.90 equiv) and an immediate color change from pink to dark red was observed. The mixture sat for 10 minutes after which NMR data was acquired. Multiple products were observed by ^{19}F NMR spectroscopy. ^{19}F NMR (376.313 MHz, CD_2Cl_2): δ = 133.67 (s, small), 130.74 (s), 119.6 (bs), -111.7 (s, small), -128.11 (s, small), -147.11 (bs), -154 (bs), -157.7 (s, $SiMe_3F$), -253.2 (dd, J = 175.7 Hz), -261.8 (d, J = 176.5 Hz), -272.0 (s, large, product), -303.5 (dbt, J = 175.3 Hz), -308.1 (dd, 177.6 Hz)

Attempts to synthesize [Ru(C-*p*-C_6H_4Me)(H_2IMes)F_3]. A stock solution of **6.8-Cl** (101.7 mg, 0.1648 mmol) was dissolved in 4.0 mL of CD_2Cl_2 and split into 0.8 mL portions (20.34 mg, 0.0330 mmol, 1.00 equiv). The reaction mixture was added to dry TAS-F ([$S(NMe_2)_3$][F_2SiMe_3]; 25.2 mg, 0.0915, 2.78 equiv) and an immediate color change from pink to dark red was observed. The mixture sat for 10 minutes after which NMR data was acquired. Multiple products were observed by ^{19}F NMR spectroscopy. ^{19}F NMR (376.313 MHz, CD_2Cl_2): δ = 119.5 (bs, 0.38F), 118.8 (bs, 1F), 113.3 (bs, 0.13F), 106.0 (d, J = 42.9 Hz, 0.59F), -121.6 (bs, 0.5F), -128.1 (s, 0.03F), -138.0 (bt, 0.27F), -146.2 (d, J = 97.5 Hz, 1.82F), -152.1 (s, small), -153.8 (d, J = 118.5 Hz, 31.8F), -157.6 (s, SiMe3F, 31.2F), -170.6 (s, 0.3F), -209.5 (bs, 0.22F), -216.4(t, J = 31-33 Hz, 1.7F), -225.3 (s, 0.28F), -252.5 (d, J = 165.6 Hz, 1.3F), -252.9 (t, J = 171-181 Hz, 3.3F), -

300.7 (d, J = 171.6 Hz, 2.09F), -303.6 (d, J = 174.6 Hz, 0.97F), -351.9 (d, J = 96.3 Hz, 0.59F), -360 (d, J = 102.4 Hz, 0.26F), -367 (bs, 0.92F), -400.4 (d, J = 102.4 Hz, 0.26F), -441.6 (s, 0.31F), -448.0 (s, 0.55F)

Attempts to synthesize [Ru(C-*p*-C_6H_4Me)(H_2IMes)(PCy_3)Cl_2F] (6.15). Method 1: A stock solution of **6.8-Cl** (101.7 mg, 0.1648 mmol) was dissolved in 4.0 mL of CD_2Cl_2 and split into 0.8 mL portions (20.34 mg, 0.0330 mmol, 1.00 equiv). The reaction mixture was mixed with tricyclohexylphosphine (9.3 mg, 0.033 mmol, 1.0 equiv) and then added to dry TAS-F ($[S(NMe_2)_3][F_2SiMe_3]$; 11.3 mg, 0.0410, 1.23 equiv). An immediate color change from orange to dark red was observed. The mixture sat for 10 minutes after which NMR data was acquired. ^{19}F NMR (376.313 MHz, CD_2Cl_2): δ = 131.0 (s, 1F), -62.5 (s, 0.06F), -64.2 (s, 0.08F), -128.0 (s, 0.04F), -153.7 (bs, 4.19F), -157 (s, TMSF, 7F), -192.6 (m, 1.12F), -197.8 (d, $^2J_{PF}$ = 53.4 Hz, 2.43F), -377.8 (d, J = 100 Hz, 0.46F). ^{31}P NMR (161.922 MHz, CD_2Cl_2): δ = 24.3 (s), 24.3 (d, $^2J_{PF}$ = 51.5 Hz, overlapping 76% total), 17.5 (d, 10%), 11.07 (free PCy_3, 14%). Method 2: Compound **6.6** (20 mg, 0.024 mmol, 1.0 equiv) was dissolved in 1 mL of CD_2Cl_2 and α-fluoro-*p*-methylstyrene (3.8 mg, 0.028 mmol, 1.2 equiv) was added. The reaction mixture was allowed to sit at room temperature over two weeks. After the 4 hours: ^{31}P NMR (161.922 MHz, CD_2Cl_2): δ = 41.0 (unknown byproduct, 3%), 30.0 (**6.6**, 67%), 24.3 (s, **6.16**, 8%), 24.3 (d, 6.15, $^2J_{PF}$ = 52 Hz, 16%) 21.3 (unknown byproduct, 2%). ^{19}F NMR (376.313 MHz, CD_2Cl_2): δ = 131 (s, **6.16**), -62 (s, small), -106 (α-fluoro-p-methylstyrene), -198 (bs, **6.15**). After 3 days: ^{31}P NMR (161.922 MHz, CD_2Cl_2): δ = 41.0 (unknown byproduct, 22%), 24.3 (s, **6.16**, 16.6%), 24.3 (d, 6.15, $^2J_{PF}$ = 52 Hz, 50%) 21.3 (unknown byproduct, 11%). ^{19}F NMR (376.313 MHz, CD_2Cl_2): δ = 131 (s, **6.16**), -

63 (dd, F_2PCy_3), -106 (α-fluoro-p-methylstyrene), -198 (bs, **6.15**). After 2 weeks in solution, the ^{31}P and ^{19}F NMR spectrum looked identical to the 3 day spectrum.

Attempts to synthesize [Ru(C-*p*-C_6H_4Me)(H_2IMes)(PCy_3)ClF_2]. A stock solution of **6.8-Cl** (101.7 mg, 0.1648 mmol) was dissolved in 4.0 mL of CD_2Cl_2 and split into 0.8 mL portions (20.34 mg, 0.0330 mmol, 1.00 equiv). The reaction mixture was mixed with tricyclohexylphosphine (17.9 mg, 0.0650 mmol, 1.97 equiv) and then added to dry TAS-F ($[S(NMe_2)_3][F_2SiMe_3]$; 11.3 mg, 0.0410, 1.23 equiv). An immediate color change from orange to brown was observed. The mixture sat for 10 minutes after which NMR data was acquired. ^{19}F NMR (376.313 MHz, CD_2Cl_2): δ = 131.0 (s, 1F), -62.5 (s, 0.08F), -64.2 (s, 0.08F), -153.7 (d, 11.3F), -157 (s, TMSF, 7.8F), -191.2 (dd, 0.25F), -192.6 (dd, J = 51.2 Hz, 103.5 Hz, 0.43F), -377.8 (d, J = 100 Hz, 0.19F). ^{31}P NMR (161.922 MHz, CD_2Cl_2): δ = 24.3 (s, 67.5%), 17.5 (d, 7.6%), 11.07 (free PCy_3, 23.8%).

Attempts to synthesize [Ru(C-*p*-C_6H_4Me)(H_2IMes)(PCy_3)F_3]. A stock solution of **6.8-Cl** (101.7 mg, 0.1648 mmol) was dissolved in 4.0 mL of CD_2Cl_2 and split into 0.8 mL portions (20.34 mg, 0.0330 mmol, 1.00 equiv). The reaction mixture was mixed with tricyclohexylphosphine (9.3 mg, 0.033 mmol, 1.0 equiv) and then added to dry TAS-F ($[S(NMe_2)_3][F_2SiMe_3]$; 11.3 mg, 0.0410, 1.23 equiv). An immediate color change from orange to dark red was observed. The mixture sat for 10 minutes after which NMR data was acquired. Multiple products were observed by ^{19}F NMR spectroscopy. ^{19}F NMR (376.313 MHz, CD_2Cl_2): δ = 131.0 (s, 0.56F), -63.3 (d, J = 637 Hz, 0.03F), -143.9

(quintet, 0.40F), -153.6 (d, $[FHF]^-$, impurity in TAS-F, 25F), -170.6 (quintet, 1.2F), -204.3 (d, J = 35.3 Hz, 0.24F). ^{31}P NMR (161.922 MHz, CD_2Cl_2): δ = 24.8 (s, 45.8%), 18.0 (d, 32.5%), 11.07 (free PCy_3, 21.6%). One possible identity of the peak at ^{31}P δ 18.0 ppm and ^{19}F δ -204.3 ppm is [Ru(CH-*p*-C_6H_4Me)(H_2IMes)(PCy_3)F_2Cl]. It is also possible that [FHF] is coordinating as a ligand.

6.7. References

1. Schrock, R. R., High oxidation state multiple metal-carbon bonds. *Chemical Reviews* **2002,** *102* (1), 145-179.
2. Furstner, A.; Davies, P. W., Alkyne metathesis. *Chem. Commun.* **2005,** (18), 2307-2320.
3. Zhang, W.; Kraft, S.; Moore, J. S., Highly active trialkoxymolybdenum(VI) alkylidyne catalysts synthesized by a reductive recycle strategy. *J. Am. Chem. Soc.* **2004,** *126* (1), 329-335.
4. Gdula, R. L.; Johnson, M. J. A., Highly Active Molybdenum-Alkylidyne Catalysts for Alkyne Metathesis: Synthesis from the Nitrides by Metathesis with Alkynes. *J. Am. Chem. Soc.* **2006,** *128*, 9614-9615.
5. Zhang, W.; Moore, J. S., Alkyne metathesis: Catalysts and synthetic applications. *Adv. Synth. Catal.* **2007,** *349* (1-2), 93-120.
6. Bunz, U. H. F., Poly(p-phenyleneethynylene)s by alkyne metathesis. *Accounts Chem. Res.* **2001,** *34* (12), 998-1010.
7. Gonzalez-Herrero, P.; Weberndorfer, B.; Ilg, K.; Wolf, J.; Werner, H., The sensitive balance between five-coordinate carbene and six-coordinate carbyne ruthenium complexes formed from ruthenium vinylidene precursors. *Organometallics* **2001,** *20* (17), 3672-3685.
8. Jung, S.; Brandt, C. D.; Werner, H., A cationic allenylideneruthenium(II) complex with two bulky hemilabile phosphine ligands. *New Journal of Chemistry* **2001,** *25* (9), 1101-1103.
9. Gonzalez-Herrero, P.; Weberndorfer, B.; Ilg, K.; Wolf, J.; Werner, H., The first example of an equilibrium between a carbene and an isomeric carbyne transition metal complex. *Angew. Chem.-Int. Edit.* **2000,** *39* (18), 3266-+.
10. Stüer, W.; Wolf, J.; Werner, H.; Schwab, P.; Schulz, M., Carbynehydridoruthenium complexes as catalysts for the selective, ring-opening metathesis of cyclopentene with methyl acrylate. *Angew. Chem.-Int. Edit.* **1998,** *37* (24), 3421-3423.
11. Castarlenas, R.; Eckert, M.; Dixneuf, P. H., Alkenylcarbene ruthenium arene complexes as initiators of alkene metathesis: An enyne creates a catalyst that promotes its selective transformation. *Angew. Chem.-Int. Edit.* **2005,** *44* (17), 2576-2579.
12. Castarlenas, R.; Vovard, C.; Fischmeister, C.; Dixneuf, P. H., Allenylidene-to-indenylidene rearrangement in arene-ruthenium complexes: A key step to highly active catalysts for olefin metathesis reactions. *J. Am. Chem. Soc.* **2006,** *128* (12), 4079-4089.
13. Rigaut, S.; Touchard, D.; Dixneuf, P. H., Amphoteric allenylidene ruthenium complexes and the first dinuclear ruthenium species with a bis-alkenyl carbyne bridging ligand. *Organometallics* **2003,** *22* (20), 3980-3984.
14. Bustelo, E.; Jiménez-Tenorio, M.; Mereiter, K.; Puerta, M. C.; Valerga, P., Reactivity of the electron-rich allenylidene-ruthenium complexes [Cp*Ru{=C=C=C(R)Ph}(dippe)][BPh4] (R = H, Ph). X-ray crystal structure of a novel dicationic ruthenium carbyne (CP* = C5Me5; dippe=1,2-bis(diisopropylphosphine)ethane). *Organometallics* **2002,** *21* (9), 1903-1911.

15. Beach, N. J.; Jenkins, H. A.; Spivak, G. J., Electrophilic attack on [Cp*Cl(PPh3)Ru(CCHR)]: Carbyne formation vs chloride abstraction. *Organometallics* **2003,** *22* (25), 5179-5181.
16. Beach, N. J.; Walker, J. M.; Jenkins, H. A.; Spivak, G. J., Ruthenium vinylidene and carbyne complexes containing a multifunctional tridentate ligand with a PNN donor set. *Journal of Organometallic Chemistry* **2006,** *691* (19), 4147-4152.
17. Beach, N. J.; Williamson, A. E.; Spivak, G. J., A comparison of Cp*- and Tp-ruthenium carbyne complexes prepared via site selective electrophilic addition to neutral ruthenium vinylidenes. *Journal of Organometallic Chemistry* **2005,** *690* (21-22), 4640-4647.
18. Cadierno, V.; Díez, J.; García-Garrido, S. E.; Gimeno, J., Efficient one-pot synthesis of alpha,beta-unsaturated carbyne complexes fac-[RuX3{ CC(H)= CR2}(dppf)] (X = Cl, Br; R = aryl, alkyl; dppf=1,1 '-bis(diphenylphosphino)ferrocene). *Organometallics* **2005,** *24* (13), 3111-3117.
19. Coalter, J. N.; Bollinger, J. C.; Eisenstein, O.; Caulton, K. G., R-Group reversal of isomer stability for RuH(X)L-2(CCHR) vs. Ru(X)L-2(CCH2R): access to four-coordinate ruthenium carbenes and carbynes. *New Journal of Chemistry* **2000,** *24* (12), 925-927.
20. Amoroso, D.; Snelgrove, J. L.; Conrad, J. C.; Drouin, S. D.; Yap, G. P. A.; Fogg, D. E., An attractive route to olefin metathesis catalysts: Facile synthesis of a ruthenium alkylidene complex containing labile phosphane donors. *Adv. Synth. Catal.* **2002,** *344* (6-7), 757-763.
21. Conrad, J. C.; Amoroso, D.; Czechura, P.; Yap, G. P. A.; Fogg, D. E., The first highly active, halide-free ruthenium catalyst for olefin metathesis. *Organometallics* **2003,** *22* (18), 3634-3636.
22. Roper, W. R., Platinum Group-Metals in the Formation of Metal-Carbon Multiple Bonds. *Journal of Organometallic Chemistry* **1986,** *300* (1-2), 167-190.
23. Roper, W. R., Carbyne Complexes of Ruthenium and Osmium. In *Transition Metal Carbyne Complexes*, Kreibl, F. R., Ed. Kluwer: Boston, 1993; Vol. 392, pp 155-168.
24. Roper, W. R.; Wright, A. H., Reactions of a Dichlorocarbene-Ruthenium Complex, Rucl2(Ccl2)(Co)(Pph3)2. *Journal of Organometallic Chemistry* **1982,** *233* (3), C59-C63.
25. Gallop, M. A.; Roper, W. R., Carbene and Carbyne Complexes of Ruthenium, Osmium, and Iridium. *Advances in Organometallic Chemistry* **1986,** *25*, 121-198.
26. Baker, L. J.; Clark, G. R.; Rickard, C. E. F.; Roper, W. R.; Woodgate, S. D.; Wright, L. J., Syntheses and reactions of the carbyne complexes, M(CR)Cl(CO)(PPh3)(2) (M = Ru, Os; R = 1-naphthyl, 2-naphthyl). The crystal structures of [Os(C-1-naphthyl)(CO)(2)(PPh3)(2)]ClO4, Os(=CH-2-naphthyl)Cl-2(CO)(PPh3)(2), and Os(2-naphthyl)Cl(CO)(2)(PPh3)(2). *Journal of Organometallic Chemistry* **1998,** *551* (1-2), 247-259.
27. Wright, A. H. Ph.D. Thesis. Ph.D. Thesis, University of Auckland, Auckland, New Zealand, 1983.
28. Clark, G. R.; Cochrane, C. M.; Marsden, K.; Roper, W. R.; Wright, L. J., Synthesis and Some Reactions of a Terminal Carbyne Complex of Osmium - Crystal-

Structures of Os(=Cr)Cl(Co)(Pph3)2 and Os(=C[Agcl]R)Cl(Co)(Pph3)2. *Journal of Organometallic Chemistry* **1986,** *315* (2), 211-230.
29. Clark, G. R.; Edmonds, N. R.; Pauptit, R. A.; Roper, W. R.; Waters, J. M.; Wright, A. H., Octahedral Carbyneosmium(Ii) Complexes. *Journal of Organometallic Chemistry* **1983,** *244* (4), C57-C60.
30. Clark, G. R.; Marsden, K.; Roper, W. R.; Wright, L. J., An Osmium-Carbene Complex. *J. Am. Chem. Soc.* **1980,** *102* (21), 6570-6571.
31. Caskey, S. R. Exploration of Ruthenium Carbon Multiple Bond Complexes: Carbenes, Carbynes, and Carbides. Ph.D., University of Michigan, Ann Arbor, 2007.
32. Caskey, S. R.; Stewart, M. H.; Ahn, Y. J.; Johnson, M. J. A.; Rowsell, J. L. C.; Kampf, J. W., Synthesis, Structure, and Reactivity of Four-, Five-, and Six-Coordinate Ruthenium Carbyne Complexes. *Organometallics* **2007,** *26*, 1912-1923.
33. Macnaughtan, M. L.; Johnson, M. J. A.; Kampf, J. W., Synthesis, Structure, and Olefin Metathesis Activity of Two Ruthenium Monofluoromethylidene Complexes. *Organometallics* **2007,** *26* (4), 780-782.
34. Macnaughtan, M. L.; Johnson, M. J. A.; Kampf, J. W., Olefin Metathesis Reactions with Vinyl Halides: Formation, Observation, Interception, and Fate of the Ruthenium-Monohalomethylidene Moiety. *J. Am. Chem. Soc.* **2007,** *129* (25), 7708-7709.
35. Sanford, M. S.; Love, J. A.; Grubbs, R. H., Mechanism and activity of ruthenium olefin metathesis catalysts. *J. Am. Chem. Soc.* **2001,** *123* (27), 6543-6554.
36. Sanford, M. S.; Ulman, M.; Grubbs, R. H., New insights into the mechanism of ruthenium-catalyzed olefin metathesis reactions. *J. Am. Chem. Soc.* **2001,** *123* (4), 749-750.
37. Sanford, M. S. Synthetic and Mechanistic Investigations of Ruthenium Olefin Metathesis Catalysts. Ph. D., California Institute of Technology, Pasadena, CA, 2001.
38. Schwab, P.; Grubbs, R. H.; Ziller, J. W., Synthesis and applications of RuCl2(=CHR')(PR(3))(2): The influence of the alkylidene moiety on metathesis activity. *J. Am. Chem. Soc.* **1996,** *118* (1), 100-110.
39. Trnka, T. M.; Morgan, J. P.; Sanford, M. S.; Wilhelm, T. E.; Scholl, M.; Choi, T. L.; Ding, S.; Day, M. W.; Grubbs, R. H., Synthesis and activity of ruthenium alkylidene complexes coordinated with phosphine and N-heterocyclic carbene ligands. *J. Am. Chem. Soc.* **2003,** *125* (9), 2546-2558.
40. Carlson, R. G.; Gile, M. A.; Heppert, J. A.; Mason, M. H.; Powell, D. R.; Vander Velde, D.; Vilain, J. M., The metathesis-facilitated synthesis of terminal ruthenium carbide complexes: A unique carbon atom transfer reaction. *J. Am. Chem. Soc.* **2002,** *124* (8), 1580-1581.
41. Gottlieb, H. E.; Kotlyar, V.; Nudelman, A., NMR chemical shifts of common laboratory solvents as trace impurities. *J. Org. Chem.* **1997,** *62* (21), 7512-7515.
42. Pangborn, A. B.; Giardello, M. A.; Grubbs, R. H.; Rosen, R. K.; Timmers, F. J., Safe and convenient procedure for solvent purification. *Organometallics* **1996,** *15* (5), 1518-1520.
43. Jung, M. E.; Light, L. A., Intramolecular Diels-alder Cyclo-additions of Perchloro(allyoxy)-cyclopentadienes and Perchlorobis(allyloxycyclopentadienes. *J. Org. Chem.* **1982,** *47* (6), 1084-1090.

44. Rosen, T. C.; Yoshida, S.; Frohlich, R.; Kirk, K. L.; Haufe, G., Fluorinated phenylcyclopropylamines. 2. Effects of aromatic ring substitution and of absolute configuration on inhibition of microbial tyramine oxidase. *Journal Of Medicinal Chemistry* **2004,** *47* (24), 5860-5871.

Chapter 7

Conclusions and Future Directions

7.1. Conclusions

Olefin metathesis (OM) is the formation of new carbon-carbon double bonds from pre-existing alkenes. OM has become a widely used tool in organic, industrial and polymer chemistry.[1-3] Current ruthenium catalysts tolerate a wide range of functional groups; however, metathesis reactions employing vinyl halides as well as other α-heteroatom-substituted olefins were not tolerated by ruthenium catalysts in cross metathesis (CM) reactions.[4-6] Our initial thesis goal was to develop methods that would allow for the formation of alkenyl halides[7] from vinyl halides in CM reactions. Effective cross metathesis, ring-opening metathesis and enyne metathesis with chlorinated olefins was accomplished by employing a catalyst with no second neutral ligand.[8,9] Vinyl fluoride participated in ring-opening metathesis and enyne metathesis.[8-10] A number of 1-fluoro-(2,)3-substituted-1,3-butadienes were synthesized through enyne metathesis with vinyl fluoride and characterized. Unfortunately, vinyl fluoride did not participate to a high degree in CM because the monofluoromethylidene intermediate was too thermodynamically stable with respect to Ru alkylidene complexes.[10,11] Fischer carbene complexes will interconvert and are thermoneutral. Fischer carbene cross-metathesis allows for productive CM of a number of directly functionalized olefins including vinyl fluoride with alkenes that are functionalized with an acetate group, increasing the

substrate scope of CM to include electron-rich olefins. Finally, the decomposition mode of the monohalomethylidene complexes studied led to facile synthesis of a number of 2nd generation Ru-benzylidyne complexes.

7.1.1. Ruthenium Monohalomethylidene Complexes

Initially, a variety of ruthenium monohalomethylidene complexes (Chart 7.1: **7.7-7.9**; X = F or Cl) were synthesized and studied to understand and address the challenges of vinyl halides in CM reactions.[8,9] Our published studies of compounds **7.7-7.9** (Chart 7.1; X = F or Cl) revealed two challenges for CM with vinyl halides. First, ruthenium monofluoromethylidene compounds (**7.7-7.9**; X = F) are thermodynamically stable relative to their Ru-alkylidene counterparts (*e.g.*, **7.1, 7.2**) and are not active intermediates in the CM cycle,[8] akin to compound **7.7-OEt**.[6] Secondly, carbon-halogen bond lability at the ruthenium carbene moiety ([Ru]CHX, X = F, Cl, Br) results in formation of the inactive carbide complex (**7.5**)[12] and/or the phosphoniomethylidene complex (**7.6**, Scheme 7.1).[9]

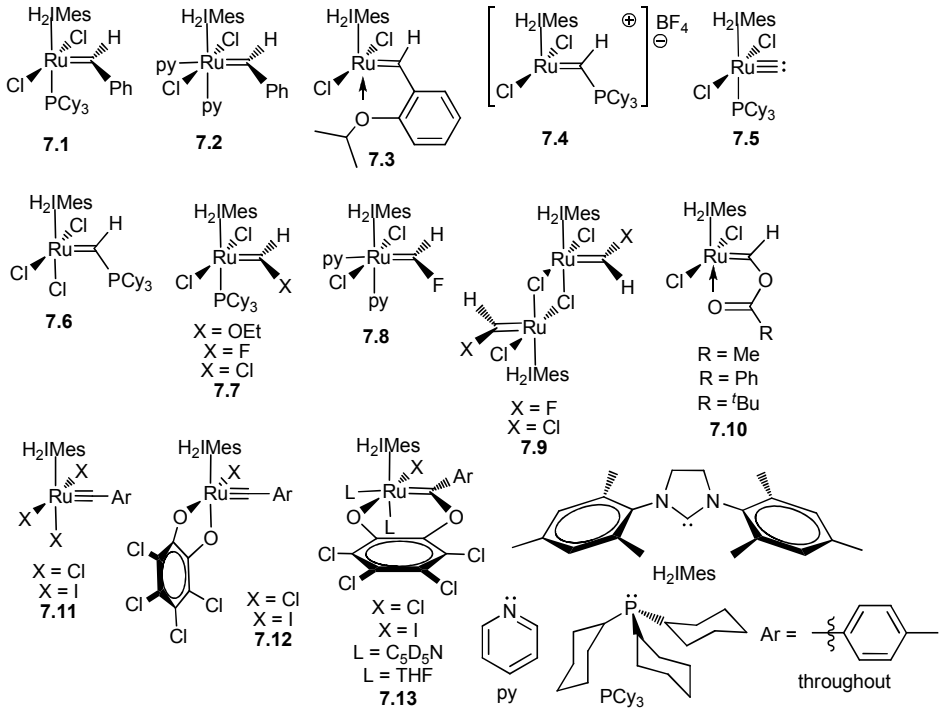

Chart 7.1. Some Important Ruthenium Complexes.

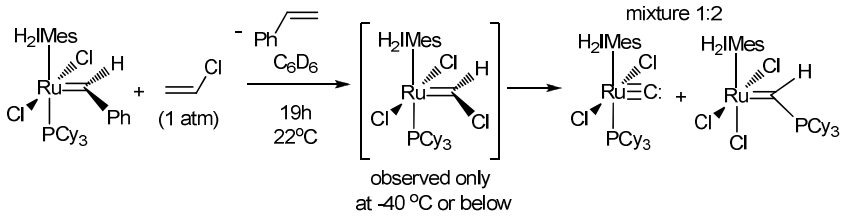

Scheme 7.1. Products of Monochloromethylidene Deactivation.[9]

However, the Ru-monochloromethylidene moiety can be stabilized by removal of a stong σ-donating neutral ligand (*e.g.*, PCy_3). Stoichiometric metathesis with **7.3** and vinyl chloride yields the μ-chloro dimer **7.9-Cl**, which is isolable and longer-lived in solution than the tricyclohexylphosphine adduct, **7.7-Cl**.[8]

7.1.2. Cross-Metathesis (CM) with Vinyl Halides.[8]

Phosphine-free catalyst **7.3** allows for productive CM of 1,2-dichloroethene with unhindered alkenes in good yields (Scheme 7.2). Conversion to the alkenyl chloride product is highly dependent on the metathesis activity of the alkene. The only alkenes that participate in CM with chlorinated olefins are those whose homodimer is also highly active for CM (*e.g.*, 1-hexene to 5-decene). Overall, 1,2-dichloroethene is a better reagent than vinyl chloride.

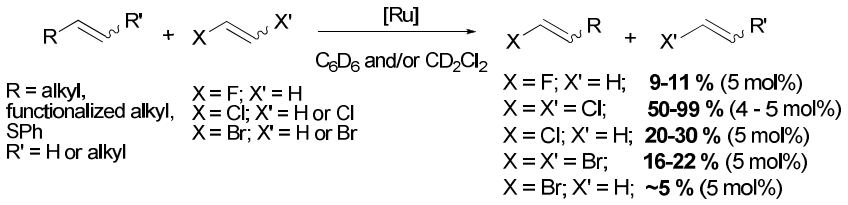

Scheme 7.2. Cross-Metathesis (CM) with Halogenated Olefins

Unfortunately, yields for CM reactions of 1,2-dibromoethene or vinyl bromide with assorted alkenes are still low, indicating that rapid catalyst decomposition still prevents productive CM with brominated olefins even when using catalyst **7.3.** CM attempts of vinyl fluoride with simple alkenes show only low conversion to alkenyl fluoride products (9-11 %; Scheme 7.2) independent of catalyst choice (**7.1, 7.2, 7.3** or **7.4**). In these cases, it is not catalyst deactivation that hinders CM but the thermodynamic stability of the monofluoromethylidene intermediate (**7.7-7.9**; X = F). Ring-opening CM of cyclooctene with vinyl fluoride is more favorable (55 %; Scheme 7.3). Release of ring strain provides an enthalpic driving force for return to the alkylidene form of the catalyst, thus encouraging productive CM.

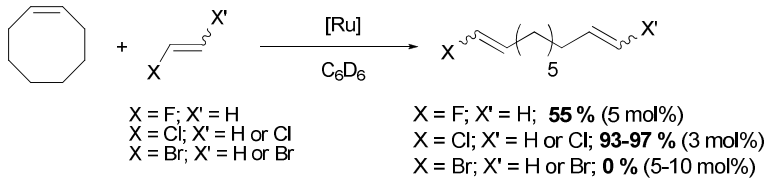

Scheme 7.3. Ring-Opening CM with Halogenated Olefins

7.1.3. Enyne Metathesis (EyM) with Vinyl Halides.

Enyne metathesis (EyM) is the insertion of an alkyne into an olefin *via* a Ru catalyst to form substituted-1,3-butadienes.[13] Vinyl halides participate in EyM reactions to form *E/Z* 1-halo-2,3-substituted-1,3-butadienes in high yields (Scheme 7.4). These reactions afforded a number of rare compounds of the form 1-fluoro-(2,)3-substituted-1,3-butadiene.

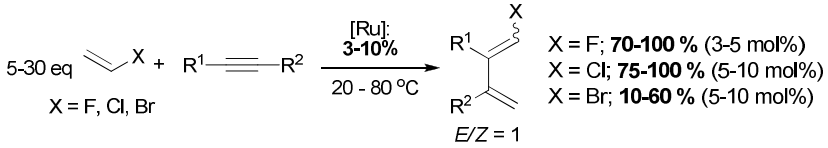

Scheme 7.4. Enyne Metathesis with Vinyl Halides

Several alkynes are tolerated including but not limited to 3-hexyne, phenylacetylene, diphenylacetylene, trimethylsilylacetylene, and propargyl benzoate. Terminal alkynes formed the 1-halo-3-substituted isomer with >95% regioselectivity. The *E/Z* ratio of butadiene products was usually around unity with the exception of 1-fluoro-2,3-diphenyl-1,3-butadiene which had an *E/Z* ratio of 5. Vinyl fluoride gave

excellent yields with catalysts **7.1** though **7.4**. High yields with vinyl chloride were obtained with only catalyst **7.3.** Yields for vinyl bromide were low.

7.1.4. Fischer to Fischer Cross-Metathesis (FCM)

Olefins with α-heteroatom-substituents do not undergo CM with other alkenes because their corresponding Fischer carbene complexes (*e.g.,* **7.7**; X = OEt or F and **7.10**) are thermodynamically stable with respect Ru-alkylidene complexes. However, Fischer carbene complexes can be interconverted.[6,10] Using this principle, CM with electron-rich olefins is possible by altering the second alkene substrate (Scheme 7.5). Using β-acetate-functionalized alkenes allows for productive CM with ethyl vinyl ether, phenyl- or ethyl vinyl sulfide, vinyl benzoate, vinyl pivalate, *N*-vinyl-pyrrolidinone, or vinyl fluoride using catalyst **7.3**. As with other CM reactions, Fischer CM reactions are in equilibrium and so excess functionalized olefin is used.

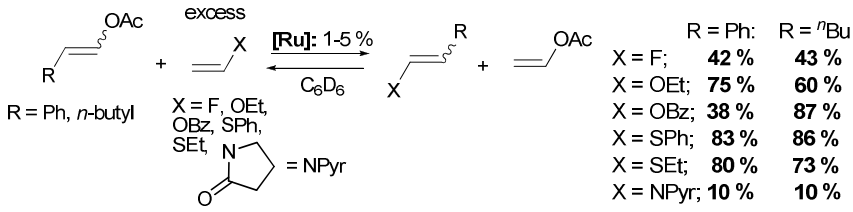

Scheme 7.5. FCM with a Variety of Directly Functionalized Olefins.

7.1.5. Facile Synthesis of Ruthenium Benzylidyne Complexes

Alkyne metathesis (AM) has been restricted for the most part to W and Mo alkylidyne catalysts.[14,15] Because Ru is less oxophilic than W and Mo, AM with Ru catalysts would expand functional group tolerance and solvent choices. However, very few Ru alkylidyne compounds have displayed any alkyne metathesis activity.[16,17] The

propensity of the carbon-halogen bond on the Ru-carbene moiety to cleave allows for direct access to new Ru-benzylidyne species **7.7-Cl** (Scheme 7.6). Ligand substitution attempts with alkoxides and aryloxides have been somewhat successful. Both reversible and irreversible ligand migration was observed between the Ru and α-carbon. Reaction conditions can be tuned so that the tetrachlorocatecholate ligand binds η^2 to the Ru-center (**7.12**) or binds η^1-Ru/η^1-α-C (**7.13**).

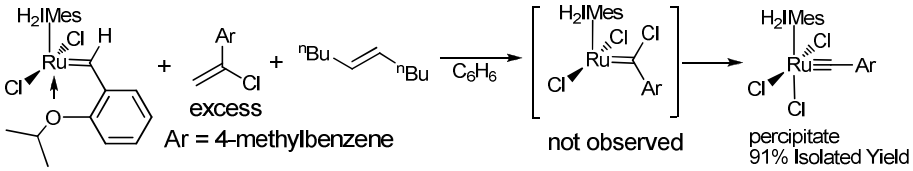

Scheme 7.6. Synthesis of a Ruthenium Benzylidyne Compound

7.2. Future Directions

This project has been extremely fruitful and has generated a great deal of results in an area of metathesis that had not until now been fully explored. These exciting results have also generated a great deal of questions still to be answered particularly in the case of Chapter 5 and Chapter 6.

7.2.1. Metathesis with Vinyl Halides

Enyne metathesis and ring-opening cross metathesis with vinyl fluoride and vinyl chloride give excellent yields and should be highly useful for organic syntheses with the current catalysts. Cross-metathesis of simple alkenes with vinyl chloride and 1,2-dichloroethylene also gives reasonable to excellent yields; however, at this time, the

substrate scope for alkenes that will participate in CM with chlorinated olefins is limited to highly-active alkenes. In addition, metathesis reactions with vinyl bromides still give only low yields of product if they work at all. In order to increase substrate scope for CM with chlorinated olefins and begin to use brominated olefins more effectively in metathesis reactions, new catalysts will need to be synthesized. Catalyst design should be focused on making the 2nd generation Blechert/Hoveyda-Grubbs catalyst, **7.3**, with more electron-withdrawing ligands. This can be accomplished by placing electron-withdrawing groups on either the *N*-heterocyclic carbene backbone and/or on the aryl rings of the NHC ligand (Figure 7.1). This should help to further stabilize the ruthenium monohalomethylidene complex with respect to decomposition through C-X bond scission.

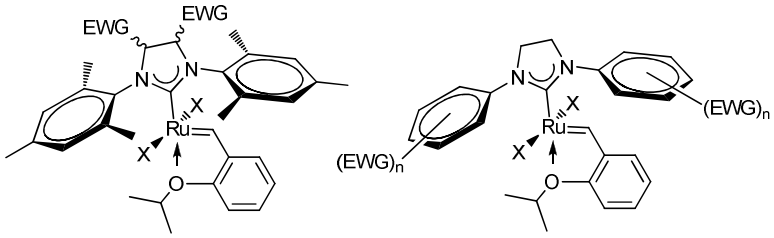

Figure 7.1. Placement of Electron-Withdrawing Groups on the NHC Ligand.

7.2.2. Metathesis with Electron-Rich Olefins

For the first time, we have demonstrated catalytic cross-metathesis of alkenes with electron-rich olefins such as ethyl vinyl ether, ethyl- and phenyl vinyl sulfide and vinyl fluoride. This was accomplished by alteration of the alkene substrate so that the metathesis can go through a Fischer-to-Fischer carbene mechanism. The ability to now use electron-rich olefins in Fischer-to-Fischer cross-metathesis (FCM) opens a new subfield in olefin metathesis chemistry. For FCM, further substrate scope testing and

optimization is needed. Also, elucidation of the factors controlling the equilibrium of the system is needed in order to determine how to drive the system to complete product formation. A great deal of experimental and computational work will be needed to accomplish this task. Future goals for this chemistry also include testing FCM as a selection tool to selectively functionalize one olefin in a molecule with multiple olefinic sites. Ring-opening metathesis (FROM) of a heterocyclic alkene to form an acyclic diene with specific regiochemistry should be feasible (Eq. 7.1).

(7.1)

Ring-closing metathesis (FRCM) to form new heterocyclic alkenes could also prove extremely useful (Eqs. 7.2 and 7.3).

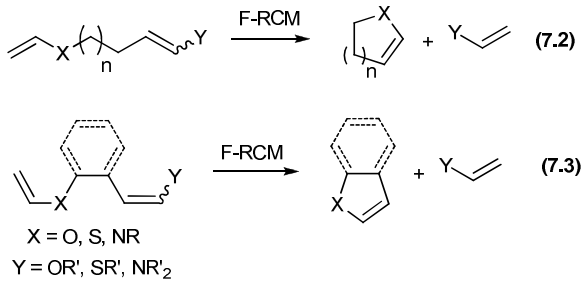

(7.2)
(7.3)

Finally, polymerization reactions could be tuned to form polymers with very precise regiochemistry incorporating heteroatoms into the main polymer chain (Eq. 7.4). We have just begun to explore the possibilities of Fischer to Fischer metathesis.

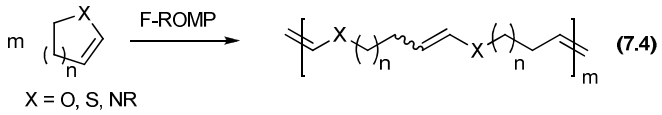

(7.4)

7.2.3. Ruthenium Benzylidyne Chemistry

A strong focus should be placed on the development of a Ru-based alkyne metathesis catalyst. To this end, we have developed a facile synthesis to form a 2nd generation benzylidyne complex and have accessed a number of Ru-benzylidyne complexes through ligand substitution. Certainly, Ru-alkylidyne chemistry is in its infancy. The reactivity of the Ru-benzylidyne complexes discussed in Chapter 6 was unique. The demonstration of reversible and irreversible Ru-αC ligand migration should be taken into consideration when designing Ru-based AM catalyst. Ultimately, the reversible migration of the catecholate ligand (**7.12** and **7.13**) or similar ligands may prove useful for alkyne metathesis. Firstly, they may help to stabilize the Ru-center towards removal of a neutral ligand in order to open a binding site for an alkyne. In our case, removal of H_2IMes ligand; this will most likely require brute force (Scheme 7.7). Secondly, the reversible migration of catecholate could be employed as an on/off switch for AM, in which the η^1-α-carbon-bound form by addition of a weakly ligating solvent would turn the AM activity off and removal of the ligands would cause the catecholate to migrate to η^2-Ru bound and reform the active catalyst. This could prove extremely useful.

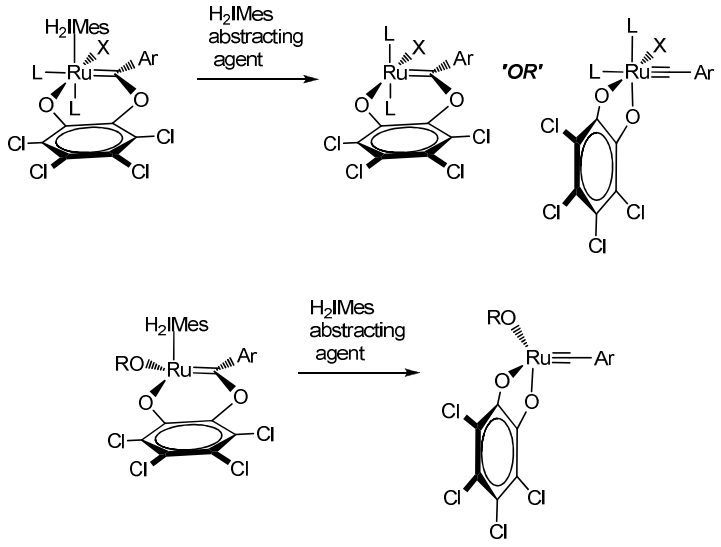

Scheme 7.7. Speculative Removal of H_2IMes

Irreversible ligand migration would be undesirable for Ru-alkylidyne catalysts as it would be detrimental to alkyne metathesis. Ligand choice for the alkyne metathesis catalyst will be very important for this reason as well as more obvious reasons such as activity of the catalyst. One possible way to prevent this type of migration is to use tridentate trianion ligands. Tethering the ancilliary ligands together will help to prevent migration through steric constraints.

At this point, treatment of different Ru-benzylidyne complexes with an activator and two alkynes to test for alkyne metathesis activity should be tested. Further attempts at ligand substitutions and removal of the PCy_3 or NHC ligand from 5-coordinate Ru-benzylidyne complexes should be investigated.

7.3. References

1. Trnka, T. M.; Grubbs, R. H., The development of L2X2Ru = CHR olefin metathesis catalysts: An organometallic success story. *Accounts Chem. Res.* **2001,** *34* (1), 18-29.
2. Fürstner, A., Olefin metathesis and beyond. *Angew. Chem.-Int. Edit.* **2000,** *39* (17), 3013-3043.
3. Grubbs, R. H., *Handbook of Metathesis*. Wiley-VCH: Weinheim, 2003; Vol. 1-3.
4. Morrill, C.; Grubbs, R. H., Synthesis of functionalized vinyl boronates via ruthenium-catalyzed olefin cross-metathesis and subsequent conversion to vinyl halides. *J. Org. Chem.* **2003,** *68* (15), 6031-6034.
5. Trnka, T. M.; Day, M. W.; Grubbs, R. H., Olefin metathesis with 1,1-difluoroethylene. *Angew. Chem.-Int. Edit.* **2001,** *40* (18), 3441-+.
6. Louie, J.; Grubbs, R. H., Metathesis of Electron-Rich Olefins: Structure and Reactivity of Electron-Rich Carbene Complexes. *Organometallics* **2002,** *21*, 2153.
7. Tsuji, J., Reactions of Organic Halides and Pseudohalides. In *Transition Metal Reagents and Catalysts: Innovations in Organic Synthesis*, Wiley: New York, 2000; pp 27-108.
8. Macnaughtan, M. L.; Gary, J. B.; Gerlach, D. L.; Johnson, M. J. A.; Kampf, J. W., Cross-Metathesis of Vinyl Halides. Scope and Limitations of Ruthenium-based Catalysts. *Organometallics* **2009,** *ASAP*.
9. Macnaughtan, M. L.; Johnson, M. J. A.; Kampf, J. W., Olefin Metathesis Reactions with Vinyl Halides: Formation, Observation, Interception, and Fate of the Ruthenium-Monohalomethylidene Moiety. *J. Am. Chem. Soc.* **2007,** *129* (25), 7708-7709.
10. Macnaughtan, M. L.; Johnson, M. J. A.; Kampf, J. W., Synthesis, Structure, and Olefin Metathesis Activity of Two Ruthenium Monofluoromethylidene Complexes. *Organometallics* **2007,** *26* (4), 780-782.
11. Fomine, S.; Ortega, J. V.; Tlenkopatchev, M. A., Metathesis of halogenated olefins - A computational study of ruthenium alkylidene mediated reaction pathways. *Journal Of Molecular Catalysis A-Chemical* **2007,** *263* (1-2), 121-127.
12. Carlson, R. G.; Gile, M. A.; Heppert, J. A.; Mason, M. H.; Powell, D. R.; Vander Velde, D.; Vilain, J. M., The metathesis-facilitated synthesis of terminal ruthenium carbide complexes: A unique carbon atom transfer reaction. *J. Am. Chem. Soc.* **2002,** *124* (8), 1580-1581.
13. Diver, S. T.; Giessert, A. J., Enyne metathesis (Enyne Bond Reorganization). *Chemical Reviews* **2004,** *104* (3), 1317-1382.
14. Schrock, R. R., High-Oxidation-State Molybdenum and Tungsten Alkylidyne Complexes. *Accounts Chem. Res.* **1986,** *19* (11), 342-348.
15. Furstner, A.; Davies, P. W., Alkyne metathesis. *Chem. Commun.* **2005,** (18), 2307-2320.

16. Caskey, S. R. Exploration of Ruthenium Carbon Multiple Bond Complexes: Carbenes, Carbynes, and Carbides. Ph.D., University of Michigan, Ann Arbor, 2007.
17. Caskey, S. R.; Stewart, M. H.; Ahn, Y. J.; Johnson, M. J. A.; Rowsell, J. L. C.; Kampf, J. W., Synthesis, Structure, and Reactivity of Four-, Five-, and Six-Coordinate Ruthenium Carbyne Complexes. *Organometallics* **2007,** *26*, 1912-1923.

Appendix 1

Crystal Data for [Ru(CHF)(H_2IMes)(PCy_3)Cl_2] (mma)

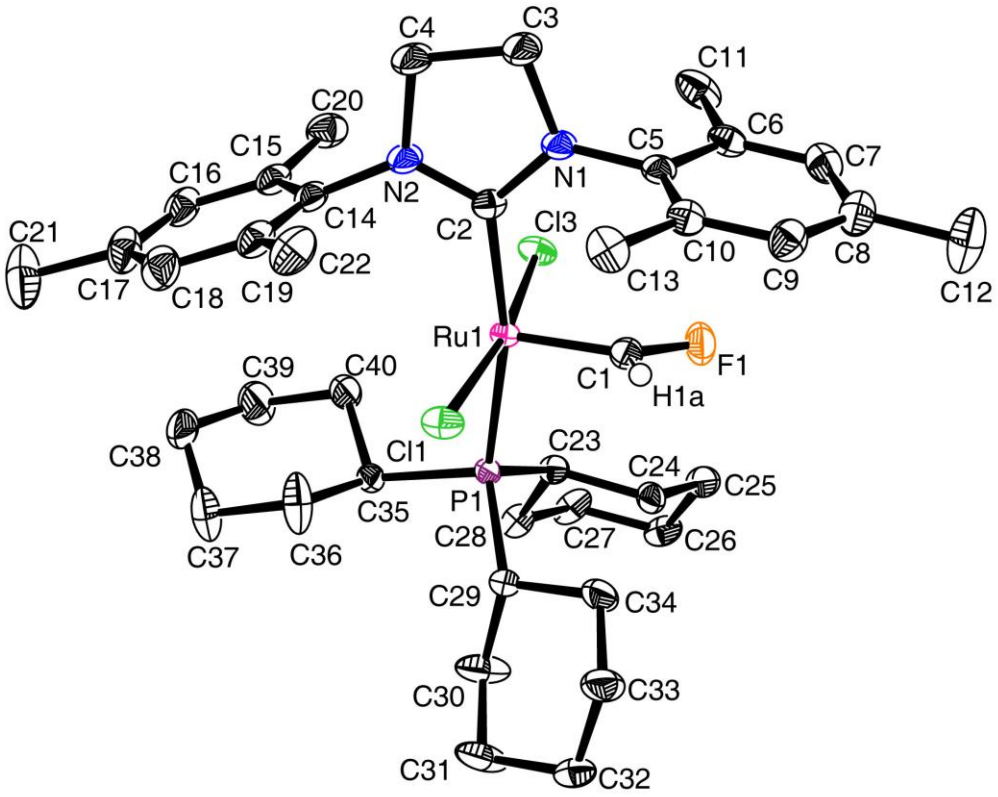

Figure A1.1. X-ray crystal structure of [Ru(CHF)(H_2IMes)(PCy_3)Cl_2] (mma) (50% thermal ellipsoid plot). Hydrogen atoms are omitted for clarity.

A1.1. Structure Determination

Orange prismatic crystals of **mma** were grown from a pentane/benzene (20:1) solution at 28 °C. A crystal of dimensions 0.48 x 0.40 x 0.34 mm was mounted on a

standard Bruker SMART 1K CCD-based X-ray diffractometer equipped with a LT-2 low temperature device and normal focus Mo-target X-ray tube (λ = 0.71073 Å) operated at 2000 W power (50 kV, 40 mA). The X-ray intensities were measured at 108(2) K; the detector was placed at a distance 4.969 cm from the crystal. A total of 4095 frames were collected with a scan width of 0.5° in ω and φ with an exposure time of 10 s/frame. The integration of the data yielded a total of 146343 reflections to a maximum 2θ value of 58.78° of which 12154 were independent and 10539 were greater than $2\sigma(I)$. The final cell constants (**A1.2**) were based on the xyz centroids of 9630 reflections above $10\sigma(I)$. Analysis of the data showed negligible decay during data collection; the data were processed with SADABS and corrected for absorption. The structure was solved and refined with the Bruker SHELXTL (version 6.12) software package, using the space group P2(1)/n with Z = 4 for the formula $C_{40}H_{60}N_2FPCl_2Ru\bullet(C_6H_6)_{0.5}$. All nonhydrogen atoms were refined anisotropically with the hydrogen atoms placed in idealized positions. The fluoro-methylidene is disordered over two positions related by a pseudomirror plane. One cyclohexyl group is also disordered. Full matrix least-squares refinement based on F^2 converged at R1 = 0.0341 and wR2 = 0.0992 [based on $I > 2\sigma(I)$], R1 = 0.0418 and wR2 = 0.1049 for all data. Additional details are presented in **A1.2**.

Sheldrick, G.M. SHELXTL, v. 6.12; Bruker Analytical X-ray, Madison, WI, 2001.

Sheldrick, G.M. SADABS, v. 2.10. Program for Empirical Absorption Correction of Area Detector Data, University of Gottingen: Gottingen, Germany, 2003.

Saint Plus, v. 7.01, Bruker Analytical X-ray, Madison, WI, 2003.

A1.2. Crystal data and structure refinement for mma.

Identification code	mma
Empirical formula	C_{43} H_{63} C_{l2} F N_2 P Ru
Formula weight	829.89
Temperature	108(2) K
Wavelength	0.71073 Å
Crystal system, space group	Monoclinic, P2(1)/n
Unit cell dimensions	a = 11.7509(9) Å alpha = 90 °
	b = 21.2958(15) Å beta = 95.055(4)°
	c = 17.7264(13) Å gamma = 90 °
Volume	4418.7(6) $Å^3$
Z, Calculated density	4, 1.247 Mg/m^3
Absorption coefficient	0.546 mm^{-1}
F(000)	1748
Crystal size	0.48 x 0.40 x 0.34 mm
Theta range for data collection	1.91 to 29.39 deg.
Limiting indices	-16<=h<=16, -29<=k<=29, -24<=l<=24
Reflections collected / unique	146343 / 12154 [R(int) = 0.0396]
Completeness to θ = 29.39	99.7 %
Absorption correction	Semi-empirical from equivalents
Max. and min. transmission	0.8361 and 0.7796
Refinement method	Full-matrix least-squares on F^2
Data / restraints / parameters	12154 / 0 / 537

Goodness-of-fit on F^2	1.071
Final R indices [$I>2\sigma(I)$]	R1 = 0.0341, wR2 = 0.0992
R indices (all data)	R1 = 0.0418, wR2 = 0.1049
Largest diff. peak and hole	1.179 and -0.753 e* $Å^{-3}$

A1.3. Atomic coordinates (x 10^4) and equivalent isotropic displacement parameters ($Å^2$ x 10^3) for mma.

U(eq) is defined as one third of the trace of the orthogonalized Uij tensor.

	x	y	z	U(eq)
P(1)	5007(1)	1391(1)	2062(1)	16(1)
Ru(1)	5103(1)	293(1)	2422(1)	16(1)
Cl(1)	6532(1)	567(1)	3406(1)	25(1)
Cl(3)	3918(1)	24(1)	1304(1)	24(1)
F(1)	2823(2)	352(1)	2825(2)	36(1)
F(1')	3862(3)	476(2)	3686(2)	40(1)
C(1)	3937(2)	324(1)	3000(1)	25(1)
C(2)	5470(2)	-661(1)	2563(1)	20(1)
C(3)	5309(2)	-1744(1)	2811(2)	35(1)
C(4)	6390(2)	-1631(1)	2412(2)	38(1)
C(5)	3891(2)	-1010(1)	3310(1)	21(1)
C(6)	2769(2)	-1097(1)	2990(1)	25(1)
C(7)	1882(2)	-1017(1)	3455(1)	29(1)
C(8)	2088(2)	-861(1)	4216(1)	33(1)
C(9)	3214(2)	-799(1)	4521(1)	29(1)
C(10)	4129(2)	-875(1)	4078(1)	24(1)
C(11)	2516(2)	-1269(1)	2168(1)	36(1)
C(12)	1120(3)	-763(2)	4712(2)	55(1)
C(13)	5338(2)	-797(1)	4426(1)	31(1)
C(14)	7352(2)	-652(1)	2006(1)	24(1)
C(15)	7371(2)	-592(1)	1219(1)	25(1)
C(16)	8371(2)	-372(1)	942(1)	31(1)
C(17)	9335(2)	-217(1)	1418(2)	36(1)
C(18)	9287(2)	-282(1)	2194(2)	35(1)
C(19)	8311(2)	-513(1)	2501(1)	28(1)
C(20)	6372(2)	-789(1)	682(1)	32(1)
C(21)	10427(2)	3(2)	1098(2)	55(1)
C(22)	8348(2)	-641(1)	3341(1)	37(1)

C(23)	3685(2)	1625(1)	1479(1)	20(1)
C(24)	2690(3)	1741(2)	1981(2)	23(1)
C(25)	1563(3)	1830(3)	1494(3)	31(1)
C(26)	1656(9)	2385(4)	946(6)	28(2)
C(27)	2630(6)	2290(3)	454(3)	29(1)
C(28)	3766(4)	2189(3)	931(3)	24(1)
C(24')	2594(6)	1419(6)	1838(5)	29(2)
C(25')	1531(6)	1554(6)	1285(6)	32(2)
C(26')	1475(18)	2231(7)	1062(10)	24(3)
C(27')	2527(11)	2404(6)	682(7)	29(2)
C(28')	3633(9)	2285(5)	1197(7)	26(2)
C(29)	5292(2)	1940(1)	2868(1)	18(1)
C(30)	5400(3)	2639(1)	2677(1)	40(1)
C(31)	5869(3)	3002(1)	3384(1)	44(1)
C(32)	5114(2)	2928(1)	4021(1)	27(1)
C(33)	4952(3)	2237(1)	4207(1)	39(1)
C(34)	4506(3)	1867(1)	3502(2)	44(1)
C(35)	6155(2)	1569(1)	1440(1)	20(1)
C(36)	7357(2)	1566(2)	1842(2)	44(1)
C(37)	8228(2)	1770(2)	1292(2)	44(1)
C(38)	8172(2)	1346(1)	594(2)	46(1)
C(39)	6972(3)	1324(2)	205(2)	54(1)
C(40)	6101(2)	1123(1)	762(1)	43(1)
C(94)	9504(2)	1810(1)	3586(1)	44(1)
C(95)	9827(6)	1200(3)	3405(3)	52(2)
C(96)	10867(5)	993(3)	3712(4)	51(2)
C(97)	11583(6)	1322(4)	4100(5)	66(2)
C(98)	11366(6)	1897(4)	4292(5)	67(2)
C(99)	10266(7)	2177(3)	4044(4)	59(2)
N(1)	4826(2)	-1105(1)	2858(1)	23(1)
N(2)	6378(2)	-943(1)	2302(1)	25(1)

A1.4. Bond lengths [Å] and angles [deg] for mma.

P(1)-C(29)	1.8544(19)
P(1)-C(35)	1.856(2)
P(1)-C(23)	1.8566(19)
P(1)-Ru(1)	2.4238(5)
Ru(1)-C(1)	1.783(2)
Ru(1)-C(2)	2.0872(19)
Ru(1)-Cl(1)	2.3853(5)
Ru(1)-Cl(3)	2.3901(5)

F(1)-C(1)	1.320(3)
F(1')-C(1)	1.269(4)
C(2)-N(2)	1.342(3)
C(2)-N(1)	1.346(3)
C(3)-N(1)	1.479(3)
C(3)-C(4)	1.527(3)
C(4)-N(2)	1.476(3)
C(5)-C(10)	1.396(3)
C(5)-C(6)	1.400(3)
C(5)-N(1)	1.430(3)
C(6)-C(7)	1.395(3)
C(6)-C(11)	1.506(3)
C(7)-C(8)	1.390(3)
C(8)-C(9)	1.391(3)
C(8)-C(12)	1.512(3)
C(9)-C(10)	1.395(3)
C(10)-C(13)	1.507(3)
C(14)-C(19)	1.397(3)
C(14)-C(15)	1.403(3)
C(14)-N(2)	1.441(3)
C(15)-C(16)	1.394(3)
C(15)-C(20)	1.504(3)
C(16)-C(17)	1.391(4)
C(17)-C(18)	1.388(4)
C(17)-C(21)	1.522(4)
C(18)-C(19)	1.401(3)
C(19)-C(22)	1.511(3)
C(23)-C(28')	1.491(10)
C(23)-C(24')	1.545(8)
C(23)-C(24)	1.551(4)
C(23)-C(28)	1.552(6)
C(24)-C(25)	1.527(5)
C(25)-C(26)	1.540(9)
C(26)-C(27)	1.513(11)
C(27)-C(28)	1.531(8)
C(24')-C(25')	1.545(10)
C(25')-C(26')	1.496(17)
C(26')-C(27')	1.50(2)
C(27')-C(28')	1.543(16)
C(29)-C(34)	1.524(3)
C(29)-C(30)	1.535(3)
C(30)-C(31)	1.534(3)
C(31)-C(32)	1.503(3)
C(32)-C(33)	1.524(3)
C(33)-C(34)	1.530(3)

C(35)-C(36)	1.525(3)
C(35)-C(40)	1.528(3)
C(36)-C(37)	1.537(3)
C(37)-C(38)	1.530(4)
C(38)-C(39)	1.515(5)
C(39)-C(40)	1.544(3)
C(94)-C(99)	1.394(8)
C(94)-C(95)	1.401(7)
C(95)-C(96)	1.366(9)
C(96)-C(97)	1.253(10)
C(97)-C(98)	1.303(10)
C(98)-C(99)	1.455(11)
C(29)-P(1)-C(35)	103.77(9)
C(29)-P(1)-C(23)	110.18(9)
C(35)-P(1)-C(23)	103.38(9)
C(29)-P(1)-Ru(1)	113.81(6)
C(35)-P(1)-Ru(1)	109.52(6)
C(23)-P(1)-Ru(1)	115.04(6)
C(1)-Ru(1)-C(2)	97.36(8)
C(1)-Ru(1)-Cl(1)	95.63(8)
C(2)-Ru(1)-Cl(1)	91.49(6)
C(1)-Ru(1)-Cl(3)	93.71(8)
C(2)-Ru(1)-Cl(3)	87.98(5)
Cl(1)-Ru(1)-Cl(3)	170.63(2)
C(1)-Ru(1)-P(1)	95.52(6)
C(2)-Ru(1)-P(1)	167.08(6)
Cl(1)-Ru(1)-P(1)	88.287(17)
Cl(3)-Ru(1)-P(1)	90.147(17)
F(1')-C(1)-F(1)	93.6(3)
F(1')-C(1)-Ru(1)	133.0(2)
F(1)-C(1)-Ru(1)	131.5(2)
N(2)-C(2)-N(1)	108.03(17)
N(2)-C(2)-Ru(1)	123.89(14)
N(1)-C(2)-Ru(1)	127.85(15)
N(1)-C(3)-C(4)	102.68(17)
N(2)-C(4)-C(3)	102.65(18)
C(10)-C(5)-C(6)	121.52(19)
C(10)-C(5)-N(1)	118.55(19)
C(6)-C(5)-N(1)	119.77(18)
C(7)-C(6)-C(5)	118.0(2)
C(7)-C(6)-C(11)	120.4(2)
C(5)-C(6)-C(11)	121.5(2)
C(8)-C(7)-C(6)	121.9(2)
C(7)-C(8)-C(9)	118.5(2)
C(7)-C(8)-C(12)	121.5(2)

C(9)-C(8)-C(12)	120.0(2)
C(8)-C(9)-C(10)	121.6(2)
C(9)-C(10)-C(5)	118.3(2)
C(9)-C(10)-C(13)	120.18(19)
C(5)-C(10)-C(13)	121.5(2)
C(19)-C(14)-C(15)	121.5(2)
C(19)-C(14)-N(2)	118.93(19)
C(15)-C(14)-N(2)	119.0(2)
C(16)-C(15)-C(14)	117.9(2)
C(16)-C(15)-C(20)	120.4(2)
C(14)-C(15)-C(20)	121.6(2)
C(17)-C(16)-C(15)	122.2(2)
C(18)-C(17)-C(16)	118.3(2)
C(18)-C(17)-C(21)	120.7(3)
C(16)-C(17)-C(21)	121.0(3)
C(17)-C(18)-C(19)	121.8(2)
C(14)-C(19)-C(18)	118.2(2)
C(14)-C(19)-C(22)	122.2(2)
C(18)-C(19)-C(22)	119.5(2)
C(28')-C(23)-C(24')	113.3(5)
C(28')-C(23)-C(24)	91.8(5)
C(24')-C(23)-C(24)	27.5(4)
C(28')-C(23)-C(28)	20.7(4)
C(24')-C(23)-C(28)	125.2(4)
C(24)-C(23)-C(28)	109.1(2)
C(28')-C(23)-P(1)	116.5(4)
C(24')-C(23)-P(1)	112.2(3)
C(24)-C(23)-P(1)	111.08(17)
C(28)-C(23)-P(1)	117.5(2)
C(25)-C(24)-C(23)	110.8(3)
C(24)-C(25)-C(26)	110.2(5)
C(27)-C(26)-C(25)	111.1(7)
C(26)-C(27)-C(28)	111.5(5)
C(27)-C(28)-C(23)	110.8(4)
C(23)-C(24')-C(25')	109.8(5)
C(26')-C(25')-C(24')	111.1(10)
C(25')-C(26')-C(27')	109.6(14)
C(26')-C(27')-C(28')	112.1(11)
C(23)-C(28')-C(27')	111.1(7)
C(34)-C(29)-C(30)	109.25(19)
C(34)-C(29)-P(1)	115.07(14)
C(30)-C(29)-P(1)	116.99(14)
C(31)-C(30)-C(29)	109.8(2)
C(32)-C(31)-C(30)	111.6(2)
C(31)-C(32)-C(33)	110.95(19)

C(32)-C(33)-C(34)	111.2(2)
C(29)-C(34)-C(33)	111.26(19)
C(36)-C(35)-C(40)	109.8(2)
C(36)-C(35)-P(1)	114.39(15)
C(40)-C(35)-P(1)	110.94(14)
C(35)-C(36)-C(37)	110.0(2)
C(38)-C(37)-C(36)	111.3(2)
C(39)-C(38)-C(37)	111.0(2)
C(38)-C(39)-C(40)	111.1(3)
C(35)-C(40)-C(39)	110.23(19)
C(99)-C(94)-C(95)	118.7(4)
C(96)-C(95)-C(94)	117.4(5)
C(97)-C(96)-C(95)	124.9(6)
C(96)-C(97)-C(98)	122.1(7)
C(97)-C(98)-C(99)	119.7(7)
C(94)-C(99)-C(98)	117.1(6)
C(2)-N(1)-C(5)	127.15(17)
C(2)-N(1)-C(3)	113.17(17)
C(5)-N(1)-C(3)	118.62(16)
C(2)-N(2)-C(14)	127.81(17)
C(2)-N(2)-C(4)	113.45(18)
C(14)-N(2)-C(4)	118.46(17)

A1.5. Anisotropic displacement parameters ($Å^2$ x 10^3) for mma.

The anisotropic displacement factor exponent takes the form:
-2 pi^2 [h^2 a*^2 U11 + ... + 2 h k a* b* U12]

	U11	U22	U33	U23	U13	U12
P(1)	15(1)	15(1)	18(1)	0(1)	0(1)	0(1)
Ru(1)	18(1)	13(1)	15(1)	0(1)	0(1)	-1(1)
Cl(1)	29(1)	21(1)	22(1)	0(1)	-8(1)	0(1)
Cl(3)	29(1)	20(1)	22(1)	-1(1)	-5(1)	-5(1)
F(1)	24(1)	32(1)	53(2)	7(1)	15(1)	2(1)
F(1')	51(2)	40(2)	30(2)	4(1)	19(1)	15(2)
C(1)	29(1)	16(1)	31(1)	4(1)	10(1)	1(1)
C(2)	26(1)	17(1)	16(1)	0(1)	2(1)	1(1)
C(3)	46(1)	17(1)	46(1)	4(1)	24(1)	2(1)
C(4)	51(2)	15(1)	53(2)	5(1)	27(1)	4(1)
C(5)	27(1)	14(1)	22(1)	2(1)	5(1)	-1(1)
C(6)	31(1)	19(1)	23(1)	4(1)	0(1)	-5(1)

C(7)	24(1)	28(1)	35(1)	7(1)	1(1)	-1(1)
C(8)	30(1)	37(1)	33(1)	4(1)	9(1)	5(1)
C(9)	33(1)	33(1)	22(1)	1(1)	5(1)	2(1)
C(10)	27(1)	22(1)	22(1)	5(1)	1(1)	0(1)
C(11)	45(1)	36(1)	27(1)	0(1)	-1(1)	-18(1)
C(12)	34(1)	84(2)	49(2)	-3(2)	17(1)	9(2)
C(13)	30(1)	36(1)	26(1)	6(1)	-2(1)	-2(1)
C(14)	28(1)	16(1)	28(1)	2(1)	9(1)	5(1)
C(15)	31(1)	18(1)	27(1)	2(1)	8(1)	6(1)
C(16)	35(1)	27(1)	33(1)	9(1)	14(1)	10(1)
C(17)	28(1)	36(1)	47(1)	15(1)	13(1)	10(1)
C(18)	26(1)	35(1)	44(1)	5(1)	2(1)	8(1)
C(19)	31(1)	24(1)	30(1)	2(1)	6(1)	9(1)
C(20)	44(1)	29(1)	25(1)	-4(1)	7(1)	0(1)
C(21)	29(1)	73(2)	66(2)	26(2)	16(1)	6(1)
C(22)	40(1)	41(1)	29(1)	3(1)	2(1)	14(1)
C(23)	18(1)	19(1)	23(1)	0(1)	-2(1)	2(1)
C(24)	17(1)	21(2)	31(2)	1(2)	2(1)	1(1)
C(25)	18(2)	28(2)	45(2)	-10(2)	-3(1)	2(1)
C(26)	25(4)	26(4)	32(3)	-5(2)	-9(2)	10(2)
C(27)	32(2)	36(3)	18(2)	-4(2)	-6(2)	16(2)
C(28)	26(2)	27(2)	18(2)	2(2)	-1(2)	6(1)
C(24')	17(3)	37(6)	33(4)	7(4)	0(2)	5(3)
C(25')	13(3)	41(6)	41(4)	-1(4)	-5(3)	7(3)
C(26')	20(5)	27(8)	24(5)	-9(5)	-3(4)	5(5)
C(27')	38(6)	21(4)	26(6)	1(4)	-11(5)	0(4)
C(28')	26(4)	19(4)	31(5)	6(4)	-10(4)	-1(3)
C(29)	20(1)	16(1)	19(1)	-1(1)	1(1)	-1(1)
C(30)	78(2)	20(1)	21(1)	-1(1)	4(1)	-14(1)
C(31)	77(2)	31(1)	27(1)	-9(1)	15(1)	-31(1)
C(32)	32(1)	22(1)	25(1)	-7(1)	-5(1)	2(1)
C(33)	58(2)	30(1)	31(1)	-11(1)	20(1)	-17(1)
C(34)	48(2)	42(1)	47(2)	-26(1)	26(1)	-27(1)
C(35)	19(1)	18(1)	22(1)	1(1)	4(1)	-1(1)
C(36)	19(1)	80(2)	35(1)	16(1)	5(1)	2(1)
C(37)	22(1)	68(2)	42(1)	6(1)	9(1)	-7(1)
C(38)	41(1)	31(1)	73(2)	-1(1)	36(1)	-2(1)
C(39)	50(2)	71(2)	45(2)	-31(2)	28(1)	-24(2)
C(40)	37(1)	46(2)	49(2)	-26(1)	23(1)	-18(1)
C(94)	69(4)	26(2)	35(3)	16(2)	-7(2)	7(2)
C(95)	83(4)	41(3)	30(2)	4(2)	-5(3)	-23(3)
C(96)	31(2)	32(2)	95(5)	27(3)	32(3)	5(2)
C(97)	38(3)	52(4)	109(6)	-5(4)	22(3)	8(3)
C(98)	48(4)	64(4)	89(6)	-23(4)	7(3)	-14(3)
C(99)	83(5)	35(3)	57(4)	-6(3)	1(3)	8(3)

N(1)	32(1)	15(1)	25(1)	1(1)	9(1)	-1(1)
N(2)	33(1)	15(1)	29(1)	3(1)	12(1)	2(1)

A1.6. Hydrogen coordinates (x 10^4) and isotropic displacement parameters ($Å^2$ x 10^3) for mma.

	x	y	z	U(eq)
H(1A)	4157	318	3529	30
H(1B)	3229	202	2742	30
H(3A)	4775	-2027	2511	42
H(3B)	5492	-1926	3321	42
H(4A)	7080	-1766	2731	46
H(4B)	6359	-1854	1921	46
H(7A)	1116	-1070	3245	35
H(9A)	3364	-701	5043	35
H(11A)	2735	-1707	2092	55
H(11B)	2950	-995	1856	55
H(11C)	1697	-1218	2023	55
H(12A)	1419	-776	5245	83
H(12B)	551	-1097	4613	83
H(12C)	762	-354	4599	83
H(13A)	5690	-435	4195	47
H(13B)	5777	-1177	4336	47
H(13C)	5333	-728	4972	47
H(16A)	8395	-326	411	37
H(18A)	9933	-168	2526	42
H(20A)	6486	-640	171	48
H(20B)	5669	-607	846	48
H(20C)	6312	-1248	679	48
H(21A)	10992	119	1515	83
H(21B)	10260	368	771	83
H(21C)	10733	-337	802	83
H(22A)	7572	-622	3502	55
H(22B)	8827	-325	3617	55
H(22C)	8670	-1060	3448	55
H(23A)	3455	1255	1154	24
H(23B)	3688	1365	1010	24
H(24A)	2624	1379	2325	28
H(24B)	2854	2120	2295	28
H(25A)	941	1912	1824	37
H(25B)	1373	1442	1202	37

H(26A)	931	2428	621	34
H(26B)	1782	2778	1240	34
H(27A)	2692	2662	125	35
H(27B)	2466	1920	123	35
H(28A)	3967	2574	1227	29
H(28B)	4377	2109	593	29
H(24C)	2533	1650	2317	35
H(24D)	2635	965	1955	35
H(25C)	1560	1291	826	39
H(25D)	833	1440	1528	39
H(26C)	1424	2496	1517	29
H(26D)	786	2308	712	29
H(27C)	2487	2853	539	35
H(27D)	2548	2155	212	35
H(28C)	4303	2370	911	32
H(28D)	3666	2577	1634	32
H(29A)	6065	1818	3103	22
H(30A)	5920	2691	2271	48
H(30B)	4642	2809	2490	48
H(31A)	6645	2847	3550	53
H(31B)	5929	3453	3258	53
H(32A)	4361	3121	3875	32
H(32B)	5462	3149	4475	32
H(33A)	4404	2199	4598	47
H(33B)	5691	2057	4416	47
H(34A)	4448	1417	3634	53
H(34B)	3731	2018	3324	53
H(35A)	6011	2002	1235	23
H(36A)	7547	1139	2035	53
H(36B)	7391	1857	2280	53
H(37A)	8070	2209	1132	53
H(37B)	9006	1754	1555	53
H(38A)	8703	1506	235	56
H(38B)	8417	916	747	56
H(39A)	6946	1023	-222	65
H(39B)	6762	1743	-4	65
H(40A)	5321	1127	501	51
H(40B)	6271	689	941	51
H(94A)	8779	1972	3400	53
H(95A)	9343	939	3081	62
H(96A)	11062	568	3624	61
H(97A)	12308	1146	4260	79
H(98A)	11923	2133	4592	81
H(99A)	10076	2591	4188	70

Appendix 2

Crystal Data for [Ru(CHF)(H_2IMes)(py)$_2$Cl$_2$]

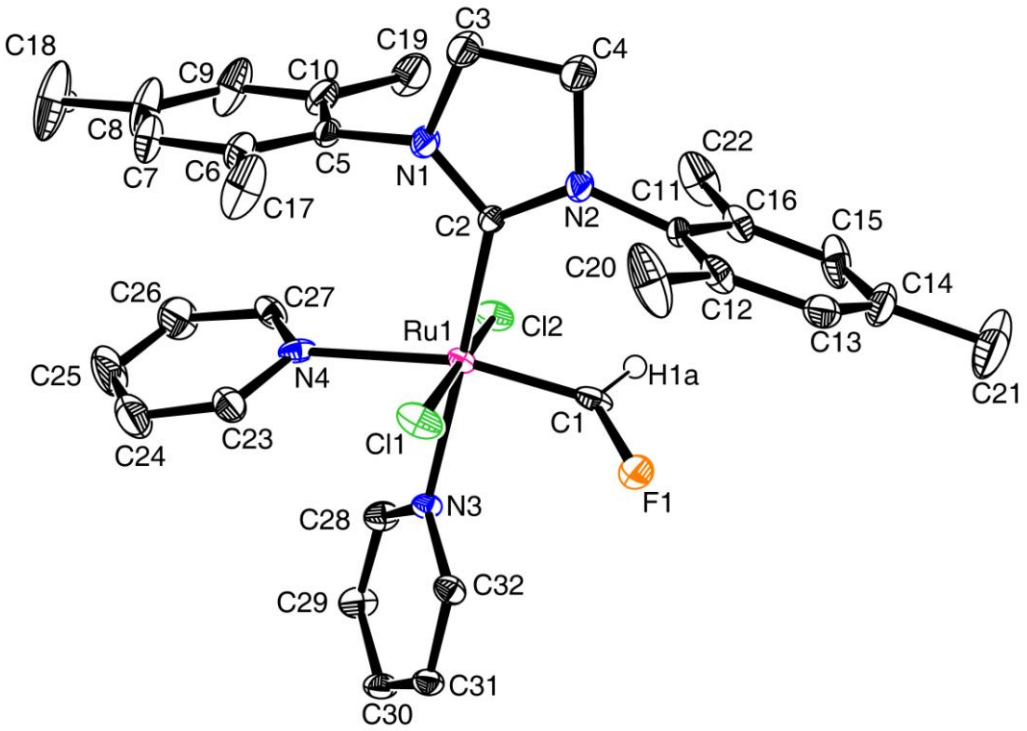

Figure A2.1. X-ray crystal structure of [Ru(CHF)(H_2IMes)(py)$_2$Cl$_2$] (mm716) (50% thermal ellipsoid plot). Hydrogen atoms are omitted for clarity.

A2.1. Structure Determination.

Orange plates of **mm716** were grown by slow diffusion of pentane into a pyridine solution at 25 °C. A crystal of dimensions 0.23 x 0.12 x 0.06 mm was mounted on a Bruker SMART APEX CCD-based X-ray diffractometer equipped with a low

temperature device and fine focus Mo-target X-ray tube (λ = 0.71073 Å) operated at 1500 W power (50 kV, 30 mA). The X-ray intensities were measured at 85(1) K; the detector was placed at a distance 5.055 cm from the crystal. A total of 2875 frames were collected with a scan width of 0.5° in ω and 0.45° in φ with an exposure time of 25 s/frame. The integration of the data yielded a total of 74027 reflections to a maximum 2θ value of 56.62° of which 7575 were independent and 7145 were greater than $2\sigma(I)$. The final cell constants (**A2.2**) were based on the xyz centroids of 9915 reflections above $10\sigma(I)$. Analysis of the data showed negligible decay during data collection; the data were processed with SADABS and corrected for absorption. The structure was solved and refined with the Bruker SHELXTL (version 6.12) software package, using the space group P2(1)/n with Z = 4 for the formula $C_{32}H_{37}N_4FCl_2Ru$. All non-hydrogen atoms were refined anisotropically with the hydrogen atoms placed in idealized positions. The monofluoromethylidine ligand and one pyridyl ligand are disordered 50/50 over two coordination sites in the equatorial plane containing the ruthenium and two chlorides. Full matrix least-squares refinement based on F^2 converged at R1 = 0.0434 and wR2 = 0.0991 [based on $I > 2\sigma(I)$], R1 = 0.0464 and wR2 = 0.1005 for all data. Additional details are presented in **A2.2**.

Sheldrick, G.M. SHELXTL, v. 6.12; Bruker Analytical X-ray, Madison, WI, 2001.

Sheldrick, G.M. SADABS, v. 2007/4. Program for Empirical Absorption Correction of Area Detector Data, University of Gottingen: Gottingen, Germany, 2007.

Saint Plus, v. 7.34, Bruker Analytical X-ray, Madison, WI, 2006.

A2.2. Crystal data and structure refinement for mm716.

Identification code	mm716
Empirical formula	C_{32} H_{37} C_{l2} F N_4 Ru
Formula weight	668.63
Temperature	85(2) K
Wavelength	0.71073 Å
Crystal system, space group	Monoclinic, P2(1)/n
Unit cell dimensions	a = 8.8643(6) Å alpha = 90 deg.
	b = 17.115(1) Å beta = 95.070(1) deg.
	c = 20.147(1) Å gamma = 90 deg.
Volume	3044.5(3) $Å^3$
Z, Calculated density	4, 1.459 Mg/m^3
Absorption coefficient	0.725 mm^{-1}
F(000)	1376
Crystal size	0.23 x 0.12 x 0.06 mm
Theta range for data collection	1.56 to 28.31 deg.
Limiting indices	-11<=h<=11, -22<=k<=22, -26<=l<=26
Reflections collected / unique	74027 / 7575 [R(int) = 0.0519]
Completeness to θ = 28.31	100.0 %
Absorption correction	Semi-empirical from equivalents

Max. and min. transmission	0.9578 and 0.8510
Refinement method	Full-matrix least-squares on F^2
Data / restraints / parameters	7575 / 0 / 439
Goodness-of-fit on F^2	1.143
Final R indices [I>2σ(I)]	R1 = 0.0434, wR2 = 0.0991
R indices (all data)	R1 = 0.0464, wR2 = 0.1005
Largest diff. peak and hole	0.623 and -0.726 e*Å^{-3}

A2.3. Atomic coordinates (x 10^4) and equivalent isotropic displacement parameters (Å^2 x 10^3) for mm716.

U(eq) is defined as one third of the trace of the orthogonalized Uij tensor.

	x	y	z	U(eq)
Ru(1)	4327(1)	900(1)	2315(1)	13(1)
Cl(1)	2629(1)	-193(1)	2201(1)	24(1)
Cl(2)	6160(1)	1939(1)	2414(1)	21(1)
C(1)	4590(12)	869(6)	3239(5)	20(2)
C(2)	2474(3)	1637(2)	2303(1)	14(1)
C(3)	345(4)	2387(3)	1895(2)	37(1)
C(4)	399(4)	2378(3)	2647(2)	39(1)
C(5)	2169(3)	2038(2)	1091(2)	17(1)
C(6)	1579(4)	1510(2)	607(2)	20(1)
C(7)	1985(4)	1599(2)	-40(2)	26(1)
C(8)	2913(5)	2201(3)	-213(2)	38(1)
C(9)	3411(5)	2737(3)	277(2)	39(1)
C(10)	3040(4)	2673(2)	930(2)	25(1)
C(11)	1979(3)	1680(2)	3521(1)	15(1)
C(12)	1161(4)	1099(2)	3816(2)	22(1)
C(13)	1371(4)	1024(2)	4507(2)	27(1)
C(14)	2333(4)	1502(3)	4897(2)	32(1)
C(15)	3111(4)	2074(3)	4586(2)	32(1)
C(16)	2934(4)	2188(2)	3901(2)	21(1)

C(17)	560(5)	857(3)	775(2)	41(1)
C(18)	3392(6)	2265(4)	-910(2)	63(2)
C(19)	3615(6)	3261(2)	1446(2)	39(1)
C(20)	81(5)	578(3)	3407(2)	46(1)
C(21)	2538(6)	1412(4)	5645(2)	60(2)
C(22)	3765(5)	2832(2)	3584(2)	38(1)
C(23)	4397(9)	113(4)	885(3)	26(1)
C(23A)	3927(17)	95(13)	3724(9)	32(3)
C(24)	4843(12)	-36(5)	254(4)	43(2)
C(24A)	4304(10)	-180(6)	4372(4)	42(2)
C(25)	5600(12)	535(6)	-69(4)	46(2)
C(25A)	5538(11)	137(6)	4734(4)	49(3)
C(26)	5888(10)	1233(5)	252(4)	37(2)
C(26A)	6390(11)	695(5)	4435(4)	41(2)
C(27)	5400(20)	1315(10)	906(12)	21(3)
C(27A)	5918(9)	932(5)	3782(4)	31(2)
C(28)	7437(4)	229(2)	1987(2)	20(1)
C(29)	8620(4)	-292(2)	1958(2)	23(1)
C(30)	8554(4)	-1003(2)	2273(2)	20(1)
C(31)	7307(3)	-1171(2)	2607(2)	17(1)
C(32)	6154(3)	-623(2)	2607(2)	17(1)
C(1A)	4270(11)	936(5)	1399(5)	24(2)
F(1)	4358(10)	239(6)	3627(4)	31(2)
F(1A)	5348(17)	1240(8)	1021(8)	50(4)
N(1)	1739(3)	1976(2)	1759(1)	22(1)
N(2)	1671(3)	1822(2)	2822(1)	20(1)
N(3)	6207(3)	76(1)	2305(1)	14(1)
N(4)	4655(8)	789(4)	1205(4)	17(1)
N(4A)	4704(11)	640(5)	3417(5)	22(2)

A2.4. Bond lengths [Å] and angles [deg] for mm716.

Ru(1)-C(1A)	1.841(10)
Ru(1)-C(1)	1.857(11)
Ru(1)-C(2)	2.069(3)
Ru(1)-N(3)	2.184(2)
Ru(1)-N(4A)	2.260(10)
Ru(1)-N(4)	2.288(8)
Ru(1)-Cl(1)	2.3995(8)
Ru(1)-Cl(2)	2.4057(8)
C(1)-F(1)	1.358(11)

C(2)-N(2)	1.353(4)
C(2)-N(1)	1.355(4)
C(3)-N(1)	1.469(4)
C(3)-C(4)	1.511(5)
C(4)-N(2)	1.494(4)
C(5)-C(10)	1.388(5)
C(5)-C(6)	1.396(4)
C(5)-N(1)	1.436(4)
C(6)-C(7)	1.391(4)
C(6)-C(17)	1.495(5)
C(7)-C(8)	1.382(5)
C(8)-C(9)	1.391(6)
C(8)-C(18)	1.506(5)
C(9)-C(10)	1.388(5)
C(10)-C(19)	1.503(5)
C(11)-C(12)	1.393(4)
C(11)-C(16)	1.395(4)
C(11)-N(2)	1.432(4)
C(12)-C(13)	1.393(5)
C(12)-C(20)	1.501(5)
C(13)-C(14)	1.377(6)
C(14)-C(15)	1.379(6)
C(14)-C(21)	1.511(5)
C(15)-C(16)	1.389(5)
C(16)-C(22)	1.498(5)
C(23)-N(4)	1.334(10)
C(23)-C(24)	1.388(10)
C(23A)-N(4A)	1.342(13)
C(23A)-C(24A)	1.40(2)
C(24)-C(25)	1.380(13)
C(24A)-C(25A)	1.371(15)
C(25)-C(26)	1.372(13)
C(25A)-C(26A)	1.387(14)
C(26)-C(27)	1.43(2)
C(26A)-C(27A)	1.405(10)
C(27)-N(4)	1.29(2)
C(27A)-N(4A)	1.346(13)
C(28)-N(3)	1.338(4)
C(28)-C(29)	1.382(4)
C(29)-C(30)	1.375(4)
C(30)-C(31)	1.374(4)
C(31)-C(32)	1.386(4)
C(32)-N(3)	1.346(4)
C(1A)-F(1A)	1.377(18)

C(1A)-Ru(1)-C(1)	174.4(5)
C(1A)-Ru(1)-C(2)	91.0(3)
C(1)-Ru(1)-C(2)	93.3(3)
C(1A)-Ru(1)-N(3)	88.0(3)
C(1)-Ru(1)-N(3)	87.9(3)
C(2)-Ru(1)-N(3)	177.09(10)
C(1A)-Ru(1)-N(4A)	168.2(3)
C(1)-Ru(1)-N(4A)	9.8(4)
C(2)-Ru(1)-N(4A)	100.3(2)
N(3)-Ru(1)-N(4A)	80.5(2)
C(1A)-Ru(1)-N(4)	11.1(3)
C(1)-Ru(1)-N(4)	164.2(4)
C(2)-Ru(1)-N(4)	102.05(19)
N(3)-Ru(1)-N(4)	76.97(18)
N(4A)-Ru(1)-N(4)	157.4(3)
C(1A)-Ru(1)-Cl(1)	88.2(3)
C(1)-Ru(1)-Cl(1)	95.5(3)
C(2)-Ru(1)-Cl(1)	89.06(8)
N(3)-Ru(1)-Cl(1)	88.18(7)
N(4A)-Ru(1)-Cl(1)	88.7(2)
N(4)-Ru(1)-Cl(1)	88.54(18)
C(1A)-Ru(1)-Cl(2)	91.0(3)
C(1)-Ru(1)-Cl(2)	85.0(3)
C(2)-Ru(1)-Cl(2)	94.60(8)
N(3)-Ru(1)-Cl(2)	88.15(7)
N(4A)-Ru(1)-Cl(2)	91.4(2)
N(4)-Ru(1)-Cl(2)	89.95(18)
Cl(1)-Ru(1)-Cl(2)	176.27(3)
F(1)-C(1)-Ru(1)	126.0(8)
N(2)-C(2)-N(1)	106.1(2)
N(2)-C(2)-Ru(1)	127.2(2)
N(1)-C(2)-Ru(1)	126.5(2)
N(1)-C(3)-C(4)	103.2(3)
N(2)-C(4)-C(3)	101.5(3)
C(10)-C(5)-C(6)	121.7(3)
C(10)-C(5)-N(1)	118.4(3)
C(6)-C(5)-N(1)	119.6(3)
C(7)-C(6)-C(5)	118.2(3)
C(7)-C(6)-C(17)	120.4(3)
C(5)-C(6)-C(17)	121.5(3)
C(8)-C(7)-C(6)	121.8(3)
C(7)-C(8)-C(9)	118.2(3)
C(7)-C(8)-C(18)	120.8(4)
C(9)-C(8)-C(18)	121.0(4)
C(10)-C(9)-C(8)	122.3(3)

C(5)-C(10)-C(9)	117.7(3)
C(5)-C(10)-C(19)	121.7(3)
C(9)-C(10)-C(19)	120.6(3)
C(12)-C(11)-C(16)	121.6(3)
C(12)-C(11)-N(2)	118.6(3)
C(16)-C(11)-N(2)	119.2(3)
C(13)-C(12)-C(11)	117.6(3)
C(13)-C(12)-C(20)	121.0(3)
C(11)-C(12)-C(20)	121.3(3)
C(14)-C(13)-C(12)	122.4(3)
C(13)-C(14)-C(15)	118.1(3)
C(13)-C(14)-C(21)	121.5(4)
C(15)-C(14)-C(21)	120.3(4)
C(14)-C(15)-C(16)	122.4(3)
C(15)-C(16)-C(11)	117.8(3)
C(15)-C(16)-C(22)	120.7(3)
C(11)-C(16)-C(22)	121.5(3)
N(4)-C(23)-C(24)	123.4(7)
N(4A)-C(23A)-C(24A)	125.0(16)
C(25)-C(24)-C(23)	119.5(9)
C(25A)-C(24A)-C(23A)	118.4(11)
C(26)-C(25)-C(24)	118.1(7)
C(24A)-C(25A)-C(26A)	118.8(7)
C(25)-C(26)-C(27)	117.5(9)
C(25A)-C(26A)-C(27A)	118.4(9)
N(4)-C(27)-C(26)	124.6(11)
N(4A)-C(27A)-C(26A)	124.2(9)
N(3)-C(28)-C(29)	123.3(3)
C(30)-C(29)-C(28)	119.2(3)
C(31)-C(30)-C(29)	118.6(3)
C(30)-C(31)-C(32)	119.0(3)
N(3)-C(32)-C(31)	123.1(3)
F(1A)-C(1A)-Ru(1)	127.5(8)
C(2)-N(1)-C(5)	130.0(3)
C(2)-N(1)-C(3)	114.0(3)
C(5)-N(1)-C(3)	115.9(3)
C(2)-N(2)-C(11)	130.7(3)
C(2)-N(2)-C(4)	113.8(3)
C(11)-N(2)-C(4)	114.5(2)
C(28)-N(3)-C(32)	116.9(3)
C(28)-N(3)-Ru(1)	122.2(2)
C(32)-N(3)-Ru(1)	120.9(2)
C(27)-N(4)-C(23)	116.8(10)
C(27)-N(4)-Ru(1)	120.7(9)
C(23)-N(4)-Ru(1)	120.8(5)

C(23A)-N(4A)-C(27A)	115.1(12)
C(23A)-N(4A)-Ru(1)	123.5(11)
C(27A)-N(4A)-Ru(1)	120.4(7)

A2.5. Anisotropic displacement parameters ($Å^2$ x 10^3) for mm716.

The anisotropic displacement factor exponent takes the form:
-2 pi^2 [h^2 a*^2 U11 + ... + 2 h k a* b* U12]

	U11	U22	U33	U23	U13	U12
Ru(1)	12(1)	10(1)	16(1)	-1(1)	3(1)	0(1)
Cl(1)	17(1)	16(1)	38(1)	-4(1)	5(1)	-4(1)
Cl(2)	19(1)	13(1)	32(1)	-2(1)	2(1)	-3(1)
C(1)	22(4)	10(4)	30(5)	1(3)	10(4)	4(4)
C(2)	15(1)	13(1)	12(1)	2(1)	2(1)	0(1)
C(3)	28(2)	65(3)	19(2)	6(2)	5(1)	29(2)
C(4)	29(2)	69(3)	20(2)	4(2)	4(1)	32(2)
C(5)	16(1)	24(2)	12(1)	2(1)	2(1)	6(1)
C(6)	16(1)	27(2)	17(1)	3(1)	-1(1)	-4(1)
C(7)	25(2)	39(2)	14(1)	-2(1)	-1(1)	-10(2)
C(8)	33(2)	69(3)	14(2)	5(2)	2(1)	-22(2)
C(9)	45(2)	51(3)	21(2)	13(2)	-3(2)	-29(2)
C(10)	32(2)	23(2)	19(2)	5(1)	-5(1)	-2(1)
C(11)	17(1)	19(1)	10(1)	0(1)	3(1)	4(1)
C(12)	24(2)	20(2)	23(2)	-5(1)	11(1)	0(1)
C(13)	35(2)	24(2)	26(2)	8(1)	16(1)	10(1)
C(14)	24(2)	57(3)	14(2)	6(2)	2(1)	14(2)
C(15)	21(2)	56(3)	19(2)	-16(2)	0(1)	-5(2)
C(16)	19(2)	24(2)	21(2)	-6(1)	6(1)	0(1)
C(17)	43(2)	53(3)	26(2)	10(2)	-5(2)	-29(2)
C(18)	62(3)	111(4)	16(2)	6(2)	6(2)	-45(3)
C(19)	65(3)	20(2)	30(2)	2(2)	-12(2)	-6(2)
C(20)	49(3)	49(3)	46(2)	-26(2)	31(2)	-29(2)
C(21)	40(2)	123(5)	19(2)	15(2)	1(2)	10(3)
C(22)	42(2)	31(2)	44(2)	-14(2)	22(2)	-17(2)
C(23)	36(4)	20(3)	22(3)	-2(3)	6(3)	3(3)

C(23A)	26(6)	45(8)	27(6)	10(5)	16(4)	11(5)
C(24)	73(6)	30(4)	28(4)	-5(3)	16(4)	9(4)
C(24A)	42(5)	54(5)	32(4)	20(4)	16(4)	23(4)
C(25)	70(6)	44(5)	27(4)	-6(4)	27(4)	6(4)
C(25A)	62(6)	71(6)	16(3)	12(4)	8(4)	45(5)
C(26)	50(5)	34(4)	29(4)	7(3)	19(4)	2(4)
C(26A)	49(5)	42(5)	28(4)	-1(3)	-8(4)	18(4)
C(27)	17(5)	19(4)	26(7)	-9(4)	1(4)	-1(4)
C(27A)	41(4)	28(4)	24(3)	-5(3)	2(3)	8(3)
C(28)	18(2)	18(1)	24(2)	5(1)	4(1)	-1(1)
C(29)	18(2)	23(2)	30(2)	7(1)	9(1)	2(1)
C(30)	20(2)	17(1)	24(2)	2(1)	3(1)	7(1)
C(31)	20(1)	12(1)	20(1)	1(1)	1(1)	1(1)
C(32)	16(1)	15(1)	20(1)	-1(1)	5(1)	0(1)
C(1A)	19(4)	23(4)	29(5)	-3(3)	3(3)	12(3)
F(1)	38(5)	34(5)	21(4)	5(3)	7(3)	16(4)
F(1A)	47(5)	71(7)	32(5)	0(4)	13(3)	24(5)
N(1)	19(1)	35(2)	14(1)	3(1)	5(1)	12(1)
N(2)	17(1)	30(2)	13(1)	1(1)	2(1)	8(1)
N(3)	16(1)	9(1)	18(1)	3(1)	4(1)	-1(1)
N(4)	14(3)	14(3)	24(4)	9(3)	5(2)	2(3)
N(4A)	29(4)	9(4)	29(5)	6(3)	15(3)	6(4)

A2.6. Hydrogen coordinates (x 10^4) and isotropic displacement parameters ($Å^2$ x 10^3) for mm716.

	X	y	z	U(eq)
H(1A)	4918	1337	3461	24
H(3A)	-562	2109	1693	44
H(3B)	340	2928	1722	44
H(4A)	622	2903	2837	47
H(4B)	-564	2184	2801	47
H(7A)	1615	1236	-372	31
H(9A)	4027	3161	161	47
H(13A)	831	628	4716	33
H(15A)	3791	2401	4849	39
H(17A)	-404	1071	896	62

H(17B)	1043	558	1151	62
H(17C)	372	512	388	62
H(18A)	3631	1744	-1073	94
H(18B)	4291	2599	-907	94
H(18C)	2567	2494	-1202	94
H(19A)	2766	3462	1676	59
H(19B)	4103	3693	1229	59
H(19C)	4352	3011	1770	59
H(20A)	-347	193	3698	70
H(20B)	623	306	3071	70
H(20C)	-736	893	3184	70
H(21A)	2054	927	5774	91
H(21B)	2072	1857	5855	91
H(21C)	3621	1393	5793	91
H(22A)	4382	3121	3929	57
H(22B)	3034	3187	3349	57
H(22C)	4422	2608	3266	57
H(23A)	3881	-287	1101	31
H(23B)	3055	-121	3483	38
H(24A)	4630	-527	47	52
H(24B)	3718	-576	4558	50
H(25A)	5912	446	-502	55
H(25B)	5805	-23	5180	59
H(26A)	6394	1645	48	44
H(26B)	7272	912	4667	49
H(27A)	5631	1790	1137	25
H(27B)	6493	1325	3586	37
H(28A)	7501	720	1771	24
H(29A)	9468	-162	1723	28
H(30A)	9354	-1371	2260	24
H(31A)	7236	-1654	2834	21
H(32A)	5286	-748	2831	20
H(1B)	3396	719	1161	28

Appendix 3

Crystal Data for [Ru(CHPCy$_3$)(H$_2$IMes)Cl$_3$]

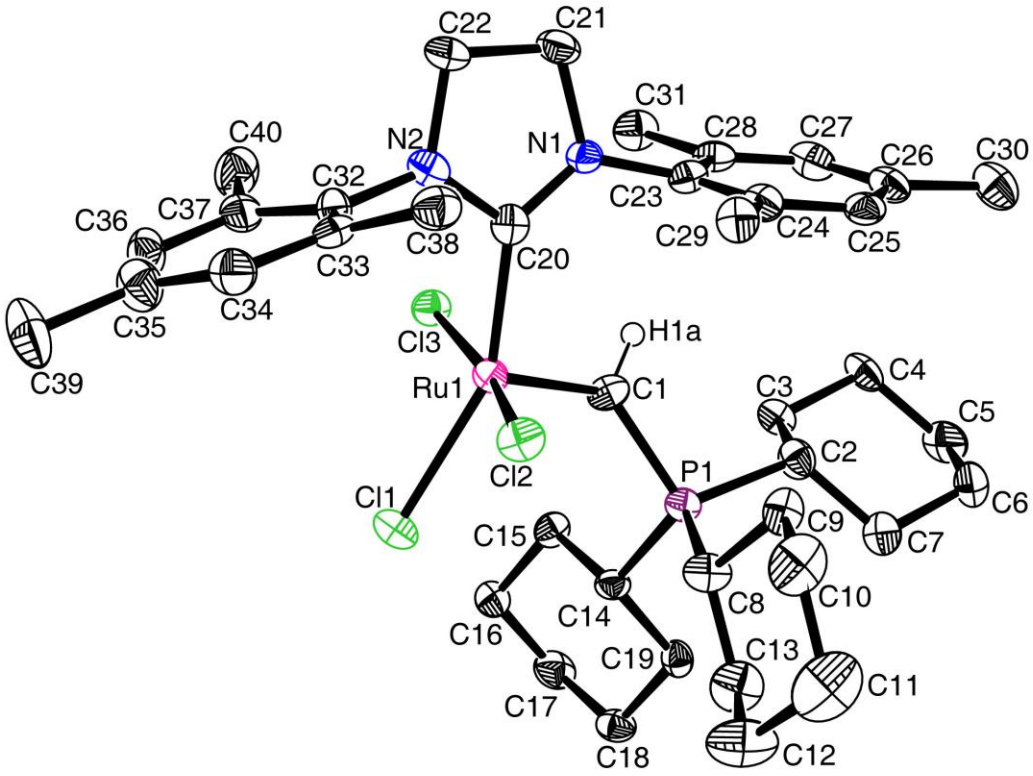

Figure A3.1. X-ray crystal structure of [Ru(CHPCy$_3$)(H$_2$IMes)Cl$_3$] (mm426) (50% thermal ellipsoid plot). Hydrogen atoms are omitted for clarity.

A3.1. Structure Determination.

Yellow needles of **mm426** were grown by diffusion of pentane into a THF-d_8 solution at 28 deg. C. A crystal of dimensions 0.40 x 0.12 x 0.08 mm was mounted on a

standard Bruker SMART 1K CCD-based X-ray diffractometer equipped with a LT-2 low temperature device and normal focus Mo-target X-ray tube (λ = 0.71073 Å) operated at 2000 W power (50 kV, 40 mA). The X-ray intensities were measured at 108(2) K; the detector was placed at a distance 4.969 cm from the crystal. A total of 2346 frames were collected with a scan width of 0.5° in ω and φ with an exposure time of 60 s/frame. The integration of the data yielded a total of 88175 reflections to a maximum 2σ value of 46.62° of which 6506 were independent and 5493 were greater than 2σ(I). The final cell constants (**A3.2**) were based on the xyz centroids of 6411 reflections above 10σ(I). Analysis of the data showed negligible decay during data collection; the data were processed with SADABS and corrected for absorption. The structure was solved and refined with the Bruker SHELXTL (version 6.12) software package, using the space group P6(1) with Z = 6 for the formula $C_{40}H_{60}N_2PCl_3Ru\bullet(C_4H_8O)_{0.33}$. All non-hydrogen atoms were refined anisotropically with the hydrogen atoms placed in idealized positions. The equivalent of two THF lattice solvates, disordered about the origin of the crystal lattice was modeled by use of the SQUEEZE subroutine of the PLATON program suite. Full matrix leastsquares refinement based on F^2 converged at R1 = 0.0440 and wR2 = 0.0922 [based on I > 2σ(I)], R1 = 0.0587 and wR2 = 0.0968 for all data. Additional details are presented in **A3.2**.

Sheldrick, G.M. SHELXTL, v. 6.12; Bruker Analytical X-ray, Madison, WI, 2001.

PLATON, A.L. Spek, Acta Cryst. (1990) A46, C-34.

Sheldrick, G.M. SADABS, v. 2.10. Program for Empirical Absorption Correction of Area Detector Data, University of Gottingen: Gottingen, Germany, 2003.

Saint Plus, v. 7.01, Bruker Analytical X-ray, Madison, WI, 2003.

A3.2. Crystal data and structure refinement for mm427

Identification code	mm426
Empirical formula	$C_{41.33}$ $H_{62.67}$ Cl_3 N_2 $O_{0.33}$ P Ru
Formula weight	831.32
Temperature	108(2) K
Wavelength	0.71073 Å
Crystal system, space group	Hexagonal, P6(1)
Unit cell dimensions	a = 20.7728(8) Å alpha = 90 deg.
	b = 20.7728(8) Å beta = 90 deg.
	c = 18.1437(16) Å gamma = 120 deg.
Volume	6780.3(7) $Å^3$
Z, Calculated density	6, 1.222 Mg/m^3
Absorption coefficient	0.588 mm^{-1}
F(000)	2624
Crystal size	0.40 x 0.12 x 0.08 mm
Theta range for data collection	1.96 to 23.31 deg.
Limiting indices	-23<=h<=23, -23<=k<=22, -20<=l<=20
Reflections collected / unique	88175 / 6506 [R(int) = 0.1470]
Completeness to θ = 23.31	99.7 %
Absorption correction	Semi-empirical from equivalents
Max. and min. transmission	0.9544 and 0.7987

Refinement method	Full-matrix least-squares on F^2
Data / restraints / parameters	6506 / 1 / 431
Goodness-of-fit on F^2	1.005
Final R indices [I>2σ(I)]	R1 = 0.0440, wR2 = 0.0922
R indices (all data)	R1 = 0.0587, wR2 = 0.0968
Absolute structure parameter	-0.01(4)
Extinction coefficient	0.0022(2)
Largest diff. peak and hole	0.363 and -0.329 e*Å^{-3}

A3.3. Atomic coordinates (x 10^4) and equivalent isotropic displacement parameters (Å^2 x 10^3) for mm426.

U(eq) is defined as one third of the trace of the orthogonalized Uij tensor.

	x	y	z	U(eq)
P(1)	9988(1)	4624(1)	9592(1)	22(1)
Ru(1)	9982(1)	6136(1)	9060(1)	21(1)
Cl(1)	11312(1)	6691(1)	9042(1)	32(1)
Cl(2)	9984(1)	5810(1)	7815(1)	29(1)
Cl(3)	10050(1)	6707(1)	10229(1)	26(1)
N(1)	8320(2)	5659(2)	9253(2)	22(1)
N(2)	8993(3)	6721(3)	8698(3)	27(1)
C(1)	9647(3)	5281(3)	9583(3)	24(1)
C(2)	9270(3)	3808(3)	10090(3)	28(2)
C(3)	9218(3)	3966(3)	10917(3)	25(1)
C(4)	8563(3)	3313(3)	11298(3)	30(2)
C(5)	8606(4)	2608(4)	11194(4)	39(2)
C(6)	8657(4)	2441(3)	10390(4)	39(2)
C(7)	9320(3)	3095(3)	10002(3)	29(2)
C(8)	10112(3)	4402(4)	8665(3)	29(2)
C(9)	9363(3)	3941(3)	8267(3)	30(2)

C(10)	9464(4)	3834(4)	7451(4)	45(2)
C(11)	9989(4)	3534(5)	7314(4)	61(2)
C(12)	10738(4)	4034(4)	7693(3)	49(2)
C(13)	10622(4)	4089(4)	8528(3)	40(2)
C(14)	10893(3)	5073(3)	10055(3)	22(1)
C(15)	10966(3)	5601(3)	10686(3)	24(1)
C(16)	11765(3)	6012(3)	10966(3)	26(1)
C(17)	11997(3)	5457(3)	11250(4)	34(2)
C(18)	11915(3)	4910(3)	10650(3)	26(1)
C(19)	11121(3)	4505(3)	10350(3)	24(1)
C(20)	9004(3)	6120(3)	8982(3)	23(1)
C(21)	7795(3)	5935(3)	9133(4)	29(1)
C(22)	8273(3)	6688(3)	8775(4)	33(2)
C(23)	8006(3)	4899(3)	9489(3)	25(1)
C(24)	7782(3)	4346(3)	8966(3)	26(1)
C(25)	7393(3)	3609(3)	9203(3)	26(2)
C(26)	7189(3)	3409(3)	9931(3)	26(1)
C(27)	7428(3)	3979(4)	10435(4)	33(2)
C(28)	7833(3)	4721(3)	10247(3)	25(1)
C(29)	7915(3)	4526(3)	8159(3)	29(2)
C(30)	6730(3)	2607(3)	10159(4)	39(2)
C(31)	8084(3)	5340(3)	10814(3)	33(2)
C(32)	9559(3)	7309(3)	8274(3)	22(1)
C(33)	9554(3)	7210(3)	7506(4)	27(2)
C(34)	10099(3)	7797(3)	7083(4)	32(2)
C(35)	10617(3)	8452(3)	7396(4)	36(2)
C(36)	10575(4)	8553(3)	8124(4)	38(2)
C(37)	10035(3)	7995(3)	8591(4)	29(2)
C(38)	8952(3)	6514(3)	7120(3)	33(2)
C(39)	11216(4)	9071(4)	6935(4)	54(2)
C(40)	9963(4)	8167(4)	9385(4)	41(2)

A3.4. Bond lengths [Å] and angles [deg] for mm426.

P(1)-C(8)	1.796(6)
P(1)-C(1)	1.825(6)
P(1)-C(14)	1.833(6)
P(1)-C(2)	1.841(6)
Ru(1)-C(1)	1.815(6)
Ru(1)-C(20)	2.021(5)
Ru(1)-Cl(2)	2.3590(15)

Ru(1)-Cl(3)	2.3991(15)
Ru(1)-Cl(1)	2.4038(14)
N(1)-C(20)	1.348(7)
N(1)-C(23)	1.441(7)
N(1)-C(21)	1.479(7)
N(2)-C(20)	1.363(7)
N(2)-C(32)	1.425(7)
N(2)-C(22)	1.468(7)
C(2)-C(7)	1.543(8)
C(2)-C(3)	1.551(8)
C(3)-C(4)	1.525(8)
C(4)-C(5)	1.521(8)
C(5)-C(6)	1.515(9)
C(6)-C(7)	1.538(8)
C(8)-C(13)	1.516(8)
C(8)-C(9)	1.538(8)
C(9)-C(10)	1.526(9)
C(10)-C(11)	1.522(10)
C(11)-C(12)	1.536(10)
C(12)-C(13)	1.546(9)
C(14)-C(15)	1.541(7)
C(14)-C(19)	1.569(8)
C(15)-C(16)	1.525(8)
C(16)-C(17)	1.542(8)
C(17)-C(18)	1.520(8)
C(18)-C(19)	1.528(8)
C(21)-C(22)	1.517(8)
C(23)-C(24)	1.379(8)
C(23)-C(28)	1.423(8)
C(24)-C(25)	1.395(8)
C(24)-C(29)	1.502(8)
C(25)-C(26)	1.386(8)
C(26)-C(27)	1.378(9)
C(26)-C(30)	1.506(8)
C(27)-C(28)	1.379(8)
C(28)-C(31)	1.521(8)
C(32)-C(37)	1.390(8)
C(32)-C(33)	1.407(8)
C(33)-C(34)	1.407(8)
C(33)-C(38)	1.528(8)
C(34)-C(35)	1.366(9)
C(35)-C(36)	1.348(10)
C(35)-C(39)	1.517(9)
C(36)-C(37)	1.421(9)
C(37)-C(40)	1.510(9)

C(8)-P(1)-C(1)	110.1(3)
C(8)-P(1)-C(14)	108.5(3)
C(1)-P(1)-C(14)	107.9(3)
C(8)-P(1)-C(2)	112.1(3)
C(1)-P(1)-C(2)	104.8(3)
C(14)-P(1)-C(2)	113.3(3)
C(1)-Ru(1)-C(20)	97.4(2)
C(1)-Ru(1)-Cl(2)	105.92(19)
C(20)-Ru(1)-Cl(2)	94.24(16)
C(1)-Ru(1)-Cl(3)	85.48(19)
C(20)-Ru(1)-Cl(3)	83.11(16)
Cl(2)-Ru(1)-Cl(3)	168.57(6)
C(1)-Ru(1)-Cl(1)	105.28(18)
C(20)-Ru(1)-Cl(1)	155.79(16)
Cl(2)-Ru(1)-Cl(1)	87.61(6)
Cl(3)-Ru(1)-Cl(1)	90.31(5)
C(20)-N(1)-C(23)	128.6(5)
C(20)-N(1)-C(21)	113.1(4)
C(23)-N(1)-C(21)	116.9(4)
C(20)-N(2)-C(32)	127.2(5)
C(20)-N(2)-C(22)	113.9(5)
C(32)-N(2)-C(22)	118.5(5)
Ru(1)-C(1)-P(1)	129.3(3)
C(7)-C(2)-C(3)	110.4(5)
C(7)-C(2)-P(1)	114.9(4)
C(3)-C(2)-P(1)	113.0(4)
C(4)-C(3)-C(2)	112.0(5)
C(5)-C(4)-C(3)	110.2(5)
C(6)-C(5)-C(4)	112.7(5)
C(5)-C(6)-C(7)	111.8(5)
C(6)-C(7)-C(2)	109.9(5)
C(13)-C(8)-C(9)	111.2(5)
C(13)-C(8)-P(1)	119.1(4)
C(9)-C(8)-P(1)	111.7(4)
C(10)-C(9)-C(8)	112.1(5)
C(11)-C(10)-C(9)	113.4(6)
C(10)-C(11)-C(12)	109.9(6)
C(11)-C(12)-C(13)	110.2(6)
C(8)-C(13)-C(12)	111.2(5)
C(15)-C(14)-C(19)	108.8(5)
C(15)-C(14)-P(1)	114.4(4)
C(19)-C(14)-P(1)	113.2(4)
C(16)-C(15)-C(14)	109.8(4)
C(15)-C(16)-C(17)	110.6(5)

C(18)-C(17)-C(16)	111.1(5)
C(17)-C(18)-C(19)	110.7(5)
C(18)-C(19)-C(14)	110.9(5)
N(1)-C(20)-N(2)	107.0(5)
N(1)-C(20)-Ru(1)	133.0(4)
N(2)-C(20)-Ru(1)	119.3(4)
N(1)-C(21)-C(22)	103.5(4)
N(2)-C(22)-C(21)	102.4(5)
C(24)-C(23)-C(28)	120.9(5)
C(24)-C(23)-N(1)	119.1(5)
C(28)-C(23)-N(1)	119.3(5)
C(23)-C(24)-C(25)	118.1(6)
C(23)-C(24)-C(29)	121.4(5)
C(25)-C(24)-C(29)	120.4(6)
C(26)-C(25)-C(24)	123.1(6)
C(27)-C(26)-C(25)	116.7(6)
C(27)-C(26)-C(30)	121.7(6)
C(25)-C(26)-C(30)	121.5(6)
C(26)-C(27)-C(28)	123.5(6)
C(27)-C(28)-C(23)	117.6(5)
C(27)-C(28)-C(31)	122.6(6)
C(23)-C(28)-C(31)	119.8(5)
C(37)-C(32)-C(33)	120.6(6)
C(37)-C(32)-N(2)	121.0(5)
C(33)-C(32)-N(2)	117.8(5)
C(32)-C(33)-C(34)	118.0(6)
C(32)-C(33)-C(38)	122.4(5)
C(34)-C(33)-C(38)	119.5(6)
C(35)-C(34)-C(33)	121.9(6)
C(36)-C(35)-C(34)	118.8(6)
C(36)-C(35)-C(39)	119.8(6)
C(34)-C(35)-C(39)	121.3(7)
C(35)-C(36)-C(37)	123.0(6)
C(32)-C(37)-C(36)	117.1(6)
C(32)-C(37)-C(40)	122.3(6)
C(36)-C(37)-C(40)	120.5(6)

A3.5. Anisotropic displacement parameters ($Å^2$ x 10^3) for mm426.

The anisotropic displacement factor exponent takes the form:
-2 pi^2 [h^2 a*^2 U11 + ... + 2 h k a* b* U12]

	U11	U22	U33	U23	U13	U12
P(1)	22(1)	25(1)	19(1)	-1(1)	0(1)	12(1)
Ru(1)	20(1)	23(1)	19(1)	0(1)	0(1)	10(1)
Cl(1)	21(1)	38(1)	31(1)	2(1)	2(1)	11(1)
Cl(2)	36(1)	36(1)	19(1)	2(1)	2(1)	21(1)
Cl(3)	26(1)	29(1)	26(1)	-5(1)	-3(1)	15(1)
N(1)	20(3)	23(3)	25(3)	-1(2)	-2(2)	12(2)
N(2)	21(3)	31(3)	27(3)	-1(2)	-1(2)	12(2)
C(1)	30(3)	31(4)	18(3)	1(3)	-5(3)	21(3)
C(2)	27(4)	27(3)	27(4)	5(3)	1(3)	11(3)
C(3)	22(3)	31(4)	18(4)	-1(3)	-1(3)	11(3)
C(4)	19(3)	33(4)	30(4)	10(3)	4(3)	7(3)
C(5)	37(4)	39(4)	40(4)	23(3)	17(3)	19(3)
C(6)	31(4)	24(4)	56(5)	0(3)	-1(3)	8(3)
C(7)	32(4)	28(4)	24(4)	3(3)	-1(3)	13(3)
C(8)	30(4)	41(4)	19(3)	-3(3)	-3(3)	21(3)
C(9)	35(4)	27(4)	26(4)	-1(3)	-6(3)	15(3)
C(10)	60(5)	52(4)	25(4)	-14(4)	-15(4)	29(4)
C(11)	95(7)	74(6)	27(4)	-11(4)	-6(5)	51(5)
C(12)	59(5)	84(6)	18(4)	-9(4)	5(3)	46(5)
C(13)	49(4)	50(5)	22(4)	-7(3)	-1(3)	25(4)
C(14)	21(3)	25(3)	22(3)	-3(3)	2(3)	13(3)
C(15)	28(3)	25(3)	19(3)	-6(3)	-3(3)	14(3)
C(16)	25(3)	27(3)	25(3)	1(3)	-1(3)	12(3)
C(17)	25(4)	39(4)	35(4)	-10(3)	-7(3)	13(3)
C(18)	25(3)	34(3)	25(4)	6(3)	2(3)	18(3)
C(19)	25(3)	21(3)	20(3)	0(3)	3(3)	8(3)
C(20)	27(3)	25(3)	15(3)	-3(3)	-3(3)	12(3)
C(21)	20(3)	34(4)	35(4)	-3(3)	3(3)	14(3)
C(22)	20(3)	36(4)	47(4)	2(3)	-1(3)	16(3)
C(23)	25(3)	27(4)	27(4)	0(3)	-1(3)	17(3)
C(24)	24(3)	29(4)	24(4)	5(3)	0(3)	14(3)
C(25)	21(3)	31(4)	30(4)	-5(3)	-7(3)	16(3)
C(26)	20(3)	33(4)	26(4)	9(3)	2(3)	12(3)

C(27)	26(4)	43(4)	31(4)	8(3)	2(3)	17(3)
C(28)	23(3)	35(4)	24(4)	0(3)	-2(3)	19(3)
C(29)	31(4)	29(4)	25(4)	1(3)	-2(3)	14(3)
C(30)	30(4)	40(4)	38(4)	8(3)	5(3)	10(3)
C(31)	37(4)	40(4)	25(4)	-8(3)	-3(3)	22(3)
C(32)	23(3)	20(3)	21(3)	-1(3)	-2(3)	8(3)
C(33)	27(3)	27(3)	37(4)	2(3)	3(3)	20(3)
C(34)	33(4)	35(4)	28(4)	5(3)	3(3)	18(3)
C(35)	35(4)	36(4)	31(4)	10(4)	2(4)	14(3)
C(36)	28(4)	23(4)	54(5)	3(3)	-13(3)	6(3)
C(37)	22(4)	31(4)	35(5)	5(3)	-6(3)	14(3)
C(38)	33(4)	36(4)	32(4)	-3(3)	1(3)	20(3)
C(39)	41(5)	38(4)	58(5)	17(4)	8(4)	1(4)
C(40)	43(4)	30(4)	47(5)	-10(3)	-11(3)	16(3)

A3.6. Hydrogen coordinates (x 10^4) and isotropic displacement parameters ($Å^2$ x 10^3) for mm426.

	x	y	z	U(eq)
H(1A)	9235	5159	9896	29
H(2A)	8785	3694	9866	34
H(3A)	9684	4073	11168	30
H(3B)	9165	4412	10961	30
H(4A)	8569	3420	11830	36
H(4B)	8091	3240	11088	36
H(5A)	9046	2662	11460	47
H(5B)	8159	2184	11414	47
H(6A)	8192	2330	10135	47
H(6B)	8711	1994	10356	47
H(7A)	9317	2980	9473	35
H(7B)	9791	3173	10220	35
H(8A)	10356	4890	8403	35
H(9A)	9081	3449	8507	36
H(9B)	9069	4195	8315	36
H(10A)	8973	3487	7235	54
H(10B)	9660	4317	7195	54
H(11A)	10066	3517	6778	73

H(11B)	9766	3021	7510	73
H(12A)	10977	4536	7471	59
H(12B)	11070	3826	7618	59
H(13A)	10405	3589	8752	48
H(13B)	11109	4413	8765	48
H(14A)	11271	5383	9675	26
H(15A)	10825	5964	10508	29
H(15B)	10627	5313	11094	29
H(16A)	11811	6353	11370	31
H(16B)	12102	6314	10563	31
H(17A)	12521	5733	11417	41
H(17B)	11684	5182	11677	41
H(18A)	12039	4543	10854	32
H(18B)	12266	5179	10245	32
H(19A)	10775	4199	10746	28
H(19B)	11085	4168	9946	28
H(21A)	7586	5984	9606	35
H(21B)	7383	5598	8804	35
H(22A)	8071	6716	8290	40
H(22B)	8315	7094	9094	40
H(25A)	7261	3226	8849	31
H(27A)	7309	3855	10940	40
H(29A)	7636	4766	7998	43
H(29B)	7750	4066	7878	43
H(29C)	8447	4862	8073	43
H(30A)	6203	2434	10071	59
H(30B)	6809	2559	10684	59
H(30C)	6881	2305	9870	59
H(31A)	7777	5575	10771	49
H(31B)	8606	5712	10725	49
H(31C)	8032	5133	11310	49
H(34A)	10108	7736	6565	38
H(36A)	10923	9017	8335	46
H(38A)	8470	6356	7354	49
H(38B)	9072	6115	7159	49
H(38C)	8928	6626	6599	49
H(39A)	11273	9549	7089	81
H(39B)	11076	8985	6414	81
H(39C)	11688	9079	7006	81
H(40A)	9573	8299	9428	61
H(40B)	10437	8585	9554	61
H(40C)	9834	7729	9690	61

Appendix 4

Crystal data for $[Ru(CHF)(H_2IMes)(\mu\text{-}Cl)Cl]_2$ (mm773)

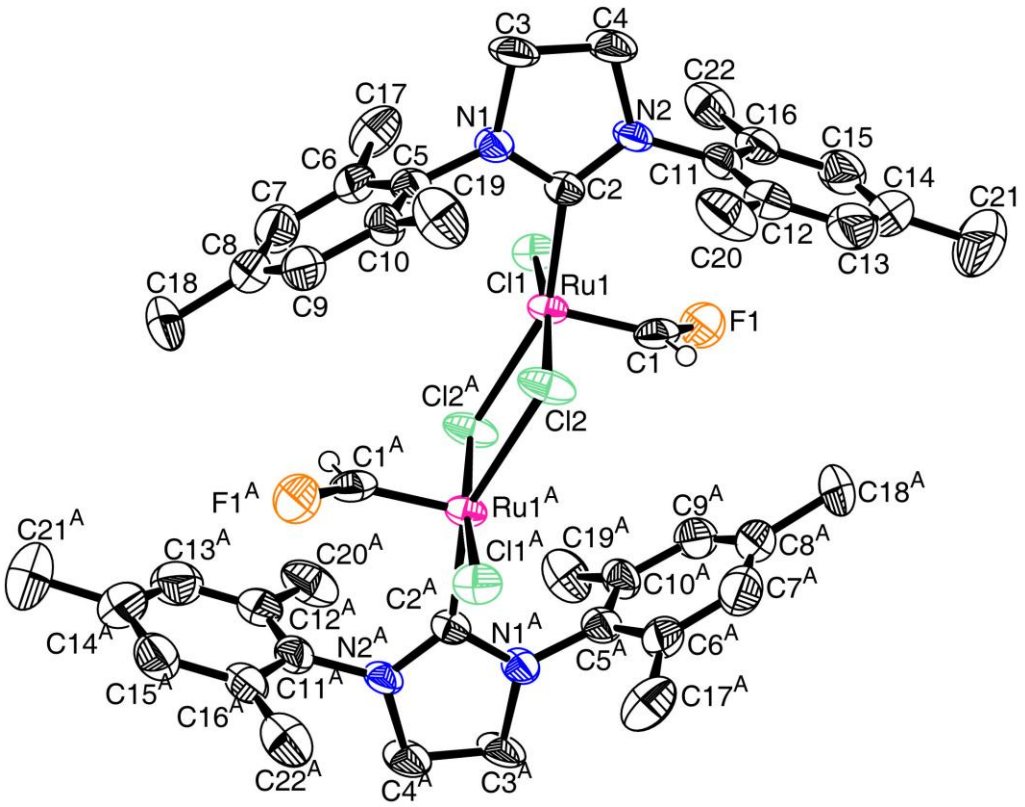

Figure A4.1. X-ray crystal structure of $[Ru(CHF)(H_2IMes)(\mu\text{-}Cl)Cl]_2$ (mm773) (50% thermal ellipsoid plot). Hydrogen atoms omitted for clarity.

A4.1. Structure Determination

Orange blocks of **mm773** were grown by diffusion of pentane into a chloroform solution at –35 °C. A crystal of dimensions 0.15 x 0.15 x 0.09 mm was mounted on a

Bruker SMART APEX CCD-based X-ray diffractometer equipped with a low temperature device and fine focus Mo-target X-ray tube (λ = 0.71073 Å) operated at 1500 W power (50 kV, 30 mA). The X-ray intensities were measured at 230(1) K; the detector was placed at a distance 5.055 cm from the crystal. Lower temperature could not be used due to a destructive phase change. A total of 930 frames were collected with a scan width of 0.5° in ω with an exposure time of 20 s/frame before sample decomposition. The integration of the data yielded a total of 31138 reflections to a maximum 2θ value of 56.68° of which 14891 were independent and 9369 were greater than 2σ(I). The final cell constants (**A4.2**) were based on the xyz centroids of 3823 reflections above 10σ(I). Analysis of the data showed approximately 15% decay during data collection; the data were processed with SADABS and corrected for absorption. The structure was solved and refined with the Bruker SHELXTL (version 6.12) software package, using the space group P1(bar) with Z = 2 for the formula $C_{44}H_{54}N_4F_2Ru_2 \cdot (CHCl_3)_2$. The structure has two independent dimers occupying inversion centers of the crystal lattice. There are two chloroform lattice solvate molecules per dimer which were modeled by use of the SQUEEZE subroutine of the PLATON program suite. All non-hydrogen atoms were refined anisotropically with the hydrogen atoms placed in idealized positions. Full matrix least-squares refinement based on F^2 converged at R1 = 0.0537 and wR2 = 0.1005 [based on I > 2σ(I)], R1 = 0.0882 and wR2 = 0.1089 for all data. Additional details are presented in **A4.2**.

Sheldrick, G.M. SHELXTL, v. 6.12; Bruker Analytical X-ray, Madison, WI, 2001.

Sheldrick, G.M. SADABS, v. 2007/4. Program for Empirical Absorption Correction of Area Detector Data, University of Gottingen: Gottingen, Germany, 2007.

Saint Plus, v. 7.34, Bruker Analytical X-ray, Madison, WI, 2006.

A.L. Spek. (2007) PLATON, A Multi-purpose Crystallographic Tool, Utrecht University, Utrecht, The Netherlands.

A4.2. Crystal data and structure refinement for mm773.

Identification code	mm773
Empirical formula	$C_{46}H_{56}Cl_{10}F_2N_4Ru_2$
Formula weight	1259.59
Temperature	230(2) K
Wavelength	0.71073 Å
Crystal system, space group	Triclinic, P-1
Unit cell dimensions	a = 12.896(3) Å alpha = 90.295(4) deg.
	b = 14.961(3) Å beta = 97.646(4) deg.
	c = 16.779(4) Å gamma = 109.138(3) deg.
Volume	3027.0(11) $Å^3$
Z, Calculated density	2, 1.382 Mg/m^3
Absorption coefficient	0.978 mm^{-1}
F(000)	1272
Crystal size	0.15 x 0.15 x 0.09 mm

Theta range for data collection	1.23 to 28.31 deg.
Limiting indices	-17<=h<=17, -19<=k<=19, -22<=l<=22
Reflections collected / unique	31138 / 14891 [R(int) = 0.0631]
Completeness to θ = 28.31	98.9 %
Absorption correction	Semi-empirical from equivalents
Refinement method	Full-matrix least-squares on F^2
Data / restraints / parameters	14891 / 0 / 517
Goodness-of-fit on F^2	1.000
Final R indices [I>2σ(I)]	R1 = 0.0537, wR2 = 0.1005
R indices (all data)	R1 = 0.0882, wR2 = 0.1089
Largest diff. peak and hole	0.927 and -0.588 e*Å $^{-3}$

A4.3. Atomic coordinates (x 10^4) and equivalent isotropic displacement parameters (Å^2 x 10^3) for mm773.

U(eq) is defined as one third of the trace of the orthogonalized Uij tensor.

	x	y	z	U(eq)
Ru(1)	9618(1)	4724(1)	5988(1)	32(1)
Ru(2)	9618(1)	9753(1)	8929(1)	32(1)
Cl(1)	8391(1)	5190(1)	6675(1)	40(1)
Cl(2)	10755(1)	4329(1)	5115(1)	48(1)
Cl(3)	10815(1)	9383(1)	10009(1)	44(1)
Cl(4)	8329(1)	10180(1)	8017(1)	45(1)
C(1)	10843(3)	5442(3)	6601(2)	42(1)
C(2)	9357(3)	3576(2)	6651(2)	32(1)
C(3)	8386(4)	2019(3)	6927(2)	60(1)
C(4)	9247(4)	2472(3)	7644(2)	52(1)
C(5)	7975(3)	2695(2)	5550(2)	39(1)

C(6)	6973(4)	2884(3)	5399(3)	48(1)
C(7)	6481(4)	2846(3)	4594(3)	59(1)
C(8)	6929(4)	2565(3)	3971(3)	63(1)
C(9)	7864(4)	2317(3)	4152(3)	59(1)
C(10)	8400(4)	2359(3)	4928(2)	45(1)
C(11)	10785(4)	4058(3)	7864(2)	41(1)
C(12)	11798(4)	4059(3)	7680(3)	51(1)
C(13)	12736(4)	4677(4)	8118(3)	70(2)
C(14)	12704(5)	5288(4)	8744(4)	80(2)
C(15)	11681(5)	5230(3)	8926(3)	66(1)
C(16)	10682(4)	4619(3)	8486(2)	46(1)
C(17)	6407(4)	3083(3)	6084(3)	68(2)
C(18)	6401(5)	2558(5)	3102(3)	99(2)
C(19)	9371(4)	2020(3)	5076(3)	64(1)
C(20)	11884(4)	3411(4)	7021(3)	71(2)
C(21)	13761(6)	5950(5)	9201(4)	136(3)
C(22)	9569(4)	4600(3)	8682(3)	59(1)
C(23)	10834(4)	10526(2)	8575(2)	42(1)
C(24)	9423(3)	8620(2)	8206(2)	34(1)
C(25)	9410(4)	7512(3)	7208(3)	57(1)
C(26)	8537(4)	7039(3)	7766(3)	55(1)
C(27)	10815(4)	9178(3)	7276(3)	47(1)
C(28)	11894(4)	9256(3)	7646(3)	59(1)
C(29)	12770(5)	9960(4)	7379(4)	82(2)
C(30)	12573(6)	10518(4)	6754(4)	90(2)
C(31)	11519(6)	10381(3)	6389(3)	76(2)
C(32)	10631(4)	9721(3)	6637(3)	53(1)
C(33)	8049(3)	7692(2)	9009(2)	39(1)
C(34)	7031(4)	7851(3)	8927(3)	45(1)
C(35)	6484(3)	7778(3)	9615(3)	51(1)
C(36)	6919(4)	7508(3)	10344(3)	52(1)
C(37)	7885(4)	7291(3)	10380(3)	49(1)
C(38)	8475(3)	7379(3)	9733(2)	42(1)
C(39)	12095(4)	8661(4)	8328(3)	74(2)
C(40)	13586(6)	11359(5)	6551(5)	145(3)
C(41)	9483(5)	9585(4)	6242(3)	72(2)
C(42)	6468(4)	8011(3)	8122(3)	63(1)
C(43)	6323(4)	7434(4)	11072(3)	83(2)
C(44)	9443(4)	7055(3)	9809(2)	46(1)
F(1)	10929(2)	6080(2)	7198(2)	57(1)
F(2)	10871(2)	11171(2)	8008(2)	61(1)
N(1)	8538(3)	2800(2)	6361(2)	37(1)
N(2)	9790(3)	3434(2)	7389(2)	37(1)
N(3)	9892(3)	8496(2)	7574(2)	40(1)
N(4)	8654(3)	7812(2)	8337(2)	38(1)

A4.4. Bond lengths [Å] and angles [deg] for mm773.

Ru(1)-C(1)	1.775(4)
Ru(1)-C(2)	2.010(3)
Ru(1)-Cl(1)	2.3483(10)
Ru(1)-Cl(2)	2.4039(11)
Ru(1)-Cl(2)#1	2.4288(10)
Ru(2)-C(23)	1.793(4)
Ru(2)-C(24)	2.007(4)
Ru(2)-Cl(4)	2.3551(10)
Ru(2)-Cl(3)	2.4078(10)
Ru(2)-Cl(3)#2	2.4244(11)
Cl(2)-Ru(1)#1	2.4289(10)
Cl(3)-Ru(2)#2	2.4244(11)
C(1)-F(1)	1.348(4)
C(2)-N(1)	1.324(4)
C(2)-N(2)	1.337(4)
C(3)-N(1)	1.489(4)
C(3)-C(4)	1.511(6)
C(4)-N(2)	1.473(4)
C(5)-C(10)	1.403(6)
C(5)-C(6)	1.403(6)
C(5)-N(1)	1.437(5)
C(6)-C(7)	1.406(6)
C(6)-C(17)	1.518(6)
C(7)-C(8)	1.386(7)
C(8)-C(9)	1.371(7)
C(8)-C(18)	1.523(6)
C(9)-C(10)	1.382(6)
C(10)-C(19)	1.491(6)
C(11)-C(12)	1.381(6)
C(11)-C(16)	1.383(5)
C(11)-N(2)	1.445(5)
C(12)-C(13)	1.371(6)
C(12)-C(20)	1.506(6)
C(13)-C(14)	1.403(7)
C(14)-C(15)	1.369(7)
C(14)-C(21)	1.502(7)
C(15)-C(16)	1.417(6)
C(16)-C(22)	1.505(6)

C(23)-F(2)	1.353(4)
C(24)-N(3)	1.329(5)
C(24)-N(4)	1.329(4)
C(25)-N(3)	1.489(5)
C(25)-C(26)	1.552(6)
C(26)-N(4)	1.454(5)
C(27)-C(32)	1.390(6)
C(27)-C(28)	1.413(6)
C(27)-N(3)	1.441(5)
C(28)-C(29)	1.395(7)
C(28)-C(39)	1.501(7)
C(29)-C(30)	1.391(8)
C(30)-C(31)	1.364(8)
C(30)-C(40)	1.565(8)
C(31)-C(32)	1.360(7)
C(32)-C(41)	1.487(7)
C(33)-C(34)	1.399(6)
C(33)-C(38)	1.414(5)
C(33)-N(4)	1.434(5)
C(34)-C(35)	1.418(6)
C(34)-C(42)	1.505(6)
C(35)-C(36)	1.395(6)
C(36)-C(37)	1.382(6)
C(36)-C(43)	1.512(6)
C(37)-C(38)	1.389(6)
C(38)-C(44)	1.470(6)

C(1)-Ru(1)-C(2)	96.58(16)
C(1)-Ru(1)-Cl(1)	95.60(14)
C(2)-Ru(1)-Cl(1)	88.86(10)
C(1)-Ru(1)-Cl(2)	88.86(14)
C(2)-Ru(1)-Cl(2)	97.60(10)
Cl(1)-Ru(1)-Cl(2)	171.69(4)
C(1)-Ru(1)-Cl(2)#1	106.86(12)
C(2)-Ru(1)-Cl(2)#1	156.56(11)
Cl(1)-Ru(1)-Cl(2)#1	88.58(4)
Cl(2)-Ru(1)-Cl(2)#1	83.41(4)
C(23)-Ru(2)-C(24)	96.88(16)
C(23)-Ru(2)-Cl(4)	96.20(14)
C(24)-Ru(2)-Cl(4)	90.12(10)
C(23)-Ru(2)-Cl(3)	88.24(14)
C(24)-Ru(2)-Cl(3)	96.09(10)
Cl(4)-Ru(2)-Cl(3)	171.90(4)
C(23)-Ru(2)-Cl(3)#2	107.63(12)
C(24)-Ru(2)-Cl(3)#2	155.46(12)

Cl(4)-Ru(2)-Cl(3)#2	88.63(4)
Cl(3)-Ru(2)-Cl(3)#2	83.55(4)
Ru(1)-Cl(2)-Ru(1)#1	96.59(4)
Ru(2)-Cl(3)-Ru(2)#2	96.45(4)
F(1)-C(1)-Ru(1)	127.6(3)
N(1)-C(2)-N(2)	109.4(3)
N(1)-C(2)-Ru(1)	117.3(3)
N(2)-C(2)-Ru(1)	132.9(3)
N(1)-C(3)-C(4)	102.8(3)
N(2)-C(4)-C(3)	103.0(3)
C(10)-C(5)-C(6)	120.8(4)
C(10)-C(5)-N(1)	119.9(4)
C(6)-C(5)-N(1)	119.2(4)
C(5)-C(6)-C(7)	118.1(4)
C(5)-C(6)-C(17)	121.1(4)
C(7)-C(6)-C(17)	120.7(4)
C(8)-C(7)-C(6)	121.1(5)
C(9)-C(8)-C(7)	118.8(4)
C(9)-C(8)-C(18)	121.1(5)
C(7)-C(8)-C(18)	120.1(5)
C(8)-C(9)-C(10)	122.9(5)
C(9)-C(10)-C(5)	117.9(4)
C(9)-C(10)-C(19)	119.3(4)
C(5)-C(10)-C(19)	122.8(4)
C(12)-C(11)-C(16)	123.0(4)
C(12)-C(11)-N(2)	118.3(4)
C(16)-C(11)-N(2)	118.7(4)
C(13)-C(12)-C(11)	117.7(5)
C(13)-C(12)-C(20)	120.5(5)
C(11)-C(12)-C(20)	121.8(4)
C(12)-C(13)-C(14)	122.8(5)
C(15)-C(14)-C(13)	117.1(5)
C(15)-C(14)-C(21)	122.5(6)
C(13)-C(14)-C(21)	120.3(6)
C(14)-C(15)-C(16)	122.6(5)
C(11)-C(16)-C(15)	116.6(4)
C(11)-C(16)-C(22)	122.2(4)
C(15)-C(16)-C(22)	121.3(4)
F(2)-C(23)-Ru(2)	126.8(3)
N(3)-C(24)-N(4)	109.6(3)
N(3)-C(24)-Ru(2)	133.1(3)
N(4)-C(24)-Ru(2)	117.3(3)
N(3)-C(25)-C(26)	101.7(3)
N(4)-C(26)-C(25)	102.6(3)
C(32)-C(27)-C(28)	122.2(4)

C(32)-C(27)-N(3)	120.1(4)
C(28)-C(27)-N(3)	117.7(4)
C(29)-C(28)-C(27)	116.5(5)
C(29)-C(28)-C(39)	121.1(5)
C(27)-C(28)-C(39)	122.2(4)
C(30)-C(29)-C(28)	120.7(6)
C(31)-C(30)-C(29)	120.5(5)
C(31)-C(30)-C(40)	121.9(7)
C(29)-C(30)-C(40)	117.4(7)
C(32)-C(31)-C(30)	121.4(5)
C(31)-C(32)-C(27)	118.6(5)
C(31)-C(32)-C(41)	121.0(5)
C(27)-C(32)-C(41)	120.4(4)
C(34)-C(33)-C(38)	121.2(4)
C(34)-C(33)-N(4)	119.7(4)
C(38)-C(33)-N(4)	119.1(4)
C(33)-C(34)-C(35)	118.2(4)
C(33)-C(34)-C(42)	121.7(4)
C(35)-C(34)-C(42)	119.8(4)
C(36)-C(35)-C(34)	121.0(4)
C(37)-C(36)-C(35)	118.6(4)
C(37)-C(36)-C(43)	121.1(4)
C(35)-C(36)-C(43)	120.3(5)
C(36)-C(37)-C(38)	122.8(4)
C(37)-C(38)-C(33)	117.8(4)
C(37)-C(38)-C(44)	118.6(4)
C(33)-C(38)-C(44)	123.3(4)
C(2)-N(1)-C(5)	122.9(3)
C(2)-N(1)-C(3)	112.2(3)
C(5)-N(1)-C(3)	124.3(3)
C(2)-N(2)-C(11)	126.5(3)
C(2)-N(2)-C(4)	112.5(3)
C(11)-N(2)-C(4)	120.4(3)
C(24)-N(3)-C(27)	126.7(3)
C(24)-N(3)-C(25)	112.4(3)
C(27)-N(3)-C(25)	120.7(3)
C(24)-N(4)-C(33)	123.4(3)
C(24)-N(4)-C(26)	113.6(3)
C(33)-N(4)-C(26)	122.9(3)

Symmetry transformations used to generate equivalent atoms:
#1 -x+2,-y+1,-z+1 #2 -x+2,-y+2,-z+2

A4.5. Anisotropic displacement parameters ($Å^2$ x 10^3) for mm773.

The anisotropic displacement factor exponent takes the form:
-2 pi^2 [h^2 a*^2 U11 + ... + 2 h k a* b* U12]

	U11	U22	U33	U23	U13	U12
Ru(1)	42(1)	26(1)	31(1)	9(1)	11(1)	15(1)
Ru(2)	43(1)	24(1)	29(1)	-2(1)	1(1)	12(1)
Cl(1)	51(1)	34(1)	41(1)	1(1)	17(1)	17(1)
Cl(2)	68(1)	52(1)	45(1)	24(1)	28(1)	41(1)
Cl(3)	57(1)	45(1)	37(1)	-10(1)	-7(1)	29(1)
Cl(4)	57(1)	36(1)	39(1)	6(1)	-4(1)	16(1)
C(1)	43(2)	33(2)	51(3)	19(2)	16(2)	12(2)
C(2)	43(2)	26(2)	30(2)	3(2)	8(2)	15(2)
C(3)	99(4)	29(2)	33(2)	13(2)	6(3)	-1(2)
C(4)	85(3)	25(2)	40(3)	12(2)	8(2)	10(2)
C(5)	50(3)	25(2)	39(2)	7(2)	4(2)	9(2)
C(6)	47(3)	37(2)	52(3)	7(2)	1(2)	5(2)
C(7)	48(3)	53(3)	70(4)	6(3)	-2(3)	12(2)
C(8)	57(3)	57(3)	53(3)	12(2)	-6(3)	-5(3)
C(9)	67(3)	54(3)	39(3)	-4(2)	7(2)	-3(3)
C(10)	59(3)	37(2)	32(2)	-2(2)	0(2)	9(2)
C(11)	49(3)	36(2)	35(2)	9(2)	1(2)	13(2)
C(12)	58(3)	52(3)	44(3)	17(2)	8(2)	17(2)
C(13)	52(3)	90(4)	66(4)	27(3)	13(3)	22(3)
C(14)	58(4)	85(4)	74(4)	22(3)	3(3)	-4(3)
C(15)	87(4)	57(3)	39(3)	1(2)	0(3)	6(3)
C(16)	70(3)	34(2)	30(2)	2(2)	5(2)	14(2)
C(17)	44(3)	64(3)	94(4)	-3(3)	20(3)	10(2)
C(18)	70(4)	138(6)	46(3)	19(3)	-23(3)	-13(4)
C(19)	90(4)	66(3)	47(3)	-11(2)	6(3)	43(3)
C(20)	83(4)	100(4)	55(3)	29(3)	20(3)	57(3)
C(21)	97(5)	142(7)	102(6)	-10(5)	-18(4)	-37(5)
C(22)	87(4)	50(3)	46(3)	1(2)	3(3)	34(3)
C(23)	61(3)	28(2)	37(2)	-6(2)	5(2)	17(2)
C(24)	48(2)	25(2)	29(2)	2(2)	-1(2)	16(2)
C(25)	90(4)	28(2)	52(3)	-6(2)	23(3)	13(2)
C(26)	82(3)	30(2)	45(3)	-6(2)	18(3)	4(2)
C(27)	60(3)	33(2)	47(3)	-7(2)	19(2)	9(2)

C(28)	70(4)	55(3)	50(3)	-8(2)	16(3)	16(3)
C(29)	67(4)	86(4)	79(4)	-24(4)	30(3)	2(3)
C(30)	112(6)	62(4)	88(5)	0(3)	65(4)	0(4)
C(31)	120(5)	45(3)	54(3)	4(2)	31(4)	11(3)
C(32)	80(4)	39(2)	41(3)	-3(2)	19(3)	17(2)
C(33)	47(3)	26(2)	33(2)	0(2)	5(2)	-1(2)
C(34)	47(3)	31(2)	46(3)	-3(2)	-4(2)	3(2)
C(35)	34(2)	50(3)	60(3)	-4(2)	6(2)	2(2)
C(36)	50(3)	51(3)	46(3)	-3(2)	9(2)	3(2)
C(37)	61(3)	49(3)	35(2)	7(2)	5(2)	15(2)
C(38)	54(3)	30(2)	36(2)	1(2)	6(2)	6(2)
C(39)	65(4)	94(4)	67(4)	-10(3)	4(3)	32(3)
C(40)	132(6)	112(6)	156(7)	-11(5)	96(6)	-33(5)
C(41)	118(5)	68(3)	46(3)	17(2)	23(3)	46(3)
C(42)	58(3)	53(3)	62(3)	10(2)	-16(3)	6(2)
C(43)	59(3)	116(5)	69(4)	20(3)	28(3)	16(3)
C(44)	62(3)	39(2)	41(2)	3(2)	3(2)	24(2)
F(1)	63(2)	44(1)	57(2)	-1(1)	4(1)	10(1)
F(2)	79(2)	40(1)	59(2)	9(1)	19(1)	10(1)
N(1)	52(2)	22(2)	32(2)	3(1)	1(2)	7(2)
N(2)	52(2)	28(2)	27(2)	9(1)	4(2)	10(2)
N(3)	54(2)	27(2)	36(2)	-4(1)	13(2)	8(2)
N(4)	57(2)	20(2)	32(2)	-3(1)	13(2)	5(2)

A4.6. Hydrogen coordinates (x 10^4) and isotropic displacement parameters ($Å^2$ x 10^3) for mm773.

	x	y	z	U(eq)
H(1A)	11517	5367	6496	50
H(3A)	8525	1469	6690	71
H(3B)	7629	1811	7077	71
H(4A)	8897	2491	8132	62
H(4B)	9784	2126	7755	62
H(7A)	5831	3015	4476	71
H(9A)	8156	2107	3724	71
H(13A)	13438	4691	7992	83
H(15A)	11639	5614	9365	80
H(17A)	6959	3325	6564	102

H(17B)	5845	2496	6204	102
H(17C)	6052	3555	5928	102
H(18A)	5957	2982	3066	149
H(18B)	5922	1913	2922	149
H(18C)	6984	2776	2758	149
H(19A)	9517	1804	4563	96
H(19B)	9211	1495	5437	96
H(19C)	10023	2540	5324	96
H(20A)	12667	3517	6985	107
H(20B)	11519	3545	6507	107
H(20C)	11522	2751	7142	107
H(21A)	13677	6567	9299	204
H(21B)	14369	6028	8885	204
H(21C)	13928	5686	9716	204
H(22A)	9223	4011	8939	88
H(22B)	9094	4636	8185	88
H(22C)	9667	5142	9049	88
H(23A)	11524	10477	8809	50
H(25A)	9979	7199	7221	68
H(25B)	9057	7503	6645	68
H(26A)	7780	6802	7460	66
H(26B)	8704	6508	8041	66
H(29A)	13508	10060	7626	98
H(31A)	11402	10754	5951	91
H(35A)	5811	7916	9579	62
H(37A)	8158	7073	10868	59
H(39A)	11735	8776	8779	111
H(39B)	12894	8829	8503	111
H(39C)	11786	7990	8149	111
H(40A)	13832	11842	6995	217
H(40B)	13366	11635	6056	217
H(40C)	14194	11124	6475	217
H(41A)	9176	8963	5952	108
H(41B)	9497	10082	5861	108
H(41C)	9020	9620	6651	108
H(42A)	7028	8297	7773	95
H(42B)	6047	8438	8196	95
H(42C)	5962	7404	7873	95
H(43A)	6704	7989	11441	124
H(43B)	6324	6858	11346	124
H(43C)	5557	7408	10899	124
H(44A)	9979	7394	10272	69
H(44B)	9789	7183	9318	69
H(44C)	9205	6373	9889	69

Appendix 5

Crystal Data for [Ru(C-*p*-C_6H_4Me)(H_2IMes)Cl_3]

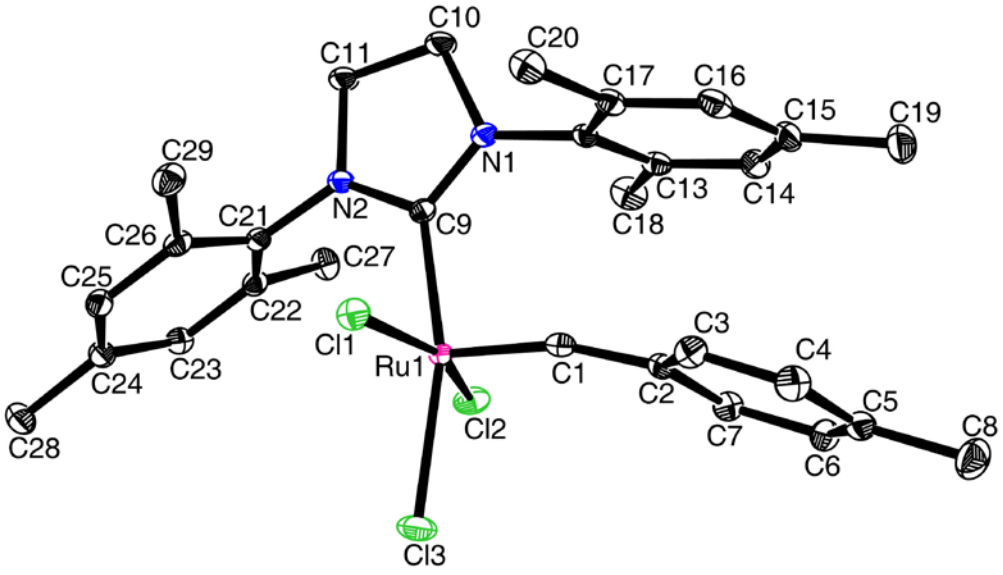

Figure A5.1. X-ray crystal structure of [Ru(C-*p*-C_6H_4Me)(H_2IMes)Cl_3] (mm668) (50% thermal ellipsoid plot). Hydrogen atoms are omitted for clarity.

A5.1. Structure Determination.

Orange needles of **mm668** were grown by diffusion of pentane into a methylene chloride solution at 23 °C. A crystal of dimensions 0.48 x 0.14 x 0.12 mm was mounted on a Bruker SMART APEX CCD-based X-ray diffractometer equipped with a low temperature device and fine focus Mo-target X-ray tube (λ = 0.71073 Å) operated at 1500 W power (50 kV, 30 mA). The X-ray intensities were measured at 85(1) K; the detector was placed at a distance 5.055 cm from the crystal. A total of 3000 frames were

collected with a scan width of 0.5° in ω and 0.45° in φ with an exposure time of 20 s/frame. The integration of the data yielded a total of 77231 reflections to a maximum 2θ value of 56.66° of which 7684 were independent and 7403 were greater than 2σ(I). The final cell constants (**A5.2**) were based on the xyz centroids of 9901 reflections above 10σ(I). Analysis of the data showed negligible decay during data collection; the data were processed with SADABS and corrected for absorption. The structure was solved and refined with the Bruker SHELXTL (version 6.12) software package, using the space group P2(1)/c with Z = 4 for the formula $C_{29}H_{33}N_2Cl_3Ru•CH_2Cl_2$. All non-hydrogen atoms were refined anisotropically with the hydrogen atoms placed in idealized positions. Full matrix least-squares refinement based on F^2 converged at R1 = 0.0317 and wR2 = 0.0776[based on I > 2σ(I)], R1 = 0.0330 and wR2 = 0.0784 for all data. Additional details are presented in **A5.2**.

Sheldrick, G.M. SHELXTL, v. 6.12; Bruker Analytical X-ray, Madison, WI, 2001.

Sheldrick, G.M. SADABS, v. 2.10. Program for Empirical Absorption Correction of Area Detector Data, University of Gottingen: Gottingen, Germany, 2003.

Saint Plus, v. 7.34, Bruker Analytical X-ray, Madison, WI, 2006.

A5.2. Crystal data and structure refinement for mm668.

Identification code	mm668
Empirical formula	C_{30} H_{35} Cl_5 N_2 Ru
Formula weight	701.92
Temperature	85(2) K
Wavelength	0.71073 Å
Crystal system, space group	Monoclinic, P2(1)/c
Unit cell dimensions	a = 8.2992(6) Å alpha = 90 deg.
	b = 22.0834(15) Å beta = 101.869(1) deg.
	c = 17.2123(12) Å gamma = 90 deg.
Volume	3087.1(4) $Å^3$
Z, Calculated density	4, 1.510 Mg/m^3
Absorption coefficient	0.963 mm^{-1}
F(000)	1432
Crystal size	0.48 x 0.14 x 0.12 mm
Theta range for data collection	1.52 to 28.33 deg.
Limiting indices	-11<=h<=11, -29<=k<=29, -22<=l<=22
Reflections collected / unique	77231 / 7684 [R(int) = 0.0416]
Completeness to θ = 28.33	100.0 %
Absorption correction	Semi-empirical from equivalents
Max. and min. transmission	0.8931 and 0.6549
Refinement method	Full-matrix least-squares on F^2

Data / restraints / parameters	7684 / 0 / 350
Goodness-of-fit on F^2	1.121
Final R indices [I>2σ(I)]	R1 = 0.0317, wR2 = 0.0776
R indices (all data)	R1 = 0.0330, wR2 = 0.0784
Largest diff. peak and hole	1.316 and -0.873 e*$Å^{-3}$

A5.3. Atomic coordinates (x 10^4) and equivalent isotropic displacement parameters ($Å^2$ x 10^3) for mm668.

U(eq) is defined as one third of the trace of the orthogonalized Uij tensor.

	x	y	z	U(eq)
Ru(1)	2667(1)	4740(1)	2207(1)	11(1)
Cl(1)	1152(1)	5527(1)	1504(1)	17(1)
Cl(2)	4292(1)	4179(1)	3219(1)	19(1)
Cl(3)	5081(1)	5275(1)	2077(1)	24(1)
Cl(4)	7467(1)	2235(1)	2475(1)	63(1)
Cl(5)	4502(1)	1736(1)	1527(1)	55(1)
N(1)	-505(2)	4026(1)	2206(1)	14(1)
N(2)	48(2)	4681(1)	3169(1)	14(1)
C(1)	2654(2)	4248(1)	1469(1)	13(1)
C(2)	3063(2)	3907(1)	840(1)	13(1)
C(3)	2421(3)	4079(1)	54(1)	17(1)
C(4)	2947(3)	3778(1)	-554(1)	18(1)
C(5)	4074(3)	3304(1)	-394(1)	17(1)
C(6)	4680(3)	3132(1)	395(1)	17(1)
C(7)	4187(2)	3428(1)	1015(1)	15(1)
C(8)	4618(3)	2973(1)	-1056(1)	26(1)
C(9)	570(2)	4444(1)	2547(1)	12(1)
C(10)	-1952(3)	3981(1)	2585(1)	19(1)
C(11)	-1514(2)	4416(1)	3283(1)	17(1)
C(12)	-362(2)	3636(1)	1560(1)	12(1)
C(13)	529(2)	3098(1)	1727(1)	15(1)
C(14)	656(3)	2721(1)	1092(1)	19(1)
C(15)	-81(3)	2866(1)	316(1)	20(1)

C(16)	-1008(3)	3394(1)	176(1)	18(1)
C(17)	-1176(2)	3786(1)	790(1)	14(1)
C(18)	1371(3)	2932(1)	2560(1)	22(1)
C(19)	171(3)	2466(1)	-361(2)	29(1)
C(20)	-2165(3)	4358(1)	620(1)	20(1)
C(21)	848(2)	5149(1)	3685(1)	13(1)
C(22)	1949(2)	4988(1)	4389(1)	14(1)
C(23)	2774(2)	5449(1)	4860(1)	14(1)
C(24)	2460(2)	6060(1)	4672(1)	15(1)
C(25)	1248(2)	6200(1)	4011(1)	15(1)
C(26)	414(2)	5754(1)	3509(1)	14(1)
C(27)	2173(3)	4342(1)	4670(1)	18(1)
C(28)	3376(3)	6558(1)	5172(1)	20(1)
C(29)	-962(3)	5936(1)	2839(1)	20(1)
C(30)	6280(3)	1582(1)	2239(2)	27(1)

A5.4. Bond lengths [Å] and angles [deg] for mm668.

Ru(1)-C(1)	1.669(2)
Ru(1)-C(9)	2.0543(19)
Ru(1)-Cl(2)	2.3282(5)
Ru(1)-Cl(1)	2.3319(5)
Ru(1)-Cl(3)	2.3764(5)
Cl(4)-C(30)	1.747(3)
Cl(5)-C(30)	1.747(3)
N(1)-C(9)	1.333(2)
N(1)-C(12)	1.431(2)
N(1)-C(10)	1.482(2)
N(2)-C(9)	1.341(2)
N(2)-C(21)	1.434(2)
N(2)-C(11)	1.472(2)
C(1)-C(2)	1.416(3)
C(2)-C(3)	1.401(3)
C(2)-C(7)	1.402(3)
C(3)-C(4)	1.383(3)
C(4)-C(5)	1.392(3)
C(5)-C(6)	1.400(3)
C(5)-C(8)	1.500(3)
C(6)-C(7)	1.382(3)
C(10)-C(11)	1.523(3)
C(12)-C(13)	1.398(3)

C(12)-C(17)	1.400(3)
C(13)-C(14)	1.393(3)
C(13)-C(18)	1.506(3)
C(14)-C(15)	1.387(3)
C(15)-C(16)	1.390(3)
C(15)-C(19)	1.510(3)
C(16)-C(17)	1.396(3)
C(17)-C(20)	1.501(3)
C(21)-C(26)	1.400(3)
C(21)-C(22)	1.404(3)
C(22)-C(23)	1.392(3)
C(22)-C(27)	1.505(3)
C(23)-C(24)	1.399(3)
C(24)-C(25)	1.390(3)
C(24)-C(28)	1.504(3)
C(25)-C(26)	1.396(3)
C(26)-C(29)	1.502(3)

C(1)-Ru(1)-C(9)	97.83(8)
C(1)-Ru(1)-Cl(2)	97.76(7)
C(9)-Ru(1)-Cl(2)	90.66(5)
C(1)-Ru(1)-Cl(1)	99.93(7)
C(9)-Ru(1)-Cl(1)	89.28(5)
Cl(2)-Ru(1)-Cl(1)	162.15(2)
C(1)-Ru(1)-Cl(3)	97.25(7)
C(9)-Ru(1)-Cl(3)	164.90(6)
Cl(2)-Ru(1)-Cl(3)	88.00(2)
Cl(1)-Ru(1)-Cl(3)	87.444(19)
C(9)-N(1)-C(12)	127.15(16)
C(9)-N(1)-C(10)	112.49(16)
C(12)-N(1)-C(10)	120.34(16)
C(9)-N(2)-C(21)	126.33(16)
C(9)-N(2)-C(11)	112.89(16)
C(21)-N(2)-C(11)	120.78(16)
C(2)-C(1)-Ru(1)	164.21(16)
C(3)-C(2)-C(7)	120.99(18)
C(3)-C(2)-C(1)	119.46(18)
C(7)-C(2)-C(1)	119.41(18)
C(4)-C(3)-C(2)	118.95(19)
C(3)-C(4)-C(5)	121.01(19)
C(4)-C(5)-C(6)	119.23(19)
C(4)-C(5)-C(8)	120.72(19)
C(6)-C(5)-C(8)	120.0(2)
C(7)-C(6)-C(5)	121.07(19)
C(6)-C(7)-C(2)	118.74(18)

N(1)-C(9)-N(2)	108.98(16)
N(1)-C(9)-Ru(1)	128.65(14)
N(2)-C(9)-Ru(1)	122.33(14)
N(1)-C(10)-C(11)	102.78(16)
N(2)-C(11)-C(10)	102.63(15)
C(13)-C(12)-C(17)	121.88(18)
C(13)-C(12)-N(1)	118.56(17)
C(17)-C(12)-N(1)	119.48(18)
C(14)-C(13)-C(12)	117.93(19)
C(14)-C(13)-C(18)	120.46(19)
C(12)-C(13)-C(18)	121.59(19)
C(15)-C(14)-C(13)	121.9(2)
C(14)-C(15)-C(16)	118.60(19)
C(14)-C(15)-C(19)	120.3(2)
C(16)-C(15)-C(19)	121.0(2)
C(15)-C(16)-C(17)	121.82(19)
C(16)-C(17)-C(12)	117.77(19)
C(16)-C(17)-C(20)	120.72(19)
C(12)-C(17)-C(20)	121.50(18)
C(26)-C(21)-C(22)	121.45(18)
C(26)-C(21)-N(2)	119.15(18)
C(22)-C(21)-N(2)	119.20(18)
C(23)-C(22)-C(21)	118.11(18)
C(23)-C(22)-C(27)	119.50(18)
C(21)-C(22)-C(27)	122.26(18)
C(22)-C(23)-C(24)	121.67(19)
C(25)-C(24)-C(23)	118.24(18)
C(25)-C(24)-C(28)	120.09(19)
C(23)-C(24)-C(28)	121.67(19)
C(24)-C(25)-C(26)	122.18(19)
C(25)-C(26)-C(21)	117.80(18)
C(25)-C(26)-C(29)	119.25(18)
C(21)-C(26)-C(29)	122.85(18)
Cl(5)-C(30)-Cl(4)	110.88(14)

A5.5. Anisotropic displacement parameters (Å^2 x 10^3) for mm668.

The anisotropic displacement factor exponent takes the form:
-2 pi^2 [h^2 a*^2 U11 + ... + 2 h k a* b* U12]

	U11	U22	U33	U23	U13	U12
Ru(1)	9(1)	12(1)	12(1)	-1(1)	3(1)	-1(1)
Cl(1)	16(1)	15(1)	18(1)	4(1)	3(1)	1(1)
Cl(2)	12(1)	27(1)	16(1)	4(1)	0(1)	1(1)
Cl(3)	13(1)	20(1)	39(1)	2(1)	6(1)	-4(1)
Cl(4)	78(1)	46(1)	73(1)	-18(1)	37(1)	-34(1)
Cl(5)	29(1)	67(1)	70(1)	43(1)	10(1)	5(1)
N(1)	12(1)	17(1)	14(1)	-2(1)	5(1)	-2(1)
N(2)	11(1)	17(1)	14(1)	-4(1)	4(1)	-3(1)
C(1)	10(1)	14(1)	14(1)	2(1)	2(1)	-1(1)
C(2)	13(1)	13(1)	14(1)	-2(1)	3(1)	-3(1)
C(3)	17(1)	16(1)	17(1)	2(1)	4(1)	1(1)
C(4)	20(1)	23(1)	12(1)	2(1)	2(1)	0(1)
C(5)	15(1)	19(1)	16(1)	-3(1)	5(1)	-3(1)
C(6)	17(1)	15(1)	19(1)	-1(1)	4(1)	2(1)
C(7)	15(1)	17(1)	14(1)	1(1)	3(1)	0(1)
C(8)	24(1)	36(1)	18(1)	-6(1)	6(1)	3(1)
C(9)	10(1)	13(1)	12(1)	1(1)	2(1)	1(1)
C(10)	15(1)	25(1)	20(1)	-6(1)	9(1)	-8(1)
C(11)	14(1)	22(1)	18(1)	-5(1)	8(1)	-6(1)
C(12)	12(1)	13(1)	14(1)	-2(1)	4(1)	-4(1)
C(13)	12(1)	14(1)	18(1)	1(1)	3(1)	-3(1)
C(14)	18(1)	12(1)	27(1)	-2(1)	9(1)	-3(1)
C(15)	21(1)	19(1)	22(1)	-8(1)	10(1)	-8(1)
C(16)	18(1)	22(1)	14(1)	-1(1)	3(1)	-8(1)
C(17)	14(1)	15(1)	15(1)	1(1)	3(1)	-4(1)
C(18)	22(1)	20(1)	22(1)	6(1)	-1(1)	0(1)
C(19)	33(1)	28(1)	29(1)	-15(1)	16(1)	-10(1)
C(20)	19(1)	18(1)	21(1)	3(1)	0(1)	0(1)
C(21)	12(1)	16(1)	13(1)	-3(1)	5(1)	-2(1)
C(22)	14(1)	14(1)	14(1)	0(1)	6(1)	0(1)
C(23)	14(1)	17(1)	12(1)	0(1)	3(1)	0(1)
C(24)	16(1)	16(1)	15(1)	-2(1)	6(1)	-2(1)
C(25)	15(1)	14(1)	17(1)	0(1)	4(1)	1(1)

C(26)	12(1)	18(1)	14(1)	0(1)	5(1)	1(1)
C(27)	23(1)	14(1)	16(1)	2(1)	4(1)	0(1)
C(28)	20(1)	17(1)	21(1)	-2(1)	1(1)	-3(1)
C(29)	16(1)	23(1)	18(1)	-1(1)	0(1)	5(1)
C(30)	26(1)	21(1)	37(1)	5(1)	14(1)	3(1)

A5.6. Hydrogen coordinates (x 10^4) and isotropic displacement parameters ($Å^2$ x 10^3) for mm668.

	x	y	z	U(eq)
H(3A)	1638	4397	-61	20
H(4A)	2533	3896	-1088	22
H(6A)	5442	2807	506	20
H(7A)	4603	3309	1549	18
H(8A)	4098	3156	-1565	38
H(8B)	4292	2547	-1050	38
H(8C)	5817	3001	-986	38
H(10A)	-2092	3563	2768	23
H(10B)	-2973	4108	2215	23
H(11A)	-2371	4731	3263	21
H(11B)	-1367	4198	3796	21
H(14A)	1264	2355	1194	22
H(16A)	-1541	3490	-353	21
H(18A)	1766	2513	2570	33
H(18B)	588	2970	2913	33
H(18C)	2305	3204	2740	33
H(19A)	1208	2574	-514	43
H(19B)	-745	2523	-815	43
H(19C)	213	2041	-192	43
H(20A)	-2432	4430	46	30
H(20B)	-1523	4699	885	30
H(20C)	-3185	4318	818	30
H(23A)	3572	5347	5321	17
H(25A)	978	6613	3896	18
H(27A)	3275	4292	5003	27
H(27B)	2050	4071	4211	27
H(27C)	1342	4242	4980	27

H(28A)	2981	6952	4946	29
H(28B)	4556	6521	5182	29
H(28C)	3187	6528	5715	29
H(29A)	-1958	6014	3045	29
H(29B)	-1176	5608	2447	29
H(29C)	-651	6303	2587	29
H(30A)	6938	1269	2033	32
H(30B)	5970	1420	2725	32

Appendix 6

Crystal Data for [Ru(C-*p*-C_6H_4Me)(H_2IMes)I_3] (mm841a)

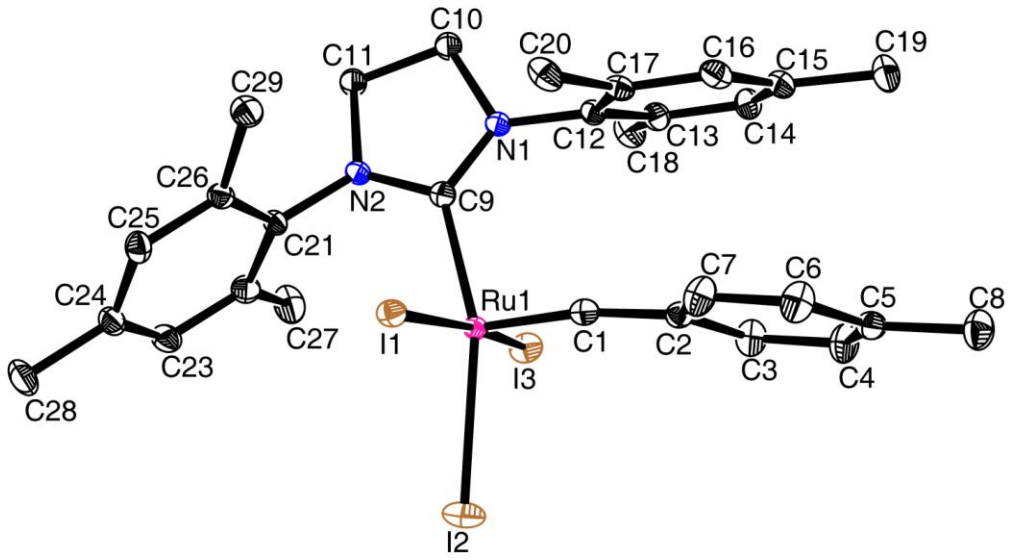

Figure A6.1. X-ray crystal structure of [Ru(C-*p*-C_6H_4Me)(H_2IMes)I_3] (mm841a) (50% thermal ellipsoid plot). Hydrogen atoms are omitted for clarity.

A6.1. Structure Determination.

Colorless plates of **mm841a** were grown by slow diffusion of pentane into a dichloromethane solution at –35 °C. A crystal of dimensions 0.22 x 0.10 x 0.07 mm was mounted on a Bruker SMART APEX CCD-based X-ray diffractometer equipped with a low temperature device and fine focus Mo-target X-ray tube (λ = 0.71073 Å) operated at 1500 W power (50 kV, 30 mA). The X-ray intensities were measured at 85(1) K; the detector was placed at a distance 5.055 cm from the crystal. A total of 3300 frames were

collected with a scan width of 0.5° in ω and 0.45° in φ with an exposure time of 20 s/frame. The integration of the data yielded a total of 48485 reflections to a maximum 2θ value of 56.70° of which 8549 were independent and 7960 were greater than 2σ(I). The final cell constants (**A6.2**) were based on the xyz centroids of 9922 reflections above 10σ(I). Analysis of the data showed negligible decay during data collection; the data were processed with SADABS and corrected for absorption. The structure was solved and refined with the Bruker SHELXTL (version 6.12) software package, using the space group P1(bar) with Z = 2 for the formula $C_{29}H_{33}N_2I_3Ru•(CHCl)_3$. All non-hydrogen atoms were refined anisotropically with the hydrogen atoms placed in idealized positions. Full matrix least-squares refinement based on F^2 converged at R1 = 0.0244 and wR2 = 0.0643 [based on I > 2σ(I)], R1 = 0.0269 and wR2 = 0.0655 for all data. Additional details are presented in **A6.2**.

Sheldrick, G.M. SHELXTL, v. 6.12; Bruker Analytical X-ray, Madison, WI, 2001.

Sheldrick, G.M. SADABS, v. 2007/4. Program for Empirical Absorption Correction of Area Detector Data, University of Gottingen: Gottingen, Germany, 2007.

Saint Plus, v. 7.34, Bruker Analytical X-ray, Madison, WI, 2006.

A6.2. Crystal data and structure refinement for mm841a.

Identification code	mm841a
Empirical formula	C_{30} H_{34} Cl_3 I_3 N_2 Ru
Formula weight	1010.71
Temperature	85(2) K
Wavelength	0.71073 Å
Crystal system, space group	Triclinic, P-1
Unit cell dimensions	a = 8.6389(6) Å alpha = 103.322(1) deg.
	b = 12.9632(9) Å beta = 103.899(1) deg.
	c = 16.5451(12) Å gamma = 97.880(1) deg.
Volume	1713.5(2) $Å^3$
Z, Calculated density	2, 1.959 Mg/m^3
Absorption coefficient	3.416 mm^{-1}
F(000)	964
Crystal size	0.22 x 0.10 x 0.07 mm
Theta range for data collection	1.81 to 28.35 deg.
Limiting indices	-11<=h<=11, -17<=k<=17, -22<=l<=22
Reflections collected / unique	48485 / 8549 [R(int) = 0.0319]
Completeness to θ = 28.35	99.8 %
Absorption correction	Semi-empirical from equivalents
Max. and min. transmission	0.7959 and 0.5203
Refinement method	Full-matrix least-squares on F^2

Data / restraints / parameters	8549 / 0 / 359
Goodness-of-fit on F^2	1.100
Final R indices [I>2σ(I)]	R1 = 0.0244, wR2 = 0.0643
R indices (all data)	R1 = 0.0269, wR2 = 0.0655
Largest diff. peak and hole	1.233 and -1.473 e*Å^{-3}

A6.3. Atomic coordinates (x 10^4) and equivalent isotropic displacement parameters (Å^2 x 10^3) for mm841a.

U(eq) is defined as one third of the trace of the orthogonalized Uij tensor.

	x	y	z	U(eq)
Ru(1)	8027(1)	3182(1)	7187(1)	12(1)
I(1)	6279(1)	1354(1)	7291(1)	15(1)
I(2)	6121(1)	4328(1)	7918(1)	25(1)
I(3)	9931(1)	5060(1)	7333(1)	20(1)
Cl(1)	5431(2)	3241(1)	1110(1)	48(1)
Cl(2)	4117(1)	956(1)	717(1)	36(1)
Cl(3)	5236(1)	1826(1)	-552(1)	36(1)
N(1)	10624(3)	2278(2)	6394(2)	14(1)
N(2)	11026(3)	2332(2)	7754(2)	14(1)
C(1)	7080(3)	3002(2)	6147(2)	14(1)
C(2)	6064(3)	2925(2)	5310(2)	15(1)
C(3)	6221(4)	3791(2)	4949(2)	20(1)
C(4)	5186(4)	3711(3)	4147(2)	22(1)
C(5)	4004(4)	2779(2)	3696(2)	18(1)
C(6)	3857(4)	1926(3)	4072(2)	23(1)
C(7)	4881(4)	1988(3)	4872(2)	22(1)
C(8)	2903(4)	2690(3)	2818(2)	24(1)
C(9)	10016(3)	2498(2)	7070(2)	13(1)
C(10)	12162(4)	1887(3)	6604(2)	20(1)
C(11)	12501(3)	2000(3)	7570(2)	18(1)
C(12)	9880(3)	2234(2)	5511(2)	14(1)
C(13)	10465(4)	3033(2)	5154(2)	17(1)
C(14)	9714(4)	2947(3)	4288(2)	21(1)

C(15)	8460(4)	2093(3)	3778(2)	21(1)
C(16)	7972(4)	1279(3)	4138(2)	19(1)
C(17)	8671(3)	1331(2)	5002(2)	16(1)
C(18)	11886(4)	3944(3)	5655(2)	23(1)
C(19)	7627(5)	2040(3)	2849(2)	29(1)
C(20)	8143(4)	427(2)	5366(2)	21(1)
C(21)	10677(3)	2283(2)	8554(2)	14(1)
C(22)	11045(4)	3210(2)	9248(2)	18(1)
C(23)	10605(4)	3112(3)	9994(2)	20(1)
C(24)	9886(4)	2120(3)	10063(2)	19(1)
C(25)	9666(4)	1204(2)	9385(2)	18(1)
C(26)	10050(3)	1257(2)	8626(2)	14(1)
C(27)	11995(5)	4280(3)	9259(2)	27(1)
C(28)	9402(4)	2029(3)	10863(2)	27(1)
C(29)	9835(4)	236(2)	7923(2)	20(1)
C(30)	4308(5)	2074(3)	291(2)	32(1)

A6.4. Bond lengths [Å] and angles [deg] for mm841a.

Ru(1)-C(1)	1.664(3)
Ru(1)-C(9)	2.067(3)
Ru(1)-I(3)	2.6702(3)
Ru(1)-I(2)	2.6802(3)
Ru(1)-I(1)	2.6941(3)
Cl(1)-C(30)	1.757(4)
Cl(2)-C(30)	1.757(4)
Cl(3)-C(30)	1.759(4)
N(1)-C(9)	1.336(3)
N(1)-C(12)	1.433(3)
N(1)-C(10)	1.478(4)
N(2)-C(9)	1.333(4)
N(2)-C(21)	1.439(3)
N(2)-C(11)	1.476(3)
C(1)-C(2)	1.423(4)
C(2)-C(3)	1.393(4)
C(2)-C(7)	1.394(4)
C(3)-C(4)	1.383(4)
C(4)-C(5)	1.393(4)
C(5)-C(6)	1.394(4)
C(5)-C(8)	1.502(4)
C(6)-C(7)	1.382(4)

C(10)-C(11)	1.522(4)
C(12)-C(13)	1.398(4)
C(12)-C(17)	1.399(4)
C(13)-C(14)	1.395(4)
C(13)-C(18)	1.501(4)
C(14)-C(15)	1.383(5)
C(15)-C(16)	1.390(4)
C(15)-C(19)	1.514(4)
C(16)-C(17)	1.395(4)
C(17)-C(20)	1.502(4)
C(21)-C(22)	1.396(4)
C(21)-C(26)	1.409(4)
C(22)-C(23)	1.403(4)
C(22)-C(27)	1.505(4)
C(23)-C(24)	1.391(4)
C(24)-C(25)	1.389(4)
C(24)-C(28)	1.504(4)
C(25)-C(26)	1.387(4)
C(26)-C(29)	1.503(4)

C(1)-Ru(1)-C(9)	100.08(12)
C(1)-Ru(1)-I(3)	93.86(9)
C(9)-Ru(1)-I(3)	86.04(7)
C(1)-Ru(1)-I(2)	99.76(10)
C(9)-Ru(1)-I(2)	159.58(8)
I(3)-Ru(1)-I(2)	87.823(10)
C(1)-Ru(1)-I(1)	94.40(9)
C(9)-Ru(1)-I(1)	93.75(7)
I(3)-Ru(1)-I(1)	171.642(11)
I(2)-Ru(1)-I(1)	89.529(10)
C(9)-N(1)-C(12)	128.6(2)
C(9)-N(1)-C(10)	112.2(2)
C(12)-N(1)-C(10)	118.6(2)
C(9)-N(2)-C(21)	126.2(2)
C(9)-N(2)-C(11)	112.8(2)
C(21)-N(2)-C(11)	120.2(2)
C(2)-C(1)-Ru(1)	170.3(2)
C(3)-C(2)-C(7)	120.7(3)
C(3)-C(2)-C(1)	120.2(3)
C(7)-C(2)-C(1)	119.1(3)
C(4)-C(3)-C(2)	119.2(3)
C(3)-C(4)-C(5)	121.0(3)
C(4)-C(5)-C(6)	119.0(3)
C(4)-C(5)-C(8)	120.7(3)
C(6)-C(5)-C(8)	120.3(3)

C(7)-C(6)-C(5)	121.0(3)
C(6)-C(7)-C(2)	119.2(3)
N(2)-C(9)-N(1)	109.2(2)
N(2)-C(9)-Ru(1)	121.1(2)
N(1)-C(9)-Ru(1)	129.2(2)
N(1)-C(10)-C(11)	103.0(2)
N(2)-C(11)-C(10)	102.4(2)
C(13)-C(12)-C(17)	121.4(3)
C(13)-C(12)-N(1)	120.0(3)
C(17)-C(12)-N(1)	118.4(2)
C(14)-C(13)-C(12)	117.8(3)
C(14)-C(13)-C(18)	119.4(3)
C(12)-C(13)-C(18)	122.7(3)
C(15)-C(14)-C(13)	122.2(3)
C(14)-C(15)-C(16)	118.5(3)
C(14)-C(15)-C(19)	121.1(3)
C(16)-C(15)-C(19)	120.4(3)
C(15)-C(16)-C(17)	121.5(3)
C(16)-C(17)-C(12)	118.4(3)
C(16)-C(17)-C(20)	120.2(3)
C(12)-C(17)-C(20)	121.4(3)
C(22)-C(21)-C(26)	121.5(3)
C(22)-C(21)-N(2)	120.9(3)
C(26)-C(21)-N(2)	117.4(2)
C(21)-C(22)-C(23)	117.8(3)
C(21)-C(22)-C(27)	123.3(3)
C(23)-C(22)-C(27)	118.8(3)
C(24)-C(23)-C(22)	121.8(3)
C(25)-C(24)-C(23)	118.4(3)
C(25)-C(24)-C(28)	120.4(3)
C(23)-C(24)-C(28)	121.2(3)
C(26)-C(25)-C(24)	122.2(3)
C(25)-C(26)-C(21)	117.9(3)
C(25)-C(26)-C(29)	120.0(3)
C(21)-C(26)-C(29)	122.1(2)
Cl(1)-C(30)-Cl(2)	110.4(2)
Cl(1)-C(30)-Cl(3)	110.3(2)
Cl(2)-C(30)-Cl(3)	110.9(2)

A6.5. Anisotropic displacement parameters ($Å^2$ x 10^3) for mm841a.

The anisotropic displacement factor exponent takes the form:
-2 pi^2 [h^2 a*^2 U11 + ... + 2 h k a* b* U12]

	U11	U22	U33	U23	U13	U12
Ru(1)	12(1)	11(1)	12(1)	3(1)	4(1)	2(1)
I(1)	14(1)	15(1)	20(1)	6(1)	8(1)	3(1)
I(2)	24(1)	18(1)	33(1)	1(1)	16(1)	5(1)
I(3)	20(1)	13(1)	28(1)	6(1)	8(1)	0(1)
Cl(1)	83(1)	29(1)	43(1)	9(1)	30(1)	21(1)
Cl(2)	40(1)	37(1)	32(1)	9(1)	13(1)	6(1)
Cl(3)	32(1)	58(1)	22(1)	14(1)	9(1)	16(1)
N(1)	13(1)	16(1)	14(1)	5(1)	5(1)	4(1)
N(2)	13(1)	17(1)	14(1)	6(1)	7(1)	4(1)
C(1)	14(1)	11(1)	19(1)	5(1)	7(1)	1(1)
C(2)	13(1)	16(1)	17(1)	5(1)	5(1)	4(1)
C(3)	20(1)	16(1)	21(1)	6(1)	2(1)	-3(1)
C(4)	24(2)	19(1)	22(2)	10(1)	3(1)	0(1)
C(5)	17(1)	19(1)	16(1)	3(1)	4(1)	6(1)
C(6)	23(2)	18(1)	24(2)	6(1)	-1(1)	-2(1)
C(7)	22(2)	17(1)	26(2)	10(1)	2(1)	0(1)
C(8)	25(2)	23(2)	18(1)	5(1)	-1(1)	2(1)
C(9)	14(1)	10(1)	16(1)	4(1)	6(1)	1(1)
C(10)	16(1)	32(2)	18(1)	11(1)	9(1)	12(1)
C(11)	12(1)	28(2)	18(1)	10(1)	7(1)	7(1)
C(12)	14(1)	18(1)	14(1)	6(1)	6(1)	5(1)
C(13)	18(1)	19(1)	18(1)	8(1)	9(1)	4(1)
C(14)	25(2)	24(2)	18(1)	11(1)	10(1)	8(1)
C(15)	22(2)	30(2)	16(1)	7(1)	9(1)	12(1)
C(16)	16(1)	21(1)	17(1)	0(1)	5(1)	3(1)
C(17)	16(1)	17(1)	17(1)	4(1)	8(1)	4(1)
C(18)	24(2)	22(2)	23(2)	8(1)	10(1)	-2(1)
C(19)	32(2)	42(2)	15(1)	9(1)	6(1)	13(2)
C(20)	28(2)	16(1)	20(1)	3(1)	12(1)	-1(1)
C(21)	14(1)	18(1)	13(1)	6(1)	6(1)	4(1)
C(22)	20(1)	16(1)	18(1)	3(1)	5(1)	4(1)
C(23)	22(2)	21(2)	15(1)	1(1)	5(1)	6(1)
C(24)	16(1)	29(2)	15(1)	8(1)	6(1)	8(1)

C(25)	17(1)	20(1)	17(1)	8(1)	6(1)	3(1)
C(26)	14(1)	16(1)	14(1)	3(1)	4(1)	4(1)
C(27)	38(2)	18(2)	21(2)	3(1)	6(1)	-2(1)
C(28)	29(2)	41(2)	16(1)	11(1)	11(1)	10(2)
C(29)	26(2)	14(1)	20(1)	4(1)	8(1)	3(1)
C(30)	30(2)	47(2)	29(2)	16(2)	12(2)	20(2)

A6.6. Hydrogen coordinates (x 10^4) and isotropic displacement parameters (Å^2 x 10^3) for mm841a.

	x	y	z	U(eq)
H(3A)	7028	4428	5250	25
H(4A)	5283	4300	3899	26
H(6A)	3042	1292	3774	28
H(7A)	4779	1400	5121	27
H(8A)	3236	2202	2374	36
H(8B)	2977	3408	2716	36
H(8C)	1777	2401	2792	36
H(10A)	13049	2339	6481	24
H(10B)	12027	1124	6274	24
H(11A)	12632	1304	7701	21
H(11B)	13490	2559	7906	21
H(14A)	10077	3493	4040	25
H(16A)	7142	674	3786	23
H(18A)	12172	3955	6268	35
H(18B)	11595	4633	5596	35
H(18C)	12820	3840	5429	35
H(19A)	6930	2576	2839	44
H(19B)	6962	1314	2553	44
H(19C)	8452	2197	2553	44
H(20A)	7305	-135	4912	32
H(20B)	7699	708	5845	32
H(20C)	9082	116	5578	32
H(23A)	10803	3739	10464	24
H(25A)	9238	518	9442	21
H(27A)	12346	4198	8730	41
H(27B)	12952	4519	9765	41

H(27C)	11304	4820	9286	41
H(28A)	8461	1432	10706	41
H(28B)	9116	2707	11127	41
H(28C)	10315	1888	11276	41
H(29A)	10847	-38	8009	30
H(29B)	9567	390	7358	30
H(29C)	8950	-310	7943	30
H(30A)	3193	2199	52	39

Appendix 7

Crystal Data for [Ru(≡C-*p*-C_6H_4Me)(H_2IMes)($O_2C_6Cl_4$)I] (mm1405a)

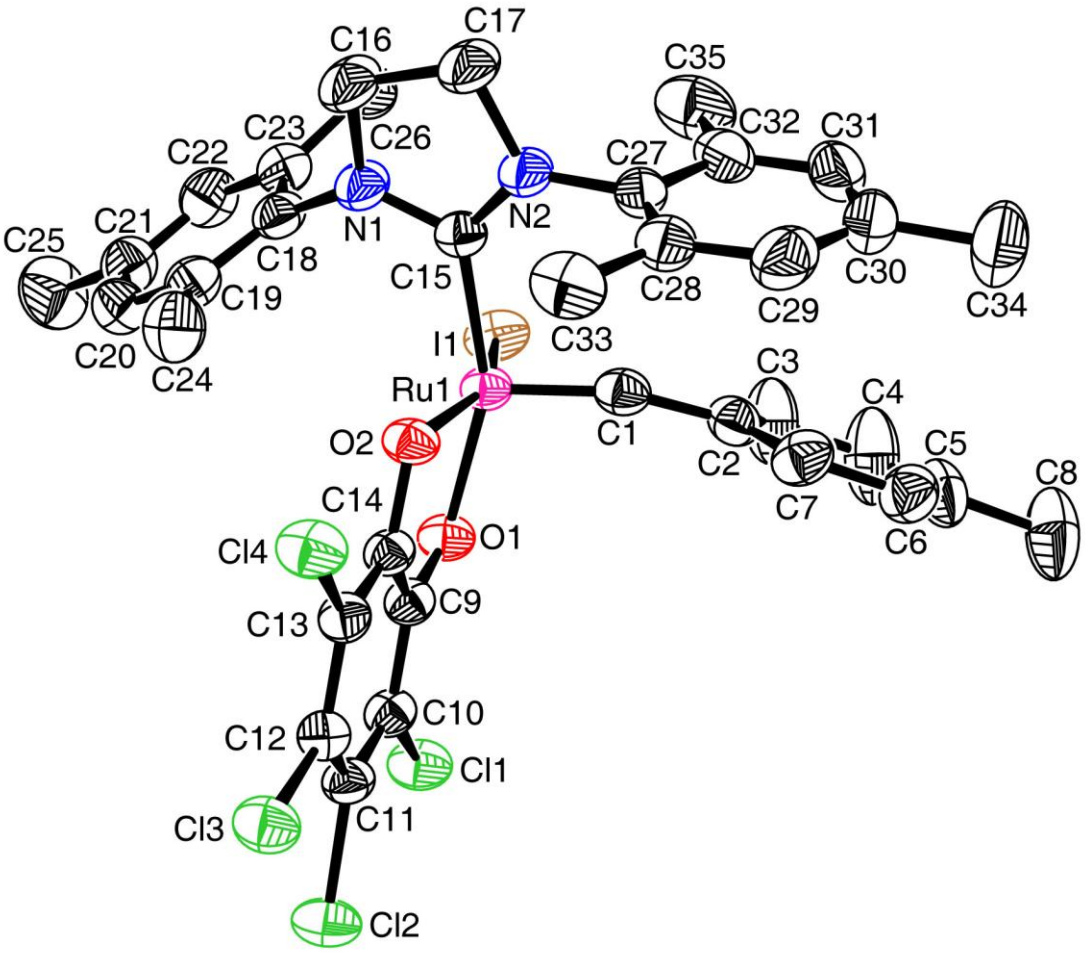

Figure A7.1. X-ray crystal structure of [Ru(≡C-*p*-C_6H_4Me)(H_2IMes)($O_2C_6Cl_4$)I] (mm1405a) (50% thermal ellipsoid plot). Hydrogen atoms are omitted for clarity.

A.7.1. Structure Determination.

Red, block-like crystals of **mm1405a** were grown from a dichloromethane/hexanes solution at −35 °C. A crystal of dimensions 0.45 x 0.23 x 0.17 mm was mounted on a Bruker SMART APEX CCD-based X-ray diffractometer equipped with a low temperature device and fine focus Mo-target X-ray tube (λ = 0.71073 Å) operated at 1500 W power (50 kV, 30 mA). The X-ray intensities were measured at 225(1) K; the detector was placed at a distance 5.055 cm from the crystal. A total of 4095 frames were collected with a scan width of 0.5° in ω and 0.45° in φ with an exposure time of 10 s/frame. The integration of the data yielded a total of 81831 reflections to a maximum 2θ value of 59.28° of which 11900 were independent and 10256 were greater than $2\sigma(I)$. The final cell constants (**A7.2**) were based on the xyz centroids of 9943 reflections above $10\sigma(I)$. Analysis of the data showed negligible decay during data collection; the data were processed with SADABS and corrected for absorption. The structure was solved and refined with the Bruker SHELXTL (version 2008/3) software package, using the space group P1bar with Z = 2 for the formula $C_{35}H_{33}N_2O_2Cl_4RuI$, (CH_2Cl_2), $(C_6H_{14})_{0.5}$. All non-hydrogen atoms were refined anisotropically with the hydrogen atoms placed in idealized positions. The hexane solvent molecule lies on an inversion center and is disordered. It was treated as diffuse scattering by use of the SQUEEZE subroutine of the PLATON program suite. Full matrix least-squares refinement based on F^2 converged at R1 = 0.0324 and wR2 = 0.0860

[based on I > 2σ(I)], R1 = 0.0379 and wR2 = 0.0897 for all data. Additional details are presented in **A7.2**.

Sheldrick, G.M. SHELXTL, v. 2008/3; Bruker Analytical X-ray, Madison, WI, 2008.

Sheldrick, G.M. SADABS, v. 2008/1. Program for Empirical Absorption Correction of Area Detector Data, University of Gottingen: Gottingen, Germany, 2008.

Saint Plus, v. 7.53a, Bruker Analytical X-ray, Madison, WI, 2008.

A.L. Spek. (2008) PLATON, v. 180108, A Multi-purpose Crystallographic Tool, Utrecht University, Utrecht, The Netherlands.

A7.2. Crystal data and structure refinement for mm1405a.

Identification code	mm1405a
Empirical formula	C_{39} H_{41} C_{l6} I N_2 O_2 Ru
Formula weight	1010.41
Temperature	225(2) K
Wavelength	0.71073 Å
Crystal system, space group	Triclinic, P-1
Unit cell dimensions	a = 8.9890(12) Å alpha = 86.304(2) deg.
	b = 12.2431(17) Å beta = 86.557(2) deg.
	c = 19.494(3) Å gamma = 81.652(2) deg.
Volume	2115.5(5) $Å^3$
Z, Calculated density	2, 1.586 Mg/m^3

Absorption coefficient	1.514 mm^{-1}
F(000)	1008
Crystal size	0.45 x 0.23 x 0.17 mm
Theta range for data collection	1.68 to 29.64 deg.
Limiting indices	-12<=h<=12, -17<=k<=17, -27<=l<=27
Reflections collected / unique	81831 / 11900 [R(int) = 0.0433]
Completeness to θ = 29.64	99.8 %
Absorption correction	Semi-empirical from equivalents
Max. and min. transmission	0.7829 and 0.5490
Refinement method	Full-matrix least-squares on F^2
Data / restraints / parameters	11900 / 0 / 440
Goodness-of-fit on F^2	1.044
Final R indices [I>2σ(I)]	R1 = 0.0324, wR2 = 0.0860
R indices (all data)	R1 = 0.0379, wR2 = 0.0897
Largest diff. peak and hole	0.905 and -0.624 e*$Å^{-3}$

A7.3. Atomic coordinates (x 10^4) and equivalent isotropic displacement parameters ($Å^2$ x 10^3) for mm1405a.

U(eq) is defined as one third of the trace of the orthogonalized Uij tensor.

	x	y	z	U(eq)
I(1)	10102(1)	3121(1)	3578(1)	53(1)
Ru(1)	8686(1)	3535(1)	2409(1)	35(1)
Cl(1)	12767(1)	5534(1)	1354(1)	50(1)

Cl(2)	11724(1)	6943(1)	8(1)	53(1)
Cl(3)	8418(1)	7045(1)	-426(1)	49(1)
Cl(4)	6168(1)	5741(1)	483(1)	50(1)
Cl(5)	495(2)	7520(1)	2646(1)	134(1)
Cl(6)	1783(2)	6301(1)	3808(1)	126(1)
N(1)	5694(2)	4002(2)	3148(1)	46(1)
N(2)	5781(2)	2484(2)	2616(1)	44(1)
C(1)	9317(2)	2261(2)	2147(1)	41(1)
C(2)	10251(2)	1298(2)	1910(1)	43(1)
C(3)	11425(4)	819(2)	2315(2)	73(1)
C(4)	12427(4)	-56(3)	2078(2)	87(1)
C(5)	12304(3)	-468(2)	1449(2)	59(1)
C(6)	11126(3)	6(2)	1052(2)	54(1)
C(7)	10106(3)	891(2)	1277(1)	50(1)
C(8)	13435(4)	-1414(3)	1190(2)	88(1)
C(9)	9954(2)	5040(2)	1495(1)	36(1)
C(10)	10948(2)	5622(2)	1101(1)	37(1)
C(11)	10475(2)	6241(2)	506(1)	38(1)
C(12)	9008(2)	6282(2)	307(1)	37(1)
C(13)	8002(2)	5693(2)	700(1)	36(1)
C(14)	8482(2)	5064(2)	1288(1)	35(1)
C(15)	6591(2)	3256(2)	2781(1)	38(1)
C(16)	4113(3)	3785(2)	3210(2)	64(1)
C(17)	4214(3)	2666(2)	2910(2)	59(1)
C(18)	6162(2)	4872(2)	3508(1)	43(1)
C(19)	6076(3)	5938(2)	3200(1)	46(1)
C(20)	6547(3)	6748(2)	3573(1)	53(1)
C(21)	7052(3)	6531(2)	4231(2)	56(1)
C(22)	7044(3)	5483(2)	4531(1)	57(1)
C(23)	6582(3)	4636(2)	4185(1)	50(1)
C(24)	5446(3)	6248(2)	2506(2)	61(1)
C(25)	7567(5)	7429(3)	4618(2)	84(1)
C(26)	6518(4)	3519(2)	4550(2)	67(1)
C(27)	6262(2)	1535(2)	2225(1)	42(1)
C(28)	5961(3)	1593(2)	1534(1)	48(1)
C(29)	6372(4)	636(3)	1173(2)	66(1)
C(30)	7049(4)	-343(2)	1490(2)	73(1)
C(31)	7293(3)	-366(2)	2175(2)	70(1)
C(32)	6913(3)	558(2)	2565(2)	55(1)
C(33)	5241(3)	2655(3)	1180(2)	63(1)
C(34)	7566(5)	-1357(3)	1083(3)	112(2)
C(35)	7259(4)	517(3)	3312(2)	80(1)
C(36)	651(4)	6274(3)	3126(2)	73(1)
O(1)	10326(2)	4443(1)	2075(1)	40(1)
O(2)	7576(2)	4479(1)	1686(1)	39(1)

A7.4. Bond lengths [Å] and angles [deg] for mm1405a.

I(1)-Ru(1)	2.6610(4)
Ru(1)-C(1)	1.681(2)
Ru(1)-O(2)	1.9854(14)
Ru(1)-O(1)	2.0249(14)
Ru(1)-C(15)	2.045(2)
Cl(1)-C(10)	1.723(2)
Cl(2)-C(11)	1.728(2)
Cl(3)-C(12)	1.722(2)
Cl(4)-C(13)	1.719(2)
Cl(5)-C(36)	1.729(4)
Cl(6)-C(36)	1.726(3)
N(1)-C(15)	1.341(3)
N(1)-C(18)	1.438(3)
N(1)-C(16)	1.480(3)
N(2)-C(15)	1.340(3)
N(2)-C(27)	1.431(3)
N(2)-C(17)	1.479(3)
C(1)-C(2)	1.430(3)
C(2)-C(7)	1.381(4)
C(2)-C(3)	1.394(4)
C(3)-C(4)	1.381(4)
C(4)-C(5)	1.372(5)
C(5)-C(6)	1.385(4)
C(5)-C(8)	1.518(4)
C(6)-C(7)	1.389(4)
C(9)-O(1)	1.339(2)
C(9)-C(10)	1.388(3)
C(9)-C(14)	1.402(3)
C(10)-C(11)	1.398(3)
C(11)-C(12)	1.390(3)
C(12)-C(13)	1.400(3)
C(13)-C(14)	1.392(3)
C(14)-O(2)	1.342(2)
C(16)-C(17)	1.511(4)

C(18)-C(19)	1.394(3)
C(18)-C(23)	1.396(3)
C(19)-C(20)	1.394(3)
C(19)-C(24)	1.503(4)
C(20)-C(21)	1.382(4)
C(21)-C(22)	1.376(4)
C(21)-C(25)	1.513(4)
C(22)-C(23)	1.397(4)
C(23)-C(26)	1.507(4)
C(27)-C(28)	1.386(3)
C(27)-C(32)	1.398(3)
C(28)-C(29)	1.398(4)
C(28)-C(33)	1.510(4)
C(29)-C(30)	1.388(5)
C(30)-C(31)	1.365(5)
C(30)-C(34)	1.516(4)
C(31)-C(32)	1.393(4)
C(32)-C(35)	1.505(5)

C(1)-Ru(1)-O(2)	111.83(9)
C(1)-Ru(1)-O(1)	104.41(8)
O(2)-Ru(1)-O(1)	81.70(6)
C(1)-Ru(1)-C(15)	98.14(9)
O(2)-Ru(1)-C(15)	84.39(7)
O(1)-Ru(1)-C(15)	156.65(7)
C(1)-Ru(1)-I(1)	92.01(7)
O(2)-Ru(1)-I(1)	155.52(5)
O(1)-Ru(1)-I(1)	87.18(4)
C(15)-Ru(1)-I(1)	98.14(6)
C(15)-N(1)-C(18)	126.32(18)
C(15)-N(1)-C(16)	112.48(19)
C(18)-N(1)-C(16)	120.96(18)
C(15)-N(2)-C(27)	128.23(18)
C(15)-N(2)-C(17)	112.65(19)
C(27)-N(2)-C(17)	119.09(18)
C(2)-C(1)-Ru(1)	163.75(18)
C(7)-C(2)-C(3)	119.5(2)
C(7)-C(2)-C(1)	122.4(2)
C(3)-C(2)-C(1)	117.8(2)
C(4)-C(3)-C(2)	119.5(3)
C(5)-C(4)-C(3)	121.7(3)
C(4)-C(5)-C(6)	118.4(3)
C(4)-C(5)-C(8)	121.0(3)
C(6)-C(5)-C(8)	120.6(3)
C(5)-C(6)-C(7)	121.1(3)

C(2)-C(7)-C(6)	119.7(2)
O(1)-C(9)-C(10)	123.16(17)
O(1)-C(9)-C(14)	117.16(17)
C(10)-C(9)-C(14)	119.68(19)
C(9)-C(10)-C(11)	120.07(18)
C(9)-C(10)-Cl(1)	118.46(16)
C(11)-C(10)-Cl(1)	121.46(15)
C(12)-C(11)-C(10)	120.30(18)
C(12)-C(11)-Cl(2)	119.73(16)
C(10)-C(11)-Cl(2)	119.97(15)
C(11)-C(12)-C(13)	119.88(19)
C(11)-C(12)-Cl(3)	120.50(16)
C(13)-C(12)-Cl(3)	119.62(16)
C(14)-C(13)-C(12)	119.71(18)
C(14)-C(13)-Cl(4)	118.80(15)
C(12)-C(13)-Cl(4)	121.48(16)
O(2)-C(14)-C(13)	122.64(17)
O(2)-C(14)-C(9)	117.02(18)
C(13)-C(14)-C(9)	120.33(17)
N(2)-C(15)-N(1)	108.50(18)
N(2)-C(15)-Ru(1)	129.00(15)
N(1)-C(15)-Ru(1)	121.36(15)
N(1)-C(16)-C(17)	102.77(19)
N(2)-C(17)-C(16)	102.70(18)
C(19)-C(18)-C(23)	121.7(2)
C(19)-C(18)-N(1)	120.0(2)
C(23)-C(18)-N(1)	118.1(2)
C(20)-C(19)-C(18)	117.5(2)
C(20)-C(19)-C(24)	119.6(2)
C(18)-C(19)-C(24)	122.9(2)
C(21)-C(20)-C(19)	122.4(2)
C(22)-C(21)-C(20)	118.4(2)
C(22)-C(21)-C(25)	120.7(3)
C(20)-C(21)-C(25)	120.9(3)
C(21)-C(22)-C(23)	122.0(3)
C(18)-C(23)-C(22)	117.8(2)
C(18)-C(23)-C(26)	122.3(2)
C(22)-C(23)-C(26)	119.9(2)
C(28)-C(27)-C(32)	122.2(2)
C(28)-C(27)-N(2)	118.7(2)
C(32)-C(27)-N(2)	118.8(2)
C(27)-C(28)-C(29)	117.5(2)
C(27)-C(28)-C(33)	121.3(2)
C(29)-C(28)-C(33)	121.2(3)
C(30)-C(29)-C(28)	121.8(3)

C(31)-C(30)-C(29)	118.5(3)
C(31)-C(30)-C(34)	120.2(4)
C(29)-C(30)-C(34)	121.2(4)
C(30)-C(31)-C(32)	122.6(3)
C(31)-C(32)-C(27)	117.3(3)
C(31)-C(32)-C(35)	121.3(3)
C(27)-C(32)-C(35)	121.4(3)
Cl(6)-C(36)-Cl(5)	110.6(2)
C(9)-O(1)-Ru(1)	110.69(11)
C(14)-O(2)-Ru(1)	111.95(12)

A7.5. Anisotropic displacement parameters ($Å^2$ x 10^3) for mm1405a.

The anisotropic displacement factor exponent takes the form:
-2 pi^2 [h^2 a*^2 U11 + ... + 2 h k a* b* U12]

	U11	U22	U33	U23	U13	U12
I(1)	39(1)	77(1)	43(1)	2(1)	-6(1)	-10(1)
Ru(1)	26(1)	42(1)	38(1)	1(1)	-2(1)	-7(1)
Cl(1)	30(1)	66(1)	56(1)	3(1)	-6(1)	-17(1)
Cl(2)	44(1)	66(1)	52(1)	7(1)	2(1)	-23(1)
Cl(3)	48(1)	55(1)	44(1)	7(1)	-6(1)	-11(1)
Cl(4)	31(1)	63(1)	57(1)	10(1)	-11(1)	-10(1)
Cl(5)	160(1)	102(1)	118(1)	11(1)	-12(1)	44(1)
Cl(6)	167(1)	103(1)	108(1)	-38(1)	-69(1)	19(1)
N(1)	33(1)	50(1)	57(1)	-13(1)	6(1)	-11(1)
N(2)	31(1)	47(1)	57(1)	-10(1)	6(1)	-11(1)
C(1)	33(1)	47(1)	44(1)	4(1)	-3(1)	-9(1)
C(2)	38(1)	40(1)	53(1)	3(1)	-2(1)	-7(1)
C(3)	77(2)	56(2)	83(2)	-18(1)	-37(2)	15(1)
C(4)	83(2)	62(2)	113(3)	-26(2)	-51(2)	26(2)
C(5)	49(1)	40(1)	88(2)	-7(1)	-12(1)	-1(1)
C(6)	46(1)	57(1)	58(1)	-7(1)	1(1)	-6(1)
C(7)	40(1)	59(1)	49(1)	2(1)	-2(1)	1(1)
C(8)	71(2)	57(2)	135(3)	-32(2)	-27(2)	14(2)
C(9)	29(1)	41(1)	38(1)	-5(1)	-2(1)	-9(1)
C(10)	27(1)	44(1)	42(1)	-6(1)	-1(1)	-10(1)
C(11)	33(1)	42(1)	39(1)	-4(1)	4(1)	-10(1)

C(12)	37(1)	40(1)	36(1)	-2(1)	-1(1)	-7(1)
C(13)	27(1)	40(1)	42(1)	-3(1)	-2(1)	-6(1)
C(14)	26(1)	40(1)	39(1)	-4(1)	0(1)	-7(1)
C(15)	32(1)	41(1)	39(1)	-1(1)	0(1)	-7(1)
C(16)	34(1)	69(2)	91(2)	-29(2)	16(1)	-16(1)
C(17)	36(1)	65(2)	80(2)	-24(1)	15(1)	-18(1)
C(18)	33(1)	49(1)	47(1)	-10(1)	5(1)	-9(1)
C(19)	37(1)	53(1)	50(1)	-4(1)	-1(1)	-6(1)
C(20)	53(1)	46(1)	61(2)	-5(1)	0(1)	-11(1)
C(21)	55(1)	56(1)	59(2)	-14(1)	-1(1)	-13(1)
C(22)	64(2)	64(2)	44(1)	-9(1)	-4(1)	-7(1)
C(23)	52(1)	52(1)	46(1)	-4(1)	6(1)	-6(1)
C(24)	60(2)	60(2)	61(2)	-2(1)	-15(1)	1(1)
C(25)	104(3)	76(2)	81(2)	-23(2)	-13(2)	-31(2)
C(26)	81(2)	60(2)	57(2)	4(1)	12(1)	-10(1)
C(27)	32(1)	39(1)	54(1)	-4(1)	2(1)	-8(1)
C(28)	39(1)	51(1)	56(1)	-6(1)	-1(1)	-12(1)
C(29)	64(2)	75(2)	65(2)	-26(1)	12(1)	-23(1)
C(30)	63(2)	51(2)	107(3)	-27(2)	27(2)	-13(1)
C(31)	55(2)	39(1)	112(3)	2(1)	16(2)	-4(1)
C(32)	44(1)	46(1)	73(2)	10(1)	1(1)	-8(1)
C(33)	54(2)	70(2)	65(2)	10(1)	-13(1)	-12(1)
C(34)	100(3)	74(2)	165(5)	-63(3)	43(3)	-17(2)
C(35)	80(2)	83(2)	73(2)	30(2)	-14(2)	-16(2)
C(36)	60(2)	79(2)	80(2)	-18(2)	-11(2)	-2(2)
O(1)	30(1)	51(1)	40(1)	2(1)	-5(1)	-11(1)
O(2)	26(1)	44(1)	45(1)	5(1)	-3(1)	-9(1)

A7.6. Hydrogen coordinates (x 10^4) and isotropic displacement parameters ($Å^2$ x 10^3) for mm1405a.

	x	y	z	U(eq)
H(3A)	11535	1090	2747	87
H(4A)	13214	-378	2355	104
H(6A)	11015	-275	623	65
H(7A)	9320	1211	999	60
H(8A)	14338	-1482	1447	132

H(8B)	13689	-1269	705	132
H(8C)	13002	-2097	1252	132
H(16A)	3458	4349	2946	76
H(16B)	3734	3760	3692	76
H(17A)	4037	2093	3268	71
H(17B)	3489	2679	2553	71
H(20A)	6521	7468	3370	64
H(22A)	7360	5333	4983	69
H(24A)	5549	5597	2239	91
H(24B)	5994	6798	2266	91
H(24C)	4390	6550	2563	91
H(25A)	8126	7097	5007	126
H(25B)	6697	7927	4781	126
H(25C)	8209	7839	4314	126
H(26A)	5564	3526	4812	100
H(26B)	7337	3353	4860	100
H(26C)	6612	2959	4214	100
H(29A)	6185	656	703	79
H(31A)	7734	-1032	2393	84
H(33A)	4236	2861	1383	94
H(33B)	5181	2550	694	94
H(33C)	5843	3237	1235	94
H(34A)	8616	-1368	931	168
H(34B)	6961	-1334	686	168
H(34C)	7453	-2018	1373	168
H(35A)	7771	-211	3447	120
H(35B)	6328	669	3590	120
H(35C)	7901	1068	3382	120
H(36A)	-351	6130	3301	87
H(36B)	1081	5675	2832	87

Appendix 8

Crystal Data for [Ru(=C(OC_6Cl_4O-)(*p*-C_6H_4Me))(H_2IMes)($C_5D_5N)_2$Cl] (mm1373)

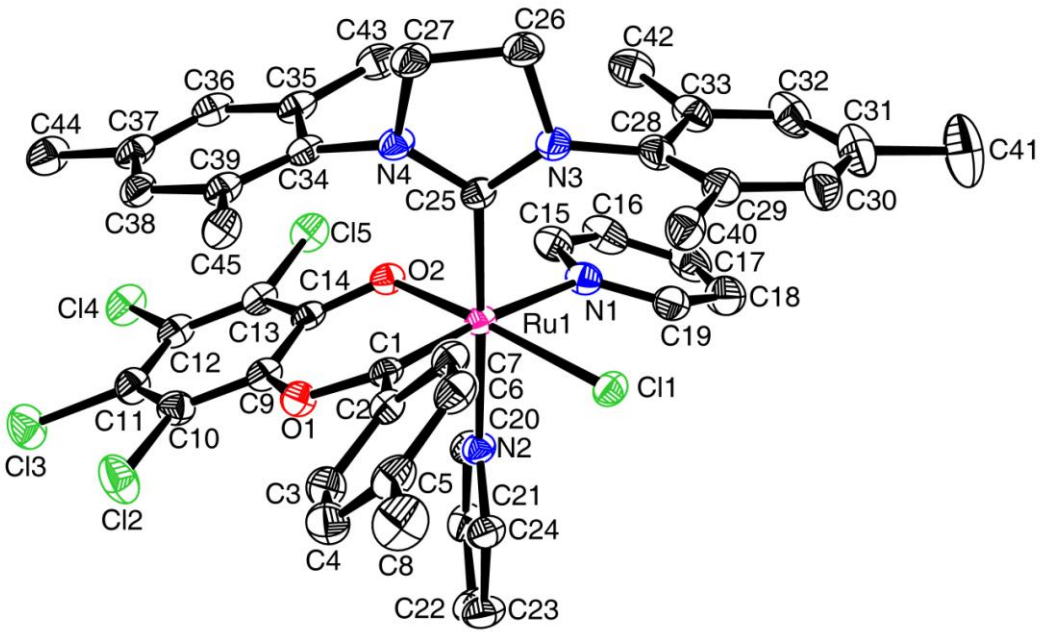

Figure A8.1. X-ray crystal structure of [Ru(=C(OC_6Cl_4O-)(*p*-C_6H_4Me))(H_2IMes)($C_5D_5N)_2$Cl] (mm1373) (50% thermal ellipsoid plot). Hydrogen atoms are omitted for clarity.

A8.1. Structure Determination.

Green needles of **mm1373** were grown from a dichloromethane/hexanes solution at –35 °C. A crystal of dimensions 0.25 x 0.10 x 0.10 mm was mounted on a Bruker SMART APEX CCD-based X-ray diffractometer equipped with a low temperature device and fine focus Mo-target X-ray tube (λ = 0.71073 Å) operated at 1500 W power (50 kV, 30 mA). The X-ray intensities were measured at 85(1) K; the detector was

placed at a distance 5.055 cm from the crystal. A total of 4095 frames were collected with a scan width of 0.5° in ω and 0.45° in φ with an exposure time of 30 s/frame. The integration of the data yielded a total of 185690 reflections to a maximum 2θ value of 56.62° of which 13022 were independent and 10983 were greater than 2σ(I). The final cell constants (**A8.2**) were based on the xyz centroids of 9171 reflections above 10σ(I). Analysis of the data showed negligible decay during data collection; the data were processed with SADABS and corrected for absorption. The structure was solved and refined with the Bruker SHELXTL (version 2008/4) software package, using the space group P2(1)/c with Z = 4 for the formula $C_{45}H_{43}N_4O_2Cl_5Ru$, (CH_2Cl_2), $(C_6H_{14})_{0.5}$. All non-hydrogen atoms were refined anisotropically with the hydrogen atoms placed in idealized positions. Full matrix least-squares refinement based on F^2 converged at R1 = 0.0478 and wR2 = 0.1300 [based on I > 2σ(I)], R1 = 0.0591 and wR2 = 0.1370 for all data. Additional details are presented in **A8.2**.

Sheldrick, G.M. SHELXTL, v. 2008/4; Bruker Analytical X-ray, Madison, WI, 2008.

Sheldrick, G.M. SADABS, v. 2008/1. Program for Empirical Absorption Correction of Area Detector Data, University of Gottingen: Gottingen, Germany, 2008.

Saint Plus, v. 7.53a, Bruker Analytical X-ray, Madison, WI, 2008.

A8.2. Crystal data and structure refinement for mm1373.

Identification code	mm1373
Empirical formula	$C_{49}\ H_{52}\ Cl_7\ N_4\ O_2\ Ru$
Formula weight	1078.17

Temperature	85(2) K
Wavelength	0.71073 Å
Crystal system, space group	Monoclinic, P2(1)/c
Unit cell dimensions	a = 10.6967(8) Å alpha = 90 deg.
	b = 25.3195(18) Å beta = 104.088(1) deg.
	c = 19.9332(14) Å gamma = 90 deg.
Volume	5236.2(7) $Å^3$
Z, Calculated density	4, 1.368 Mg/m^3
Absorption coefficient	0.697 mm^{-1}
F(000)	2212
Crystal size	0.25 x 0.10 x 0.10 mm
Theta range for data collection	1.33 to 28.31 deg.
Limiting indices	-14<=h<=14, -33<=k<=33, -26<=l<=26
Reflections collected / unique	185690 / 13022 [R(int) = 0.0623]
Completeness to θ = 28.31	99.9 %
Absorption correction	Semi-empirical from equivalents
Max. and min. transmission	0.9336 and 0.8450
Refinement method	Full-matrix least-squares on F^2
Data / restraints / parameters	13022 / 47 / 604
Goodness-of-fit on F^2	1.093
Final R indices [I>2σ(I)]	R1 = 0.0478, wR2 = 0.1300
R indices (all data)	R1 = 0.0591, wR2 = 0.1370
Largest diff. peak and hole	1.154 and -1.234 $e*Å^{-3}$

A8.3. Atomic coordinates (x 10^4) and equivalent isotropic displacement parameters ($Å^2$ x 10^3) for mm1373.

U(eq) is defined as one third of the trace of the orthogonalized Uij tensor.

	x	y	z	U(eq)
Ru(1)	7192(1)	140(1)	2230(1)	20(1)
Cl(1)	8282(1)	304(1)	1332(1)	24(1)
Cl(2)	6291(1)	-1965(1)	2832(1)	41(1)
Cl(3)	3976(1)	-2002(1)	3537(1)	40(1)
Cl(4)	2764(1)	-946(1)	3879(1)	35(1)
Cl(5)	3839(1)	132(1)	3493(1)	31(1)
Cl(6)	7595(1)	8851(1)	9823(1)	54(1)
Cl(7)	10102(1)	9284(1)	9840(1)	58(1)
O(1)	7105(2)	-964(1)	2554(1)	24(1)
O(2)	5952(2)	42(1)	2860(1)	23(1)
N(1)	6179(3)	938(1)	1989(1)	26(1)
N(2)	5579(2)	-142(1)	1418(1)	23(1)
N(3)	9629(2)	766(1)	2999(1)	24(1)
N(4)	9099(2)	154(1)	3648(1)	23(1)
C(1)	7786(3)	-559(1)	2355(1)	22(1)
C(2)	8932(3)	-819(1)	2193(2)	23(1)
C(3)	8920(3)	-1355(1)	2003(2)	29(1)
C(4)	9994(3)	-1583(1)	1849(2)	32(1)
C(5)	11117(3)	-1294(1)	1881(2)	30(1)
C(6)	11139(3)	-769(1)	2081(2)	27(1)
C(7)	10058(3)	-533(1)	2231(2)	24(1)
C(8)	12262(4)	-1543(2)	1688(2)	41(1)
C(9)	6050(3)	-908(1)	2824(2)	23(1)
C(10)	5566(3)	-1386(1)	3000(2)	28(1)
C(11)	4546(3)	-1406(1)	3321(2)	28(1)
C(12)	4010(3)	-935(1)	3470(2)	27(1)
C(13)	4485(3)	-458(1)	3298(2)	24(1)
C(14)	5534(3)	-420(1)	2980(1)	22(1)
C(15)	5262(3)	1082(1)	2310(2)	30(1)
C(16)	4442(3)	1507(1)	2101(2)	38(1)
C(17)	4557(4)	1796(1)	1532(2)	41(1)
C(18)	5510(4)	1661(2)	1208(2)	39(1)
C(19)	6309(3)	1234(1)	1451(2)	31(1)
C(20)	4346(3)	-32(1)	1413(2)	26(1)
C(21)	3307(3)	-217(1)	908(2)	30(1)
C(22)	3535(3)	-535(2)	386(2)	33(1)

C(23)	4796(3)	-654(2)	389(2)	33(1)
C(24)	5784(3)	-455(1)	908(2)	27(1)
C(25)	8722(3)	389(1)	3014(1)	21(1)
C(26)	10587(3)	826(1)	3667(2)	29(1)
C(27)	10367(3)	333(1)	4057(2)	28(1)
C(28)	9604(3)	1196(1)	2522(2)	27(1)
C(29)	10458(3)	1192(1)	2088(2)	28(1)
C(30)	10505(3)	1633(2)	1678(2)	37(1)
C(31)	9752(4)	2077(2)	1697(2)	43(1)
C(32)	8954(4)	2078(1)	2151(2)	39(1)
C(33)	8879(3)	1647(1)	2576(2)	31(1)
C(34)	8349(3)	-170(1)	3998(1)	23(1)
C(35)	7459(3)	83(1)	4310(2)	26(1)
C(36)	6769(3)	-223(1)	4675(2)	28(1)
C(37)	6940(3)	-765(1)	4743(2)	29(1)
C(38)	7869(3)	-999(1)	4465(2)	27(1)
C(39)	8605(3)	-709(1)	4103(2)	25(1)
C(40)	11323(3)	730(1)	2046(2)	30(1)
C(41)	9814(6)	2549(2)	1242(3)	68(2)
C(42)	8078(3)	1697(2)	3096(2)	36(1)
C(43)	7250(3)	669(1)	4249(2)	32(1)
C(44)	6137(3)	-1090(2)	5117(2)	36(1)
C(45)	9669(3)	-985(1)	3865(2)	28(1)
C(46)	8906(4)	9229(2)	10296(2)	38(1)
C(47)	6375(12)	2336(7)	4498(5)	113(6)
C(48)	5293(10)	2541(6)	3933(8)	113(5)
C(49)	3998(10)	2282(4)	3780(5)	84(3)
C(50)	3244(11)	2497(4)	4264(7)	91(4)
C(51)	1938(9)	2272(4)	4147(5)	75(3)
C(52)	1173(9)	2421(3)	4668(5)	51(2)

A8.4. Bond lengths [Å] and angles [deg] for mm1373.

Ru(1)-C(1)	1.876(3)
Ru(1)-O(2)	2.051(2)
Ru(1)-C(25)	2.068(3)
Ru(1)-N(2)	2.179(2)
Ru(1)-N(1)	2.288(3)
Ru(1)-Cl(1)	2.3981(7)
Cl(2)-C(10)	1.728(3)
Cl(3)-C(11)	1.723(3)
Cl(4)-C(12)	1.722(3)
Cl(5)-C(13)	1.728(3)
Cl(6)-C(46)	1.768(4)

Cl(7)-C(46)	1.746(4)
O(1)-C(9)	1.370(3)
O(1)-C(1)	1.371(4)
O(2)-C(14)	1.294(4)
N(1)-C(19)	1.342(4)
N(1)-C(15)	1.345(4)
N(2)-C(20)	1.346(4)
N(2)-C(24)	1.347(4)
N(3)-C(25)	1.366(4)
N(3)-C(28)	1.443(4)
N(3)-C(26)	1.476(4)
N(4)-C(25)	1.367(4)
N(4)-C(34)	1.439(4)
N(4)-C(27)	1.474(4)
C(1)-C(2)	1.496(4)
C(2)-C(7)	1.392(4)
C(2)-C(3)	1.407(4)
C(3)-C(4)	1.386(4)
C(4)-C(5)	1.395(5)
C(5)-C(6)	1.387(5)
C(5)-C(8)	1.507(5)
C(6)-C(7)	1.397(4)
C(9)-C(10)	1.394(4)
C(9)-C(14)	1.419(4)
C(10)-C(11)	1.394(4)
C(11)-C(12)	1.387(5)
C(12)-C(13)	1.385(5)
C(13)-C(14)	1.420(4)
C(15)-C(16)	1.388(5)
C(16)-C(17)	1.380(6)
C(17)-C(18)	1.376(6)
C(18)-C(19)	1.390(5)
C(20)-C(21)	1.387(4)
C(21)-C(22)	1.383(5)
C(22)-C(23)	1.381(5)
C(23)-C(24)	1.382(4)
C(26)-C(27)	1.518(5)
C(28)-C(33)	1.399(5)
C(28)-C(29)	1.404(4)
C(29)-C(30)	1.391(5)
C(29)-C(40)	1.507(5)
C(30)-C(31)	1.389(6)
C(31)-C(32)	1.386(6)
C(31)-C(41)	1.512(5)
C(32)-C(33)	1.395(5)
C(33)-C(42)	1.501(5)
C(34)-C(39)	1.397(4)
C(34)-C(35)	1.412(4)

C(35)-C(36)	1.392(5)
C(35)-C(43)	1.500(5)
C(36)-C(37)	1.386(5)
C(37)-C(38)	1.384(5)
C(37)-C(44)	1.511(4)
C(38)-C(39)	1.399(4)
C(39)-C(45)	1.507(4)
C(47)-C(48)	1.497(9)
C(48)-C(49)	1.497(9)
C(49)-C(50)	1.502(9)
C(50)-C(51)	1.474(9)
C(51)-C(52)	1.518(8)

C(1)-Ru(1)-O(2)	93.00(11)
C(1)-Ru(1)-C(25)	90.37(12)
O(2)-Ru(1)-C(25)	94.87(10)
C(1)-Ru(1)-N(2)	88.32(11)
O(2)-Ru(1)-N(2)	84.34(9)
C(25)-Ru(1)-N(2)	178.44(11)
C(1)-Ru(1)-N(1)	171.39(11)
O(2)-Ru(1)-N(1)	83.80(9)
C(25)-Ru(1)-N(1)	97.85(10)
N(2)-Ru(1)-N(1)	83.42(9)
C(1)-Ru(1)-Cl(1)	93.02(9)
O(2)-Ru(1)-Cl(1)	169.13(6)
C(25)-Ru(1)-Cl(1)	94.13(8)
N(2)-Ru(1)-Cl(1)	86.79(7)
N(1)-Ru(1)-Cl(1)	88.95(7)
C(9)-O(1)-C(1)	125.6(2)
C(14)-O(2)-Ru(1)	121.83(19)
C(19)-N(1)-C(15)	117.3(3)
C(19)-N(1)-Ru(1)	121.6(2)
C(15)-N(1)-Ru(1)	120.1(2)
C(20)-N(2)-C(24)	117.2(3)
C(20)-N(2)-Ru(1)	122.3(2)
C(24)-N(2)-Ru(1)	120.5(2)
C(25)-N(3)-C(28)	130.0(3)
C(25)-N(3)-C(26)	113.2(2)
C(28)-N(3)-C(26)	114.4(2)
C(25)-N(4)-C(34)	128.5(2)
C(25)-N(4)-C(27)	113.6(2)
C(34)-N(4)-C(27)	117.1(2)
O(1)-C(1)-C(2)	104.7(2)
O(1)-C(1)-Ru(1)	123.9(2)
C(2)-C(1)-Ru(1)	131.0(2)
C(7)-C(2)-C(3)	118.0(3)
C(7)-C(2)-C(1)	120.1(3)
C(3)-C(2)-C(1)	121.9(3)

C(4)-C(3)-C(2)	120.5(3)
C(3)-C(4)-C(5)	121.5(3)
C(6)-C(5)-C(4)	118.0(3)
C(6)-C(5)-C(8)	121.1(3)
C(4)-C(5)-C(8)	120.9(3)
C(5)-C(6)-C(7)	121.0(3)
C(2)-C(7)-C(6)	121.0(3)
O(1)-C(9)-C(10)	113.7(3)
O(1)-C(9)-C(14)	125.3(3)
C(10)-C(9)-C(14)	120.8(3)
C(11)-C(10)-C(9)	121.9(3)
C(11)-C(10)-Cl(2)	119.8(3)
C(9)-C(10)-Cl(2)	118.3(2)
C(12)-C(11)-C(10)	118.6(3)
C(12)-C(11)-Cl(3)	120.7(2)
C(10)-C(11)-Cl(3)	120.7(3)
C(13)-C(12)-C(11)	120.0(3)
C(13)-C(12)-Cl(4)	120.3(3)
C(11)-C(12)-Cl(4)	119.7(3)
C(12)-C(13)-C(14)	123.1(3)
C(12)-C(13)-Cl(5)	120.4(2)
C(14)-C(13)-Cl(5)	116.4(2)
O(2)-C(14)-C(9)	125.1(3)
O(2)-C(14)-C(13)	119.3(3)
C(9)-C(14)-C(13)	115.6(3)
N(1)-C(15)-C(16)	123.2(3)
C(17)-C(16)-C(15)	118.8(3)
C(18)-C(17)-C(16)	118.6(3)
C(17)-C(18)-C(19)	119.5(4)
N(1)-C(19)-C(18)	122.6(3)
N(2)-C(20)-C(21)	123.0(3)
C(22)-C(21)-C(20)	119.1(3)
C(23)-C(22)-C(21)	118.3(3)
C(22)-C(23)-C(24)	119.5(3)
N(2)-C(24)-C(23)	122.9(3)
N(3)-C(25)-N(4)	105.9(2)
N(3)-C(25)-Ru(1)	129.2(2)
N(4)-C(25)-Ru(1)	124.6(2)
N(3)-C(26)-C(27)	102.5(2)
N(4)-C(27)-C(26)	101.9(2)
C(33)-C(28)-C(29)	120.6(3)
C(33)-C(28)-N(3)	119.2(3)
C(29)-C(28)-N(3)	119.4(3)
C(30)-C(29)-C(28)	118.5(3)
C(30)-C(29)-C(40)	118.7(3)
C(28)-C(29)-C(40)	122.7(3)
C(31)-C(30)-C(29)	122.0(3)
C(32)-C(31)-C(30)	118.2(3)

C(32)-C(31)-C(41)	120.9(4)
C(30)-C(31)-C(41)	120.9(4)
C(31)-C(32)-C(33)	122.0(3)
C(32)-C(33)-C(28)	118.5(3)
C(32)-C(33)-C(42)	118.7(3)
C(28)-C(33)-C(42)	122.8(3)
C(39)-C(34)-C(35)	120.4(3)
C(39)-C(34)-N(4)	121.1(3)
C(35)-C(34)-N(4)	118.0(3)
C(36)-C(35)-C(34)	118.5(3)
C(36)-C(35)-C(43)	120.4(3)
C(34)-C(35)-C(43)	121.1(3)
C(37)-C(36)-C(35)	121.9(3)
C(38)-C(37)-C(36)	118.4(3)
C(38)-C(37)-C(44)	120.9(3)
C(36)-C(37)-C(44)	120.6(3)
C(37)-C(38)-C(39)	122.0(3)
C(34)-C(39)-C(38)	118.4(3)
C(34)-C(39)-C(45)	122.8(3)
C(38)-C(39)-C(45)	118.7(3)
Cl(7)-C(46)-Cl(6)	110.6(2)
C(49)-C(48)-C(47)	120.6(11)
C(48)-C(49)-C(50)	108.9(9)
C(51)-C(50)-C(49)	113.2(9)
C(50)-C(51)-C(52)	116.3(9)

A8.5. Anisotropic displacement parameters ($Å^2$ x 10^3) for mm1373.

The anisotropic displacement factor exponent takes the form:
-2 pi^2 [h^2 a*^2 U11 + ... + 2 h k a* b* U12]

	U11	U22	U33	U23	U13	U12
Ru(1)	18(1)	24(1)	17(1)	-1(1)	3(1)	-1(1)
Cl(1)	24(1)	30(1)	20(1)	1(1)	6(1)	-2(1)
Cl(2)	49(1)	27(1)	58(1)	-1(1)	33(1)	-3(1)
Cl(3)	40(1)	37(1)	48(1)	2(1)	22(1)	-10(1)
Cl(4)	23(1)	51(1)	34(1)	3(1)	13(1)	-1(1)
Cl(5)	26(1)	39(1)	32(1)	1(1)	12(1)	8(1)
Cl(6)	37(1)	65(1)	62(1)	-25(1)	21(1)	-15(1)

Cl(7)	38(1)	94(1)	48(1)	-21(1)	21(1)	-19(1)
O(1)	23(1)	27(1)	25(1)	-2(1)	11(1)	-2(1)
O(2)	20(1)	28(1)	21(1)	-2(1)	7(1)	-1(1)
N(1)	24(1)	26(1)	27(1)	-3(1)	3(1)	0(1)
N(2)	21(1)	27(1)	19(1)	0(1)	2(1)	-2(1)
N(3)	22(1)	27(1)	21(1)	0(1)	2(1)	-4(1)
N(4)	19(1)	31(1)	19(1)	-1(1)	2(1)	-3(1)
C(1)	21(1)	28(2)	15(1)	-2(1)	3(1)	-4(1)
C(2)	23(1)	26(1)	19(1)	1(1)	6(1)	1(1)
C(3)	28(2)	31(2)	29(2)	-1(1)	11(1)	-2(1)
C(4)	36(2)	28(2)	34(2)	-3(1)	15(1)	4(1)
C(5)	28(2)	38(2)	25(2)	2(1)	11(1)	7(1)
C(6)	22(1)	38(2)	23(1)	2(1)	8(1)	1(1)
C(7)	23(1)	29(2)	22(1)	0(1)	7(1)	1(1)
C(8)	34(2)	48(2)	45(2)	0(2)	16(2)	11(2)
C(9)	17(1)	32(2)	21(1)	-1(1)	6(1)	-1(1)
C(10)	27(2)	30(2)	28(2)	-3(1)	8(1)	-2(1)
C(11)	24(2)	34(2)	28(2)	2(1)	9(1)	-6(1)
C(12)	18(1)	41(2)	22(1)	0(1)	6(1)	-3(1)
C(13)	17(1)	34(2)	22(1)	0(1)	5(1)	2(1)
C(14)	18(1)	31(2)	16(1)	-1(1)	1(1)	-1(1)
C(15)	25(2)	29(2)	36(2)	-4(1)	6(1)	0(1)
C(16)	27(2)	31(2)	54(2)	-9(2)	7(2)	2(1)
C(17)	41(2)	26(2)	50(2)	-2(2)	2(2)	4(2)
C(18)	47(2)	31(2)	37(2)	2(1)	3(2)	5(2)
C(19)	35(2)	27(2)	29(2)	-1(1)	4(1)	-1(1)
C(20)	22(1)	32(2)	22(1)	0(1)	3(1)	2(1)
C(21)	22(2)	39(2)	28(2)	5(1)	3(1)	-1(1)
C(22)	28(2)	46(2)	22(2)	-2(1)	-1(1)	-7(1)
C(23)	32(2)	43(2)	24(2)	-8(1)	6(1)	-7(2)
C(24)	26(2)	34(2)	22(1)	-3(1)	6(1)	-4(1)
C(25)	19(1)	25(1)	19(1)	-2(1)	6(1)	1(1)
C(26)	24(2)	36(2)	24(2)	-2(1)	1(1)	-5(1)
C(27)	22(1)	37(2)	23(1)	0(1)	-1(1)	-5(1)
C(28)	23(1)	27(2)	27(2)	0(1)	2(1)	-5(1)
C(29)	24(2)	32(2)	28(2)	0(1)	4(1)	-6(1)
C(30)	33(2)	37(2)	42(2)	7(2)	10(2)	-7(1)
C(31)	39(2)	32(2)	56(2)	12(2)	9(2)	-5(2)
C(32)	37(2)	24(2)	54(2)	3(2)	5(2)	-1(1)
C(33)	27(2)	27(2)	36(2)	-3(1)	2(1)	-4(1)
C(34)	21(1)	33(2)	15(1)	-2(1)	4(1)	-2(1)
C(35)	21(1)	38(2)	18(1)	-2(1)	3(1)	2(1)
C(36)	21(1)	43(2)	21(1)	-4(1)	5(1)	-1(1)
C(37)	20(1)	47(2)	19(1)	0(1)	3(1)	-7(1)
C(38)	26(2)	33(2)	20(1)	2(1)	2(1)	-4(1)
C(39)	21(1)	34(2)	18(1)	-1(1)	3(1)	-1(1)
C(40)	24(2)	36(2)	31(2)	3(1)	7(1)	-3(1)
C(41)	76(3)	41(2)	95(4)	31(3)	33(3)	2(2)

C(42)	33(2)	34(2)	40(2)	-8(2)	9(2)	1(1)
C(43)	32(2)	38(2)	27(2)	-4(1)	9(1)	4(1)
C(44)	29(2)	51(2)	29(2)	0(2)	10(1)	-10(2)
C(45)	26(2)	33(2)	26(2)	3(1)	8(1)	4(1)
C(46)	34(2)	52(2)	29(2)	-5(2)	11(1)	-8(2)
C(47)	124(9)	187(16)	47(6)	39(8)	58(6)	36(10)
C(48)	90(8)	99(10)	144(13)	32(10)	16(8)	12(7)
C(49)	151(8)	49(5)	67(6)	31(5)	52(6)	-3(6)
C(50)	135(8)	40(5)	121(10)	37(6)	75(8)	22(6)
C(51)	95(7)	58(6)	69(6)	3(5)	13(6)	36(5)
C(52)	65(5)	35(4)	56(5)	9(4)	20(4)	4(4)

A8.6. Hydrogen coordinates (x 10^4) and isotropic displacement parameters ($Å^2$ x 10^3) for mm1373.

	x	y	z	U(eq)
H(3A)	8169	-1561	1980	35
H(4A)	9965	-1945	1719	38
H(6A)	11900	-567	2116	33
H(7A)	10092	-171	2361	29
H(8A)	12070	-1593	1186	61
H(8B)	12446	-1886	1919	61
H(8C)	13013	-1311	1834	61
H(15A)	5171	882	2699	36
H(16A)	3813	1598	2346	45
H(17A)	3991	2082	1368	49
H(18A)	5622	1858	821	47
H(19A)	6972	1148	1228	37
H(20A)	4180	183	1772	31
H(21A)	2451	-127	921	36
H(22A)	2841	-667	34	40
H(23A)	4983	-872	38	40
H(24A)	6646	-541	905	33
H(26A)	10427	1150	3911	35
H(26B)	11475	836	3602	35
H(27A)	11042	65	4061	34
H(27B)	10344	417	4539	34

H(30A)	11069	1630	1377	44
H(32A)	8442	2381	2172	47
H(36A)	6164	-56	4884	34
H(38A)	8012	-1368	4523	32
H(40A)	10843	466	1725	45
H(40B)	11626	571	2506	45
H(40C)	12065	851	1880	45
H(41A)	9177	2812	1300	103
H(41B)	9626	2436	757	103
H(41C)	10678	2704	1373	103
H(42A)	8599	1854	3522	54
H(42B)	7779	1347	3196	54
H(42C)	7333	1924	2907	54
H(43A)	6795	757	3773	48
H(43B)	8085	850	4366	48
H(43C)	6733	782	4566	48
H(44A)	5982	-1439	4903	53
H(44B)	5311	-912	5088	53
H(44C)	6598	-1127	5604	53
H(45A)	10059	-740	3595	42
H(45B)	9313	-1289	3577	42
H(45C)	10326	-1106	4269	42
H(46A)	8600	9585	10384	45
H(46B)	9269	9058	10748	45
H(47A)	6297	2478	4943	170
H(47B)	7200	2447	4412	170
H(47C)	6336	1950	4508	170
H(48A)	5164	2917	4039	136
H(48B)	5592	2536	3501	136
H(49A)	4101	1895	3842	101
H(49B)	3533	2352	3295	101
H(50A)	3721	2423	4746	109
H(50B)	3175	2885	4208	109
H(51A)	2012	1882	4142	90
H(51B)	1440	2382	3682	90
H(52A)	1631	2299	5129	76
H(52B)	321	2255	4538	76
H(52C)	1073	2806	4673	76

Appendix 9

Crystal Data for [Ru(=C(OC(CF$_3$)$_2$CH$_2$-)(*p*-C$_6$H$_4$Me))(H$_2$IMes) (OC(CF$_3$)$_2$CH$_3$)] (mm1332)

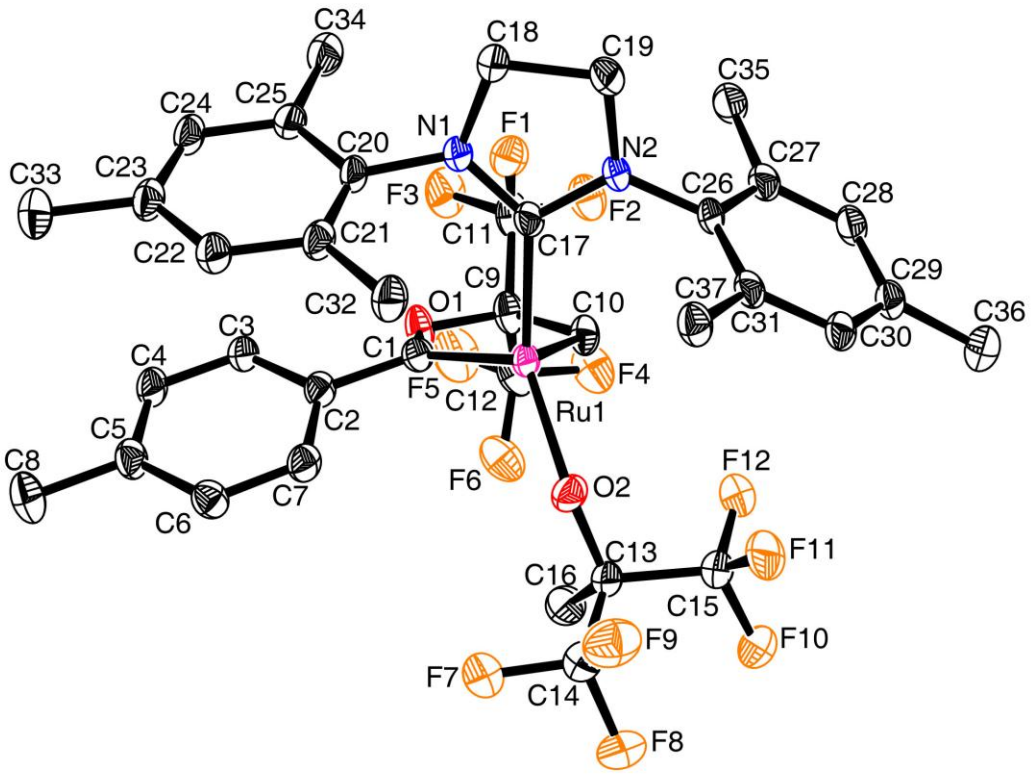

Figure A9.1. X-ray crystal structure of [Ru(=C(OC(CF$_3$)$_2$CH$_2$-)(*p*-C$_6$H$_4$Me))(H$_2$IMes) (OC(CF$_3$)$_2$CH$_3$)] (mm1332) (50% thermal ellipsoid plot). Hydrogen atoms are omitted for clarity.

A9.1. Structure Determination.

Purple plates of **mm1332** were grown from a pentane solution at –35 deg. C. A crystal of dimensions 0.21 x 0.15 x 0.05 mm was mounted on a Bruker SMART APEX CCD-based X-ray diffractometer equipped with a low temperature device and fine focus Mo-target X-ray tube (λ = 0.71073 Å) operated at 1500 W power (50 kV, 30 mA). The X-ray intensities were measured at 85(1) K; the detector was placed at a distance 5.055 cm from the crystal. A total of 3000 frames were collected with a scan width of 0.5° in ω and 0.45° in φ with an exposure time of 45 s/frame. The integration of the data yielded a total of 95604 reflections to a maximum 2θ value of 55.86° of which 9443 were independent and 7462 were greater than $2\sigma(I)$. The final cell constants (**A9.2**) were based on the xyz centroids of 9992 reflections above $10\sigma(I)$. Analysis of the data showed negligible decay during data collection; the data were processed with SADABS and corrected for absorption. The structure was solved and refined with the Bruker SHELXTL (version 2008/3) software package, using the space group P2(1)/c with Z = 4 for the formula $C_{37}H_{38}N_2O_2F_{12}Ru\bullet(C_5H_{12})_{0.5}$. All non-hydrogen atoms were refined anisotropically with the hydrogen atoms placed in idealized positions. The pentane solvent lies on an inversion center and is disordered. One carbon of the ethyl bridge of the H_2IMes ligand is also disordered. Full matrix least-squares refinement based on F^2 converged at R1 = 0.0428 and wR2 = 0.1107 [based on $I > 2\sigma(I)$], R1 = 0.0599 and wR2 = 0.1204 for all data. Additional details are presented in **A9.2**.

Sheldrick, G.M. SHELXTL, v. 2008/3; Bruker Analytical X-ray, Madison, WI, 2008.

Sheldrick, G.M. SADABS, v. 2008/1. Program for Empirical Absorption Correction of Area Detector Data, University of Gottingen: Gottingen, Germany, 2008.

Saint Plus, v. 7.53a, Bruker Analytical X-ray, Madison, WI, 2008.

A9.2. Crystal data and structure refinement for mm1332.

Identification code	mm1332
Empirical formula	$C_{39.50}$ H_{44} F_{12} N_2 O_2 Ru
Formula weight	907.84
Temperature	85(2) K
Wavelength	0.71073 Å
Crystal system, space group	Monoclinic, P2(1)/c
Unit cell dimensions	a = 12.6265(10) Å alpha = 90 deg.
	b = 17.5776(14) Å beta = 108.816(1) deg.
	c = 18.7633(15) Å gamma = 90 deg.
Volume	3941.8(5) $Å^3$
Z, Calculated density	4, 1.530 Mg/m^3
Absorption coefficient	0.492 mm^{-1}
F(000)	1852
Crystal size	0.21 x 0.15 x 0.05 mm
Theta range for data collection	1.70 to 27.93 deg.
Limiting indices	-16<=h<=16, -23<=k<=23, -24<=l<=24
Reflections collected / unique	95604 / 9443 [R(int) = 0.0693]
Completeness to θ = 27.93	99.8 %

Absorption correction	Semi-empirical from equivalents
Max. and min. transmission	0.9758 and 0.9038
Refinement method	Full-matrix least-squares on F^2
Data / restraints / parameters	9443 / 53 / 542
Goodness-of-fit on F^2	1.072
Final R indices [$I>2\sigma(I)$]	R1 = 0.0428, wR2 = 0.1107
R indices (all data)	R1 = 0.0599, wR2 = 0.1204
Largest diff. peak and hole	1.269 and -1.079 e*Å^{-3}

A9.3. Atomic coordinates (x 10^4) and equivalent isotropic displacement parameters (Å^2 x 10^3) for mm1332.

U(eq) is defined as one third of the trace of the orthogonalized Uij tensor.

	x	y	z	U(eq)
Ru(1)	5245(1)	2555(1)	2069(1)	20(1)
F(1)	6876(2)	902(1)	3039(1)	34(1)
F(2)	5952(2)	-70(1)	2462(1)	38(1)
F(3)	7520(2)	235(1)	2314(1)	45(1)
F(4)	4803(2)	64(1)	980(1)	45(1)
F(5)	6415(2)	227(1)	851(1)	52(1)
F(6)	5124(2)	1061(1)	416(1)	44(1)
F(7)	3710(2)	4151(1)	180(1)	45(1)
F(8)	1953(2)	3894(1)	-270(1)	46(1)
F(9)	2654(2)	4332(1)	860(1)	48(1)
F(10)	1232(2)	2578(2)	178(1)	60(1)
F(11)	1726(2)	3122(2)	1266(1)	55(1)
F(12)	2356(2)	2012(1)	1137(1)	45(1)
O(1)	6716(2)	1582(1)	1642(1)	31(1)
O(2)	3988(2)	3093(1)	1322(1)	28(1)
N(1)	7062(2)	2573(1)	3619(1)	26(1)

N(2)	5427(2)	2186(1)	3623(1)	24(1)
C(1)	6439(2)	2326(2)	1766(2)	24(1)
C(2)	7163(2)	2851(2)	1503(2)	24(1)
C(3)	8235(2)	2634(2)	1522(2)	26(1)
C(4)	8898(2)	3125(2)	1271(2)	28(1)
C(5)	8517(2)	3836(2)	985(2)	28(1)
C(6)	7422(2)	4047(2)	946(2)	27(1)
C(7)	6764(2)	3561(2)	1211(2)	26(1)
C(8)	9237(3)	4375(2)	709(2)	39(1)
C(9)	5940(3)	1035(2)	1736(2)	29(1)
C(10)	4936(2)	1418(2)	1885(2)	27(1)
C(11)	6581(3)	522(2)	2387(2)	33(1)
C(12)	5574(3)	590(2)	997(2)	37(1)
C(13)	3123(2)	3040(2)	654(2)	28(1)
C(14)	2846(3)	3855(2)	362(2)	37(1)
C(15)	2102(3)	2687(2)	806(2)	39(1)
C(16)	3407(3)	2567(2)	61(2)	36(1)
C(17)	6020(2)	2402(2)	3164(2)	22(1)
C(18)	7162(17)	2650(20)	4427(9)	36(5)
C(18A)	7226(6)	2380(10)	4417(5)	34(2)
C(19)	6023(3)	2337(2)	4421(2)	33(1)
C(20)	7924(2)	2960(2)	3409(2)	24(1)
C(21)	7734(2)	3702(2)	3133(2)	26(1)
C(22)	8614(2)	4083(2)	2987(2)	28(1)
C(23)	9658(2)	3751(2)	3128(2)	28(1)
C(24)	9821(2)	3020(2)	3419(2)	28(1)
C(25)	8966(2)	2605(2)	3560(2)	27(1)
C(26)	4274(2)	1964(2)	3379(2)	23(1)
C(27)	4002(2)	1202(2)	3461(2)	27(1)
C(28)	2877(2)	991(2)	3200(2)	28(1)
C(29)	2035(2)	1512(2)	2878(2)	26(1)
C(30)	2324(2)	2267(2)	2840(2)	26(1)
C(31)	3432(2)	2511(2)	3094(2)	24(1)
C(32)	6638(2)	4109(2)	3002(2)	31(1)
C(33)	10604(3)	4176(2)	2974(2)	36(1)
C(34)	9191(3)	1814(2)	3869(2)	38(1)
C(35)	4880(3)	612(2)	3826(2)	33(1)
C(36)	830(3)	1256(2)	2560(2)	35(1)
C(37)	3699(3)	3344(2)	3070(2)	28(1)
C(38)	-1645(8)	525(6)	132(8)	124(5)
C(39)	-503(7)	926(5)	227(5)	67(2)
C(40)	270(8)	270(6)	249(6)	88(3)
C(41)	1308(10)	290(7)	107(7)	106(3)
C(38A)	1641	-510	-123	153

A9.4. Bond lengths [Å] and angles [deg] for mm1332.

Ru(1)-C(1)	1.820(3)
Ru(1)-O(2)	1.986(2)
Ru(1)-C(17)	1.990(3)
Ru(1)-C(10)	2.045(3)
F(1)-C(11)	1.336(4)
F(2)-C(11)	1.343(4)
F(3)-C(11)	1.336(3)
F(4)-C(12)	1.335(4)
F(5)-C(12)	1.340(4)
F(6)-C(12)	1.340(4)
F(7)-C(14)	1.348(4)
F(8)-C(14)	1.349(4)
F(9)-C(14)	1.334(4)
F(10)-C(15)	1.340(4)
F(11)-C(15)	1.350(4)
F(12)-C(15)	1.329(4)
O(1)-C(1)	1.392(3)
O(1)-C(9)	1.424(3)
O(2)-C(13)	1.373(3)
N(1)-C(17)	1.351(4)
N(1)-C(20)	1.441(3)
N(1)-C(18A)	1.483(7)
N(1)-C(18)	1.486(14)
N(2)-C(17)	1.364(3)
N(2)-C(26)	1.432(4)
N(2)-C(19)	1.467(4)
C(1)-C(2)	1.491(4)
C(2)-C(7)	1.390(4)
C(2)-C(3)	1.397(4)
C(3)-C(4)	1.386(4)
C(4)-C(5)	1.384(4)
C(5)-C(6)	1.410(4)
C(5)-C(8)	1.515(4)
C(6)-C(7)	1.390(4)
C(9)-C(11)	1.525(5)
C(9)-C(12)	1.528(4)
C(9)-C(10)	1.538(4)
C(13)-C(16)	1.521(4)
C(13)-C(14)	1.534(5)
C(13)-C(15)	1.538(4)
C(18)-C(19)	1.533(14)
C(18A)-C(19)	1.523(8)

C(20)-C(21)	1.395(4)
C(20)-C(25)	1.401(4)
C(21)-C(22)	1.397(4)
C(21)-C(32)	1.506(4)
C(22)-C(23)	1.388(4)
C(23)-C(24)	1.385(4)
C(23)-C(33)	1.514(4)
C(24)-C(25)	1.397(4)
C(25)-C(34)	1.498(4)
C(26)-C(27)	1.403(4)
C(26)-C(31)	1.405(4)
C(27)-C(28)	1.395(4)
C(27)-C(35)	1.512(4)
C(28)-C(29)	1.387(4)
C(29)-C(30)	1.384(4)
C(29)-C(36)	1.513(4)
C(30)-C(31)	1.392(4)
C(31)-C(37)	1.506(4)
C(38)-C(39)	1.562(8)
C(39)-C(40)	1.503(8)
C(40)-C(41)	1.420(8)
C(41)-C(38A)	1.567(11)
C(41)-C(38)#1	1.599(9)

C(1)-Ru(1)-O(2)	116.05(11)
C(1)-Ru(1)-C(17)	96.40(12)
O(2)-Ru(1)-C(17)	143.97(10)
C(1)-Ru(1)-C(10)	82.10(12)
O(2)-Ru(1)-C(10)	106.34(11)
C(17)-Ru(1)-C(10)	92.61(12)
C(1)-O(1)-C(9)	113.2(2)
C(13)-O(2)-Ru(1)	146.1(2)
C(17)-N(1)-C(20)	126.8(2)
C(17)-N(1)-C(18A)	112.2(4)
C(20)-N(1)-C(18A)	120.8(4)
C(17)-N(1)-C(18)	114.1(6)
C(20)-N(1)-C(18)	114.6(7)
C(18A)-N(1)-C(18)	18.4(12)
C(17)-N(2)-C(26)	125.7(2)
C(17)-N(2)-C(19)	112.8(2)
C(26)-N(2)-C(19)	120.6(2)
O(1)-C(1)-C(2)	108.2(2)
O(1)-C(1)-Ru(1)	122.6(2)
C(2)-C(1)-Ru(1)	128.6(2)
C(7)-C(2)-C(3)	118.7(3)

C(7)-C(2)-C(1)	120.2(2)
C(3)-C(2)-C(1)	121.0(3)
C(4)-C(3)-C(2)	120.5(3)
C(5)-C(4)-C(3)	121.5(3)
C(4)-C(5)-C(6)	117.9(3)
C(4)-C(5)-C(8)	121.7(3)
C(6)-C(5)-C(8)	120.4(3)
C(7)-C(6)-C(5)	120.7(3)
C(2)-C(7)-C(6)	120.6(3)
O(1)-C(9)-C(11)	106.8(2)
O(1)-C(9)-C(12)	104.6(2)
C(11)-C(9)-C(12)	110.6(3)
O(1)-C(9)-C(10)	111.6(2)
C(11)-C(9)-C(10)	111.6(2)
C(12)-C(9)-C(10)	111.3(3)
C(9)-C(10)-Ru(1)	109.56(19)
F(1)-C(11)-F(3)	106.8(3)
F(1)-C(11)-F(2)	107.0(3)
F(3)-C(11)-F(2)	107.0(2)
F(1)-C(11)-C(9)	110.9(2)
F(3)-C(11)-C(9)	113.6(3)
F(2)-C(11)-C(9)	111.3(3)
F(4)-C(12)-F(5)	106.6(3)
F(4)-C(12)-F(6)	107.0(3)
F(5)-C(12)-F(6)	106.5(3)
F(4)-C(12)-C(9)	112.3(3)
F(5)-C(12)-C(9)	113.7(3)
F(6)-C(12)-C(9)	110.3(3)
O(2)-C(13)-C(16)	113.5(2)
O(2)-C(13)-C(14)	106.5(3)
C(16)-C(13)-C(14)	109.2(3)
O(2)-C(13)-C(15)	109.0(2)
C(16)-C(13)-C(15)	108.9(3)
C(14)-C(13)-C(15)	109.6(3)
F(9)-C(14)-F(7)	106.3(3)
F(9)-C(14)-F(8)	107.1(3)
F(7)-C(14)-F(8)	105.8(3)
F(9)-C(14)-C(13)	114.1(3)
F(7)-C(14)-C(13)	110.0(3)
F(8)-C(14)-C(13)	113.0(3)
F(12)-C(15)-F(10)	106.8(3)
F(12)-C(15)-F(11)	106.7(3)
F(10)-C(15)-F(11)	106.6(3)
F(12)-C(15)-C(13)	110.9(3)
F(10)-C(15)-C(13)	113.2(3)

F(11)-C(15)-C(13)	112.2(3)
N(1)-C(17)-N(2)	106.5(2)
N(1)-C(17)-Ru(1)	132.6(2)
N(2)-C(17)-Ru(1)	120.1(2)
N(1)-C(18)-C(19)	101.0(9)
N(1)-C(18A)-C(19)	101.6(5)
N(2)-C(19)-C(18A)	100.9(4)
N(2)-C(19)-C(18)	104.1(6)
C(18A)-C(19)-C(18)	17.8(12)
C(21)-C(20)-C(25)	121.9(3)
C(21)-C(20)-N(1)	119.3(2)
C(25)-C(20)-N(1)	118.5(3)
C(20)-C(21)-C(22)	118.0(3)
C(20)-C(21)-C(32)	122.9(3)
C(22)-C(21)-C(32)	119.1(3)
C(23)-C(22)-C(21)	121.8(3)
C(24)-C(23)-C(22)	118.5(3)
C(24)-C(23)-C(33)	120.5(3)
C(22)-C(23)-C(33)	121.0(3)
C(23)-C(24)-C(25)	122.3(3)
C(24)-C(25)-C(20)	117.5(3)
C(24)-C(25)-C(34)	119.8(3)
C(20)-C(25)-C(34)	122.7(3)
C(27)-C(26)-C(31)	120.9(3)
C(27)-C(26)-N(2)	119.0(3)
C(31)-C(26)-N(2)	120.1(3)
C(28)-C(27)-C(26)	118.3(3)
C(28)-C(27)-C(35)	119.4(3)
C(26)-C(27)-C(35)	122.4(3)
C(29)-C(28)-C(27)	121.8(3)
C(30)-C(29)-C(28)	118.6(3)
C(30)-C(29)-C(36)	120.9(3)
C(28)-C(29)-C(36)	120.5(3)
C(29)-C(30)-C(31)	122.0(3)
C(30)-C(31)-C(26)	118.2(3)
C(30)-C(31)-C(37)	120.0(3)
C(26)-C(31)-C(37)	121.8(3)
C(40)-C(39)-C(38)	103.0(7)
C(41)-C(40)-C(39)	127.4(8)
C(40)-C(41)-C(38A)	112.0(9)
C(40)-C(41)-C(38)#1	112.0(10)
C(38A)-C(41)-C(38)#1	0.3(5)

Symmetry transformations used to generate equivalent atoms: #1 -x,-y,-z

A9.5. Anisotropic displacement parameters ($Å^2$ x 10^3) for mm1332.

The anisotropic displacement factor exponent takes the form:
-2 pi^2 [h^2 a*^2 U11 + ... + 2 h k a* b* U12]

	U11	U22	U33	U23	U13	U12
Ru(1)	16(1)	28(1)	20(1)	0(1)	10(1)	2(1)
F(1)	29(1)	33(1)	39(1)	-1(1)	12(1)	3(1)
F(2)	45(1)	28(1)	49(1)	1(1)	24(1)	-3(1)
F(3)	40(1)	43(1)	64(1)	4(1)	32(1)	15(1)
F(4)	61(1)	36(1)	44(1)	-11(1)	26(1)	-15(1)
F(5)	62(1)	51(1)	58(1)	-15(1)	40(1)	8(1)
F(6)	61(1)	44(1)	35(1)	-5(1)	27(1)	-2(1)
F(7)	37(1)	52(1)	44(1)	13(1)	12(1)	-7(1)
F(8)	34(1)	56(1)	39(1)	12(1)	0(1)	4(1)
F(9)	48(1)	49(1)	45(1)	0(1)	12(1)	17(1)
F(10)	25(1)	95(2)	50(1)	25(1)	-2(1)	-17(1)
F(11)	38(1)	86(2)	55(1)	24(1)	34(1)	21(1)
F(12)	34(1)	58(1)	46(1)	18(1)	16(1)	-6(1)
O(1)	30(1)	28(1)	46(1)	-1(1)	28(1)	0(1)
O(2)	21(1)	38(1)	26(1)	0(1)	8(1)	4(1)
N(1)	18(1)	40(1)	22(1)	3(1)	9(1)	-2(1)
N(2)	20(1)	34(1)	22(1)	2(1)	12(1)	-1(1)
C(1)	22(1)	29(1)	22(1)	0(1)	11(1)	2(1)
C(2)	21(1)	32(2)	21(1)	-3(1)	11(1)	0(1)
C(3)	21(1)	33(2)	26(1)	2(1)	11(1)	1(1)
C(4)	20(1)	38(2)	30(2)	0(1)	14(1)	0(1)
C(5)	26(1)	36(2)	27(2)	-2(1)	15(1)	-4(1)
C(6)	29(2)	28(1)	27(2)	0(1)	13(1)	2(1)
C(7)	22(1)	34(2)	26(2)	-2(1)	12(1)	2(1)
C(8)	39(2)	40(2)	49(2)	2(2)	28(2)	-6(1)
C(9)	29(2)	27(1)	38(2)	-4(1)	21(1)	-1(1)
C(10)	23(1)	32(2)	31(2)	-4(1)	16(1)	-2(1)
C(11)	31(2)	29(2)	47(2)	-5(1)	24(2)	2(1)
C(12)	47(2)	34(2)	40(2)	-5(1)	28(2)	-1(1)
C(13)	19(1)	41(2)	25(2)	5(1)	9(1)	1(1)
C(14)	27(2)	49(2)	34(2)	7(2)	10(1)	2(1)
C(15)	22(2)	62(2)	36(2)	17(2)	12(1)	4(1)
C(16)	34(2)	51(2)	26(2)	0(1)	13(1)	2(1)
C(17)	19(1)	26(1)	24(1)	2(1)	12(1)	4(1)

C(18)	20(6)	61(13)	27(7)	7(7)	7(5)	-7(7)
C(18A)	23(3)	59(6)	22(3)	6(3)	8(2)	-5(3)
C(19)	29(2)	51(2)	22(2)	-1(1)	12(1)	-7(1)
C(20)	16(1)	37(2)	23(1)	-1(1)	10(1)	-3(1)
C(21)	18(1)	38(2)	25(2)	-4(1)	10(1)	-1(1)
C(22)	24(1)	33(2)	29(2)	0(1)	12(1)	-1(1)
C(23)	20(1)	39(2)	28(2)	-6(1)	11(1)	-5(1)
C(24)	17(1)	40(2)	30(2)	-2(1)	11(1)	-1(1)
C(25)	20(1)	38(2)	24(1)	0(1)	7(1)	-2(1)
C(26)	18(1)	33(2)	22(1)	1(1)	13(1)	1(1)
C(27)	25(1)	32(2)	28(2)	4(1)	15(1)	4(1)
C(28)	26(1)	31(2)	32(2)	3(1)	17(1)	0(1)
C(29)	23(1)	33(2)	28(2)	0(1)	14(1)	0(1)
C(30)	22(1)	31(1)	29(2)	3(1)	15(1)	5(1)
C(31)	24(1)	29(1)	24(1)	1(1)	15(1)	1(1)
C(32)	23(1)	35(2)	38(2)	-1(1)	15(1)	2(1)
C(33)	27(2)	40(2)	45(2)	-2(2)	19(1)	-5(1)
C(34)	24(2)	44(2)	45(2)	9(2)	11(1)	2(1)
C(35)	29(2)	34(2)	39(2)	10(1)	17(1)	5(1)
C(36)	25(2)	38(2)	44(2)	-1(1)	12(1)	-2(1)
C(37)	27(2)	28(2)	36(2)	2(1)	17(1)	2(1)
C(38)	118(7)	136(11)	123(10)	83(9)	43(8)	-2(6)
C(39)	95(5)	65(5)	33(4)	31(4)	8(4)	7(4)
C(40)	116(6)	79(6)	48(5)	35(4)	-2(5)	38(5)
C(41)	139(8)	102(7)	73(6)	39(6)	27(6)	32(7)
C(38A)	123	184	157	127	51	-2

A.9.6. Hydrogen coordinates (x 10^4) and isotropic displacement parameters ($Å^2$ x 10^3) for mm1332.

	x	y	z	U(eq)
H(3A)	8513	2145	1707	31
H(4A)	9630	2971	1297	34
H(6A)	7132	4525	738	33
H(7A)	6035	3716	1193	31
H(8A)	9966	4138	776	59
H(8B)	9345	4849	999	59

H(8C)	8867	4486	175	59
H(10A)	4810	1183	2331	32
H(10B)	4253	1342	1446	32
H(16A)	4109	2751	5	54
H(16B)	2804	2614	-421	54
H(16C)	3491	2033	217	54
H(18A)	7267	3181	4597	43
H(18B)	7785	2334	4751	43
H(18C)	7652	2781	4762	41
H(18D)	7616	1887	4558	41
H(19A)	6113	1865	4722	39
H(19B)	5618	2717	4624	39
H(19C)	5921	1918	4745	39
H(19D)	5781	2822	4587	39
H(22A)	8493	4584	2786	33
H(24A)	10538	2793	3526	34
H(28A)	2683	475	3245	34
H(30A)	1749	2630	2636	31
H(32A)	6080	3904	2549	46
H(32B)	6739	4654	2934	46
H(32C)	6381	4033	3437	46
H(33A)	11316	4033	3350	54
H(33B)	10487	4725	3003	54
H(33C)	10622	4047	2470	54
H(34A)	9909	1637	3835	57
H(34B)	8593	1474	3577	57
H(34C)	9218	1813	4397	57
H(35A)	4948	563	4360	49
H(35B)	5601	769	3782	49
H(35C)	4660	121	3575	49
H(36A)	334	1679	2578	53
H(36B)	701	831	2860	53
H(36C)	674	1092	2037	53
H(37A)	3687	3480	2561	42
H(37B)	4444	3447	3428	42
H(37C)	3141	3647	3206	42
H(38A)	-1597	-11	2	187
H(38B)	-2238	775	-271	187
H(38C)	-1816	559	605	187
H(39A)	-557	1267	-203	81
H(39B)	-249	1224	700	81
H(40A)	439	46	758	106
H(40B)	-189	-112	-105	106
H(41A)	1900	468	565	128
H(41B)	1257	658	-302	128

H(38D)	2359	-472	-216	230
H(38E)	1064	-684	-581	230
H(38F)	1706	-874	285	230